AD NUMBER	
AD380821	
CLASSIFICATION CHANGES	
TO:	unclassified
FROM:	confidential
LIMITATION CHANGES	
TO:	Approved for public release, distribution unlimited
FROM:	Distribution authorized to U.S. Gov't. agencies only; Administrative/Operational Use; 01 JUN 1964. Other requests shall be referred to US Federal Aviation Agency, Attn: Supersonic Transport Development, Washington, DC 20553.
AUTHORITY	
FAA ltr, 10 Oct 1972; FAA ltr, 10 Oct 1972	

SECURITY

MARKING

The classified or limited status of this report applies to each page, unless otherwise marked.
Separate page printouts MUST be marked accordingly.

(14)
Report No. PWA-2397 — Vol. 2 **CONFIDENTIAL**

Copy #________

(11) 30 Nov[redacted]64

(12) 1v.

AD 380821

ACCESSION FOR
CFSTI WHITE SECTION
DDC BUFF SECTION
UNANNOUNCED
JUSTIFICATION

BY
DISTRIBUTION/AVAILABILITY CODES
DIST. AVAIL. and/or SPECIAL

13

(6) SUPERSONIC TRANSPORT AIRCRAFT ENGINE

PHASE II-A DEVELOPMENT PROGRAM,
VOLUME II (U). (8)

(9) FINAL REP[redacted]T, 1 Jun-30 Nov 64.

E. H. Document Control
Eng. Sub-Control Station
MAR 8 1965
Number: 139-5-C 11 B41

(15)
Prepared Under Contract FA-SS-64-2

Period Covered
1 June 1964 through 30 November 1964

FAA SECURITY CONTROL
NO. 65 573-A-2

(FOR OFFICIAL USE ONLY)

DDC
RECEIVED
MAY 8 1967
D

This document contains information affecting the national defense of the United States within the meaning of the Espionage Laws, Title 18 U.S.C. Sections 793 and 794. Its transmission or the revelation of its contents in any manner to an unauthorized person is prohibited by law.

Reproduction, distribution and use of this document are limited as specified in the contract under which it was prepared. Use for other than U.S. Governmental purposes is subject to prior approval of United Aircraft Corporation.

Approved by R. L. Toft — R. L. Toft, Project Engineer

Pratt & Whitney Aircraft DIVISION OF UNITED AIRCRAFT CORPORATION

EAST HARTFORD • CONNECTICUT

(287500)

Best Available Copy

CONFIDENTIAL

DOWNGRADED AT 3 YEAR INTERVALS;
DECLASSIFIED AFTER 12 YEARS.
DOD DIR 5200.10

NOTICES

When Government drawings, specifications, or other data are used for any purpose other than in connection with a definitely related Government procurement operation, the United States Government thereby incurs no responsibility nor any obligation whatsoever; and the fact that the Government may have formulated, furnished, or in any way supplied the said drawings, specifications, or other data, is not to be regarded by implication or otherwise as in any manner licensing the holder or any other person or corporation, or conveying any rights or permission to manufacture, use, or sell any patented invention that may in any way be related thereto.

Copies have been placed in the DDC collection. U.S. Government agencies may obtain copies from DDC. Other qualified DDC users may request, by submission of a DDC Form 1, through:

Director of Supersonic Transport Development
Federal Aviation Agency
Washington, D.C. 20553

Defense Documentation Center release to the Clearinghouse for Federal, Scientific, and Technical Information (CFSTI) and foreign announcement and dissemination are not authorized. The distribution of this report is limited because it contains technology identifiable with items excluded from export by the Department of State (U.S. Export Control Act of 1949 as amended).

CONFIDENTIAL

Material in this publication relating to

JET FLAMEHOLDER

reveals subject matter contained in a patent application which has been placed under Secrecy Order by the Commissioner of Patents. This Secrecy Order has been modified by a "Permit A"

A Secrecy Order prohibits publication or disclosure of the invention, or any material information with respect thereto. It is separate and distinct, and has nothing to do with the classification of Government contracts

By statute, violation of a Secrecy Order is punishable by a fine not to exceed $10,000 and/or imprisonment for not more than two years

A "Permit A" authorizes disclosure of the subject matter of the patent application to any person of the classes hereinafter specified if such person is known to be concerned directly in an official capacity with the subject matter, provided that all reasonable safeguards are taken to otherwise protect the invention from unauthorized disclosure. The specified classes are:

(a) Any officer or employee of any department, independent agency or bureau of the Government of the United States.

(b) Any person designated specifically by the head of any department, independent agency or bureau of the Government of the United States, or by his duly authorized subordinate as a proper individual to receive the disclosure of the above indicated application

A "Permit A" also authorizes disclosure to the minimum necessary number of persons of known loyalty and discretion employed by or working with United Aircraft Corporation or its licensees and whose duties involve cooperation in the development, manufacture or use of the subject matter by or for the Government of the United States, provided such persons are advised of the issuance of the Secrecy Order

Should it appear necessary to make disclosures not authorized above, a request for modification of the Secrecy Order should be made through the Pratt & Whitney Aircraft Patent Engineer

The foregoing does not in any way lessen responsibility for the security of the subject matter as imposed by any Government contract or the provisions of the existing laws relating to espionage and national security.

STATEMENT #3 CLASSIFIED

In addition to security requirements which apply to this document and must be met, each transmittal outside the agencies of the U.S. Government must have prior approval of FAA, Wash. DC

CONFIDENTIAL

EXHAUST SYSTEM

EXHAUST SYSTEM

Best
Available
Copy

ITEM 8 - EXHAUST SYSTEM

OBJECTIVES

Pratt & Whitney Aircraft has conducted static (internal flow only) and wind tunnel (internal and external flow) tests of scale models of the engine exhaust system, including thrust reverser, directed toward verification of the exhaust system performance.

A. INTRODUCTION

The goal of this program was to meet or exceed the following exhaust system performance specifications expressed in terms of the thrust-minus-drag coefficient (C_{FP}) at typical power settings for the following flight conditions:

Mach Number	Condition	C_{FP} With 2% Secondary Air Flow
3.0	Cruise	0.999
2.7	Cruise	0.999
1.2	Acceleration	0.962
0.9	Cruise to Alternate	0.935
0	Sea-Level Take-Off	0.980

$$C_{FP} = \frac{\text{(Gross Thrust of Primary Flow and any Secondary Air) - (External Wave Drag and All Internal Losses)}}{\text{Ideal Gross Thrust of Primary Flow}}$$

The goal for thrust reversing is a minimum of 40 per cent reverse thrust with no significant engine airflow suppression.

During the course of the contract period, a systematic program has been followed to select and develop an operationally flexible, efficient

exhaust nozzle system. The exhaust system has been shown to be a very critical component of the propulsion unit, and, therefore, it must be capable of high performance without being excessively heavy or complex. During Phase I, the whole field of available exhaust systems was appraised in relation to the supersonic transport requirements. The two most promising systems, the blow-in-door ejector and the plug nozzle, were then selected for further investigation.

During Phase IIA, the blow-in-door ejector and the plug nozzle were compared on the basis of internal and external performance, weight, mechanical complexity, and compatibility with the airframe for the supersonic transport. Further parametric experimentation was conducted to supplement the Phase I work to define the performance potential of both exhaust systems.

B. SUMMARY

Two engine cycles were originally considered during the Phase IIA program: a duct burning turbofan and a partially augmented turbojet. Although the turbojet was later eliminated, programs were conducted to evaluate nozzles for both cycles. Neither system was studied as extensively as that selected for the STF219 engine.

The blow-in-door ejector was chosen for the STF219 duct-heating turbofan engine proposed for the supersonic transport for the following reasons.

1. Superior performance
2. Relatively light weight
3. Applicable to engines with large amounts of augmentation
4. Relative insensitivity to installation effects
5. Reliability since no linkage is required between the ejector and the activated portion of the primary nozzle
6. Convenient adaptability to a thrust reverser system
7. Effectiveness as a noise suppressor

The plug nozzle was eliminated for the co-annular duct-heating turbofan engine on the basis of the analytical, experimental, and design studies conducted during both Phase I and Phase IIA. Its performance, weight, and complexity made it completely unacceptable for the supersonic transport.

The performance obtained from scale model tests of the blow-in-door ejector selected for the STF219 engine compares very favorably with the Pratt & Whitney Aircraft model specification. At sea-level take-off, the program goal was achieved, and, at Mach 0.9 cruise, the goal was actually exceeded. The performance at Mach 1.2 was within less than one per cent of meeting the goal, and, at superaonic cruise, the performance was within approximately one per cent of the goal. The relative success in essentially meeting the goals during this phase of the supersonic transport program can be directly attributed to the wealth of background information obtained from the analyses and tests conducted under previous research and development programs. Significant progress was also made during Phase IIA in demonstrating reverse thrust coefficients compatible with the airframe requirements.

The results of the experimental program indicate that the levels of exhaust nozzle performance established as program goals can be attained through reasonable development.

C. TEST PROGRAM

1. NOZZLE DESCRIPTION

a. Blow-in-Door Ejector

The blow-in-door ejector is a variable-geometry, self-actuated nozzle, which aerodynamically adjusts itself to the correct expansion ratio as engine pressure ratio and flight Mach number vary.

b. Plug Nozzle

The plug nozzle, like the blow-in-door ejector, can provide aerodynamically adjusting performance characteristics. In this type of exhaust system, the throat is annular and the supersonic expansion of the exhaust gases takes place along a central plug.

c. Performance Definitions

The parameter used to present the exhaust nozzle performance is the gross thrust coefficient, C_{FP}. This coefficient is defined as the sum of the gross thrusts from the primary stream, the fan stream, and the secondary and tertiary streams minus the sum of the external pressure

or wave drag, the internal drag, and the ram drag of any tertiary air, all divided by the ideal gross thrust of the primary and fan streams. The reverse thrust coefficient is defined as above except that the thrust and drag are of the same sign.

2. TEST FACILITIES

The scale model exhaust nozzles and thrust reversers for the supersonic transport were tested at United Aircraft Corporation Research Laboratories. The facilities used included a static test stand, a continuous-flow interchangeable subsonic-transonic wind tunnel, and a 17-inch by 17-inch transonic-supersonic blow-down wind tunnel.

The versatility of the continuous-flow wind tunnel has been extended by the addition of a new balance that splits, meters, and throttles three concentric flows. This balance is similar to the one in use in the 17-inch by 17-inch wind tunnel.

3. DISCUSSION

During this phase of the program, the research and development programs, initiated under the previous SST contract and covered by Report PWA-2353, was extended to cover new aspects of nozzle operation. Included were studies of blow-in-door ejectors and reversers for co-annular, duct-heating turbofan engines and exhaust systems for a partially augmented turbojet engine.

a. Co-Annular Blow-In-Door Ejectors

Early Testing - Early testing under the current contract was conducted on the freely floating blow-in-door ejector for which calibration tests had been conducted under the previous contract. Testing was conducted in the eight-foot section of the main wind tunnel at the United Aircraft Corporation Research Laboratories, since better accuracy can be obtained for low power, subsonic flow with this wind tunnel than with the previously used seventeen-inch tunnel.

The results of the test series together with the results obtained previously are shown in Figure 8-1. A summary of the performance

obtained as a function of Mach number is shown in Figure 8-2. The performance indicated by these tests was as much as five per cent better than that obtained in the seventeen-inch tunnel, but it is somewhat lower than desired, particularly with high subsonic flow. Although previous tests of fixed ejectors have indicated that higher performance levels can be obtained, it is noted that the fixed version of the freely floating ejector was not tested, and that the freely floating model was designed to meet the requirements of an earlier duct-heating turbofan engine, and, therefore, does not represent the geometry or performance anticipated for the STF219 engine.

The performance obtained was lower than desired because the interactions between the ejector design variables, which were determined from parametric studies of the fixed model test results, were underestimated. Consequently, a program was undertaken to better establish the pertinent design criteria and to investigate various aspects of freely floating ejector operation.

Exploratory tests were conducted at Mach 0.9 at conditions simulating a 33 per cent power setting without duct heating to represent typical subsonic cruise operation. It was found that the compromises made in designing the shroud for supersonic operation produced greater aerodynamic losses during subsonic operation than anticipated. A three per cent loss was incurred by the increase in the external wave drag generated by the steep conical boat-tail angles associated with the trailing edge flaps in their closed position, and a two per cent loss occurred at the forward, inner portion of the shroud. Additional testing indicated that the external wave drag could be reduced by adjusting the stops on the trailing edge flaps to increase the minimum exit area. The losses at the shroud could be eliminated by redesigning the shroud leading edge. These changes were subsequently evaluated at supersonic cruise conditions and were found to have essentially no adverse effect.

Additional testing was conducted to evaluate other aspects of the ejector design during subsonic operation. The use of tandem blow-in-doors to produce a cylindrical contour during supersonic cruise, rather than a single door, produced a small loss during subsonic operation. Leakage around the blow-in-doors was found to improve the performance by approximately 0.5 per cent.

The blow-in-door area beneath the struts in the plane of the shroud leading edge was blocked off by extending the struts radially toward the centerline. This area constitutes approximately 15 per cent of the blow-in-door area, and it was desired to determine whether active flow occurred in this area. Blocking the area produced a loss of approximately one per cent, indicating that active flow does occur.

Experimental studies were conducted to investigate the effects of changes to the ejector geometry. For one test series, the trailing edge flaps were held closed and the blow-in-doors held at various positions at several important flight conditions. The results are shown in Figure 8-3. At Mach 0 with maximum duct heating and at Mach 0.9 cruise, closing the doors decreases the performance by approximately seven per cent. At Mach 1.2, however, closing the doors increases the performance by approximately three per cent. These results are not representative of normal operation, however, since normally the flaps would open as the Mach number increased.

In conjunction with the study described above, a series of tests were conducted to evaluate the effect of the trailing edge flap position at several flight conditions and with the blow-in doors permitted to float freely. The results obtained from this series are presented in Figure 8-4. At Mach 0, varying the exit area produces a negligible effect. At Mach 0.9 cruise, however, increasing the exit area from the minimum to the maximum decreases the nozzle performance by 11 per cent. At Mach 1.2 with maximum duct heating, the nozzle performance is not very sensitive to changes in the exit area except at the very low area ratios. The results shown in Figure 8-4 indicate that significant improvements in subsonic nozzle performance can be achieved by simply changing the inner stop on the trailing edge flaps. It shows that a slightly larger minimum exit area would be highly advantageous for all three operating conditions.

The secondary cooling flow associated with blow-in-door ejectors was also investigated. An attempt was made to replace the conventional secondary flow with flow through the blow-in doors. A model was modified by drilling small holes in the upstream section of the fore-body, as shown in Figure 8-5, to permit secondary air to be drawn in. The results of testing the modified ejector are shown in Figures 8-6 and 8-7 with and without duct heating at Mach 0, 0.6, and 0.9. No

significant improvement in performance was obtained, but it is believed that an improvement could be realized by resizing and relocating the holes closer to the primary nozzle assembly.

In addition to the subsonic test programs, several ejector designs were tested at Mach 2.6 to simulate operation during supersonic cruise. Attention was directed primarily to the effects produced by changing the shroud and primary nozzle geometries. The investigation of the effect of changing the shroud geometry demonstrated that the cruise performance could be predicted to within two per cent and that the change in performance resulting from a change in the minimum internal diameter of the shroud could be minimized through proper design. It was demonstrated that the minimum diameter could be moved downstream with a performance change which was no greater than one per cent providing that the translation was conducted along the estimated streamline of the primary jet. Consequently, considerable freedom may be exercised in the design of the shroud to produce an ejector capable of high performance in the subsonic, transonic, and supersonic regimes.

The configurations tested to evaluate the effect of changing the nozzle geometry are shown in Figures 8-8 and 8-9. The engine primary stream area ratio was varied from 1.00 to 2.37, and the fan stream area ratio was varied from 1.18 to 2.12. The changes to the primary stream area ratio produced a maximum performance change of 2 per cent, but most of the results were within 0.75 per cent. The over-all performance at simulated supersonic cruise conditions was within one per cent of the predicted value.

These tests indicated that, within the range considered, no single shroud design is significantly superior to the others and that the over-all ejector performance is slightly more sensitive to changes in the shroud geometry than to changes in the primary geometry. However, the two systems must act as one efficient unit and must be developed simultaneously. Although the performance improvements demonstrated were small, they must be considered at this stage of the program if the high performance goals are to be realized.

Recent Studies - STF219 Ejector Design - The early exhaust nozzle performance and parametric studies were based on some of the early SST engine and ejector concepts. When the engine cycle (STF219) was selected during the Phase IIA program, the knowledge gained from the previous exhaust system studies was used to design a series of blow-in-door ejector models to simulate the STF219 engine operating conditions. These are shown in Figure 8-10. Although the final engine parameters used in the model specification differ slightly from those used in the design of the models, the over-all effect of the differences are not considered to be significant.

The models tested had fixed geometries which simulated the geometries of a consistent variable-geometry ejector at sea-level take-off, Mach 0.9 cruise, Mach 1.2 acceleration (maximum duct heating), and Mach 2.7 cruise. The model is shown schematically in Figure 8-11.

As in the previous blow-in-door ejector programs, alternate configurations were constructed and tested to evaluate the effects of changing design parameters known to exert a strong influence on performance. Comparisons were then made with the basic design. The results are shown in Figures 8-12 through 8-15. The solid symbol on each curve denotes the basic design data.

The nozzle area ratio, A_{exit}/A^*_{total}, has a negligible effect over the range tested at both sea-level take-off and at Mach 0.9 cruise (the upper curves of Figures 8-12 and 8-13), but a somewhat more pronounced effect at Mach 1.2 (Figure 8-14). The lower value of C_{FP} shown at Mach 0.9 for the basic design is due to a difference in the internal contour of the other shrouds tested. The effect of changes to the blow-in-door area, A_{bid}/A^*_{total}, is also shown in Figures 8-12 and 8-13 at sea-level take-off and at Mach 0.9 with the effect being most pronounced at Mach 0.9. Previous tests have indicated that the blow-in-doors should be sized for optimum subsonic cruise performance. During supersonic cruise, where the blow-in doors are closed and the trailing edge flaps fully extended, the internal shroud shape is most important. One critical parameter is the location of the minimum shroud diameter location. The effect of moving the minimum shroud diameter is shown in Figure 8-15.

These tests indicated that the ejector selected for the STF219 demonstrates near maximum performance for the range of variables tested at take-off, at subsonic cruise, and at the critical Mach 1.2 acceleration condition. It appears, however, that a further optimization of the internal shroud shape may improve the performance during supersonic cruise. Comparison of the experimental results with those predicted by a theoretical analysis of three concentric flows programmed on a high-speed computer (see Figure 8-16) indicates that additional performance improvement might be made, but that the experimental levels obtained are reasonable. The performance of the STF219 ejector and the performance specified by the Phase IIA model specification are shown in Figure 8-17. As shown, at sea-level take-off, the goal has been achieved, and, at Mach 0.9, the goal was exceeded. The performance at Mach 1.2 is within less than one per cent of the goal, and, for supersonic cruise, the performance is approximately one per cent less than that specified. Consequently, the experimental program has demonstrated that, with reasonable development, the model specification goals for the STF219 blow-in-door ejector can be met.

b. Blow-In-Door Ejector Reversers

During this report period, the basic reverser program discussed in Pratt & Whitney Aircraft Report PWA-2353 was continued with new aspects of the reverser design being considered. The effect of installation blow-in-door blockage, flight Mach number, and engine-to-duct total pressure ratio were all considered. Reverse thrust coefficients of over 40 per cent (the minimum thrust reversing goal) were obtained statically, and, at Mach 0.9, coefficients in excess of 75 per cent were obtained.

Installation blockages were simulated by modifying an available model as shown in Figure 8-18. These blockages, representing two typical installations, result in large reductions in the usable blow-in-door area for thrust reversing. The blockage to the airflow necessitates that some of the flow be bled past the reverser. This flow, however, results in forward thrust. Consequently, a device was developed to spoil the forward thrust. The spoiler is shown in Figure 8-18 and the test results in Figure 8-19. With five doors blocked and without the spoiler, the reverse thrust coefficient was about 20 per cent. With the

spoiler and a 23 per cent bleed flow. however, a reverse thrust coefficient of 40 per cent was achieved. At other operating conditions than that tested when the total pressure ratio of the two streams is larger and the effect of the blow-in-door blockage is larger, the spoiler can be used to even greater advantage to maintain a satisfactory reverse thrust level.

The effect of flight Mach number on reverser performance was evaluated for an ejector with four doors blocked and with unspoiled, low bleed flow, and for an ejector with five doors blocked and with spoiled high bleed flow. The results are presented in Figures 8-20 and 8-21, respectively. In each case, the reverse thrust increases significantly with Mach number with the reverser with the unspoiled bleed showing the greater effect. The increase is caused by increased external drag and by base pressure effects. The use of large amounts of bleed flow tends to pressurize the base area and reduce the drag effect, consequently reducing the sensitivity of the reverse thrust coefficient to Mach number.

The results of exploratory tests to evaluate the effect of the total pressure ratio between the fan and engine streams are shown in Figure 8-22. The reverse thrust coefficient is essentially unaffected by the pressure ratio split, but the flow coefficients of the individual streams are affected. The engine stream becomes highly suppressed as the pressure ratio is increased above 1.0. (The STF219 engine has a fan-to-engine pressure ratio of approximately 1.1). These tests, however, were conducted without bleed flow to permit the worst case of suppression to be investigated. Bleed flow, of course, relieves the engine suppression at high pressure ratios and the fan suppression at low pressure ratios.

Since these tests were conducted on a model which closely approximates the STF219 ejector, the results obtained indicate that a satisfactory reverser can be incorporated into the STF219 ejector and that the required levels of reverse thrust can be obtained without appreciable suppression of either the engine or duct streams.

c. <u>Exhaust Systems for a Partially Augmented Turbojet Engine</u>.

Early in the Phase IIA program, before the selection of the STF219 duct heating engine, a partially augmented turbojet engine (the

STJ227) was actively considered. Consequently, an experimental investigation was conducted on exhaust systems for this engine. Two types of nozzles were considered: a blow-in-door ejector and a plug nozzle. The latter, while found to be impractical for the co-annular duct burning turbofan, was known to be competitive with the blow-in-door ejector for a low-augmentation turbojet. With low augmentation rates, cooling of the plug nozzle is not prohibitive and the jet area variations required are comparatively small so that the plug nozzle is feasible.

A series of scale models of both a blow-in-door ejector and a plug nozzle were constructed and tested at sea-level take-off, Mach 0.9 cruise, Mach 1.2 acceleration, and Mach 2.7 cruise to establish performance levels. The engine parameters used in designing the exhaust systems are shown in Table 8-1

TABLE 8-1

Partially Augmented Turbojet Engine Operating Conditions
(Nacelle Diameter = 90.3 Inches)

Mach Number	Flight Condition	Altitude (Feet)	P_{tp}/P_{am}	$A_j C_d$ (Sq. Ft.)
0	Take-Off	0	3.39	9.11
0.9	Cruise	36150	3.33	9.7
1.2	Accel.	45000	7.25	12.1
1.6	Accel.	45000	11.35	12.1
2.0	Accel.	45000	16.0	12.1
2.7	Cruise	65000	25.2	12.4
3.0	Cruise	65000	32.5	12.1

Blow-In-Door Ejector Tests - A schematic drawing of the blow-in-door ejector model designed for the STJ227 partially augmented turbojet is shown in Figure 8-23. Fixed geometry models, simulating the geometry at the various operating conditions, were used. Similar to the program for the STF219 blow-in-door ejector, the variables studied were the nozzle area ratio, the blow-in-door area ratio, and the minimum shroud diameter location. The test results appear in Figures 8-24 through 8-26.

At sea-level take-off, the performance obtained with 2.0 per cent secondary airflow was about optimum, but at Mach 0.9 and Mach 1.2, the performance was clearly not optimum. It is noted, however, that these results are for an early design, and that the development program was terminated when the STF219 engine was selected.

The large discrepancy between the basic design performance and that of the other designs tested at Mach 0.9 is primarily a result of changes in the internal shroud contour. The basic design had an over-all diverging contour such that the exit diameter was greater than the minimum shroud diameter, whereas the models had an exit diameter equal to the minimum shroud diameter.

Figure 8-26 shows the effect on performance of varying the shroud contour for Mach 2.7 cruise. As shown, the contour of the basic design provides nearly optimum performance.

The over-all performance as a function of Mach number is shown in Figure 8-27. The performance at sea-level take-off and at Mach 2.7 cruise met the specified goals. The subsonic cruise and transonic acceleration performance, however, is substantially below optimum, but examination of Figures 8-24 and 8-25 indicates that changes in the blow-in-door area, the trailing edge hinge point location, and the nozzle exit area when the flaps are fully retracted could produce large performance improvements with little or no change in the Mach 2.7 performance.

Plug Nozzle Tests - The plug nozzles tested are shown in Figure 8-28. Two test series were conducted. In the first, the effects of changes to the nozzle area ratio, the amount of plug truncation, and the plug contour were investigated using an external expansion plug nozzle. In later tests, the effects of changes to the nozzle area and the plug contour were investigated using a multiple expansion plug nozzle.

For the first series, each nozzle had the same throat or jet area but different exit areas. They were tested at Mach 0, 0.9, and 1.2 simulating non-afterburning operation. The influence of the nozzle area ratio on performance is shown in Figure 8-29. As shown, decreasing the area ratio improved the performance. Moderate amounts of plug truncation were found to have little effect on the nozzle performance. As shown in Figure 8-30, more than 50 per cent of the total plug length

can be eliminated with little or no loss. Analysis of the test data at Mach 1.2 and Mach 2.6 indicated that, with less than 50 per cent of the plug truncated, the plug base force approached the level of thrust that could be obtained from the portion of the plug that was truncated. With more than 50 per cent of the plug removed, however, the thrust that could be obtained from the removed portion exceeded the plug base force, and the over-all performance decreased. Figure 8-31 shows the thrust available on the complete plug and the force measured on the base of the truncated cones.

The effect of changes to the plug contour was studied by testing conical plugs and plugs with isentropic contours. The results, shown in Figure 8-32, show that the isentropic contour is superior to the conical contour at static conditions and is inferior at Mach 0.9. At Mach 1.2, neither plug has a distinct advantage over the other. Schlieren photographs indicated that overexpansion occurred at the upstream portion of the conical plug as a result of the reduced throat turning angle. The resulting billowing of the jet interacting with the external flow increased the external pressures and reduced the external drag. Increased pressures on the end of the plug were created by recompression of the flow, consequently, the over-all performance of the conical plug was better than that of the isentropic plug at certain operating conditions where the external drag has a large influence on the over-all performance. The drag on the isentropic and conical plugs is shown in Figure 8-33.

Initial testing with a multiple expansion plug nozzle was conducted at Mach numbers between 1.2 and 2.6. Good performance was obtained at high supersonic flows (see Figure 8-34), but the transonic performance was not as good as that of the single expansion plug nozzle.

Later testing with the multiple expansion plug nozzle was conducted to investigate the effect of changes to the area ratio produced by pivoting the shroud and by changing the plug cone angle. With low pressure ratios, the internal area ratio was found to be quite important in keeping the overexpansion losses to a minimum. At Mach 1.2 (Figure 8-35), large performance losses can occur with large internal area ratios. These losses are larger than would be expected on the basis of the area ratio alone since the portion of the plug affected by the external flow decreases as the internal area ratio increases, thereby compounding the effect.

At Mach 2.6, the data substantially agrees with the theoretical performance values. At this flight condition, the pressure ratios are greater, and, therefore, overexpansion is no longer a problem.

Figure 8-36 shows the combined effects of changes to the plug cone angle and to the internal area ratio on the nozzle performance at Mach 2.6. It can be seen that a severe decrease in performance occurred as the cone angle was increased. This drop occurred because some of the shrouds used were not long enough to accommodate the large amounts of internal expansion associated with large cone angles, that is, the last Mach line associated with the internal expansion extended out beyond the end of the shroud. It would be possible to use the shorter, steep-angle plugs by redesigning the shroud to match. In Figure 8-37, the performance at Mach 1.2 also decreases for the plugs with large cone angles. At these operating pressure ratios, the large internal area ratios associated with the steep cone angle created several overexpansion losses.

A summary of the plug nozzle tests is presented in Figure 8-38 together with the estimated blow-in-door ejector performance for the same engine cycle. For a more meaningful comparison, the plug nozzle performance has been modified to account for the thrust of the secondary cooling air used in estimating the performance of the blow-in-door ejector. This thrust is calculated for 2 per cent (temperature corrected) cooling flow at representative pressure levels. It can be seen that the plug nozzle performance is, in general, comparable to that of a blow-in-door ejector for a turbojet powerplant. Although the investigation was somewhat limited, the results indicate that high performance levels can be obtained with a plug nozzle system over the complete operating range. The required nozzle would necessarily employ geometric variations to provide a multiple expansion nozzle similar to the models tested at supersonic flight conditions and still yield the single-expansion plug nozzle performance subsonically. Weight and complexity of the mechanical arrangement, however, could reduce its over-all effectiveness.

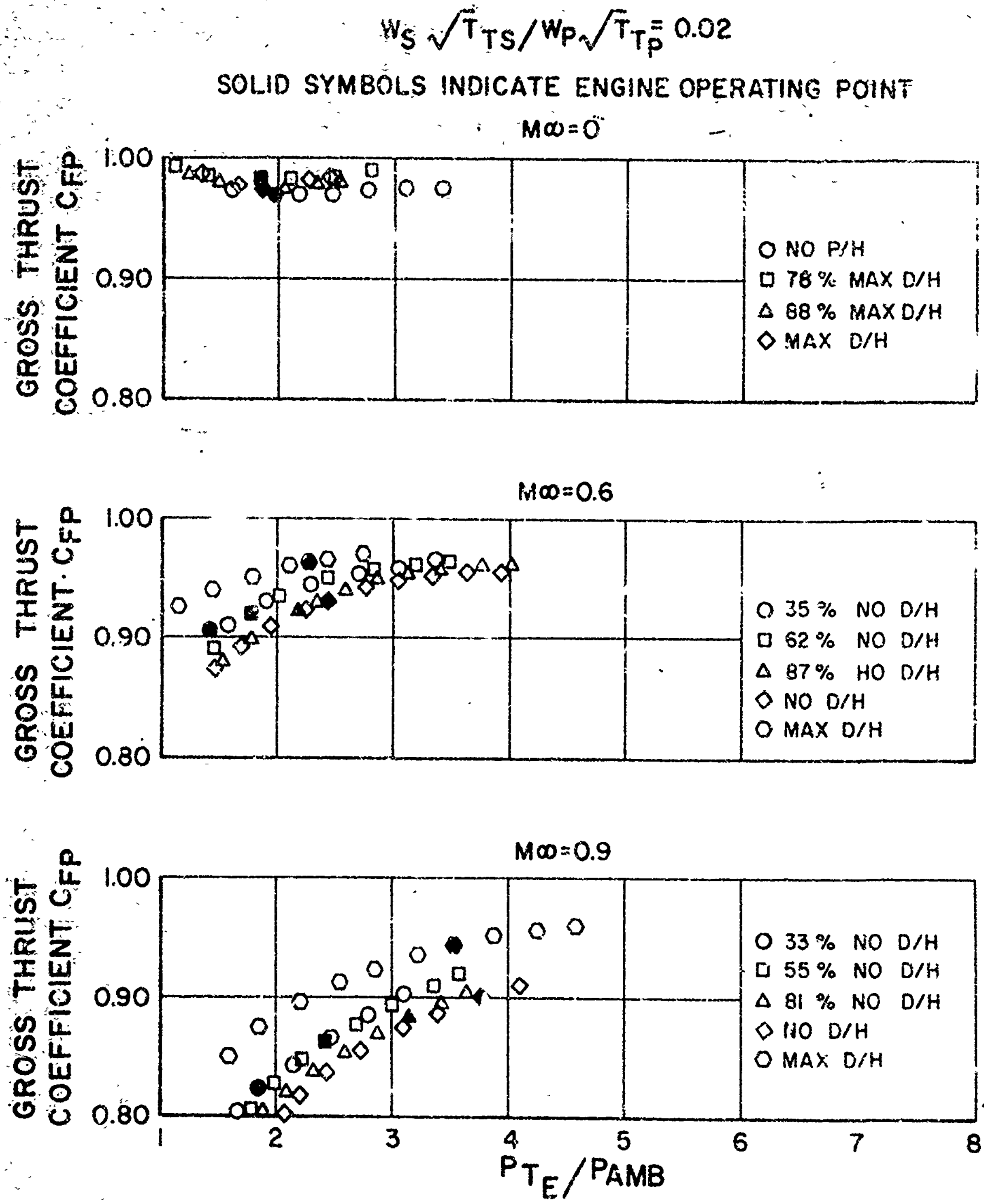

WIND TUNNEL TEST DATA OF FIRST FREELY FLOATING CO-ANNULAR BLOW-IN DOOR EJECTOR MODEL FOR SUPERSONIC TRANSPORT

Figure 8-1

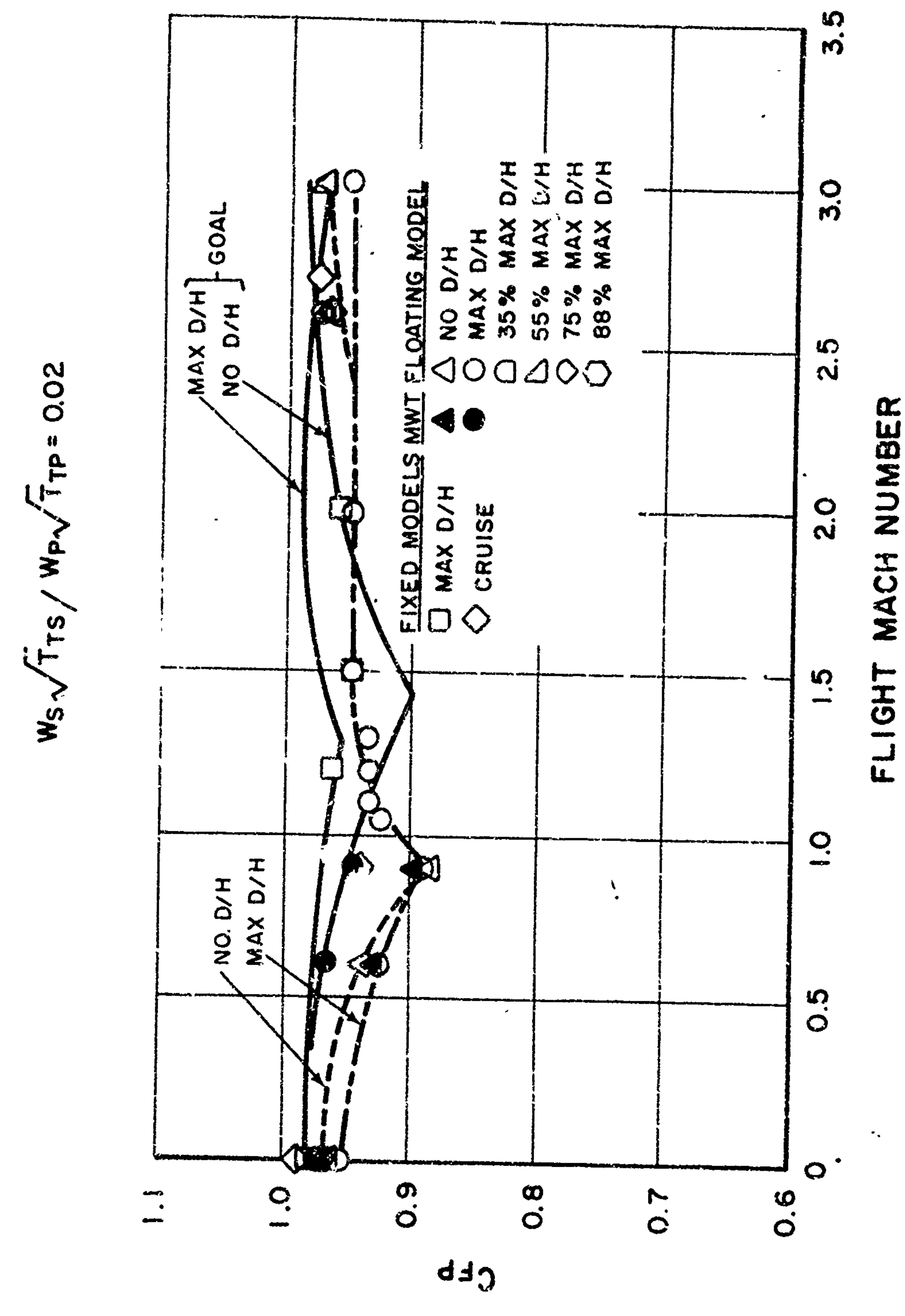

SUMMARY OF DATA FOR FREELY FLOATING CO-ANNULAR BLOW-IN DOOR EJECTOR MODEL

Figure 8-2

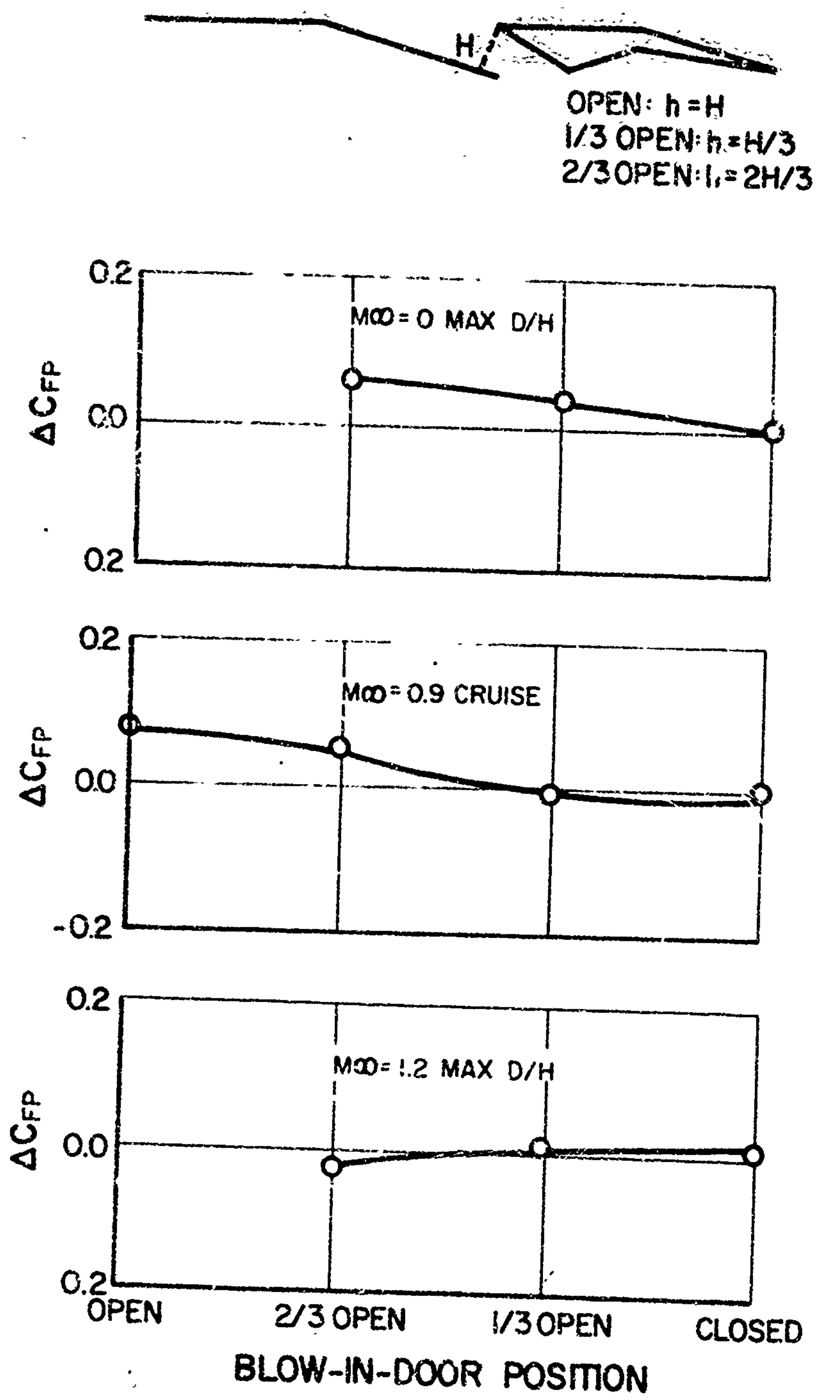

EFFECT ON PERFORMANCE OF BLOW-IN DOOR POSITION WITH TRAILING EDGE FLAPS FIXED IN CLOSED POSITION

Figure 8-3

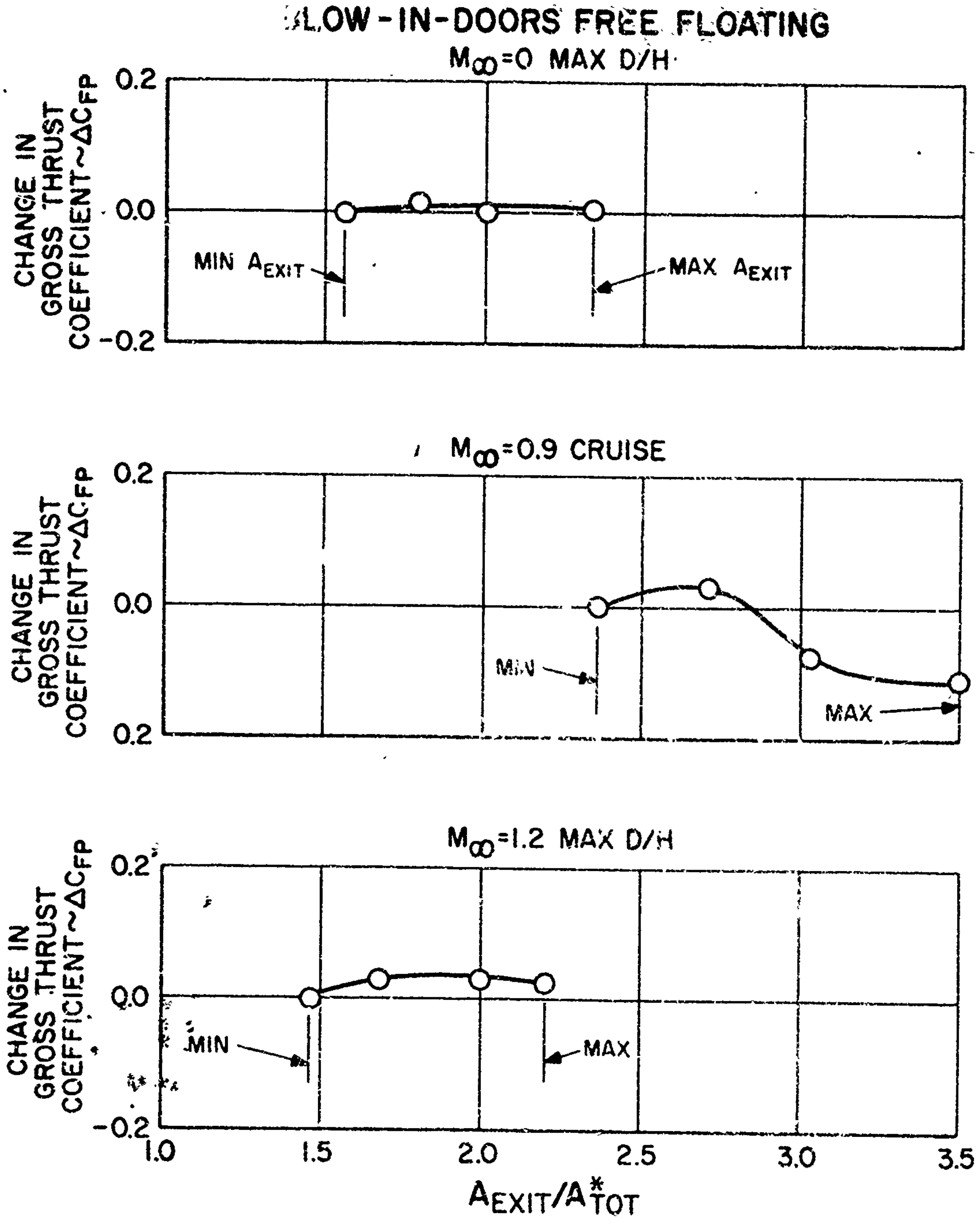

EFFECT OF VARYING TRAILING EDGE FLAP POSITION ON PERFORMANCE

Figure 8-4

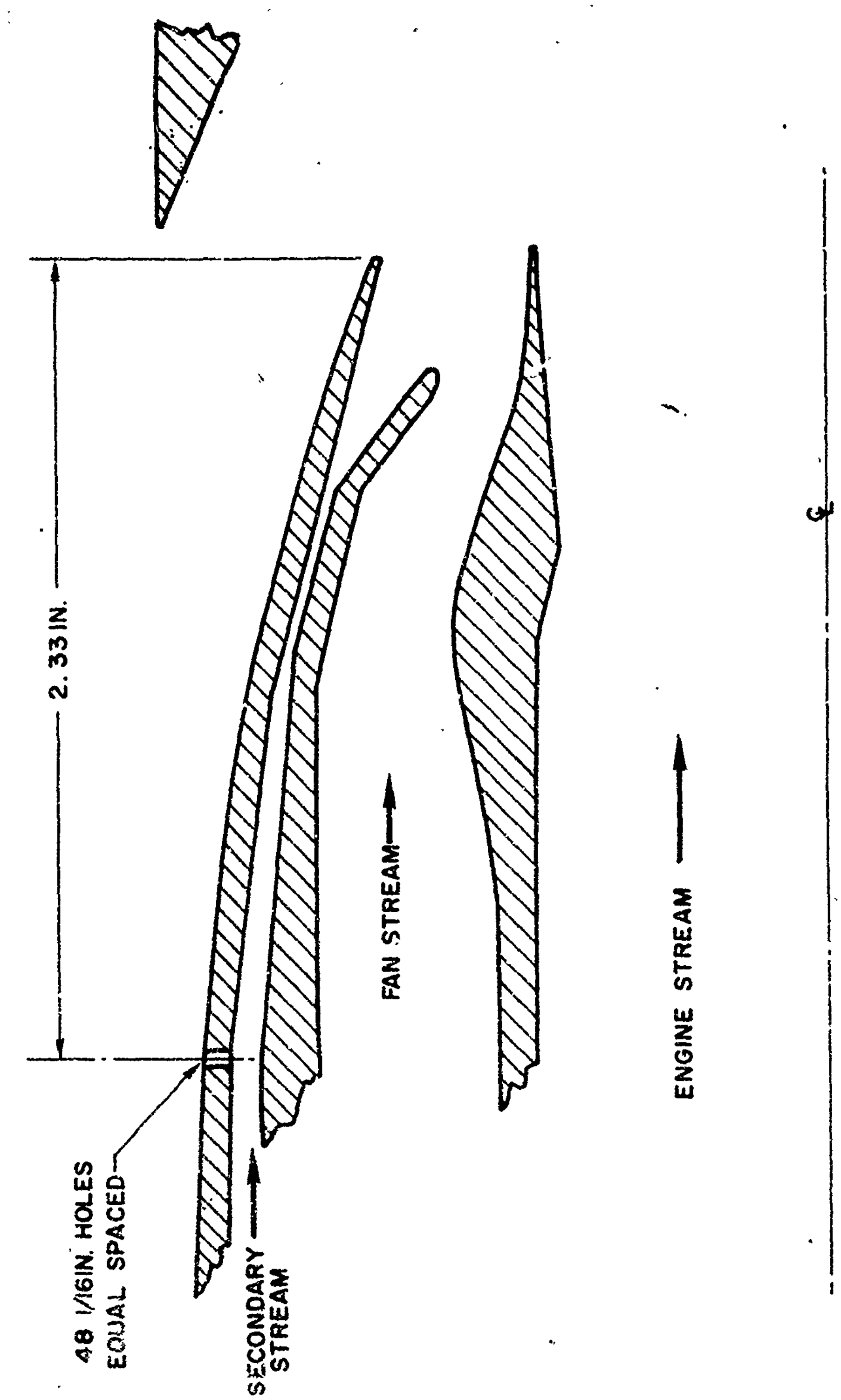

SCHEMATIC DIAGRAM OF FOREBODY VENTING DESIGN

Figure 8-5

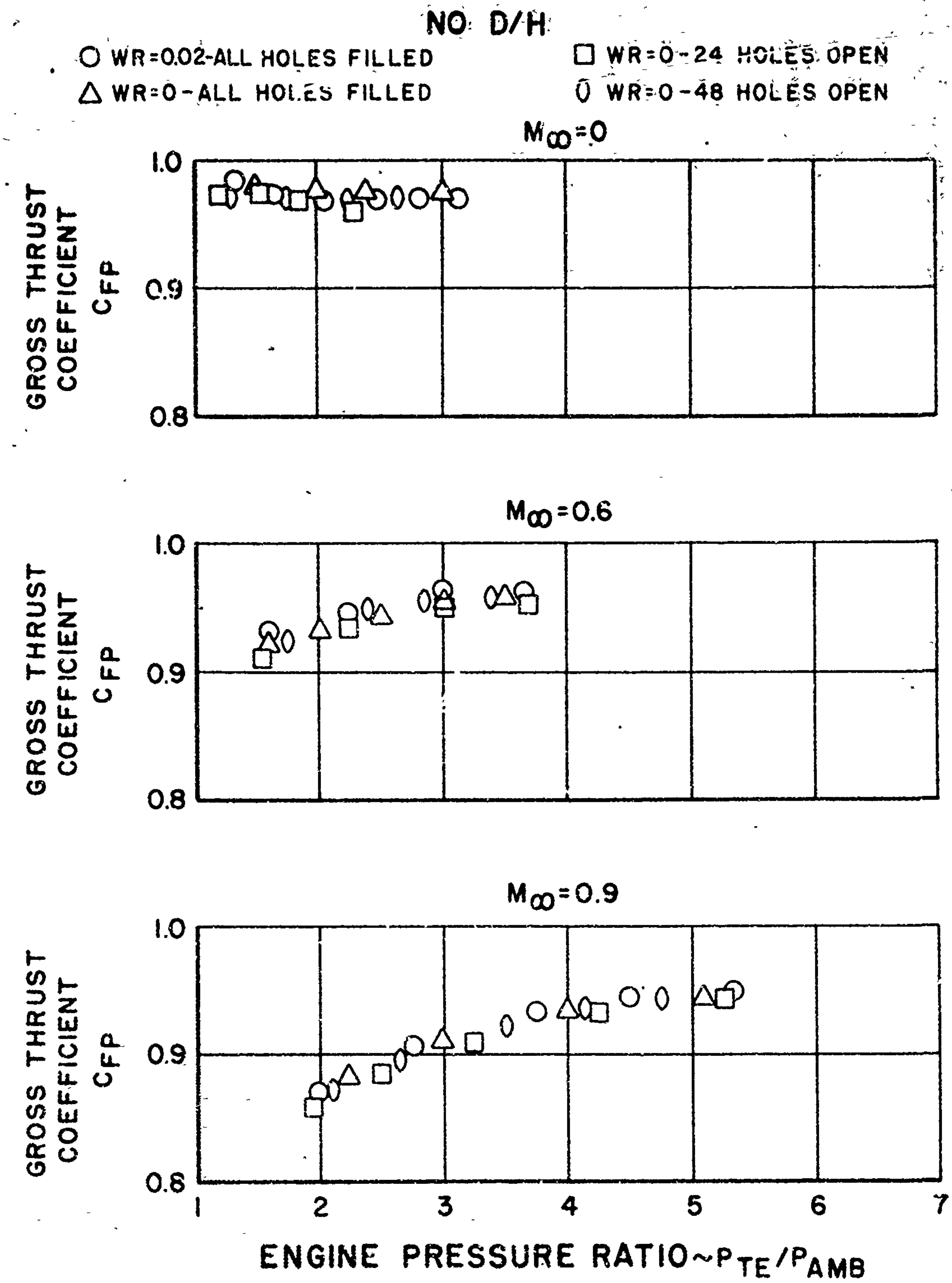

EFFECT OF FOREBODY VENTING ON PERFORMANCE WITHOUT AUGMENTATION

Figure 8-6

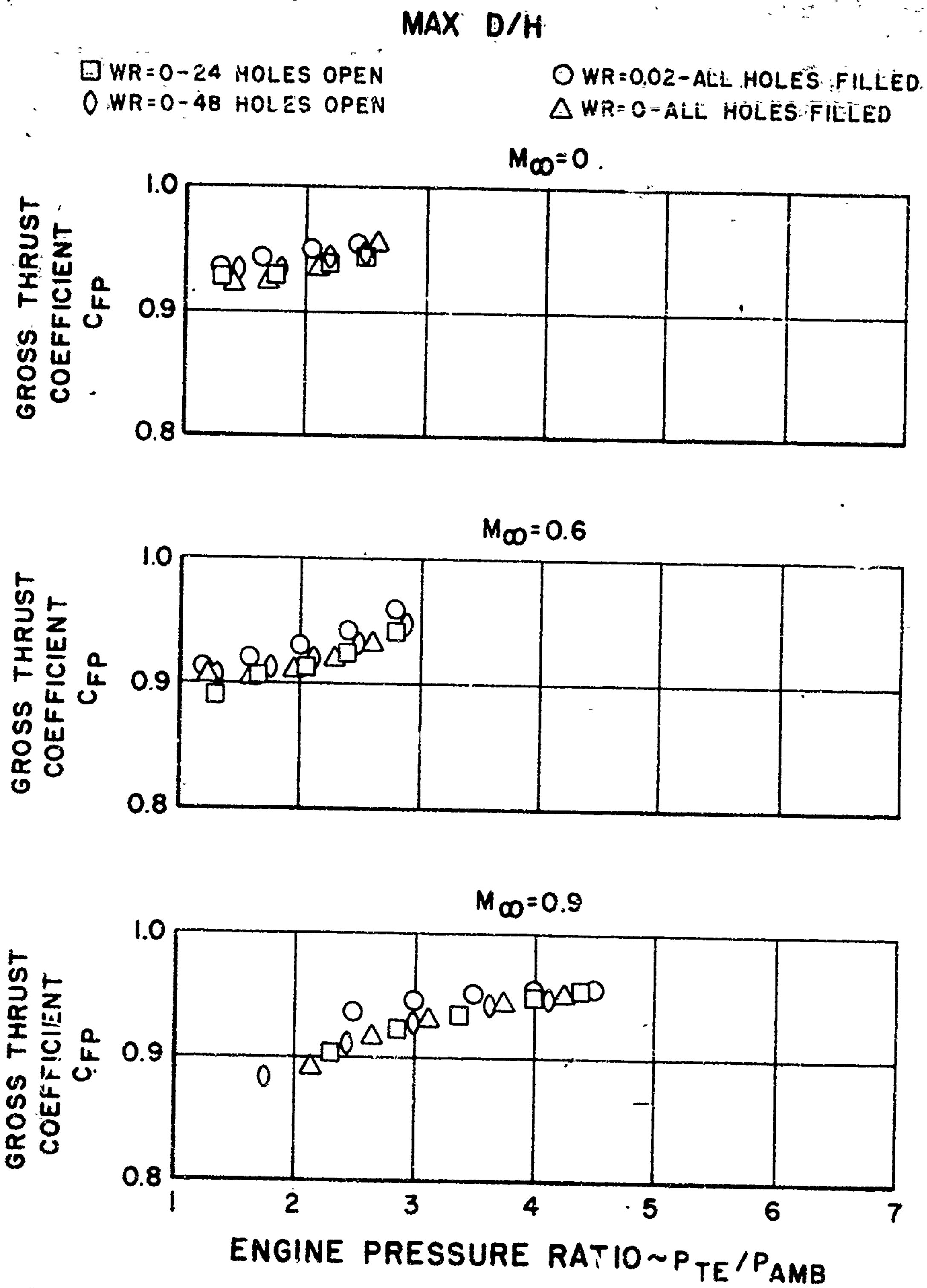

EFFECT OF FOREBODY VENTING ON PERFORMANCE
WITH MAXIMUM AUGMENTATION

Figure 8-7

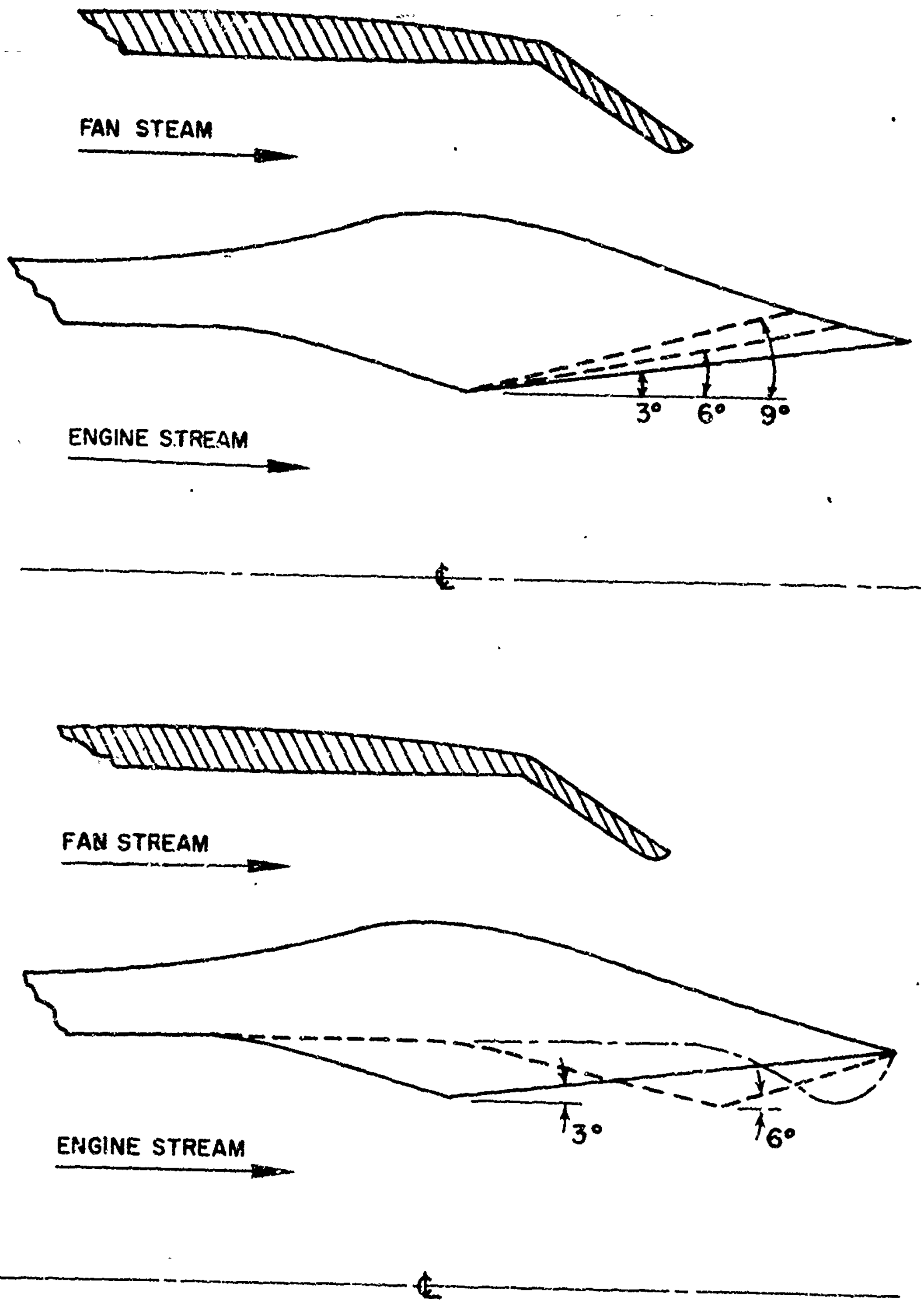

SCHEMATIC DIAGRAMS OF PRIMARY
ENGINE NOZZLES EVALUATED

Figure 8-8

M_N = 2.7 CRUISE

$(A^*/A_{MAX})ENG = 0.1660$ $(A^*/A_{MAX})FAN = 0.232$ $(R_{TE}/R_{AM}) = 9.61$ $(R_{TF}/R_{AM}) = 12.35$

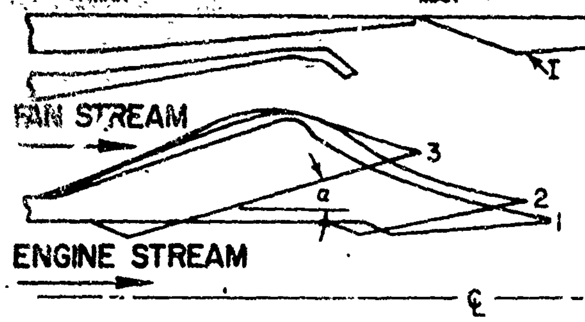

CONFIG	ENG α	$(A/A^*)E$	$(A/A^*)F$	CFP
1	3°	1.118	2.115	0.980
2	8.5°	1.374	1.687	0.985
3	15°	2.371	1.177	0.965

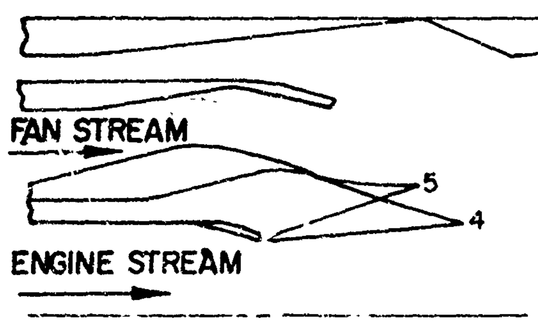

CONFIG	ENG α	$(A/A^*)E$	$(A/A^*)F$	CFP
4	3°	1.118	1.64	0.980
5	15°	1.748	1.177	0.983

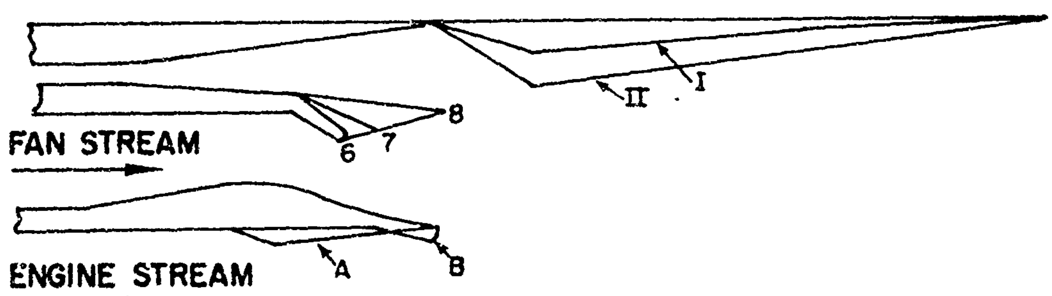

	CONFIG	ENG α	FAN α	$(A/A^*)E$	$(A/A^*)F$	CFP I	CFP II
A	6	3°	—	1.118	1.177	0.980	0.990
A	7	3°	15°	1.118	1.380	0.978	0.990
A	8	3°	15°	1.118	1.663	0.978	0.990
B	6	—	—	1.000	1.177	0.978	0.990
B	7	—	15°	1.000	1.380	—	0.990
B	8	—	15°	1.000	1.663	—	0.990

CHARACTERISTICS OF PRIMARY ENGINE NOZZLES EVALUATED

Figure 8-9

Mach Number	Flight Condition	P_{te}/P_{am}	P_{tf}/P_{am}	$A_j Cd_e$ (sq ft)	$A_j Cd_f$ (sq ft)
0	Sea Level	2.13	2.42	4.96	8.33
0.9	Cruise	2.90	3.48	4.96	4.36
1.2	Accel	5.19	5.84	4.96	8.47
2.7	Cruise	14.68	29.08	4.96	5.46

Note: The final engine conditions used in the model specification differ slightly from these values.

STF219 ENGINE OPERATING CONDITIONS USED FOR EXHAUST NOZZLE MODELS

Figure 8-10

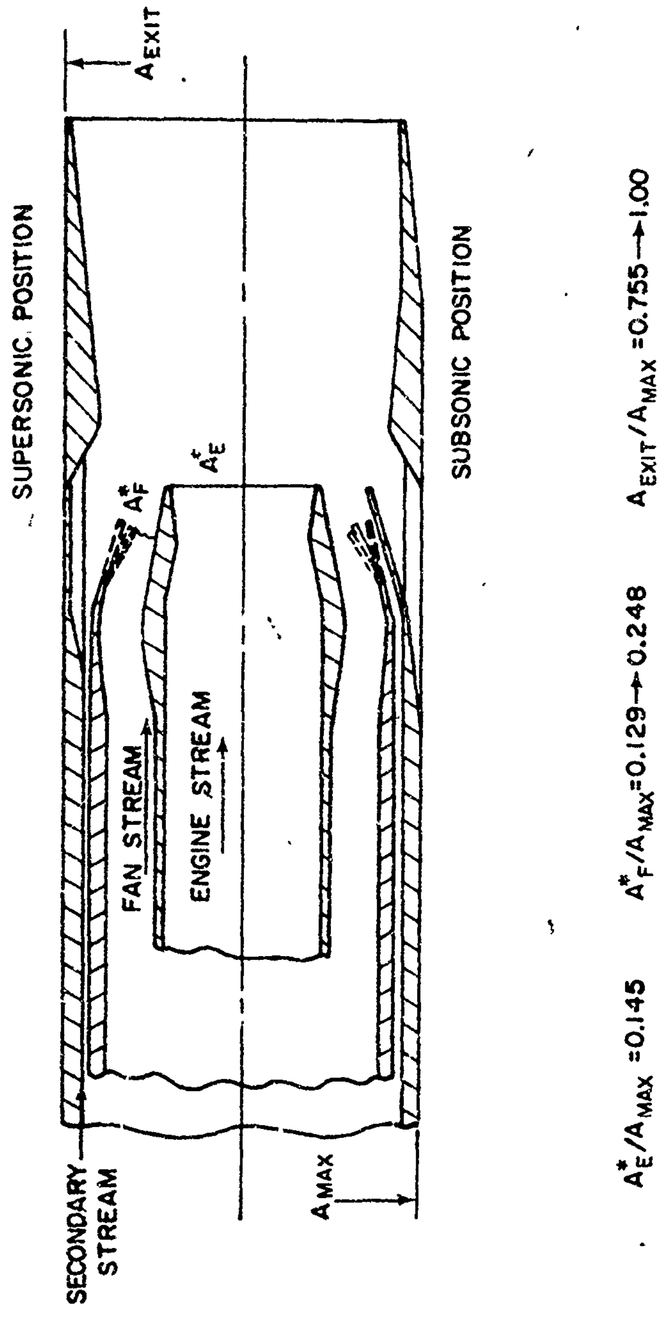

SCHEMATIC DIAGRAM OF MODEL SIMULATING STF219 EJECTOR

Figure 8-11

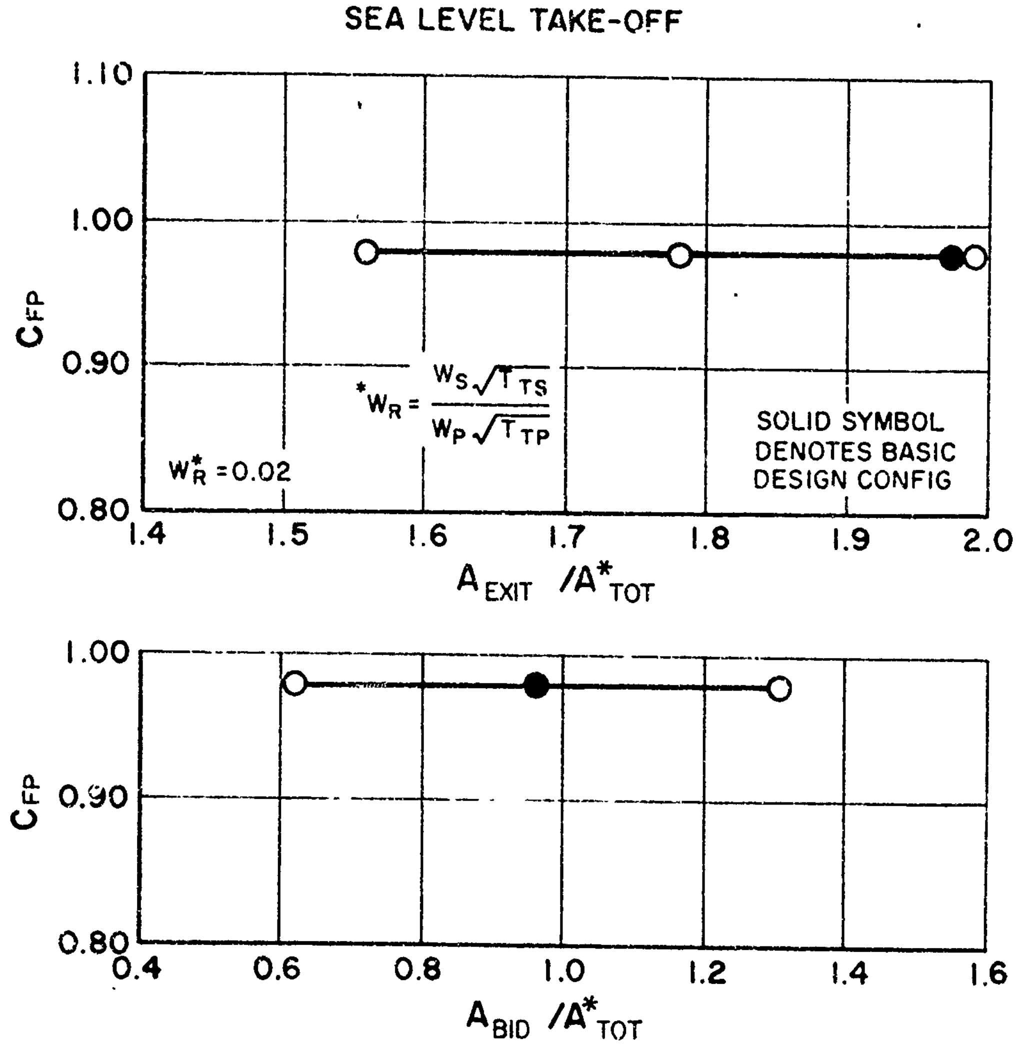

TYPICAL EFFECTS OF SHROUD EXIT AREA AND BLOW-IN DOOR AREA ON EJECTOR PERFORMANCE AT SEA LEVEL TAKE-OFF

Figure 8-12

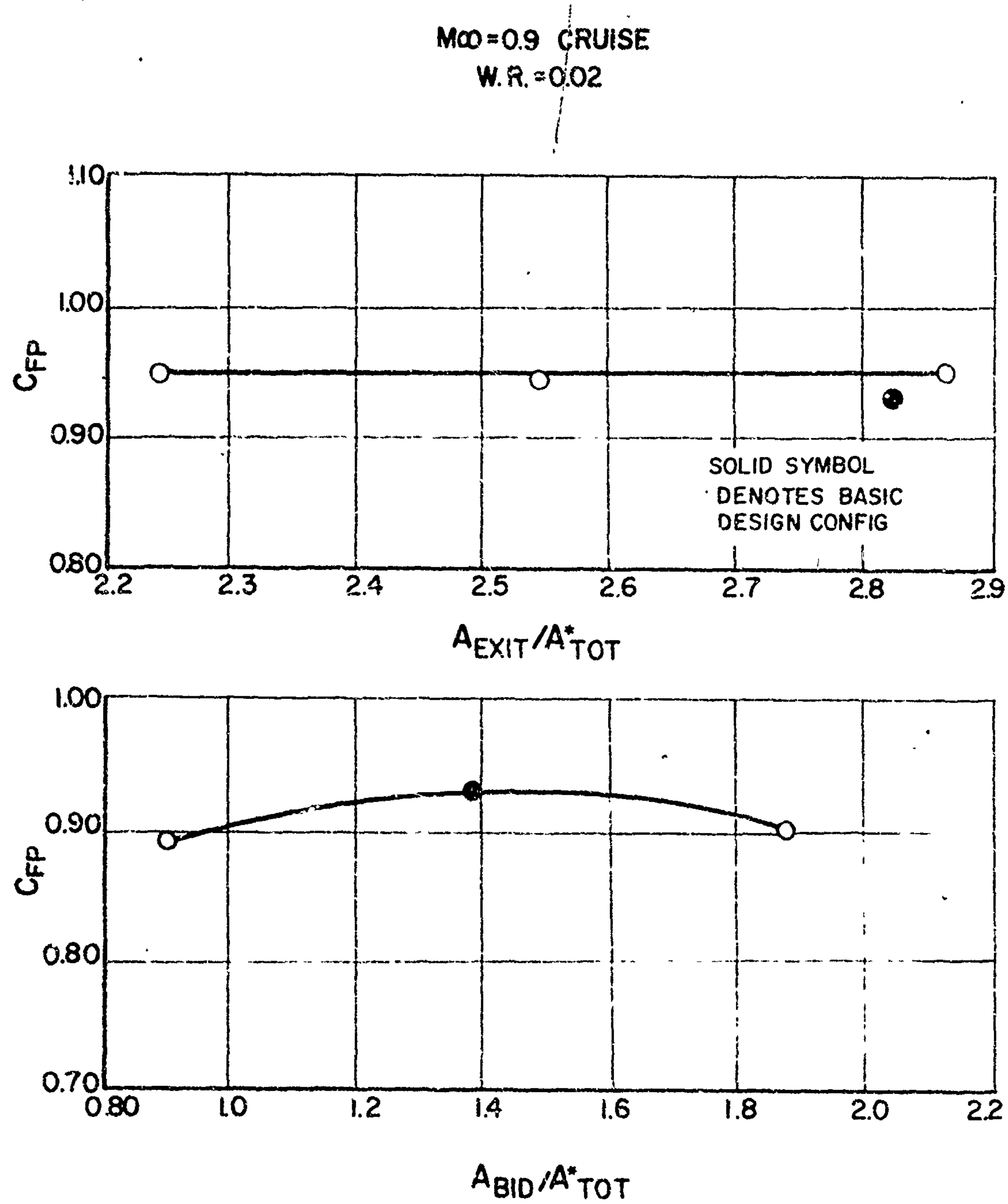

TYPICAL EFFECTS OF SHROUD EXIT AREA AND BLOW-IN DOOR AREA ON EJECTOR PERFORMANCE AT MACH 0.9 CRUISE

Figure 8-13

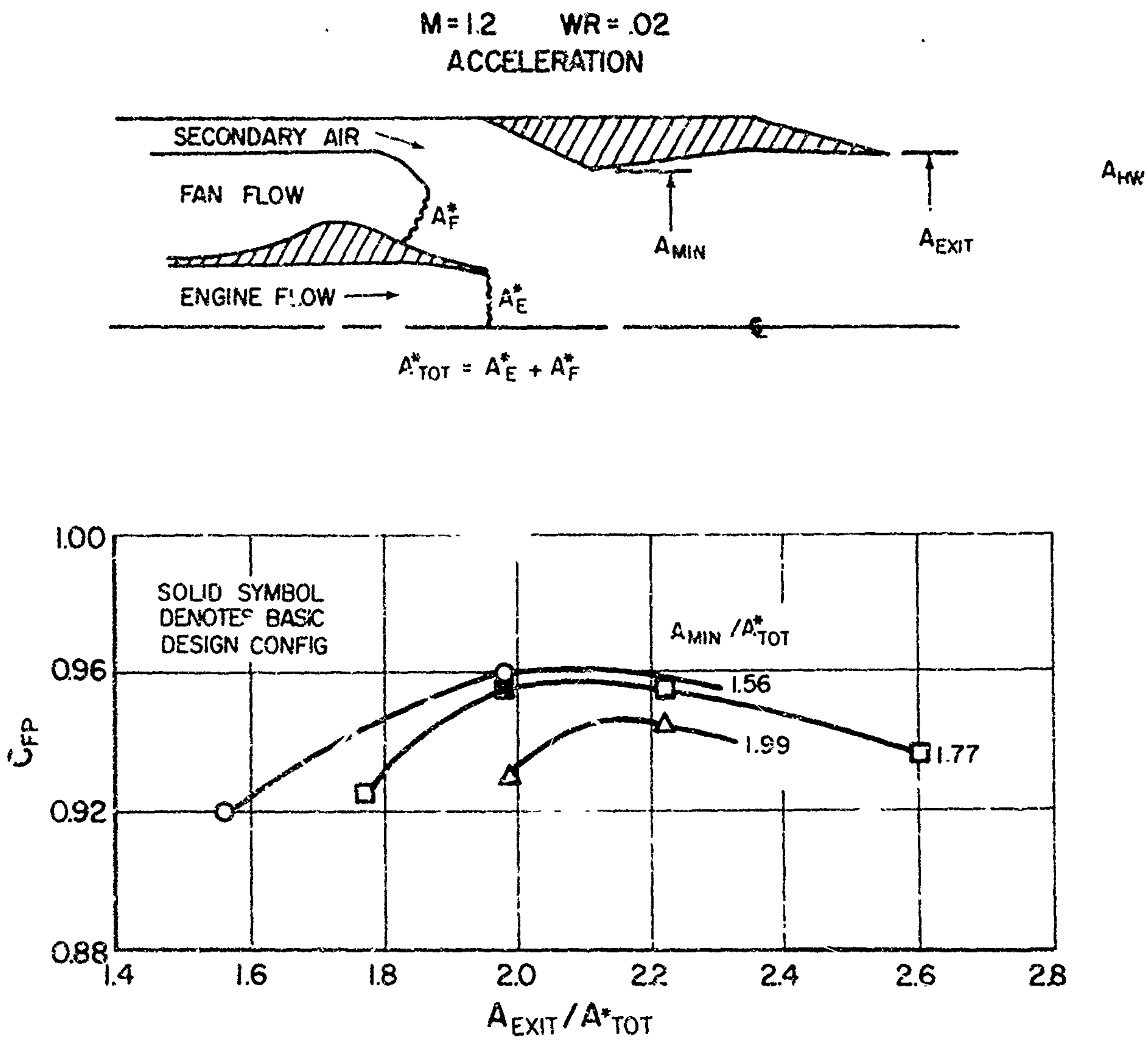

EFFECT OF SHROUD GEOMETRY ON TRANSONIC BLOW-IN DOOR EJECTOR PERFORMANCE AT MACH 1.2

Figure 8-14

M_∞ = 2.7 CRUISE

W.R. = 0.02

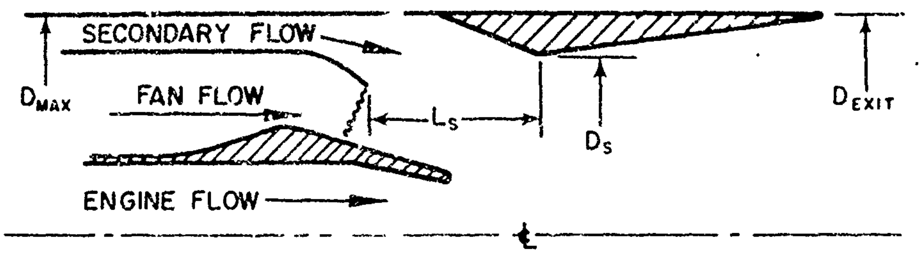

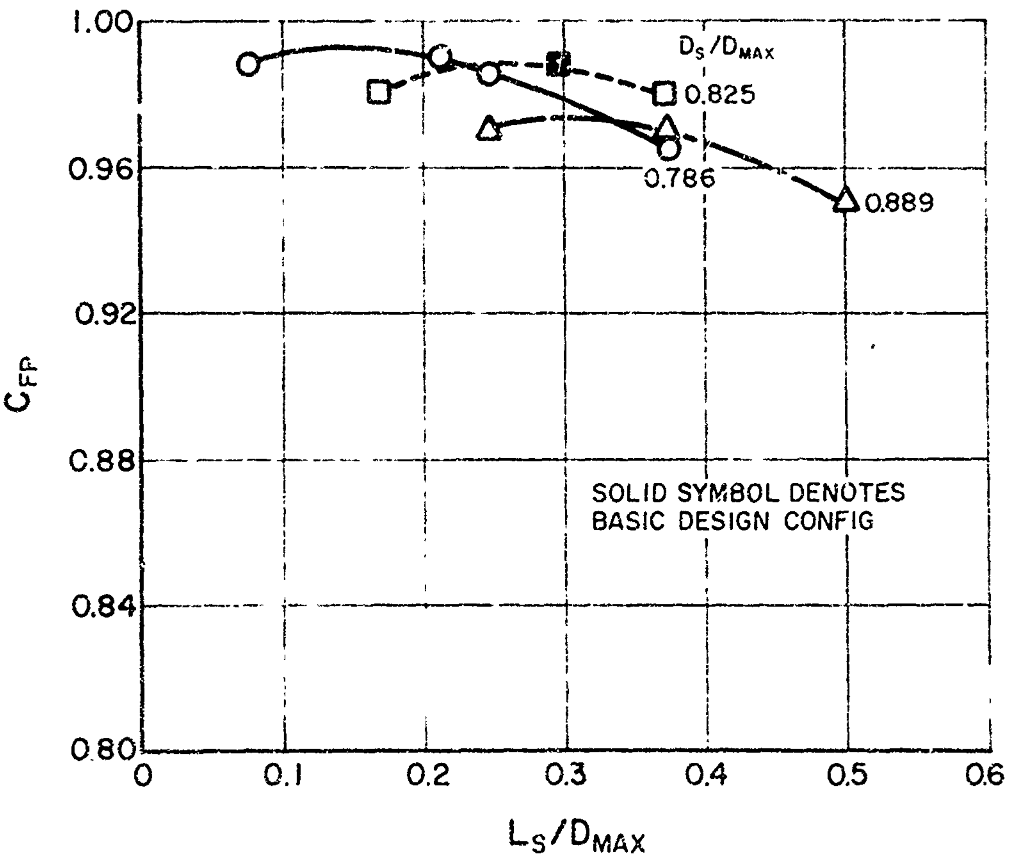

EFFECT OF SHROUD GEOMETRY ON SUPERSONIC BLOW-IN DOOR EJECTOR PERFORMANCE AT MACH 2.7 CRUISE

Figure 8-25

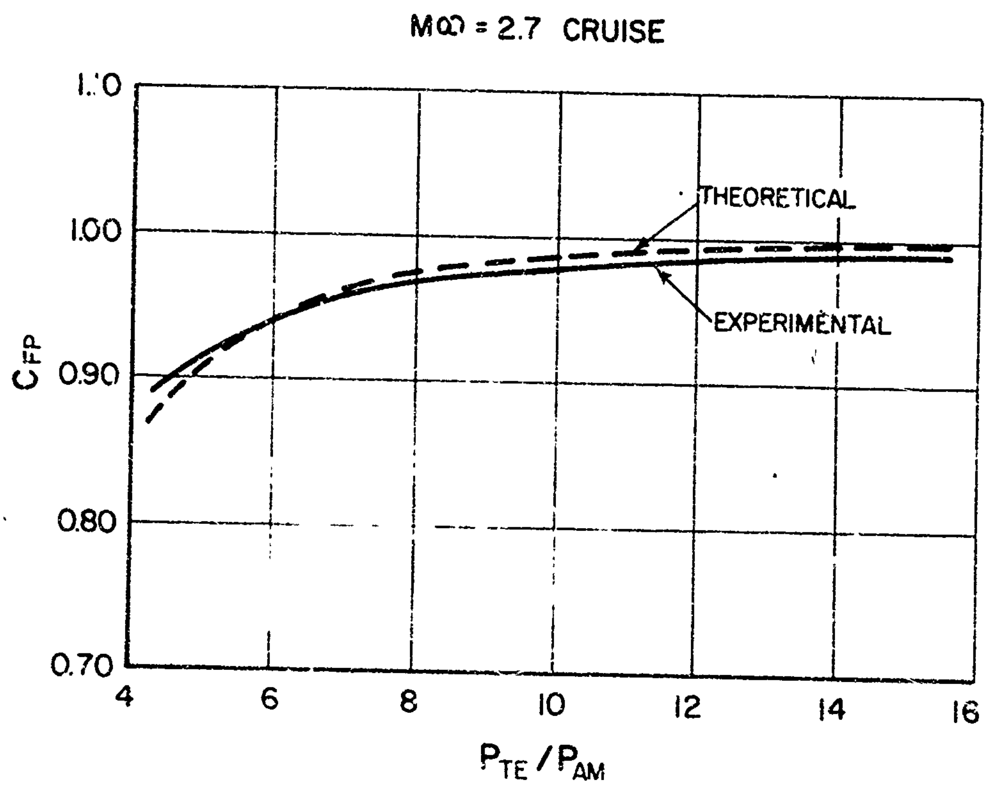

THEORETICAL AND EXPERIMENTAL EJECTOR PERFORMANCE AT MACH 2.6 CRUISE

Figure 8-16

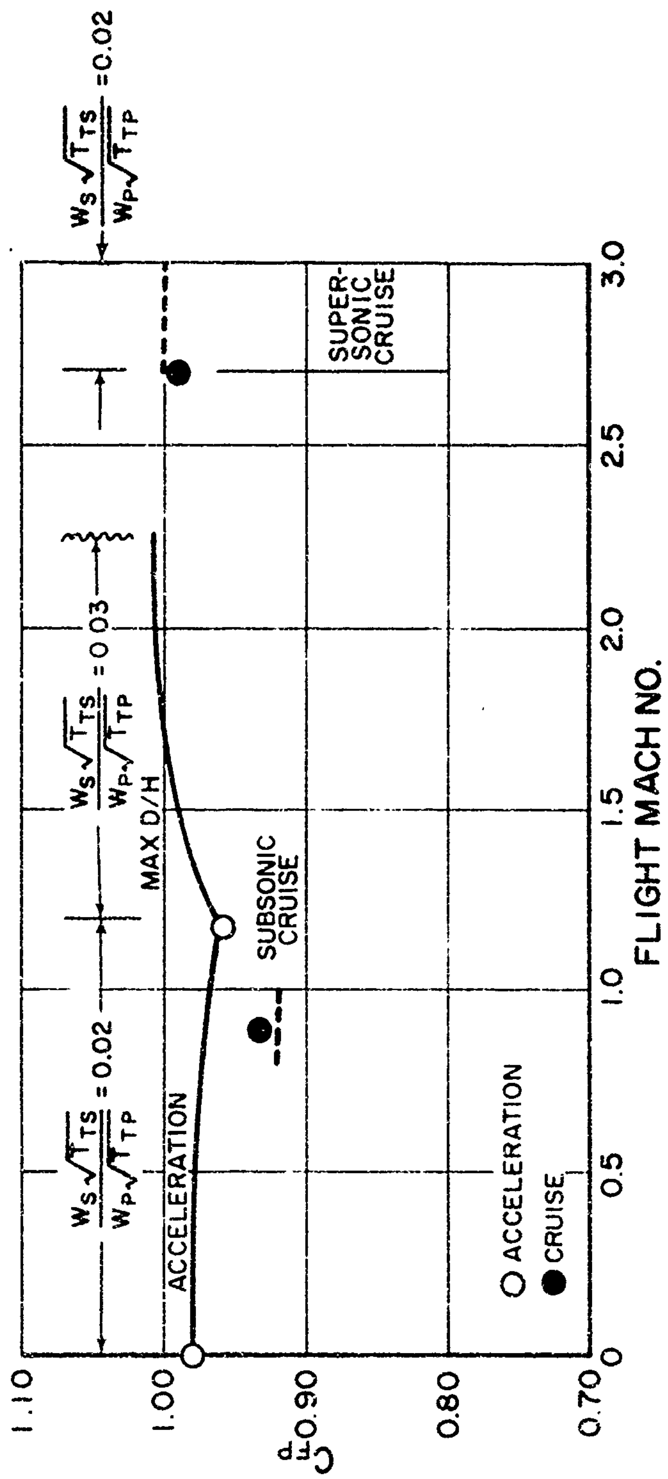

SCALE MODEL STF219 BLOW-IN DOOR EJECTOR PERFORMANCE AND PHASE IIA MODEL SPECIFICATION PERFORMANCE REQUIREMENTS

Figure 8-17

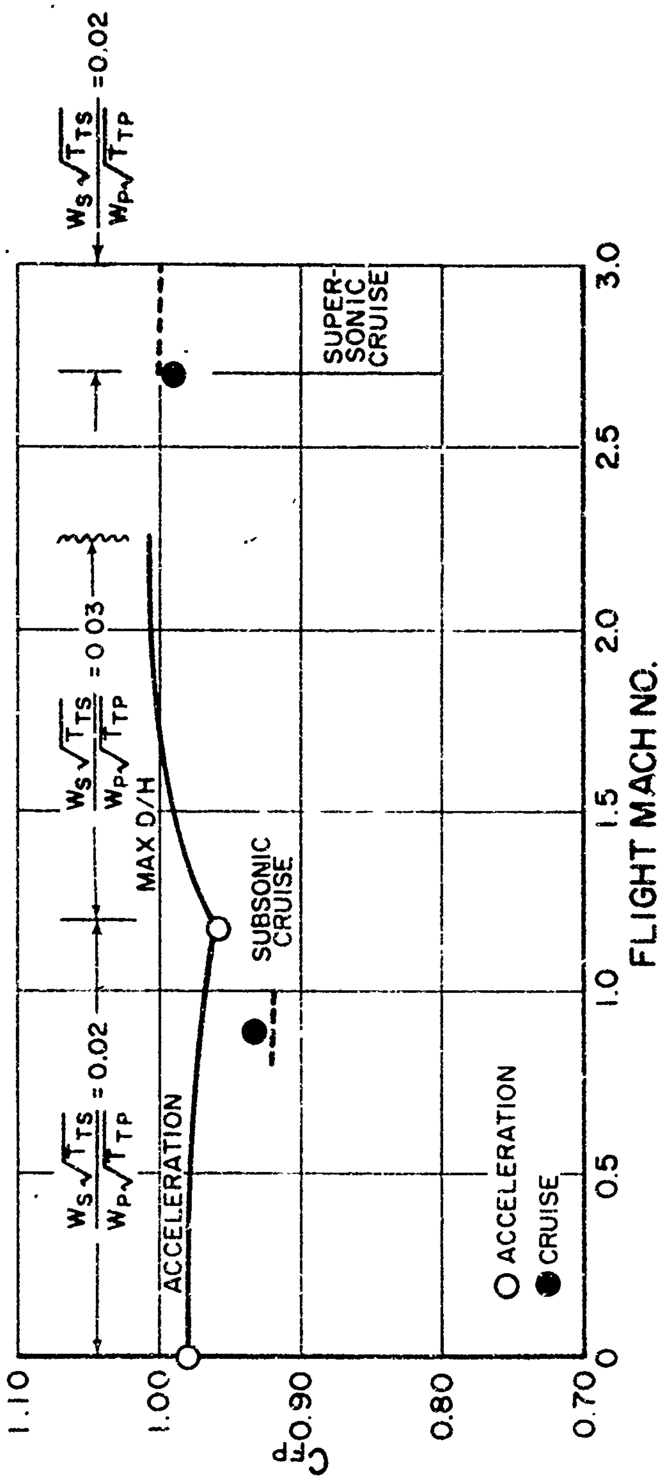

SCALE MODEL STF219 BLOW-IN DOOR EJECTOR PERFORMANCE AND PHASE IIA MODEL SPECIFICATION PERFORMANCE REQUIREMENTS

Figure 8-17

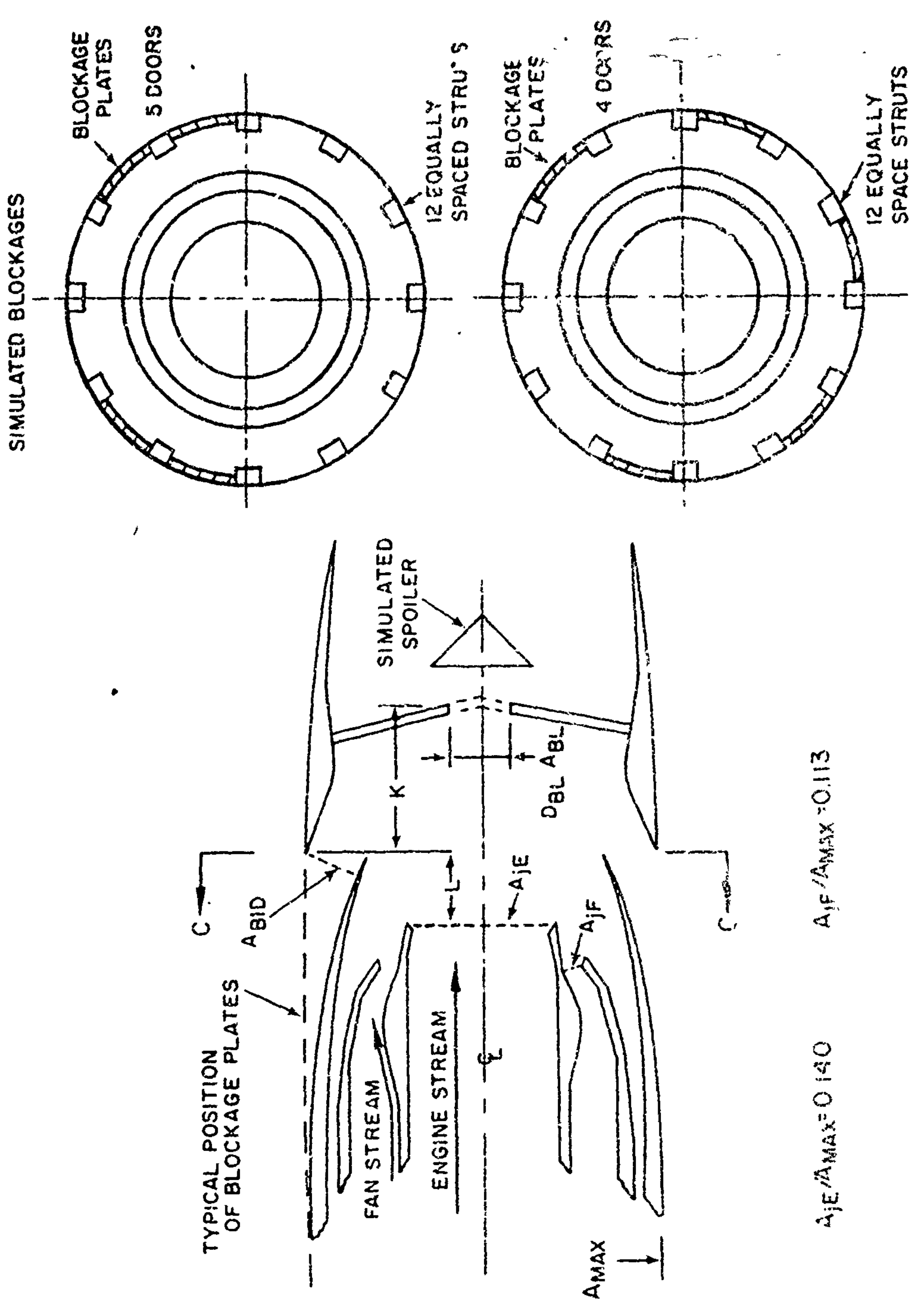

SCHEMATIC DIAGRAM OF CO-ANNULAR BLOW-IN DOOR EJECTOR-REVERSER MODELS

Figure 8-18

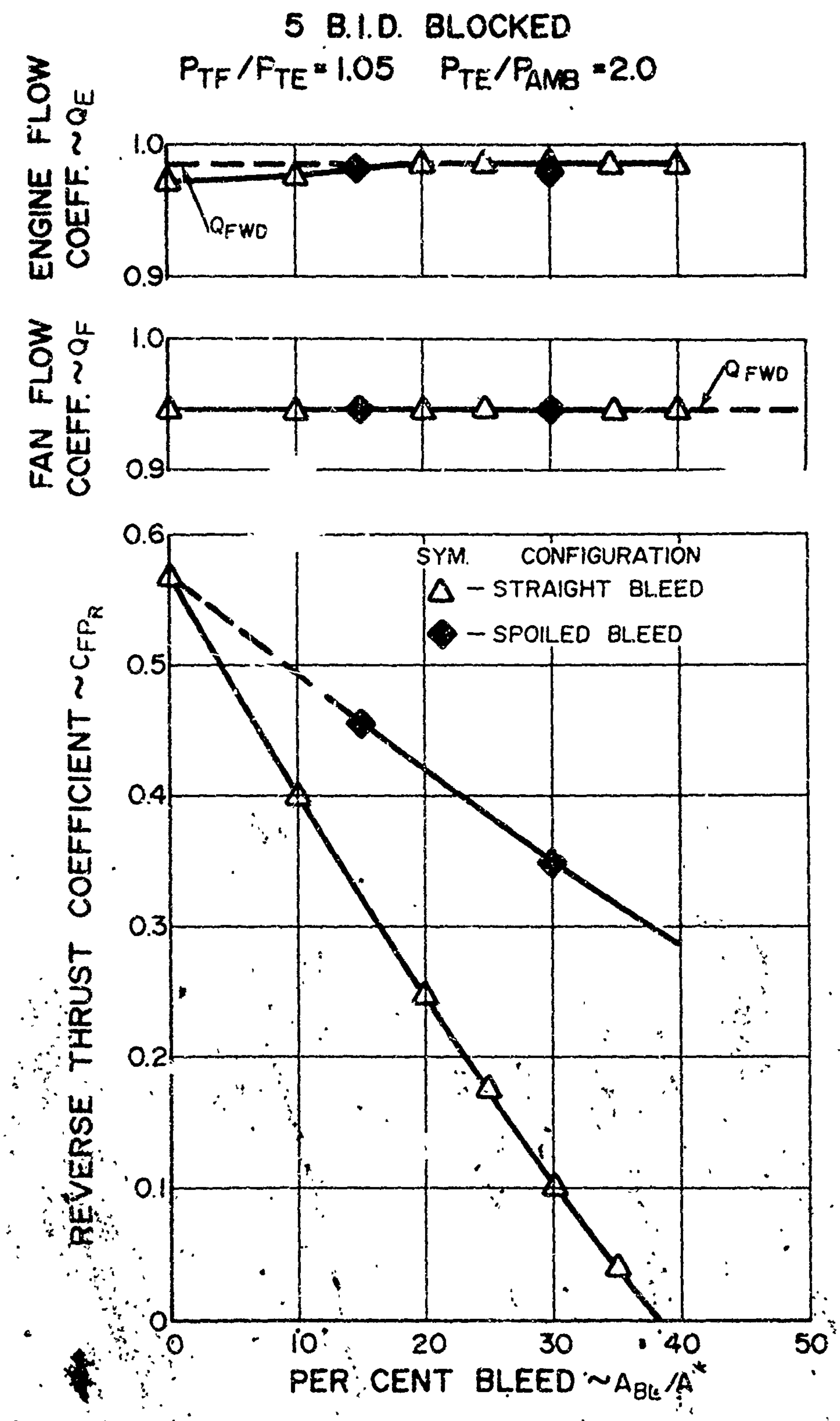

TYPICAL EFFECT OF BLEED FLOW SPOILER

Figure 8-19

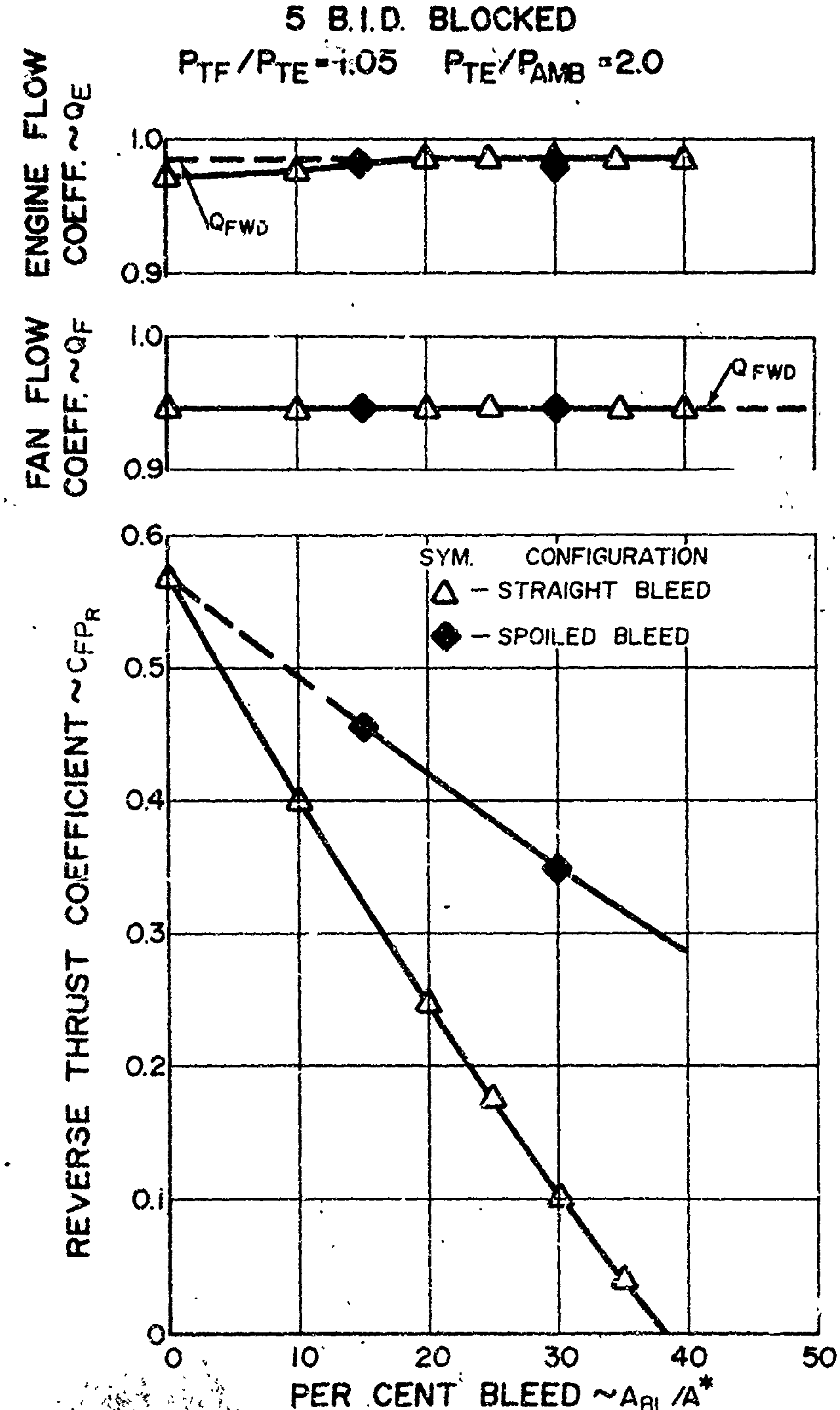

TYPICAL EFFECT OF BLEED FLOW SPOILER

Figure 8-19

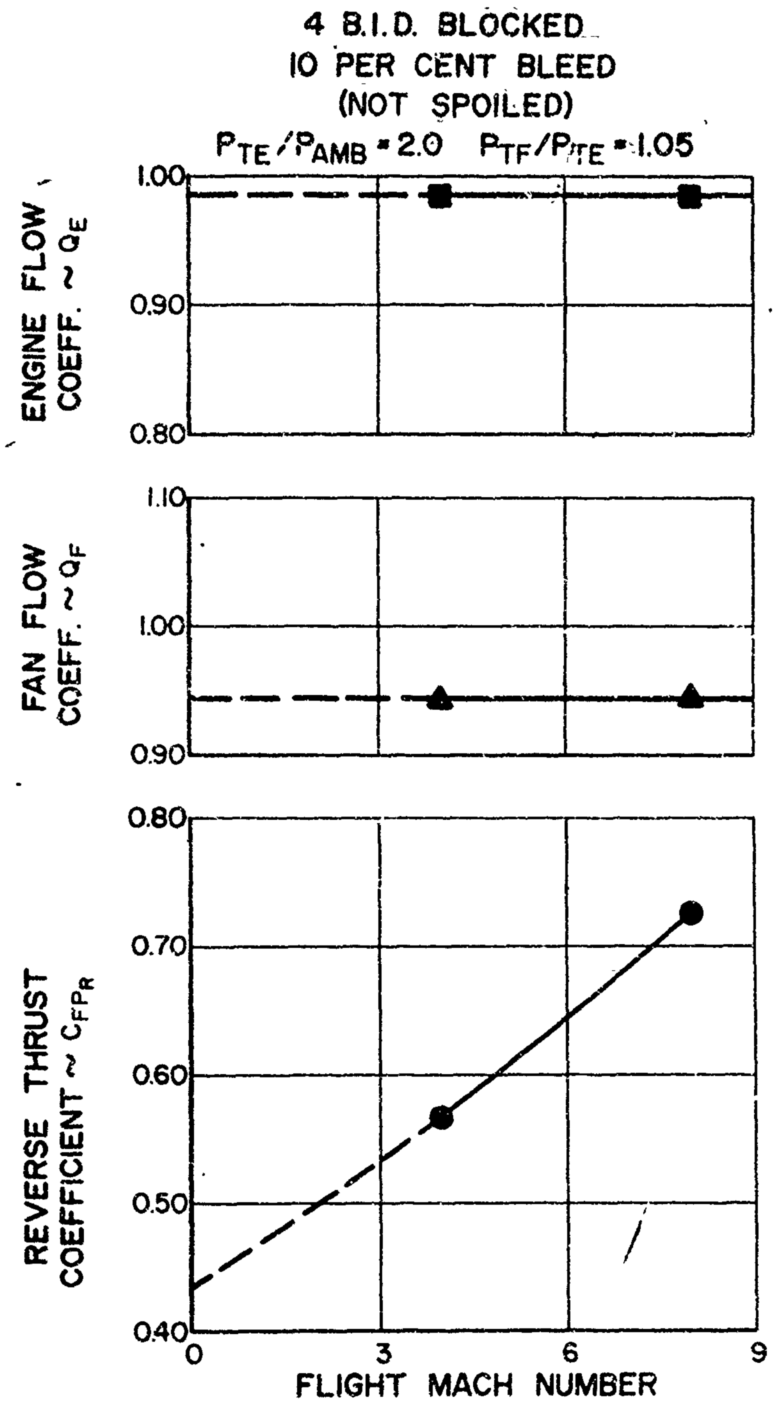

TYPICAL EFFECT OF FLIGHT MACH NUMBER ON ENGINE FLOW, FAN FLOW, AND REVERSE THRUST COEFFICIENTS WITH FOUR BLOW-IN DOORS BLOCKED

Figure 8-20

5 B.I.D. BLOCKED
30 PER CENT BLEED
(SPOILED)
$P_{TE}/P_{AMB} = 2.0 \quad P_{TF}/P_{TE} = 1.05$

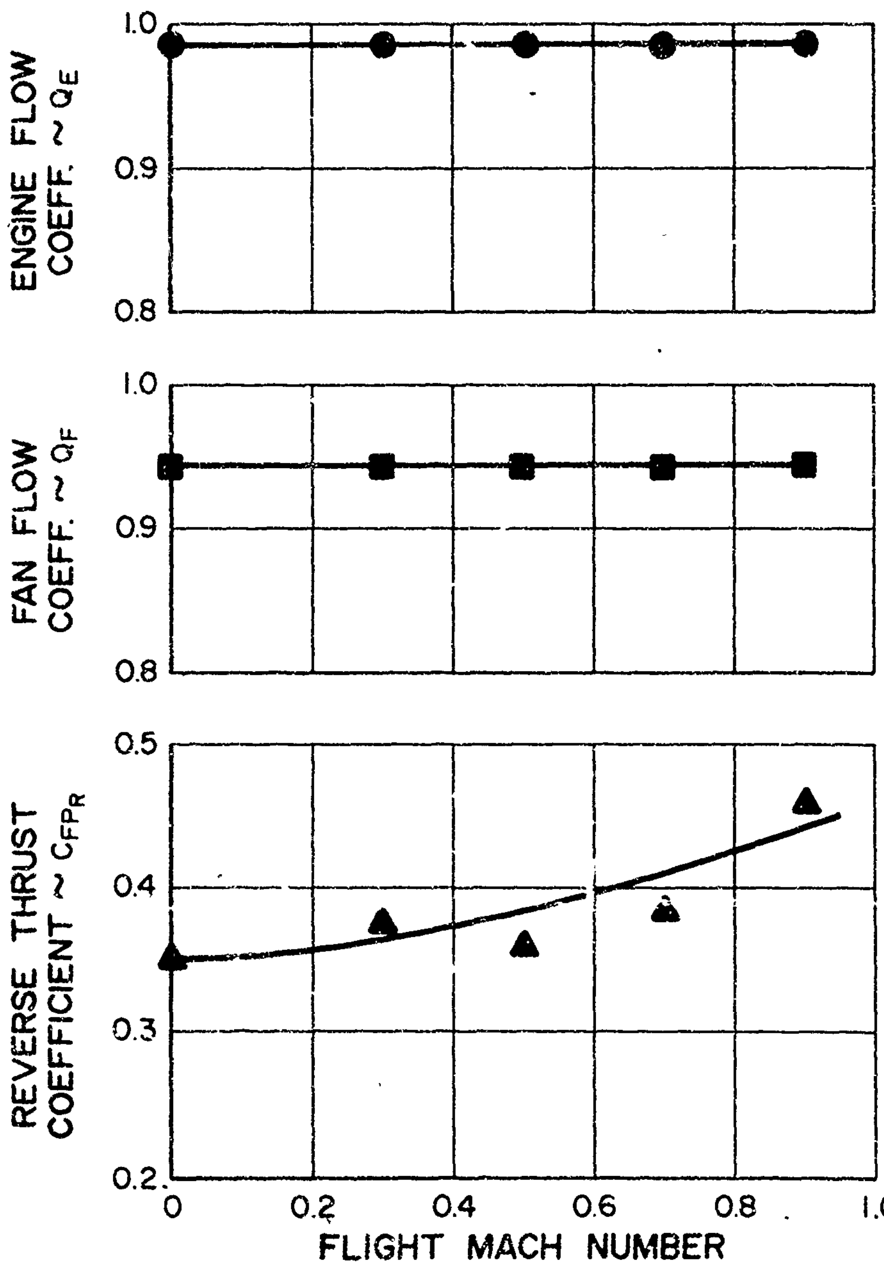

TYPICAL EFFECT OF FLIGHT MACH NUMBER ON ENGINE FLOW, FAN FLOW, AND REVERSE THRUST COEFFICIENTS WITH FIVE BLOW-IN DOORS BLOCKED

Figure 8-21

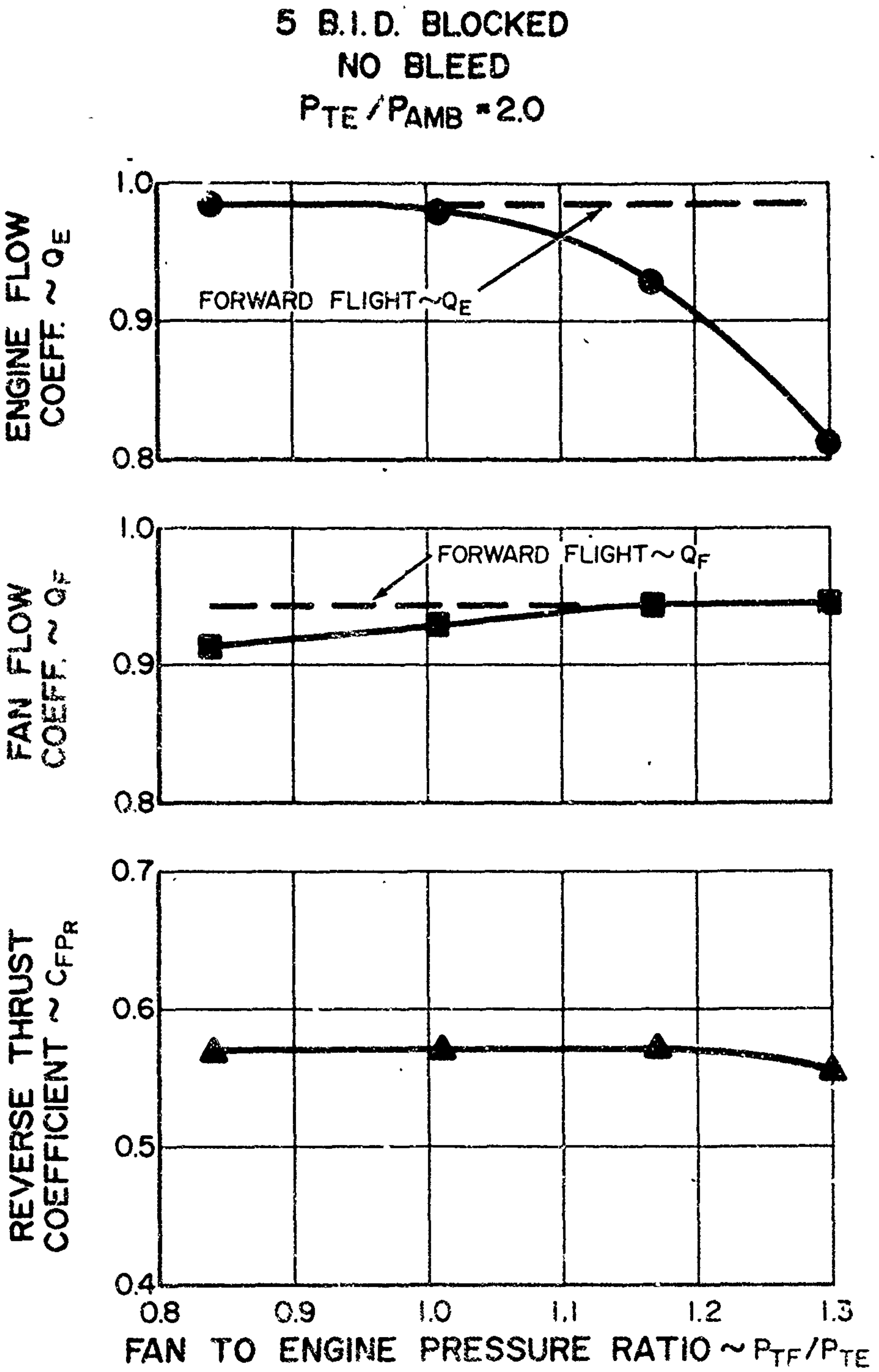

TYPICAL EFFECT OF FAN-TO-ENGINE PRESSURE RATIO ON ENGINE FLOW, FAN FLOW, AND REVERSE THRUST COEFFICIENTS WITH FIVE BLOW-IN DOORS BLOCKED

Figure 8-22

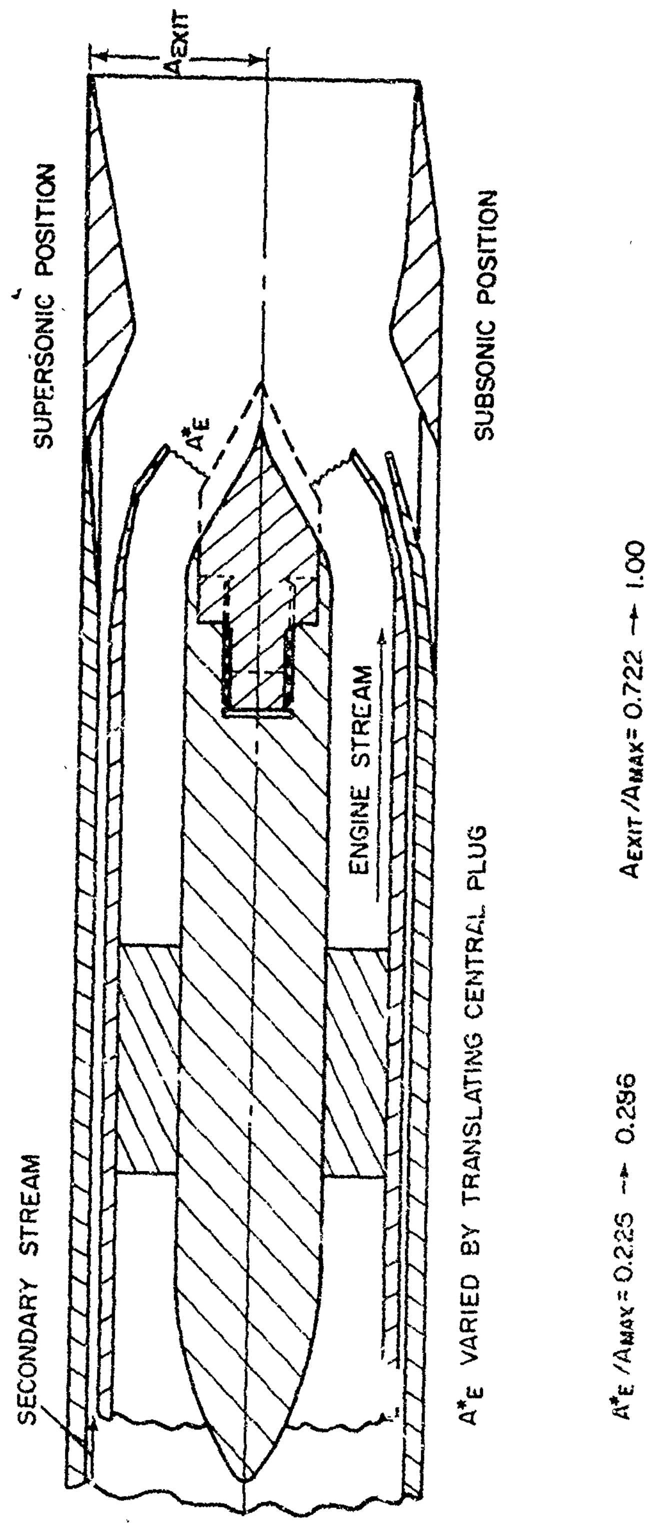

SCHEMATIC DIAGRAM OF MODEL USED TO SIMULATE PARTIALLY AUGMENTED TURBOJET

Figure 8-23

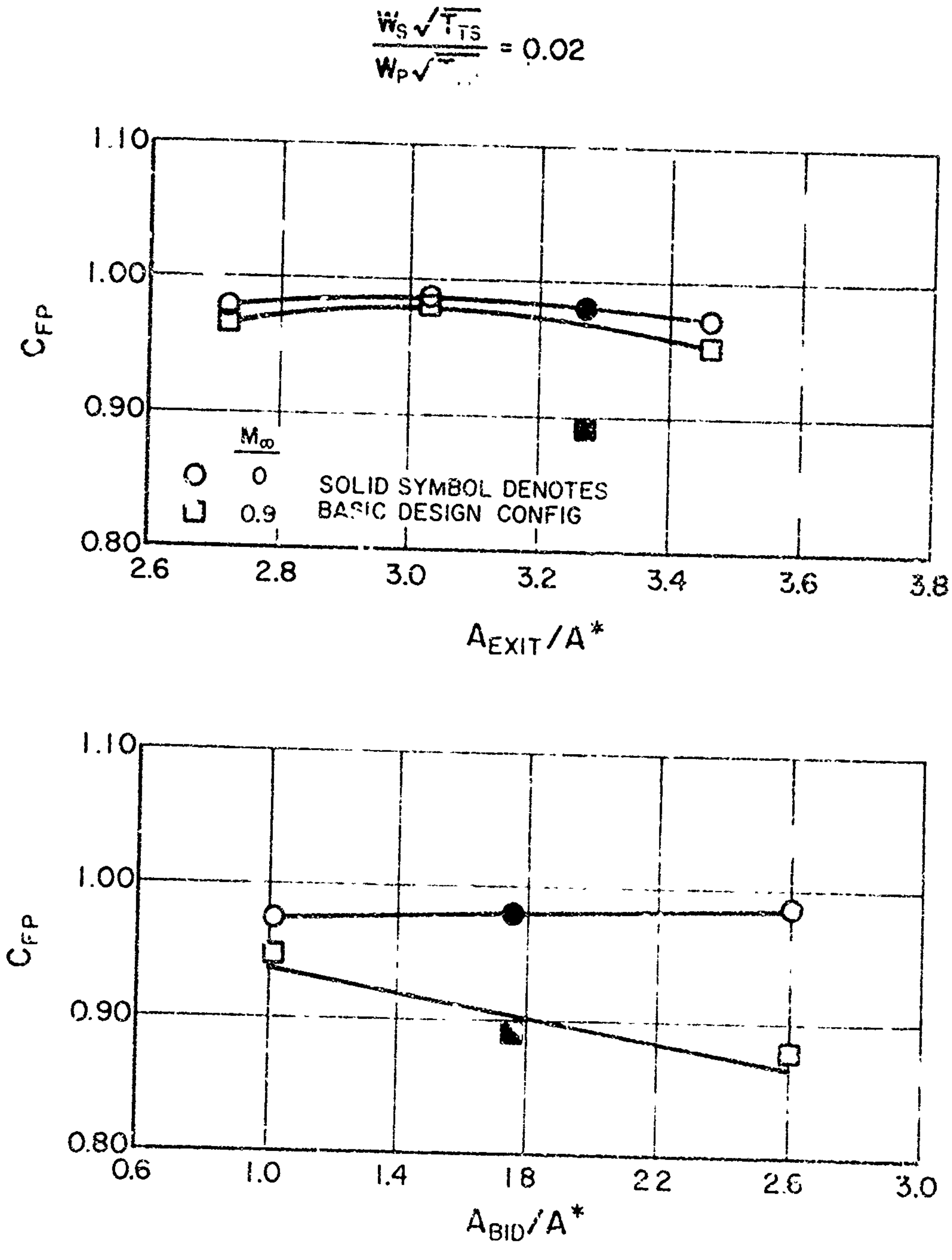

TYPICAL EFFECTS OF SHROUD EXIT AREA AND BLOW-IN DOOR AREA ON STJ227 EJECTOR PERFORMANCE

Figure 8-24

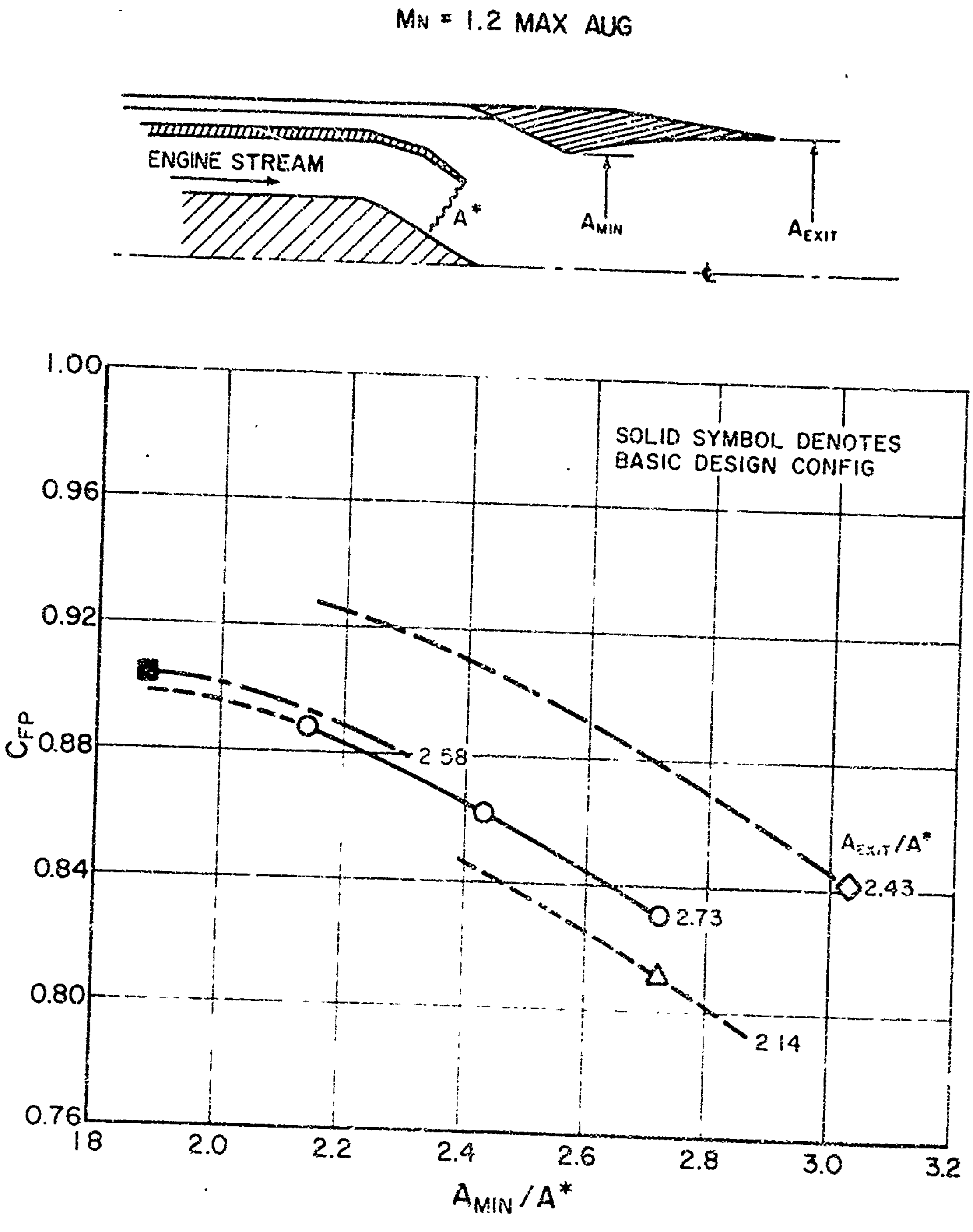

EFFECT OF SHROUD GEOMETRY ON TRANSONIC BLOW-IN-DOOR EJECTOR PERFORMANCE OF STJ 227

Figure 8-25

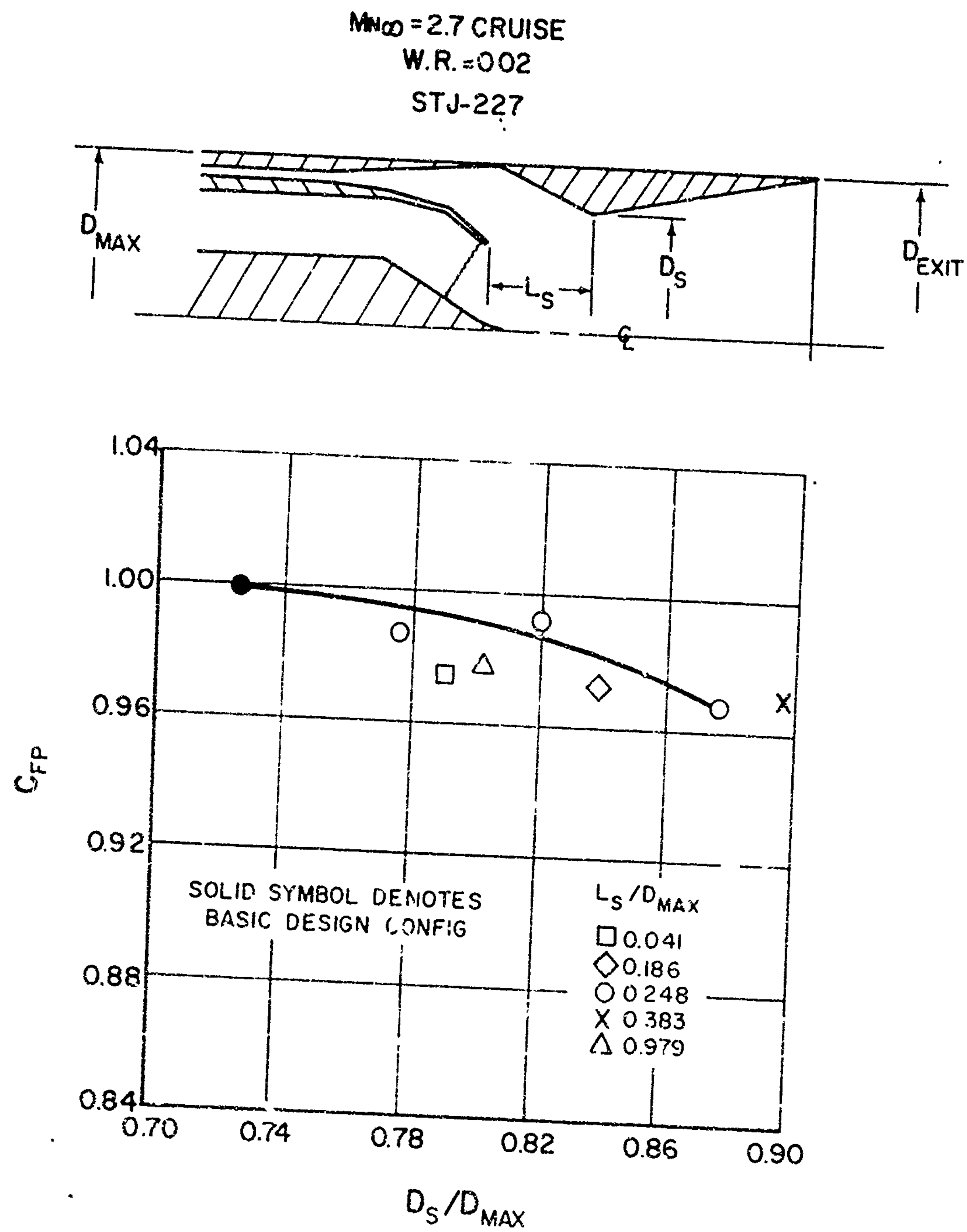

EFFECT OF SHROUD GEOMETRY ON SUPERSONIC BLOW-IN-DOOR EJECTOR PERFORMANCE

Figure 8-26

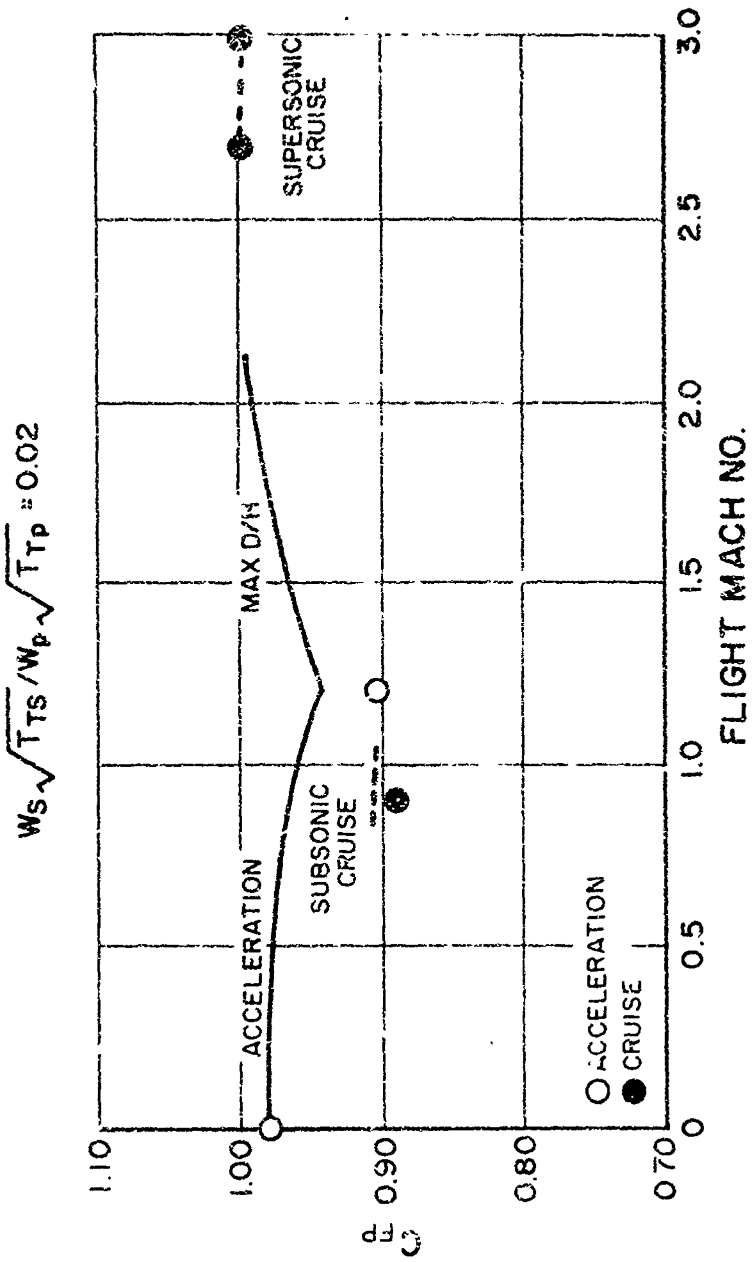

SCALE MODEL STJ227 BLOW-IN-DOOR EJECTOR PERFORMANCE AND PHASE IIA MODEL SPECIFICATION PERFORMANCE REQUIREMENTS

Figure 8-27

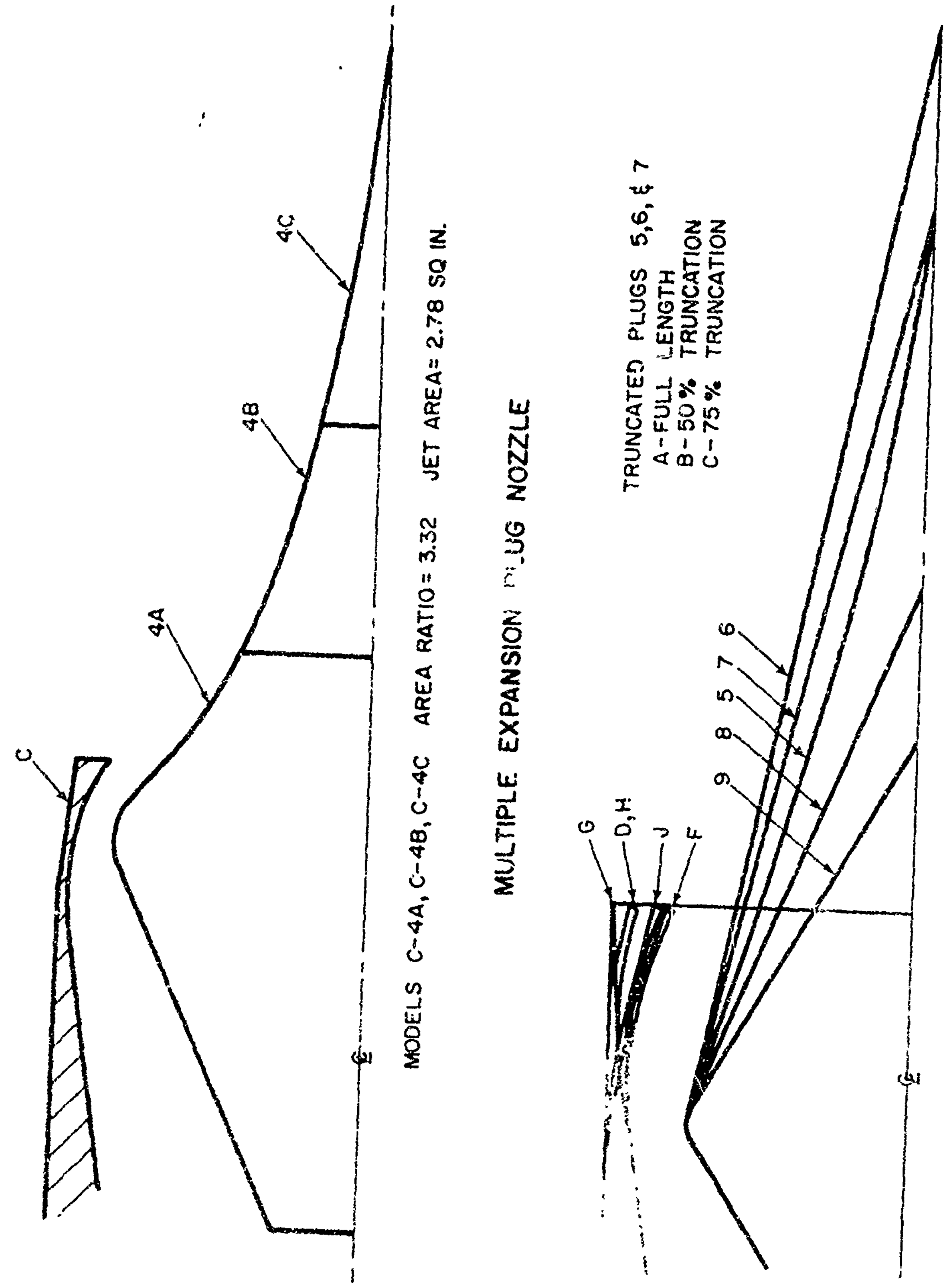

SCHEMATIC DIAGRAMS OF PLUG NOZZLES TESTED

Sheet 1 of 2

Figure 8-

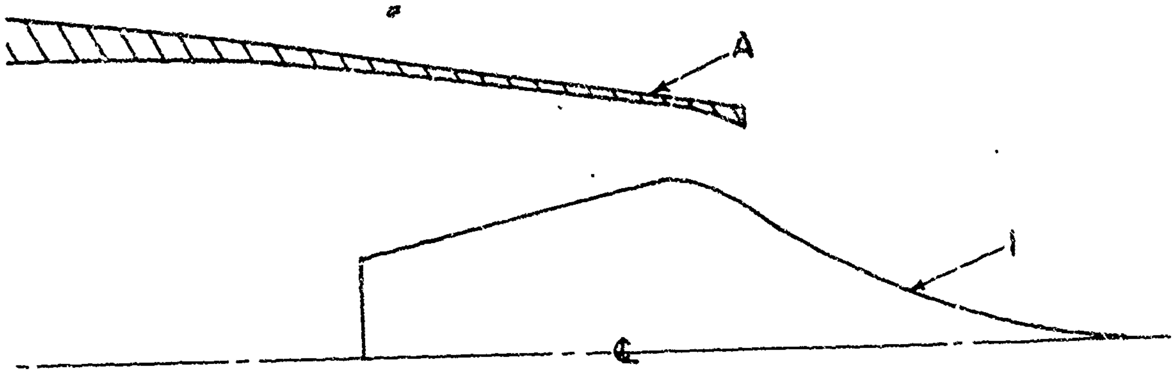

MODEL A-1 AREA RATIO = 1.72 JET AREA = 2.78 SQ IN.

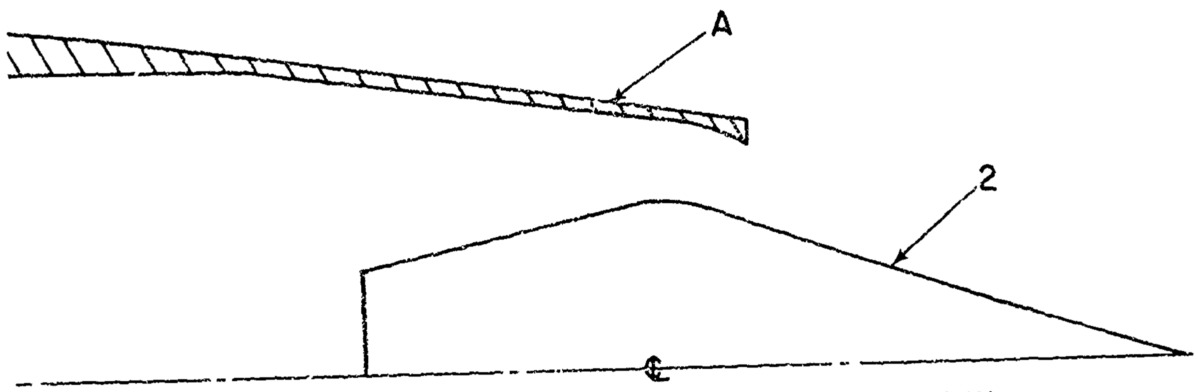

MODEL A-2 AREA RATIO - 1.72 JET AREA = 2.78 SQ IN.

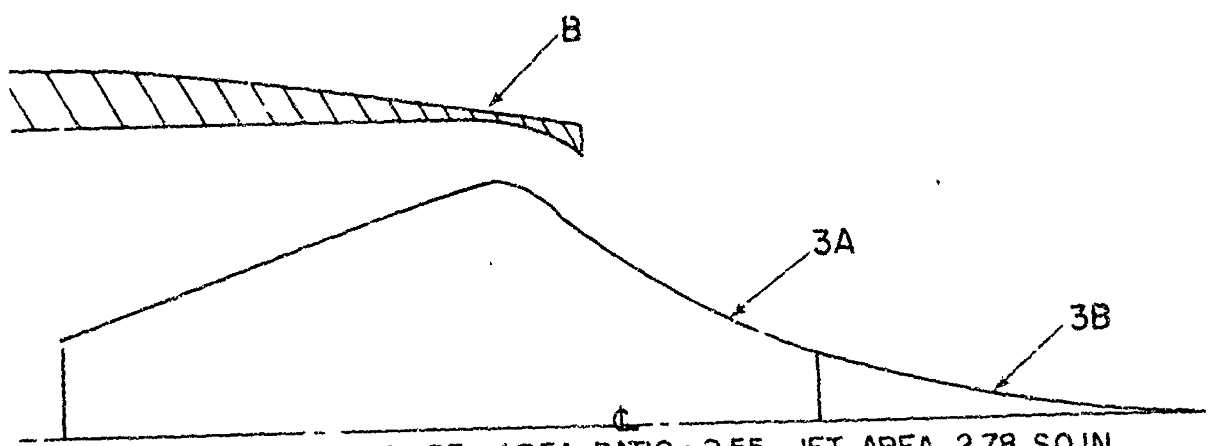

MODEL B-3A & B-3E AREA RATIO = 2.55 JET AREA 2.78 SQ IN.

SCHEMATIC DIAGRAMS OF PLUG NOZZLES TESTED

Sheet 2 of 2

Figure 8-28

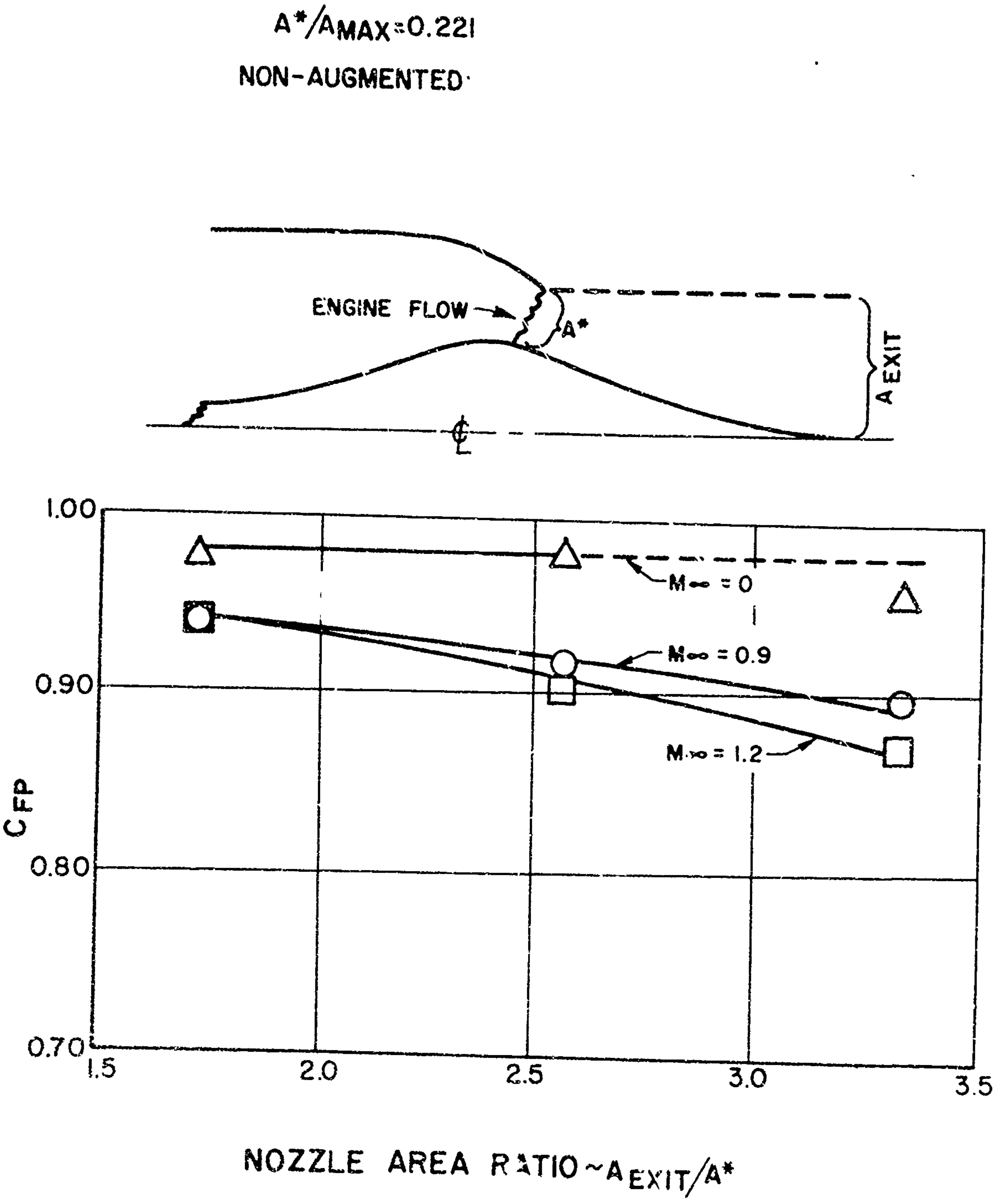

TYPICAL EFFECT OF NOZZLE AREA RATIO ON PERFORMANCE

Figure 8-29

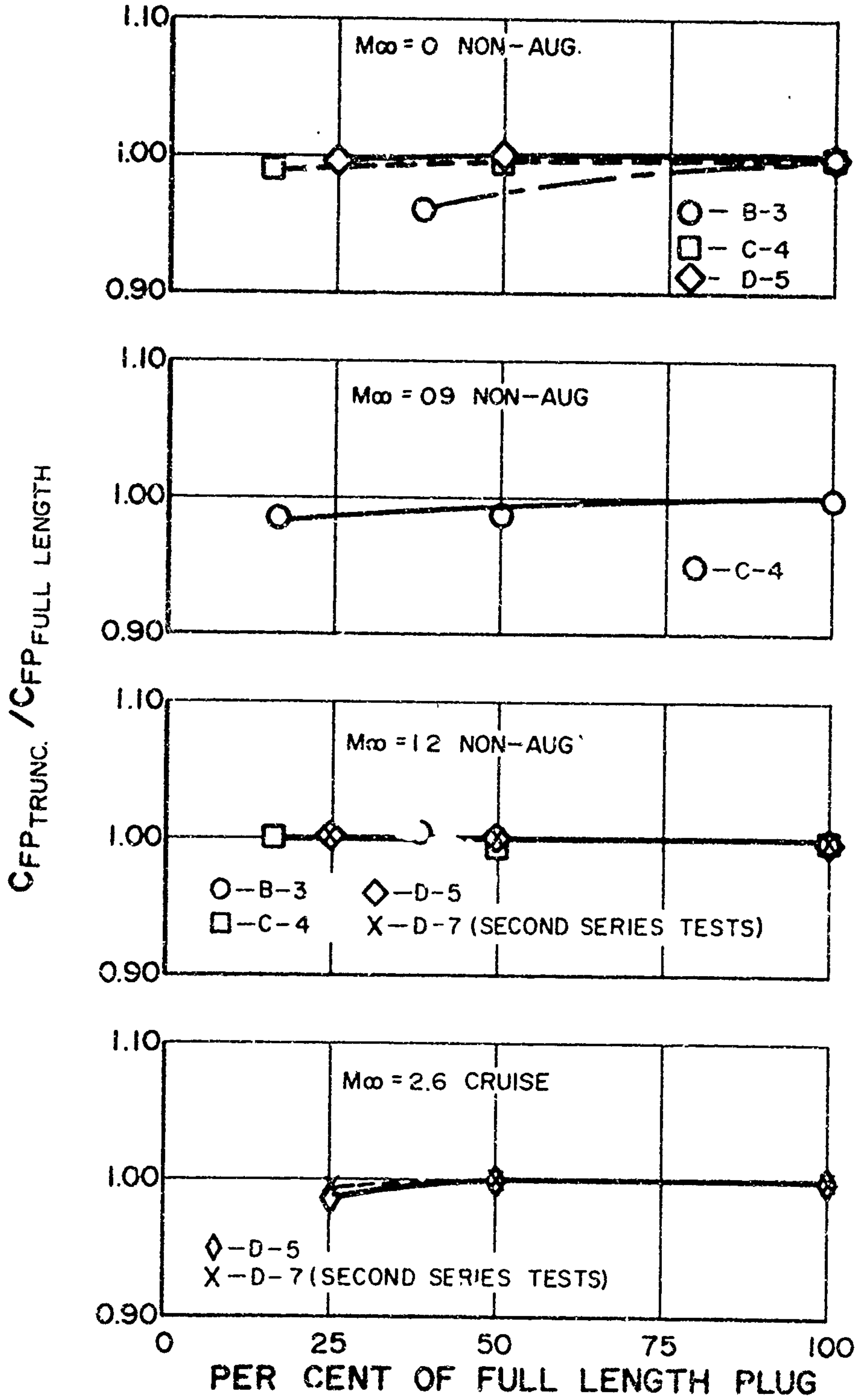

NOZZLE PERFORMANCE WITH TRUNCATED PLUG

Figure 8-30

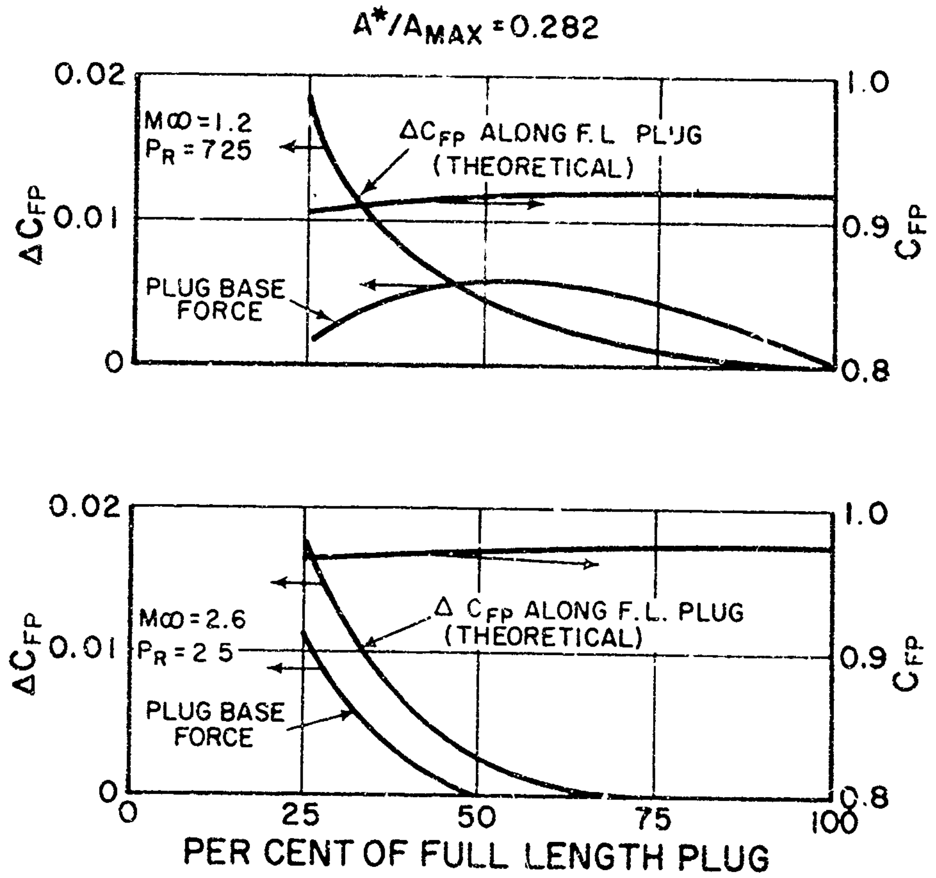

EFFECT OF PLUG TRUNCATION ON NOZZLE PERFORMANCE

Figure 8-31

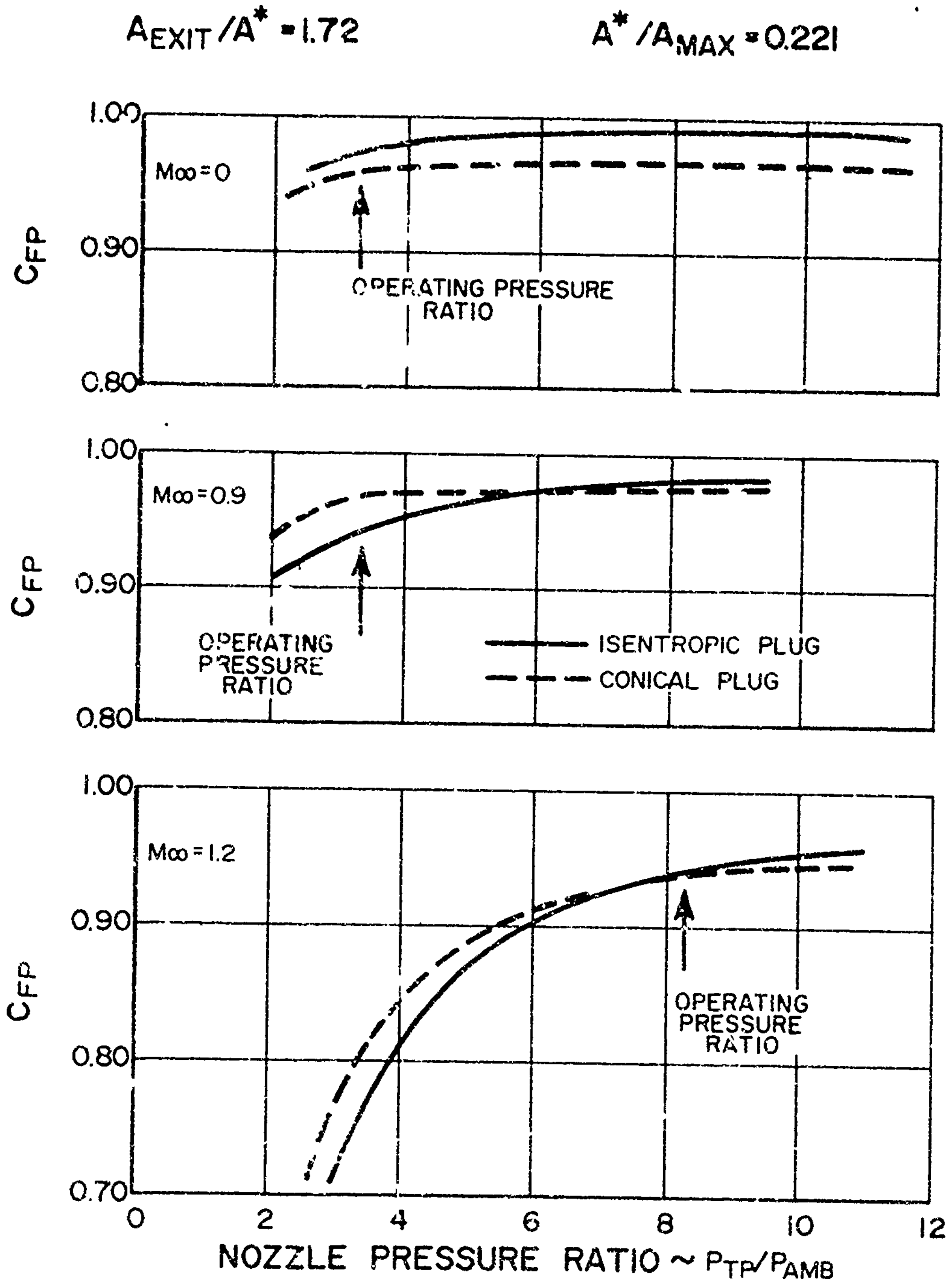

EFFECT OF PLUG CONTOUR ON NOZZLE PERFORMANCE

Figure 8-32

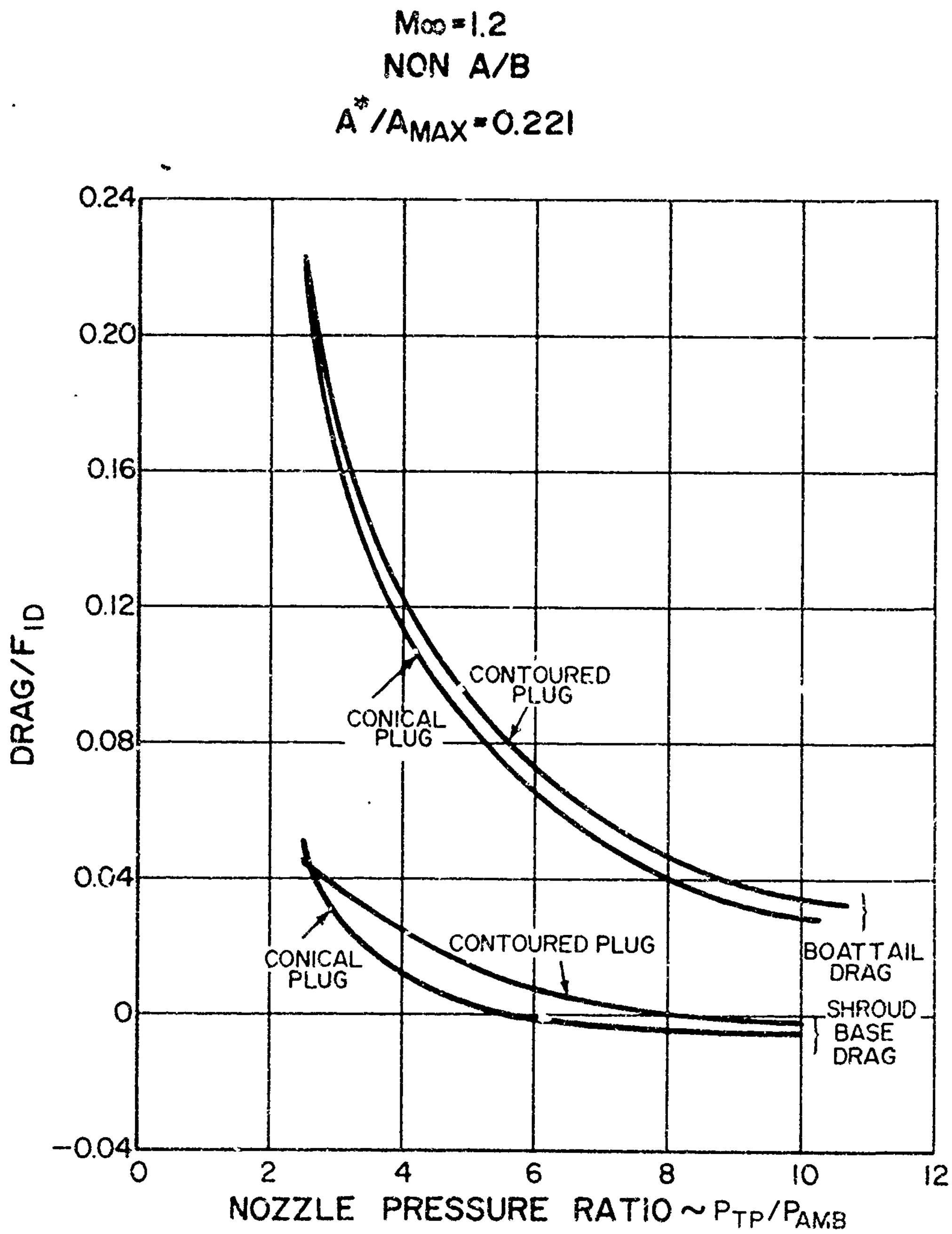

BOAT-TAIL AND SHROUD BASE DRAG

Figure 8-33

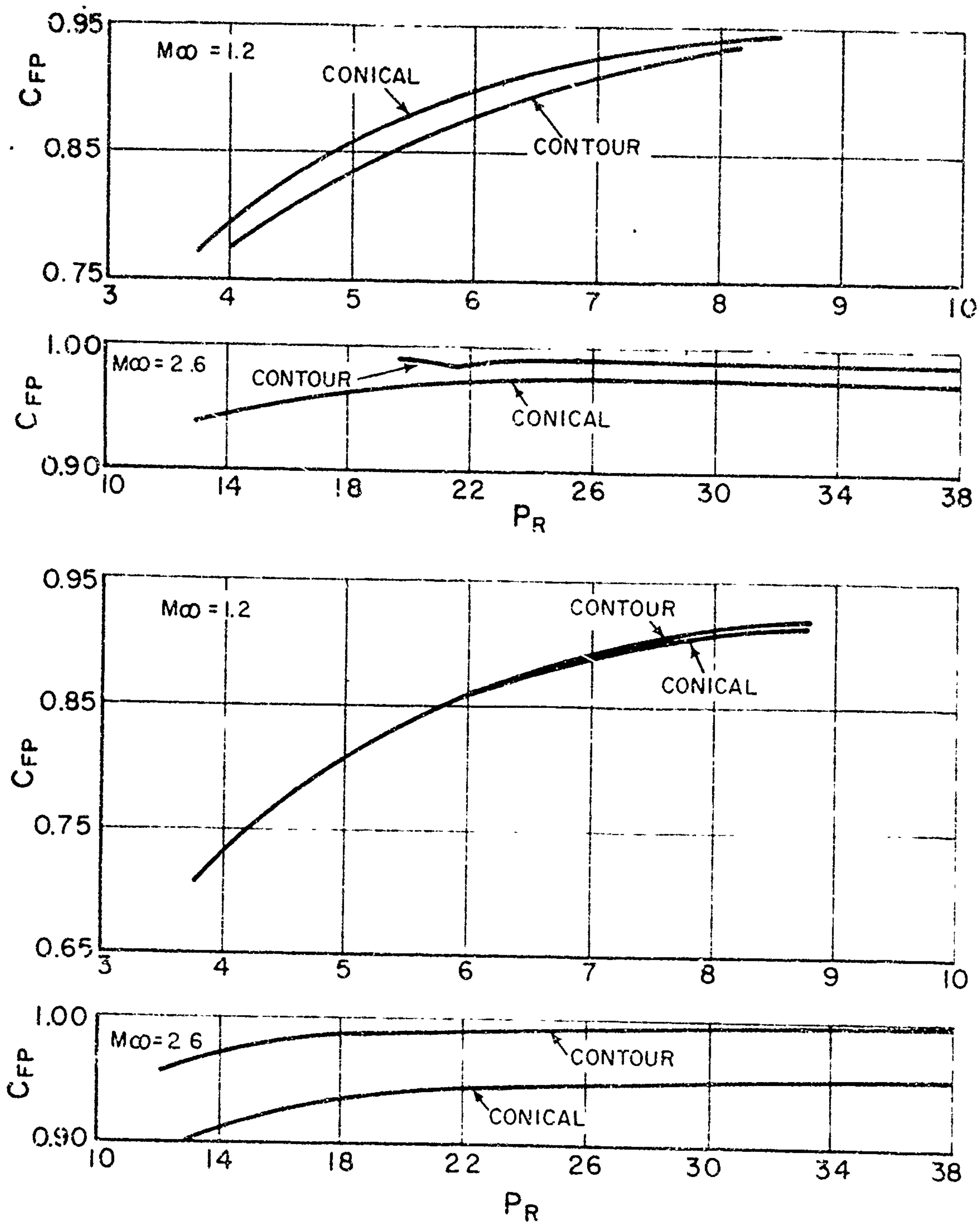

MULTIPLE EXPANSION PLUG NOZZLE PERFORMANCE

Figure 8-34

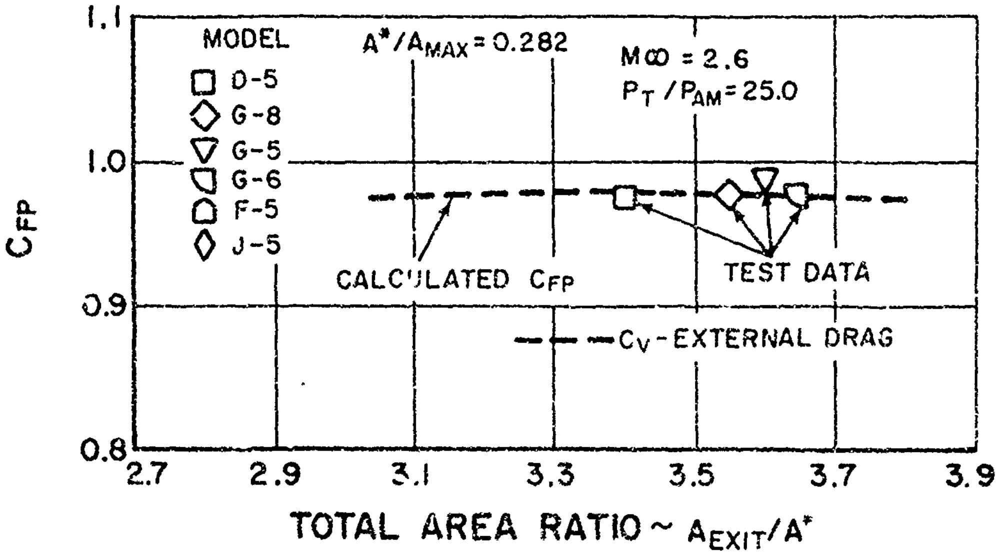

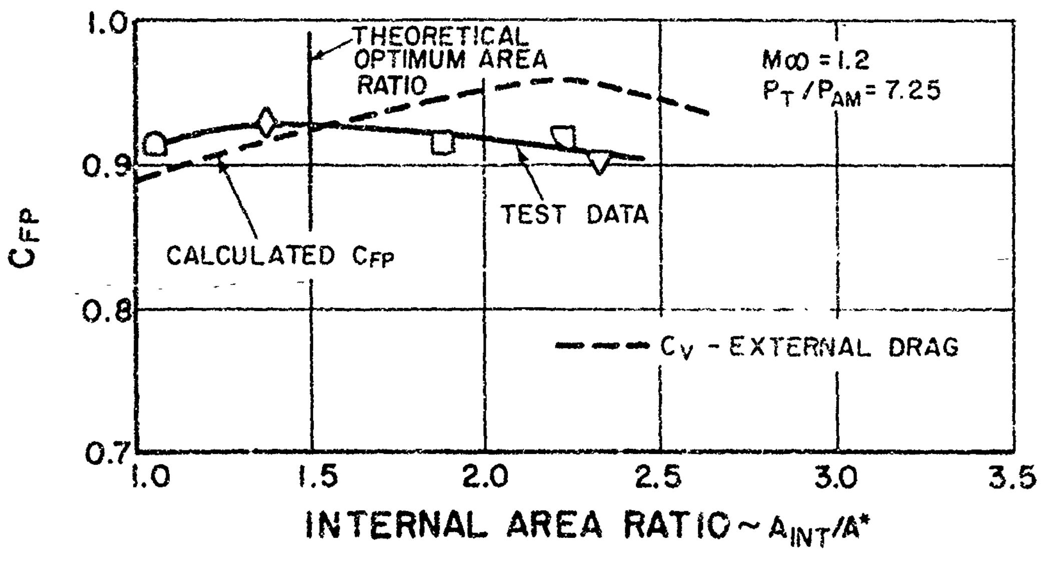

EFFECT OF AREA RATIO ON MULTIPLE EXPANSION PLUG NOZZLE PERFORMANCE

Figure 8-35

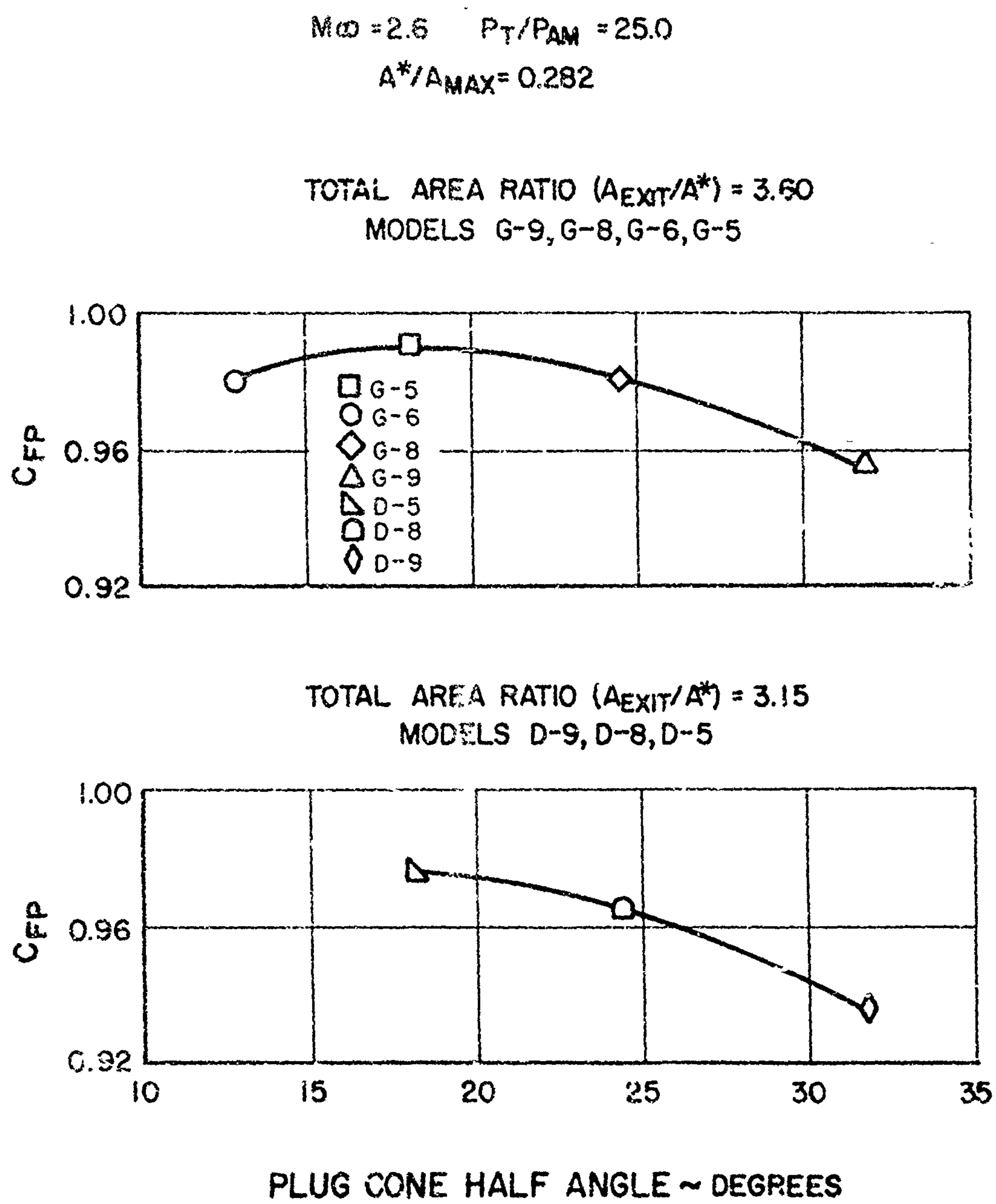

EFFECT OF PLUG CONE HALF ANGLE ON MULTIPLE EXPANSION PLUG NOZZLE PERFORMANCE

Figure 8-36

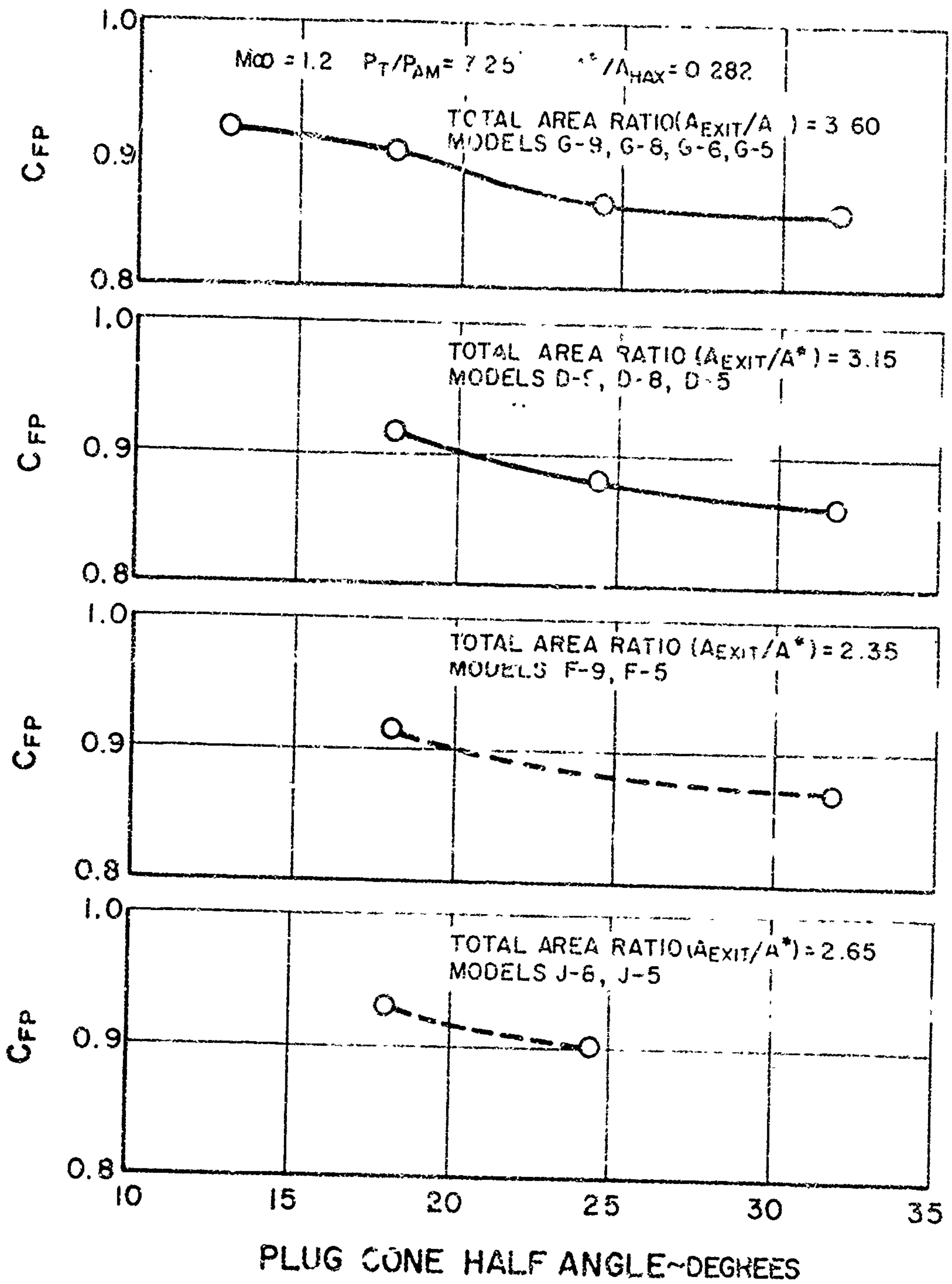

EFFECT OF PLUG CONE ANGLE ON MULTIPLE EXPANSION PLUG NOZZLE PERFORMANCE

Figure 8-37

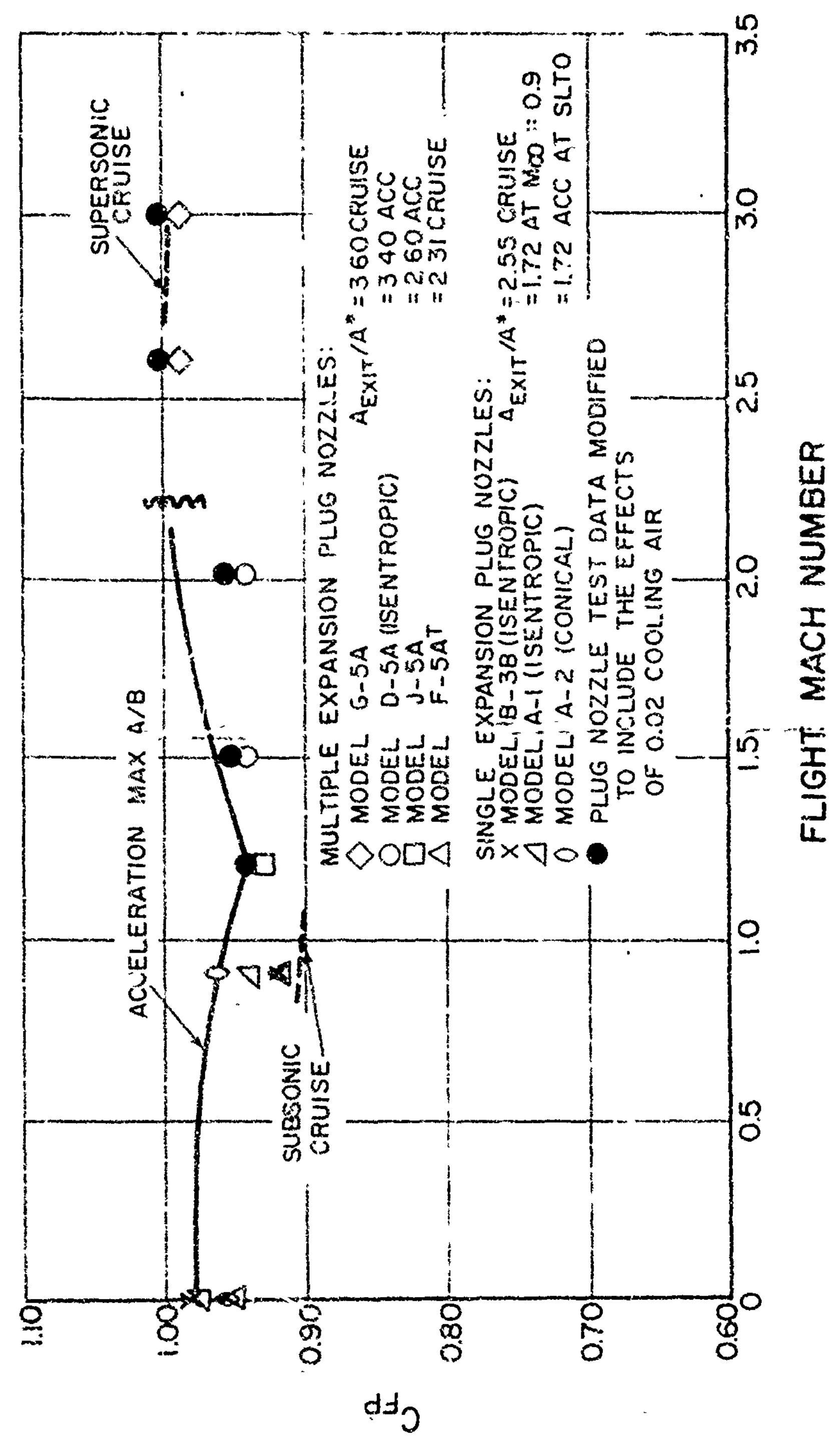

SCALE MODEL PLUG NOZZLE PERFORMANCE AND PHASE IIA MODEL SPECIFICATION PERFORMANCE REQUIREMENTS

Figuer 8-38

NOISE

ITEM 9 - NOISE REDUCTION

OBJECTIVE

The objective of the noise reduction work was to obtain information on noise suppression devices and techniques which could be incorporated into the design of the SST airplane. During Phase II-A of the program, variations of model inlets and nozzles and fan duct treatments were tested to determine their effect on noise generation. The goal of this program was to obtain information which may be used to design a SST airplane that will meet or better the FAA specified noise levels of: 1) 118 PNdb at 1500 feet from the centerline of the runway during the take-off roll, 2) 108 PNdb at a point three miles from the start of the take-off roll, and 3) 118 PNdb at a point one mile from the end of the runway beneath the approach flight path.

A. INTRODUCTION

The ability of the SST airplane to have acceptable noise levels depends on its low speed performance characteristics, the engine size, and the noise radiated from the engine at take-off and approach power settings. A satisfactory solution to the aircraft noise problem can be obtained by the joint efforts of the airplane and engine manufacturers.

In order that the SST airplane be capable of profitable operation, numerous features of the engine and airframe design must be optimized for the many operating regimes involved in a complete mission. Design of the airframe and engine must also be optimized from the noise standpoint, without violating any of the economic or safety ground rules. To obtain low noise levels, the engine size and cycle should be selected and developed to produce minimum noise while meeting the other requirements of the airplane. A high thrust engine installed in an aircraft with satisfactory climb characteristics will be at a relatively high altitude at the three mile point. At this point, power can be safely reduced so that acceptable noise levels will result in the community beneath the flight path.

As the ILS glide slope is fixed at from 2.5 to 3.0 degrees, little can be done to increase the altitude of the airplane on the approach over the community. However, as noise increases with thrust, the airplane should be designed to require as little thrust as possible during approach. Thus the engine for the SST must have high thrust for ground roll and initial climb, and low engine noise levels per pound of thrust.

The STF219 engine proposed by Pratt & Whitney Aircraft for use in SST airplanes incorporates the turbofan, or ducted fan, engine cycle. This cycle has several inherent advantages over a turbojet cycle engine, one of which is lower engine noise levels. Conversion of subsonic jet transport engines from the turbojet to the turbofan cycle resulted in the most significant noise reduction to date in the populated areas beneath the take-off flight path.

Because of the increased turbine inlet temperature and lower compressor compression ratio required for economical supersonic flight, the engines designed for use in the SST will be noisier at maximum power than those used in current subsonic jets. Figure 9-1 shows estimated noise versus thrust for the STF219 engine as well as several current Pratt & Whitney Aircraft jet engines. Although the proposed SST powerplant is more noisy at maximum power, it compares favorably when the noise level per pound of thrust is considered. It must also be kept in mind that the SST airplane will be overpowered for takeoff. Some flexibility regarding the thrust used for ground roll versus that used during reduced power climb is therefore available.

Three major sources of noise are inherent in the design of the STF219 engine. These sources are: 1) noise from the compressor radiated out the inlet, 2) noise from the compressor radiated out the fan ducts, and 3) noise generated in the jet exhaust wake.

Because the intent of Phase II-A of the study contract was to produce results directly applicable to the SST engine, test programs were initiated to investigate noise reduction techniques suitable for use in each of the three major regions. In addition to the test program, analytical studies were conducted to assess the potential improvement from suppression devices.

B. REVIEW OF NOISE SUPPRESSION DEVICES

The necessity for minimizing the noise from aircraft engines has long been recognized by Pratt & Whitney Aircraft. Noise reduction work on reciprocating engines was begun in 1938, and methods were established for gearing a propeller to an engine so as to obtain acceptable noise characteristics. Jet engine noise studies began in 1953, several years before the operation of scheduled jet transports in this country. Tests were conducted to gain an understanding of the jet engine noise generating mechanisms, and many suppressor devices were tested and evaluated. As a part of Phase II-A of the SST engine study contract, results of previous tests on suppressor devices were reviewed to determine whether they could be beneficially integrated into the design of the SST engine.

1. EXHAUST NOISE

The noise heard from the exhaust of a jet engine is characterized by a spectral composition which contains random acoustic energy throughout a broad frequency band. Turbulence generated by mixing of the high velocity engine exhaust gas with the atmosphere provides the source of this noise. This turbulent mixing region may extend 20 nozzle diameters downstream of the engine nozzle exit. Small size turbulent eddies result from the high shear gradients near the nozzle exit and act as a source for high frequency noise. Low frequency noise results from the large turbulent eddies that exist further downstream from the nozzle exit. The sound pressure level of the noise generated by this mixing process has been shown to be related to the relative velocity between the jet and the ambient air and varies as shown in Figure 9-2.

a. Exhaust Noise Suppression Techniques

Because exhaust noise is generated external to the engine, only three general approaches to exhaust noise reduction appear feasible. These approaches are: 1) reduce the jet velocity, 2) change the mixing process, and 3) change the directivity. These three approaches and the effect of internal mixing are discussed in the following paragraphs.

b. Jet Velocity

The forward thrust generated by a jet engine results from the summation of the differential pressures acting on the engine. This thrust is equal to the increase in momentum of the gas passing through the engine, or, in other words, the product of the mass flow and increase in gas velocity. Each pound of air entering the engine during static operation produces a thrust proportional to its exit velocity. Small, light, high-thrust jet engines are possible because of high exit velocities.

For a given nonaugmented thrust, turbine inlet temperature, and compressor pressure ratio, a turbofan cycle engine will always have a lower jet velocity than a turbojet cycle engine and will therefore be less noisy. After the operating cycle and size of an engine are fixed, the jet velocity depends on the engine thrust setting and may be reduced only by decreasing the thrust.

The size of the engines which will be used on the SST will be determined by transonic climb requirements, not by take-off power requirements as is the case for the subsonic transports. As an excess of take-off thrust will be available, it can therefore be adjusted to meet noise limits during take-off. Fly-over noise beyond the three mile point will be determined by the thrust used during ground roll and initial climb and the performance of the airplane. A large airflow engine will have a lower jet velocity and therefore create less noise than a smaller airflow engine at the same thrust. The relationships between jet exhaust velocity, airplane performance, and fly-over noise must all be considered in sizing an engine for a particular airplane. After an engine-airframe combination is selected, there is little possibility of further reductions in noise by reducing jet velocity.

c. Changing the Mixing Process

Although several types of suppressors are currently in use, the operating principles of all the devices are similar. Basically, the perimeter of the jet nozzle in the exit plane is substantially increased by replacing the standard circular nozzle with an irregularly shaped nozzle. This procedure changes the shape of the mixing boundary and creates a greater surface area between the exhaust stream and the ambient air. As aerodynamic shear forces act over this increased surface area, the stream is decelerated within a much shorter distance behind the nozzle exit than is the stream from a standard convergent circular nozzle.

The effect of this nozzle change on jet noise is twofold. Less energy is radiated as noise because of the more rapid deceleration of the stream, and the noise generated is higher in frequency because of the irregular nozzle shape. High frequency noise is attenuated more rapidly with distance than is low frequency noise. The noise reduction obtained from a typical multitube suppressor, as compared to a convergent circular nozzle, can be seen on Figure 9-3.

From 1953 to 1960, Pratt & Whitney Aircraft maintained an extensive acoustics program to study the effect of nozzle shape on jet noise. In the anechoic chamber shown in Figure 9-4, models of over 1200 variations of 150 basic configurations were tested. A few of these models are shown in Figure 9-5. As a result of model tests, about 200 variations of 50 basic suppressor nozzles were built and tested on JT3 and JT4 engines. Typical full-scale suppressor configurations are shown in Figure 9-6. Many of these suppressors were tested to better establish jet noise theories, and were not intended to be prototypes of flight suppressors.

During the tests on suppressors, it was learned that a sizeable reduction in noise measured during a ground sound test does not necessarily mean that the noise levels during flight will be reduced. Severe performance and weight penalties, associated with the use of an inefficient device, may actually cause an increase in noise beneath the take-off flight path. This subject is discussed further in Part F of this item of the report.

d. Change in Directivity

The rectangular nozzle shown in Figure 9-7 was designed to take advantage of changes in the exhaust noise directivity pattern. This device had an asymmetrical noise radiation pattern, and was mounted so as to minimize the noise radiated toward the ground beneath the airplane.

e. Internal Flow Stream Mixing

The exhaust noise level of a nonaugmented turbofan cycle engine depends on engine size, turbine inlet temperature, by-pass ratio, and fan exit velocity (fan pressure ratio). As explained below, noise levels can be shown to decrease when either fan exit velocity or by-pass ratio are increased. Potential for additional exhaust noise re-

duction may also be realized by complete mixing of the primary engine and fan duct streams. As the exit velocity of the mixed stream is usually lower than that of the primary, a net reduction in noise usually results.

Increasing either the by-pass ratio or fan duct flow exit velocity on a fixed airflow-size gas generator is usually accompanied by a decrease in noise and an increase in thrust. These effects are shown in Figure 9-8. A reduction in noise results because additional energy is extracted from the primary engine stream to drive the fan stages, reducing the primary-jet exit velocity. Additional noise reduction potential may be realized from internally mixing the two streams, and is shown in the shaded area of the curve. Noise reduction from mixing is shown to depend on both by-pass ratio and fan duct velocity.

In plotting the curves, a fixed airflow-size gas generator engine with a fixed turbine inlet temperature was assumed. Practical considerations affecting the engine performance parameters and mechanical design were not considered. The physical means of increasing the "fully expanded" fan exit velocity would be to add fan stages or increase the work done per stage. An increase in by-pass ratio could be achieved by increasing the fan diameter. The effect of by-pass ratio and fan exit velocity on noise will vary as other engine performance parameters are varied, but the trends shown in Figure 9-8 will hold true.

Experience has shown that little mixing takes place between two streams in a short common-flow cylindrical duct. However, tests have shown that it is possible to achieve effective mechanical mixing of the two streams in a reasonably short length of duct by the use of special mixing devices.

Several variations of three basic types of mixing devices shown in Figure 9-9 were sound tested on a full-scale turbofan engine. Test results showed that many of the devices reduced the exhaust noise level by an amount consistent with theory, but excessive performance penalties were associated with some of these configurations.

2. COMPRESSOR NOISE

a. Blade and Vane Number Changes

From an analysis of the theory presented in SAE report 345D, it would appear that the use of either a large number of vanes (more than twice the number of blades), or else no vanes in a compressor would result in the propagation of no fundamental blade-passing frequency noise out the inlet duct at subsonic blade tip speeds. Experimental tests (on both rigs and engines) have verified this conclusion. Unfortunately, in previous engine designs the choice of a compressor configuration which did not generate propagating noise was not possible because of structural considerations, but small changes in the number of blades and vanes could be made.

Small changes in numbers of either blades or vanes can make significant changes in both the radial and circumferential distribution of sound energy in the interaction generated "spinning modes". In many practical cases, four or more circumferential modes may be present, some forward spinning and some backward spinning, each having a complex radial pressure distribution. In this complex situation, it is not feasible to estimate analytically the result of a small change in blade or vane number on the far field noise.

In practice, the optimum blade-vane combination is best determined by a series of acoustic tests involving hardware changes in full scale. Basic theory can be used to identify the significant noise generating modes, and the results of the far field sound measurements will establish the optimum configuration.

A series of tests on different blade-vane combinations provided the data used to select the final configuration used in the JT3D "hush kit" fan. Two of the many stator vanes tested in full scale are shown in Figure 9-10. A series of rotors, having from 30 to 36 blades, was also evaluated in conjunction with the vane assemblies. Results of the tests showed that a 35-blade rotor used in conjunction with a 55-vane stator resulted in the lowest far field noise levels and had no adverse affect on performance.

It was also learned during development of the JT3D turbofan engine for minimum noise that the annoyance of the noise as judged by listeners was reduced when different numbers of blades were used in the

two fan stage rotors. Two discrete tones sufficiently separated in frequency had a less piercing quality than the single frequency tone generated when both fan stage rotors had the same number of blades. This feature was also incorporated in the final configuration.

b. Spacing

Rotor blade-stator vane spacing has been shown to have a significant effect on compressor noise level. Tests on ten-inch diameter models, 28-inch diameter rigs, and full-scale engines have verified that noise levels are reduced as spacing is increased. Results of a series of spacing tests were included in the Phase I final report, PWA-2353. These test results showed a significant noise reduction with increased spacing at low rotor tip speeds, but that spacing had a relatively negligible effect when rotor blade tip velocities were near and above supersonic. Figure 9-11 shows the average results of increased spacing on noise as determined from a wide variety of model, rig, and engine tests.

c. Blade Tip Clearance

Extensive tests to measure the effect of blade tip clearance on noise levels were conducted using compressor rigs. Tests were conducted using excessive tip clearances as limited by compressor efficiency down to a "negative" tip clearance obtained by operating with the blade tips running in a trough as shown in Figure 9-12. Tests were also conducted using slightly eliptical rotor ducts which caused a variable tip clearance. Results of these tests showed that tip clearance was not a significant variable in noise generation.

d. Variable Vane Angle of Attack

A variation in vane angle can be expected to have an effect on the pressure field upstream of the vane and the wake downstream from it. As noise is generated by the aerodynamic interaction of the upstream pressure and the downstream wake with the rotor pressure field, it is fair to assume that some change in noise intensity would result from vane angle changes. To evaluate this effect experimentally, sound tests were run on both rigs and engines fitted with variable angle vanes. Typical full-scale experimental hardware is shown on Figure 9-13. Results of constant rotor-speed tests on this type of hardware have shown small, unpredictable changes in noise with changes in vane angles.

In many instances where a noise reduction was measured at a fixed rotor speed, this reduction could not be realized at a constant thrust condition. This was because the vane angle changes also resulted in reduced performance. The higher rotor speeds and exhaust velocities needed to maintain constant thrust with the vanes in an off-design position tended to increase noise levels and offset part or all of the expected reduction in noise.

e. Vane Slant Angle

As noise is generated by an interaction of the blade-vane wakes, an obvious way to change the nature of this interaction is to slant the stator vanes. Figure 9-14 shows slanted vane assemblies which were tested in full-scale fan engines. A wide variety of slanted vane stators was also tested on rigs. Results of the tests on rigs where only one well defined spinning mode was generated indicated some significant reductions from changes in slant angle as was indicated by theory. Tests of slanted vanes in full-scale engines showed little improvement in far field noise. Analysis of these test results indicated that the large number of spinning modes present made it impossible to select a vane angle which would reduce the intensity of all the modes at the same time.

f. Blade Shape

Several different types of blades which were acoustically tested are shown in Figure 9-15. Results of the tests showed no significant improvements in noise, although some significant changes in performance were measured. Because of the necessity of obtaining good compressor performance, the possible variations in blade shape are quite limited, so this avenue of potential noise reduction is not promising.

g. Vane Shape

As vane shape determines the wake from the vane, it could affect the noise generated. A series of vanes of various shapes were tested on a ten-inch model to check the effect of vane shape on noise level. Some of the assemblies tested are shown on Figure 9-16. Results of these tests indicated that the nonstandard vane shapes did affect the details of the sound pressure distribution in the duct, and some significantly influenced the noise level and the radiation pattern in the far field. Some vane shapes which showed good results in the model tests were

tested in full scale, but they were found to be relatively ineffective because of the complicated modal structure of the engine compressor noise field. Full-scale engines were tested with both blunt and sharp edged inlet guide vanes. A small reduction in noise was measured with the sharp vanes as a result of a weaker vane wake.

h. Indexing

Tests were conducted on ten-inch model compressors with the same number of vanes in front of and behind a rotor. Each set of vanes was individually spaced from the rotor so that noise of equal strength was generated. Both sets of vanes were then installed in the model. At a fixed speed, one set of vanes was circumferentially rotated until an index position was found that resulted in minimum noise levels in the far field. At this vane position, the noise generated by the rotor and the upstream vanes was out of phase with that generated by the downstream vanes, resulting in cancellation of the noise fields. A very significant reduction in noise was measured with the ten-inch model with the vanes set at the optimum index position.

Similar tests were run on a full-scale engine with a 51-inch diameter fan, but a significant reduction in far field noise could not be obtained. After detailed investigations, it was found that differences in the radial pressure distribution in the spinning mode sound patterns in front of and behind the rotor prevented effective noise cancellation. The necessary changes to make the upstream and downstream sound fields similar could not be effectively achieved, indicating that this scheme would be very difficult to use on a full-scale engine.

i. Coanda Inlet Guide Vane

Figure 9-17 shows a cross sectional view of Coanda vane assembly. Pressure air is blown through slots in the vane trailing edge, causing significant changes in the vane air-exit angle and the vane wake. This type of device was built and tested on compressor rigs, but showed no significant effect on noise. Further tests on this type device would probably be necessary to fully evaluate its effect on noise.

j. Sound Absorbing Rotor Duct Shrouds

Tests were run with resonant absorber material installed on the compressor blade shrouds. Typical full-scale and rig parts are shown in Figure 9-18. Many configurations were tested with a wide variety of

shroud treatment constructions. Results of this series of tests showed that the use of sound absorbing material in this location was not significantly effective.

3. INLET NOISE

a. Sound Absorbing Inlets

One of the more effective means of reducing compressor noise is the use of sound absorbing inlets. Both Fiberglas-lining and resonant-tuned-absorber lining materials have been tested and were shown to be effective These two types of inlets as well as a Fiberglas-lined "bulb type" inlet are shown in Figure 9-19. The bulb inlet, which prevented line-of-sight sound propagation, was quite effective acoustically but was not practical for flight use in subsonic inlet configurations.

b. Choked Inlets

Several types of inlets shaped to provide a sonic flow section between the face of the compressor and the inlet opening are shown in Figure 9-20. Results of the tests have shown that the sonic section acts as an effective blockage to the propagation of sound out of the inlet. A mechanism to cause sonic flow in the inlet ducts of subsonic transports was not considered practical because a relatively elaborate and heavy structure would be required compared with conventional subsonic inlets and because the additional control devices required might impair the safety of the airplane.

4. FAN DISCHARGE NOISE

On a turbofan engine, discrete frequency compressor noise is radiated rearward from the fan ducts as well as forward from the inlet duct. The level of this noise is related to compressor design as is that radiated out the inlet. Specific items that were tested to determine their effect on fan discharge noise levels are discussed below.

a. Turbulence Generators

Devices were attached to the fan duct exit to cause the exit airflow to be turbulent. Some of these devices are shown in Figure 9-21. No reduction in discrete frequency noise level was measured during sound tests with these devices installed.

b. Reflecting Exit Vanes

A fan exit guide vane assembly with sound reflecting vanes is shown in Figure 9-22. This assembly was installed in conjunction with a sound absorbing inner shroud. The vanes were designed to offer little resistance to airflow but to reflect sound into the absorbing panels (not shown). Tests of this device showed a relatively small reduction of noise in the far field, due to the propagation characteristics of the many spinning modes.

c. Sound Absorbing Fan Discharge Ducts

Tests were run using both fiberglass-lined and resonant-tuned-absorber lined fan ducts. From five to ten db noise reduction was measured using the Fiberglas-lined ducts. Less attenuation was measured using the tuned-absorber-lined ducts because of the effect of flow velocities on the attenuating properties of the material. Tests of the acoustic properties of materials with flow indicate that they can be designed to work, but the design parameters are not yet clearly established.

5. APPLICATION OF ACOUSTIC TEST EXPERIENCE TO THE SST ENGINE

Results of past acoustic tests have been incorporated in the STF219 engine design, and will be of value during the engine development program. The acoustic test program conducted during Phase II-A was designed to pursue methods of noise reduction which experience has shown to be most effective. Specific instances where past test results were incorporated in the engine design are discussed below.

a. Nozzle Design

Models of blow-in-door ejector nozzles incorporating suppression devices were designed during Phase II-A. Experience gained during previous tests of suppressor nozzles and mixing devices was incorporated in the design of these ejector nozzles.

b. Compressor Design

Inlet guide vanes, which usually provide the strongest noise source during low power operation, were not included in the compressor design. Different numbers of blades were used in the two-stage fan to improve the characteristics of the noise generated, and provisions were made to allow variations in the number of stator vanes to optimize noise levels during the development phase of the engine.

c. Acoustical Materials

The effectiveness of acoustical linings in inlet and fan discharge ducts has been demonstrated in the past, but the effects of flow velocity were not well understood. Tests to screen many types of acoustical materials and constructions with high flow velocities were planned and conducted during Phase II-A to determine which are most satisfactory for use in the SST engine.

d. Inlet Ducts

An effective means of reducing compressor noise is by the use of sound attenuating inlet ducts. A program to determine the effects of SST inlet ducts on noise was planned and conducted during Phase II-A. As the SST engine inlet incorporates variable geometry which may be used to increase the duct Mach number, tests were conducted to determine the effect of duct Mach numbers of up to 1.0 (or choked) on noise propagation. Previous testing had suggested some noise reduction could be expected at near-choked conditions and complete blockage of noise at the choke point.

C. INLET DUCT PROPAGATION CHARACTERISTICS

1. GENERAL DISCUSSION

During the approach to landing, the most noticeable engine noise is the compressor whine radiated from the inlet duct. Compressor noise is generated by blades passing stationary vanes and is annoying because of its high frequency. Propagation of compressor noise through inlets of the type used on subsonic aircraft is fairly well understood, but very little data are available on the propagation of sound through complex supersonic inlets of the type designed for the SST airplane.

Several features of a supersonic inlet could influence the propagation of inlet noise. An inlet with significant changes in cross section along its length could be expected to have a sound radiation pattern somewhat different from a short circular inlet. Since a variable area inlet is required to assure good ram pressure recovery over a wide range of flight Mach numbers, the possibility exists of using this variable area feature to control noise during approach. Theory and experimental data both verify that noise is not propagated out of choked inlet, but the effect on noise of operation near a choked condition has not been well documented. A boundary layer bleed system incorporated in the SST inlet design to prevent boundary layer build up at high flight speeds could also be expected to have some effect on noise.

In addition to the features inherent in a supersonic inlet which could affect noise, it may be possible to improve its noise propagation properties by the use of acoustical treatment. The size and shape of the supersonic inlets provide opportunities for the use of acoustical treatment which are not inherent in subsonic inlets.

It is also possible that wakes produced by structures in a supersonic inlet could interact with the compressor rotor pressure field to provide additional noise sources. Tests were conducted to investigate both the favorable and the unfavorable effects of the inlet on noise generation.

As the inlets designed by the two competing airplane manufacturers are quite dissimilar, it was decided to build and test models of each. Data from tests of the supersonic inlets were compared to noise levels measured from a conventional bellmouth inlet, which has been shown to have acoustical properties similar to subsonic transport inlets. Sound data presently used to estimate inlet noise levels were obtained

during tests of bellmouth and subsonic flight inlets. In order to conduct a realistic test of the inlets, it was necessary to install them on a compressor rig capable of simulating inlet flow velocities similar to those in the inlets to be used on the SST engine. Results of the tests provided better insight into the effect of the supersonic inlet on noise propagation and methods of reducing this noise.

2. FACILITIES

The 28-inch diameter compressor rig, used to study the effect of compressor design features on noise during Phase I of the SST development program, was assigned to the Phase II-A inlet test program. As this rig had been used for extensive acoustic tests, its performance and acoustic characteristics were well known. The compressor rig and drive engine are shown in Figure 9-23.

One major modification to the test facility had to be made for this series of tests. Previous tests were conducted to assess the effects of configuration changes on the energy converted to noise by the rig, so a reverberant plenum room led to the most repeatable results. To determine the effectiveness of a supersonic inlet, its influence on directivity as well as sound level must be measured. To measure directivity, it is necessary to eliminate the reflection of sound from the walls toward the microphone. This situation was achieved by the installation of Fiberglas wool on all surfaces of the plenum room.

Prior to the start of tests, a loudspeaker was used to check the room for reflections, and the environment was found to be satisfactory. Tests showed that sound measurements taken along an arc about seven feet from the rig inlet were free from distortion by the room shape and reflectivity.

3. EXPERIMENTAL PROGRAM

a. Test Models

Two basic SST models were fabricated to fit the 28-inch diameter compressor rig. One model was patterned after a two-dimensional inlet designed for the Lockheed airplane and the other was patterned after the Boeing axisymmetrical design. A view of each is shown in Figures 9-24 through 9-26. Other inlets that have been tested are shown in Figures 9-27 and 9-28.

Lockheed Inlet Duct - In the Lockheed inlet model, provisions were made to vary the shape of the duct inner body to determine the effect of flow velocity on noise. Because of the lack of symmetry on the Lockheed inlet, noise was measured in both the horizontal and vertical plane to determine the assymetry of the noise radiation pattern.

First tests of the Lockheed inlet showed a high turbulence noise level which was thought to be the result of the airflow across the square corners on the inlet lip. During later tests on this model, a one-inch radius lip was added to the inlet to decrease the inlet airflow turbulence. At approach flight speeds, the stream tube swallowed by the engine is significantly larger than the inlet, but incoming air streamlines would be considerably smoother than those during static operation. It was felt that the small radius added to the lip would better simulate air entry during flight conditions by reducing the turbulence generated by the flow over the inlet lip.

Boeing Inlet Duct - The design of the Boeing inlet incorporates several features which permitted configuration changes to be quickly made. Inserts with various surface treatment were designed to slide into the cylindrical outer support duct to check their effects on noise attenuation through the duct. Provisions were also made to evaluate the effects on noise of centerbody size, and boundary layer bleed systems.

This cylindrical inlet was selected over the Lockheed model for assessing effects on noise of design variations because its shape made it much easier to make configuration changes. It was considered reasonable to assume that any of the schemes tested on this inlet would have about the same effect on noise when properly applied to the geometry of the Lockheed inlet.

b. Compressor Configuration

Two compressor configurations were used during this series of tests. The first tests were run with a 32-blade rotor, a 46-vane stator and no inlet guide vanes. This configuration was used during a series of tests to determine the effect of wakes from structures inside the inlet.

The second series of tests was designed to study the acoustical effects of the inlet geometry, and inlet guide vanes were installed in the com-

pressor for this series of tests. The noise level from inlet guide vanes is generally higher than noise from stator vanes. More accurate measurements can be made because of the improved signal-to-background-noise ratio.

Both the inlet guide vane assembly and the stator vane assembly had 46 vanes. A 14-lobe backward spinning pressure pattern was generated by the interactions of the vane assemblies with the 32-blade rotor.* The choice of blades and vanes was made to approximate the type of spinning modes expected in the SST engine.

Typical performance data from the 28-inch diameter compressor rig are shown on Figure 9-29. At 10,000 rpm, or 100 percent speed, the rotor blade tips are well above sonic velocities. Performance of this rig is typical of that expected from axial flow compressors.

c. Data Recording

All inlet configurations were tested over a range of duct flow velocities at a series of rotor speeds from 4000 to 10,000 rpm. Signals from a microphone, traversed slowly through 90 degrees along an arc forward of the rig, were tape recorded along with an indication of the microphone position. Data on rig operating parameters and inlet duct velocity were recorded at each test point.

d. Data Analysis

Tape recordings of the noise from the rig were analyzed using a 50 cycle fixed band-width filter to obtain plots of the level of fundamental blade-passing frequency noise and its harmonic versus angle from the inlet. A comparison of noise levels from different inlets attached to the same compressor, operating at a specific condition, provided a measure of the effectiveness of the inlet. Spectral analysis of the noise, using a "Panoramic" Sonic Analyzer, was made in some instances to document the spectrum shape.

e. Test Results

Tests of 16 different inlet configurations were conducted, and a total test time of 112 hours was accumulated.

---

*SAE report 345D; Axial Flow Compressor Noise Studies, Tyler and Sofrin.

Summaries of the test results and schematic drawings of the inlet duct configurations tested are shown in Figure 9-30.

f. Conclusions

From the results of the tests, the following conclusions can be drawn:

- Duct length has no substantial effect on noise at approach power conditions.
- A significant increase in noise did not result from wakes from the four struts in the Boeing shape inlet or from the centerbody wake in the Lockheed inlet.
- Inlet noise levels are significantly reduced as the duct flow velocity is increased above a Mach number of about 0. 7.
- Essentially no discrete noise is propagated out of a choked inlet.
- A significant reduction in inlet noise can be obtained with an acoustically lined inlet.
- A sharp-lip inlet tends to redistribute the discrete compressor noise into bands of random noise, causing a considerably different sound quality.
- The inlet shape had a small effect on the sound radiation pattern.
- Tests on one configuration having a boundary layer bleed system showed only a small effect on noise.
- Centerbody shape had little effect on the effectiveness of duct lining.

4. RECOMMENDATIONS

Although many configu ations have been tested, there are still many other tests that must be conducted to determine:

- The optimum location for acoustical treatment.
- The effectiveness of various types of treatment.
- The effect of inlet blow-in doors on noise.
- The effects of various boundary layer bleed system designs with different bleed flows.
- How inlet duct shape and compressor-generated "spining mode" sound patterns affect the attenuation of sound with increasing duct-flow Mach number.
- The otpimum combinations of design features for low noise levels.

5. ANALYSIS OF RESULTS

Several methods of reducing the noise radiated out of a SST inlet duct are suggested by the results of these tests. As shown by Figure 9-31, one of the most effective methods would be to expand the centerbody and obtain a choked throat section in the inlet, effectively blocking the discrete frequency noise. It is also shown in Figure 9-32 that significant reductions may be obtained with a nearly choked inlet, which may be more desirable than a fully choked inlet from safety considerations.

The length of the supersonic inlets provides a considerable area where acoustical treatment materials may be installed and, as was shown by the tests, substantial noise reductions can be achieved.

When the sharp inlet lip was tested, a very significant change in the quality of the noise from the inlet was observed. This change in quality would probably not result in a lower calculated PNdb level because the octave band noise levels were not changed. However, the sound was judged by observers to be considerably less annoying because of the absence of the discrete tones. The spectral composition is shown in Figure 9-33.

Estimates of noise from the STF219 engine have been made by Pratt & Whitney Aircraft using both full values of inlet compressor noise and with the inlet noise reduced by ten db. This ten db reduction was expected to be obtained by development of the acoustical qualities of both the engine compressor and the inlet duct. Results of these tests, as shown in Figure 9-34, indicate the ten db reduction should be obtainable from the inlet duct alone, if necessary, by acoustical treatment of the duct.

6. DISCUSSION OF RESULTS

a. Repeatability

Results of the test program are felt to be repeatable to within ±3 db, which is quite good for inlet noise measurements. Directivity patterns measured in the acoustically treated plenum room are sharply defined, indicating little interference from unwanted sound reflecting surfaces.

b. Sources for Error

One of the largest sources for error in these tests results from the relatively short distance between the microphone and the inlet. If the microphone is still in the "near field" of the inlet duct opening, the directivity patterns measured may not be representative of those in the far field. As the size of the plenum room is the limiting factor, it is not possible to positively check this feature. In either instance, the measurements taken are consistent and should provide a good indication of the relative effects of the inlets on far field noise.

Another possible source for small errors is the change in the noise energy generated by the compressor when inlet ducts having differing pressure recovery characteristics are compared. Source strength is very difficult to monitor as the readings from stationary micropohones mounted in the inlet duct have little meaning; small changes in microphone position, either axial or radial, may show a large difference in db indication due to standing sound pressure patterns resulting from combinations of "spinning modes". Future tests using devices to purposely reduce the inlet recovery factor should be run, and the effect on generated sound should be documented.

c. Two-Dimensional Inlet Sound Directivity

Measurements of noise in both the horizontal and vertical plane from the two-dimensional model inlet showed a reduction in peak fly-over noise of about six db when compared with the axisymmetrical model (see Figure 9-35). To determine whether the noise radiation pattern from the two-dimensional inlet was symmetrical, microphones were simultaneously traversed along arcs in both the horizontal and vertical planes. This test was also repeated with the pivot point of the microphones moved about two feet forward from the standard location, centered beneath the widest section of the duct opening. Although near field effects were suggested by apparent differences in sound radiation patterns observed after moving the microphone arc pivot point, significant differences in the hotizontal and vertical planes were not suggested.

d. Sharp Lip Inlets

Although substantial changes in noise because of a sharp lip were noted, the in-flight effect of forward velocity will result in less turbulence over the inlet lip than during ground operation. Opening the inlet blow-in doors may also have a substantial effect on air velocities over the lip, and tests of this configuration are planned. However, some turbulent flow over the inlet lip can be expected at approach flight speeds and approach thrust settings, and the effect of this on the sound quality will probably be favorable.

e. Effect of Inlet Mach Number

Results of acoustic tests with high velocity flow in both the axisymmetric and the two-dimensional inlet ducts are shown in Figure 9-32. More complete analysis of the data from tests on the axisymmetrical inlet suggested the curve shown in the preliminary report, dated 1 November 1964, be revised as now shown.

Theories to describe the flow of acoustical energy, contained in "spinning mode" pressure patterns, upstream through a duct with a varying flow Mach number are not well established. As the acoustic energy is contained in the "spinning modes", sound is not propogated directly opposite to the direction of flow, but at some angle to it. This angle is governed by the rotational speed of the "spinning mode" and also by the flow velocity. Increased flow velocity tends to shift the mode propagation direction, and may reduce the acoustical energy propogated toward the duct opening.

It is possible that compressors having different blade-vane numbers may require different inlet-duct flow Mach numbers to obtain equal values of noise reduction. The least desirable compressor configuragion would have equal numbers of blades and vanes and generate plane waves which would probably require nearly sonic duct velocity to achieve complete blockage. The "spinning mode" helix angle can be varied at a given rotor speed by changing the number of vanes. Consequently, the duct Mach numbers required to block the propagation of sound through the inlet may depend on the rotor-vane configuration.

From the results of the test, duct shape appeared to have a relatively small effect on the reduction of noise with increasing Mach number. However, much more data were available from the two-dimensional inlet than from the axisymmetrical inlet. A better comparison to determine the effect of inlet shape can be obtained only after further tests of the axisymmetrical inlet at several additional duct-flow Mach numbers.

A better understanding of the effect of inlet-duct flow Mach number on compressor noise propogation is desirable. This approach may well provide the means for obtaining low airplane noise levels during landing approach without affecting the safety of operation or necessitating the inclusion of devices in the inlet for the sole purpose of noise attenuation. Future tests should be conducted with more instrumentation to allow detailed study of the inlet-duct flow conditions and sound propagation characteristics. Variations in blade and vane numbers should also be tested to better establish the relationships between compressor design and the attenuation of sound with inlet-duct flow velocity. Results of these tests would be of interest for the design of both SST airplane inlets and engine compressors.

f. Inlet Length

The small change in noise with inlet length, shown in Figure 9-36, could have resulted from a build up of the boundary layer in the long duct. Theoretical analysis indicates that inlet length should have no effect on noise.

g. Sound Absorbing Materials

Results of acoustic tests of inlet ducts having perforated-sheet walls backed by Fiberglas showed significant noise reductions. Although these tests showed the use of acoustical treatment is effective, further tests must be conducted to evaluate the effectiveness of various types of materials and to determine their optimum location in the inlet. The high temperatures in the inlet of a SST during cruise rule out the use of many familiar acoustic materials including Fiberglas.

To evaluate the effect of a perforated-sheet wall on noise propagated out of an inlet duct, the Fiberglas filling material was removed from the inlet. Results of tests on the revised inlet showed some discrete noise attenuation when compared with a hard-walled duct, but much less attenuation than was measured with the Fiberglas in place. Re-

moval of the Fiberglas wool from the perforated duct lining also caused a sizeable increase in turbulence noise. The apparent reduction in discrete noise may have been the result of the more random character of the inlet noise, as only a portion of the total energy was passed through the 50 cycle band-width filter. The turbulence was probably the result of flow through the holes in the duct surface. Perforated duct liners having less open area should be evaluated for acoustical effectiveness.

D. SOUND ABSORBING MATERIALS

1. OBJECTIVES OF TESTS

Compressor discrete-frequency noise will be the limiting source of engine noise during the SST landing approach and may also contribute to the overall PNdb level at the three mile point for reduced power climb-out. This noise radiates from both the engine inlet and the fan discharge duct. Tests have shown that properly designed acoustic absorbing treatments can be incorporated as inlet and fan duct linings to provide significant reductions in this component of the noise.

The effect of airflow on the sound absorbing properties of linings has been found to be important. A lining which is effective under no-flow conditions gradually loses its absorbing properties when air is flowing in the same direction as the sound is propagating. The effect of flow on sound propagation in an upstream direction is much less pronounced. Therefore, it is a more difficult matter to evolve a satisfactory absorbing liner for the fan discharge duct than for the engine inlet.

The object of this portion of the Phase IIA program was to develop sound absorbing treatments applicable to the STF219. Since the fan discharge application is the more difficult, efforts were concentrated on this application.

2. DESCRIPTION OF FACILITIES

Early tests of sound absorbing materials for use in lining fan inlet and discharge ducts in the first commercial turbofan engines were made in simple, small-scale rectangular ducts using loud-speaker noise sources. At the frequencies of interest, the wave lengths were small compared to the duct cross-section dimensions, so that the sound pressure field was distributed over the cross section in complicated patterns. These patterns were very sensitive to the loud-speaker

operation and made repeatable results extremely difficult to obtain. Further difficulties arose in comparing results measured on full-scale engine ducts with predictions based on the small-scale test ducts. It was found essential to evolve a model technique in which the dimension between the treated surfaces is the same in the model test as in the full-scale application. The effect of treating the walls of the fan discharge annulus can be realistically studied if an annular segment having the full-scale annular width and a convenient length is used as a model. In practice, for ducts of large diameter-to-annulus-width ratio, the annular segment can be developed into a rectangular duct for convenience of model tests.

To avoid complicated sound pressure distributions in the test duct which would differ from the distribution in the full-scale engine, it is essential to supply the duct entrance section with a diffuse sound field. Such a field is characterized by a slightly fluctuating sound pressure level at all points in the entrance cross section but has the property that the time averaged levels are the same at all these points. This diffuse field is conveniently supplied by connecting the test duct entrance section to a reverberent chamber in which is operated a random noise source. By surveying the sound field radiated from the exit of the test duct, in both the treated and untreated conditions, an assessment of the absorbtion can be obtained from the differences of the levels at corresponding locations around the exit. Providing that the radiation directivity patterns are not too different in shape for the hard- and treated-wall ducts, this procedure gives an effective insertion loss but necessitates taking readings at a relatively large number of angular locations, during which time the acoustic source level must remain constant. To eliminate the complications of this procedure, a method was developed for utilizing a well-known acoustic technique wherein the test duct exit is terminated in a duplicate reverberation chamber. By means of this technique the insertion loss of a treated duct can be obtained by comparing readings from a single microphone located in the downstream chamber with those obtained with the untreated reference duct. Figure 9-37 shows the two chambers and the interconnecting test duct.

3. METHOD OF TEST

The theory of the two-room insertion testing is based on the use of a diffuse sound field in the two reverberant chambers, with rms sound pressures in the source and receiving chambers of p_s and p_r, respectively. The duct to be studied, having a cross-section area of A_d, is inserted between two chambers having wall surface areas A_s and A_r.

The incident sound intensity per unit wall area is then proportional to p^2 and we set

$$I = K p^2$$

where I = sound intensity, p = rms sound pressure, and K = constant. If A_d is the cross sectional area of the duct, then the acoustic power, P, transmitted into the duct from the source chamber is

$$P_{in} = K A_d p_s^2.$$

As a result of the sound attenuation in the duct, the power leaving the duct in the receiving room is reduced by a factor B. The equation for the energy balance is

$$B K A_d p_s^2 = K (A_r \alpha_r) p_r^2 + K A_d p_r^2.$$

where α_r is the wall absorbtion coefficient.

The left hand side of this equation represents the acoustic power transmitted out from the duct into the receiving chamber. (It equals the incident power from the source room reduced by the factor B.) The first term on the right hand side of the equation is the power absorbed by the walls in the receiving chamber and the second term is the power going back into the duct. From this equation we can now express the factor B in terms of the measured quantities, p_s and p_r, as follows:

$$B = \frac{p_r^2}{p_s^2} \quad \frac{1}{(A_r \alpha_r / A_d) + 1}$$

Expressed in decibels,

$$10 \log_{10} \left(\frac{1}{B}\right) = 20 \log_{10} \left(\frac{p_s}{p_r}\right) + 10 \log_{10} \left(1 + \frac{A_r \alpha_r}{A_d}\right)$$

The first term on the right hand side of this equation is simply the difference between the sound pressure levels in the source and the receiver chambers, L_s and L_r in db. Thus,

$$10 \log_{10} \left(\frac{1}{B}\right) = L_s - L_r + 10 \log_{10} \left(1 + \frac{A_r \alpha_r}{A_d}\right)$$

The incident sound intensity per unit wall area is then proportional to p^2 and we set

$$I = K\,p^2$$

where I = sound intensity, p = rms sound pressure, and K = constant. If A_d is the cross sectional area of the duct, then the acoustic power, P, transmitted into the duct from the source chamber is

$$P_{in} = K\,A_d\,p_s^2.$$

As a result of the sound attenuation in the duct, the power leaving the duct in the receiving room is reduced by a factor B. The equation for the energy balance is

$$B\,K\,A_d\,p_s^2 = K\,(A_r\,\alpha_r)\,p_r^2 + K\,A_d\,p_r^2.$$

where α_r is the wall absorbtion coefficient.

The left hand side of this equation represents the acoustic power transmitted out from the duct into the receiving chamber. (It equals the incident power from the source room reduced by the factor B.) The first term on the right hand side of the equation is the power absorbed by the walls in the receiving chamber and the second term is the power going back into the duct. From this equation we can now express the factor B in terms of the measured quantities, p_s and p_r, as follows:

$$B = \frac{p_r^2}{p_s^2} \quad \frac{1}{(A_r\,\alpha_r/A_d) + 1}$$

Expressed in decibels,

$$10\log_{10}\left(\frac{1}{B}\right) = 20\log_{10}\left(\frac{p_s}{p_r}\right) + 10\log_{10}\left(1 + \frac{A_r\,\alpha_r}{A_d}\right)$$

The first term on the right hand side of this equation is simply the difference between the sound pressure levels in the source and the receiver chambers, L_s and L_r in db. Thus,

$$10\log_{10}\left(\frac{1}{B}\right) = L_s - L_r + 10\log_{10}\left(1 + \frac{A_r\,\alpha_r}{A_d}\right)$$

The correction term, $10 \log_{10} (1 + A_r \alpha_r / A_d)$, can be determined from reverberation measurements in the receiving chamber. The purpose of such a measurement is of course to measure the wall absorption ($A_r \alpha_r$). Thus if the reverberation time is T_r we obtain

$$T_r = \frac{0.05V}{A_r \alpha_r}, \qquad A_r \alpha_r = \frac{0.05V}{T_r} .$$

where V = chamber volume.

A model pulse-jet engine ("Dyna-jet") was used as the noise source in one of these chambers. The pulse-jet is shown in Figure 9-38. The fundamental frequency of the pulses was about 225 cycles per second, and all harmonics are present up to frequencies above the range of interest. Using this noise source, one-third octave band measurements were made from 2000 through 6000 cycles per second. Air flow through the reverberant chamber and duct system was supplied by a 300 HP low pressure blower. The sound source can be transferred from one chamber to the other for study of sound attenuation against the flow.

Since the test method is predicated on the existence of a diffuse sound in the reverberant chamber, several tests of the reverberant field decay were made. In each case, chart recordings of the level in the chambers showed a smooth uniform decay. Also, several microphone positions were tested with nearly identical results. The sound pressure levels in each of the chambers were monitored by a 21 BR-180 microphone. The output of these microphones was fed to a General Radio one-third octave band filter and Graphic Level Recorder. With the pulse-jet operating, the difference in sound pressure levels between the source and receiving chamber was measured for both the hard wall duct and its treated counterpart. The difference was then attributed to the treatment in the duct.

4. RESULTS

A sketch of a portion of the fan discharge duct of the STF219 engine is shown in Figure 9-39. With this design it is possible to insert splitters which can be treated with absorbing material. These splitters have the dual effect of eliminating line of sight transmission of the noise and increasing the amount of absorptive surface. Two models were tested, one with the flow split into three channels and the other split into two channels. A photograph of the model SST engine fan-discharge duct with a channel having one-third of the duct width and two splitters for the full-scale engine is shown in Figure 9-40.

The duct linings used for the tests are described in Figure 9-41. The acoustic treatment (Feltmetal) shown in Figure 9-40 was made of 420 stainless steel. All of the feltmetal had a 20 percent density and an average pore size of 500 microns. The test results for the duct equivalent in width to one-third of the fan exhaust duct are shown in Figures 9-42 through 9-45 for an airflow through the duct of 300 feet per second.

Figure 9-42 shows the insertion loss with lining A. Since this lining is very thin the low frequency absorption is negligible. Because of the elimination of line of sight and the better absorption at the high end of the spectrum, the insertion loss improves with frequency. Figure 9-43 shows the effect of an increased lining thickness by spacing the feltmetal from the back surface with honeycomb. The improvement at the low end of the spectrum is particularly important. Figure 9-44 shows even better low frequency attentuation. The thicker layer of feltmetal is a decided improvement over lining A. Note that the upper range of frequency still show the effect of the elimination of the line of sight through the duct. Figure 9-45 shows the results of tests with lining D, the thickest lining tested. Again the improvement at the low frequencies is noticeable. Background noise due to flanking sound limited the insertion loss that could be measured.

Figure 9-46 shows the effect of duct air velocity. Little or no change in insertion loss was noted over the range of velocities tested (100 to 300 feet per second). It might be noted that the phenomenon of attenuation remaining constant with duct velocity has not been observed in previous work on flow through straight ducts.

Figure 9-47 gives the results of a model duct having one-half the width of the STF219 duct. The line of sight was not eliminated completely so that the high frequency end of the spectrum is not attenuated as much as the one-third size duct model. However, there is more attenuation available in the high frequency range than is needed to reduce the fan discharge noise below the exhaust noise background level.

Several tests were conducted on straight ducts lined with tuned absorbing liners consisting of a perforated facing spaced from the hard walls, in which a small quantity of air was pumped through the duct perforations. The program was designed to explore possible increases in acoustic resistance by the presence of a steady flow superposed on the oscillatory sound particle velocity through the facing perforations. Since none of the configurations tested gave significant sound absorbtion no test results are presented here.

5. EFFECT OF RESULTS ON SST AIRPLANE DESIGN

The results of the tests have shown that use of a curved duct with narrower channels created by treated splitters will yield excellent attenuation of fan noise. The elimination of line-of-sight transmission of noise together with channels whose width is near the wave length of the sound to be attenuated are important considerations in the design of the duct.

Straight ducts were not nearly as effective. They would require narrower channels and are affected much more by the flow. Use of bleed air in an absorbing duct gave no substantial results.

6. RECOMMENDATIONS

These preliminary results have indicated that the discrete frequencies in the SST engine fan-discharge duct can be effectively reduced. Further work to fully exploit the findings on the curved duct-feltmetal combination should be continued. This work should be directed toward optimizing the attenuation while minimizing the weight of the treatment.

The use of bleed air through the treatment should also be explored further. Although preliminary results are discouraging it is believed that satisfactory results may be achieved, thus providing another technique for noise reduction.

E. EXHAUST NOISE

1. INTRODUCTION

The object of the Phase II-A model exhaust noise program was to study the noise characteristics of exhaust nozzle systems designed for the SST powerplant and to explore some means for optimizing exhaust noise suppression.

While the SST airplane-powerplant configurations in design will be able to meet the appropriate community noise limits, any noise reduction that can be achieved without penalizing performance is a valuable contribution.

A limited amount of fly-over noise data on powerplants equipped with an exhaust nozzle system of the type designed for the SST were obtained which indicated a significant reduction in expected noise levels (see Appendix B). The model nozzle program was intended to more fully explore this area.

2. DESCRIPTION OF FACILITIES

An overall diagram of the anechoic chamber test facility is shown in Figure 9-48. Basically the facility consists of a compressed air supply a natural gas fuel supply system, and a burner section in which the natural gas is mixed with compressed air and burned to be exhausted through the test nozzle.

a. Compressed Air Supply

The compressed air is supplied through a plenum chamber to provide uniform flow at the airflow measuring venturis. A system of duct work divides the air flow into a primary and two secondary streams before entering the burner section. The air supply delivers five pounds per second at 37 psia.

b. Fuel Supply System

The natural gas fuel system was developed and built during the contract period to replace the previously used JP-4 jet fuel system. This modification was necessary to obtain the high temperature required to simulate the SST engine cycle. The natural gas is received through city gas lines after which it is compressed to 120 psi, cooled and piped to a surge tank. A photograph of the gas supply equipment is shown in Figure 9-49. A regulator system on the outlet of the surge tank provides the main gas stream which is divided into three individually regulated streams to the burner section. Inherent in the natural gas system is the threat of explosions or serious leaks. Accordingly, an extensive network of safety devices was installed in conjunction with the gas system.

c. Test Rig and Anechoic Chamber

The burner section and test nozzle are mounted in an anechoic chamber wherein acoustic measurements of the jet noise are made. The anechoic chamber is constructed of wedge-shaped sections of Fiberglas and is designed to prevent reflections of frequencies above 300 cps.

The hot gases exhausted through the nozzle are carried out of the anechoic chamber by exhaust fans in the roof. To assure proper cooling and purging of the chamber, an additional 300 hp centrifugal blower provides air flowing from the floor up over the burner section and through the chamber.

A more detailed drawing of the burner section with a test nozzle mounted is shown in Figure 9-50. Here it is shown how the compressed air supply stream is divided into a primary stream and two secondary streams. The primary stream passes through a throttling valve to the fuel injector where natural gas is mixed with the air stream. In the burner section combustion takes place and the hot combustion products are exhausted through the primary nozzle. Air flow and combustion occurs in the same manner in the two secondary duct sections. Following combustion, the two hot secondary streams combine in the collector ring and pass on through the secondary or duct nozzle.

The flexibility of a test rig constructed in this way should be noted. The throttling valves shown in Figure 9-50 and photographed in Figure 9-51 allow control of the by-pass ratio, the ratio of secondary air to primary air. In addition, the secondary airflow can be shut off completely to study primary jet noise. Since the burner and fuel supply systems for the primary and secondary streams are separate units, it is also possible to run different air-fuel ratios in the two sections.

As a consequence of the extremely high temperatures required at the nozzle in simulating the duct heating engine cycle, about 3000°F, some of the test nozzles had to be constructed with water cooled walls. The intricate nozzle cooling system required the installation of a fairly sophisticated water system in the anechoic chamber wherein control of several waterflow rates and water stream temperatures are maintained. A photograph of the water cooled nozzle designed for maximum duct heat operation is shown in Figure 9-52.

3. METHOD OF TEST

In evaluating model nozzle configurations it is necessary to consider both sound and performance. Accordingly, the test program was laid out to document both of these considerations for each model tested. Rig operating points were selected in the light of the SST engine operating schedule. The engine nozzle pressure ratio versus tailpipe temperature relation in the operating range was simulated by the particular model. At each operating point two duct pressures were used, one where duct

The preceding calculations have been programed for an IBM 1620 computer.

b. Sound Data System

The procedure involved in measuring noise levels of model jet nozzles and converting the results to permit predictions of full-scale engine noise is best illustrated in Figure 9-55. Three steps in the process are:

- Tape recording of model jet noise in actave bands.
- One-third octave spectral analysis and conversion of the recorded data to IBM cards by SNORE.
- Processing of the model data and calculation of full-scale predictions by IBM 1620.

The sound data recording system is shown schematically in Figure 9-56 and photographically in Figure 9-57. For the one-fourteenth scale models used to predict full-scale results, the full-scale seventh octave maximum frequency of 4800 cps requires a measurement of model jet noise up to about 65,000 cps.

Response limitations of the tape recorder and related equipment set an upper frequency limit of about 65,000 cps. This allowed recording of the first seven octaves of noise scaled up in frequency for the model to full-scale size ratio. As noise in the eighth octave is usually of no importance in a jet noise spectrum, no useful information was lost by not measuring it.

A B&K one-quarter-inch diameter high-frequency microphone was used to survey the sound field. Figure 9-58 shows the microphone mounted on a boom, which swings in an arc over the model nozzle, to measure the sound radiation pattern at constant radius. The boom is positioned in five-degree increments over a 90-degree arc, and a 50-second recording of the noise is made at each position. A network of prefilters separate the noise into eight octave bands. These bands are individually amplified and recorded on the 14-channel tape recorder along with one unfiltered overall channel. This scheme is used to overcome the ultrasonic dynamic range limitations of the tape recorder.

The recording system is calibrated with a known sound pressure level fed into the system through the microphone. In addition, a pink noise signal, equal energy per octave, is recorded on tape to determine the frequency response of the system.

The magnetic tapes are transported to Pratt & Whitney Aircraft's data handling system, SNORE (Sequential Noise Output Recording Equipment), shown in Figure 9-59. This system divides the eight recorded octave bands into one-third octave bands and converts the sound levels, recorded on a linear voltage scale, to a logarithmic decibel scale. The output of this information from SNORE is in the form of IBM punched cards.

An IBM 1620 has been programmed to process model jet noise data recorded on punched cards by SNORE. In the program, appropriate microphone response and attenuator corrections are applied to the recorded noise levels. In addition, corrections to the measured noise level are applied to account for attenuation in the chamber which is significant in the ultrasonic range for the ten-foot nozzle-to-microphone distance. The resulting sound pressure levels are printed out in tabular form giving one-third octave spectra for each boom angle at a constant radius. In addition, an integrated overall sound pressure level is computed for each microphone position. These results are then scaled to give predictions of noise for the full-scale engine at a 150-foot constant radius and PNdb at constant altitudes. The constant altitude results give the PNdb for a simulated fly-over at several altitudes. These results are shown schematically in Figure 9-60.

4. RESULTS

Acoustic test results are available in the primary velocity range of 1200 to 2000 feet per second on two versions of the basic SST blow-in-door ejector nozzle in a configuration without duct heat.

Over the entire operating range without duct heating, the primary stream velocity is sufficiently higher than that of the secondary so that it is the only significant source of noise. Previous experiments have shown, however, that surrounding the primary stream with secondary or by-pass air can modify the basic primary jet noise. This change, which is called the secondary interaction effect depends on the geometric details of the by-pass nozzle configuration. Therefore, to evaluate this effect, the test program included noise surveys of; 1) the primary stream only 2) both primary and secondary streams and 3) the complete system with ejector shroud attached.

The two basic SST nozzle systems for operation without duct heating that were tested were designated (1, 1, 1) and (1, 2, 1). The first digit refers to the primary nozzle, the second digit designates the secondary nozzle, and the final digit identifies the ejector shroud. Configuration (1, 1, 1) had a secondary-area-to-primary-area ratio of approximately 0.5, and configuration (1, 2, 1) incorporated a reworked

secondary area giving a ratio of approximately 0.8. Common to both secondaries were the same primary and ejector shroud. Runs were made on the following combinations of components (see figures 9-61 and 9-62):

(1,0,0) primary nozzle only
(1,1,0) with secondary stream blocked
(1,1,0) both streams
(1,1,1) ejector added

(1,2,0) with secondary blocked
(1,2,0) both streams
(1,2,1) ejector added

The operating stream conditions are given in the performance curves Figures 9-63 through 9-66. These curves are presented as functions of the primary stream total pressure ratio, P_{TE}/P_{AMB}, and include the following essential properties: primary total temperatures, and the duct preesure ratio and temperature. Two schedules of duct pressure ratio were followed for the same engine pressure-temperature operating line, one corresponding to essentially equal primary and secondary pressures and the other giving a higher duct pressure ratio. The range of primary velocity explored was from 1200 to 2100 feet per second.

Of the many possible ways of presenting the large amount of sound data, it was decided to present 200-foot altitude maximum PNdb versus primary pressure ratio, P_{TE}/P_{AMB}, corresponding to the full-scale configuration. As described previously in detail, these values were obtained by an IBM program using a 14:1 scale factor and transforming model one-third octave sound levels to full-scale complete octaves. By cross-referencing the corresponding performance curves, PNdb can be correlated with other properties such as jet velocity or percent thrust.

Data for configurations using the smaller secondary nozzle, (1, 1, 0) and (1, 1, 1), were similar to the data for the larger secondary, (1, 2, 0) and (1, 2, 1), and are therefore not included here. Referring to the PNdb curves for configurations (1, 2, 0) and (1, 2, 1), Figures 9-67 through 9-70, it can be seen that:

1) The secondary interaction is essentially negligible.

2) In the primary velocity range from 1200 to 2000 feet per second, the addition of the ejector does not change the noise when compared at the same pressure ratio. On the basis of equal thrust, there appears to be a small (order of 1 PNdb) reduction when operating at the low duct pressure schedule, but since this effect is not evident for the high duct pressure schedule, it is considered unreliable.

Concerning the lack of interaction effect, it appears that the upstream spacing of the secondary annular nozzle with respect to the primary discharge plane is large enough to prevent an increase in noise. Previous tests of a coplanar discharge nozzle have indicated an increase on the order of two db over the primary noise. For a configuration having a separation distance of about three primary diameters, a decrease of about two db has been observed. It would appear that the separation distance of about one-third diameter in models (1,1,1) and (1,2,1) represents a null situation in which the secondary interaction neither reduces nor increases the primary jet noise.

Figure 9-71 presents normalized maximum OASPL data versus relative jet velocity for three model configurations. These data fall on a curve which is about four db below the curve for standard nozzles adopted by the SAE A-21 committee. It is to be expected that data taken in an anechoic environment will be on the average three db lower than data taken in the presence of a reflecting ground surface, since the effect of the ground is to add the reflected field pressure to the duct sound pressure. Under the usual conditions, this addition is incoherent and raises the measured overall level by three db. The data obtained with the anechoic chamber model system are thus within one db of the SAE A-21 standard.

The behavior of the complete exhaust system is a more involved situation. The complication results from the larger number of parameters required to describe the ejector configuration. Three basic ratios specify a simple cylindrical ejector, obtained by dividing each of the following dimensions by nozzle diameter: 1) ejector diameter, 2) ejector length, 3) separation between nozzle exit plane and ejector entrance plane. On most ejectors the interior contour generally differs from a simple conical surface.

Some fly-over noise data from aircraft equipped with blow-in-door ejectors have shown noise reductions (see Appendix B), although previous noise tests of other ejectors* have shown inconsistent results. Further investigation is needed to provide a better understanding of noise generation phenomena with blow-in-door ejectors.

---

* NACA Report TN-3573; "Effect of Exhaust Nozzle Ejectors on Turbojet Noise Generation". Also, Activities Reports on Jet Noise Projects, UAC Research Laboratories, period September to December 1956.

Some variations of model SST exhaust configurations have been fabricated which have not been tested due to lack of time. Essentially, they involve schemes for changing the cross-sectional shape of the primary and/or by-pass streams, addition of channels and scoops to the ejector shroud to introduce supplementary air into the jet stream, and variation of the shroud terminal nozzle shape. These modifications would be applied to the full-scale engine in the form of two-position devices which would be operated for noise suppression during take-off and climb-out and would be retracted for all other flight conditions.

5. RECOMMENDATIONS

On the basis of the model results, it appears probable that secondary interaction effects and basic ejector suppression are negligible in the operating range without duct heat, whereas some full-scale fly-over data indicate noise reductions (see Appendix B). It remains to explore devices built for improving the mixing of the primary, secondary, and induced streams for the purpose of noise suppressions.

Nozzles built but not tested due to lack of time are:

- Two basic duct-heat nozzle systems, incorporating a common water-cooled primary nozzle, a common ejector, and 2 water-cooled secondary nozzles, one for maximum duct heat and one for partial duct heat.

- Four scalloped nozzles which promote the mixing of the primary and secondary streams. These are for operation without duct heat to study the effect of primary-secondary stream interfaces on noise, both with and without the inclusion of an ejector shroud.

Asymmetrical nozzles have previously been explored in full-scale and model programs for straight jet and by-pass exhaust systems. Rectangular nozzles, for example have been shown to give significant noise suppression with excellent performance characteristics.* If additional testing is requested, a model ejector shroud terminating in a rectangular shape should be used to explore the possibilities of noise suppression by modifying the final shape. Previous model tests have

* "Rectangular Nozzles for Jet Noise Suppression"; Tyler, Sofrin and Davis, SAE Paper 57T, 1959.

shown that asymmetrical arrangements of the primary and secondary streams can materially affect the jet noise by modifying the interaction effect. A model should be constructed to study the effect of displacing the center of the circular fan discharge nozzle with respect to the primary so that most of the by-pass stream discharges on the top or alternatively, on the bottom of the primary jet.

Looking beyond the program currently planned for Phase II-A, it is expected that further explanation along the lines dicussed below will be necessary to evolve optimized noise suppression techniques.

A more complete documentation of the effect of simple ejectors in combination with by-pass nozzles is needed. Other past studies of the use of ejectors on single stream nozzles have indicated the importance of three basic geometric parametrics: ejector diameter, length, and spacing, in terms of jet nozzle diameter. Additionally, the ejector surface contour and the jet pressure ratio and temperature are important. For by-pass nozzles, two additional independent variables enter the picture: by-pass stream pressure ratio and temperature. A program to systematically explore the effect of these variables is needed to determine optimum ejector operation from the standpoint of noise. Results of this program must clearly be coordinated with thermodynamic performance requirements to insure practical applicability to efficient full-scale engines. Variations of exhaust system geometry which incorporate devices to alter the mixing processes should continue to be explored in model form. From the point of practical application, such a device must have retractable features to avoid performance penalties in all flight regimes where noise suppression is irrelevant. The use of models permits testing of a variety of ideas to define arrangements that provide effective suppression. After basic promising configurations have been selected, a model program is needed to explore the possible reductions in suppression that result from compromising the geometry to conform with full-scale practical limitations.

A limited amount of large-scale testing is recommended to assure the carry-over of effects determined from small models. It is conceivable that some of the full-scale construction details cannot be adequately simulated in small size models. A few of the interesting configurations evolved from model studies should be fabricated for evaluation on experimental turbofan engines currently available.

Questions remain on the limits of applicability of noise data obtained from static tests to predict results when the airplane moves through the air during climb-out. To clarify this subject it is advisable to

conduct a limited number of scale model tests in which the test nozzle is placed in a stream of moving ambient air. Facilities exist in the anechoic chamber for simulating the flight condition by surrounding the model nozzle with a stream of ambient air supplied by a large nozzle surrounding the rig and discharging upstream of the model nozzle. Experiments to evaluate this method of flight simulation should be conducted and tests run on the effect of moving air on model straight jets, by-pass jets, and jets with ejector-suppressor devices.

F. ANALYSIS OF TOTAL SST AIRPLANE NOISE

The noise at the three locations where limits have been established (1500 feet to the side of the runway during take-off ground roll, under the take-off flight path three miles from start of take-off roll, and under the approach flight path one mile from touch-down) are a function of three main variables. These variables are: 1) engine noise as a function of thrust for the thrust level at the FAA specified conditions, 2) airplane climb capability which is in turn dependent on engine thrust during ground roll and initial climb and on airplane aerodynamic characteristics, 3) airplane thrust requirements during approach. Obviously the engine and airplane characteristics are intimately interrelated.

To obtain low noise levels from the engine, the fan engine cycle should be used and the by-pass ratio should be as large as is compatible with the requirements of other aspects of the airplane flight mission. Beyond this, the engine must be designed and developed to minimize the exhaust and inlet noise radiated from the engine to the ground.

Recognizing that low noise is not the only important requirement of the airplane, it must also be recognized that the compromise take-off and approach flight paths and thrust requirements will be important factors in determining the noise levels on the ground under the FAA specified conditions. The operation of SST airplanes from existing airports can be acceptably quiet only if the following four criteria are met:

1) Low noise engine cycle.

2) Engine noise minimized by use of attenuating features.

3) High thrust available for ground roll and initial climb.

4) Flight operation to produce minimum noise on the ground.

A violation of any one of these criteria will result in excess noise from the airplane.

1. ENGINE SIZE

High engine thrust for take-off and initial climb is necessary to assure low noise levels over the community. Figure 9-72 shows the change in community noise with engine size if airplane size is held constant. The increase in community noise that accompanies a decrease in engine size results from: 1) a lower altitude over the community, and 2) a higher exit gas velocity needed to maintain sufficient thrust for a safe minimum climb speed. Because gas temperature is a limiting feature in the design of both turbines and duct heaters, a practical limit exists on the thrust obtained per pound of airflow. Because of this limit, the maximum thrust an engine can produce is closely related to its basic airflow size. Therefore, a given weight airplane with a larger sized, or higher thrust, engine will climb faster and be at a higher altitude before it overheads the community. After power cut-back, a large airflow engine will have a lower thrust per pound of airflow, and therefore a lower jet velocity, than a smaller engine when both are providing equal thrust. As noise decreases much faster with reduced velocity than it increases with engine size, the airplane with large sized engines will be generating lower noise levels than the same airplane would be if fitted with smaller engines. The relationships between airplane flight characteristics, climb rate, noise, and engine size must be considered in the selection of an engine for use on a specific airplane.

2. ENGINE NOISE LEVELS

Noise must also be a basic consideration in the design of the SST engine. The engine operating cycle has an effect on noise, the turbofan cycle generally showing lower levels. Compressor design details, inlet and duct geometry, and the exhaust nozzle characteristics are other design features which can affect the noise levels from an engine. The use of noise suppression devices not inherent in the design of the engine should be avoided if at all possible. In most cases, some weight and performance penalties are associated with suppressor devices, which can adversely affect the operating costs of the SST. The development cycle of the SST engine will be first directed toward

obtaining as efficient an engine as possible, and then optimizing the design for noise without compromising performance. At this point, the engine noise characteristics can be documented to determine if the need for further noise suppression exists. If added suppression is needed, development of acoustically treated inlets or fan ducts or possible further development of the acoustical properties of the exhaust nozzle can be pursued.

3. NOISE SUPPRESSION

A great deal of care must be used in determining whether the incorporation of suppressor devices in the SST engine are of real benefit. Most suppressor devices have performance losses and weight penalties associated with them which can seriously affect the overall performance of the airplane. Besides introducing serious economic penalties in the operation of the SST, it is also possible that the suppressor devices do considerably less good in flight than ground sound tests may suggest, unless all ground to flight variables are taken into account.

a. Exhaust Suppressors

Unfortunately, the noise reductions measured during ground tests of suppressor nozzles may not be completely realized in flight because of reduced airplane performance resulting from:

- Aerodynamic losses - Loss of available take-off thrust and cruise thrust generally result from the use of suppressor devices. In flight, these devices have also been shown to have a greater drag than a simple nozzle.

- Weight - To accomplish a specific mission, a suppressor equipped airplane will generally have higher take-off gross weight than one without suppressors. This weight increase results from the added weight of the suppressors, the heavier airplane structure needed to carry the suppressors, and the increased fuel load needed because of the added weight, reduced thrust and increased drag.

For a specific fixed range and payload mission, the result of this weight and drag increase and thrust loss is to reduce the airplane rate of climb during take-off. Since the airplane has less altitude over the populated areas around the airport, the attenuation of noise due to distance is less than for an airplane at a higher altitude equipped

with standard nozzles. This offsets the noise reduction obtained from the suppressors, and illustrates why ground sound test data may be misleading if not properly interpreted.

The weight and drag increase and thrust loss associated with exhaust noise suppressors also result in increased airplane operating costs. In the case of the supersonic transport, virtually no factors which could increase the aircraft operating costs can be tolerated.

The most satisfactory suppressor for use on the SST would probably be one that is retractable or disposable. With this type of device the significant loss in performance and efficiency would occur during only the initial, low-altitude climb phase of take-off. As well as providing a noise reduction, a satisfactory design would also incorporate low performance losses, light weight, and fail safe operation.

b. Discrete Noise Attenuation

The same considerations apply to the use of special acoustical construction in the inlet and fan ducts of the SST as were applied to the exhaust suppressors. Devices which result in an excessive weight increase or performance losses will not be acceptable in the SST engine.

c. Operator Technique

There is little doubt that excessive community noise levels would result from a full power take-off of the SST without a power cut-back near the three mile point. If large size engines are used on the SST, it will be possible to reduce thrust to a value which will allow an acceptable climb rate with tolerable noise levels.

For a given SST airplane, there is a trade-off between airport sideline noise and community noise which is accomplished by operator technique. Figure 9-73 shows the trade-off for a typical SST airplane. Higher airport sideline noise levels are the penalty paid for low community noise levels. The use of higher power during take-off is necessary to obtain a high altitude at the three mile point at which power is cut back. It is quite possible that the operation of the SST may be tailored to the requirements of each airport from which it is operated, taking into account the noise requirements of specific airports.

4. STF219 ENGINE NOISE LEVELS

Estimated noise levels for the STF219 engine versus engine thrust are shown on Figures 9-74 and 9-75 No reduction in noise from either a blow-in-door ejector or compressor noise attenuating devices was assumed. Figure 9-74 shows estimated sideline noise at 1500 feet from the engine centerline versus static thrust. In-flight noise level estimates are shown on Figure 9-75. At comparable engine percent power settings, a 640 lbs/sec max. airflow engine will be about one PNdb less noisy than a 700 lbs/sec engine. Levels were shown for 300 feet altitude as it is representative of the approach point, and the levels at altitudes of from 1500 to 3000 feet generally bracket those expected at three miles from the start of take-off roll.

Figures 9-76 and 9-77 are similar to those described above, except that noise attenuation was assumed for the blow-in-door ejector, the supersonic inlet, and reduced noise out the fan ducts. The noise attenuation assumed from the blow-in-door ejector varies with velocity as shown on Figure 9-78 A ten db reduction in both inlet and fan discharge discrete frequency compressor noise was also assumed as being obtainable using present state of the art methods. Inlet noise attenuation can be achieved by the combination of compressor design optimization for low noise, and also by development of a supersonic inlet with sound absorbing features. Complete attenuation of inlet noise is possible if a choked inlet duct is used during approach. Results of tests on inlet ducts are contained in Part C of Item 9.

Attenuation of compressor noise radiated out the fan discharge ducts can be attained by proper design. Some attenuation can be obtained by optimization of the compressor geometry for minimum noise, and it has been demonstrated that the desired amount of attenuation can be obtained by installation of acoustically treated flow splitters in the fan duct diffuser section between the compressor discharge and the duct heaters. Results of Phase II-A tests of a treated diffuser section have shown attenuations of about 10 to 15 db at 2000 cps and more at higher frequencies. These results are presented in Part D of Item 9.

Noise estimates shown on the curves were calculated using the procedures outlined by the SAE A-21 Committee. These procedures are in general agreement with noise estimating procedures previously used by Pratt & Whitney Aircraft and are expected to give fairly reliable results. Figure 9-79 compares the noise levels estimated for an unsuppressed STF219 engine using the A-21 Committee method with those estimated using the Pratt & Whitney Aircraft method.

Compressor noise levels were estimated using procedures developed by Pratt & Whitney Aircraft from sound measurements on several engines. These procedures are described in Appendix A.

5. AIRPLANE FLY-OVER NOISE LEVELS

In order to calculate the noise beneath the flight path of an airplane, it is necessary to have complete information on the airplane flight paths and thrust requirements. These data were not generally available during Phase II-A because of the continual improvements and modifications being made in the airplane designs. For this reason, data on the noise levels for specific airplane designs fitted with STF219 engines will not be reported by Pratt & Whitney Aircraft. These data will probably be reported by each airframe contractor using the latest airplane configuration and performance.

Compressor noise levels were estimated using procedures developed by Pratt & Whitney Aircraft from sound measurements on several engines. These procedures are described in Appendix A.

5. AIRPLANE FLY-OVER NOISE LEVELS

In order to calculate the noise beneath the flight path of an airplane, it is necessary to have complete information on the airplane flight paths and thrust requirements. These data were not generally available during Phase II-A because of the continual improvements and modifications being made in the airplane designs. For this reason, data on the noise levels for specific airplane designs fitted with STF219 engines will not be reported by Pratt & Whitney Aircraft. These data will probably be reported by each airframe contractor using the latest airplane configuration and performance.

APPENDIX A

ESTIMATION OF COMPRESSOR NOISE

The need to estimate compressor noise levels of advanced engines led to the establishment of an estimating [illegible]edure based on both theory and empirical data from current eng[illegible] The estimating procedure relates compressor noise levels to th[illegible]echanical tip velocity of the first rotor and the inlet diameter. It is recognized that the engine design and additional performance parameters such as blade loading and blade and vane aerodynamics influence the compressor noise levels. At the present time, these effects are not completely predictable. Due to these unpredictable factors, it is much more difficult to accurately estimate compressor noise levels than it is to estimate exhaust noise levels from a circular nozzle.

Inlet and fan discharge compressor noise levels from current engines of various sizes and types, normalized to a constant inlet diameter, are shown on Figure 9-A-1 as a function of mechanical tip velocity. The spread in the noise levels from the various engines shown on the curve indicates that factors other than mechanical tip speed and inlet diameter are contributing to the compressor noise levels.

The estimating procedure is thus designed to best fit the measured data from current engines equipped with subsonic inlets and inlet guide vanes. The compressor noise estimation procedure is outlined as follows:

1) Calculate the fundamental blade passing frequency, f.

$$f = \frac{BN}{60}$$

B = number of first rotor blades
N = mechanical rotor speed, rpm

This establishes which octave band contains the fundamental blade passing frequency.

2) Calculate the mechanical tip velocity, V_T.

$$V_T = \frac{D \pi N}{720}$$

D = inlet diameter, inches
N = mechanical rotor speed, rpm

3) Enter Figure 9-A-1 at V_T and read from the curve the maximum compressor noise levels from the inlet and fan discharge normalized to a 51-inch inlet diameter.

$$(\text{OBSPL} + 20 \log 51/D)_{\text{inlet}}, \quad (\text{OBSPL} + 20 \log 51/D)_{\text{fan}}$$

4) Calculate the inlet diameter correction, C.

$$C = 20 \log D/51$$

D = inlet diameter, inches

5) Add the inlet diameter correction to find the maximum inlet and fan discharge compressor noise levels for the octave band containing the fundamental blade passing frequency (OBSPL inlet, OBSPL fan).

$$\text{OBSPL inlet} = (\text{OBSPL} + 20 \log \frac{51}{D})_{\text{inlet}} + C$$
$$\text{OBSPL fan} = (\text{OBSPL} + 20 \log \frac{51}{D})_{\text{fan}} + C$$

6) Calculate maximum compressor noise levels for the octaves above and below the octave containing the fundamental blade passage noise.

Octave above = OBSPL - 2 db
Octave below = OBSPL - 7 db

The above octave band noise levels are the estimated maximum compressor noise levels along a parallel line 200 feet from the engine.

These levels are then added to the exhaust noise levels estimated according to the SAE A-21 Committee procedures.

APPENDIX B

YF-12A FLY-OVER NOISE MEASUREMENTS

Fly-over noise levels during take-off and landing operations were recorded during the YF-12A airplane flight test program. Noise levels from this aircraft were of interest to the SST project because the YF-12A was designed to operate in the same range of flight Mach numbers as the SST, and details of the engine installation resembled that planned for the SST. Some observers reported that the YF-12A airplane, powered by two large J58 afterburning engines was less noisy than the F-104 chase airplane which had only one afterburning J79 engine. The YF-12A airplane engine installation differed from that of the F-104 in that blow-in-door ejector (BIDE) exhaust nozzles were used on the high Mach number airplane.

1. METHOD OF TEST

Sound measurements were taken at Edwards Air Force Base by Pratt & Whitney Aircraft acoustics engineers. The signals from four microphones positioned beneath the flight path were recorded on magnetic tape during take-off and landings. Acoustic data recording and analysis was done in accordance with standard Pratt & Whitney Aircraft procedures which provide accuracies of about ±2 db. Aircraft altitudes were scaled from photographs taken of the aircraft at the overhead position. Engine performance parameters which are related to noise were obtained for each flight from recorders installed in the airplane.

Of the several flights recorded, twelve were suitable for detailed acoustic analysis. Eight of these flights were afterburning take-offs, three were nonafterburning take-offs, and four were landing approaches. The flights selected for analysis were recorded during low wind conditions and were free from interference by noise from other airplanes. Some flight altitudes were as low as 250 feet where the effects of temperature and humidity on sound propagation are of little significance.

2. EXHAUST NOISE

Exhaust noise levels from the flight tests, normalized for jet density and nozzle area, are plotted Figure 9-B-1. The solid line shown on this figure is identical with that used in the SAE A-21 Committee noise calculating procedure. Also shown are data from static ound tests of a

J58 engine with a circular nozzle. As shown on the curve, the measured YF12-A flight noise levels were lower than would be expected from either the ground tests or from the use of the A-21 Committee calculating procedure. The reduction in noise was attributed to some effect of the BIDE.

3. INLET NOISE

Noise from the YF-12A airplane during approach was characterized by an almost complete lack of compressor whine. This characteristic was observed on both the J58 engine powered YF-12A and a prototype airplane powered by a J75 engine which has a compressor identical with that used in the Pratt & Whitney Aircraft JT4 commercial transport jet engine. Narrow frequency band analysis techniques were used to isolate and measure the fundamental blade passing fequency from approach fly-over tape recordings of the J75 powered YF-12A airplane, and the levels were compared with similar results from fly-overs of JT4 powered 707 airplanes. Results of the analysis is shown on Figure 9-B-2. A similar comparison for the J58 compressor noise was not possible as noise from this engine was not recorded during fly-overs of any aircraft other than the YF-12A. Ground sound tests have shown bellmouth-inlet-equipped J58 engines to have compressor noise levels comparable to those of the J75 engine.

The significant lack of inlet noise from the YF-12A airplane was attributed to the presence of the supersonic inlet. Details of the design of the inlet were not available so an analysis could not be made to determine specific features which may have affected its acoustical characteristics. It is, however, a fairly safe assumption that noise control features were not a consideration in the inlet design. It is known that the inlet was not in a choked condition during approach.

Results of the YF-12A fly-over noise tests are of particular significance to the SST engines being designed by Pratt & Whitney Aircraft. Incorporated in the design of the SST engine is a BIDE nozzle. In addition to the beneficial effects of this nozzle on performance, the tests show that its use results in some reduction in jet noise which will improve the SST take-off noise characteristics. Approach noise levels would be drastically reduced if the SST inlet has acoustic characteristics similar to those of the supersonic YF-12A inlet.

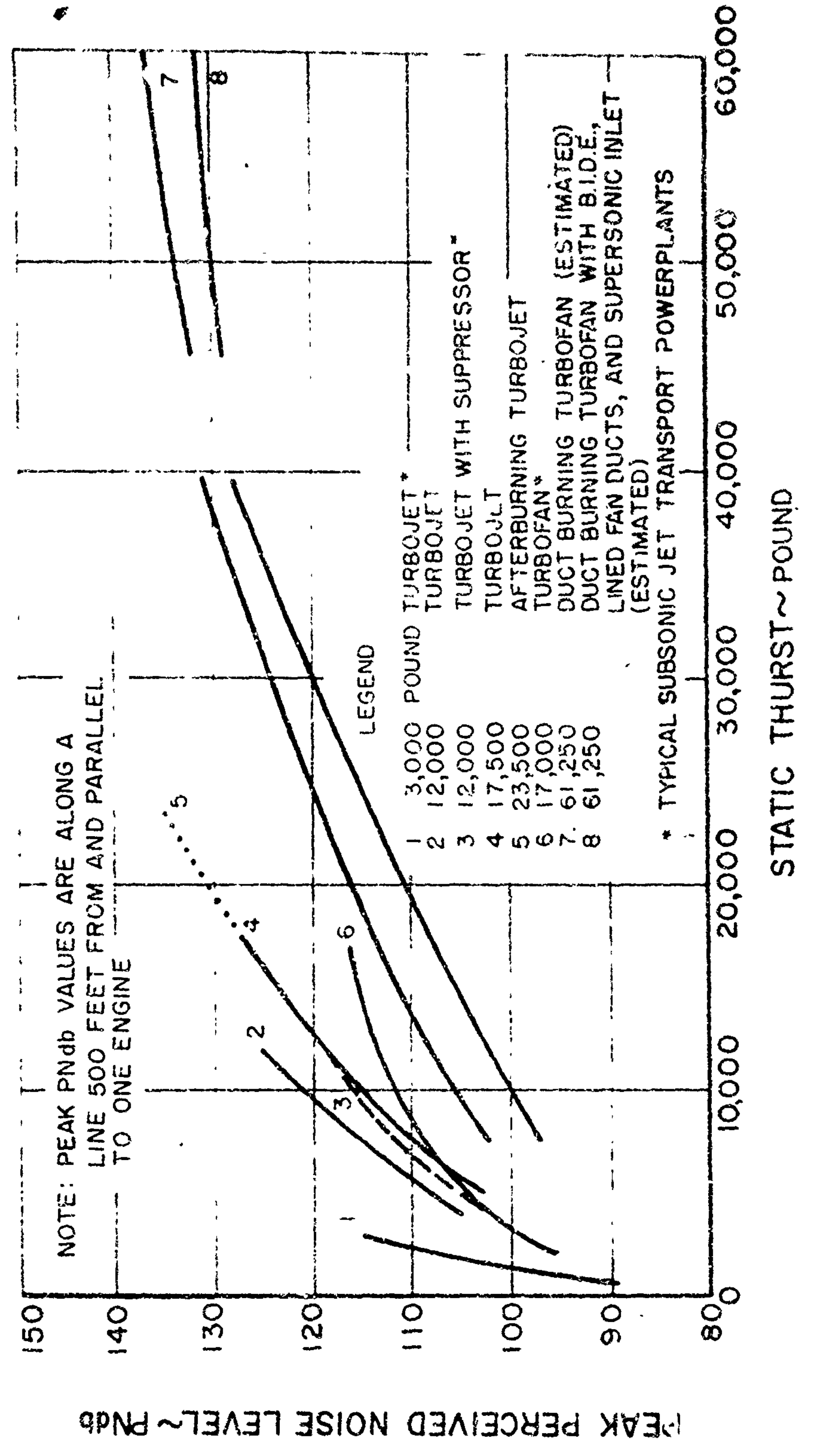

ESTIMATED STF219 ENGINE NOISE LEVELS COMPARED WITH CURRENT TURBOJET AND TURBOFAN ENGINE NOISE LEVELS

Figure 9-1

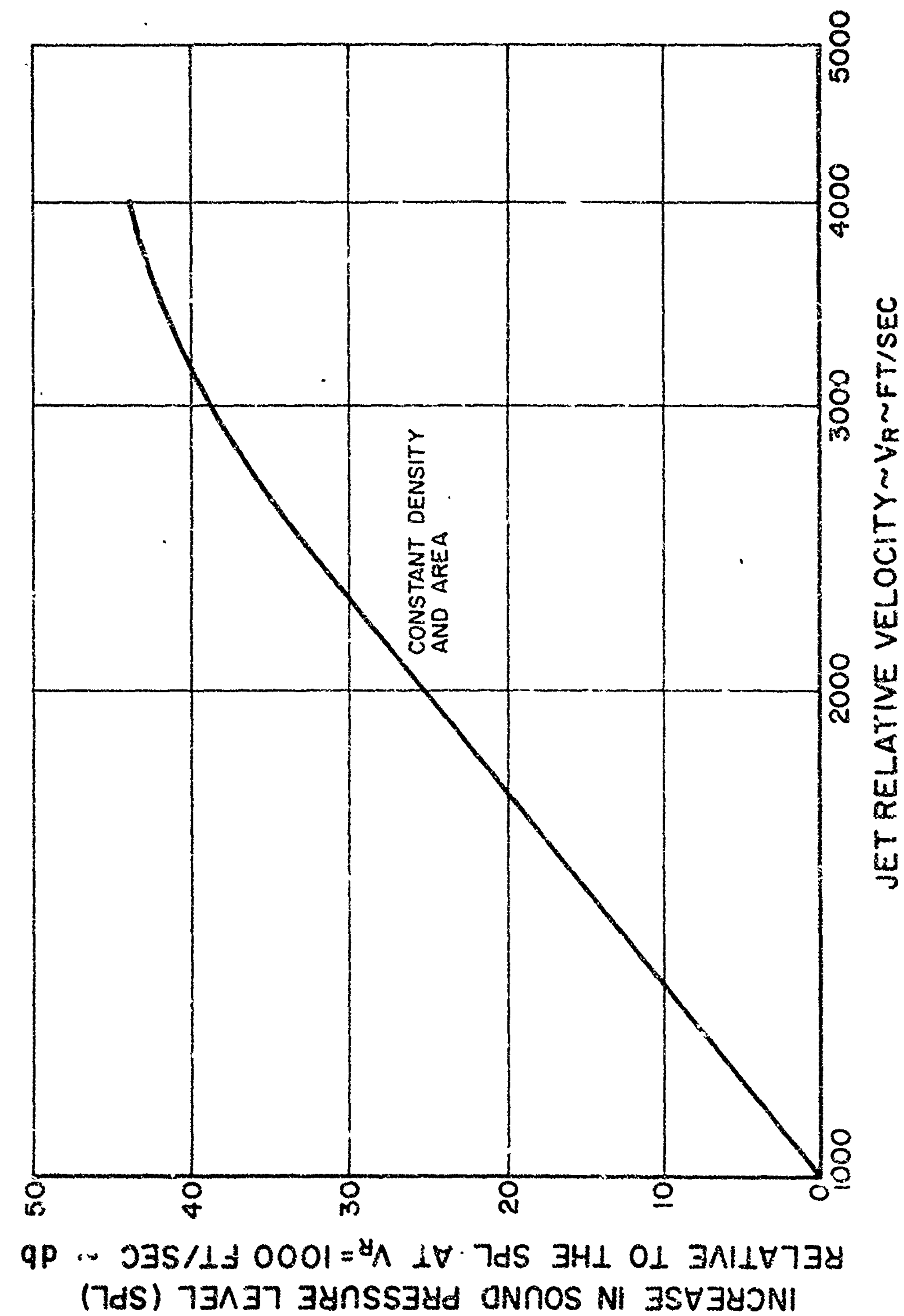

EFFECT OF JET RELATIVE VELOCITY ON SOUND PRESSURE LEVEL

Figure 9-2

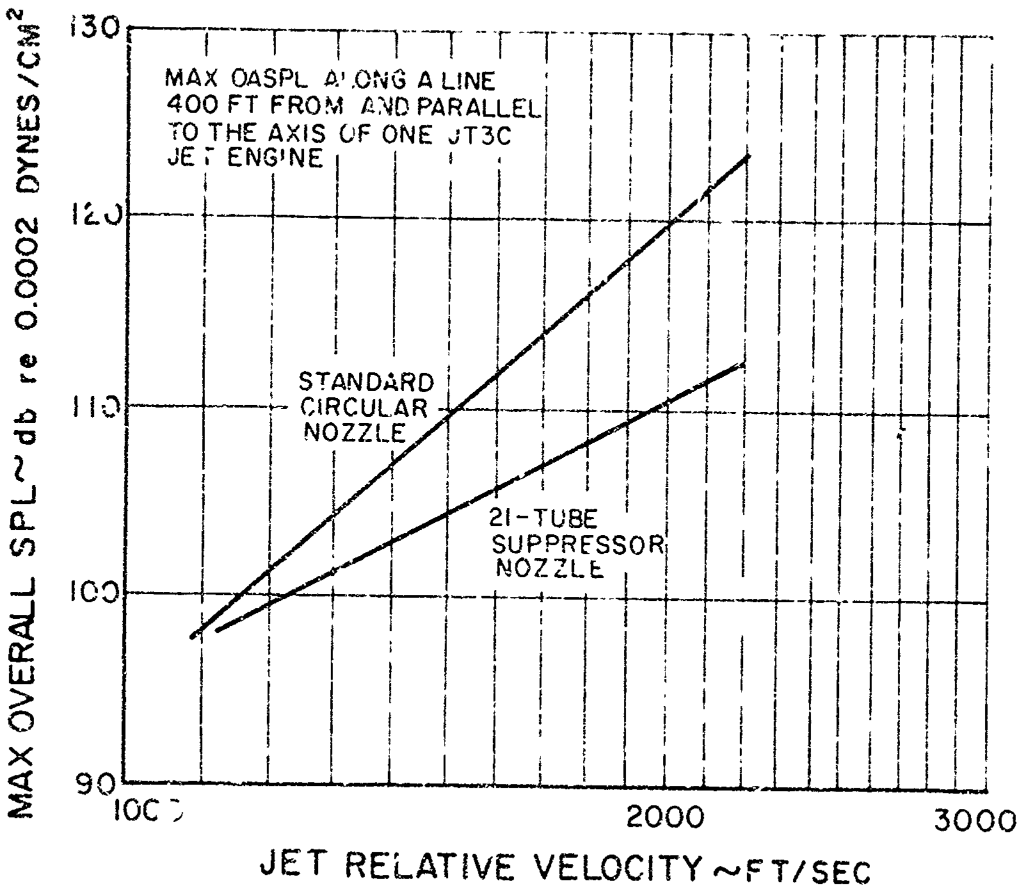

21-TUBE NOISE SUPPRESSOR PERFORMANCE

Figure 9-3

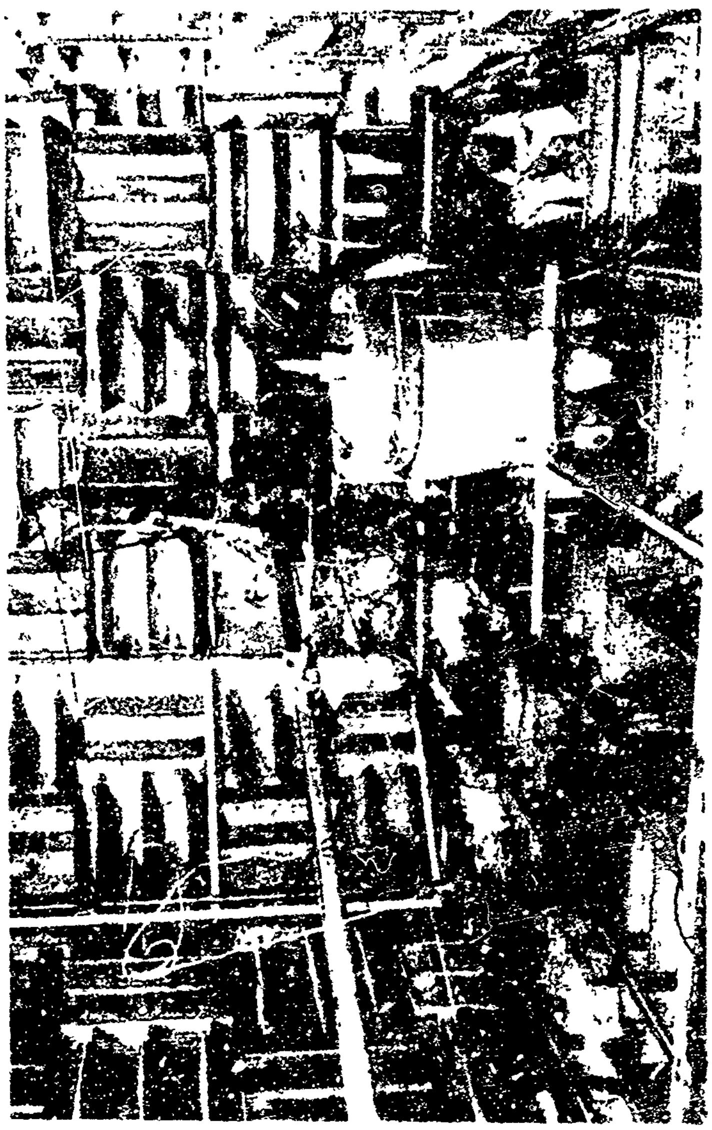

ANECHOIC CHAMBER SHOWING SCALE MODEL EXHAUST NOZZLE
AND TRAVERSING MICROPHONE BOOM

Figure 4

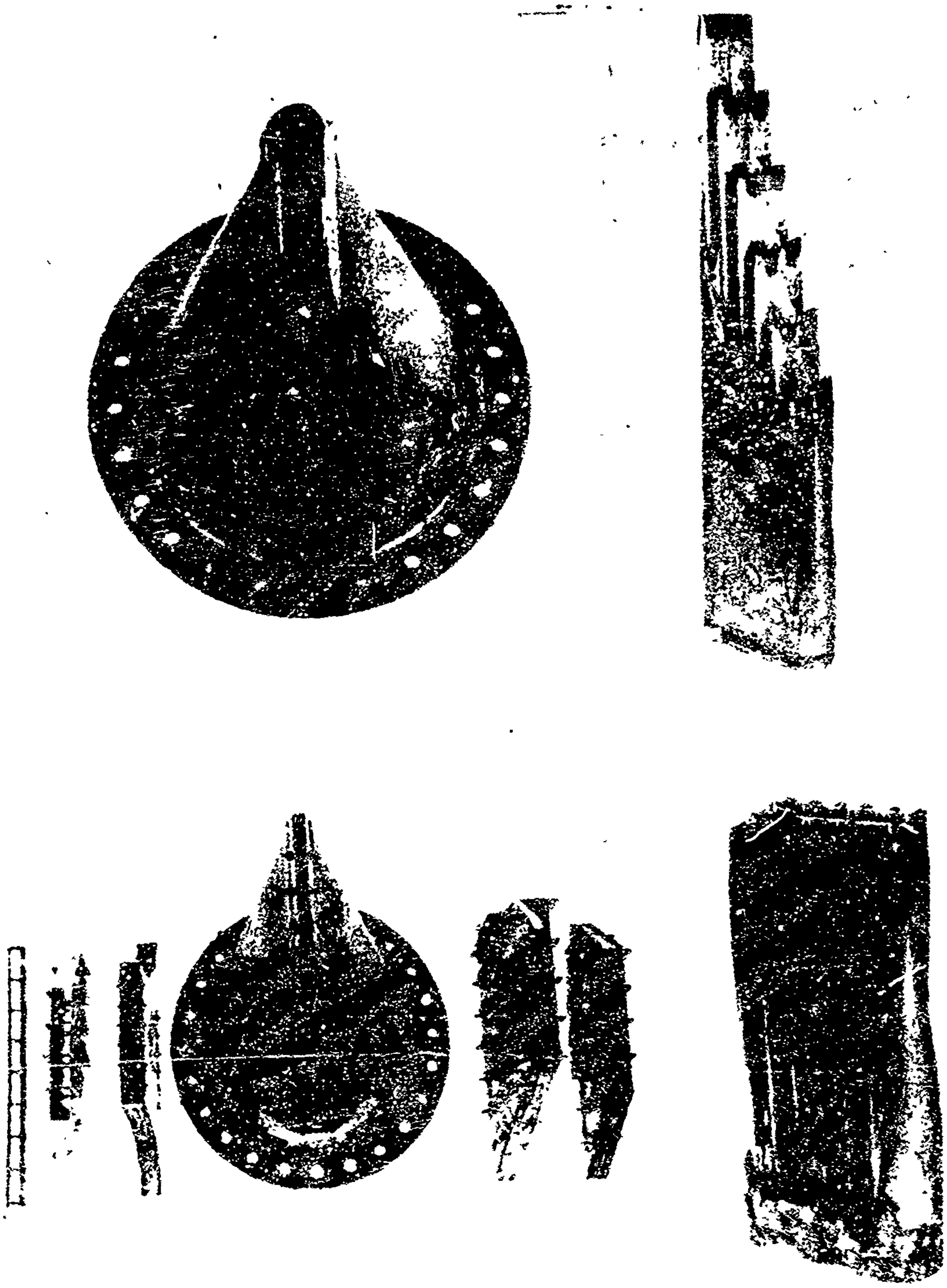

XP-7473

SCALE MODEL EXHAUST NOZZLES; AREA
EQUIVALENT TO THREE-INCH DIAMETER CIRCULAR NOZZLE

Figure 9-5

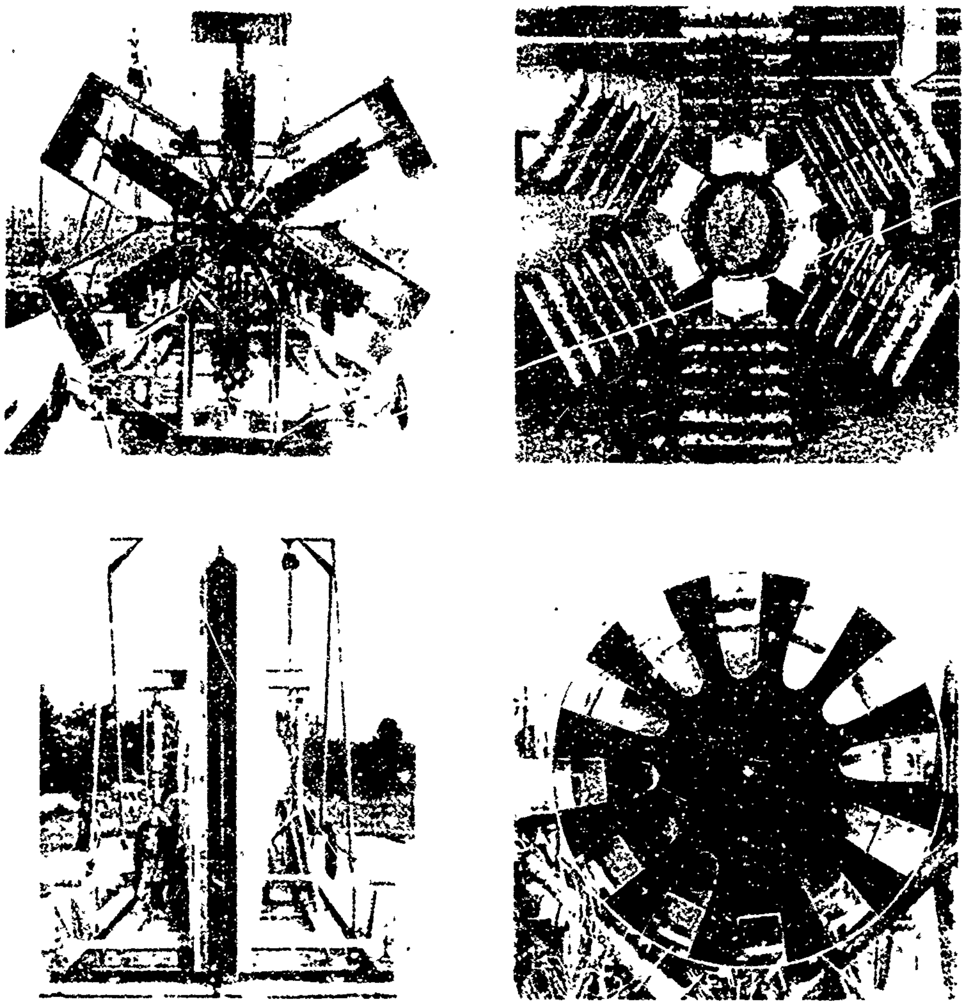

Various Experimental Jet Noise Suppressors Acoustically Tested in Full Scale

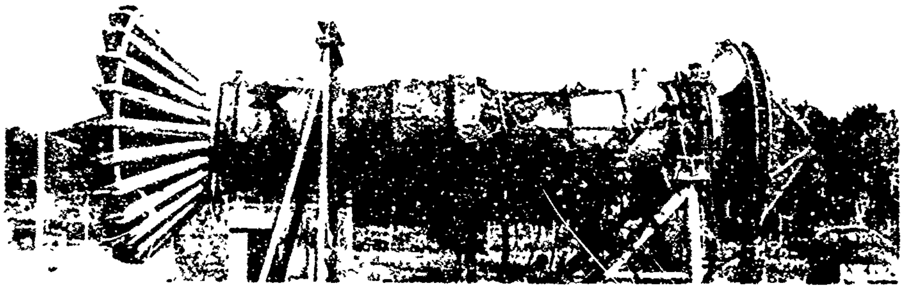

Side View of Engine with Test Suppressor

EXPERIMENTAL JET NOISE SUPPRESSORS

Figure 9-6

RECTANGULAR NOISE SUPPRESSOR NOZZLE

Figure [illegible]-7

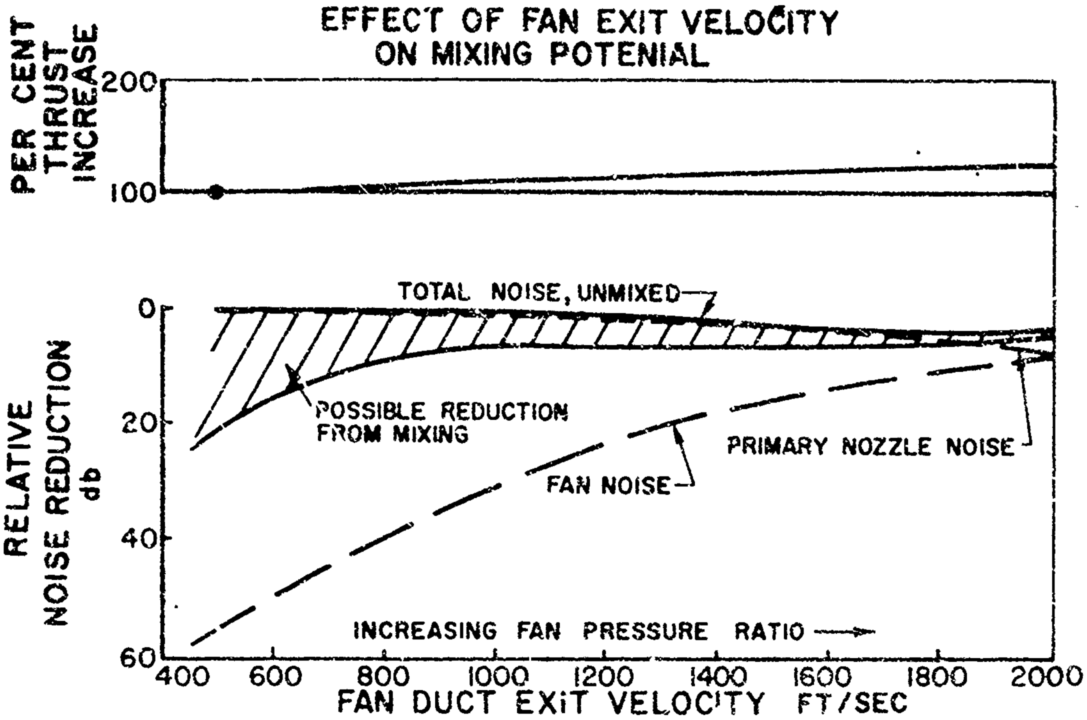

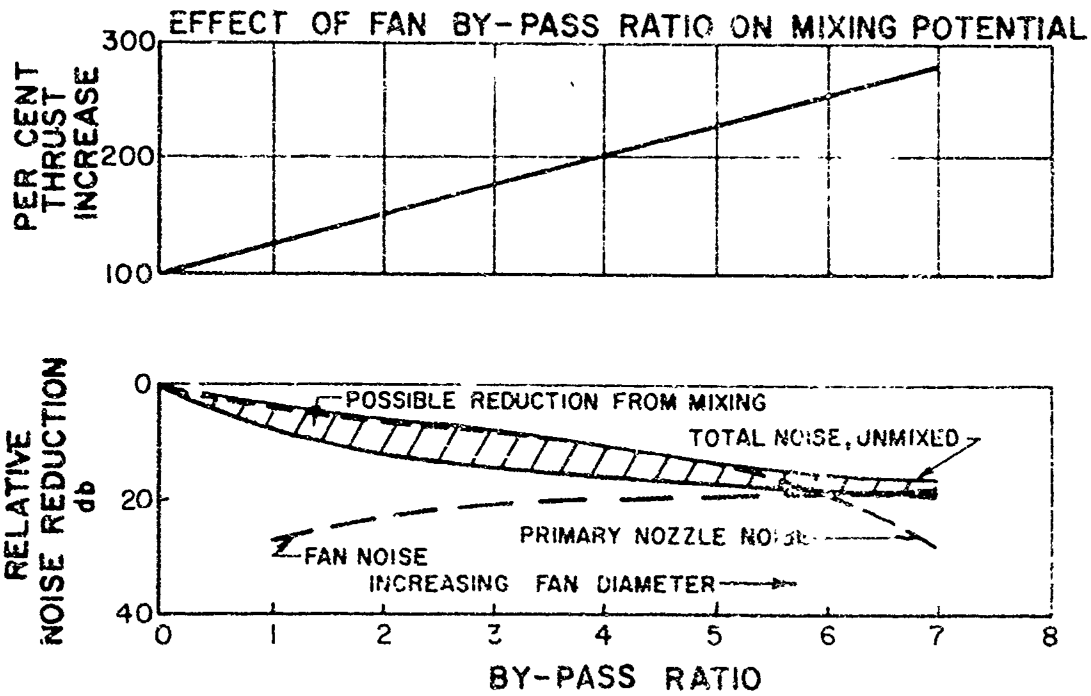

POTENTIAL NOISE REDUCTION FROM MIXING

Figure 9-8

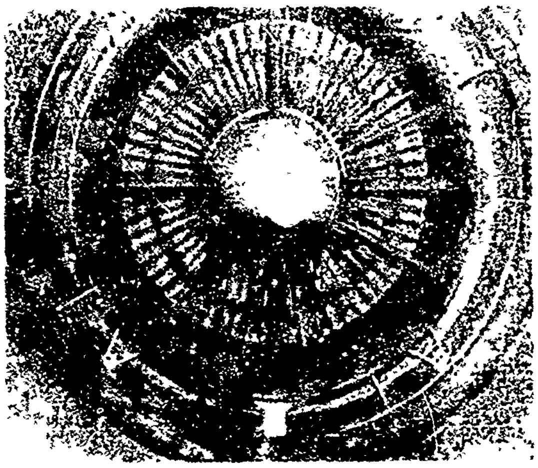

Baesline Configuration, No Mixer

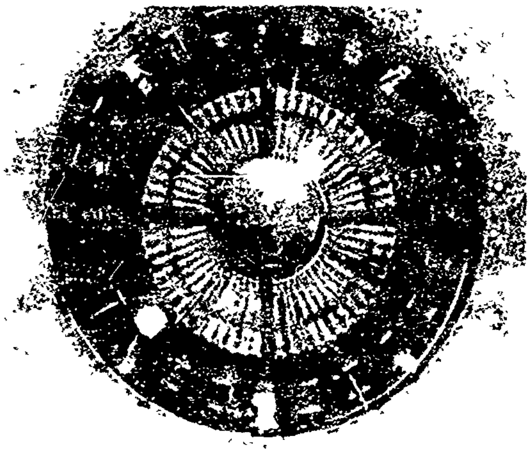

Finger Mixer

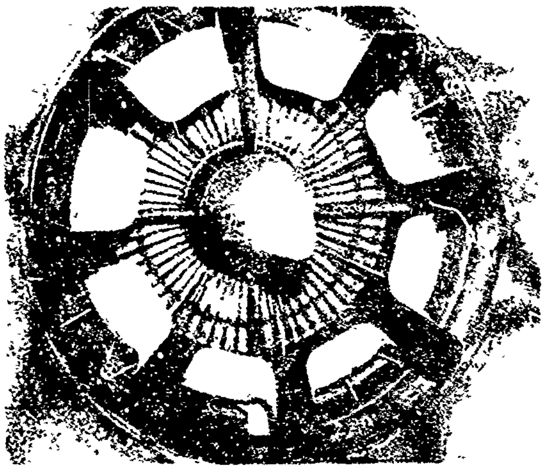

8-Lobe Mixer

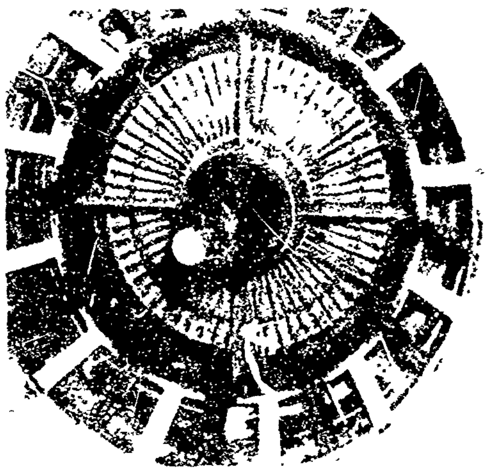

24-Strut Mixer

EXPERIMENTAL MIXING DEVICES
ACOUSTICALLY TESTED IN FULL SCALE

Figure 9-[illegible]

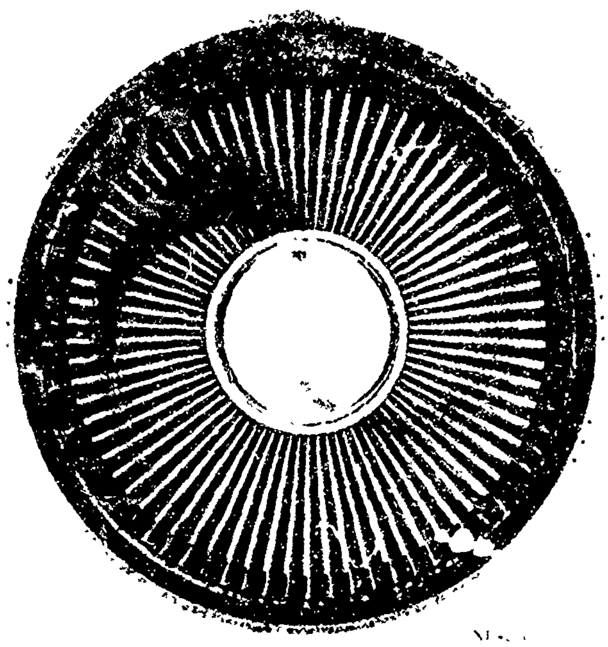

74-Vane

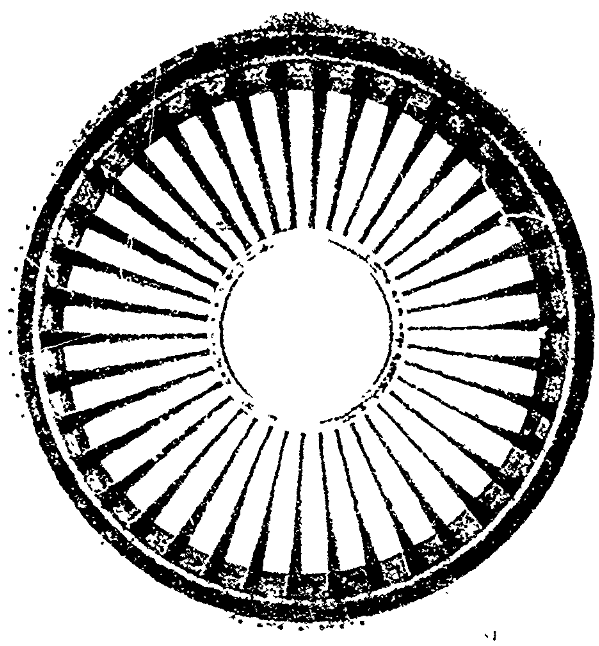

38-Vane

JT D STATOR VANE ASSEMBLIES

Figure [illegible]-11

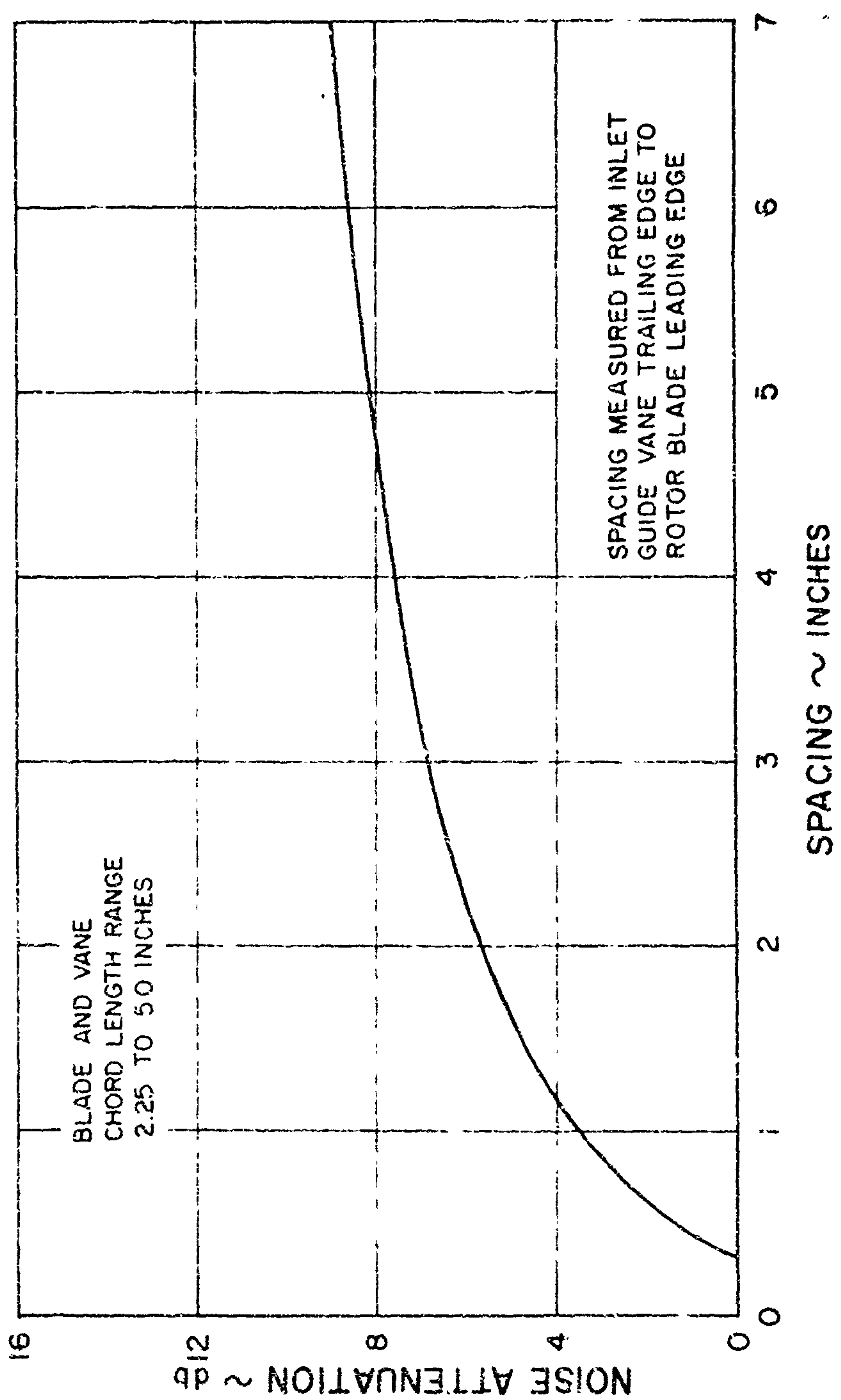

EFFECT OF VANE-TO-BLADE SPACING ON NOISE LEVEL AT SUBSONIC BLADE TIP SPEEDS

Figure 9-11

EXP-97374

COMPRESSOR ROTOR WITH BLADE TIPS IN SHROUDED TROUGH

Figure 9-12

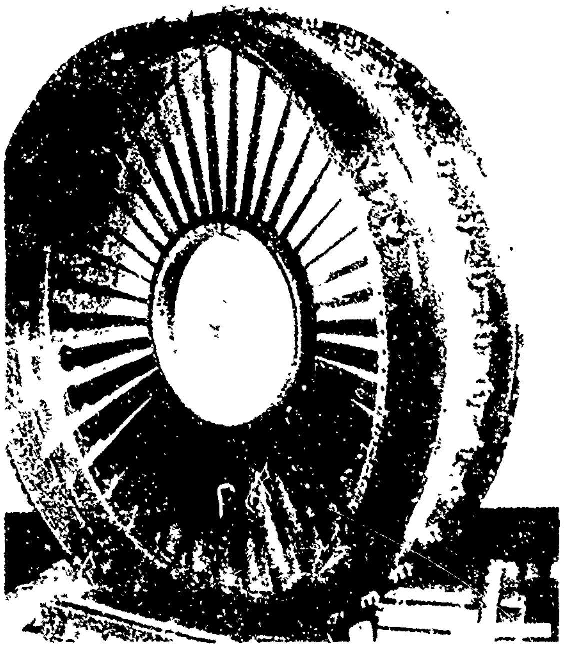

JT3D Variable Angle Stator Vane Assembly

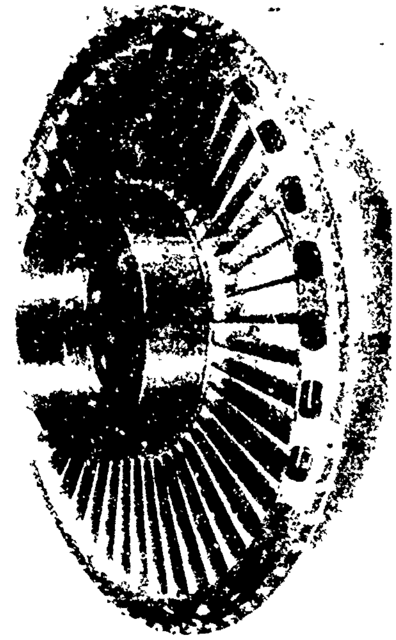

Variable Angle Stator Vane Assembly for Rig

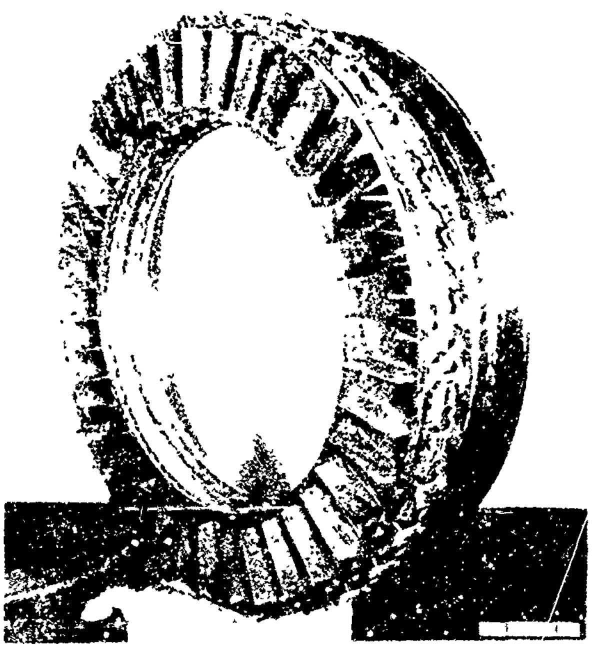

JT3D Variable Trailing Edge Exit Guide Vane Assembly

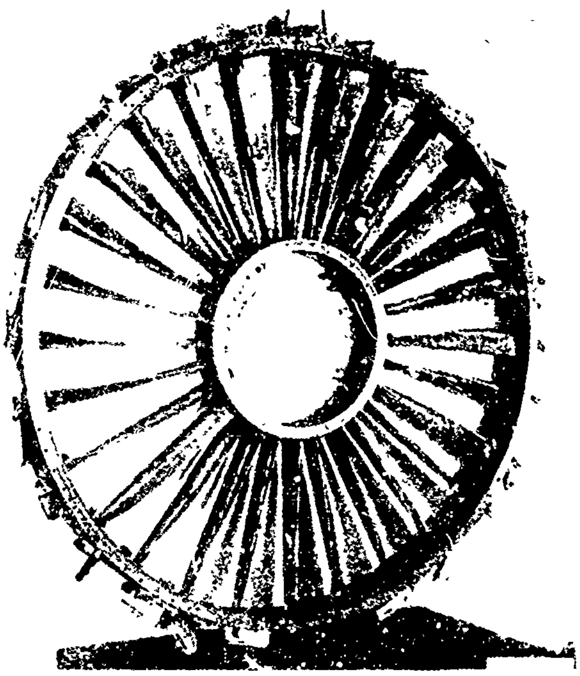

JT3D Variable Trailing Edge Inlet Guide Vane Assembly

FULL-SCALE VARIABLE-ANGLE VANE ASSEMBLIES

Figure 2-13

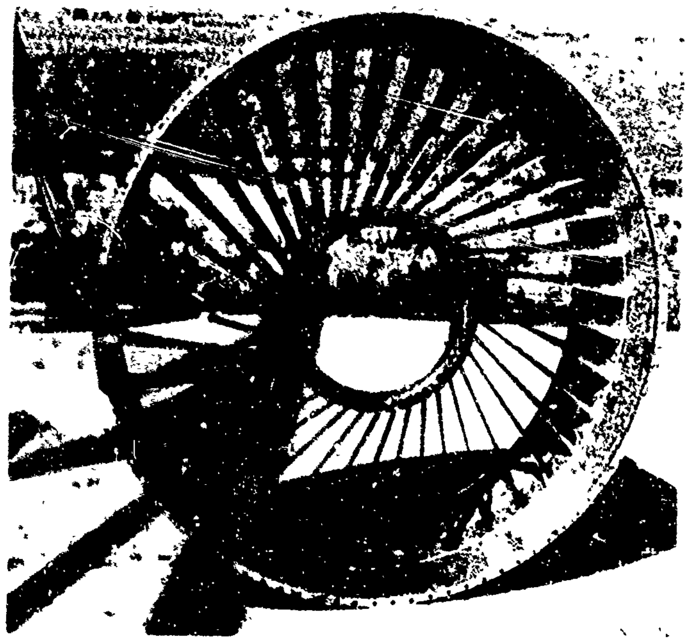

JT3D 38-Vane, 30° Slant Stator

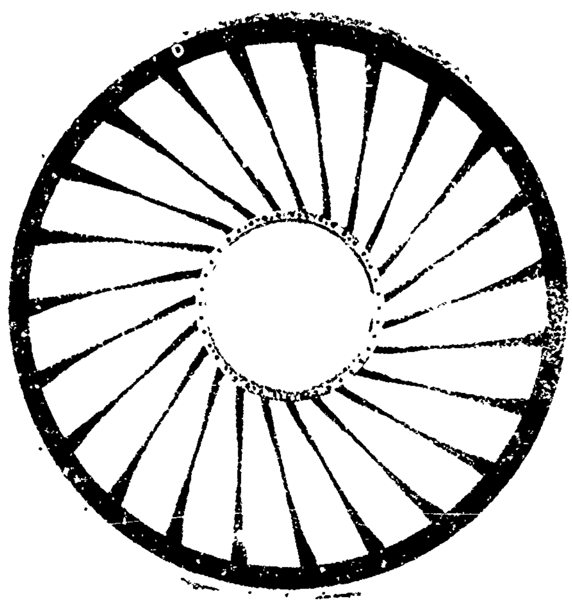

JT3D 23-Vane 30° Slant Inlet Guide Vane

FULL-SCALE SLANTED VANE ASSEMBLIES

Figure 9-11

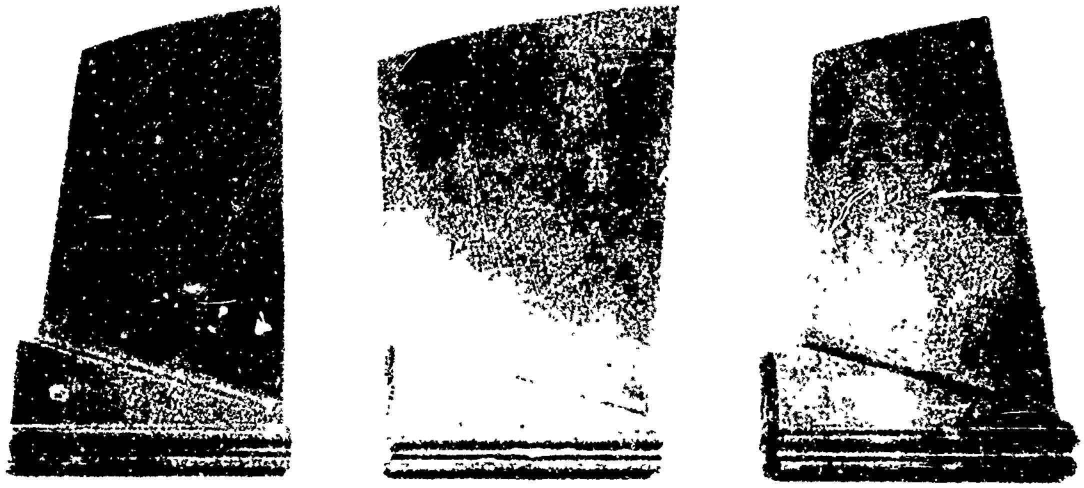

M-46 [illegible]

Blades with Various Taper Ratios

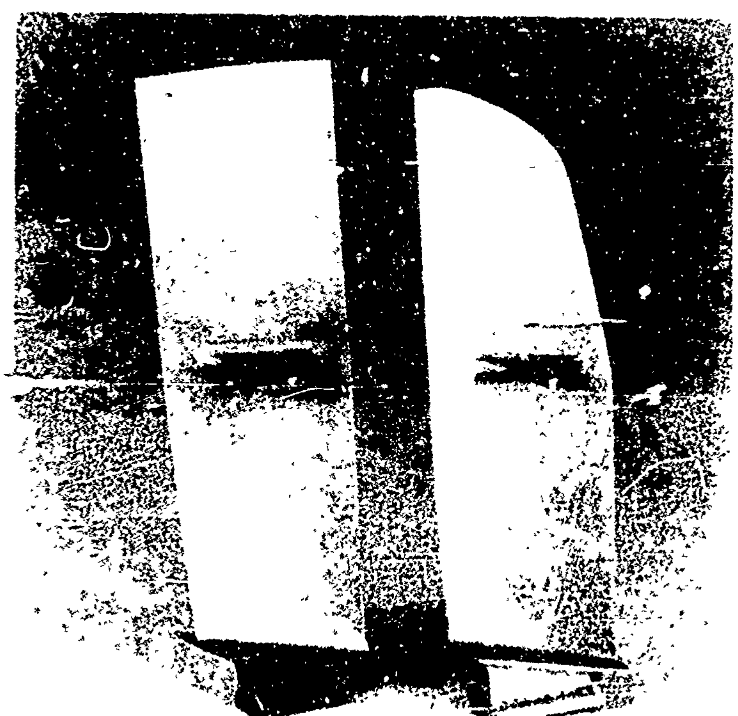

Standard Blade and Blade with Cut-Back Leading Edge

VARIOUS BLADE PLAN FORMS TESTED FOR NOISE GENERATION

Figure 9-15

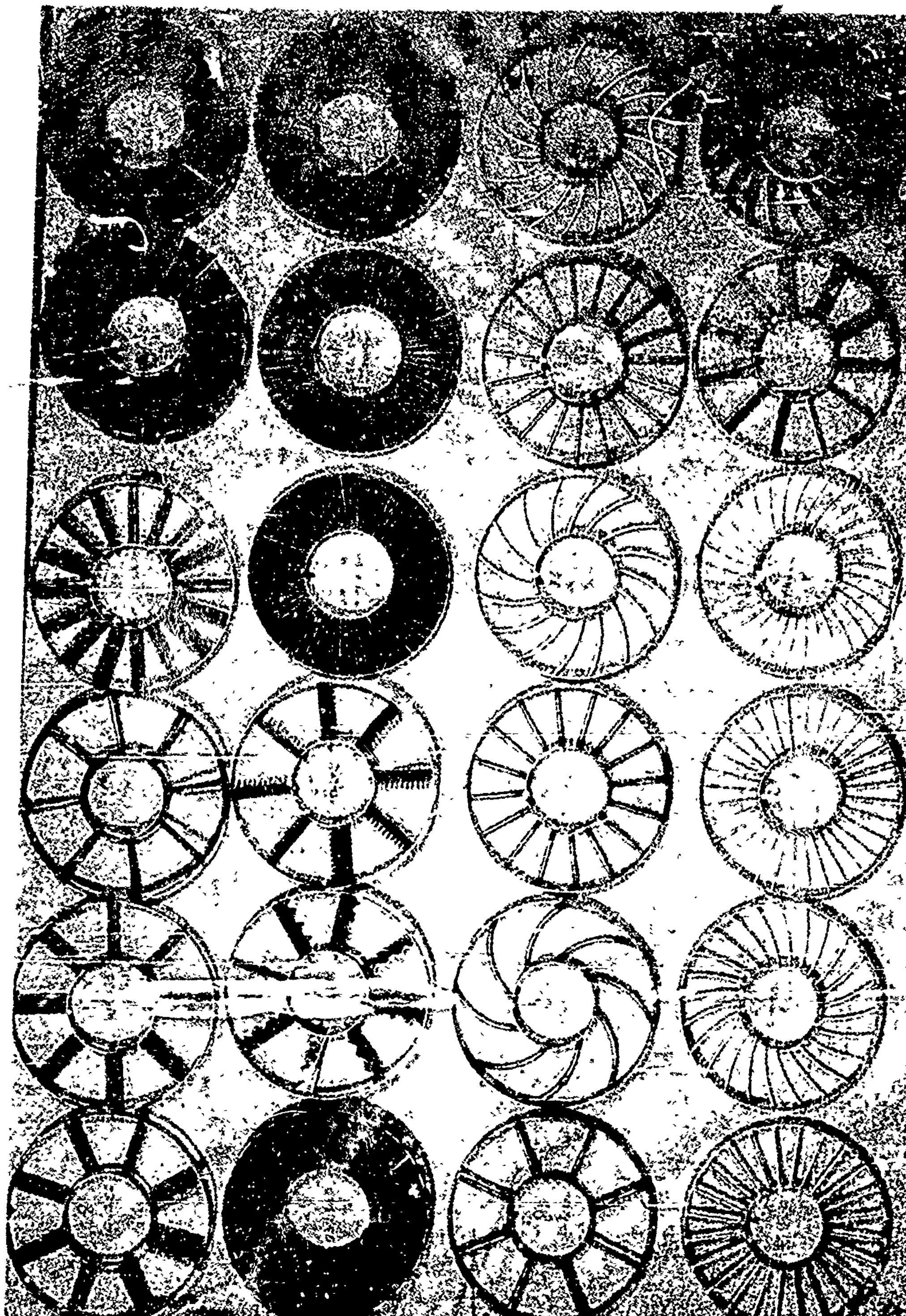

STATOR AND TURBULENCE-GENERATOR VANE CONFIGURATIONS

Figure 9-16

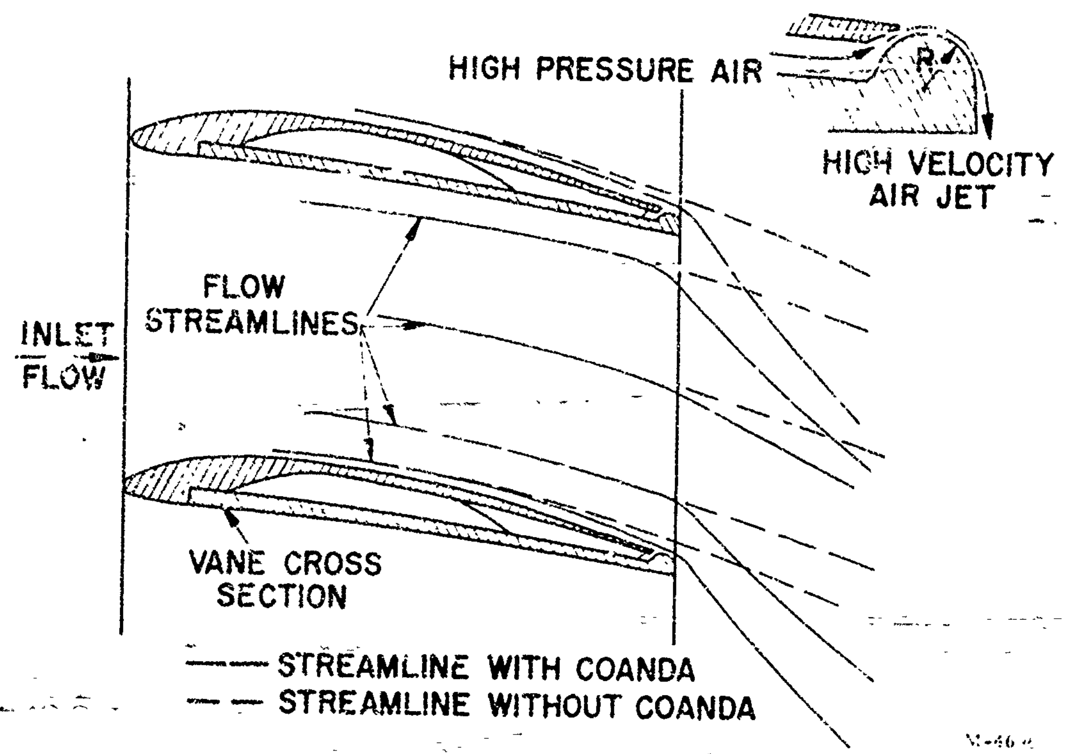

COANDA INLET GUIDE VANE

Figure 9-17

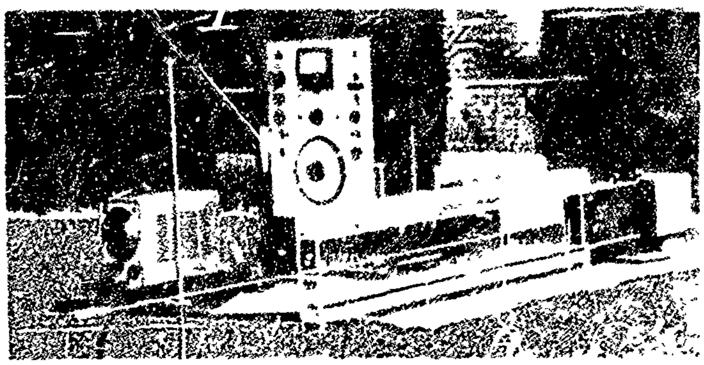

Research Rig

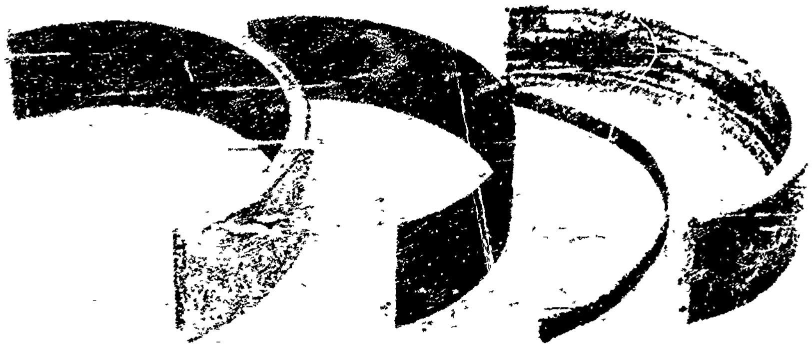

Compressor Rig (28 inches)

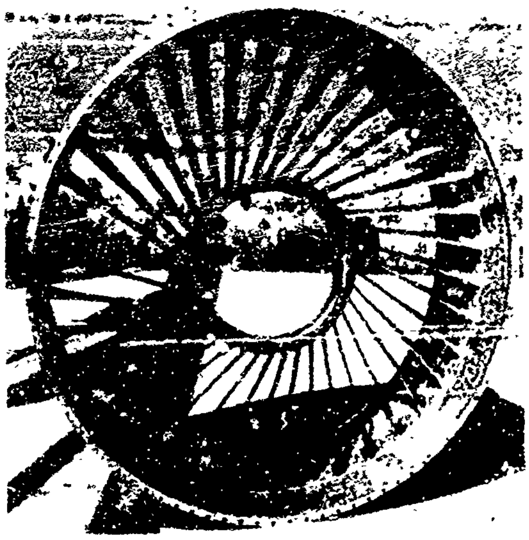

Full Scale (50 inches)

M-4889

RESONANT ABSORBER SHROUDS

Figure 9-18

Flight Type Inlets

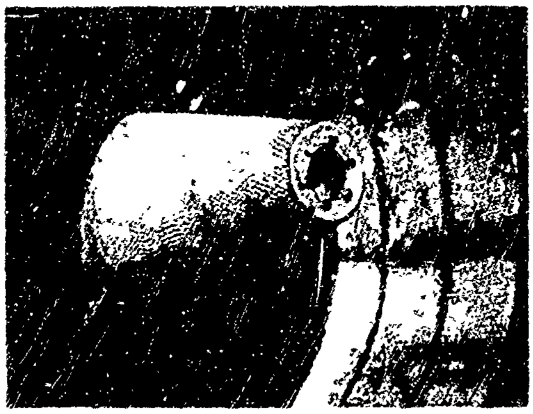

Fiberglas Lined

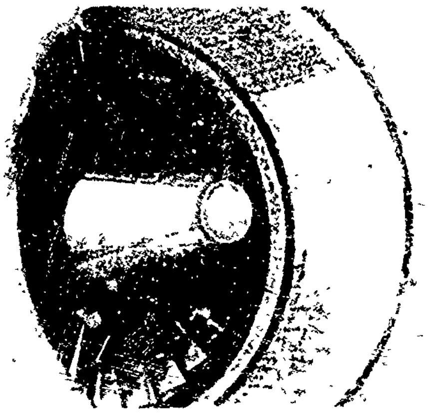

Resonant Tuned Absorber
M-4889

Fiberglas Lined Bulb Inlet

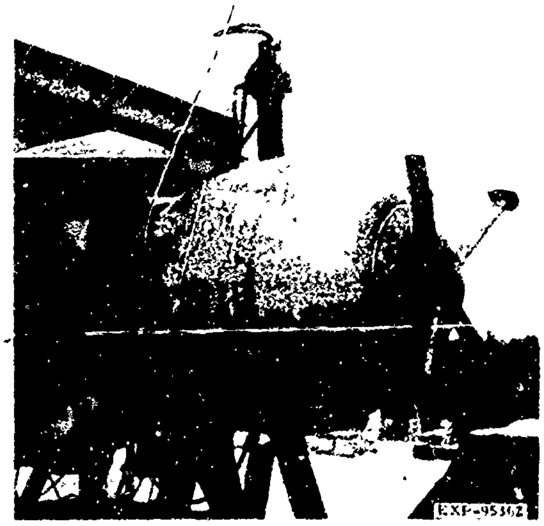

Bulb Type Nose Cone
Outer Duct Removed

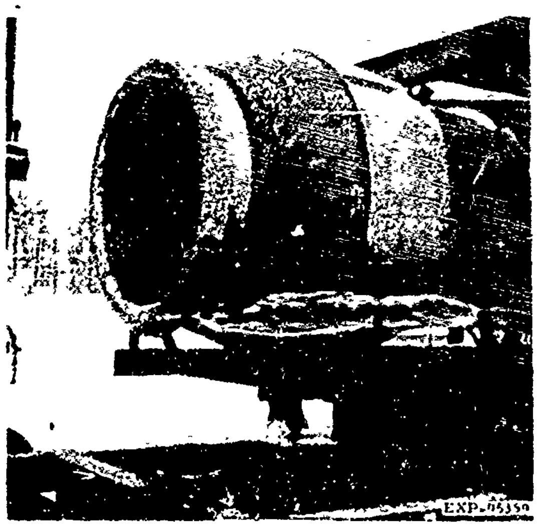

Bulb Type Duct and Nose Cone

SOUND ABSORBENT INLETS

Figure 9-19


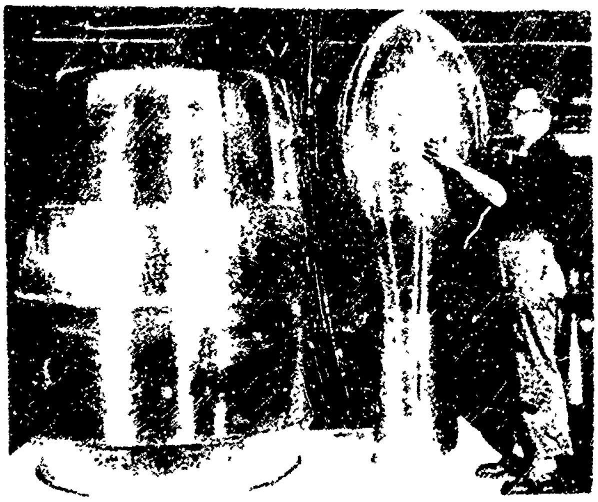

M-4895

Full Scale Variable Cone

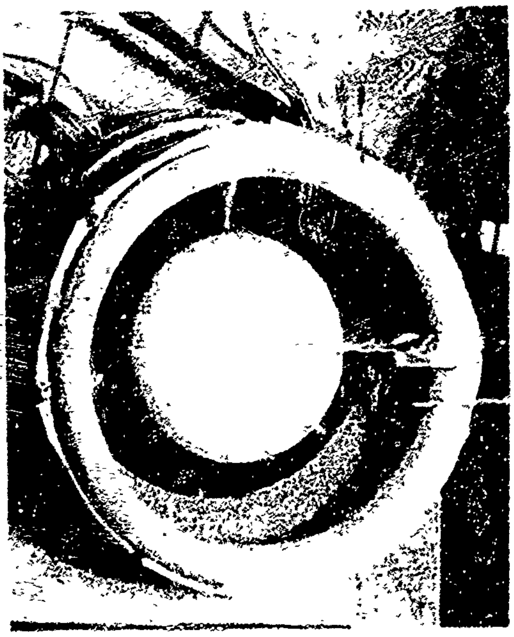

1/3 Scale Model

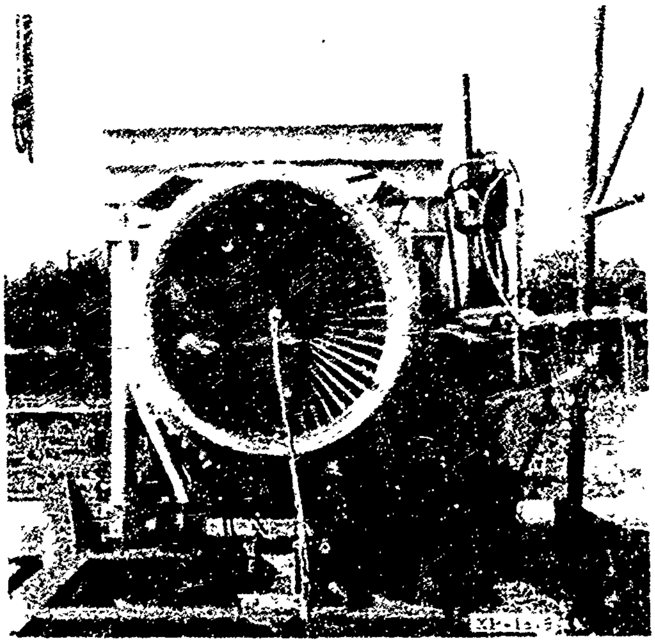

48-Strut Choked Inlet

SONIC INLET COWLS

Figure 9-20

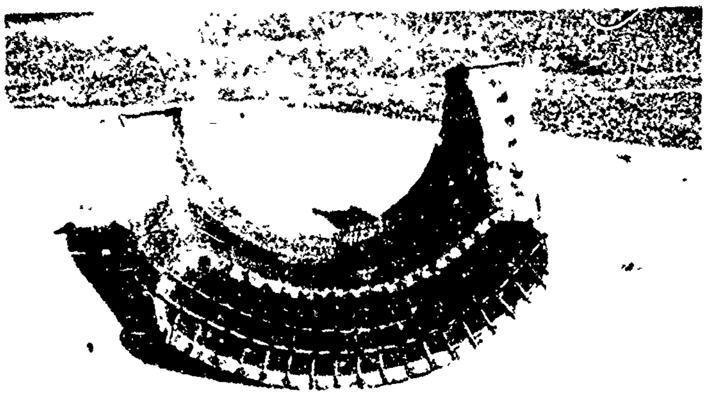

Rod Type

Sawtooth

FULL-SCALE FAN EXIT DUCT TURBULENCE GENERATORS

Figure 9-21

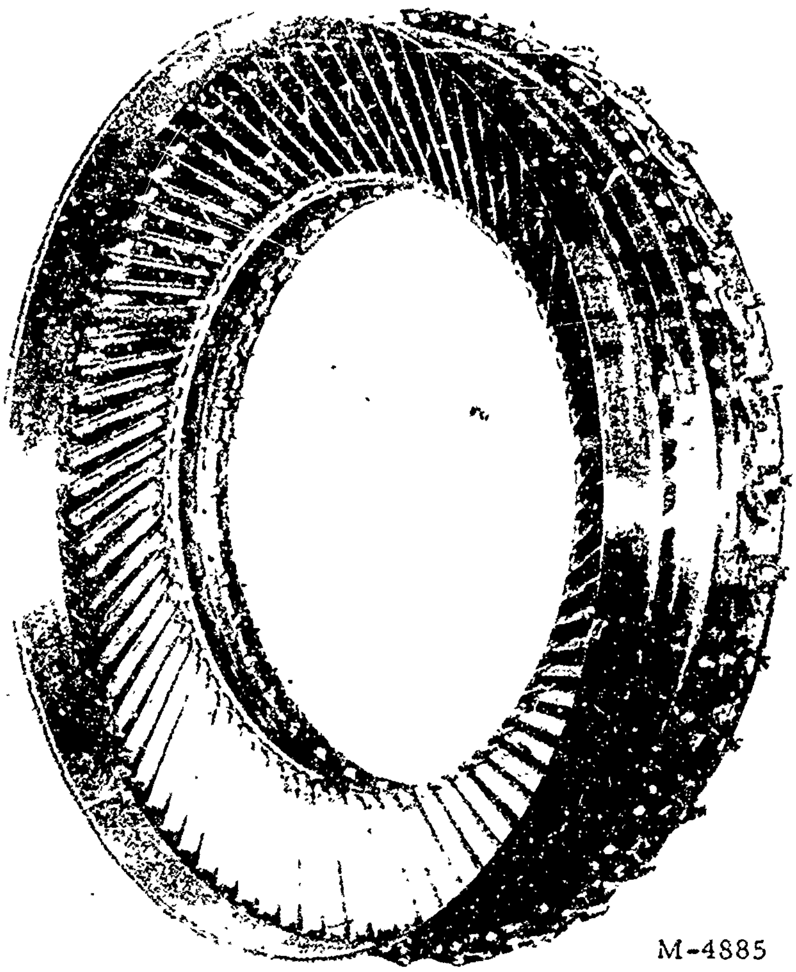

M-4885

SOUND-REFLECTING FAN EXIT STATOR

Figure 9-22

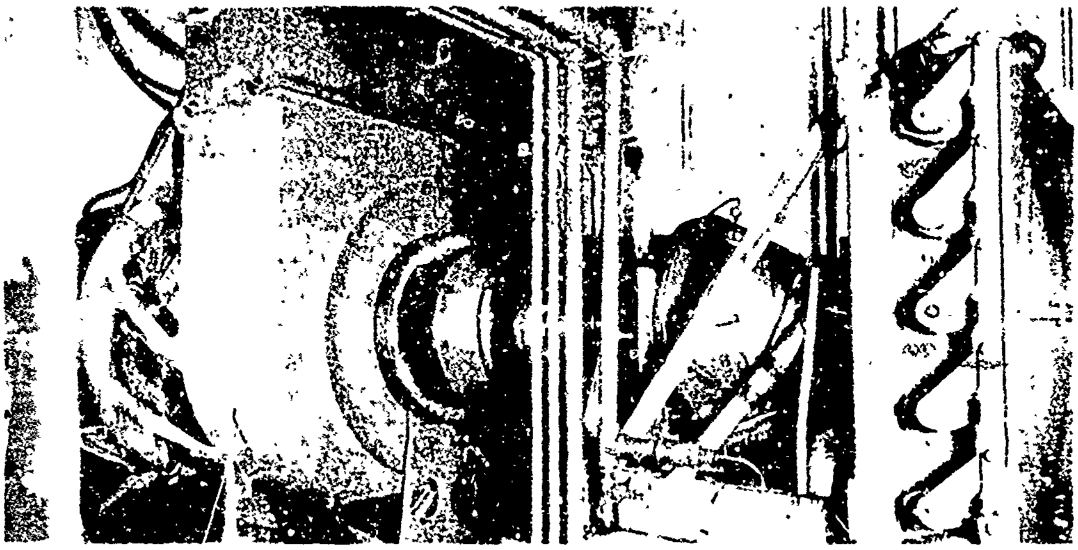

Drive Engine and Gearbox

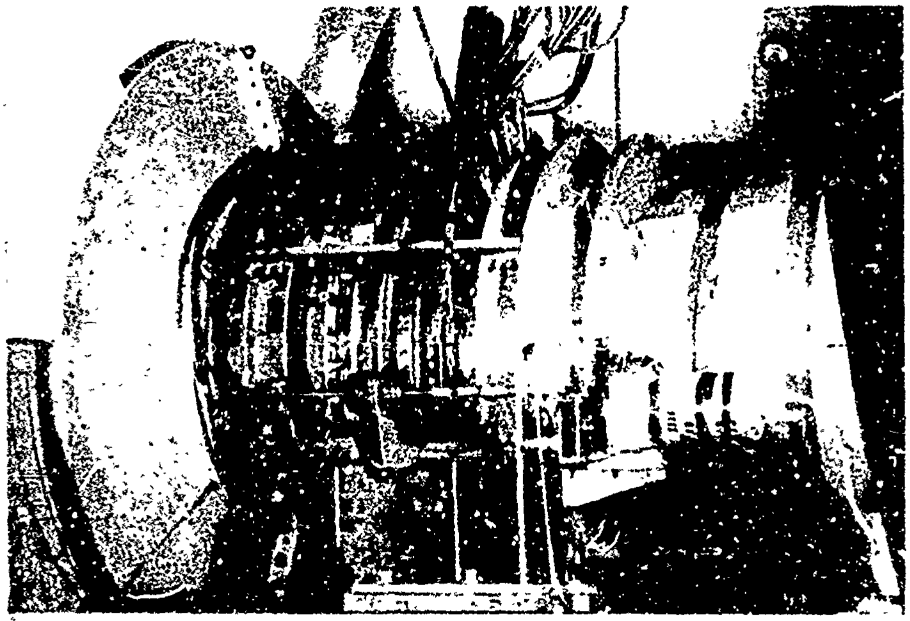

Compressor Rig

-INCH DIAMETER COMPRESSOR RIG AND DRIVE ENGINE

Figure 9-23

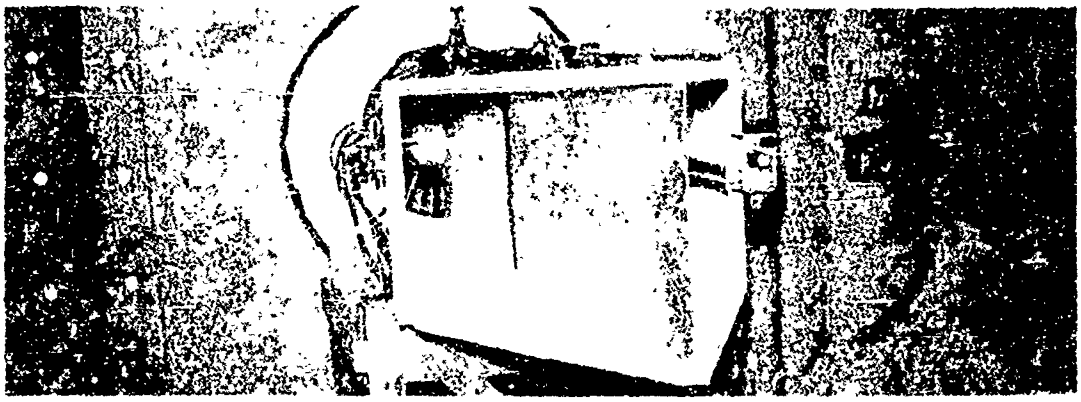

Inlet with Centerbody Collapsed; Configuration 1-L-1

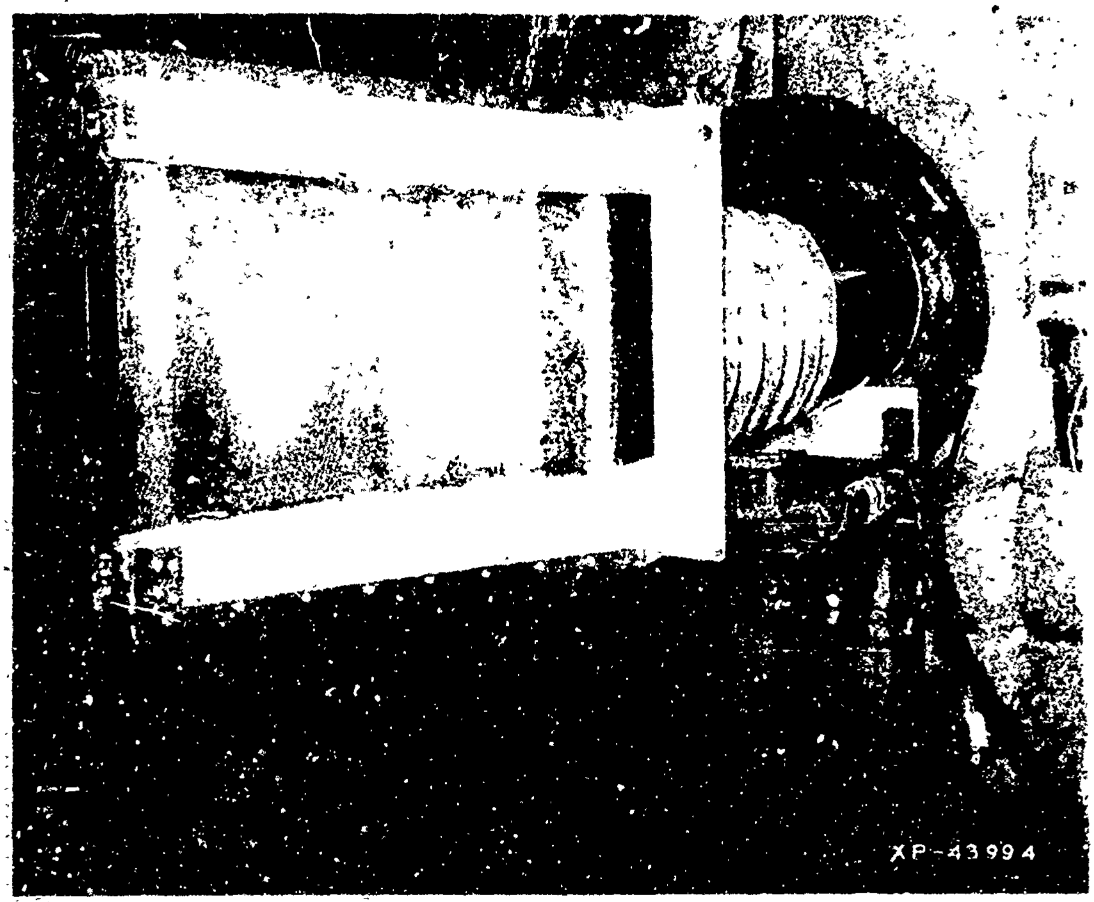

LOCKHEED SHAPE INLET

Figure 9-24

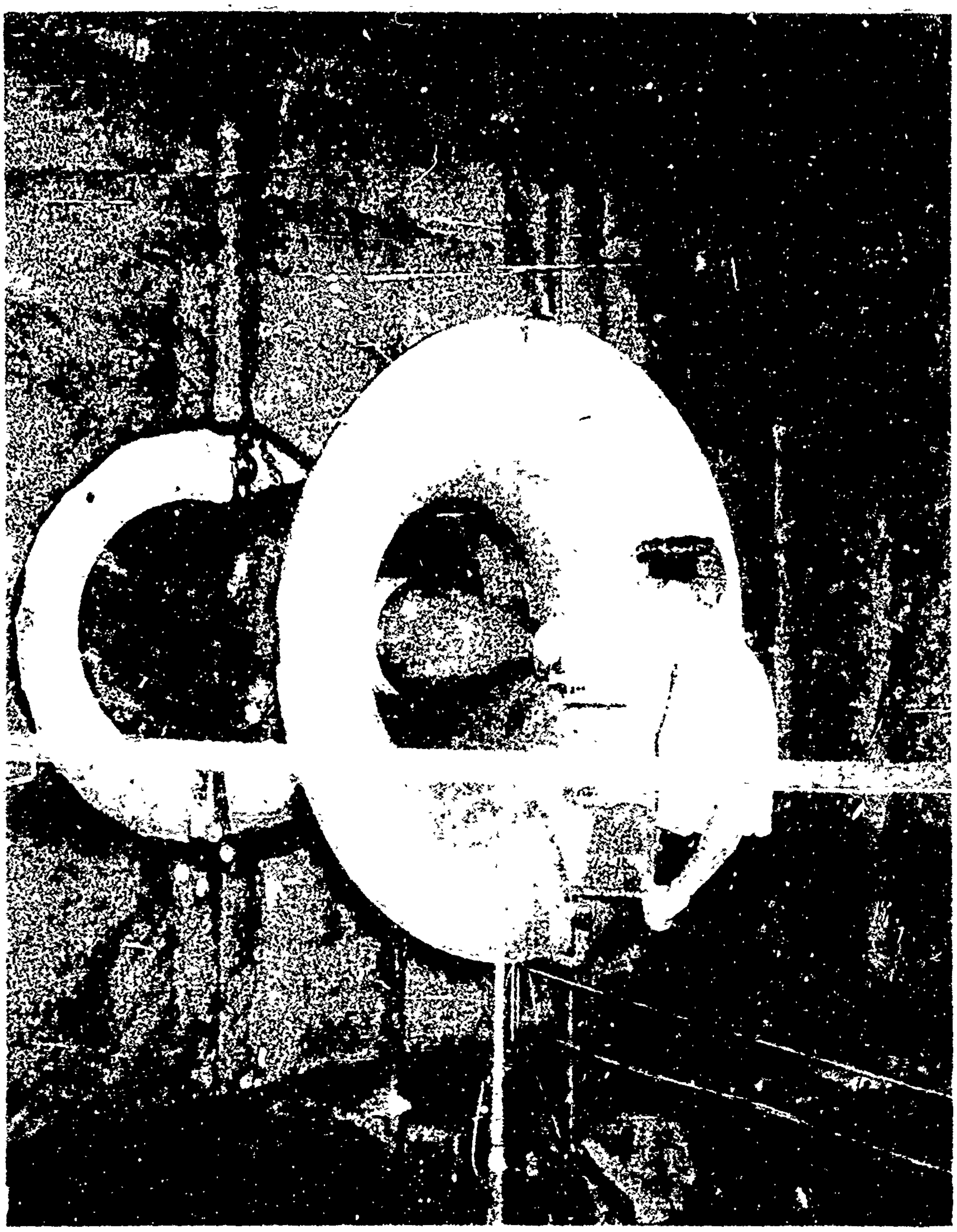

BOEING SHAPE INLET WITH PARTIALLY EXPANDED CENTERBODY

CONFIGURATION 2-B-2

Figure 9-25

Rear View of Configuration 1-B-1 with Collapsed Centerbody

Alternate Centerbodies   Airflow Areas: 3.5 ft^2, 2.5 ft^2, and 1.4 ft^2

BOEING SHAPE INLET AND ALTERNATE CENTERBODIES

Figure 9-26

Side View

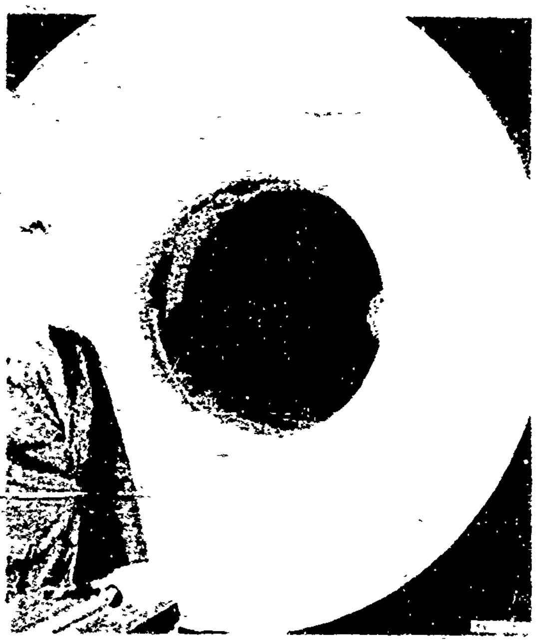

Front View

LONG INLET, CONFIGURATION 1-B-0

Figure 9-27

SHARP LIP INLET: CONFIGURATION 2-B-0A

Figure 9-28

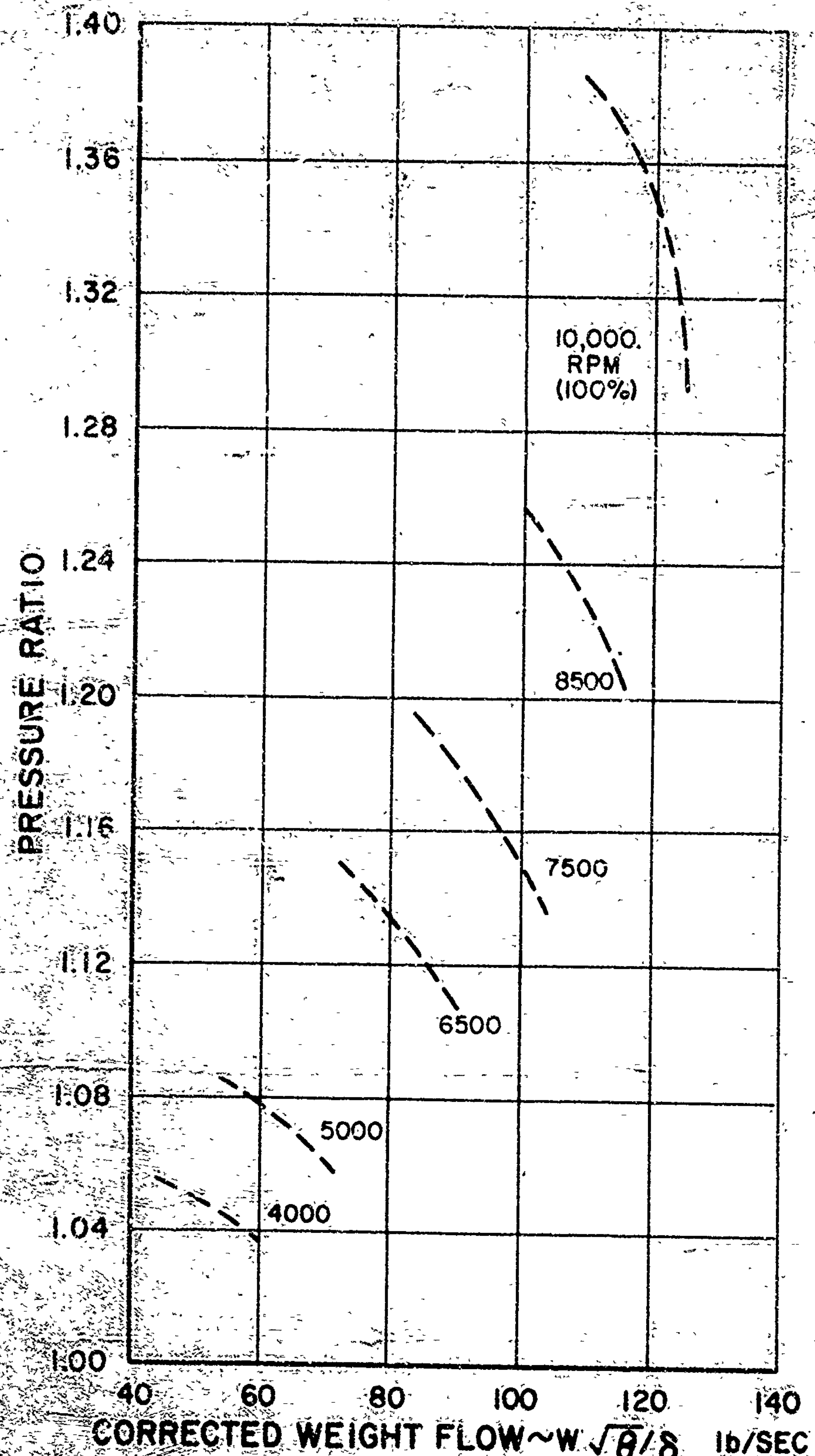

PERFORMANCE MAP OF 28-DIAMETER COMPRESSOR USED FOR NOISE INVESTIGATIONS

Figure 9-29

Object of Test	Result of Test	Test Configuration
To obtain a baseline for tests of the effect of inlet shape on a rig without inlet guide vanes	**Baseline Configuration** Sound documented over rig operating range	Reference Long Inlet Conf. 1-B-O 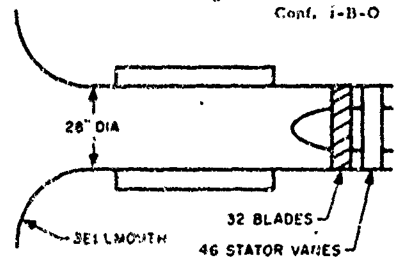 See Figure 9-27
To evaluate effects of the 4 equally spaced struts and long centerbody on discrete frequency noise.	**Compared with 1-B-O** Very little change in discrete noise levels or directivity. A level increase of 2 to 3 db occurred at low rig speeds, and a decrease of 3 to 4 db occurred at maximum rig speeds	Boeing Shape Inlet, Center Body Collapsed, with Struts Conf 1-B-1 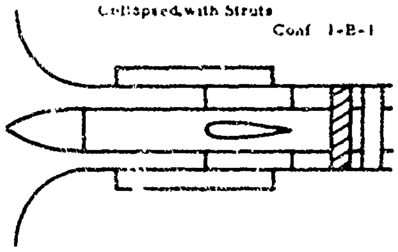 See Figure 9-26
To evaluate the effect of the Lockheed two-dimensional shaped inlet on discrete noise	**Compared with 1-B-1** No significant changes in sound level or directivity over the speed range surveyed (40 to 65% maximum rpm)	Lockheed Shape Inlet, Center Body Collapsed Conf 1-L-1 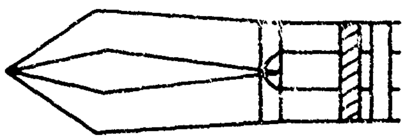 See Figure 9-24
To obtain a baseline for long duct tests on a rig with inlet guide vanes.	**Baseline Configuration** Sound documented over rig operating range.	Standard Rig Bellmouth Inlet Conf. 2R 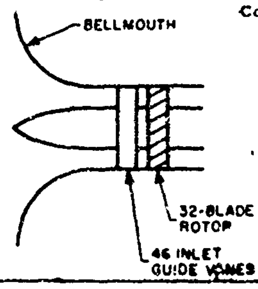
To determine the effect of a 54-inch cylindrical extension of the inlet duct on the propagation of discrete noise and to provide a baseline for further tests	**Compared with Conf. 2R** Levels of discrete noise were essentially similar at low rig speeds, increased slightly at 65% max. speed, and were reduced by 6 to 8 db at maximum rig speed. See Figure 9-36.	Reference Long Duct Conf. 2-B-O 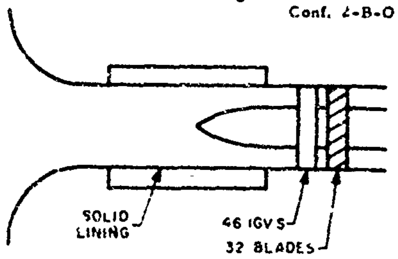

RESULTS OF NOISE TESTS
Figure 9-30
Sheet 1 of 3

Object of Test	Results of Test	Test Configuration
To evaluate the effects of a sharp lipped air intake.	Compared with 2-B-O Essentially no change in sound energy propagated but considerable change in sound quality. Discrete frequencies were not audible. See spectrum display, Figure 9-33.	Sharp Lip Inlet Conf. 2-B-OA 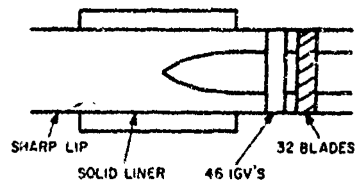 See Figure 9-28
To determine the effects of the cylindrical center body	Compared with 2-B-O No significant change in either level or directivity pattern	Boeing Shaped Inlet, Center Body Collapsed, No Struts 3.5 sq. ft. Airflow Area Conf. 2-B-1 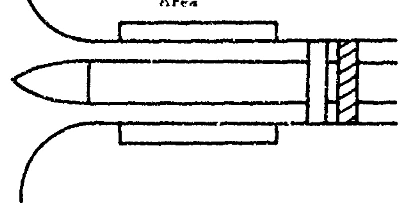
To determine the effect of centerbody shape and inlet duct velocity on noise	Compared with 2-B-1 No significant changes when throat Mach number was below 0.5. Effectively no discrete noise propagated when inlet choked. *	Boeing Shaped Inlet with Partially Expanded Center Body, 2.5 sq. ft. Thrust Area Conf. 2-B-2 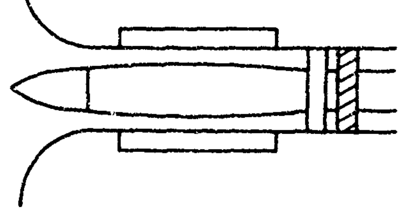 See Figure 9-25
To determine the effect of centerbody shape and inlet duct velocity on noise	Compared with 2-B-1 and 2-B-2 No significant changes where throat Mach number was below 0.5. Substantial reductions occurred where throat mach numbers approached unity. Essentially no discrete noise propagated when inlet choked *	Boeing Shaped Inlet with Fully Expanded Center Body, 1.4 ft.^{2} Throat Area Conf 2-B-3 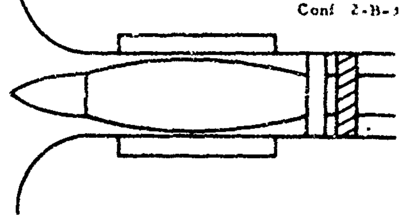 See Figure 9-26
To determine the effects of acoustical lining in an inlet duct.	Compared with 2-B-1 Discrete noise levels at angles of 30 to 90 degrees from the compressor centerline were reduced by 10 to 15 db at rig speeds up to 75% of maximum, and by 5 to 10 db at 85% of maximum to maximum rig speeds. See Figure 9-34	Fiberglas Lined Boeing Shaped Inlet With Collapsed Center Body 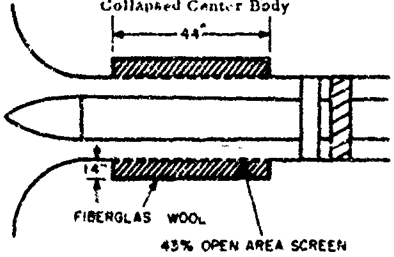 Conf. 2-BA1-1

*See Panoramic spectrum display, Figure 9-31, and curve, Figure 9-32, showing the effect of inlet Mach number on noise.

RESULTS OF NOISE TESTS (Cont'd.)

Figure 9-30

Sheet 2 of 3

Object of Test	Results of Test	Test Configuration
To determine the effect of a convergent-divergent type center body on the sound attenuation characteristics of an acoustically lined duct.	Compared with Conf. 2-BA1-1 No significant changes in the effectiveness of the lining.	Fiberglas Lined Boeing Shaped Inlet With Partially Expanded Center Body 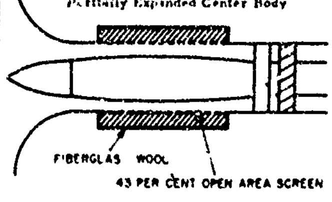 Conf. 2-BA1-2
To determine the effect of lining the duct with 43% open area screen.	Compared with Conf. 2-B-2 The discrete frequencies in the noise spectrum were replaced by bands of high frequency random noise. The levels of the discrete noise were reduced by 4 to 7 db, but the overall noise level was not reduced.	Screen Lined Boeing Shaped Inlet With Partially Collapsed Center Body Conf. 2-BA2-2 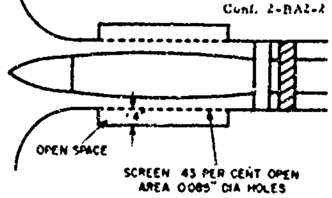
To determine the effects of a combination of 43% open area screen and 1.2% open area perforated metal liners	Compared with 2-B-2 No significant noise reduction	Boeing Shaped Inlet with Combination Perforated Lining, No Air Bleed Conf. 2-BA3-2 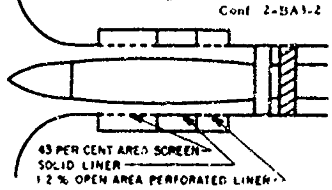
To determine the effects of natural bleed flow through the 1.2% open area perforated liner	Compared with 2-BA3-2 Consistent noise reduction of 2 to 4 db at all conditions	Boeing Shaped Inlet Combination Perforated Lining with Bleed Air Flow Conf. 2-BA3B-2 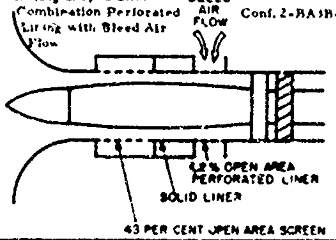
To further evaluate the effects of the Lockheed two-dimensional shaped inlet on the propagation of compressor noise To determine if the sound patterns were symmetrical in the horizontal and vertical planes.	Compared with Conf. 2-L-1 Little change in sound spectra properties, but an improved directivity pattern showed lower peak for lower noise levels about 4 db. See Figure 9-45. Near field effects excluded, the horizontal and vertical radiation patterns were similar.	Lockheed Model Inlet with Collapsed Centerbody Conf. 2-L-1 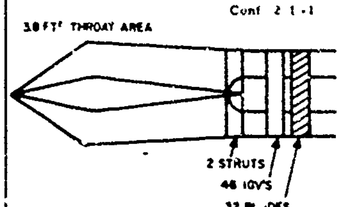
To measure the attenuation of inlet noise due to inlet throat Mach number rear units.	Compared with Conf. 2-L-1 Significant sound attenuation occurred at throat Mach numbers above 0.7, with complete sonic blockage occurring near Mach 0.9. See Figure 9-32	Lockheed Model Inlet with Fully Expanded Centerbody Conf. 2-L-3 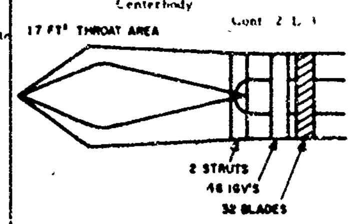

RESULTS OF NOISE TESTS (Cont'd.)

Figure 9-30

Sheet 3 of 3

Effect of Choked Inlet on Noise

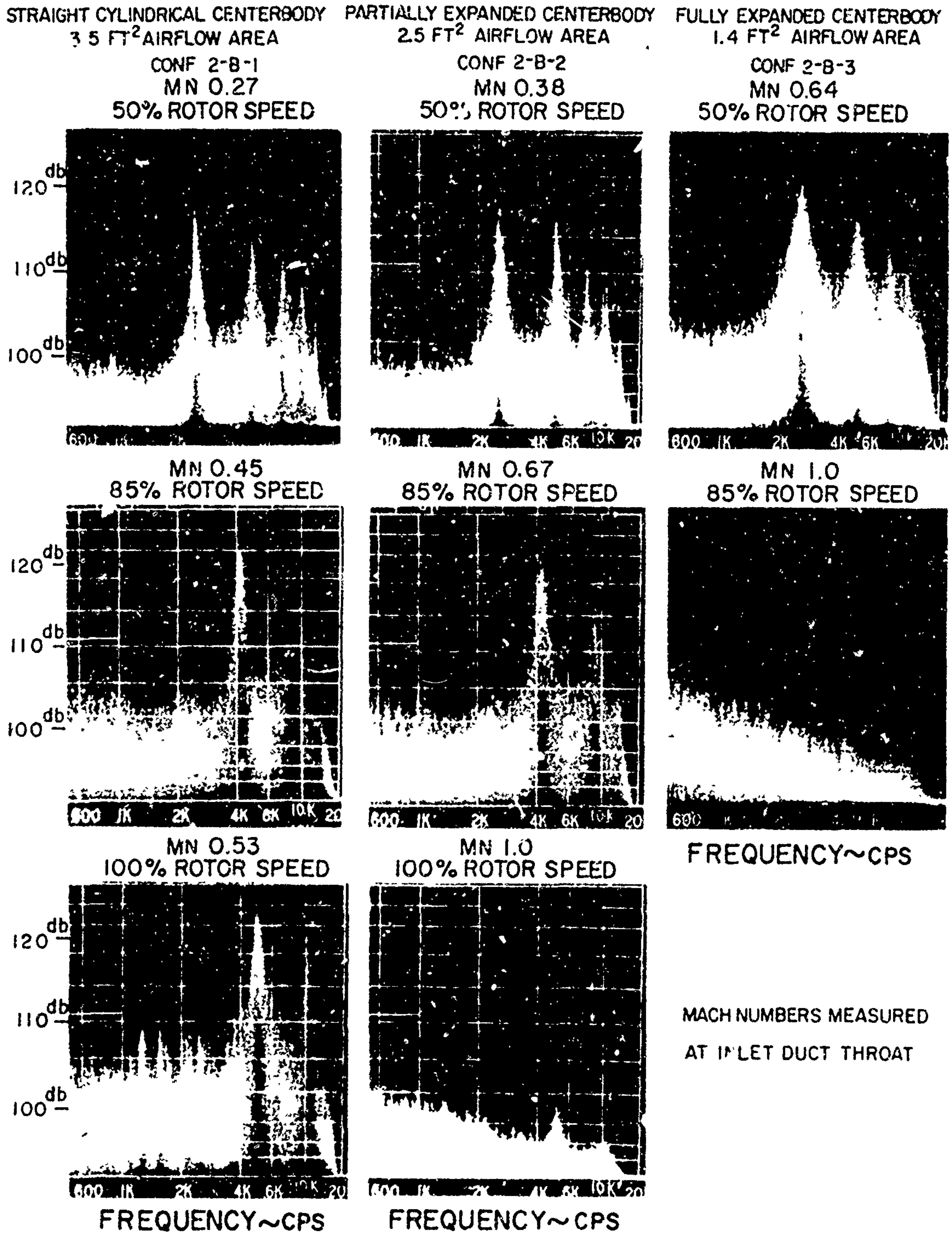

SOUND SPECTRUM OF 28-INCH DIAMETER NOISE RIG

Figure 9-31

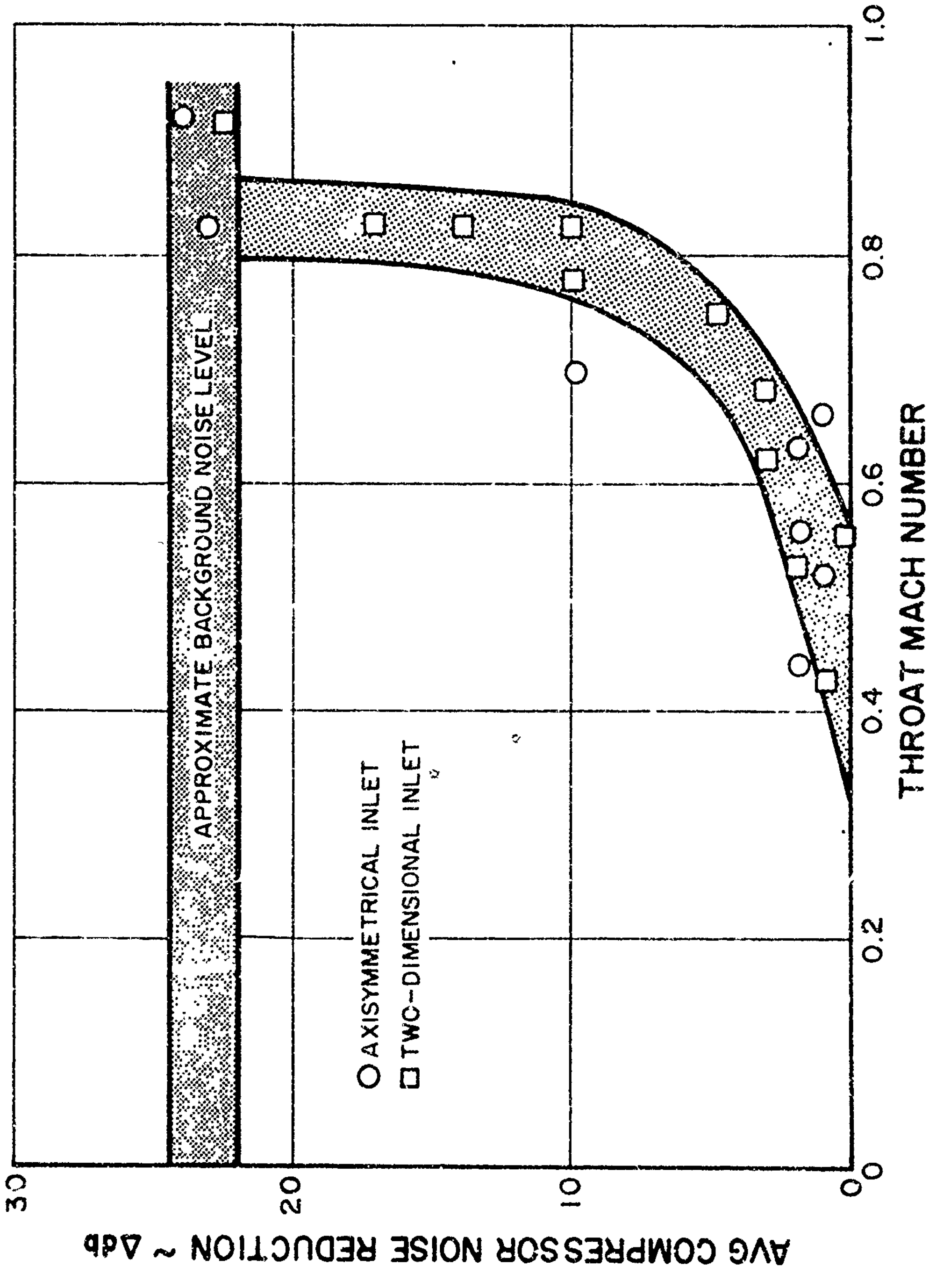

EFFECT OF INLET MACH NUMBER ON NOISE PROPAGATION

Figure 9-32

Effect of Sharp Lip Inlet on Noise Spectrum

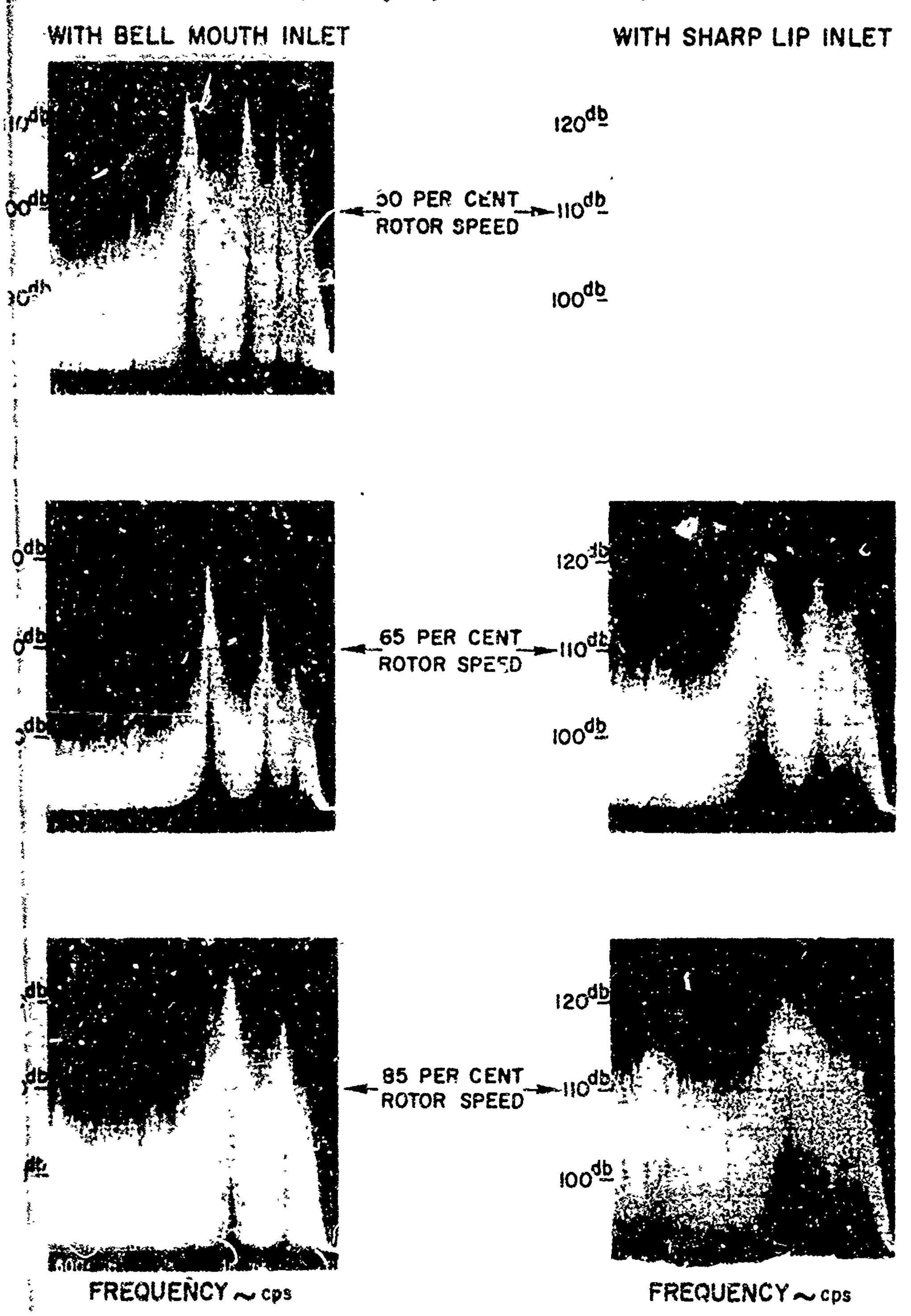

SOUND SPECTRUM OF 28-INCH DIAMETER NOISE RIG
WITH 54-INCH CYLINDRICAL EXTENSION
Figure 9-33

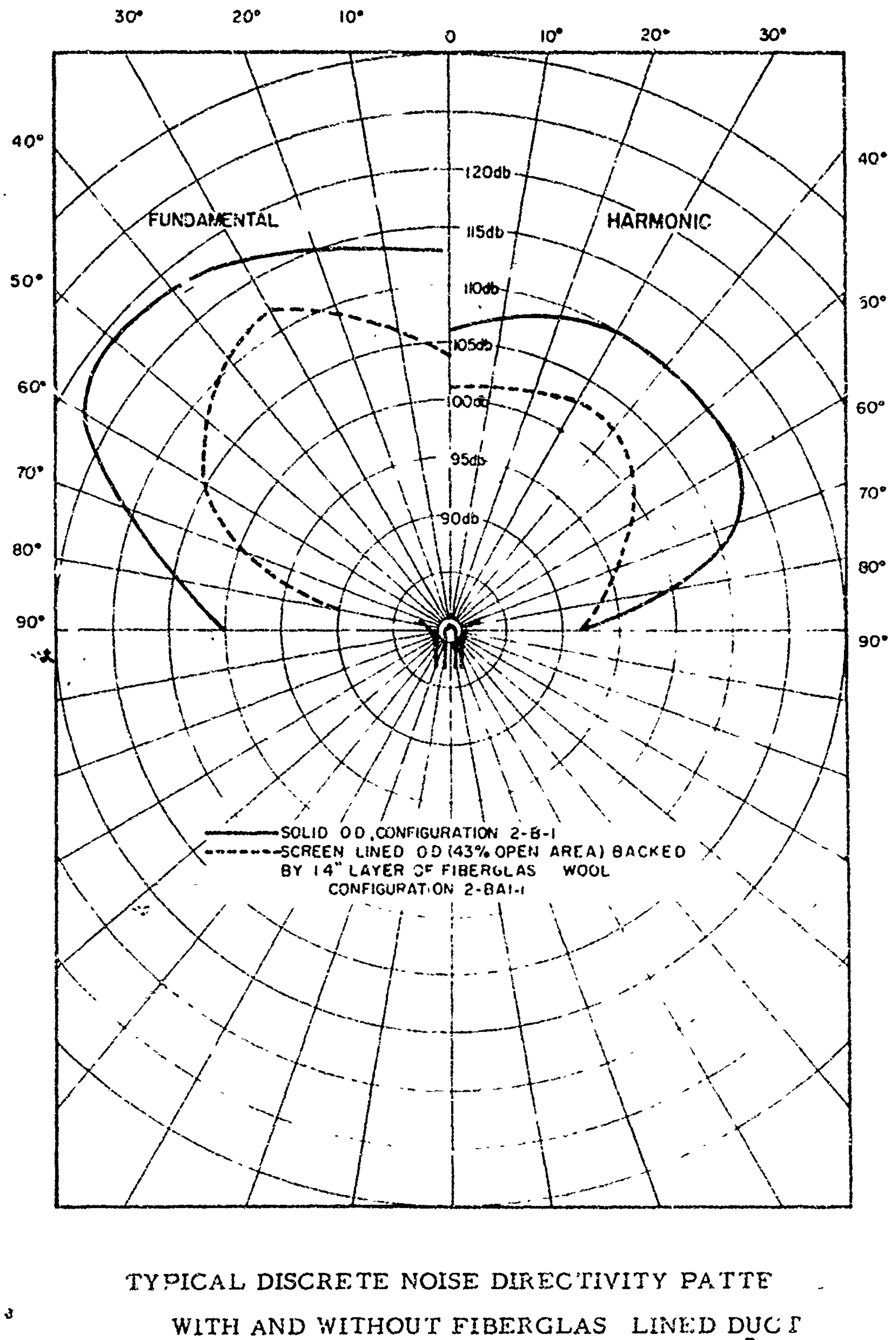

TYPICAL DISCRETE NOISE DIRECTIVITY PATTE
WITH AND WITHOUT FIBERGLAS LINED DUCT

Figure 9-34

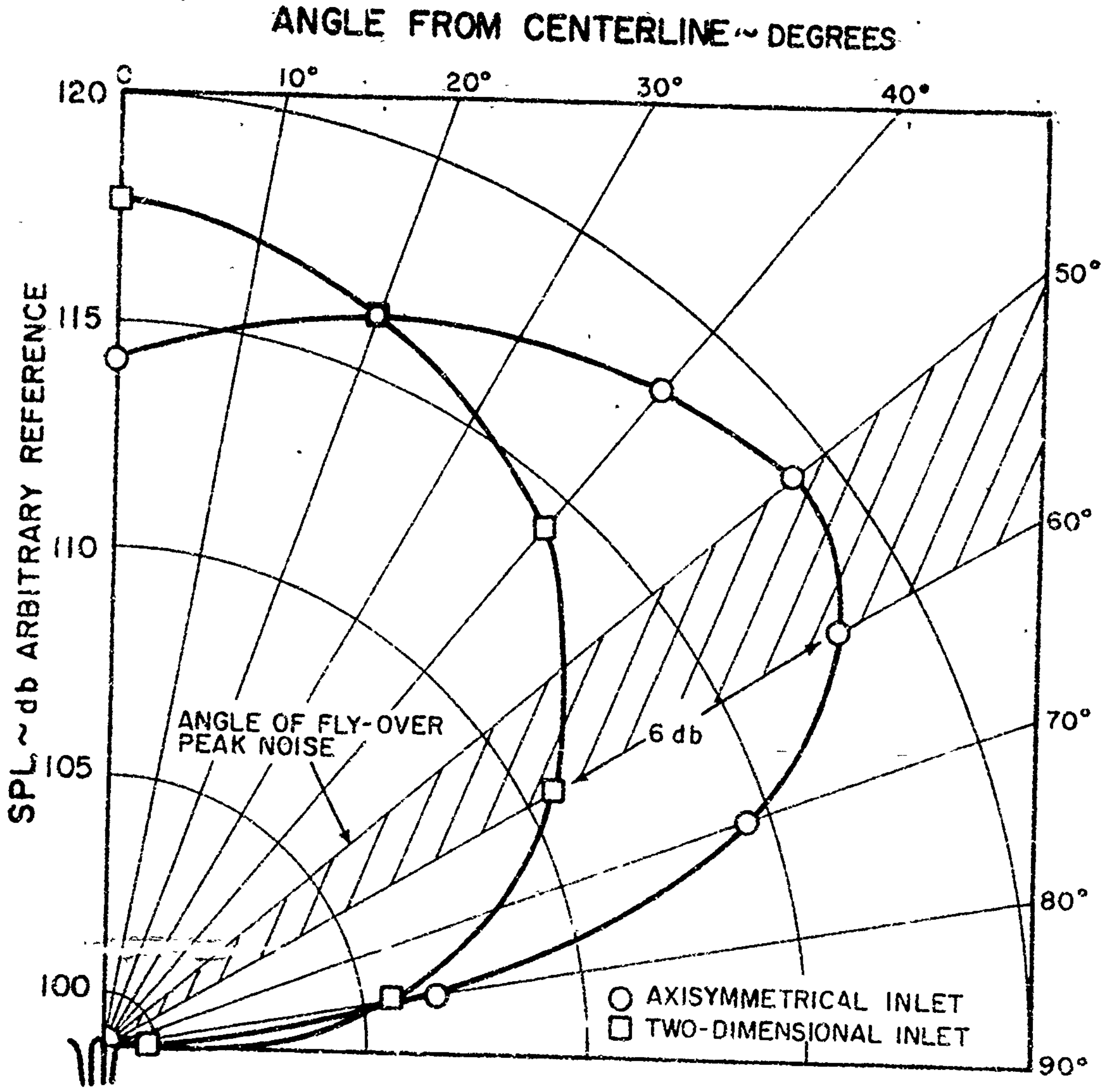

TYPICAL DIRECTIVITY OF FUNDAMENTAL DISCRETE FREQUENCY NOISE FOR AXISYMMETRICAL AND TWO-DIMENSIONAL INLETS

Figure 9-35

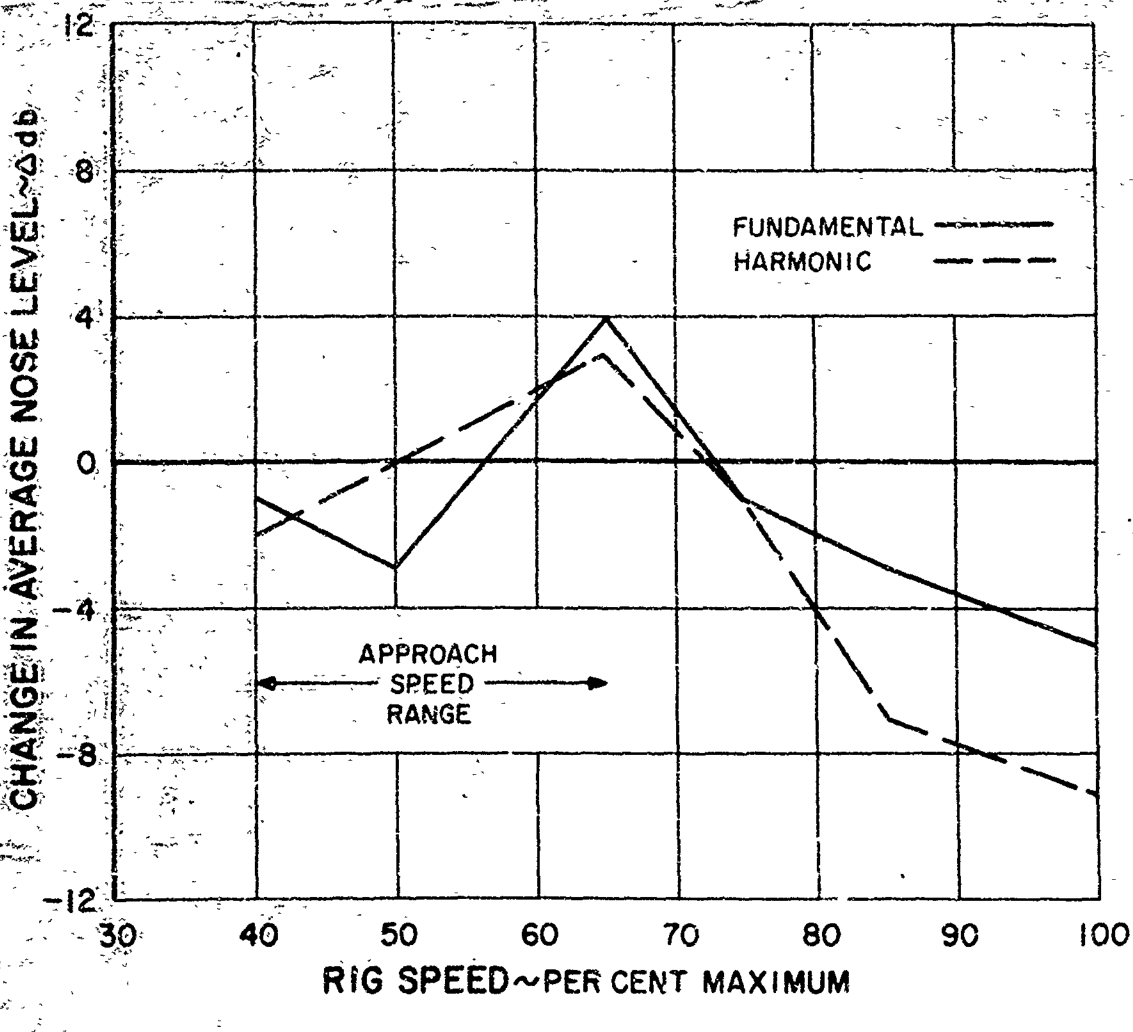

EFFECT ON AVERAGE NOISE LEVEL
OF 54-INCH EXTENSION OF INLET DUCT
Figure 9-36

X-18294

REVERBERATION CHAMBER TEST FACILITY

Figure 9-37

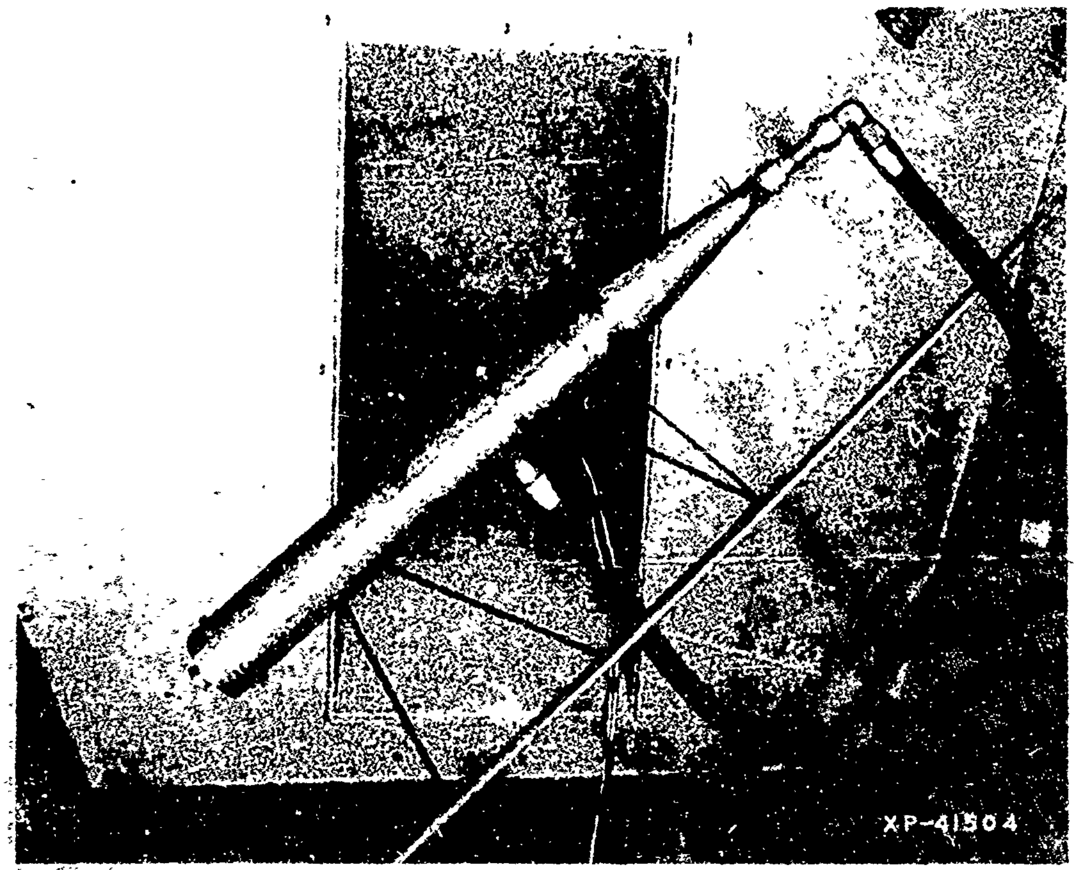

MODEL PULSE-JET USED AS NOISE SOURCE
IN REVERBERATION CHAMBER TESTING
Figure 9-38

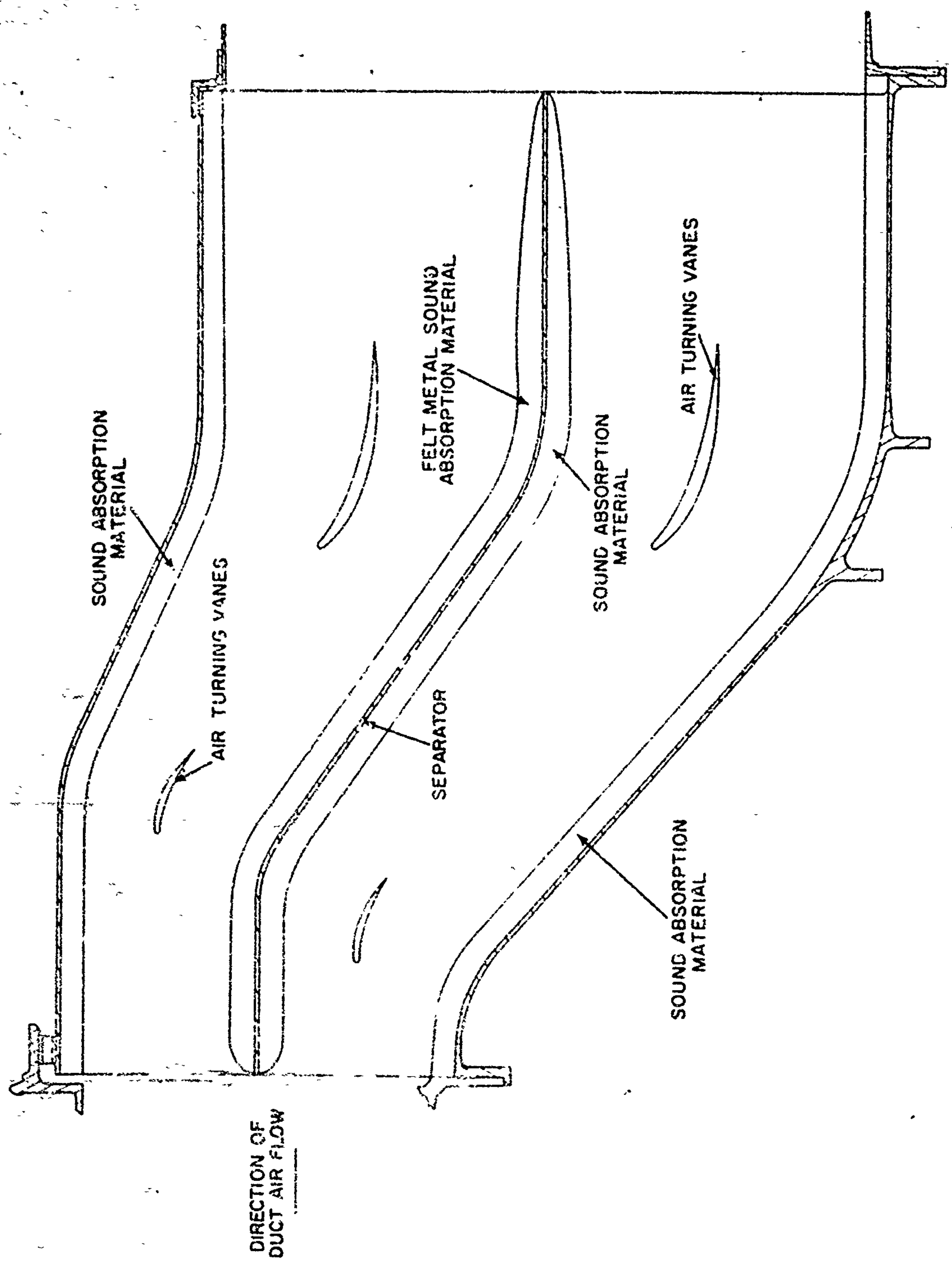

STF219 FAN DISCHARGE DUCT
SHOWING LOCATION OF SOUND ABSORPTION MATERIALS

Figure 9-39

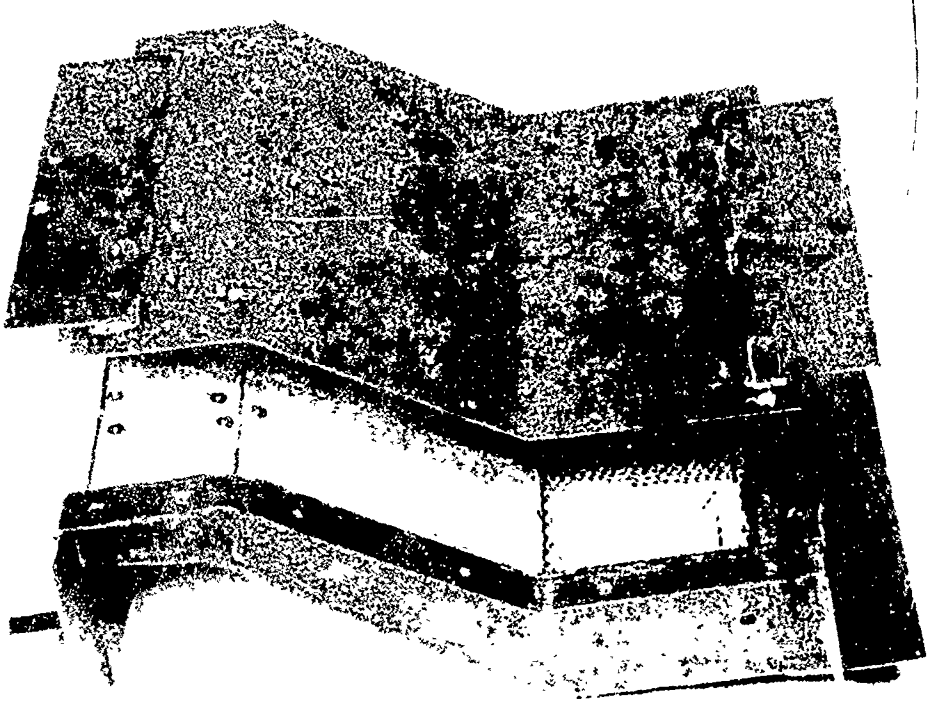

XP-45412

FAN DISCHARGE DUCT MODEL

FOR TESTING OF SOUND ABSORPTION MATERIALS

Figure 9-40

SOUND ABSORPTION MATERIALS
TESTED IN FAN DISCHARGE DUCT MODEL

Treatment	Absorbent	Backing Material	Total Thickness
A	0.125 in. Feltmetal	None	0.125 in.
B	0.125 in. Feltmetal	0.125 in. Honeycomb	0.250 in.
C	0.375 in. Feltmetal	None	0.375 in.
D.	0.125 in. Feltmetal	0.375 in. Honeycomb	0.500 in.

Feltmetal - 430 stainless steel felted fibers with 20% density

Honeycomb - 0.250 in. center Hex aluminum

Figure 9-41

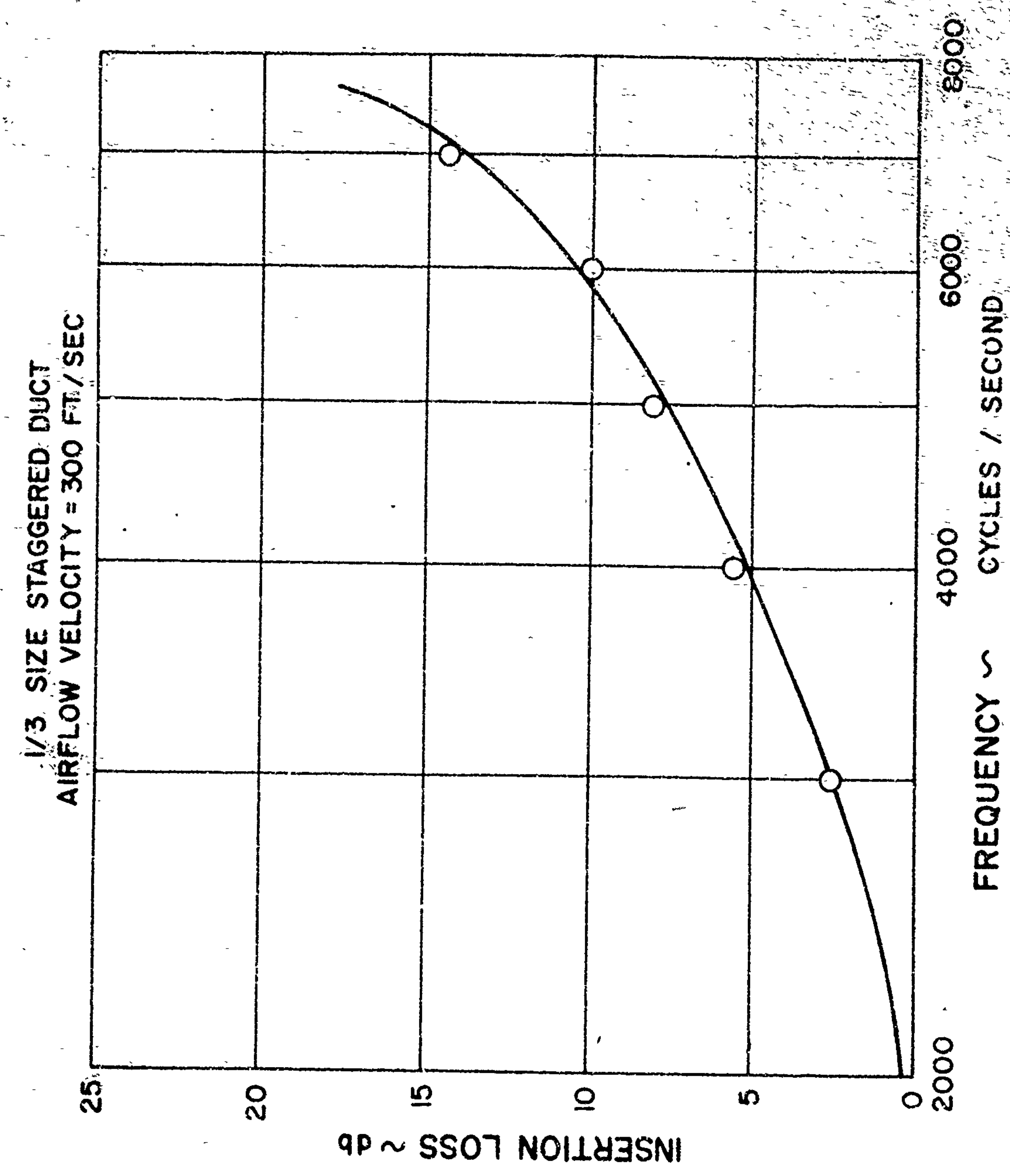

INSERTION LOSS WITH FAN DUCT LINING A

Figure 9-42

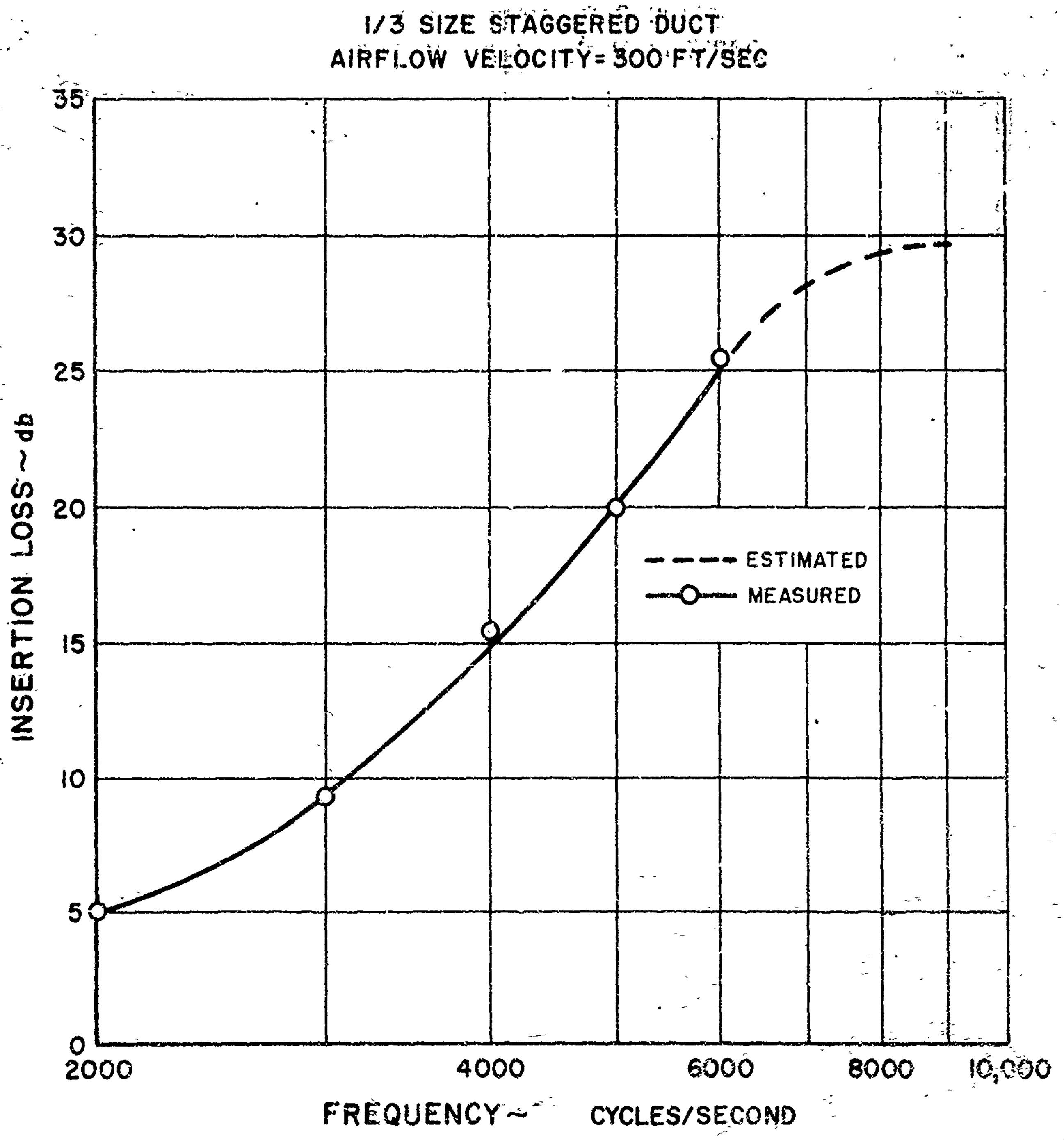

INSERTION LOSS WITH FAN DUCT LINING B

Figure 9-43

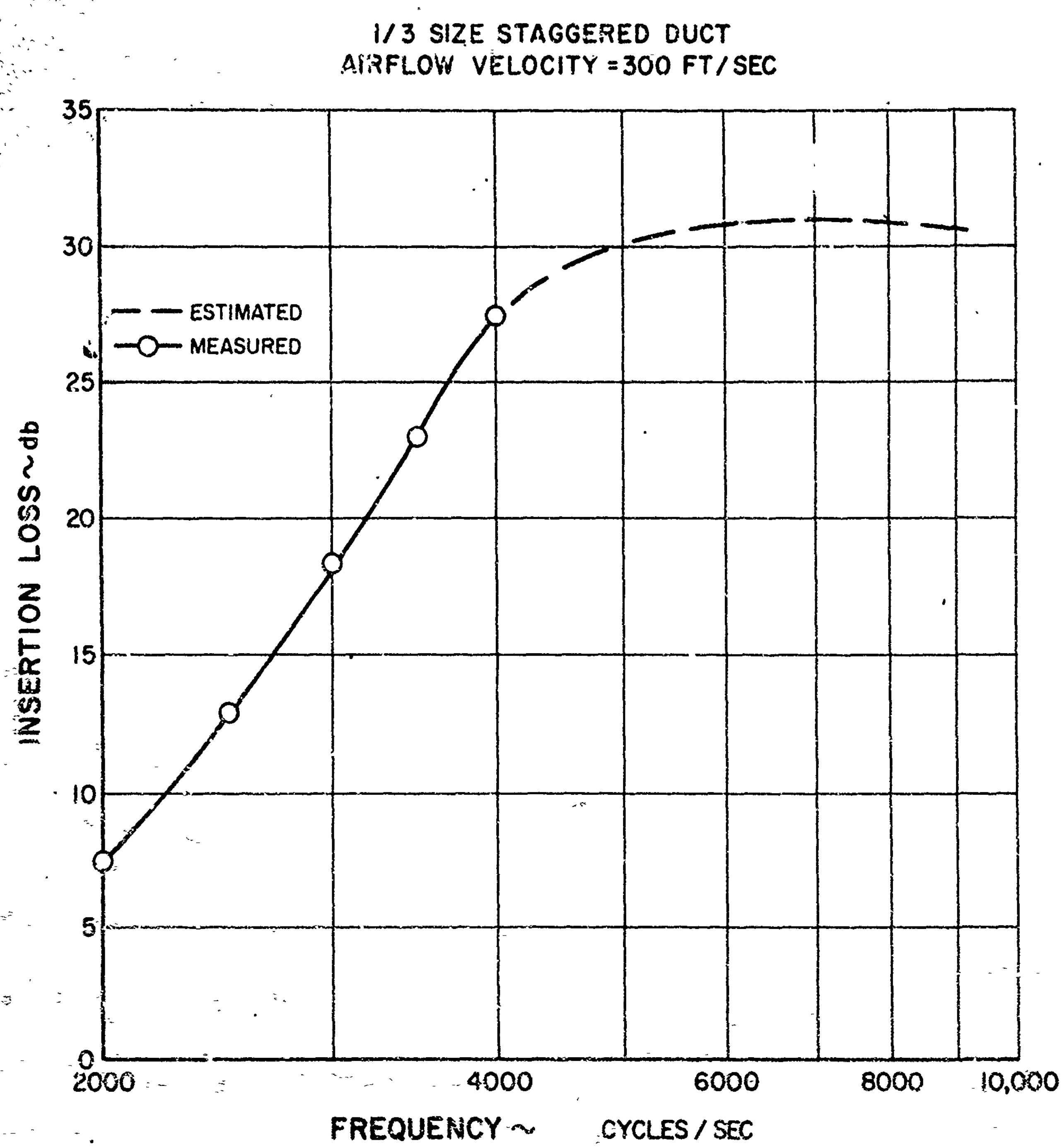

INSERTION LOSS WITH FAN DUCT LINING C

Figure 9-44

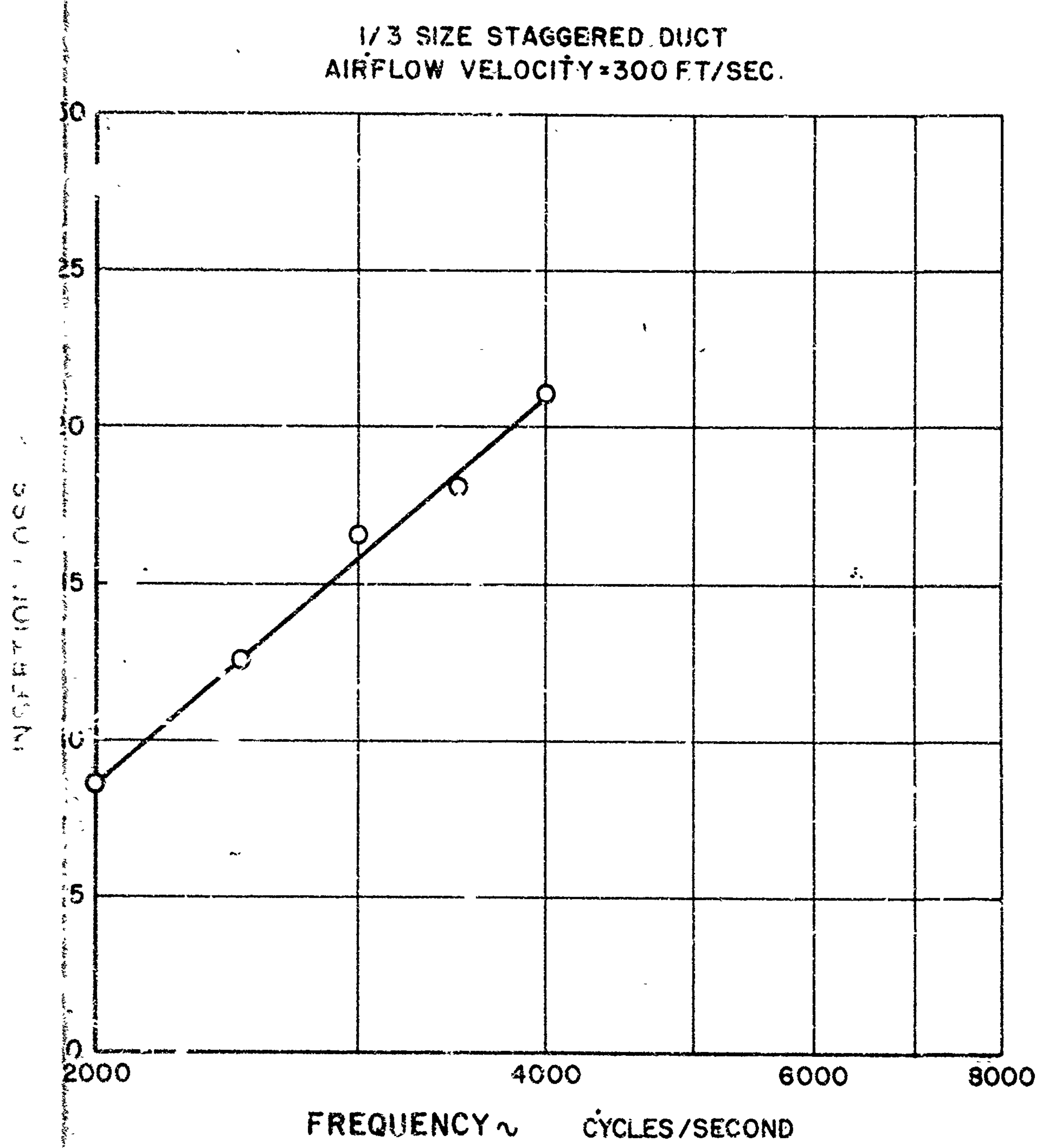

INSERTION LOSS WITH FAN DUCT LINING D

Figure 9-45

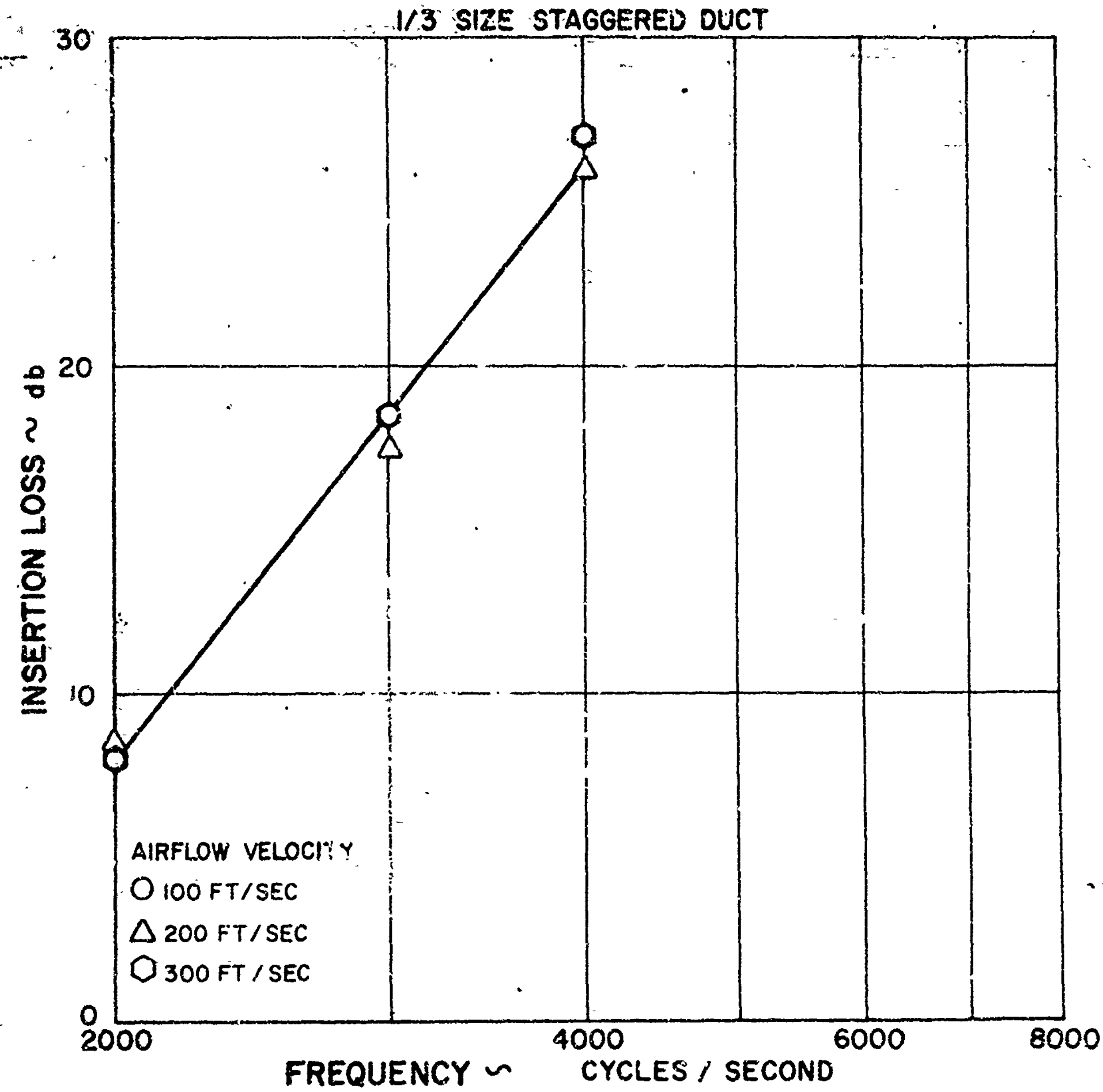

EFFECT OF FLOW VELOCITY ON INSERTION LOSS
WITH FAN DUCT LINING C

Figure 9-46

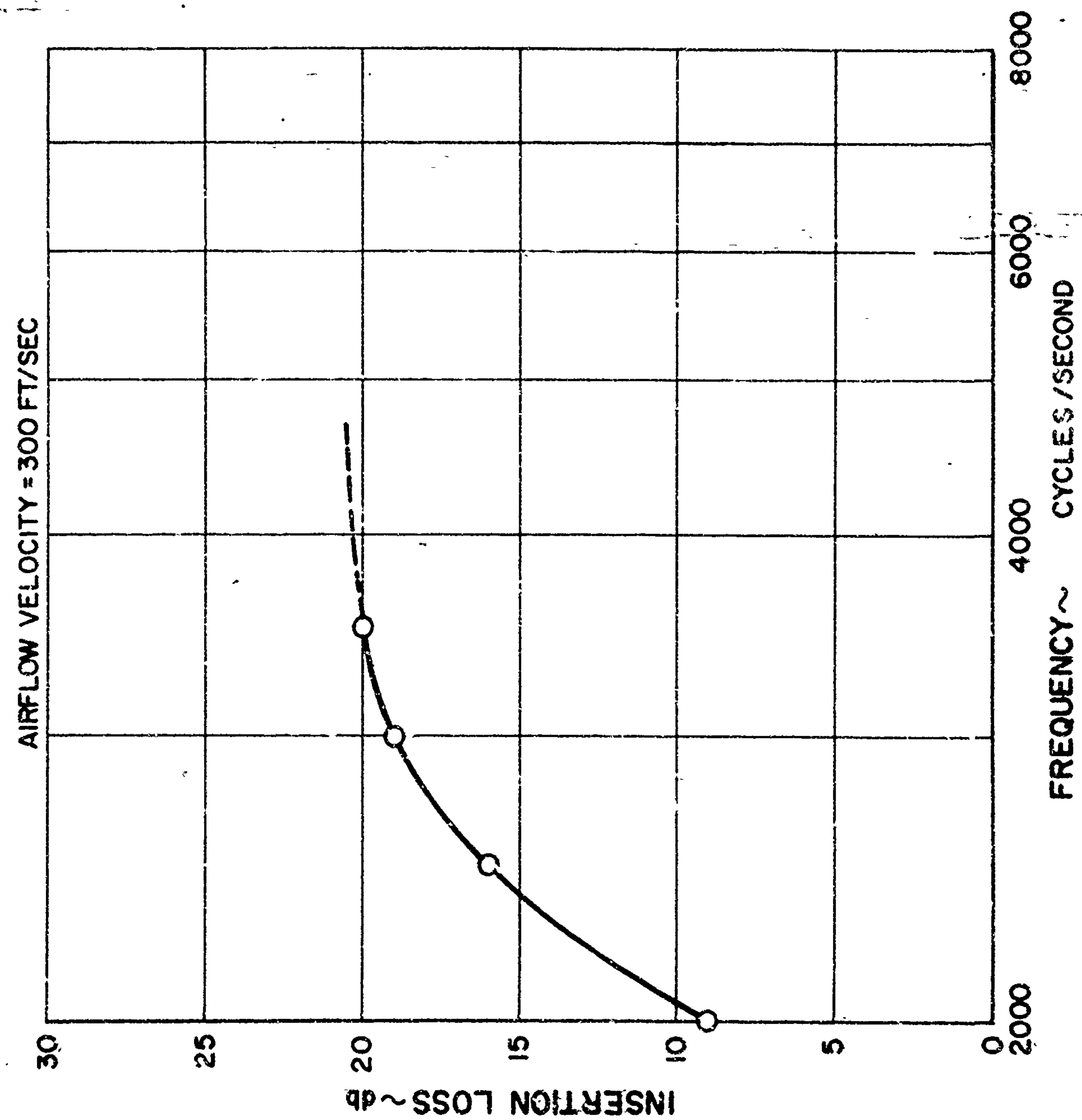

INSERTION LOSS WITH FAN DUCT LINING C
IN ONE-HALF SIZE STAGGERED DUCT
Figure 9-47

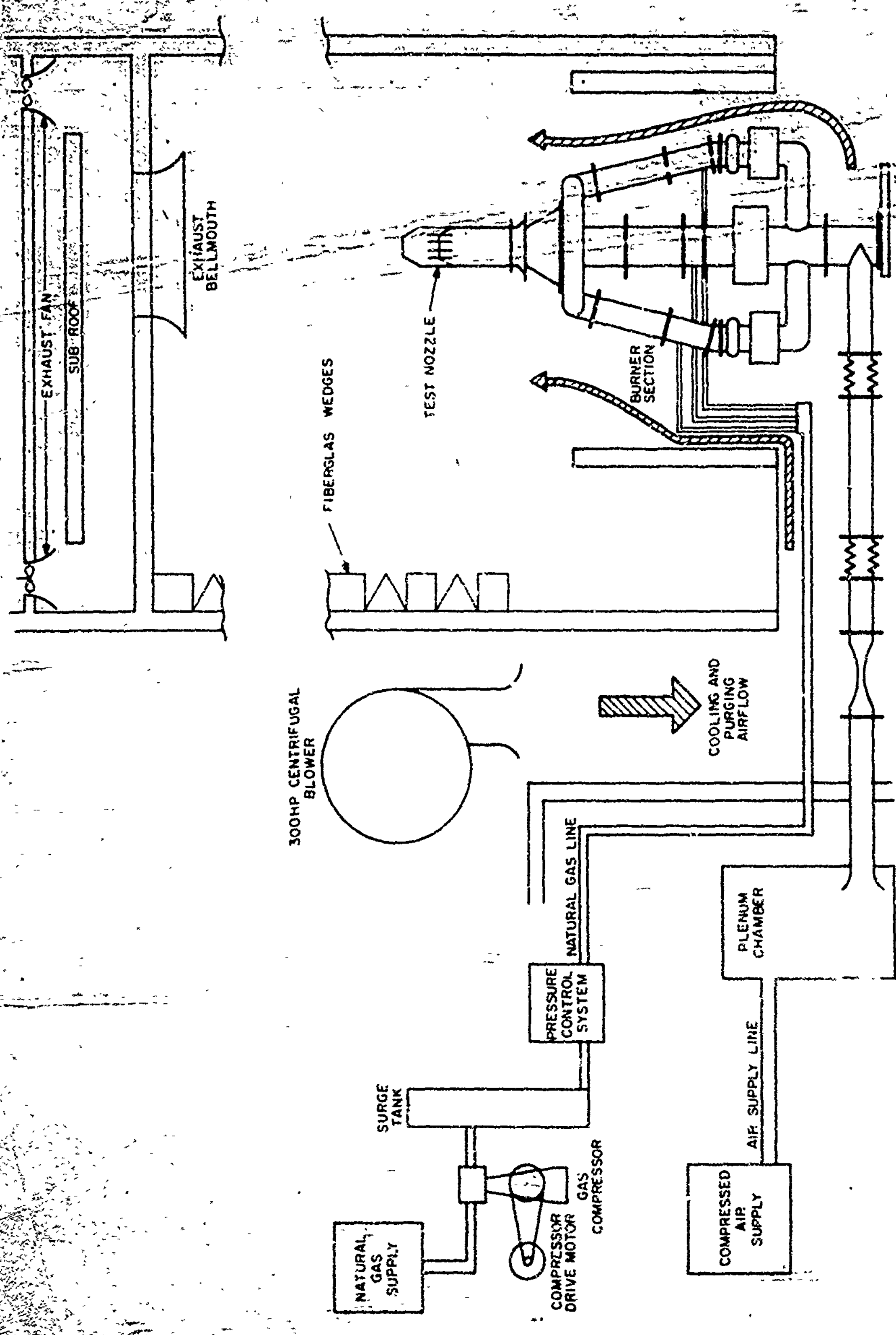

OVERALL DIAGRAM OF ANECHOIC CHAMBER TEST FACILITY

Figure 9-48

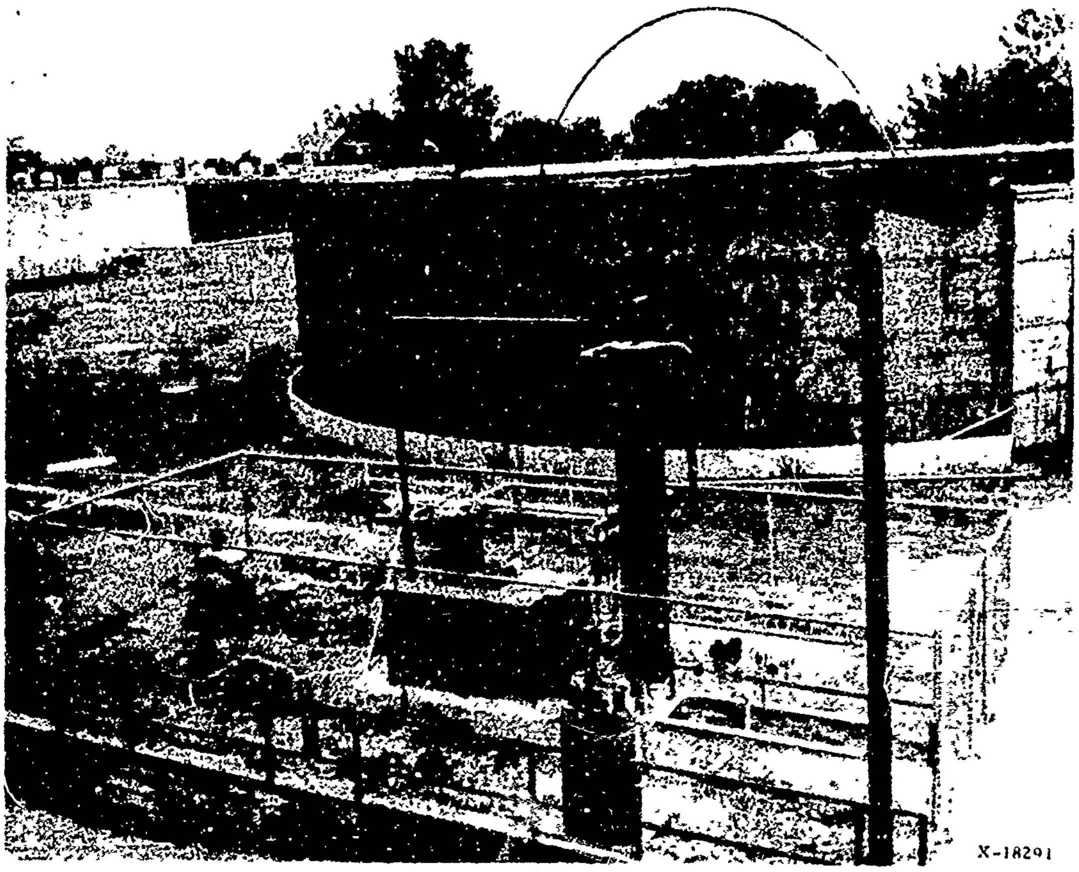

X-18291

NATURAL GAS FUEL SUPPLY SYSTEM

Figure 9-49

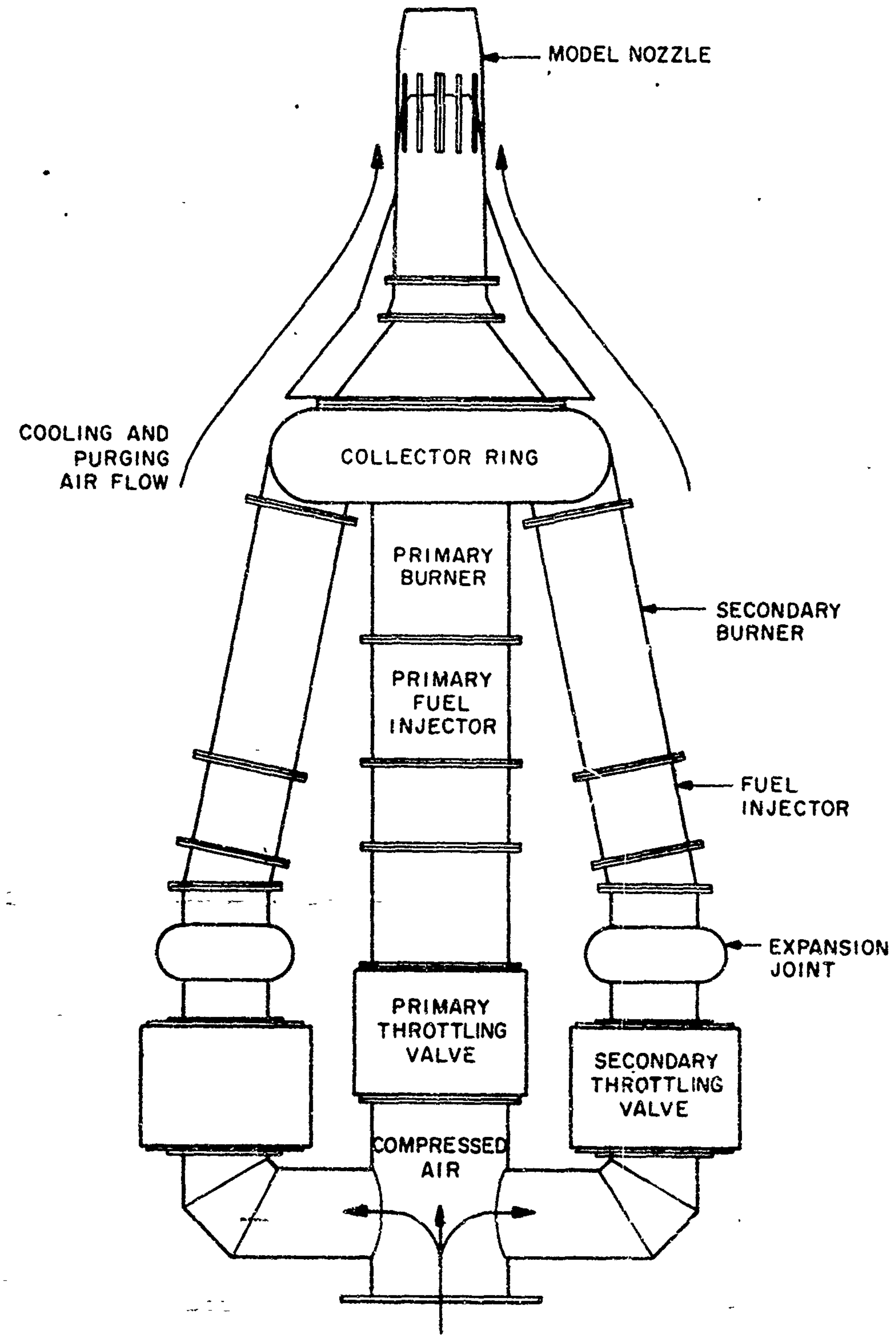

SCHEMATIC DIAGRAM OF BURNER SECTION
IN ANECHOIC CHAMBER
Figure 9-50

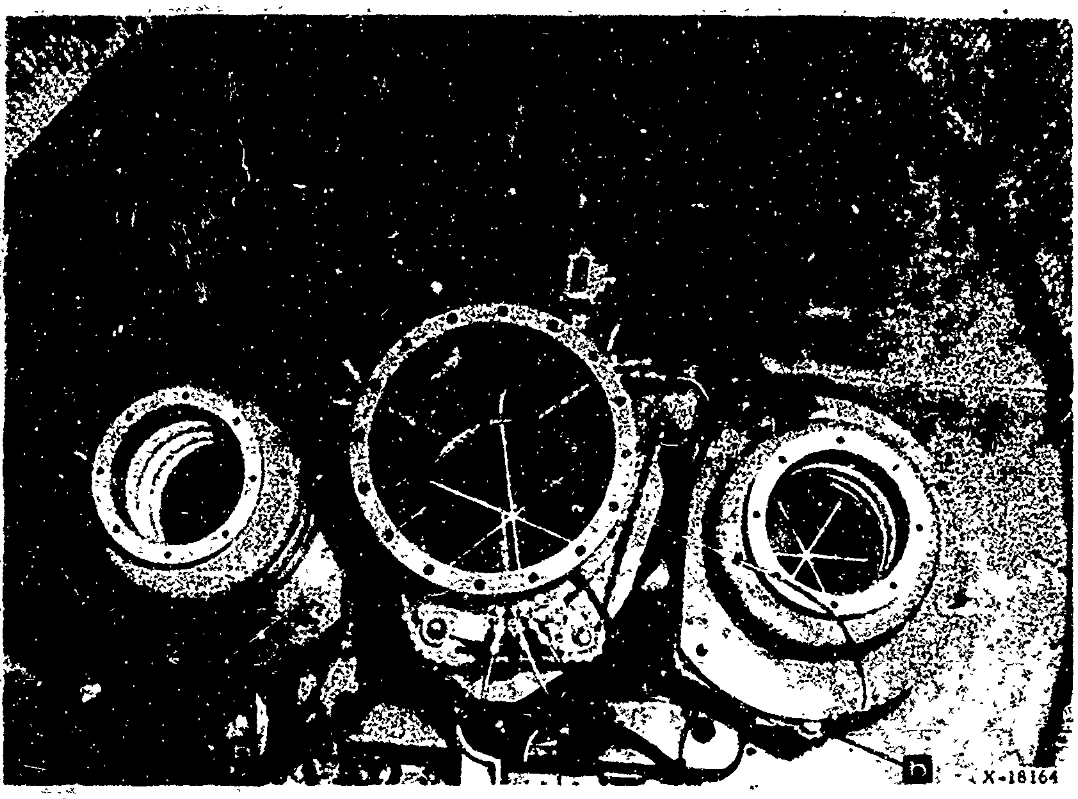

a. Chain drive for primary valve

b. Chain drives for secondary valves

PRIMARY AND SECONDARY THROTTLING VALVES

Figure 9-51

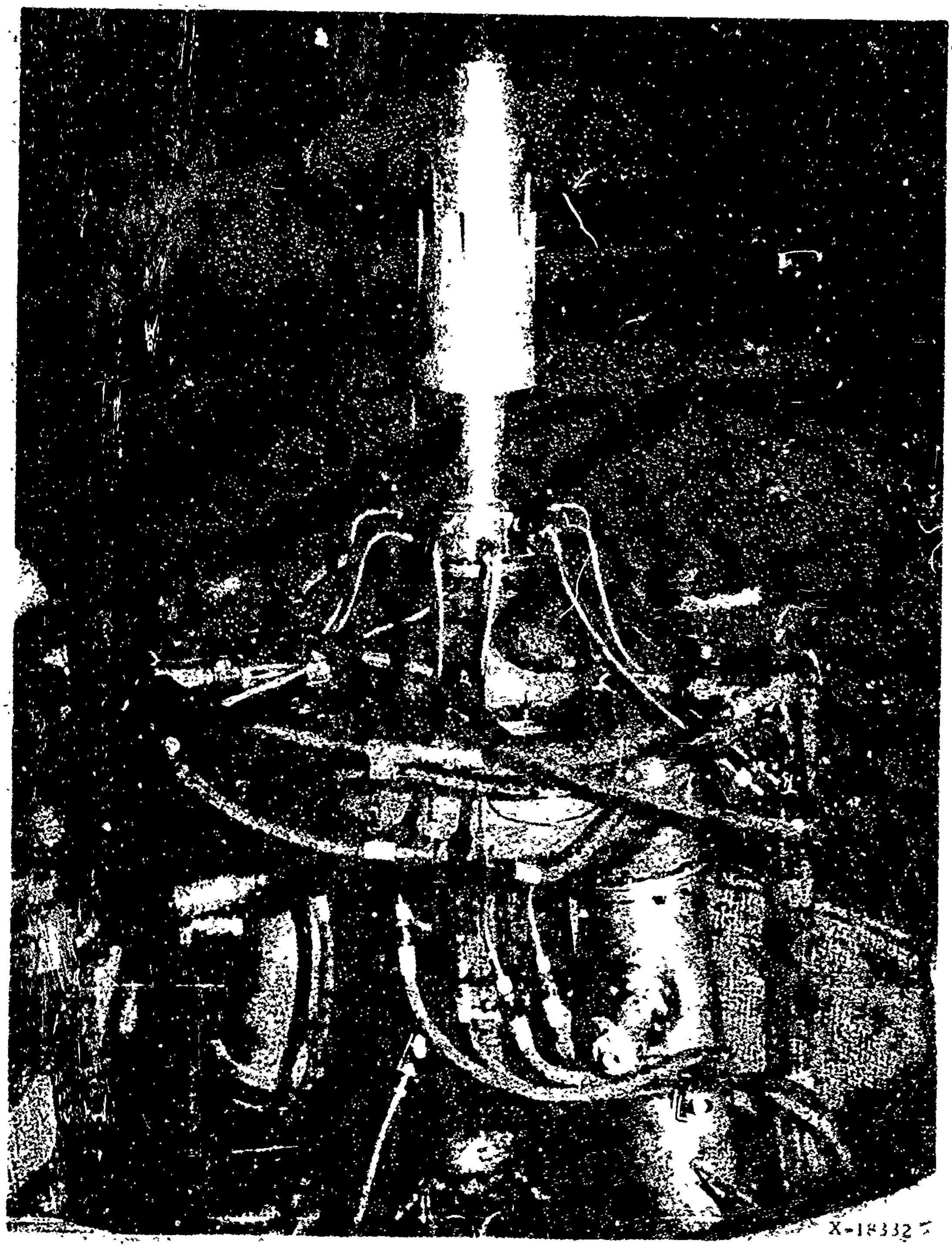

WATER-COOLED MAXIMUM DUCT-HEATING NOZZLE MODEL
MOUNTED ON TEST RIG
Figure 9-52

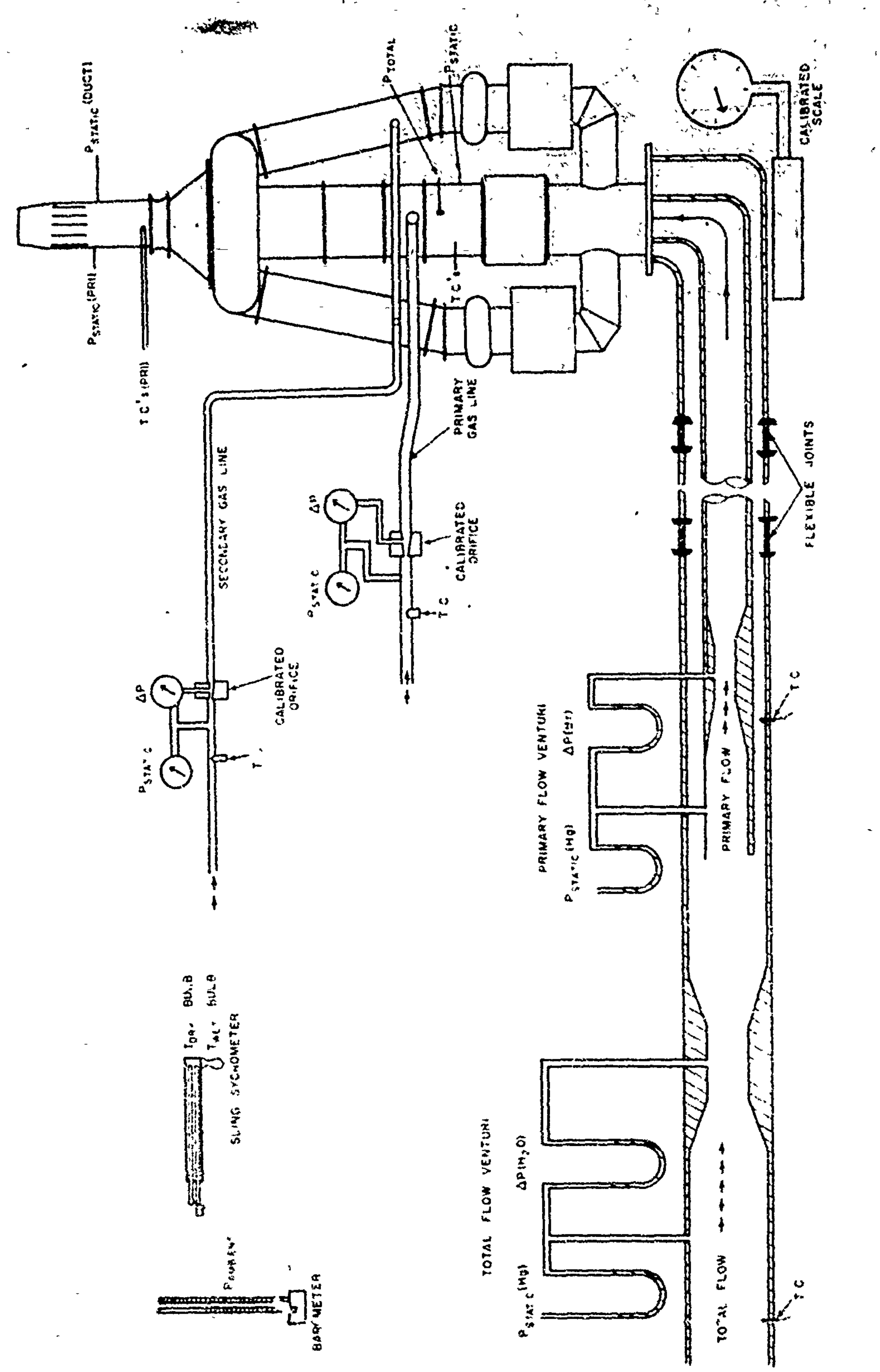

SCHEMATIC DIAGRAM OF PERFORMANCE INSTRUMENTATION IN ANECHOIC CHAMBER

Figure 9-53

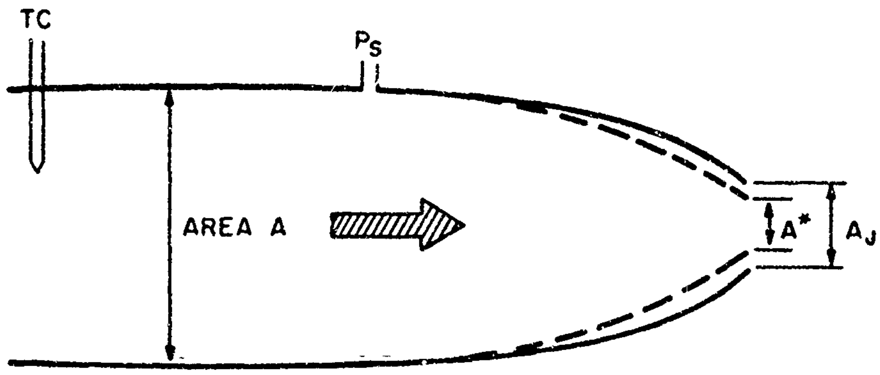

NOZZLE AERODYNAMIC DIAGRAM

Figure 9-54

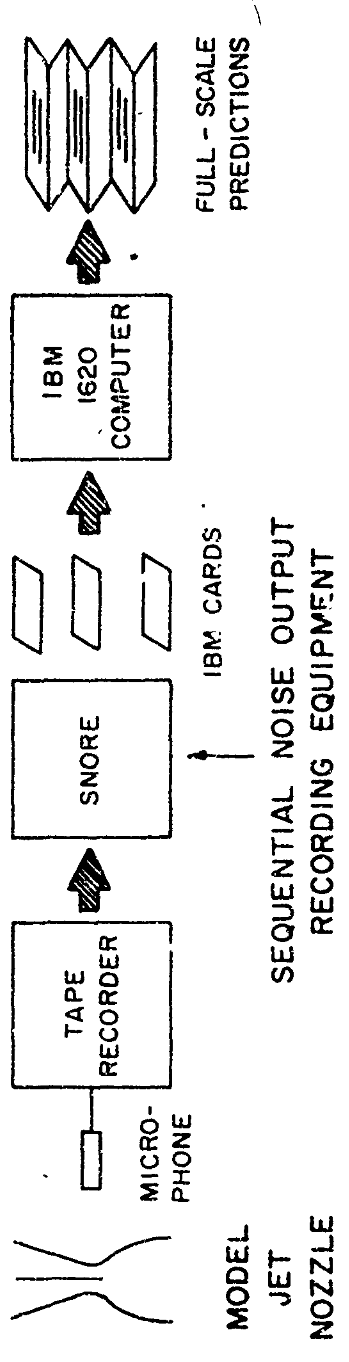

SCHEMATIC DIAGRAM OF SOUND DATA PROCESSING SYSTEM

Figure 9-55

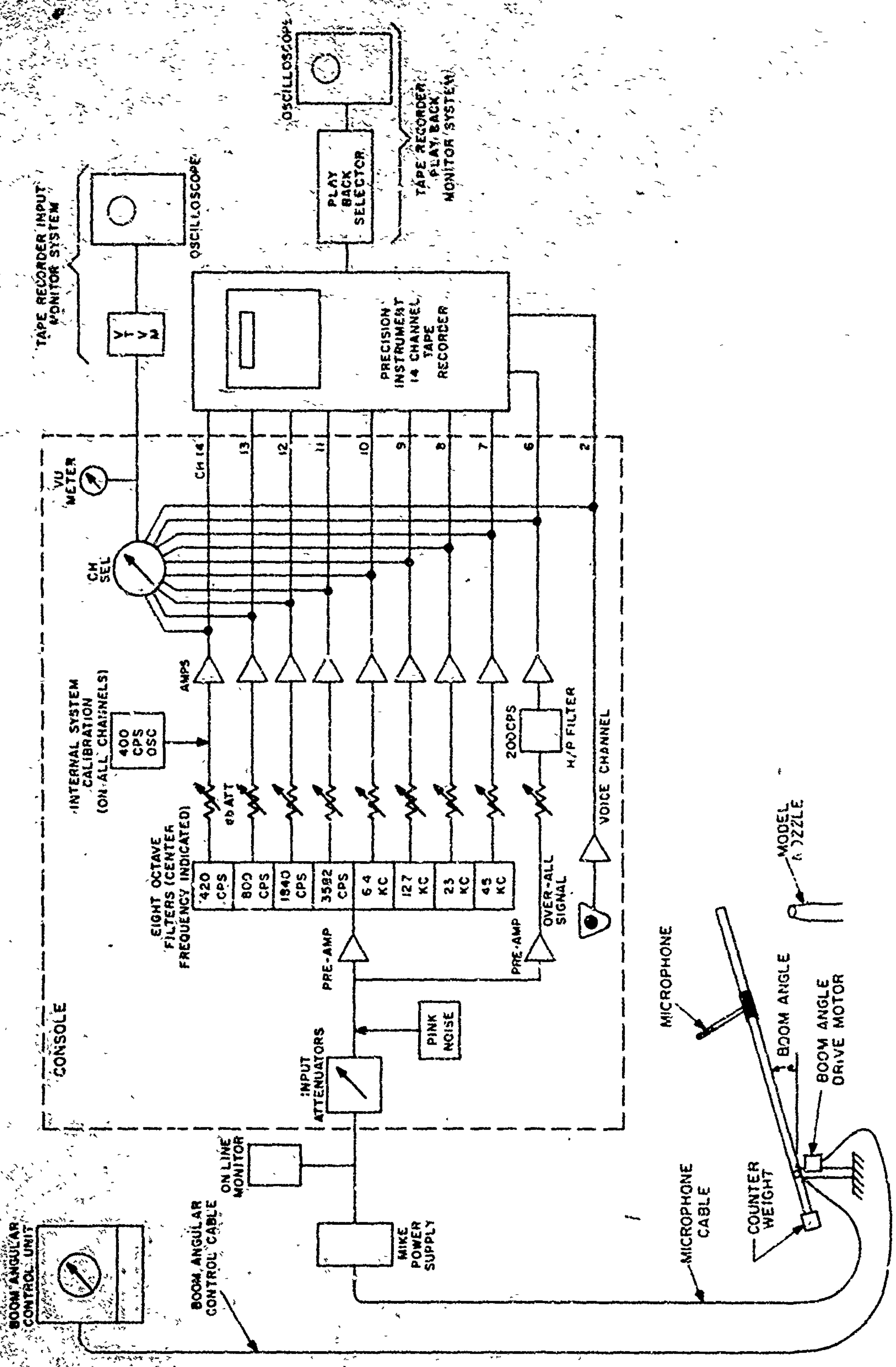

SCHEMATIC DIAGRAM OF SOUND DATA RECORDING SYSTEM

Figure 9-56

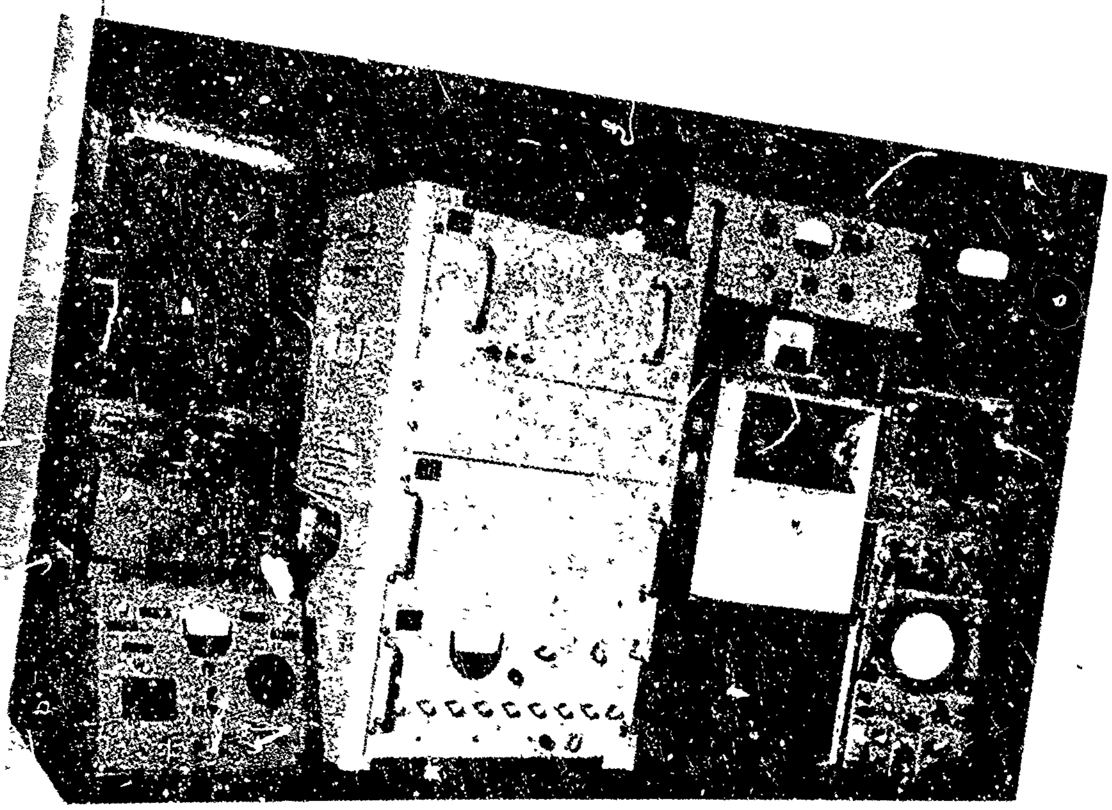

X-18290

SOUND DATA RECORDING SYSTEM

Figure 9-57

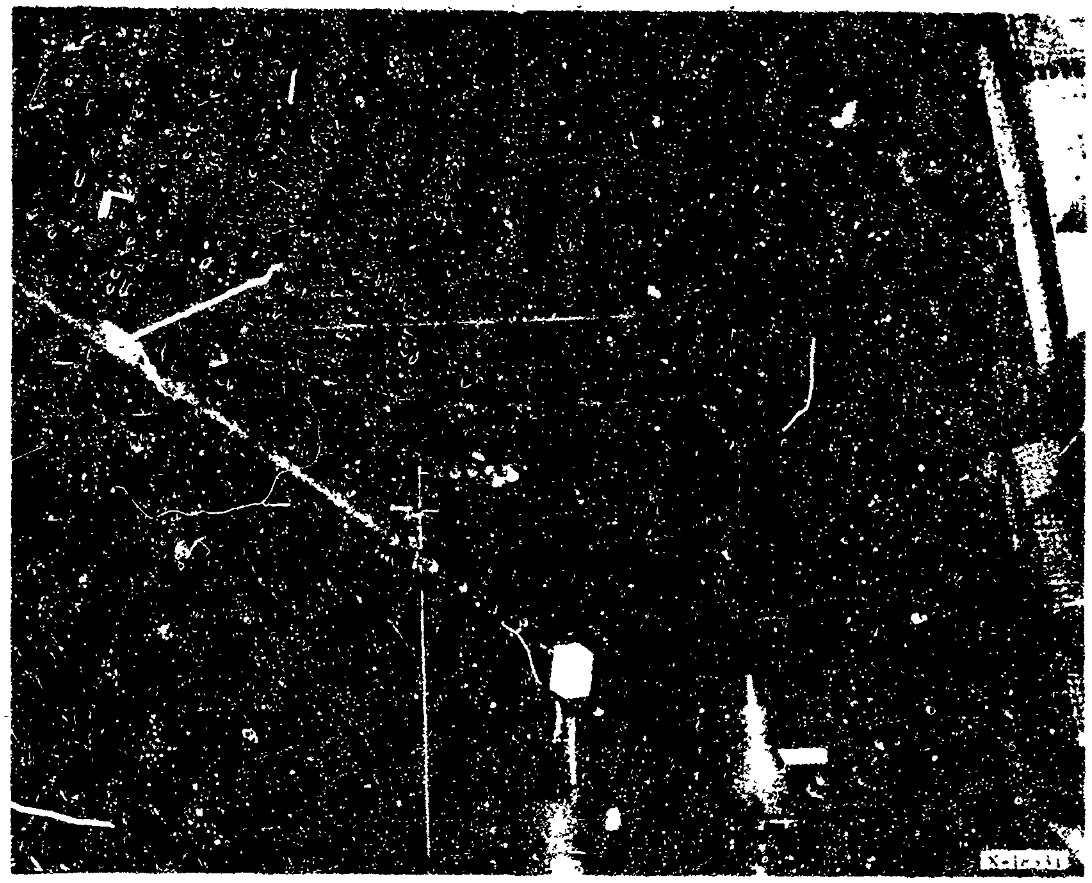

INTERIOR OF ANECHOIC CHAMBER
SHOWING MICROPHONE BOOM AND TEST MODEL

Figure 9-58

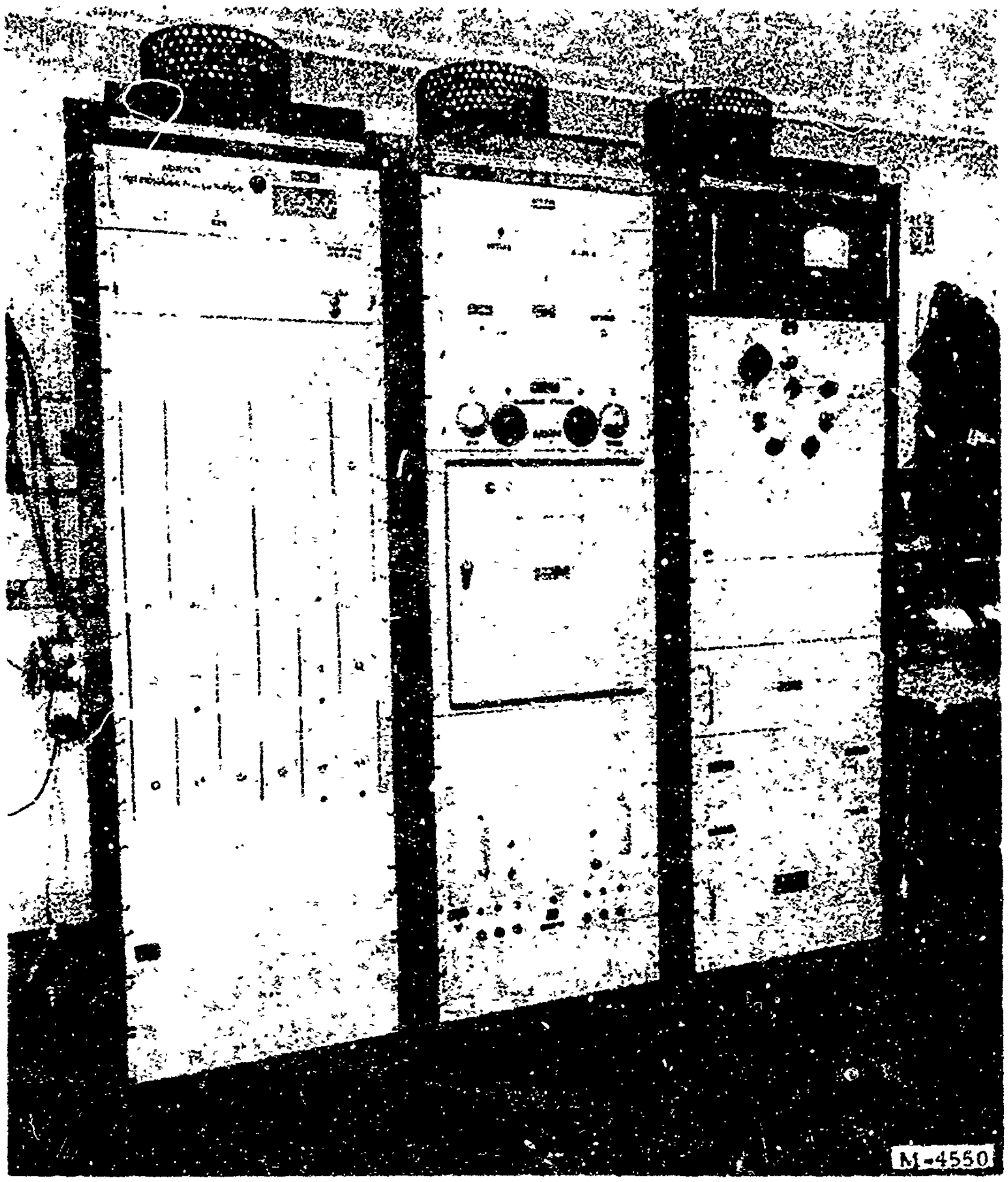

PHOTOGRAPH OF SNORE
(SEQUENTIAL NOISE OUTPUT RECORDING EQUIPMENT)

Figure 9-59

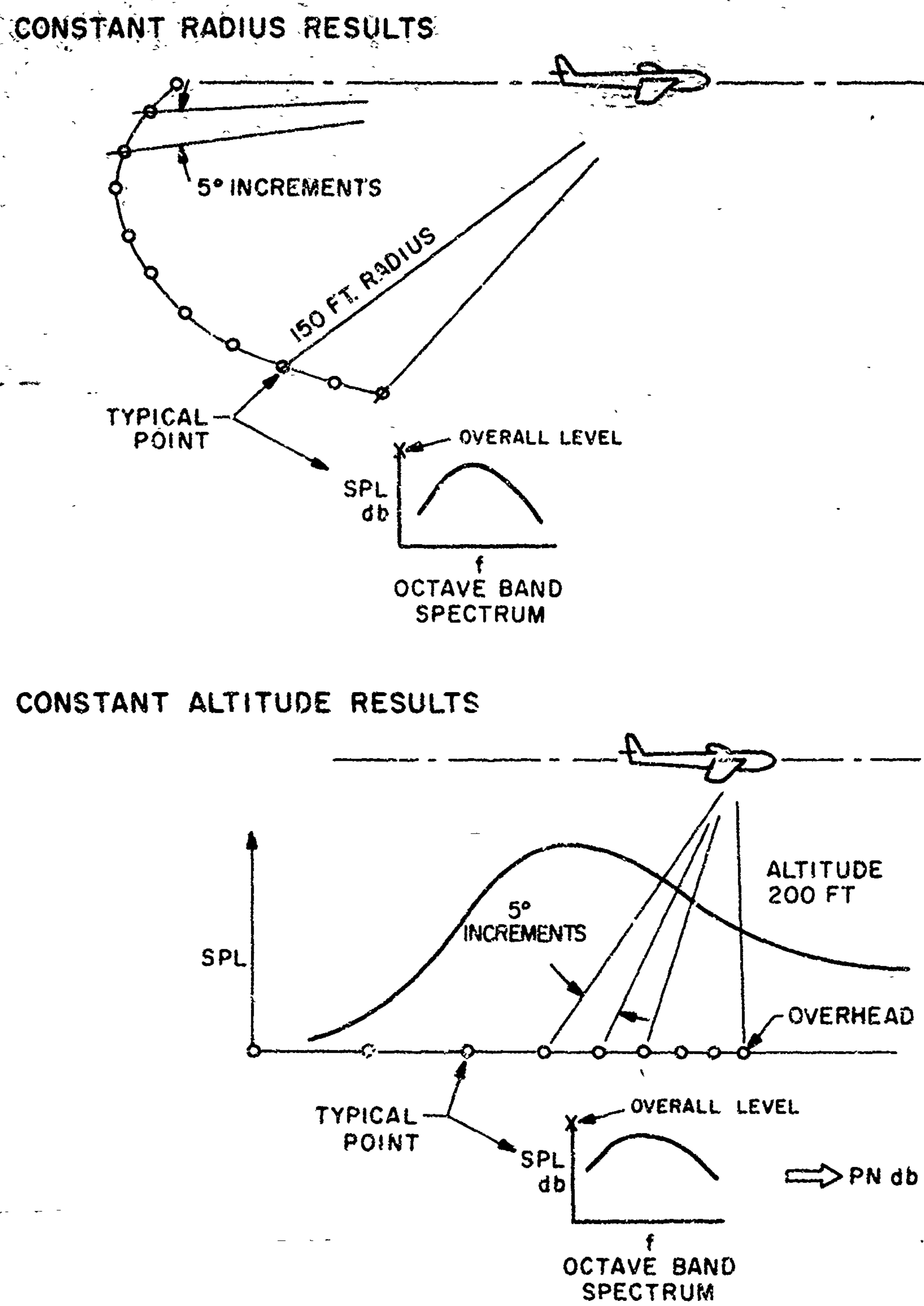

FULL-SCALE NOISE PREDICTIONS

Figure 9-60

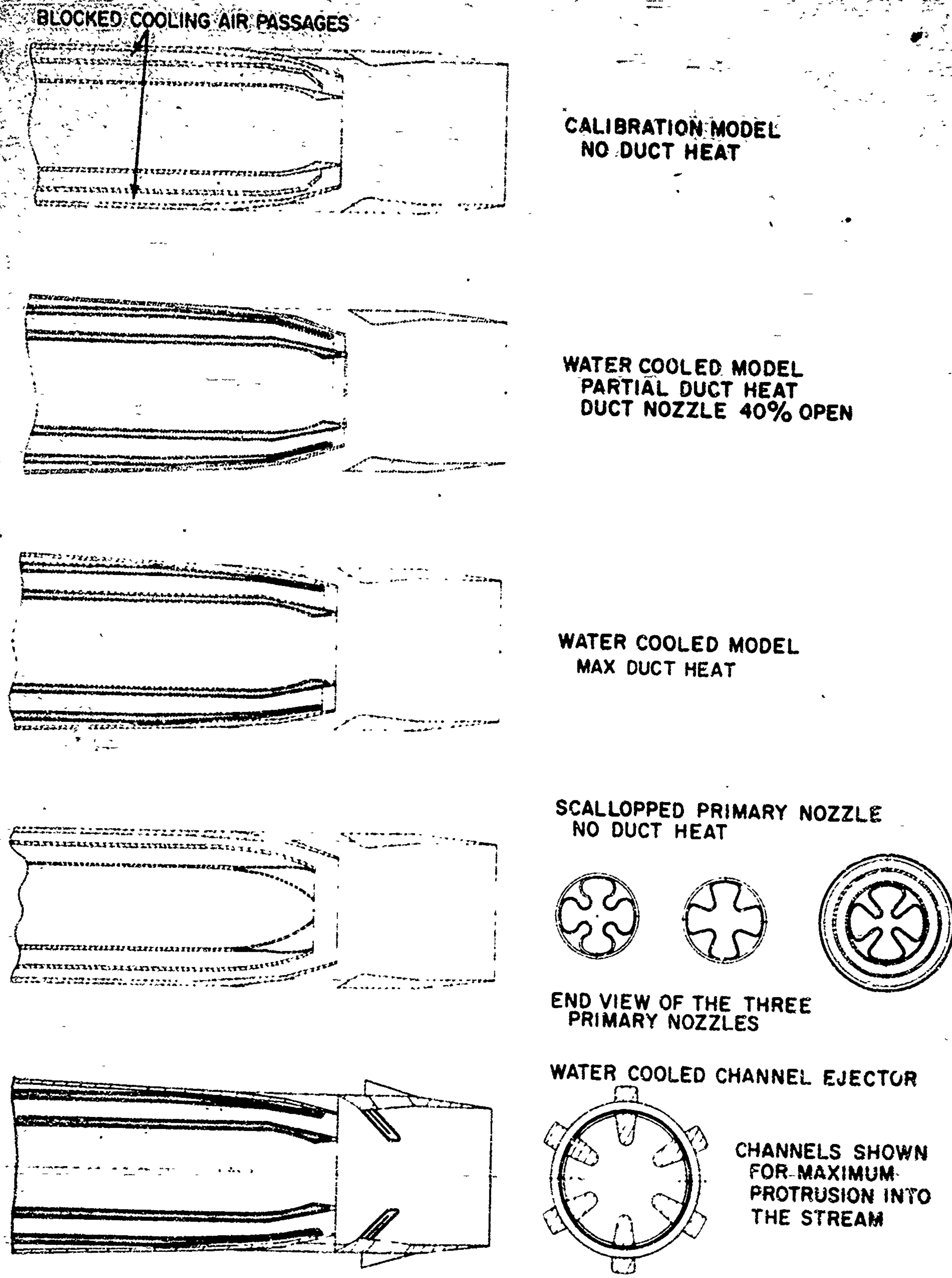

BLOW-IN-DOOR EJECTOR NOZZLE MODELS FOR NOISE TESTS

Figure 9-61

Primary Only

Primary and Secondary

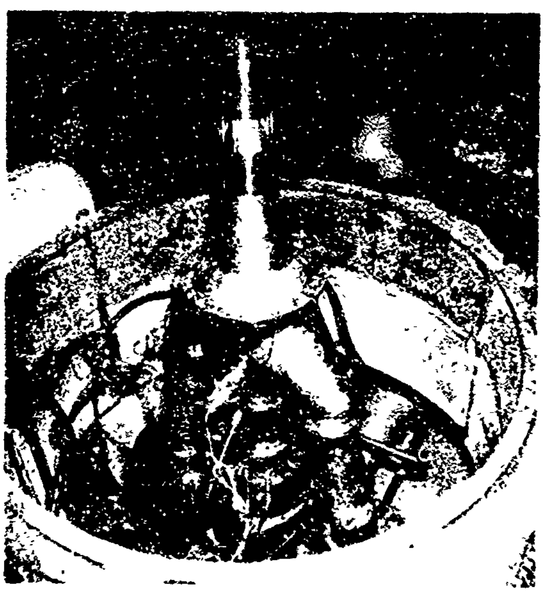

Primary, Secondary, and Ejector Shroud

NOZZLE TEST MODELS MOUNTED ON RIG

Figure 9-62

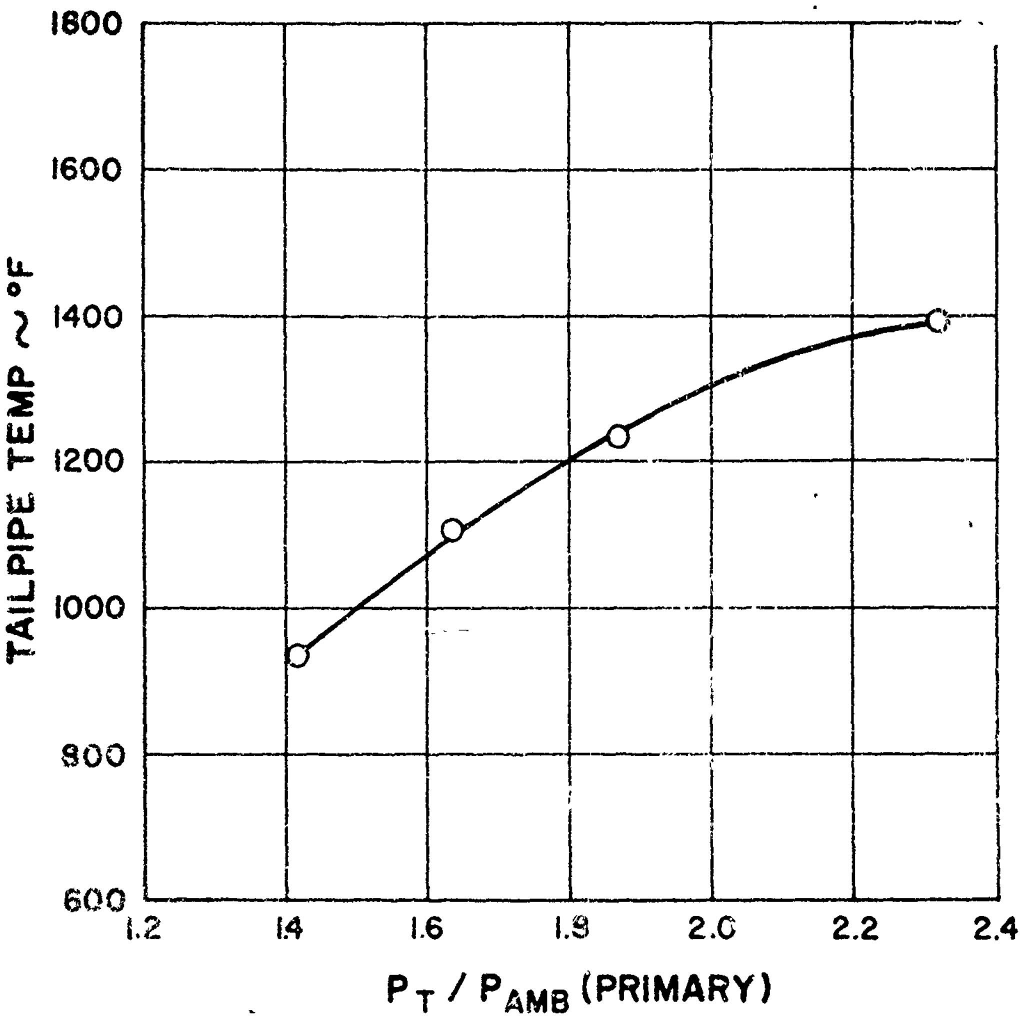

TAILPIPE TEMPERATURE VS PRIMARY PRESSURE RATIO

Figure 9-63

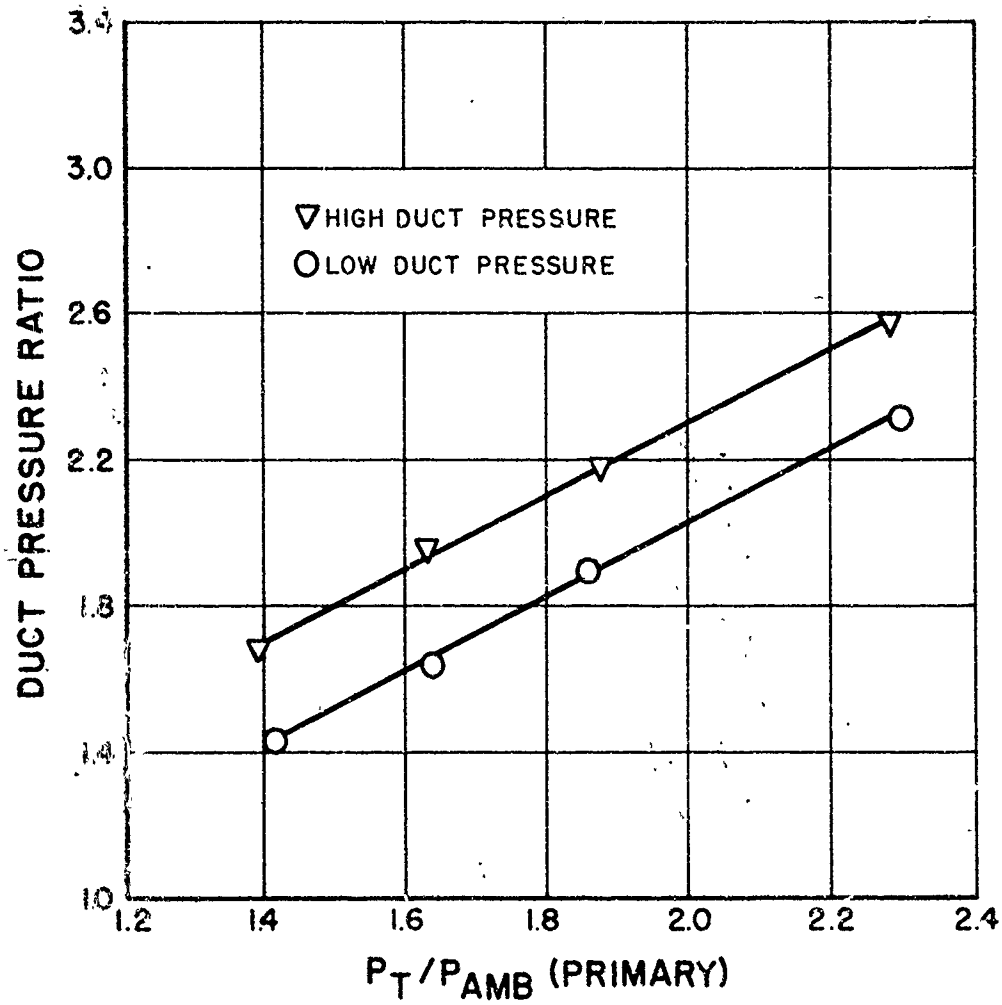

DUCT PRESSURE RATIO VS PRIMARY PRESSURE RATIO

Figure 9-64

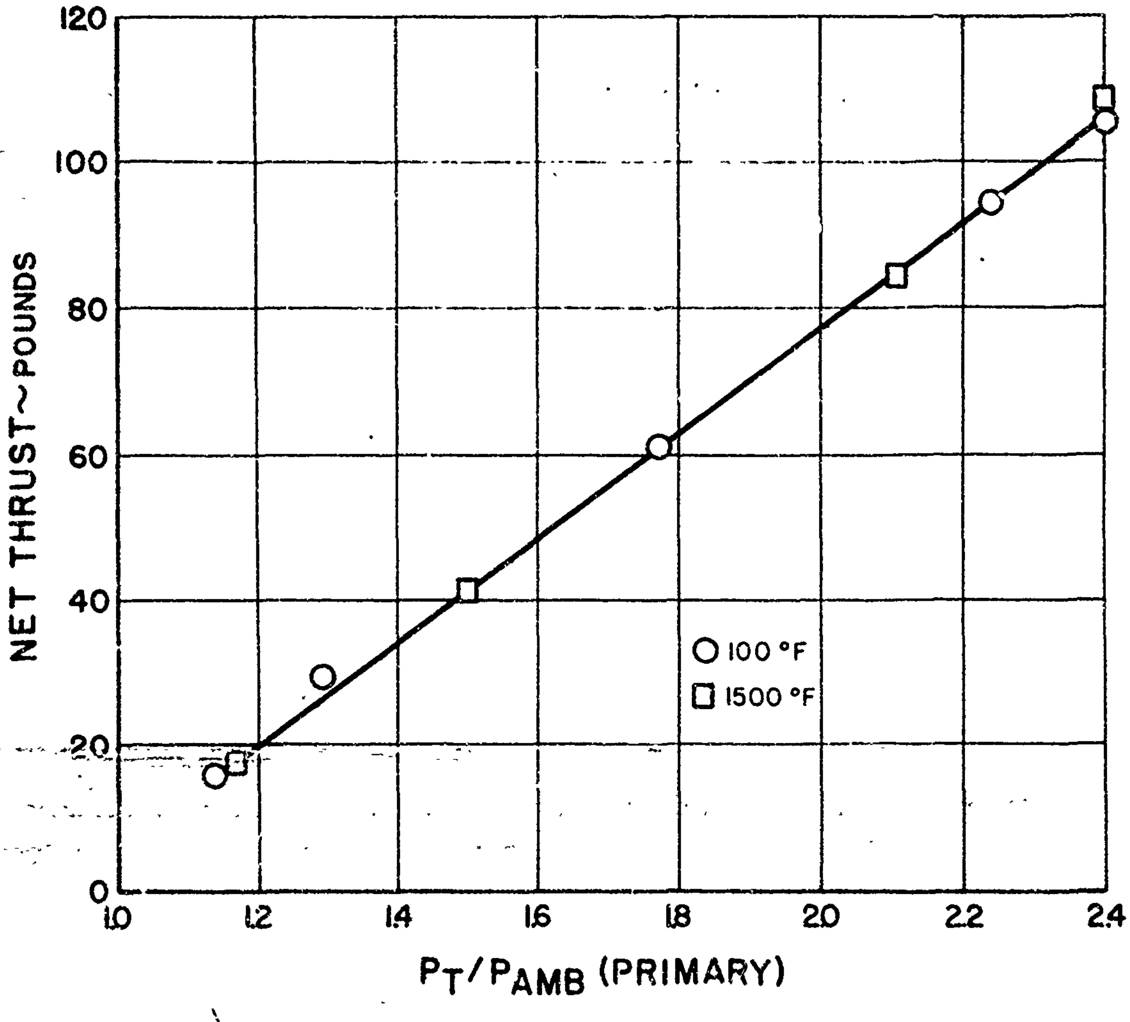

NET THRUST VS PRIMARY PRESSURE RATIO

Figure 9-65

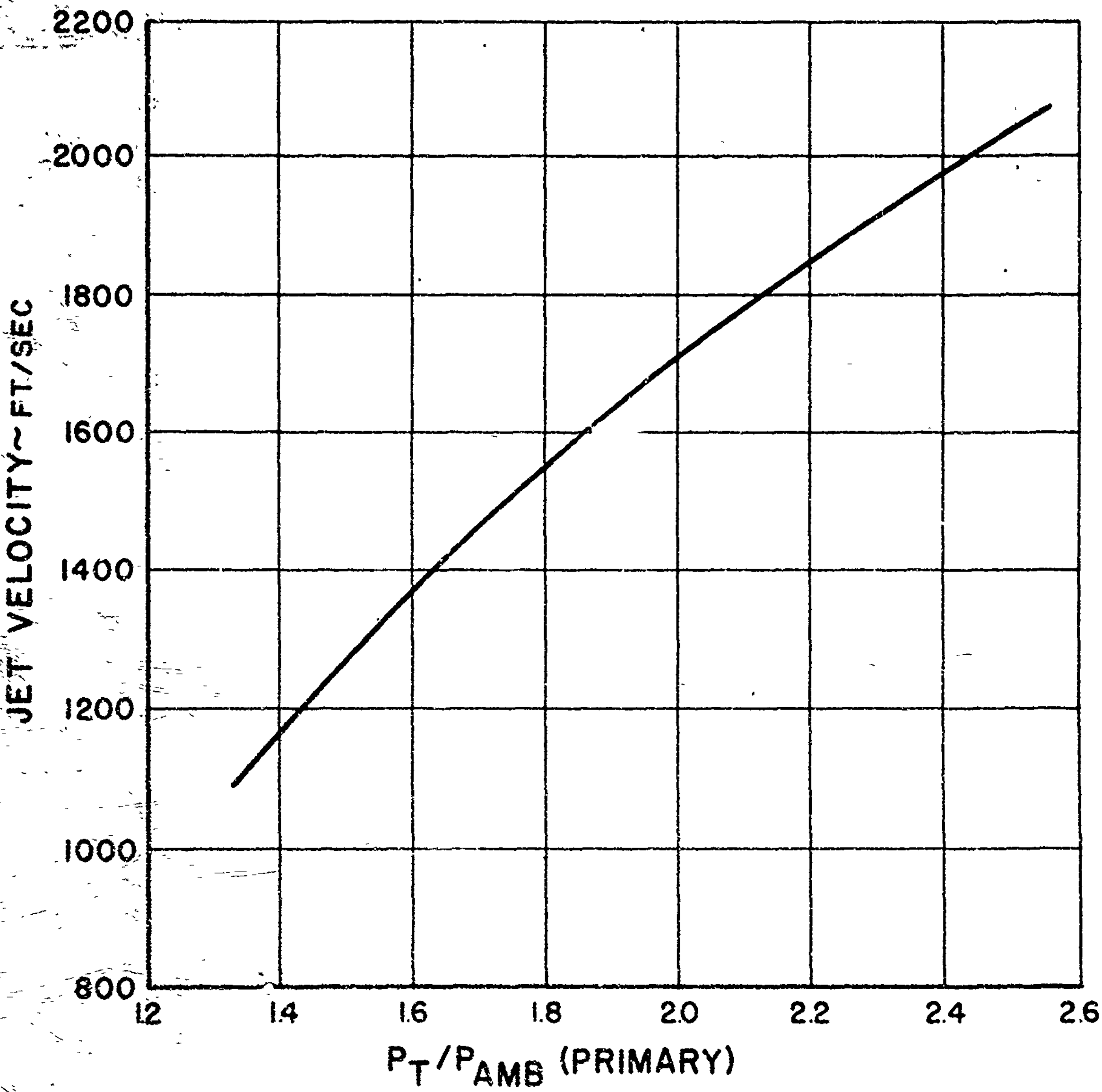

JET VELOCITY VS PRIMARY PRESSURE RATIO

Figure 9-66

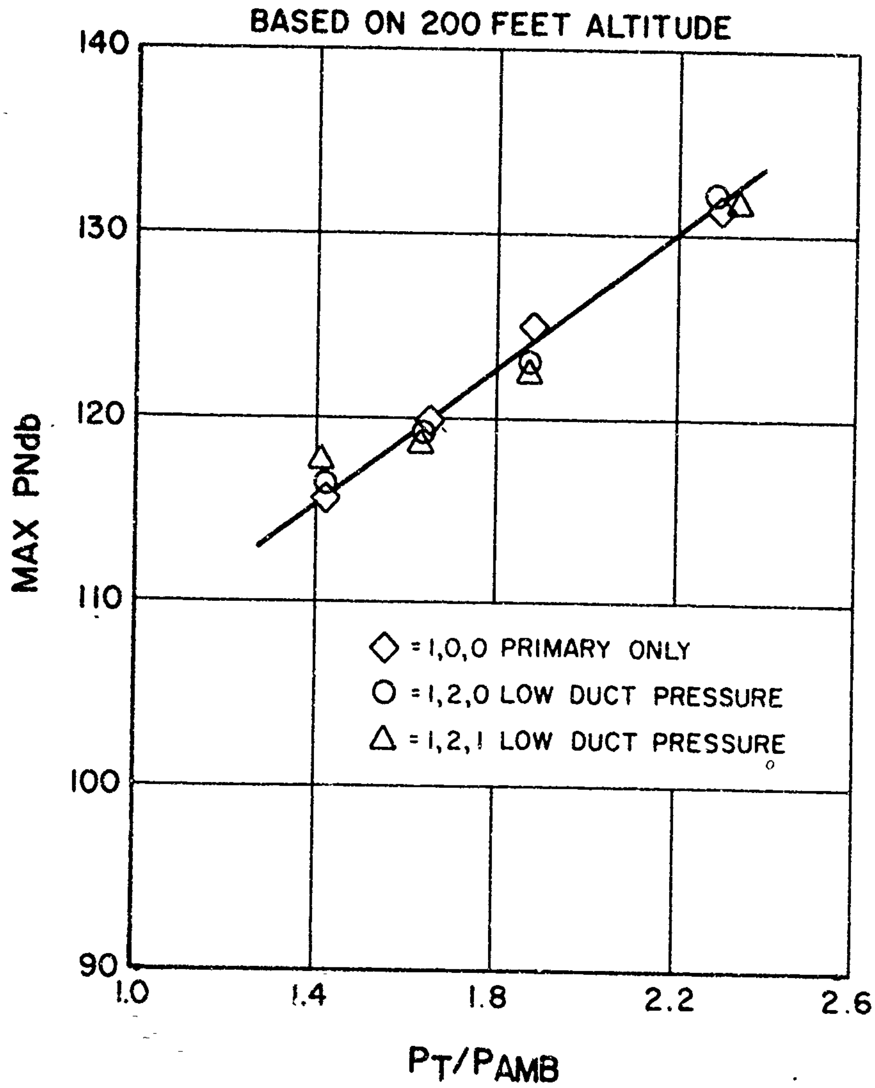

JET NOISE VS PRESSURE RATIO FOR LOW DUCT PRESSURE

Figure 9-67

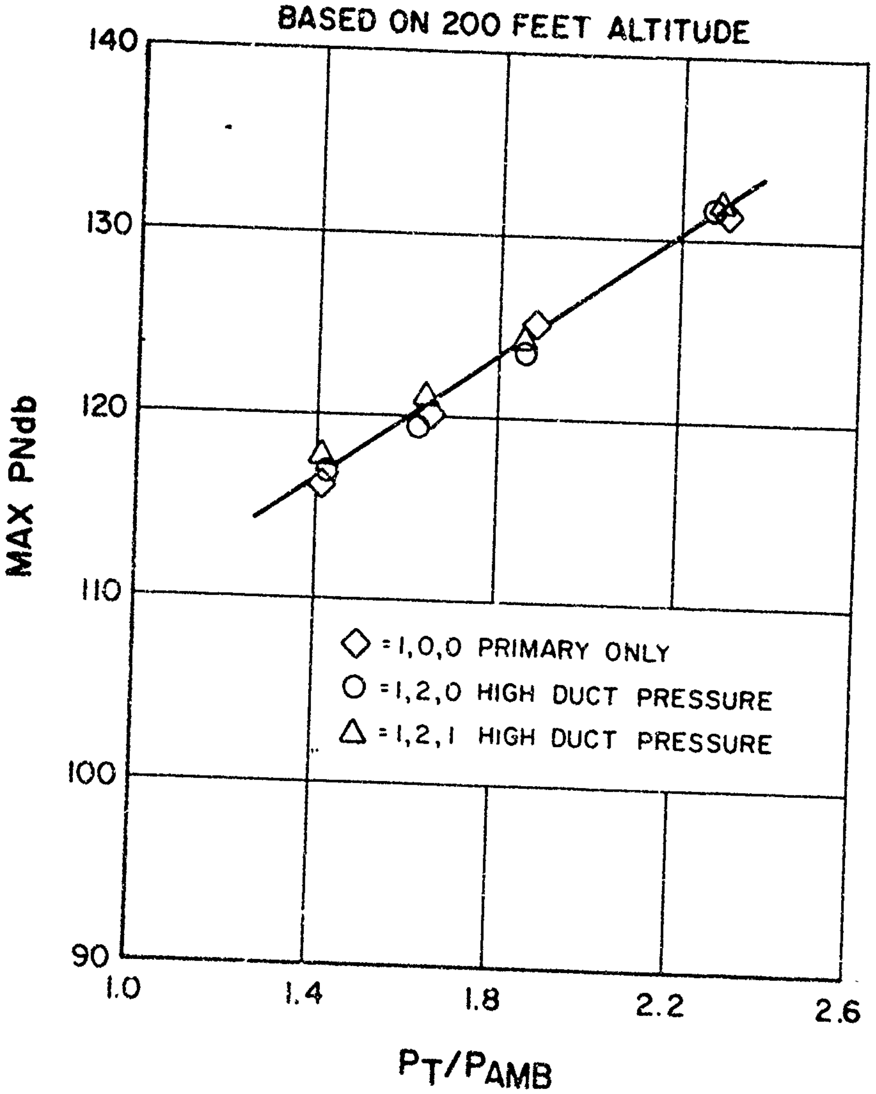

JET NOISE VS PRESSURE RATIO FOR HIGH DUCT PRESSURE

Figure 9-68

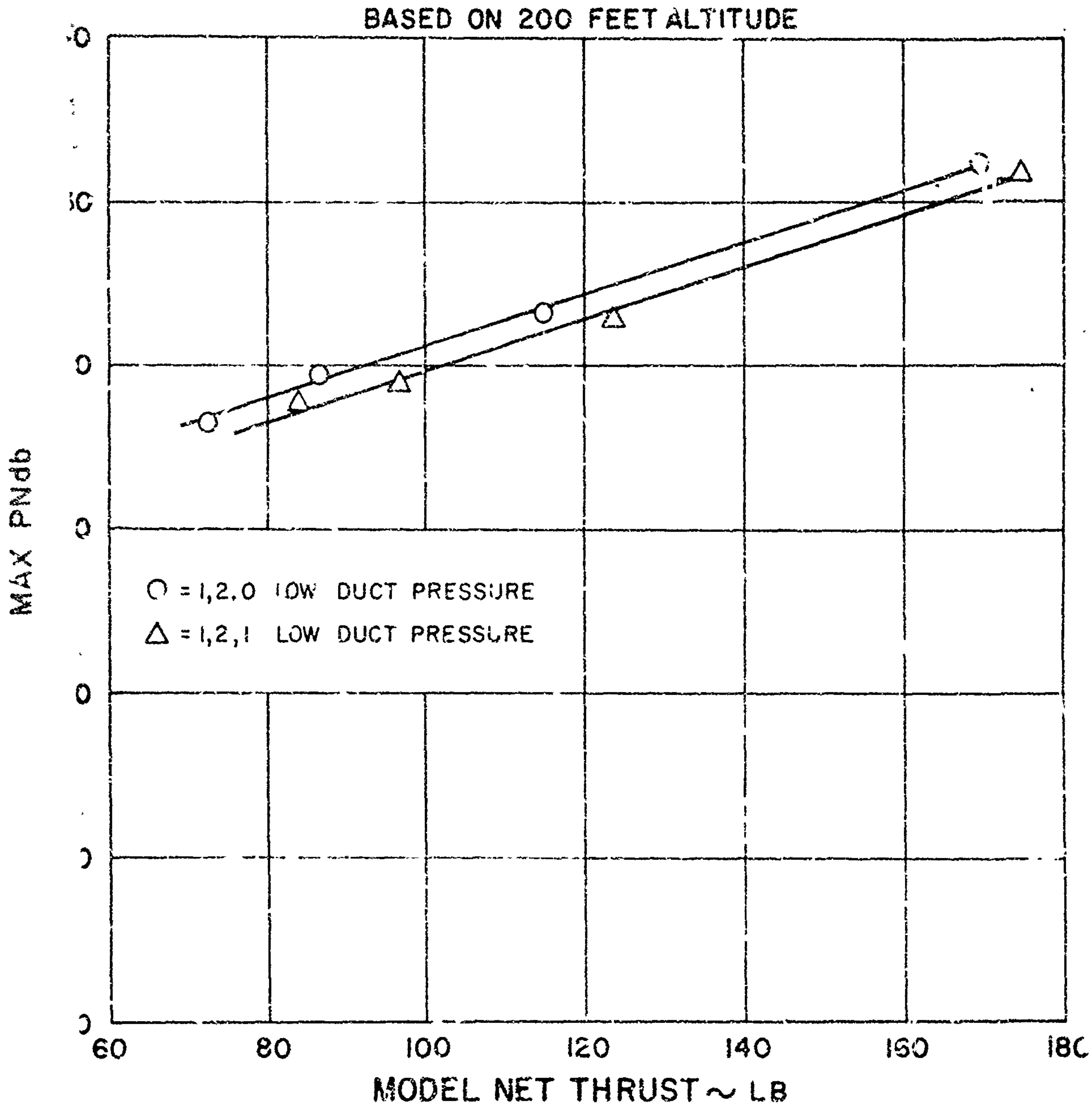

JET NOISE VS NET THRUST FOR LOW DUCT PRESSURE

Figure 9-69

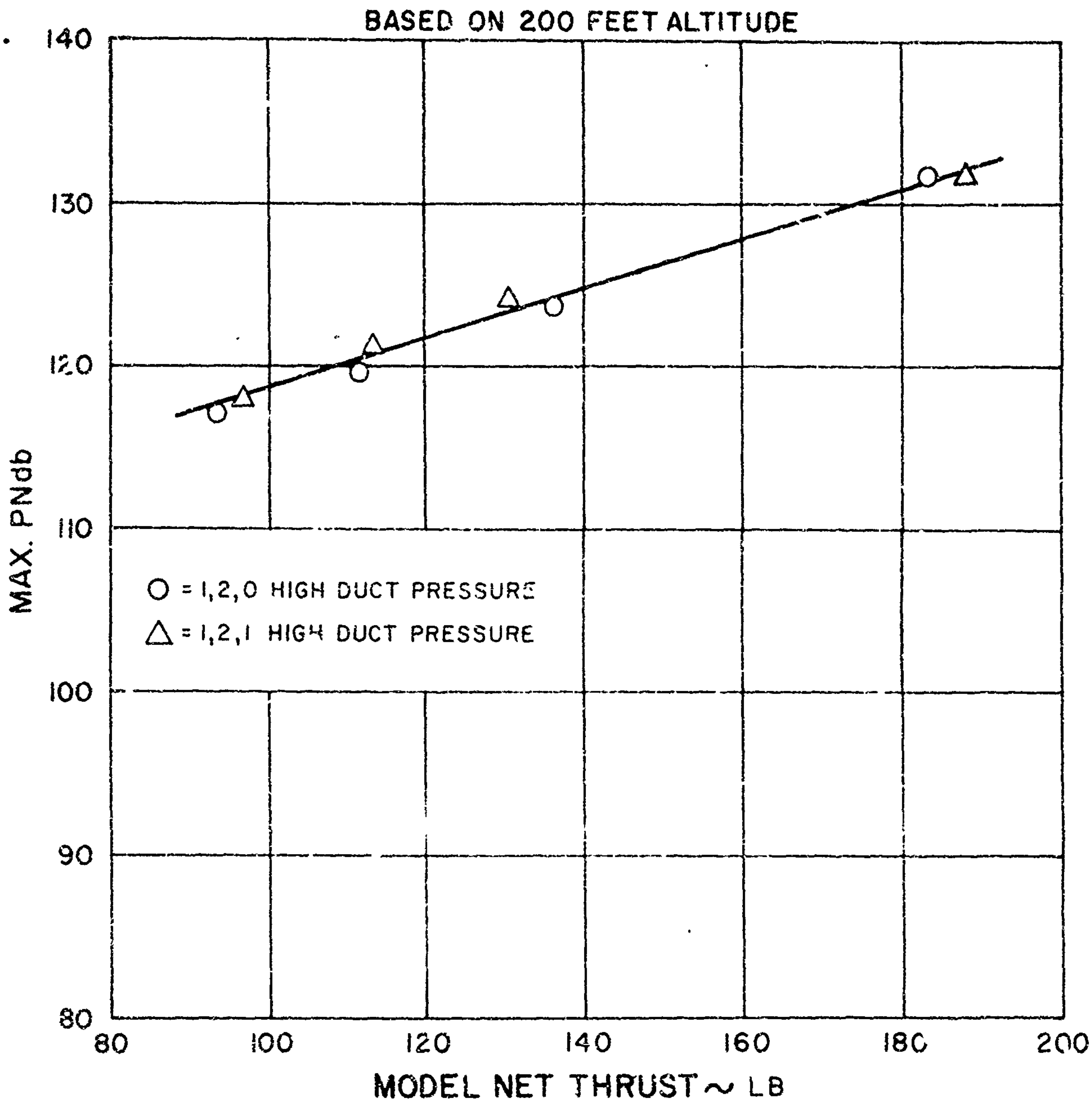

JET NOISE VS NET THRUST FOR HIGH DUCT PRESSURE

Figure 9-70

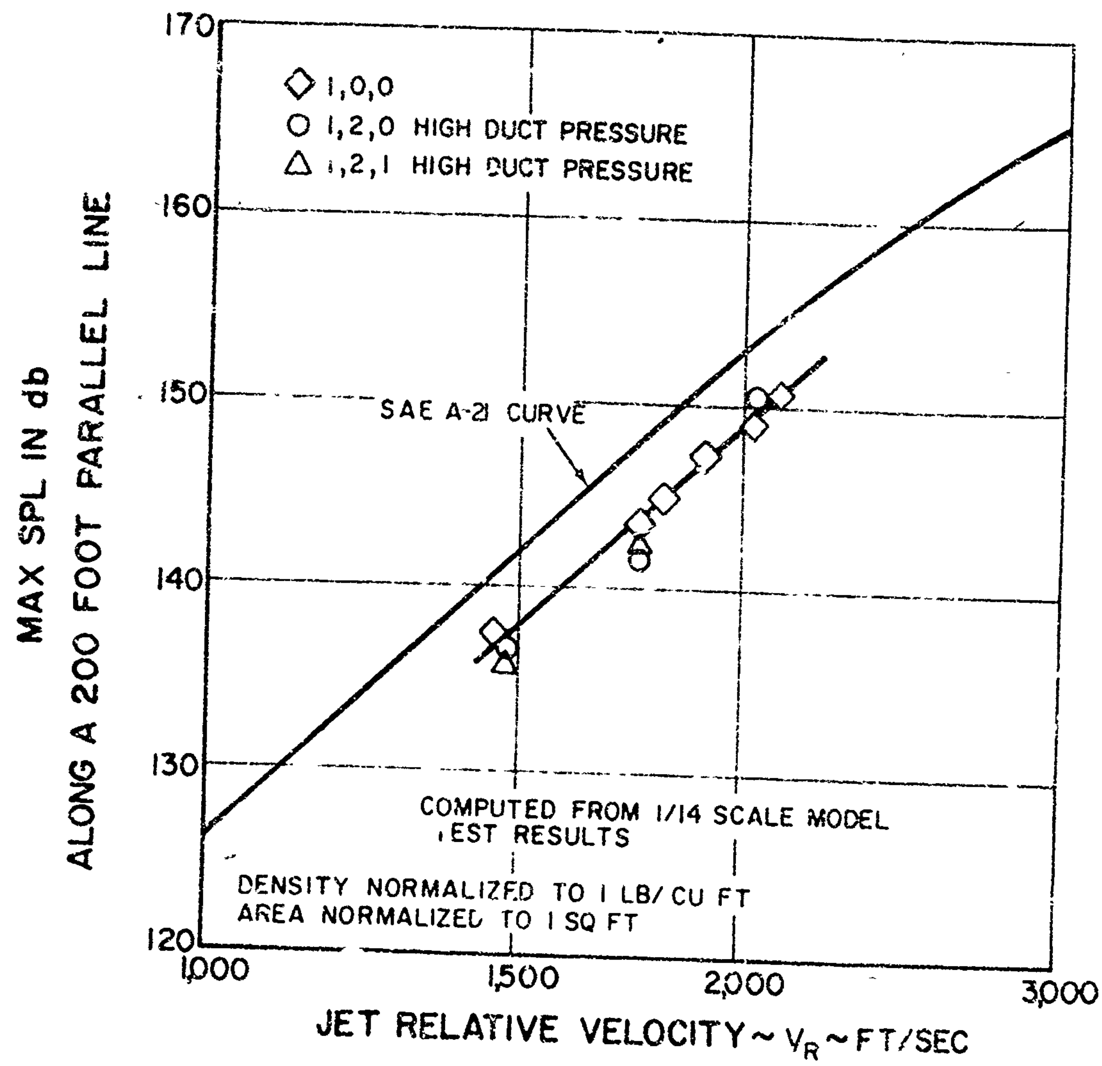

COMPARISON OF SST NOZZLE MODELS WITH SAE A-21 COMMITTEE PREDICTIONS

Figure 9-71

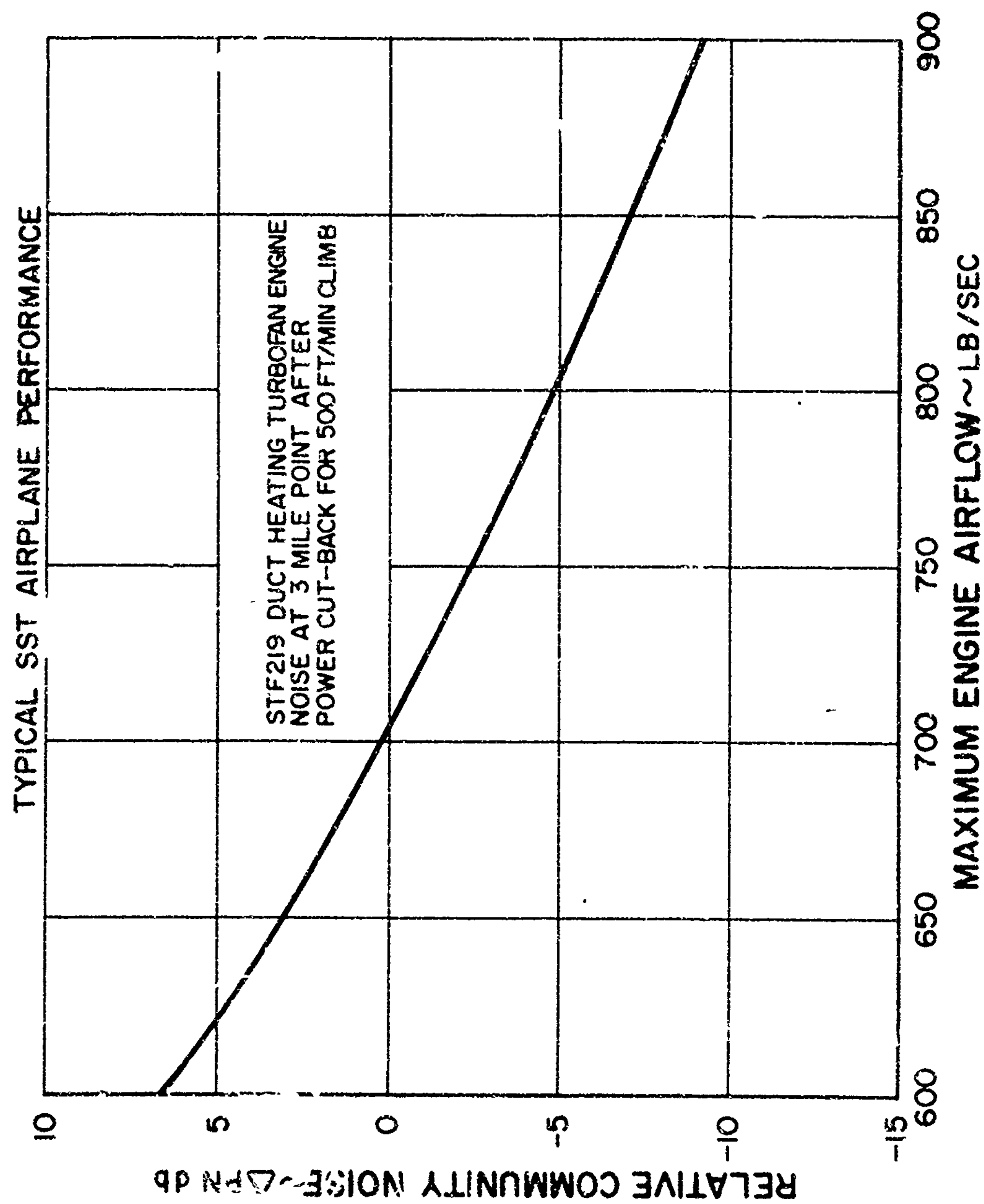

EFFECT OF ENGINE SIZE ON COMMUNITY NOISE

Figure 9-72

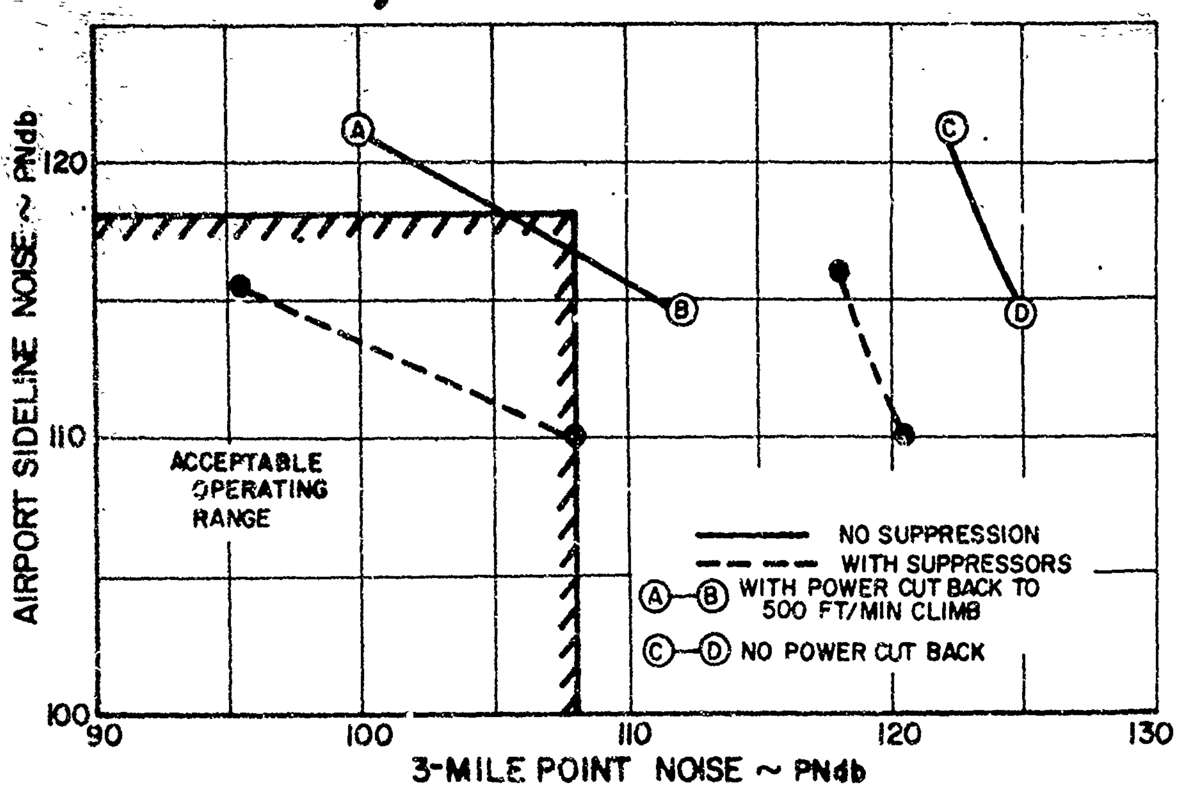

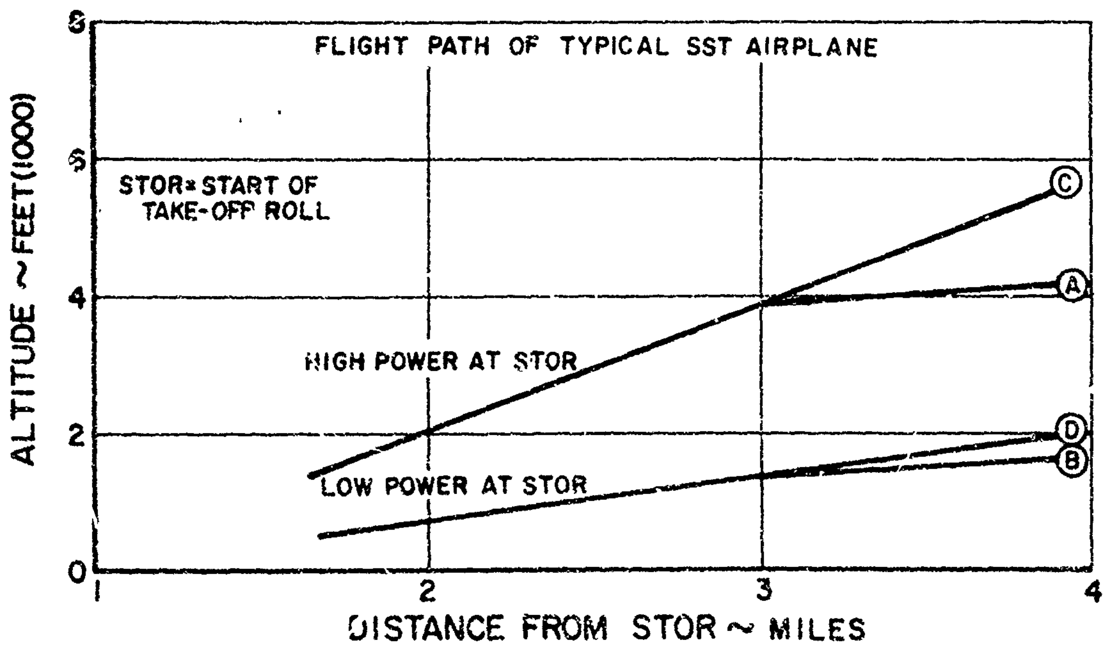

TRADE-OFF BETWEEN COMMUNITY NOISE AND AIRPORT NOISE FOR A TYPICAL SST AIRPLANE

Figure 9-73

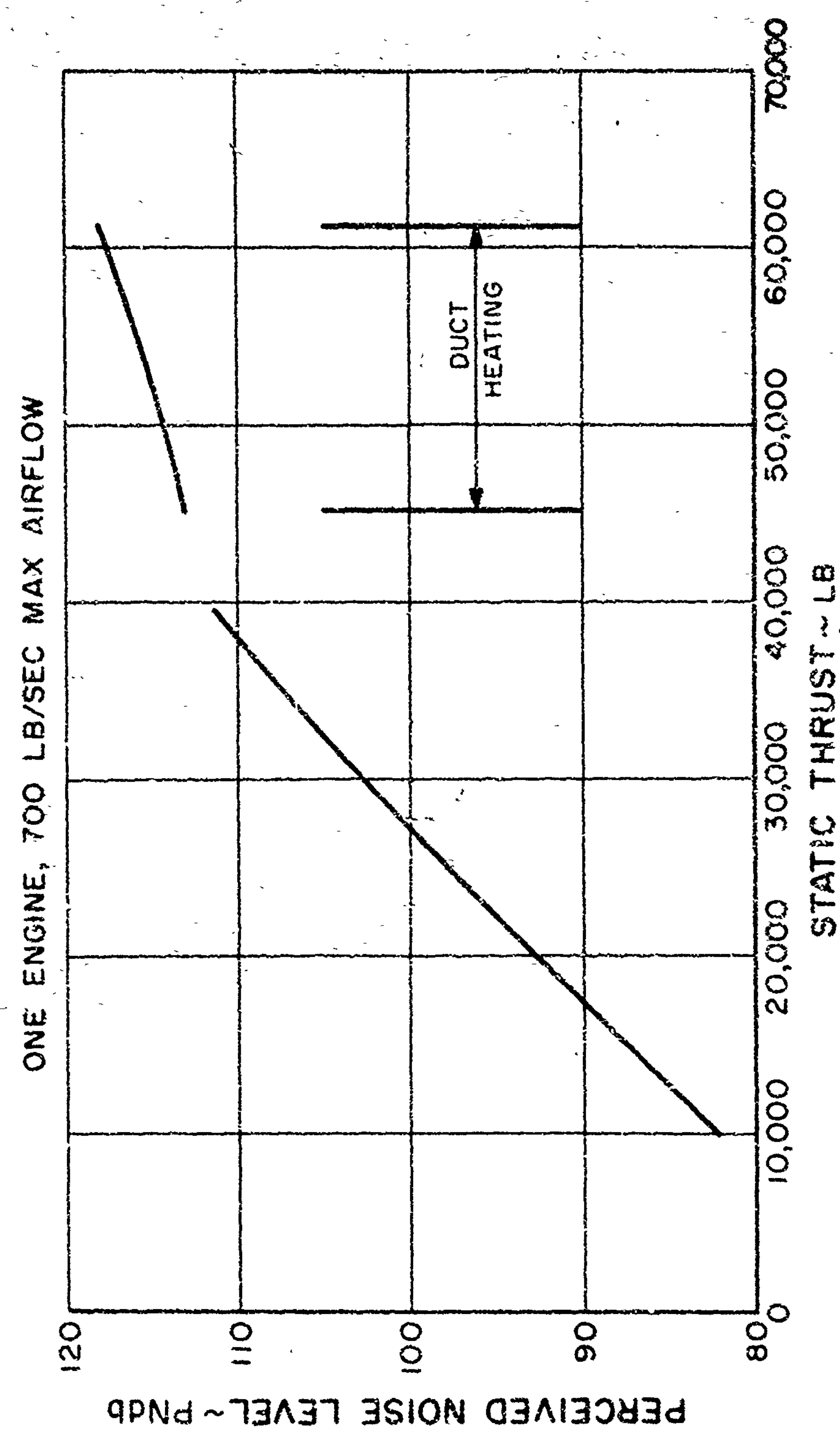

SIDELINE NOISE AT 1500 FEET FROM CENTERLINE OF STF219 ENGINE WITH NO NOISE SUPPRESSION

Figure 9-74

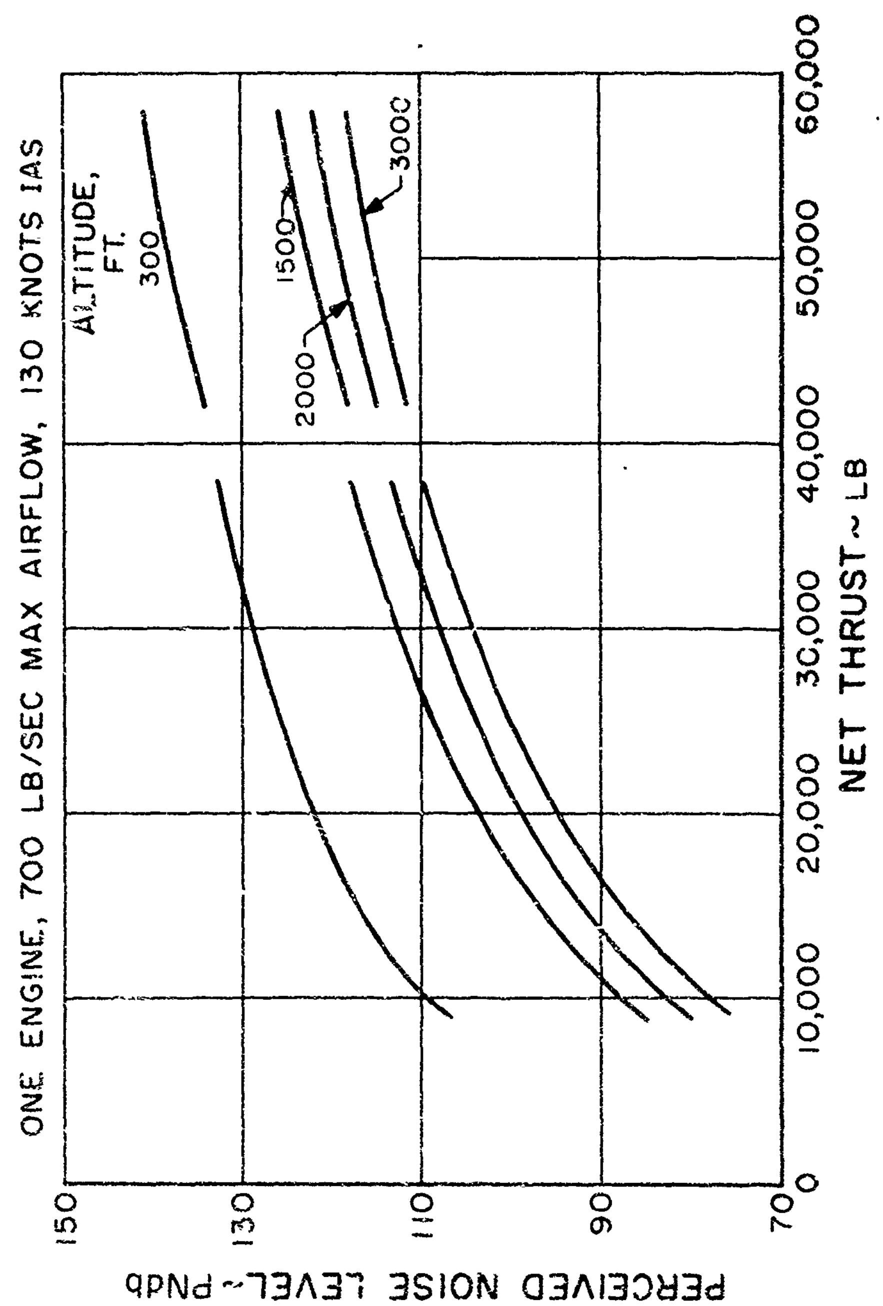

IN-FLIGHT NOISE FROM STF219 ENGINE
WITH NO NOISE SUPPRESSION

Figure 9-75

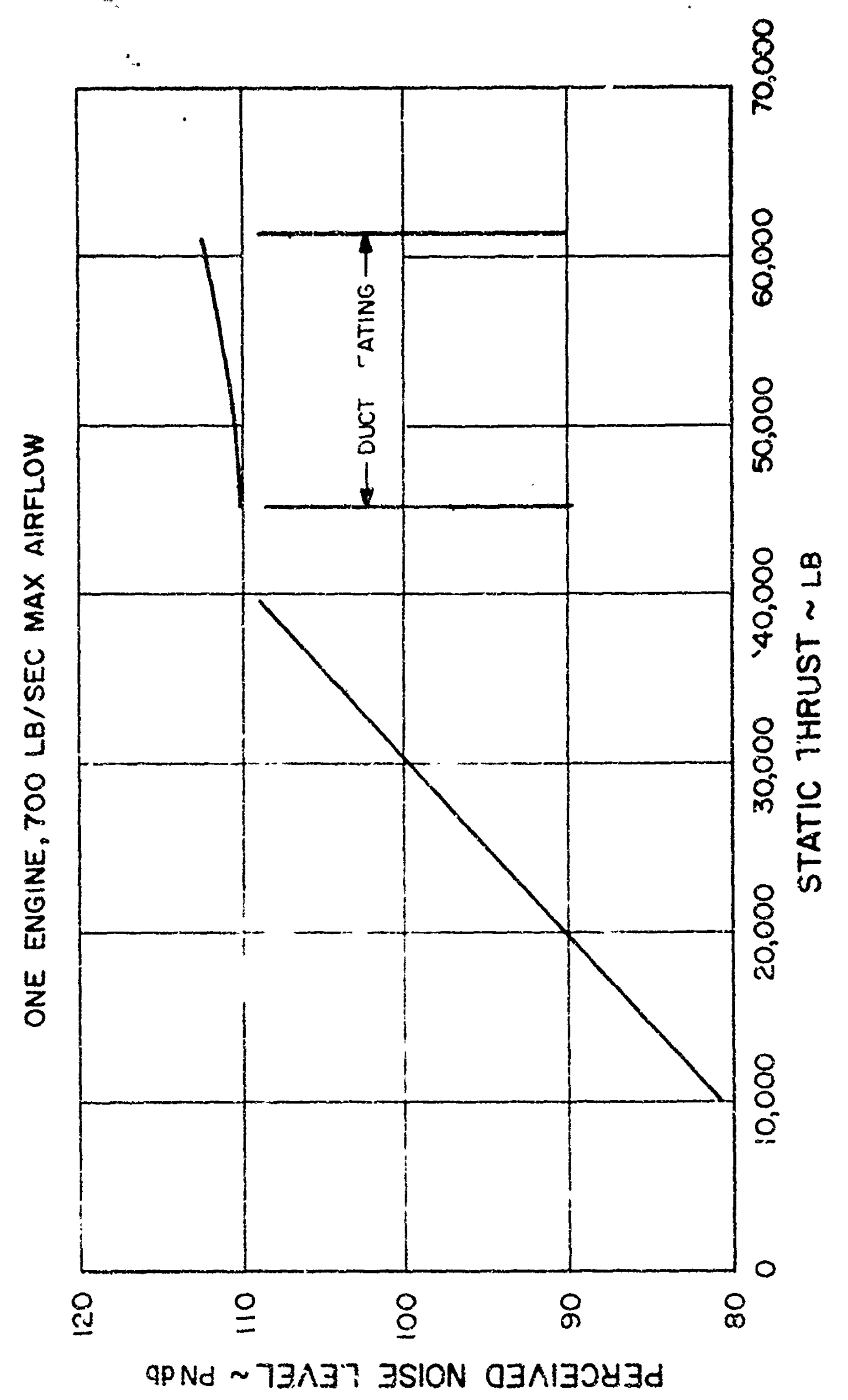

SIDELINE NOISE AT 1500 FEET FROM CENTERLINE OF

STF219 ENGINE WITH NOISE SUPPRESSION

Figure 9-76

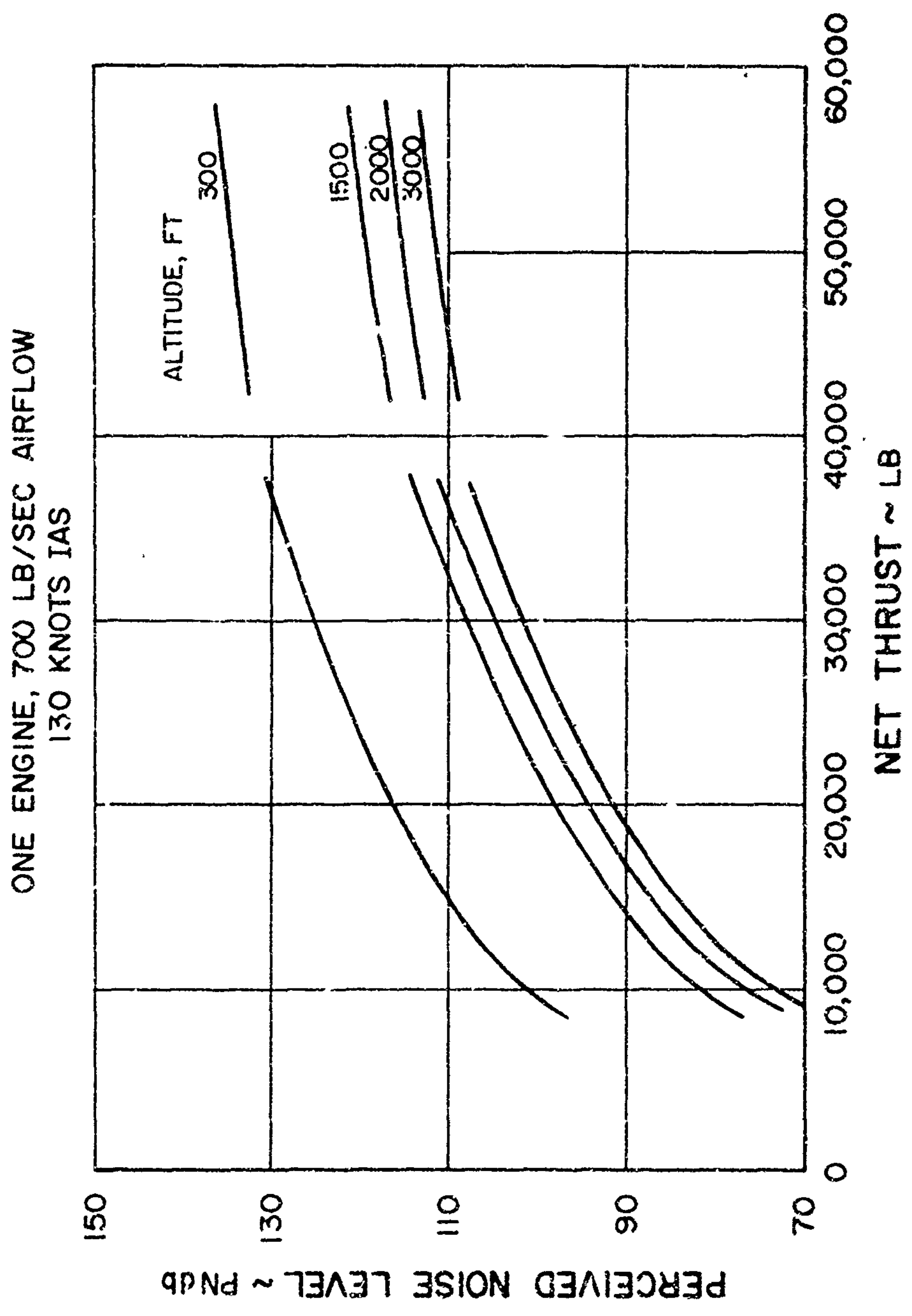

IN-FLIGHT NOISE FROM STF219 ENGINE
WITH NOISE SUPPRESSION
Figure 9-77

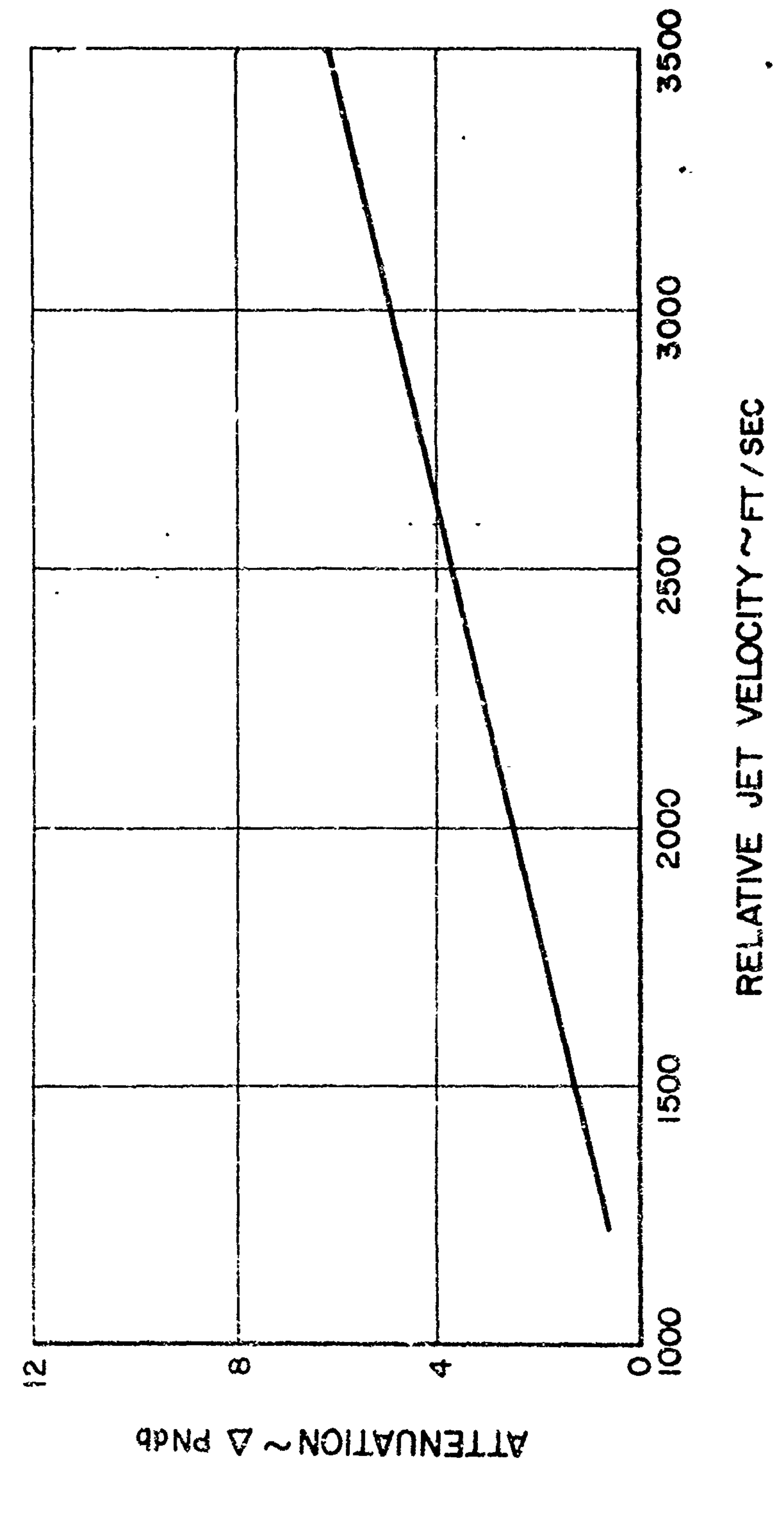

NOISE ATTENUATION DUE TO BLOW-IN-DOOR EJECTOR

Figure 9-78

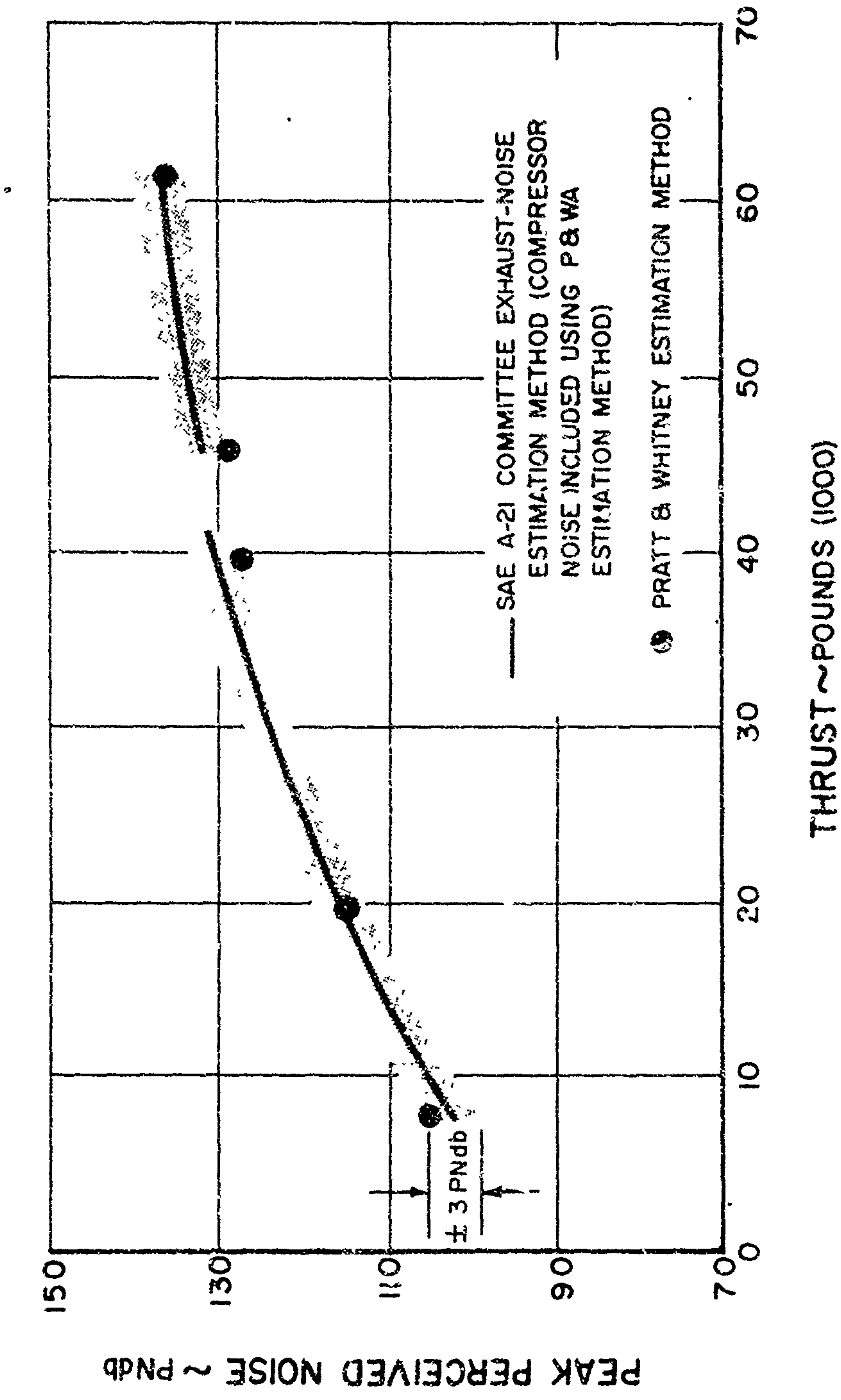

ESTIMATED STF219 ENGINE NOISE LEVELS ALONG A LINE 500 FEET FROM AND PARALLEL TO ONE ENGINE

Figure 9-79

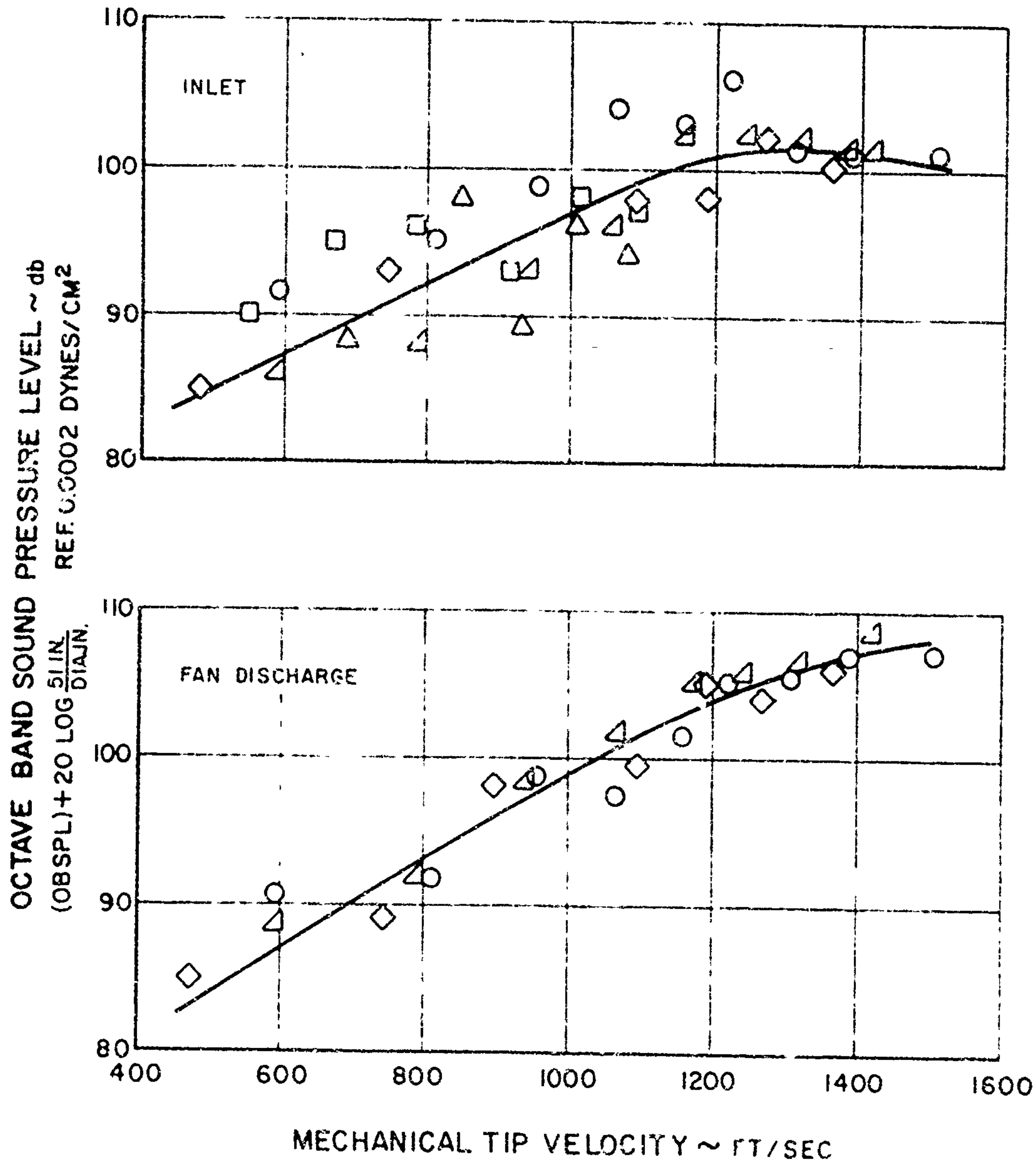

SOUND PRESSURE LEVELS OF OCTAVE BAND CONTAINING FUNDAMENTAL BLADE-PASSING NOISE

Figure 9-A-1

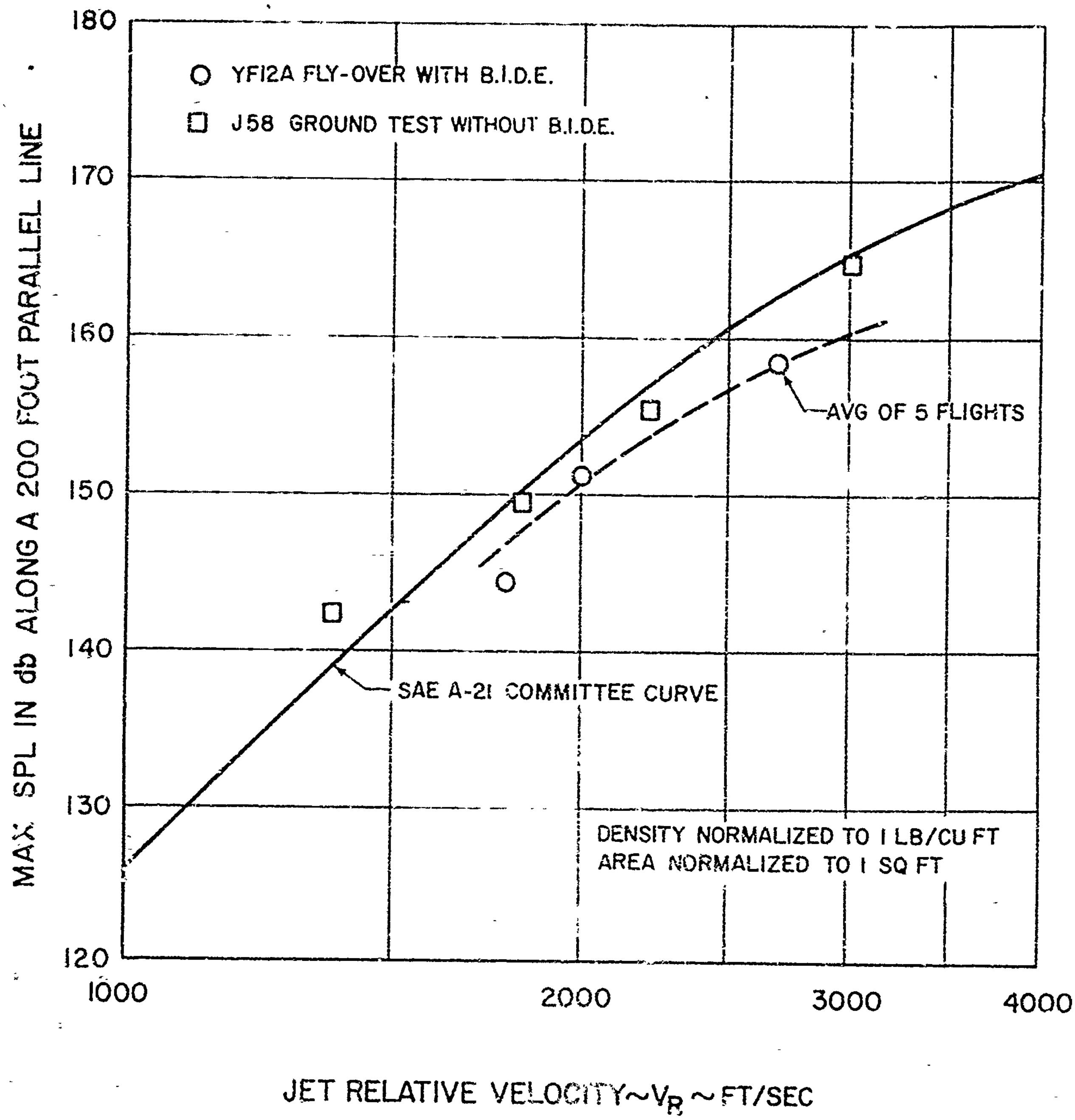

EFFECT OF BLOW-IN-DOOR EJECTOR ON EXHAUST NOISE

Figure 9-B-1

ONE ENGINE APPROACH THRUST
CONSTANT ALTITUDE

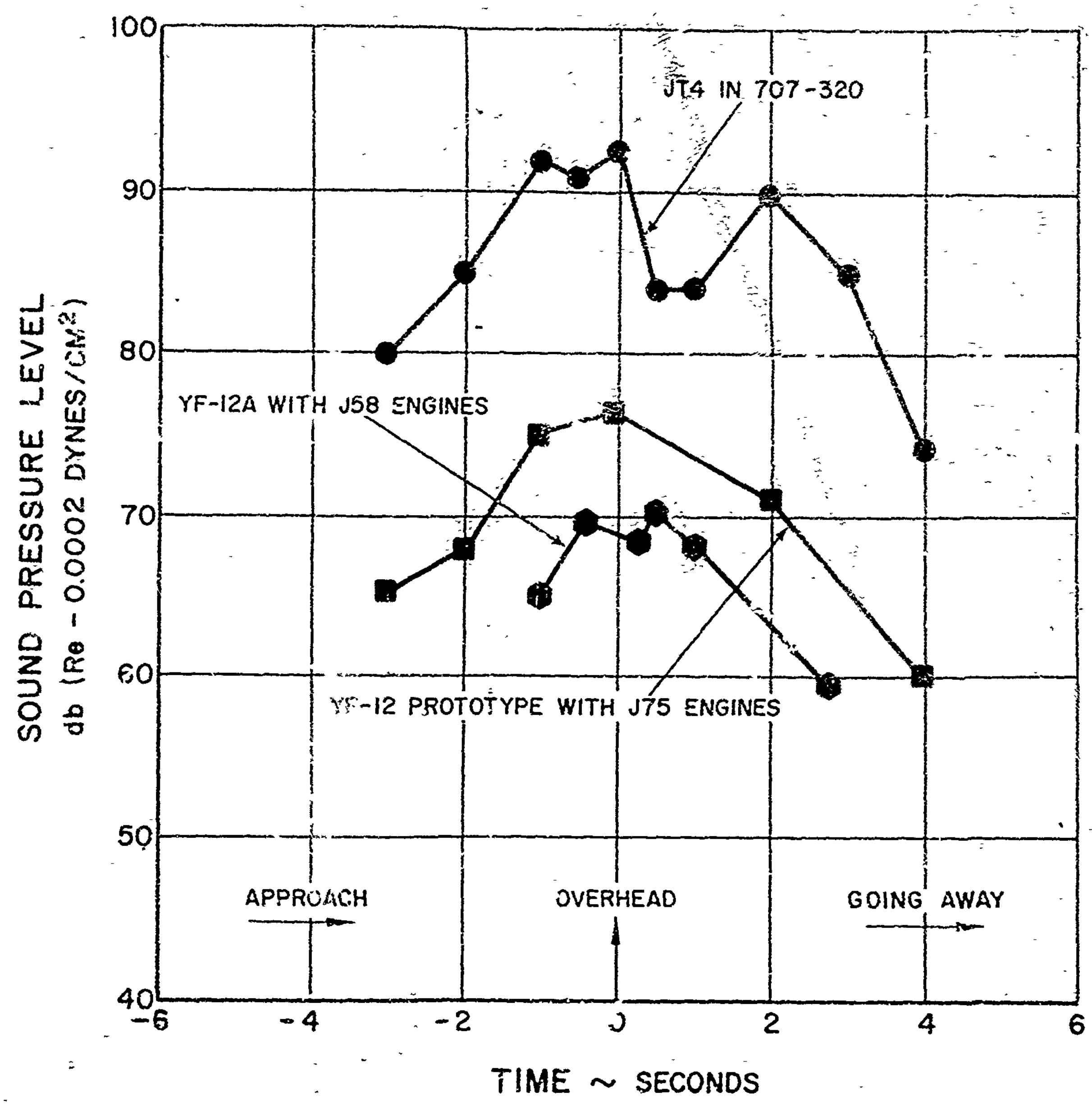

PEAK DISCRETE FREQUENCY FLY-OVER NOISE COMPARISON
FOR ONE ENGINE AT APPROACH THRUST

Figure 9-B-2

CONTROLS

CONTROLS

ITEM 10 - CONTROLS AND ACCESSORIES

OBJECTIVE

The program is being conducted to determine the system requirements of the controls and accessories and to establish the design requirements with the sub-contractors.

A. CONTROLS

1. INTRODUCTION

The fuel system for the STF219 engine is a hydromechanical system employing the same fundamental principles as used for the JT11F-11, -12 engine.

The control system has four basic functions:

1. It controls the engine speed between idle and maximum gas generator power.

2. It schedules the main engine fuel flow within the desired limits during transient operation.

3. It sequences the scheduled duct burner flow, supplied from an air driven turbopump, over the operating envelope between augmentation cut-off and maximum augmentation to two individual fuel manifolds.

4. It positions the exhaust nozzle area to maintain the desired engine operating condition.

The requirements will be established such that the thrust varies essentially linearly with the power lever position and that the air flows are compatible with the air induction system over the range of the flight envelope. Further, the fuel system must provide rapid thrust modulation of the engine while ensuring safe, reliable regulation during transient operation.

2. DESCRIPTION OF COMPONENTS

Packaging and Operation - A schematic diagram of the fuel system for the supersonic transport is shown in Figure 10-1. The system is basically the same as was proposed for the Phase I program. The gas generator fuel control, the duct heater fuel control, and the duct exhaust nozzle area control are all packaged in a single unit consisting of a computer section, a gas generator fuel metering system, and a duct heater fuel metering and nozzle control system.

Packaging the three systems together results in a system which is smaller and lighter than that using separate packages. The weight savings is realized by the full utilization of the servos and cams common to each control unit and by the elimination of the fuel line connection between separate units. Further, the single unit may be removed for servicing the fuel metering subassemblies without disturbing the settings of the control system.

The major changes to the system were the removal of the trimming power lever, the relocation of the fuel-oil coolers to a position downstream of the main fuel pump, the addition of an air induction system signal input for airflow control, and an aircraft signal for control of the landing approach velocity.

With the present control, the thrust level of the STF219 engine is controlled by a single power lever. The power lever sets the absolute power available from the gas generator and the duct burner in the range from full reverse to full forward. The relationship between the power lever and the relative thrust levels of the gas generator and the duct heater is shown in Figure 10-2. The relationship is such that the thrust changes essentially linearly with changes in power lever position. For non-augmented operation, thrust is controlled directly by the power lever in the conventional manner. For take-off, the power lever is advanced to the maximum non-duct heating position. If duct heating is desired, the power lever is advanced into the duct heating regime. As the duct heater lights, the gas generator thrust level is cut back as the control resets the turbine inlet temperature to its cruising value. The desired thrust is attained by duct heater modulation. Maximum engine power may be obtained by moving the power lever to the full forward position. At this setting, the turbine inlet temperature is set to its maximum value, and the duct heater provides maximum power. When cruise flight conditions are reached, the

power lever is repositioned in the duct heater modulation range. In this range, the turbine inlet temperature is set at its cruising value, and the desired thrust is obtained by duct heater modulation. For descent, holding, approach, landing, and reverse, the required power can be obtained by adjusting the power lever position in a conventional manner.

With the removal of the trimming function from the control, it is still necessary to provide for operation of the fuel shut-off valve and actuation of the inflight windmilling brake. This is accomplished by the use of the fuel shut-off lever similar to that used in present-day commercial engine controls.

<u>Gas Generator Fuel System</u> - The gas generator fuel control system for the supersonic transport engine consists of an engine driven fuel pump, an optional fuel de-icing system, a fuel-oil heat exchanger, a gas generator fuel control, a manifold check and dump valve, fuel nozzles, and the associated lines and manifolds. It is basically the same as the system for the JT11F engine, since the control requirements for the STF219 and JT11F engines are similar.

Fuel enters the inlet port of the fuel pump where it is driven by a centrifugal boost stage pumping element. The fuel is discharged into the fuel de-icing heat exchanger, if included, through a fuel filter, and is then fed back into a spur gear pumping stage. This stage delivers fully pressurized fuel through a fuel-oil cooler to the main fuel metering valve.

On the earlier version of the system, the main engine fuel oil cooler was located between the centrifugal boost pump and the gear-type pump. With this arrangement, however, failure of the centrifugal pump would cause the fuel to be bypassed directly to the gear-type pump around the fuel-oil cooler. By positioning the fuel-oil cooler downstream of the gear-type pump, fuel is supplied to the fuel-oil cooler independent of the operation of the centrifugal boost pump.

The high-setting fuel temperature control bypass valve has also been modified. This valve limits the fuel system temperature by returning fuel to the aircraft fuel tanks or another supplementary cooling source when required. Originally, the valve was thermostatically operated. To increase the reliability of the system, however, provision has now been made for the addition of a manually operated backup valve which would be actuated whenever the power lever was plac~~ed in~~ the idle position.

The original system also included a low-setting fuel temperature-controlled bypass valve and on-off valve. This valve transferred the fuel flow which was bypassed by the main fuel control to the inlet of the high-pressure stage of the duct fuel pump when the fuel temperature exceeded a preset value. Transferring the higher temperature bypass fuel flow to the duct burner during augmented operation resulted in the fuel-oil cooler receiving cooler fuel from the main fuel pump. For the modified system, the transfer line has been eliminated and a second fuel oil cooler has been added between the duct fuel pump and the duct fuel metering valve. The modification reduces the bulk oil temperature and produces a simpler, more reliable system.

Duct Heater Exhaust Nozzle and Fuel Control System - The duct heater fuel and exhaust nozzle control system consists of a bleed air turbine driven duct heater fuel pump, a hydraulic pump, a duct exhaust nozzle control, a duct heater fuel control, a fuel oil cooler, manifold dump valves, and appropriate fuel injection devices. The system is designed to provide the correct amount of properly atomized fuel to the duct heater in order to establish and maintain the augmentation thrust level selected by the pilot, and to position the exhaust nozzle to establish and maintain the proper engine airflow.

Fuel is supplied to the duct heater nozzle system by a hydraulic pump which in turn is supplied with fuel from the boost stage or the impeller bypass line of the gas generator fuel pump. Pressurized fuel from the hydraulic pump is supplied to the hydraulic system controls where it is used as a power source to adjust the exhaust nozzle and nozzle reverser. During duct heating, fuel is supplied to the duct fuel pump where it is pumped by centrifugal pumping stages to the desired pressure and delivered to the duct fuel control. The duct fuel pump is driven by an auxiliary turbine which receives its power from a controlled amount of bleed air flow taken from the discharge of the engine high-pressure compressor. The duct heater fuel control schedules the augmentation fuel flow and supplies it through manifold dump valves to two individual fuel injection systems at a rate which is a function of engine burner pressure, inlet pressure and temperature, and power lever position. Fuel flow variations with changes in the power lever position are rate limited.

The duct exhaust nozzle area is positioned to maintain a desired engine inlet airflow during both non-duct heating and duct heating engine operation. The duct exhaust nozzle control properly positions the duct exhaust nozzle area by monitoring the engine high speed rotor speed, the engine inlet temperature, the fan discharge total-to-static pressure ratio, flight Mach number, and power lever position.

The system meets the transient requirements of the engine by using the rate limited power lever concept and a series of interlocks.

3. CONTROL METHODS

The engine control methods are similar to those of the JT11F engines. Unlike the earlier control, however, the present control maintains a constant inlet corrected airflow with cruising flight Mach number, automatically adjusts the thrust to maintain a constant cruise flight Mach number and a constant landing approach velocity, and provides low idle operation during descent.

Airflow Control - It is desirable to maintain a constant engine inlet corrected airflow for a given cruising flight Mach number, regardless of the free stream ambient conditions, in order to provide a better match between the inlet and the engine at non-standard conditions. Better matching reduces the aircraft drag and compressor inlet distortion. In order to meet the cruising inlet design point airflow requirements, it is necessary that the total airflow entering the inlet (minus bleed air for boundary layer control and secondary cooling) equal the airflow entering the engine and that the static pressure at the compressor face be such that the shock is placed at its optimum position. These requirements may be met either by using separately scheduled engine and inlet airflow controls or by using an engine airflow control which is dependent on the inlet conditions.

For the first method, the engine airflow is controlled by adjusting the duct exhaust nozzle area as a function of flight Mach number, high speed rotor speed, and engine inlet total temperature during engine operation above Mach 2. (The primary gas stream area is not variable.) Below Mach 2, the area is varied only as a function of the high speed rotor speed and the engine inlet total temperature. The transition Mach number is somewhat arbitrary and was selected for convenience. In both regions, the monitored parameters are used to

schedule the control parameter $(P_{t3}-P_{s3})/P_{s3}$. In the low Mach number region, the engine corrected airflow is maintained constant for a given inlet temperature, whereas, for the high Mach number region, the airflow is maintained constant for a given Mach number. The required Mach number signal will be obtained from the inlet system as shown in Figure 10-3.

For this method, the aircraft inlet airflow is independently controlled as a function of Mach number. The controlled airflow for the engine is estimated to be accurate within ±2 per cent, and the aircraft inlet should provide an airflow at the level of the high tolerance engine airflow. When the engine requires less airflow, the bypass doors will open to satisfy continuity and to position the shock at the optimum station.

For the second method, the engine airflow is controlled by varying the duct exhaust nozzle area as a function of the duct area control parameter, $(P_{t3} - P_{s3})/P_{s3}$, and the time integral of the inlet shock position error. The duct area control parameter would be scheduled from the high-speed rotor speed and the engine inlet total temperature, without the incorporation of the inlet shock position reset, this would result in the engine corrected airflow being a direct function of the engine inlet temperature. Thus, the engine corrected airflow would change with the ambient temperature for a constant flight Mach number during cruise. However, with the incorporation of the inlet shock position error reset, the engine corrected airflow is held constant for a given cruise Mach number despite decreases in the engine inlet temperature level.

When the engine requires less airflow than the inlet is passing, the bypass doors open, and, when more airflow is required, the bypass doors close. With the bypass doors closed, the normal shock moves downstream, producing a higher total pressure loss. It is required, however, that with the inlet bypass doors closed, the shock be positioned at its optimum station. Therefore, as shown in Figure 10-4, the shock position error acts as a bias on the duct area control parameter error to change the airflow required by the engine until the shock position error is reduced to zero. The biasing signal is prevented from reaching the area control when the bypass doors are open by a switching function in the inlet control.

Cruising Flight Mach Number Control - Both airframe manufacturers expressed a desire for a system that would modulate the engine thrust to hold the Mach number constant and provide cruise speed stability. A system was, therefore, designed which reduces the fuel supplied to the duct heater when the inlet total temperature exceeds a predetermined value. The fuel is reduced by resetting the duct fuel flow bias schedule (see Figure 10-5). The rate of change would depend upon the stability of the system and on the physical limits associated with high-rise cam contours.

Figure 10-6 shows the characteristics of the constant cruising Mach number control. During cruise, the power lever would be positioned for the desired engine thrust in the conventional manner. Normally, without the constant Mach number control feature, the net thrust delivered would increase with the flight Mach number until the increase in drag offset the increase in thrust. With the constant Mach number control feature, however, the thrust would be reduced for inlet total temperatures above the cut-off value by a proportional-gain fuel trimming hook. Resetting the power lever causes the cut-back to occur at a different engine thrust level. The thrust decreases with inlet total temperature at the same rate as previously, however, and therefore a different cruising Mach number would be obtained.

Constant Aircraft Approach Velocity Control - Lockheed requested that the feasibility of controlling the engine thrust to provide a constant approach velocity to a landing be studied. Such a feature was found to be feasible.

A rotor-speed governor hook reset by an error in flight speed was developed. The reset circuit would be supplied by the airframe manufacturer. The reset signal would be received by a lever on the outside of the control which would reset the engine power setting in accordance with the schedule shown in Figure 10-7. The effect of the system is shown in Figure 10-8. The reset system would not operate at idle or at maximum rated power. The slope of the governor hook should be as large as possible to a[illegible] a rapid engine reaction to compensate for aircraft drag characteristics and produce an effective velocity correction. The steepness of the slope would be limited by the stability requirements.

Low Idle - In accordance with a request from Boeing, a system has been devised to permit reduced fuel flow during descent. The system provides two idle levels, the lower of which uses a fuel flow which is one-quarter of that of the other.

Low idle operation can be obtained by placing the power lever in the idle position and the fuel cut-off lever in the low idle position, providing that the high-speed rotor speed is at least 50 per cent of the maximum speed. During initial descent, the rotor speed is above the 50 per cent value and low idle may be obtained. When the aircraft speed drops to about Mach 0.8, however, the rotor speed will decrease below the 50 per cent value and normal idle power will be developed. Advancing the power lever overrides the low idle settings. Further, low idle cannot be re-obtained after being overridden either by a change in the power lever setting or by a decrease in rotor speed unless the fuel cut-off lever is cycled between normal and low idle.

4. ENGINE TRANSIENT PERFORMANCE

The engine performance levels required by the supersonic transport during steady-state and commercial operation are higher than those for any existing commercial aircraft engine. To evaluate and optimize the transient performance of the combined engine, inlet, and control systems, a computer program was developed simulating each of the components. The program permitted the interactions of the inlet and engine systems to be studied as a working unit.

Computer Program - The STF219 engine and inlet performance was simulated on an electrical analog computer coupled with a digital computer. The analog computer was used primarily for integrations whereas the digital computer was used for algebraic calculations and to provide the non-linear functions and the selected time constants.

The calculation procedure used for the engine program is shown in Figures 10-9 through 10-16. It incorporates all recognizable effects including mass storage during transients, temperature lags, and rotor inertial effects. Provision is made for the simulation of surge in the low- and high-pressure compressors. The surge system is actuated when the calculated value of the average compressor pressure rise exceeds the surge value for a given corrected speed. The surge value shifts to account for the effects of inlet distortion and the value for the low-pressure compressor shifts when the high-pressure compressor is surging.

The engine program was combined with programs for fuel and exhaust nozzle controls and sent to Lockheed and Boeing. Lockheed supplied a program simulating a two-dimensional mixed compression inlet and a bypass door control.

The control vendors subsequently conducted transient performance studies using programs for their respective control systems in conjunction with the engine programs. The studies were directed primarily toward operation during augmentation to determine the compatibility of the engine with the inlet, but attention was also directed toward operation during duct heater lighting, duct heater blow-out, engine accelerations and decelerations, compressor surge, and engine flame-out. The results of these studies are presented in Appendices A and B for Bendix and Hamilton Standard, respectively.

Duct Heater Lighting - It is required that the duct heater be capable of being lit at all flight conditions. Lighting the duct heater, however, raises the back pressure on the fan, and, when the engine is operating at the maximum turbine inlet temperature, might drive the fan into the surge region. Protection will be obtained by lighting the duct burner at its leanest fuel-air ratio. Additional surge margin will be obtained by increasing the duct exhaust area before lighting the duct burner.

Figure 10-17 is a plot of the duct exhaust nozzle control parameter vs the corrected rotor speed for operation without duct heating and with duct heating using the minimum fuel-to-air ratio. The amount of duct nozzle area reset required depends on the rotor speed and on the fuel-to-air ratio at lighting.

When zone lighting is selected, the fan discharge pressure ratio reset valve is activated by the rate limiting power lever through a sequencing valve. This changes the requested $(P_{t3} - P_{s3})/P_{s3}$ to produce an error signal which causes the duct area to be reset. When zone lighting is achieved, the error signal is removed and the duct area readjusts to a value compatible with the temperature in the duct.

Zone lighting has a direct effect on the airflow required by the engine. Increasing the duct nozzle area prior to duct lighting increases the engine corrected airflow, whereas zone light up reduces the airflow for a fixed nozzle position. Figure 10-18 shows the calculated and analog computer values of airflow during these operations. The two sets of data differ because the calculated data assumed instantaneous combustion, an instantaneous rise in back pressure on the fan, and no change in the exhaust nozzle area as shown in Figure 10-19. However, combustion may require as long as 0.1 second to reach its proper level because of drooling effects of the manifold during the filling and lighting period. Also, the

pressure rise does not coincide with the temperature rise, but lags behind by about 0.01 second. Further, the engine airflow change lags behind the pressure rise by about 0.02 second. The total transient, therefore, requires about 0.13 second, but since the duct exhaust nozzle responds during the first 0.04 second, the airflow distrubance is reduced. Figures 10-20 and 10-21 show typical traces for duct heater lighting and thrust modulation.

Typical inlets are not expected to retain the shock wave when subjected to step airflow changes greater than 2 per cent or smooth changes at rates greater than 10 per cent per second. Duct burner lighting could exceed these limits, and therefore the augmentation control system will provide a signal for the supersonic inlet control system before duct burner lighting. This will permit the inlet control to anticipate the burner lighting and prevent the shock wave from being expelled. After lighting has been achieved, the resetting signal will be removed. The Lockheed inlet which incorporates stabilizing throat bleed can tolerate greater airflow distrubance rates than those listed above and thus requires no anticipation signal.

<u>Engine Accelerations and Decelerations</u> - The engine is expected to accelerate from idle through maximum non-augmented thrust to maximum thrust in accordance with the curve shown in Figure 10-22. The speed transient is shown in Figure 10-23.

The gas generator acceleration is limited by a fuel flow acceleration schedule which maintains an adequate surge margin for the high pressure compressor and ensures that the turbine inlet temperature limit is not exceeded. The acc leration schedule closely approximates the steady-state operating line for the fan.

The augmentation acceleration is limited by the time required to fill the individual zone manifolds. At the flight conditions on which Figures 10-23 and 10-24 are based, the time to fill each manifold is one second. The remaining acceleration time is a result of the rate limiting of the power lever motion to minimize the airflow disturbance.

During engine deceleration, the airflow remains essentially constant since the duct exhaust nozzle area is varied to maintain the prescheduled fan discharge pressure parameter. However, when the limit of the exhaust nozzle area change is reached, the airflow will be reduced.

During decelerations, the permissable rate of airflow change does not exceed 10 per cent per second, and therefore the system is compatible with the inlet.

Compressor Surge - Should compressor surge occur, it will occur during engine accelerations or decelerations, or as a result of inlet distortion, duct heater lighting, or inadequate duct nozzle exhaust area.

If the fuel control does not adequately limit the rate of fuel flow increase during acceleration, the rapid rise in burner temperature and pressure will accelerate the high-pressure compressor with its relatively low inertia into the surge region since the flow is restricted by the turbine nozzle vanes. The fan, however, is driven toward choked operation since its relatively high inertia restricts its acceleration rate, and the increased airflow demanded by the high-pressure compressor reduces the pressure between the compressors. During deceleration, the high-speed rotor decelerates faster than the low-speed rotor, restricting the engine flow. With these conditions, the fan may surge unless the duct exhaust nozzle area is increased.

Inlet flow distortions may cause slightly reduced flows and have a tendency, therefore, to induce surge. The effects of surge on the inlet were determined during several computer runs. Surge was induced by altering the control limits so that either duct lighting occurred with too rich a mixture or that the duct exhaust nozzle area was too small. In each case, the engine surged violently enough to disgorge the normal shock, producing high normal shock total pressure losses and consequently reduced compressor inlet total pressure and engine airflow. The traces for shock expulsion are not included in Appendices A and B since the computer was not programmed to compute for a shock position outside the cowl lip.

With normal control operation, the reduced engine airflow would be sensed by the duct area control which would increase the duct area and permit the engine to recover. The engine power lever angle might also be reduced at the first indication of disturbance to make the engine requirements more compatible with the inlet.

5. THRUST REVERSER

Boeing has requested a three-position thrust reverser. The positions are stow, null thrust, and reverse thrust. The position of the thrust reverser is controlled by the power lever as shown in Figure 10-23.

The reverser is stowed for all power lever angles greater than 35 degrees. The null position is provided for power lever angles between 35 and 23 degrees with a rotor speed approximately 80 per cent of the maximum speed being obtained at the 25 degree point. Retarding the power lever further selects the full reverse thrust position and in-

creases the rotor speed until 100 per cent of the available reverse thrust is obtained at a power lever angle of 0 degrees. The fuel control limits the rate of change of the power lever until the selected position of the reverser is achieved. The reverser requirements for the Lockheed installation are conventional in that only two positions, stow and reverse, are required. The system operates essentially the same as the current subsonic jet reversers and is the same as the system described above except for the omission of the null thrust position.

6. CONTROL VENDOR STATUS

Contracts for the continuation of the work funded by contract AF33(657)-11189 and reported in Technical Report PWA-2353, Appendices A and B, were placed with the Bendix Products Aerospace Division and with the Hamilton Standard Division. The contracts provided for each vendor to continue the testing of their respective pressure ratio sensor designs in order to more fully explore the problem areas. It was intended that this phase of the program would reveal which engine control is better suited for the proposed engine, thus enabling a selection of one of the vendors.

The vendors have completed their studies and have submitted their reports. The reports submitted by the vendors are included in this report as Appendices A and B and contain the results of analytical, design, and experimental efforts conducted to develop a control system which will meet the engine requirements and provide optimum engine performance. Included are the results of control mode studies, analog computer control simulation, and studies of control configurations and installation arrangements.

7. CONTROL SYSTEM COMPONENTS

Studies were conducted to define the design and performance requirements of the primary components of the control system. The main fuel control, duct area control, and duct fuel control requirements were issued to the vendors early enough to permit them to study the requirements and develop a mathematical model of the control for computer representation. The preliminary purchase specification for the control system, PPS 819D, is presented in Appendix 10-A.

Additional specification (also included in Appendix 10-A) have been issued for the system pumps. The main fuel pump is an engine-driven high-pressure single stage unit fed by a single-stage centrifugal pump. The requirements for this pump are specified in PPS 858. The engine-driven hydraulic pump requirements are specified in PPS 859. The duct heater fuel pump is a centrifugal unit driven by an auxiliary air turbine. The requirements for this pump are specified in PPS 860.

B. ACCESSORIES - IGNITION SYSTEM

1. INTRODUCTION

The design of the SST engine ignition system was predicated on the requirements for high reliability and long life under the extreme environmental conditions of this installation. Consideration was given to methods of reducing the system complexity to produce a system with low weight and low cost when such reductions could be made without sacrificing performance or reliability.

A high and a low tension system were designed. The low tension system appeared to be the better suited for the intended application. The low tension system is a 4-joule dual ignition system using fuel to cool the critical exciter components. Two versions of the system were designed and tested. By using fuel cooling, electrical components similar to those used on existing commercial engines could be used at their maximum operating temperatures, and the low tension leads and igniters required no technological advances to permit operation at the anticipated temperature levels.

The high tension system was designed as a backup system in case the low tension system is found to be inadequate for engine ignition under certain operating conditions. The high tension system is somewhat larger, more expensive, and more complex than the low tension system. Furthermore, a larger development effort would be necessary to perfect a high tension transformer capable of withstanding the SST environmental temperatures without electrical breakdown. One vendor has proposed a high tension ignition system in which the high tension transformer is housed in the fuel-cooled exciter. The vendor has started development of the high temperature, high tension lead required to supply power to the ignitor. A second vendor has designed and fabricated a high tension, high temperature transformer, and tests have been conducted.

Augmentor rig ignition by a resistance element glow plug was demonstrated following a laboratory evaluation of the glow plug temperature and warm-up characteristics.

2. COMPONENTS

The low tension ignition system consists of two independent AC powered, 4-joule low tension capacitance discharge type ignition circuits designed to fire two igniters continuously. Both circuits are contained in a single exciter package. Two cooling systems were designed. For the first, shown in Figure 10-25, fuel circulates in an annular passage around the exciter. For the second, shown in Figure 10-26, the fuel flows through a spiral-wound tube brazed to the exciter body. The exciters are enclosed in a thermally insulating blanket in both designs.

Two high-tension ignition systems were designed. The first consists of a low tension exciter, similar to that used for the low tension system, driving two separate voltage transformer-capacitor-igniter packages as shown in Figure 10-27. The transformer-igniter system is designed to operate in environments up to 1000°F and provision is made for the replacement of the igniter plug in the field. For the second system, the high-tension transformer is housed in the cooled exciter package. High temperature, high tension leads, still in the development stage, will connect the exciter to the igniters.

The 24-volt DC powered glow plug for augmentor ignition consists of a dual helically wound resistance coil recessed in a steel shell.

3. FACILITIES

An altitude chamber consisting of a 3.5-foot diameter sphere was used to obtain a pressure level equivalent to the pressure at an altitude of 80,000 feet. The chamber cannot simulate the cold ambient temperature associated with the high altitude, however.

A 4-cubic foot chamber, thermostatically maintained at -65°F, was used to cold soak components a minimum of 48 hours before low-temperature testing.

The radio frequency interference shielded room is constructed to comply with the requirements of MIL-E-1957A. The equipment, radio receiver, antennas, stabilization networks, and signal generator comply with the requirements of MIL-I-6181D.

The heat transfer capabilities of the fuel-cooled exciter were evaluated on a rig using water instead of fuel as the heat sink while the exciter was mounted in an electrically heated oven. The heat added to the water as it was pumped through the exciter in the oven was removed in a secondary heat exchanger. The temperatures of the exciters, water, and oven were measured with thermocouples and with a potentiometer pyrometer. Water flow rates and pressure drop through the exciter cooling passages were measured with a flow meter and differential pressure gage, respectively.

4. TEST PROCEDURE

The igniters were evaluated for spark repetition rate, breakdown voltage as a function of pressure, radio frequency interference, and heat transfer characteristics.

The spark repetition rate was determined at sea level ambient pressure and temperature, at sea level ambient temperature but a pressure altitude of 80,000 feet, and at sea level ambient pressure and -65°F. Tests were conducted at each of the above conditions with minimum, nominal, and maximum input power. Open circuit voltages were measured by an oscilloscope fed by a voltage divider.

The igniter breakdown voltage was measured at atmospheric pressure, 100 psig, 200 psig, and 500 psig. Voltages were measured by an oscilloscope fed by a voltage divider in the igniter input lead.

Because of the method of constructing the high voltage transformer-capacitor-igniter package, the open circuit voltage could not be readily measured without destroying the igniter. Consequently, the open circuit voltage was determined by measuring the minimum pressure at which the igniter fails to fire. This value was then correlated to the cut-off pressures for igniters with similar gap designs for which the breakdown voltage is known.

The spark energy of the high-tension ignition system was determined by integrating the power-vs-time curve produced from an oscillograph display of the voltage and current during igniter firing.

Radio frequency interference tests were conducted in accordance with MIL-I-6181D.

Heat transfer characteristics were evaluated in an oven with the exciters protected from direct contact with the oven floor by a fire brick. A water flow rate of 250 pph was established on the basis of the ratio

of the specific heats of water and fuel and was equivalent to a fuel flow of 500 pph. The oven was then set at 750°F and the water temperature into the exciter maintained at 90°F. The data taken included the water temperature into and out of the exciter, the exciter internal temperature, the temperature profile of the exciter skin, and the pressure drop through the exciter cooling passage. Readings were taken every 15 minutes. The exciter was not energized until after the temperature had been stable for at least one hour.

Inasmuch as the ability of water to remove heat from the surface over which it is passing differs from that of fuel, the temperature of the exciter internal components when using fuel cooling could not be computed directly from the data based on using water as the coolant. Instead, the temperature of the effective portion of the exciter wall adjacent to the internal components was computed from the data obtained with water as the coolant. Based on the fact that the temperature differential between internal components and the exciter wall must be the same regardless of coolant in order to remove a given amount of heat from within the exciter, the internal component temperature was then calculated assuming a fuel coolant flow of 500 pph at 250°F.

Glow plug element temperatures were measured under ambient pressure and temperature as a function of power input by an optical pyrometer. Transient as well as stabilized characteristics were determined. The augmentor rig described in Item 7 was lit by injecting atomized fuel onto the glow [illegible] set at approximately 2300°F.

5. DISCUSSION OF RESULTS

Low-Tension Ignition System - The results of testing the two low-tension ignition systems are shown in Table 10-1. These results indicate that both low-tension ignition systems have the capability of meeting all SST requirements with respect to spark repetition rate and open circuit voltage. Both systems operated satisfactorily at altitude, cold, and sea-level ambient conditions. The spark rate checks made during heat transfer tests with the component temperatures between 250 and 300°F never fell below the minimum requirement of one spark per second or went above the maximum of 2.5 sparks per second. The voltage required to make the low tension igniter spark was less than 1 KV for any pressure up to 200 psig, and only rose to 1.1 KV at 500 psig.

TABLE 10-1

Low-Tension Ignition System Test Results

Spark Repetition Rate (Sparks Per Minute)

	Annular-Cooled Exciter		Spiral Tubing-Cooled Exciter	
Sea Level Ambient	Circuit A	Circuit B	Circuit A	Circuit B
360 CPS 90 VAC	109	118	72	78
400 CPS 115 VAC	154	161	88	93
440 CPS 124 VAC	160	175	82	87
Altitude (80,000 Feet)				
360 CPS 90 VAC	112	119	72	76
400 CPS 115 VAC	159	173	92	88
440 CPS 124 VAC	158	172	36	88
Cold (-65°F)				
360 CPS 90 VAC	121	125	83	80
400 CPS 115 VAC	168	181	88	94
440 CPS 124 VAC	167	177	87	93

Other Characteristics

	Annular-Cooled Exciter		Spiral Tubing-Cooled Exciter	
Open Circuit Voltage (volts)	2980	2980	2980	2980
Total Hot Time to Date (Hours)	65		124	
Total Electrical Time to Date (Hours)	20.5		49	

Typical SST Low Tension Igniter

Pressure (psig)	0	100	200	500
Breakdown Voltage (KV)	0.6	0.7	0.9	1.1

High-Tension Ignition System - The high-tension ignition system met the same spark repetition rate standards set for the low tension system and continues to meet these requirements during a duty cycle operation of 2 minutes on, 3 minutes off, 2 minutes on, and 23 minutes off. The test was conducted at 1000°F and indicated that the high temperature, high-tension transformer design is a feasible method of supplying a high-tension ignition system if required for the SST engine. The high-tension igniter power was 38.5 Kw and the spark energy was 0.6 Joules, indicating that some improvement in high-tension transformer efficiency is required.

TABLE 10-2

High-Tension Ignition System Test Results

	Spark Repetition Rate (Sparks Per Minute)		
	360 CPS 90 VAC	400 CPS 115 VAC	440 CPS 124 VAC
Sea Level Ambient	75	91	90
Altitude (80,000 Feet)	72	88	68
Cold (-65°F)	71	86	94
Hot (1000°F)	-	78	-

Other Characteristics

Igniter Pressure (psig)	100	200	300	350	375
Sparks Per Minute	84	8[illegible]	85	81	Igniter fires Intermittently

Total Time at 1000°F to Date 43.5 Hours
Total Electrical Time to Date 5.2 Hours

	First Loop	Second Loop	Third Loop	Total
Power at Igniter (Kw)	28	7.1	3.4	38.5
Energy at Igniter (Joules)	0.35	0.15	0.10	0.60

Radio Frequency Interference - Radio frequency interference testing has established that neither radiated nor conducted noise is a problem for the SST ignition system. All recorded noise levels were well below the limits of acceptable noise as established in MIL-E-5007B.

Glow-Plug Testing - The results of testing the glow plug are shown in Figure 10-23. These results indicate that the glow plug has the ability to reach and exceed the temperature required to ignite the SST augmentor. The test results were confirmed by the successful glow plug lighting of the augmentor test rig. Current development of the glow plug is being directed toward decreasing the warm-up time and improving the durability.

Exciter Cooling Tests - The results of heat transfer testing the exciter are shown in Table 10-3. The results indicate that fuel cooling allows the internal exciter components to operate at or below the temperature levels of current engine ignition systems. The annular cooling method was somewhat more effective than the spiral-wound-tube method, primarily because a higher percentage of the area cooled directly by the fuel is adjacent to the interior components in the annular cooling design, whereas in the wrapped tube design a large portion of the tubing removes ambient heat through the insulation resulting in cooler insulation but a higher fuel temperature rise. Both cooling schemes maintained satisfactory internal temperatures with the ignition system energized. Investigation of the construction of the wrapped-tube exciter by the vendor has revealed deviations from the design, which, when corrected, will improve the ability of the exciter to cool the internal components.

The low tension leads continued to function satisfactorily at the maximum temperature level to which they will be exposed on the SST engine.

TABLE 10-3

Exciter Cooling Test Results

	Annular Cooled Exciter		Spiral Tubing Cooled Exciter	
	With Insulation (est.)	Without Insulation	With Insulation	Without Insulation
Max Internal Component Temperature - Ignition On (°F)	[illegible]	[illegible]	[illegible]	342
Heat Removed by Cooling Fluid (BTU)	[illegible]	[illegible]	397	[illegible]
Temperature Rise Across Exciter Cooling Fluid (°F)	[illegible]	14	4	11
Pressure Drop Across Exciter (psi)	1.5	1.5	4.0	4.0
Spark Rate (Sparks Per Minute)	[illegible]	144	92	94
Predicted Component Temperatures (°F)				
Tank Capacitor	320		338	
Power Coil Rectifier	240			
Rectifier Compartment			256	
Transformer Compartment			29?	

Note: Data for operation at ambient temperature of 750°F and equivalent of cooling with fuel at 250°F and flow rate of 500 pph.

6. RECOMMENDATIONS

The favorable results obtained with the initial combustor and augmentor ignition system hardware confirms that development of these systems should continue.

Development of the low tension ignition system should be directed toward:

1. Further improvement of the exciter design to reduce the size and weight below the current acceptable levels and to improve heat transfer characteristics and field maintenance capabilities,

2. Investigations of actual ignition capabilities in combustor rig testing, and

3. Endurance testing of acceptable designs to prove long term reliability.

High-tension ignition system development should include investigation of the effects of high temperature on the high-tension components with particular emphasis on the development of high-temperature transformers and high-tension leads. High-temperature endurance testing will be necessary to prove the reliability of the high-tension components.

The augmentor ignition system glow plug requires rig development to optimize the plug temperature, configuration, and location. Development efforts should be directed toward improving the durability and reducing the warm-up time.

NOMENCLATURE

Primary Symbols

A	Area (ft^2)
C_p	Specific heat at constant pressure (Btu/lb°R)
C_v	Specific heat at constant volume (Btu/lb°R)
F	Thurst (lb)
h	Enthalpy (But/lb)
K	Constant
KBL	Duct flameholder bleed air factor. KBL = 1 - (bleed airflow/ total airflow)
Mn	Mach number
N_1	Low-speed rotor speed (rpm)
N_2	High-speed rotor speed (rpm)
P	Total pressure (lb/ft^2)
P_s	Static pressure (lb/ft^2)
R	Gas constant ($\bar{R}$/MW) (ft lb/lb°R)
S	Laplace complex operator (sec^{-1})
T	Total temperature (°R)
V	Volume (ft^3)
V_o	Air velocity relative to aircraft (ft/sec)
W_a	Airflow (lb/sec)
W_f	Fuel flow (lb/sec)
γ	C_p/C_v
δ	P/2116
η	Efficiency
θ	T/519
τ	Time constant (sec)
$\mathcal{P}$	Power (Btu/sec)

Subscripts

am	Ambient
av	Average
b	Burner
bd	Duct diffuser discharge
ch	High-pressure compressor
d	Fan duct exit section
e	Primary burner section
g	Gross
ID	Radial section passing primary airflow
n	Net
OD	Radial section passing duct airflow

op	Optimum
r	Ram
s	Static
t	Total
2	Fan inlet
3	Fan discharge
4	High-pressure compressor discharge
5	Primary burner discharge
6	High-pressure turbine discharge
7	Low-pressure turbine discharge
9	Primary tailpipe discharge

Superscript

1	Ideal

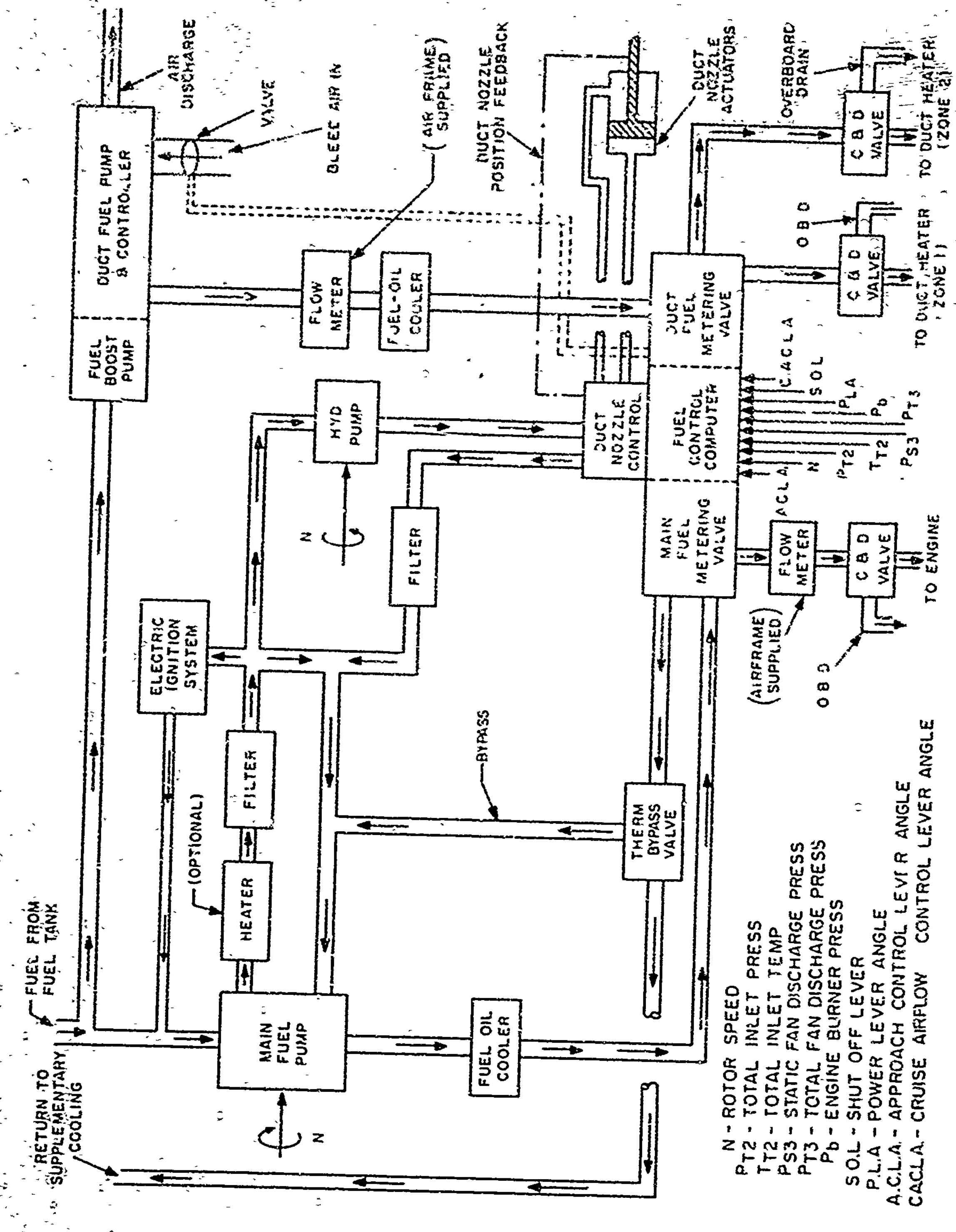

SCHEMATIC DIAGRAM OF ENGINE CONTROL SYSTEM

Figure 10-1

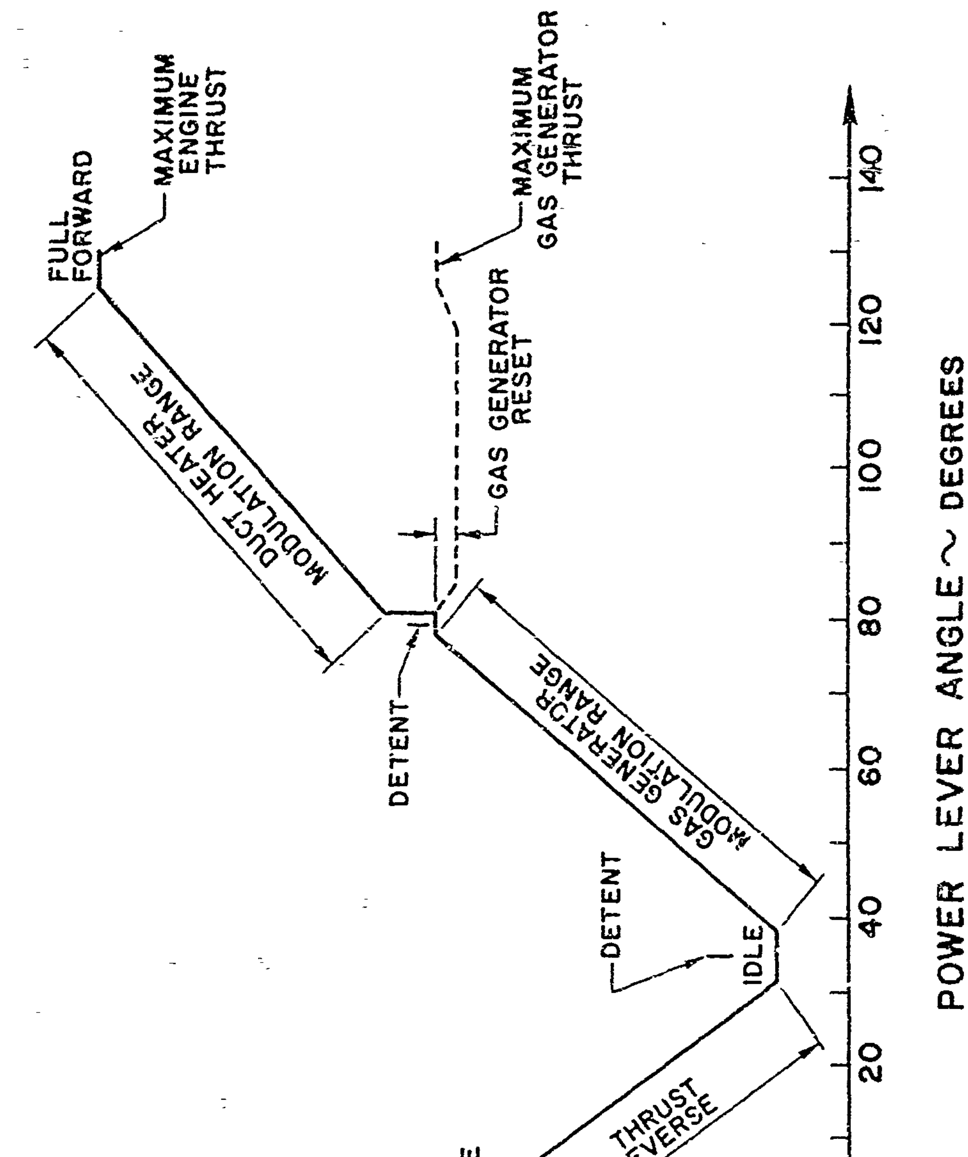

ILLUSTRATION OF POWER LEVER OPERATION

Figure 10-2

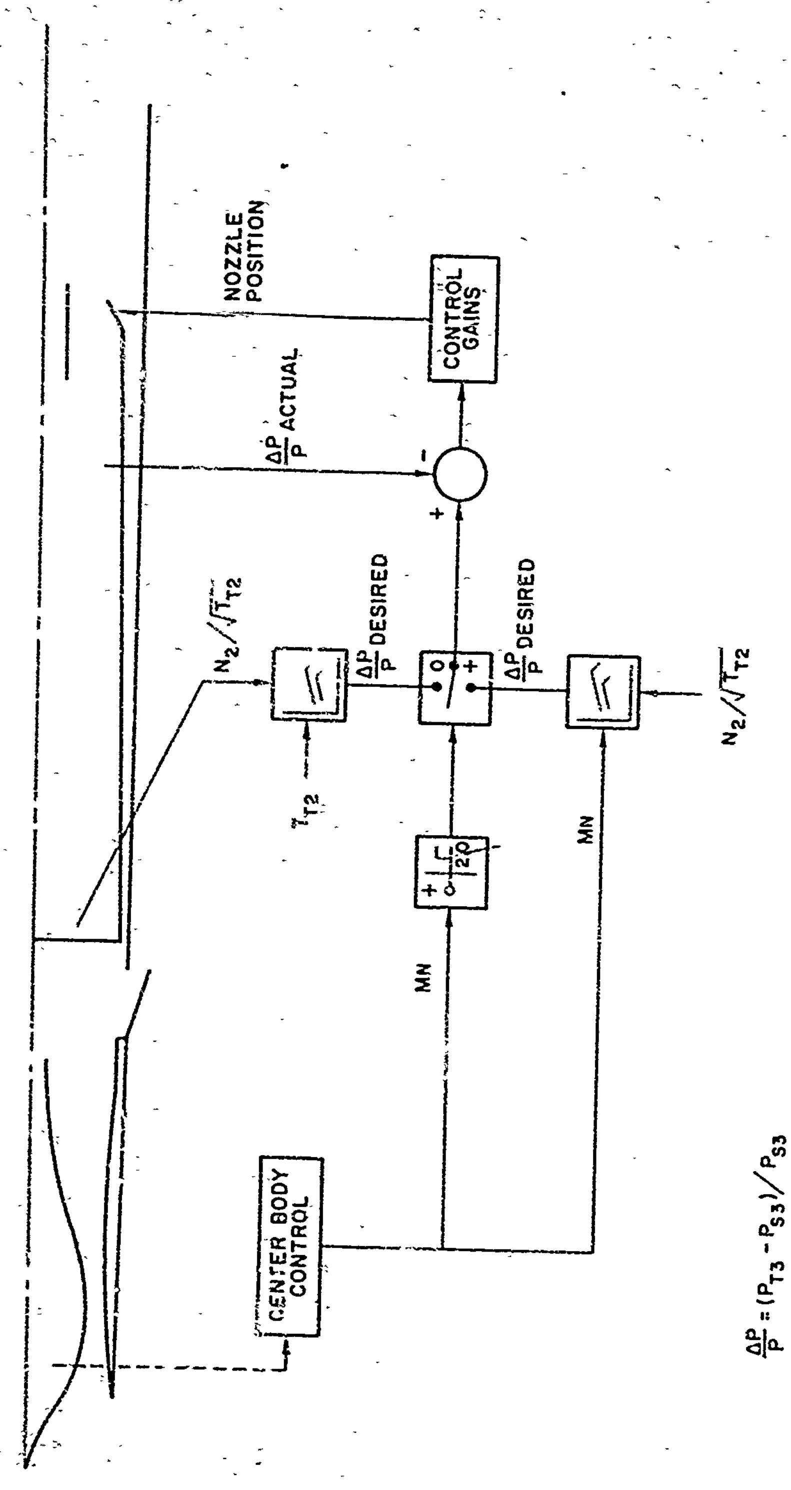

ENGINE AIRFLOW CONTROL - METHOD I

Figure 10-3

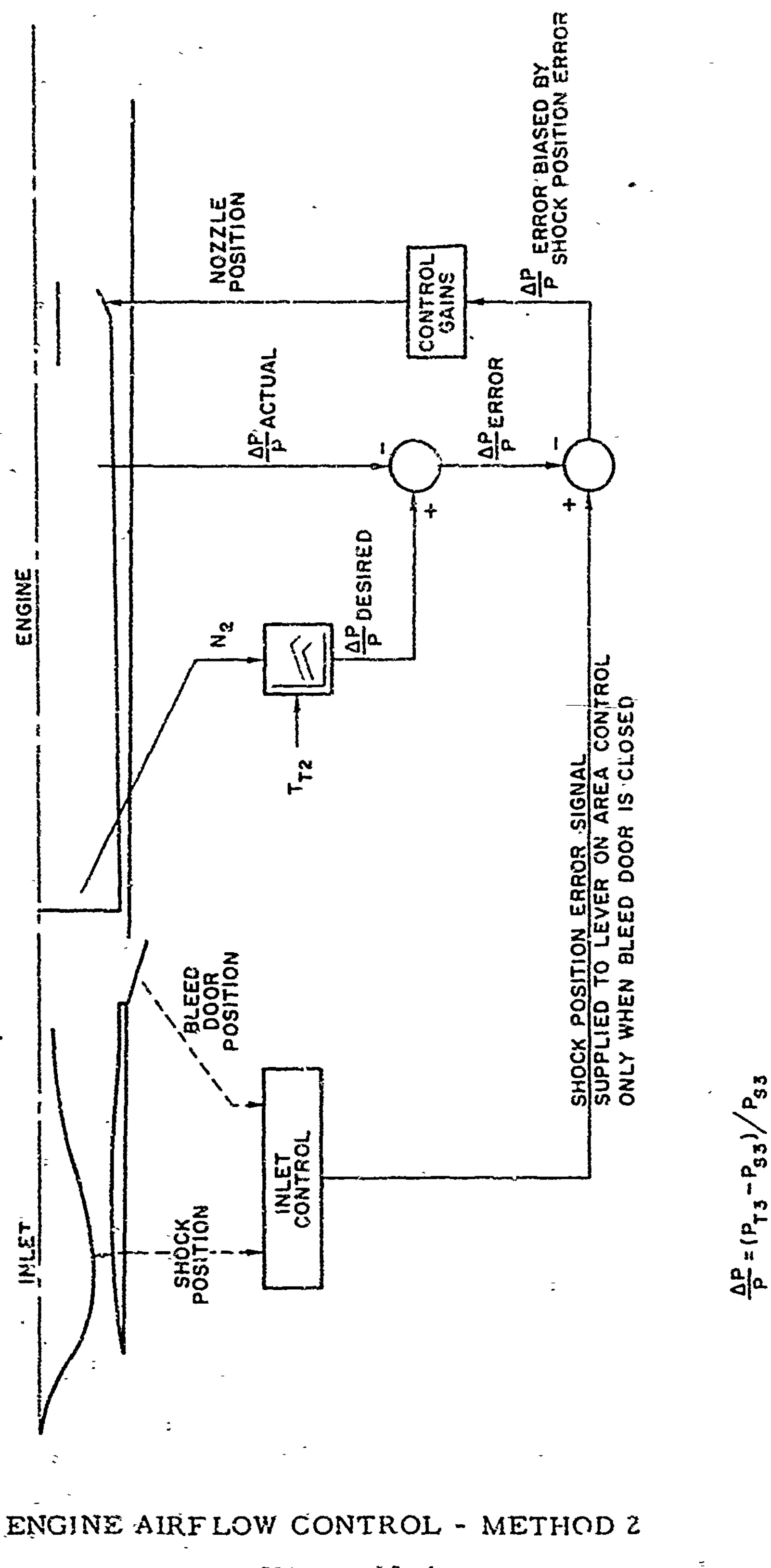

ENGINE AIRFLOW CONTROL - METHOD 2

Figure 10-4

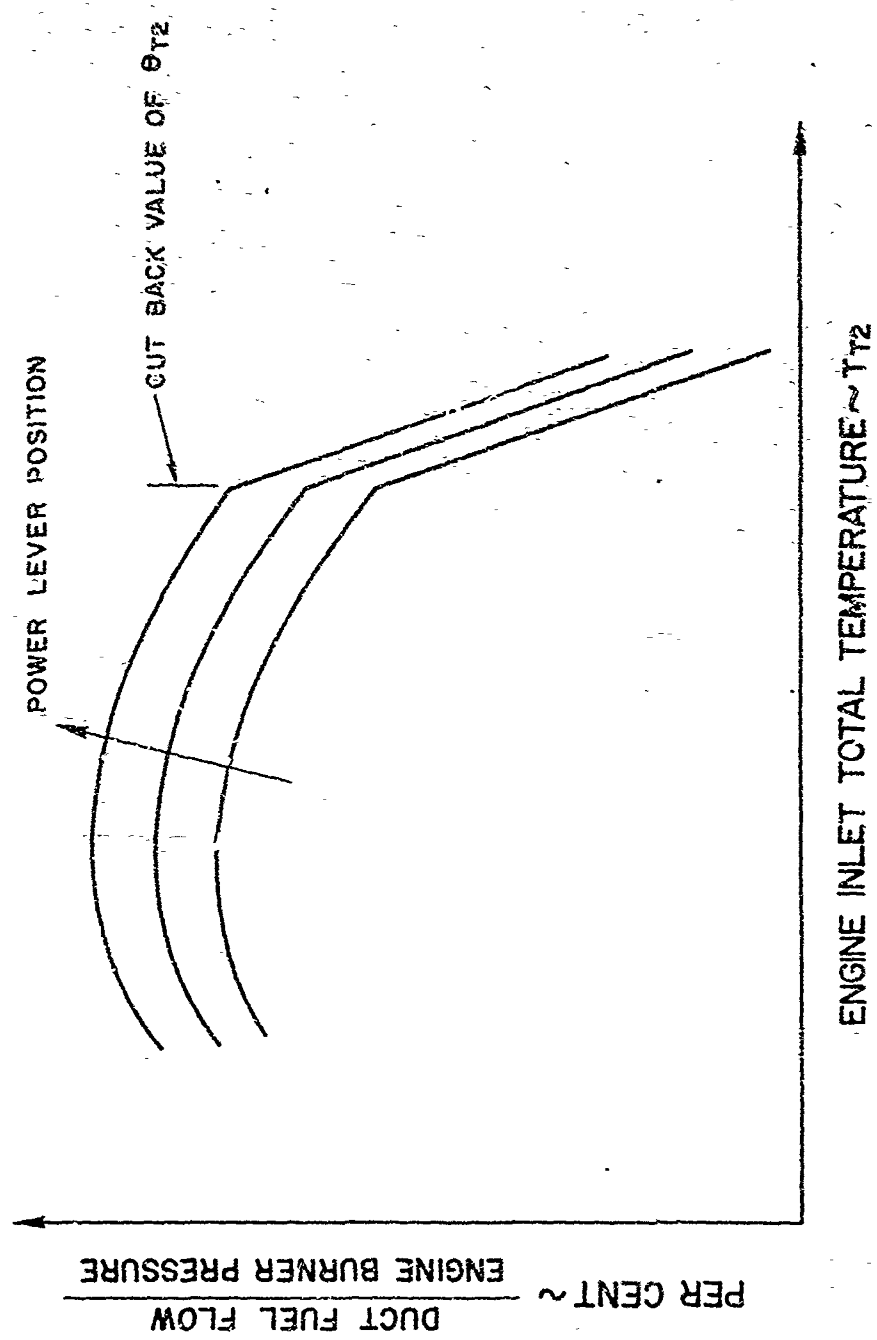

ILLUSTRATION OF DUCT FUEL FLOW RATIO BIAS RESET
FOR THRUST CUT-BACK

Figure 10-5

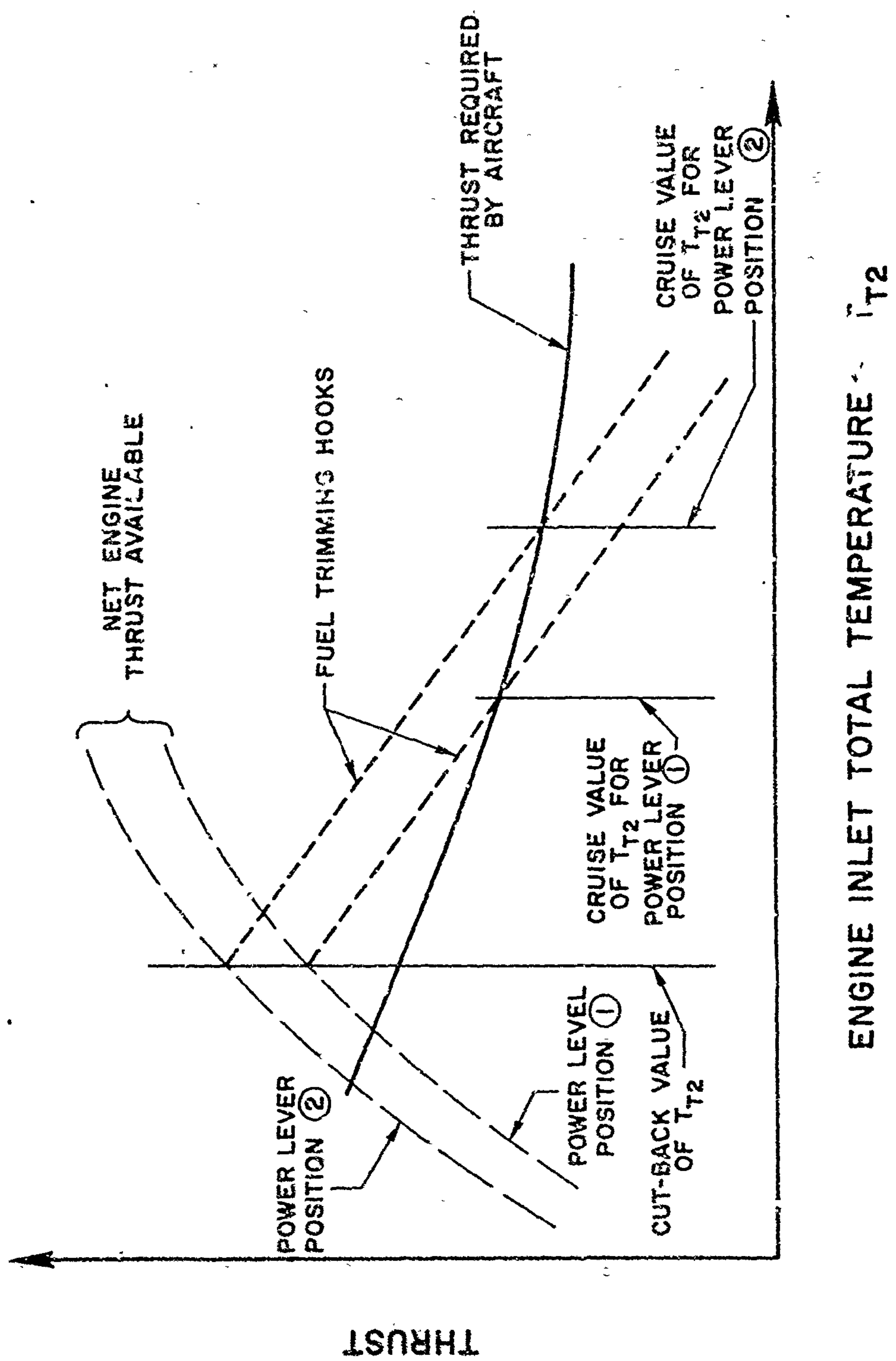

CONSTANT CRUISING MACH NUMBER CONTROL CONCEPT

Figure 10-6

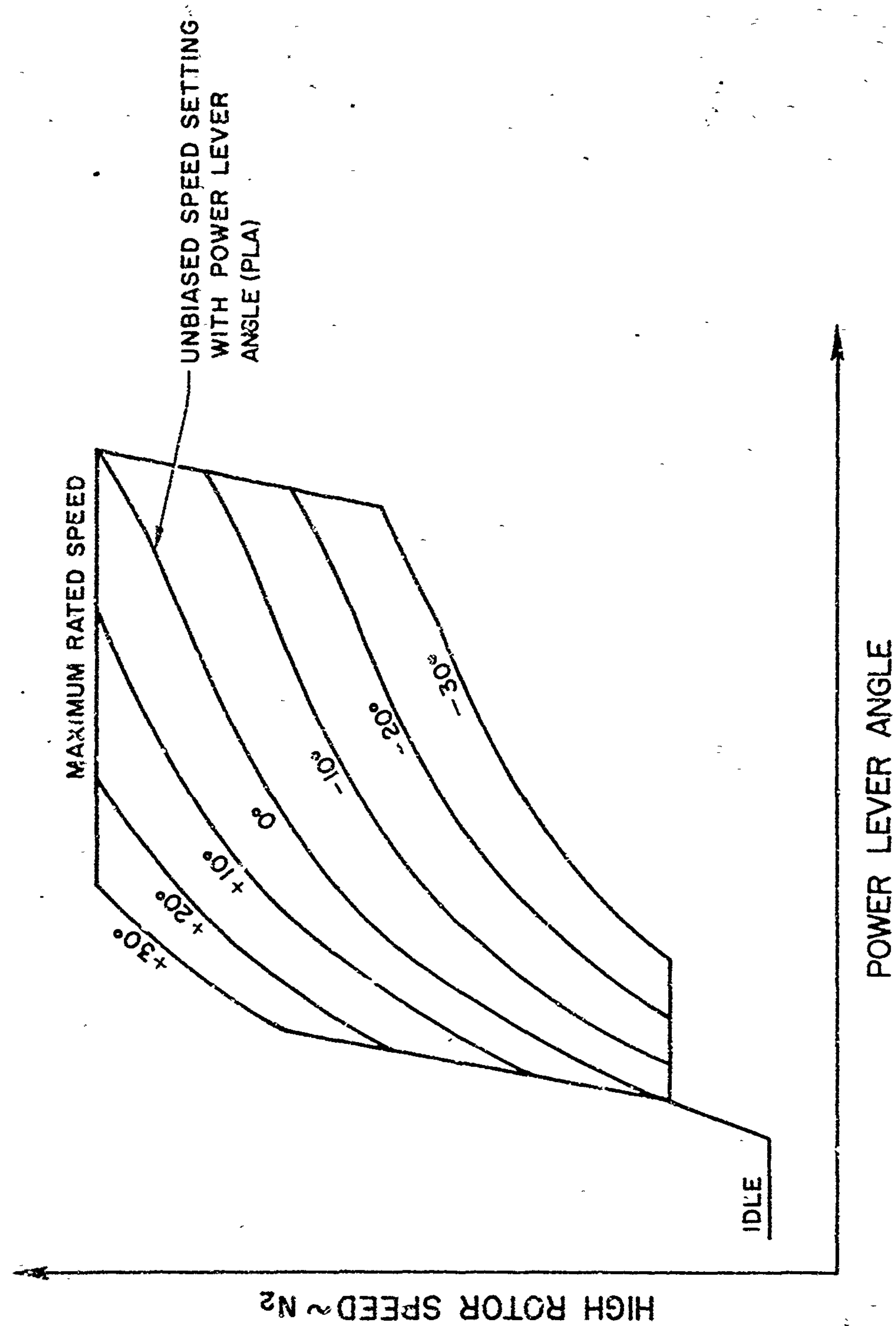

ILLUSTRATION OF ROTOR SPEED BIAS WITH APPROACH SPEED RESET LEVER ANGLE

Figure 10-7

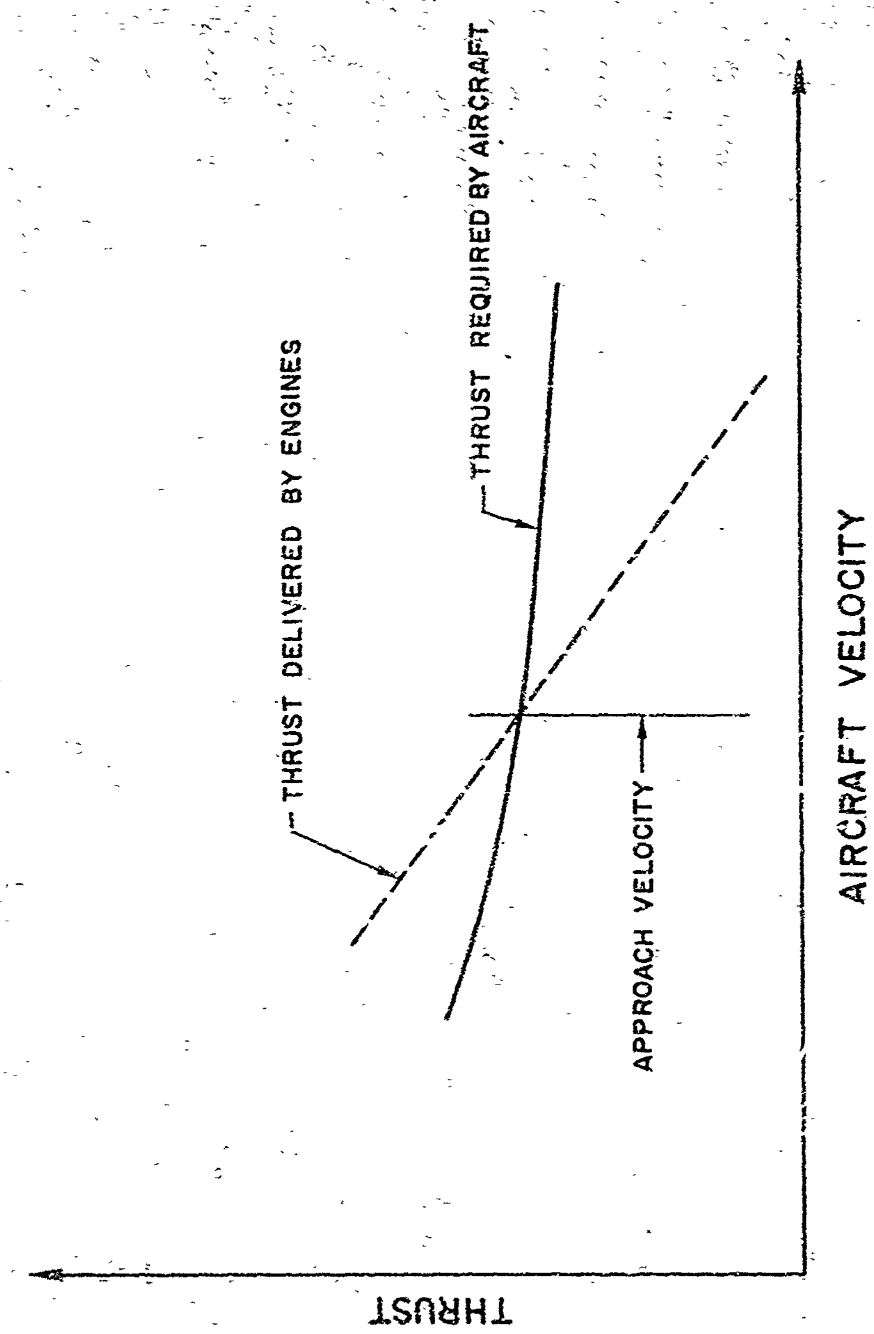

ILLUSTRATION OF APPROACH VELOCITY CONTROL CONCEPT

Figure 10-8

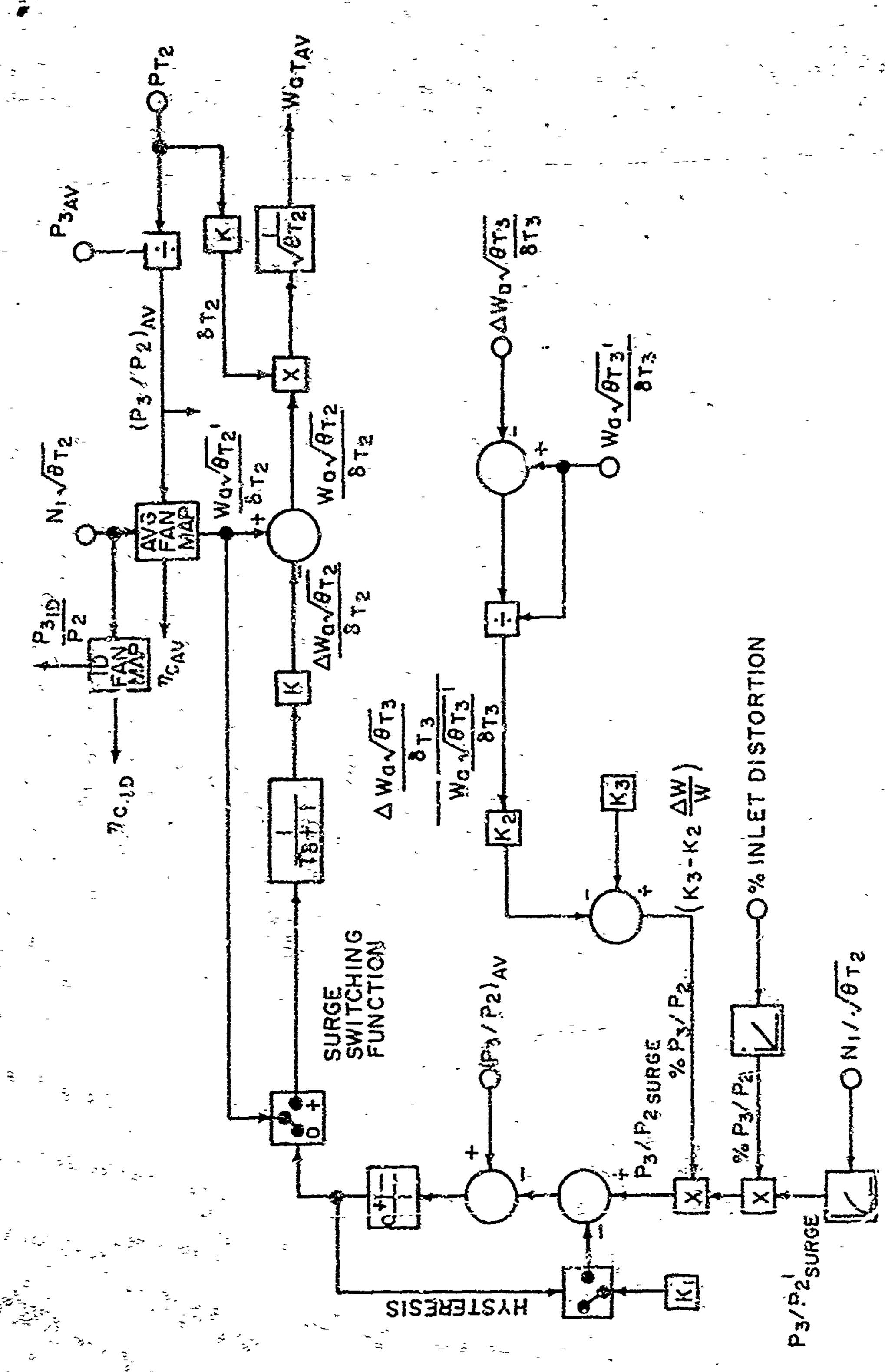

ANALOG PROGRAM FOR STF219
ENGINE LOW-PRESSURE COMPRESSOR

Figure 10-9

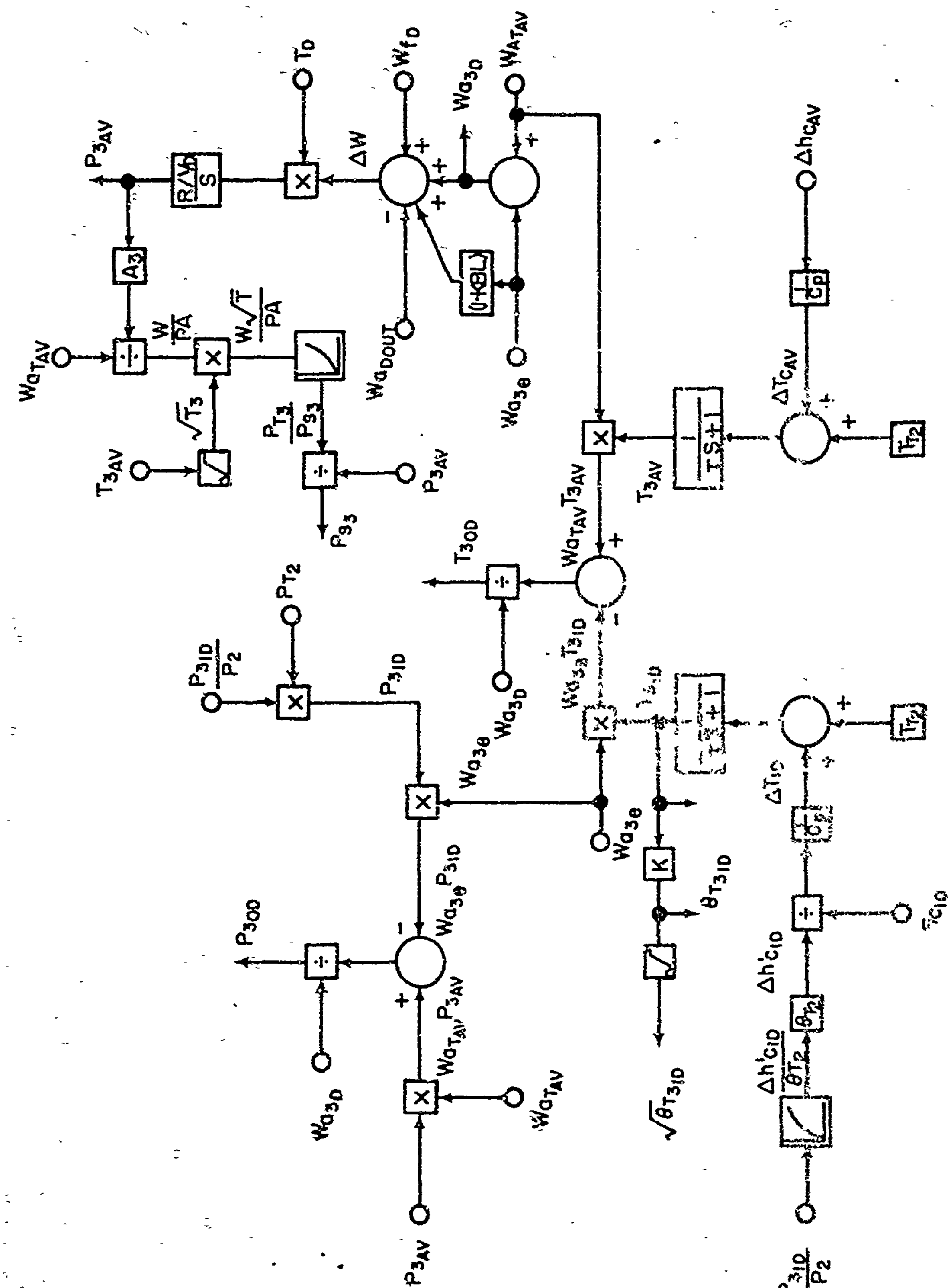

ANALOG PROGRAM FOR STF219 ENGINE
LOW-PRESSURE COMPRESSOR DISCHARGE

Figure 10-10

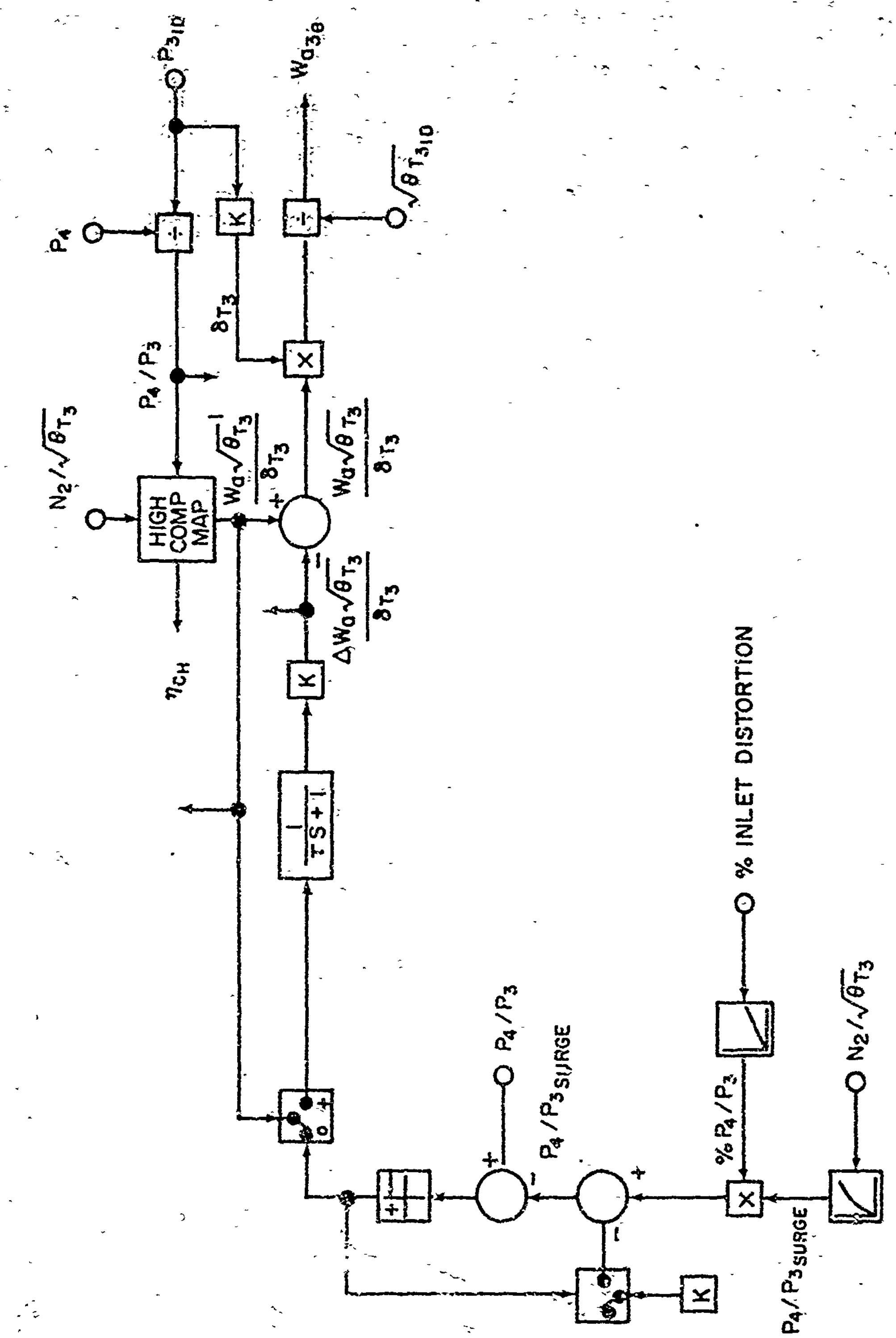

ANALOG PROGRAM FOR STF219 ENGINE
HIGH-PRESSURE COMPRESSOR

Figure 10-11

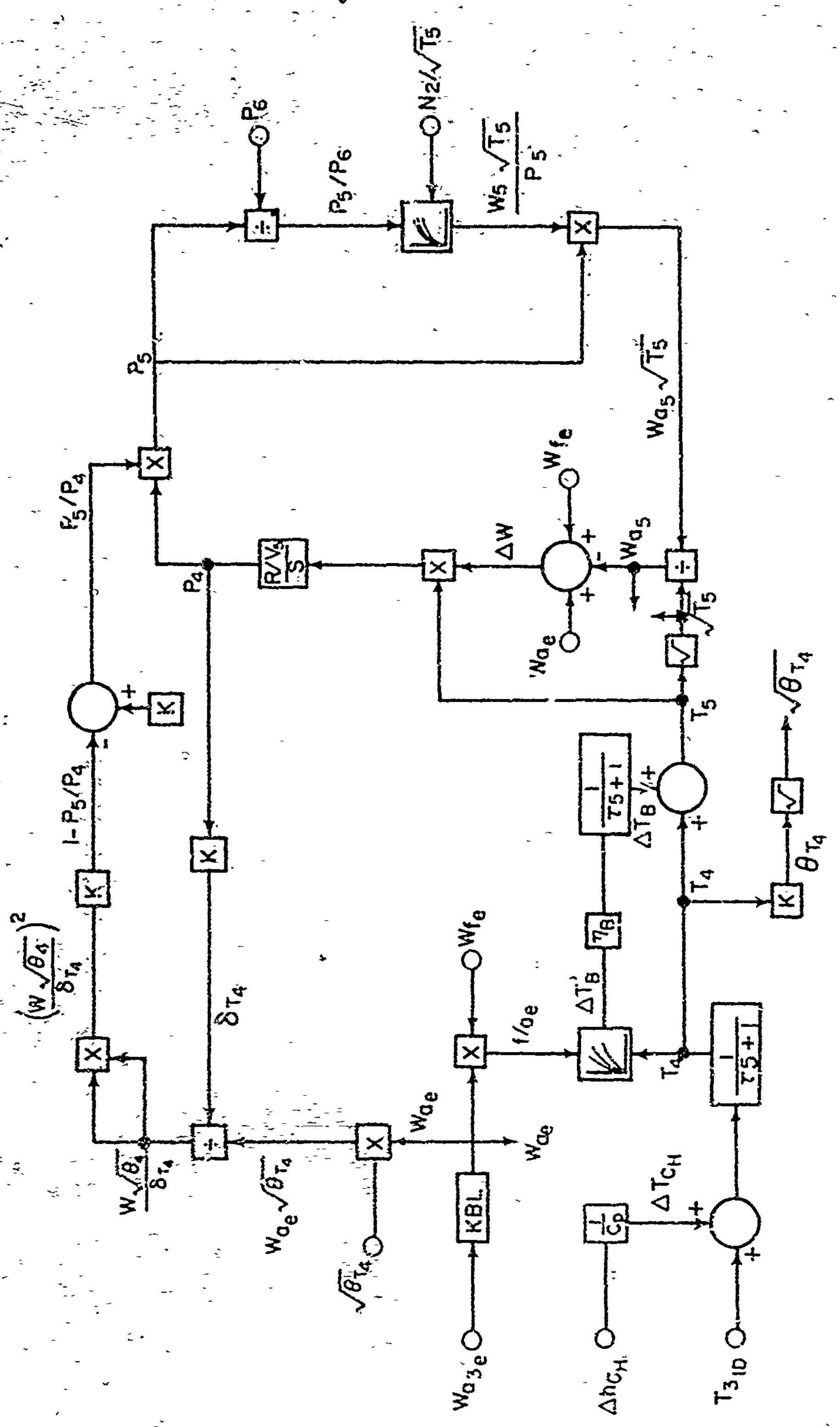

ANALOG PROGRAM FOR STF219 ENGINE
PRIMARY COMBUSTOR SECTION

Figure 10-12

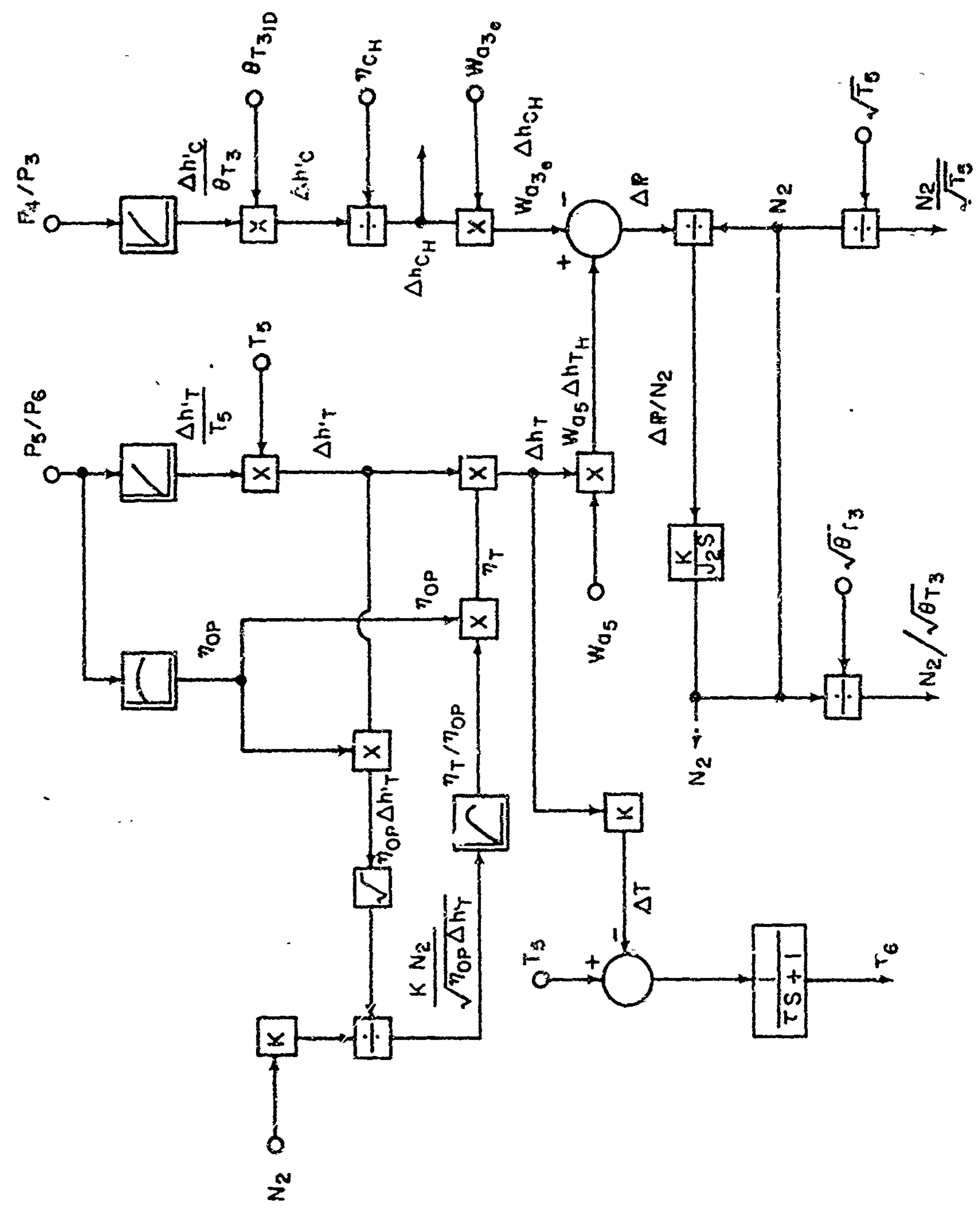

ANALOG PROGRAM FOR STF219 ENGINE
HIGH-PRESSURE ROTOR TORQUE BALANCE

Figure 10-13

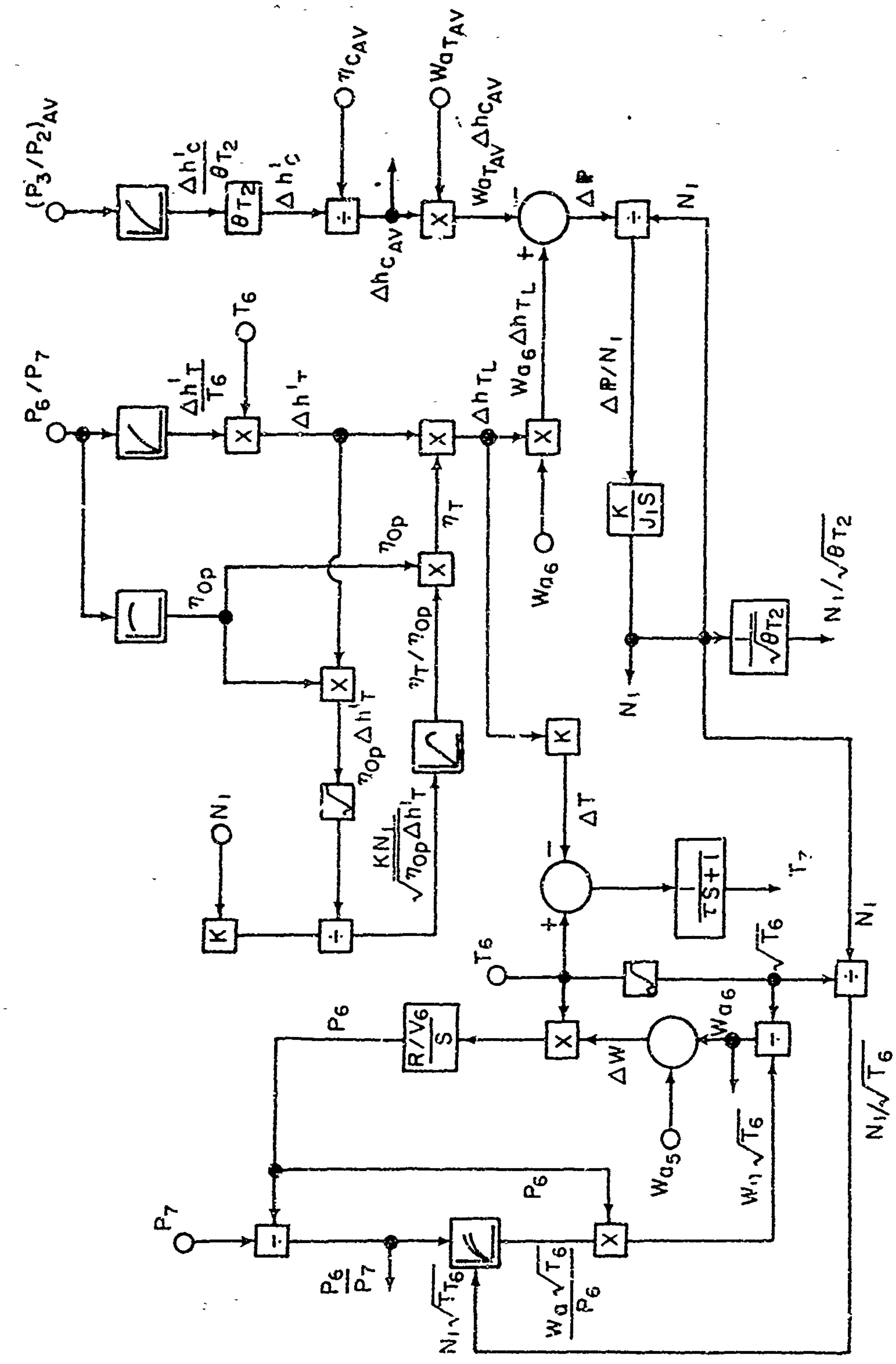

ANALOG PROGRAM FOR STF219 ENGINE
LOW-PRESSURE ROTOR TORQUE BALANCE

Figure 10-14

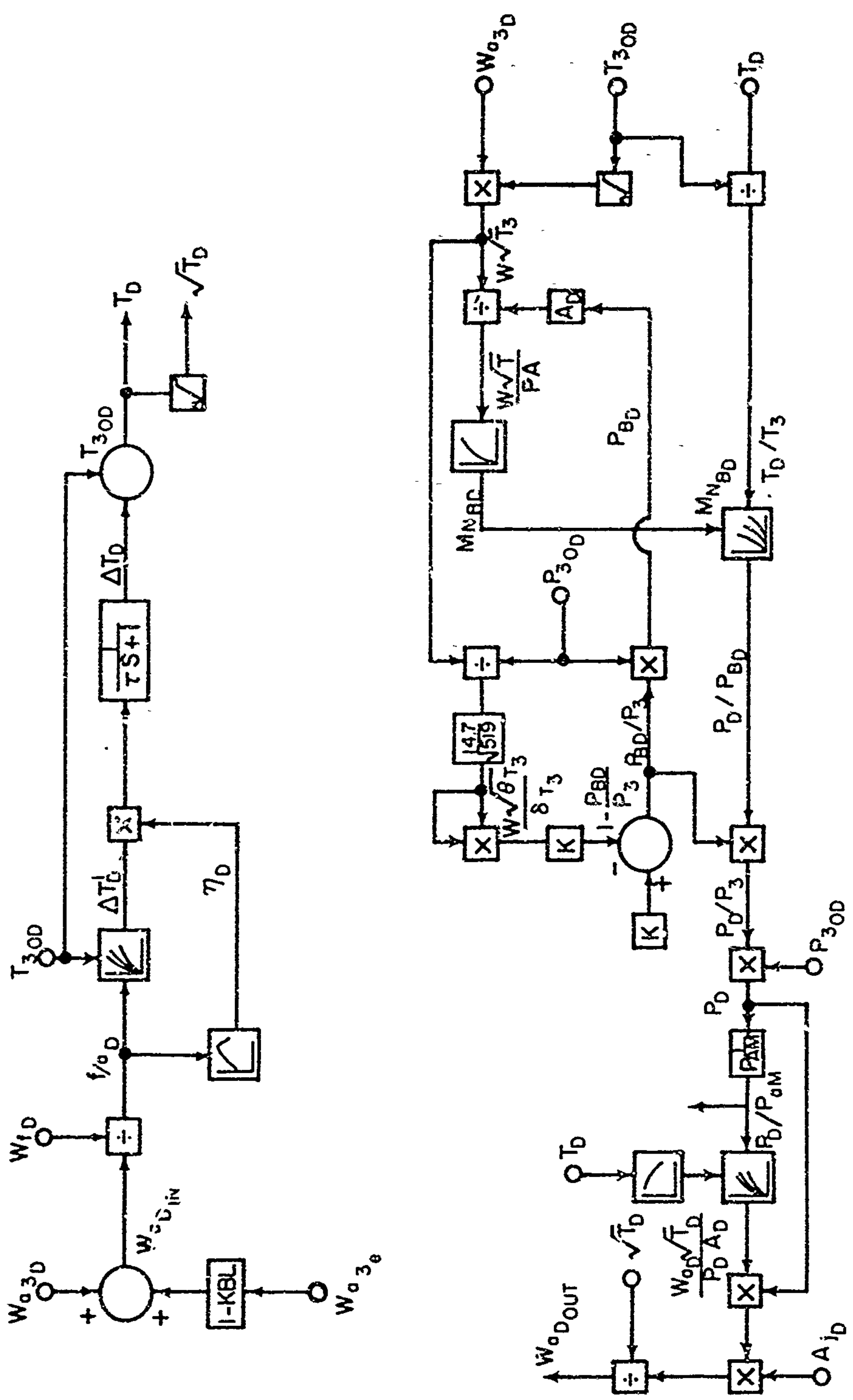

ANALOG PROGRAM FOR STF219 ENGINE
DUCT COMBUSTOR SECTION

Figure 10-15

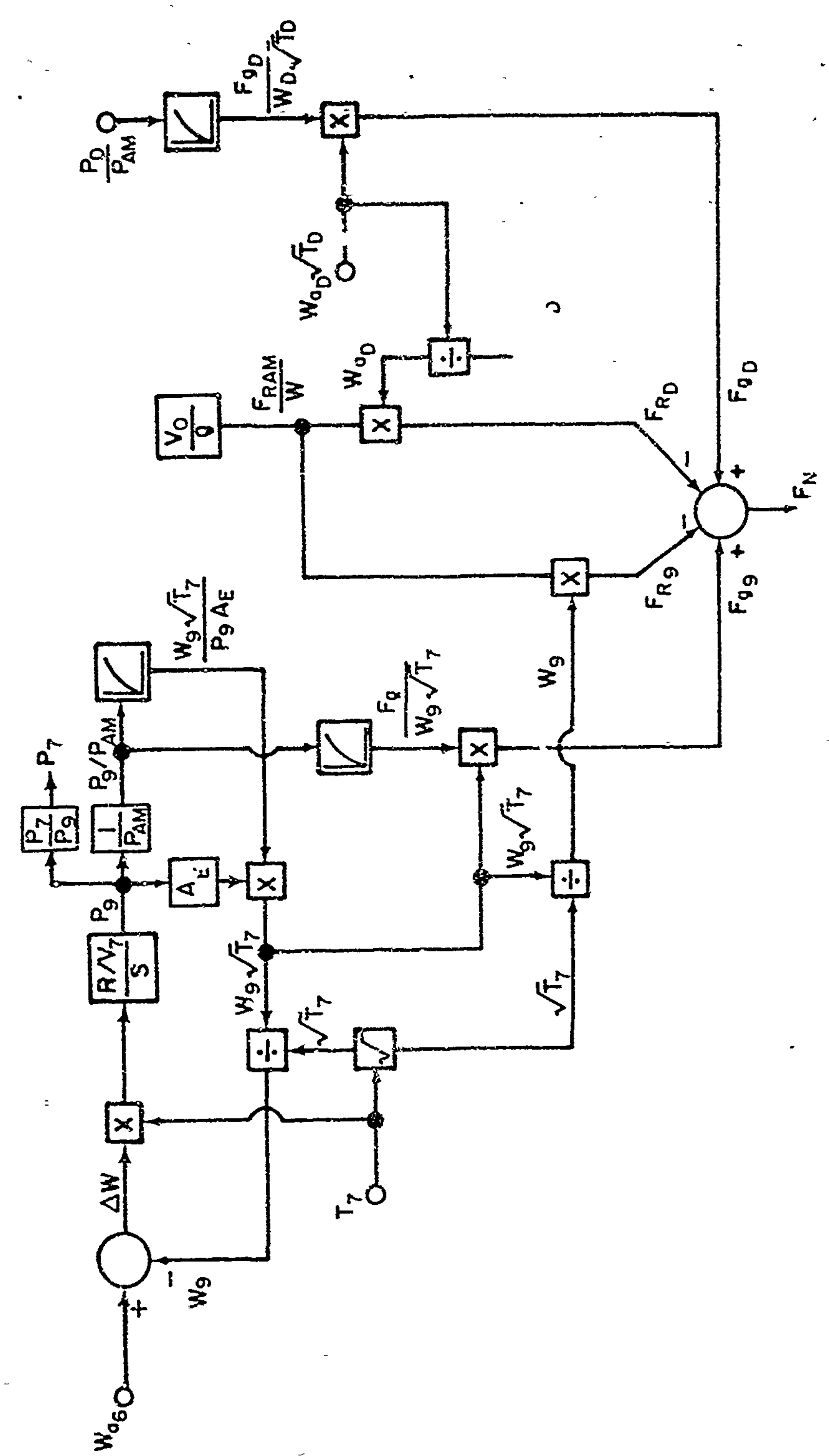

ANALOG PROGRAM FOR STF219 ENGINE
TAILPIPE AND THRUST CALCULATION

Figure 10-16

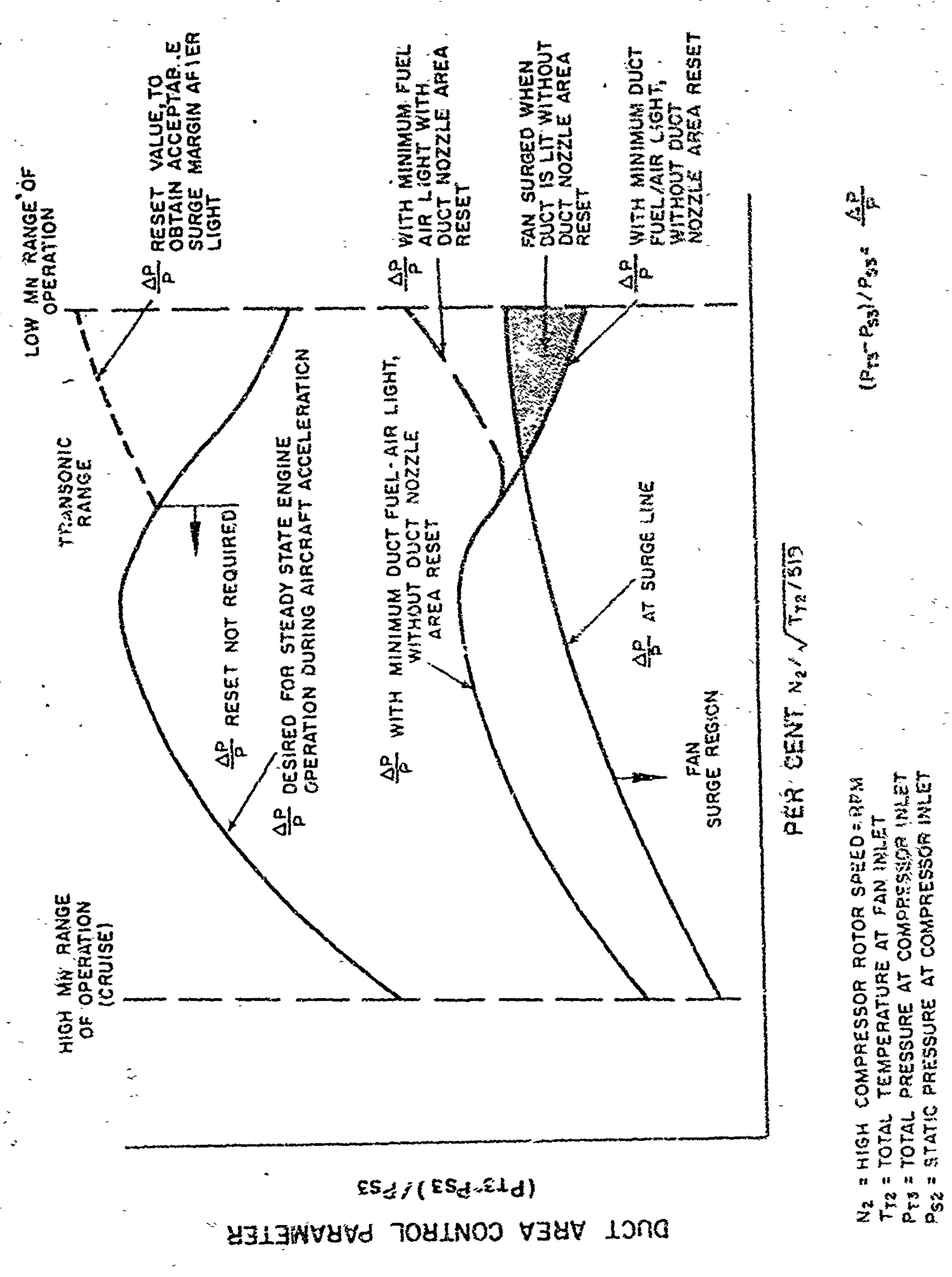

VARIATION IN DUCT AREA CONTROL PARAMETER WITH ROTOR SPEED SHOWING EFFECT OF DUCT LIGHTING

Figure 10-17

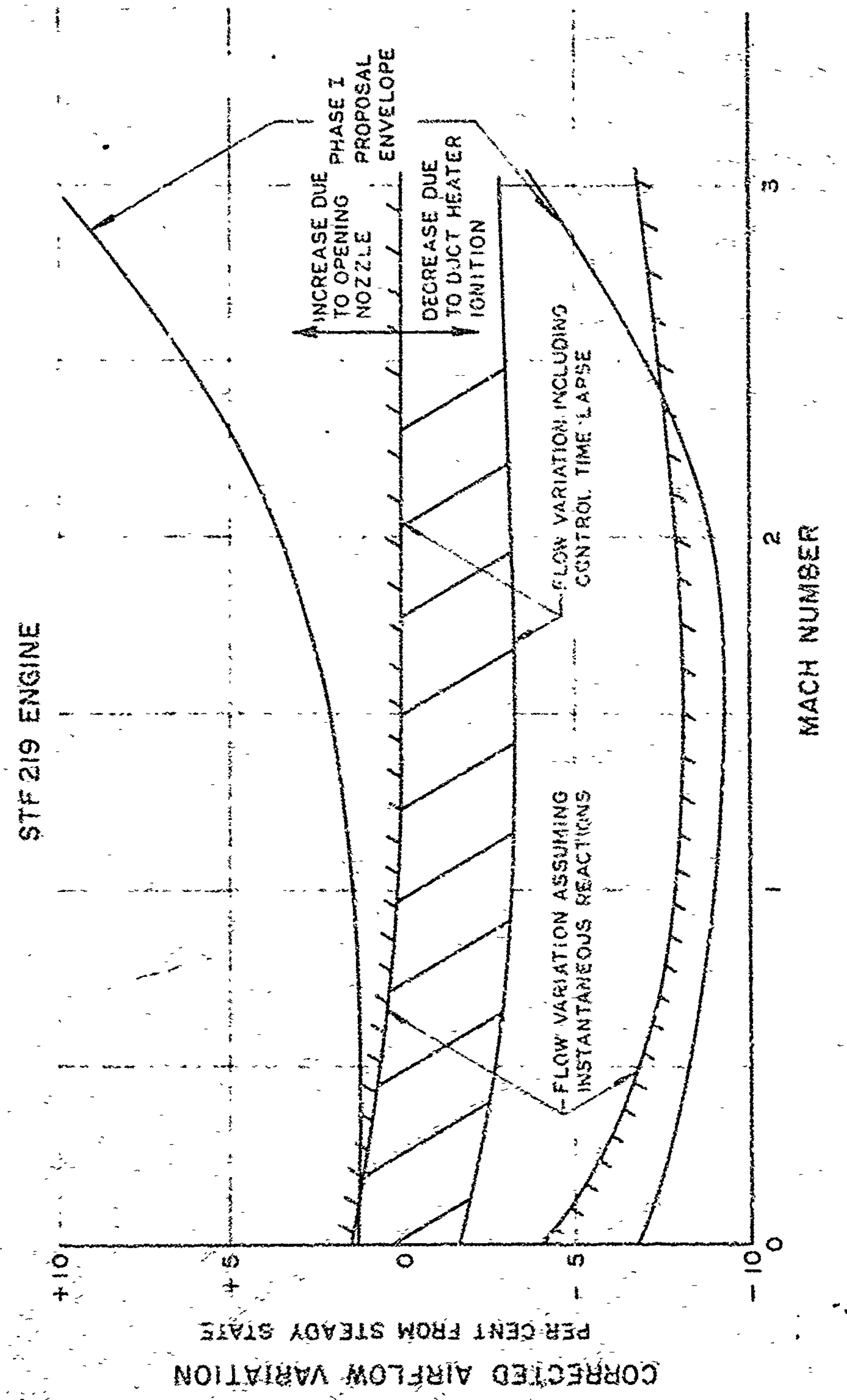

AIRFLOW CHANGES DURING DUCT LIGHTING

Figure 10-18

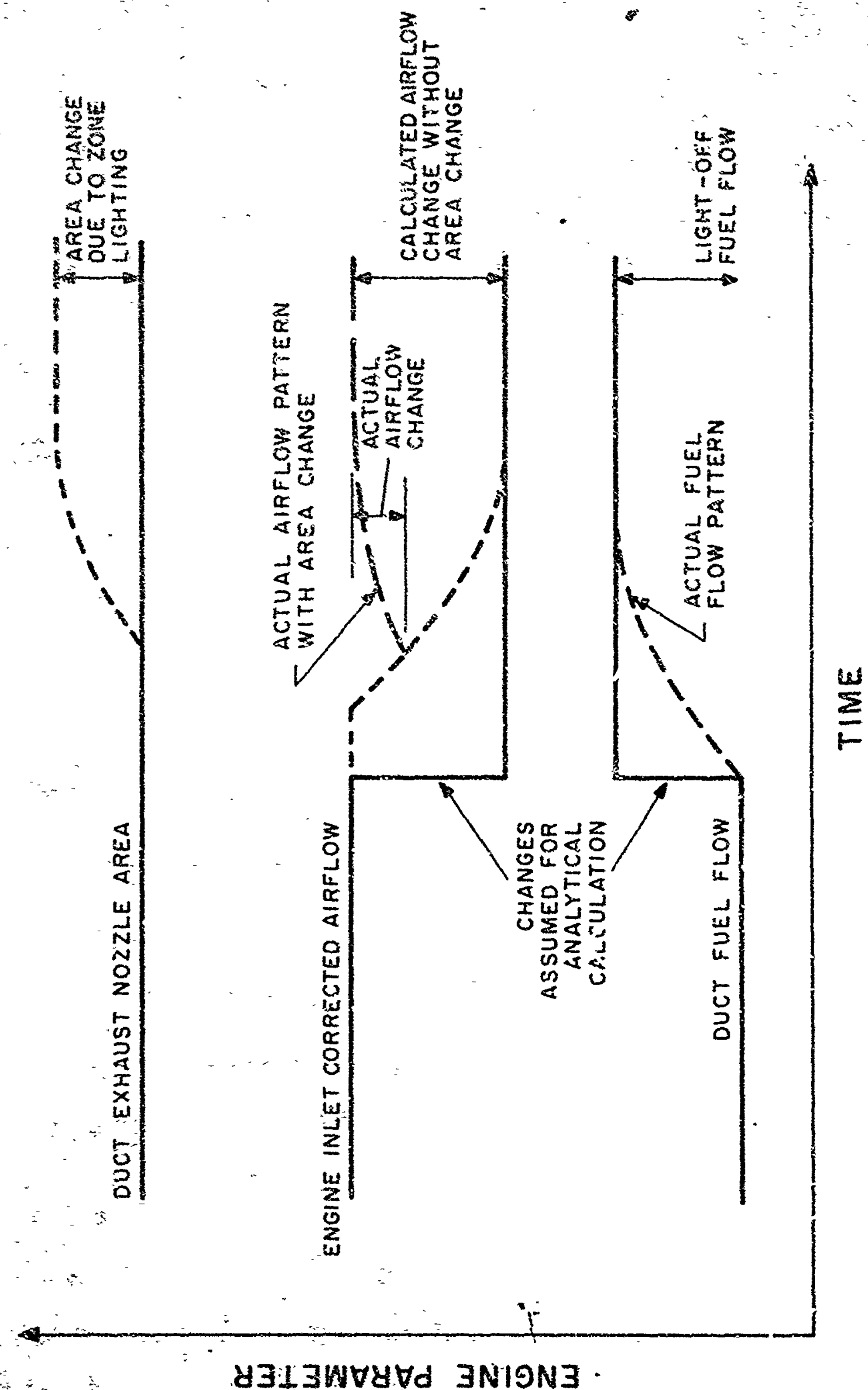

ILLUSTRATION OF TRANSIENT RESPONSE DURING LIGHTING

Figure 10-19

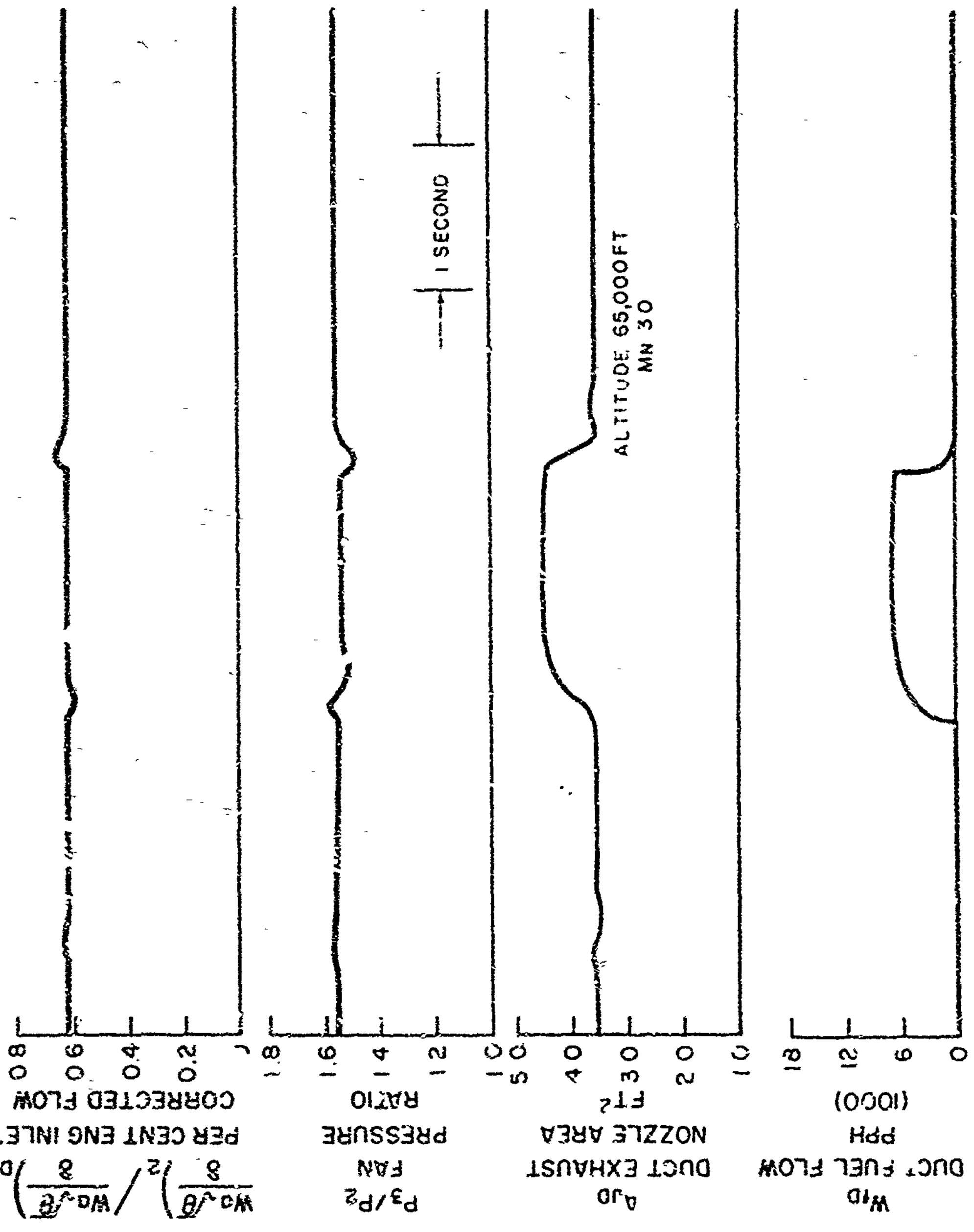

DUCT HEATER TRANSIENT RESPONSE DURING LIGHTING

Figure 10-26

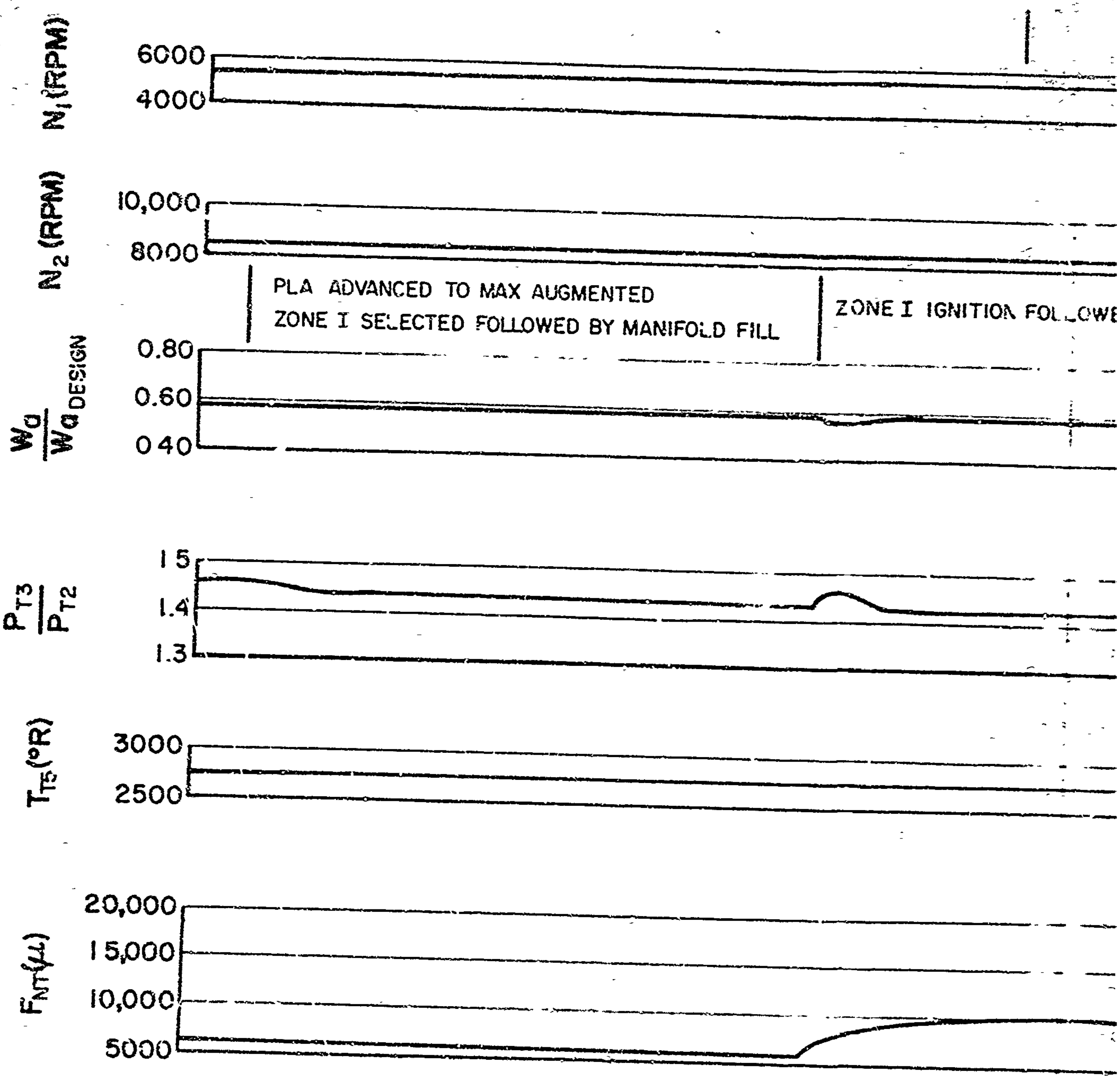

N_1 (RPM)
6000
4000
N_2 (RPM)
10,000
8000
PLA ADVANCED TO MAX AUGMENTED
ZONE I SELECTED FOLLOWED BY MANIFOLD FILL
ZONE I IGNITION FOLLOWE
$\frac{W_a}{W_{a_{DESIGN}}}$
0.80
0.60
0.40
$\frac{P_{T3}}{P_{T2}}$
1.5
1.4
1.3
T_{T5} (°R)
3000
2500
F_{NT} (lb)
20,000
15,000
10,000
5000

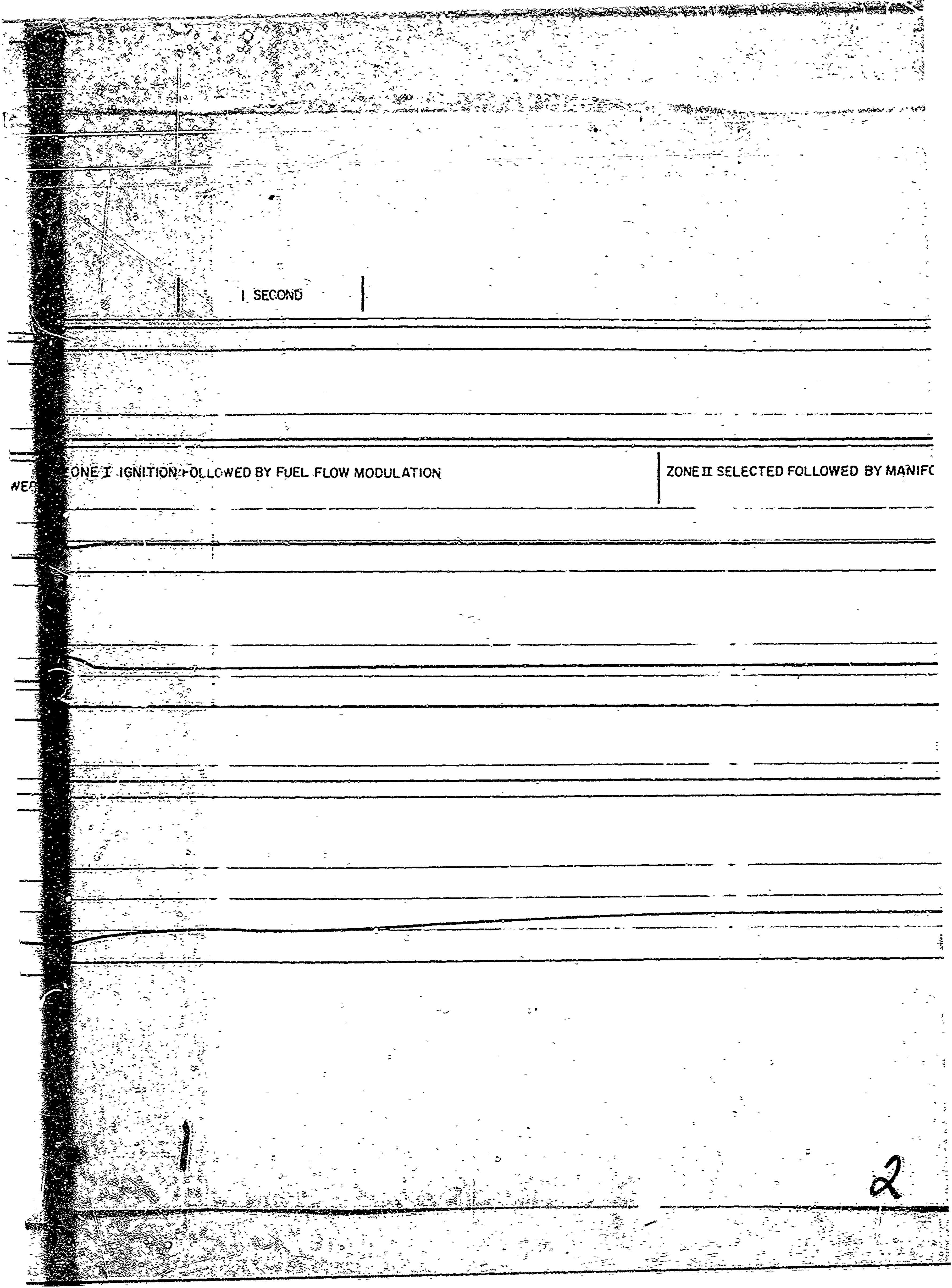
1 SECOND
WEF
ONE I IGNITION FOLLOWED BY FUEL FLOW MODULATION
ZONE II SELECTED FOLLOWED BY MANIFC
2

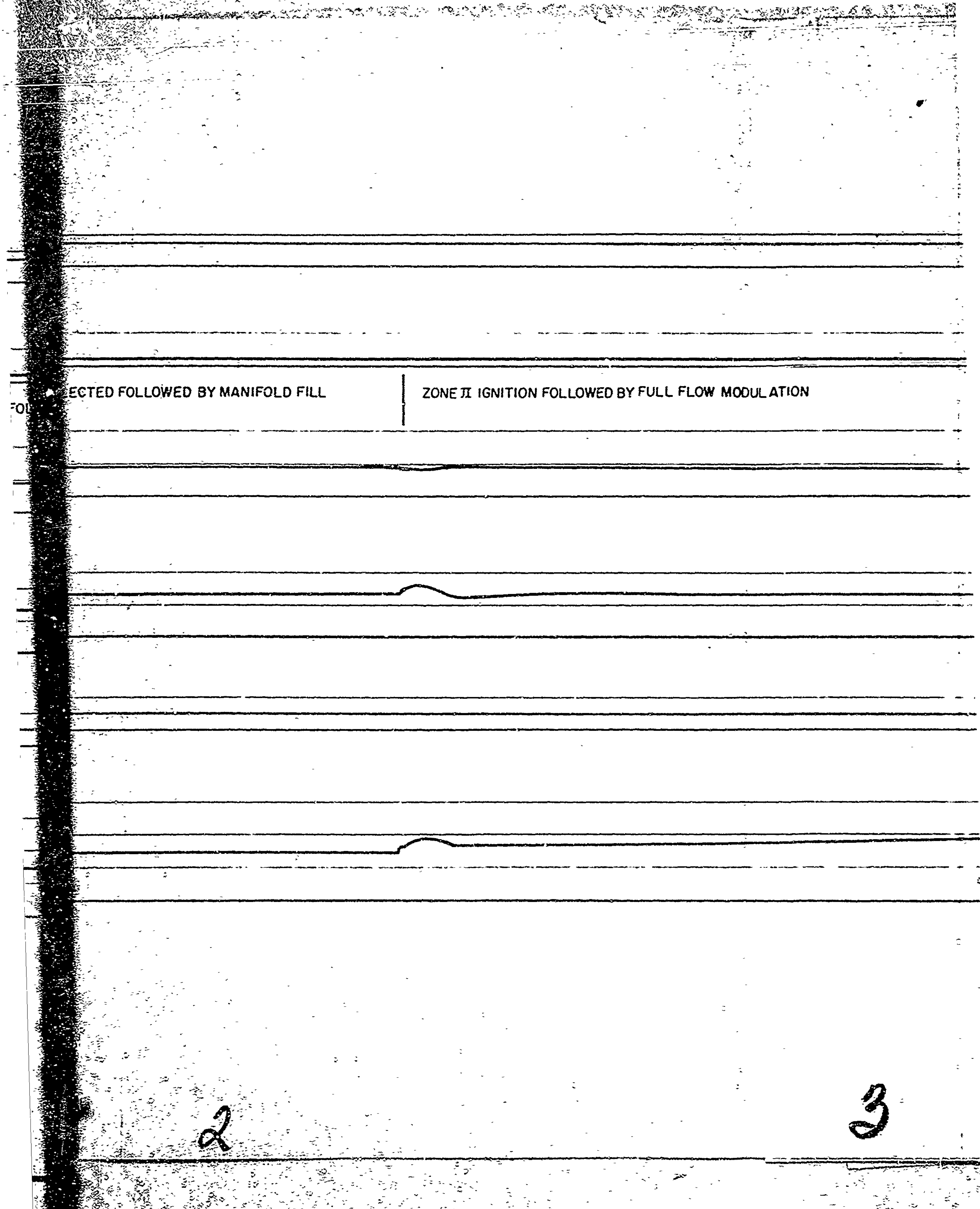

FOL
ECTED FOLLOWED BY MANIFOLD FILL
ZONE II IGNITION FOLLOWED BY FULL FLOW MODULATION
2
3

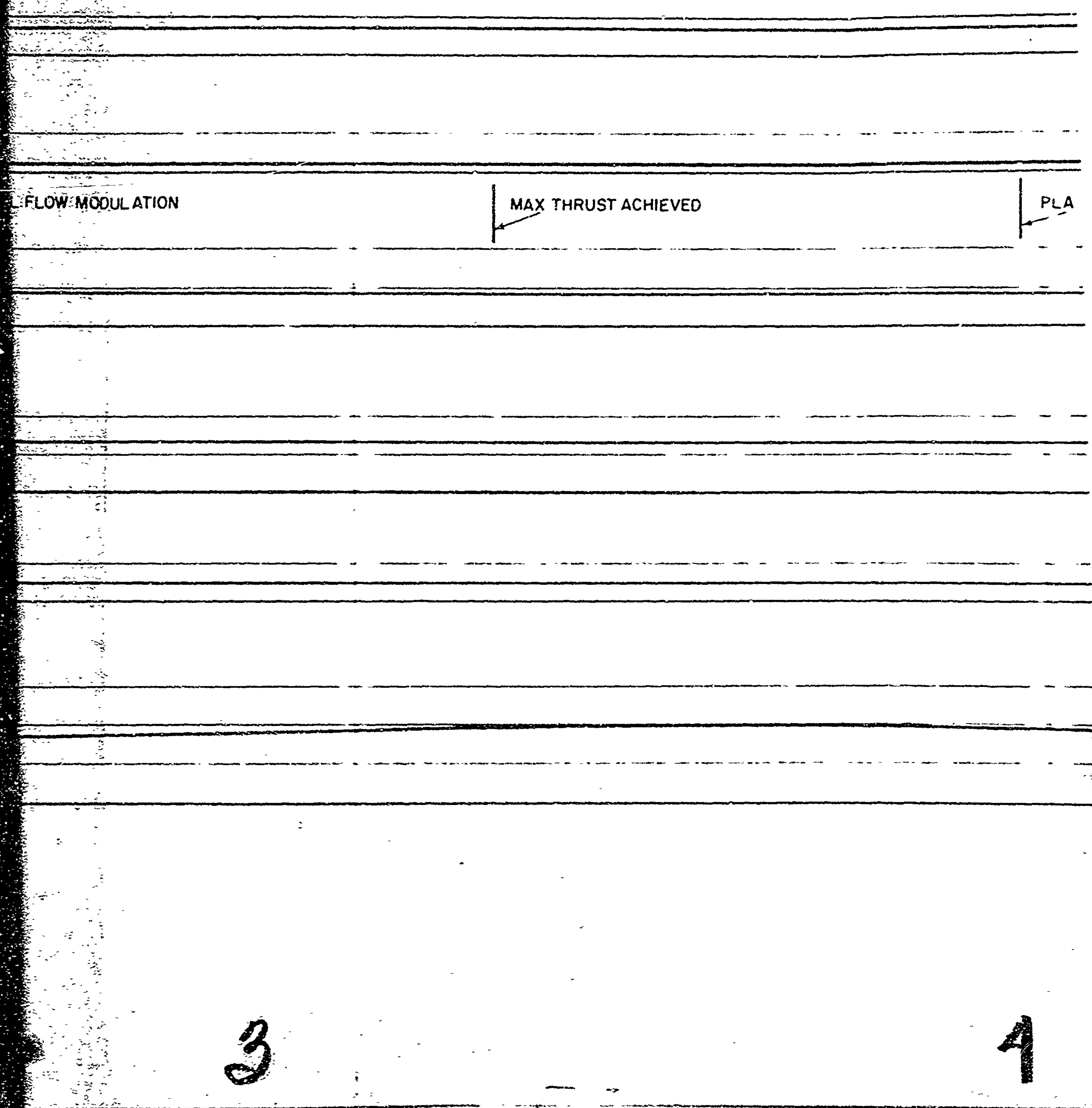
FLOW MODULATION
MAX THRUST ACHIEVED
PLA
3
4

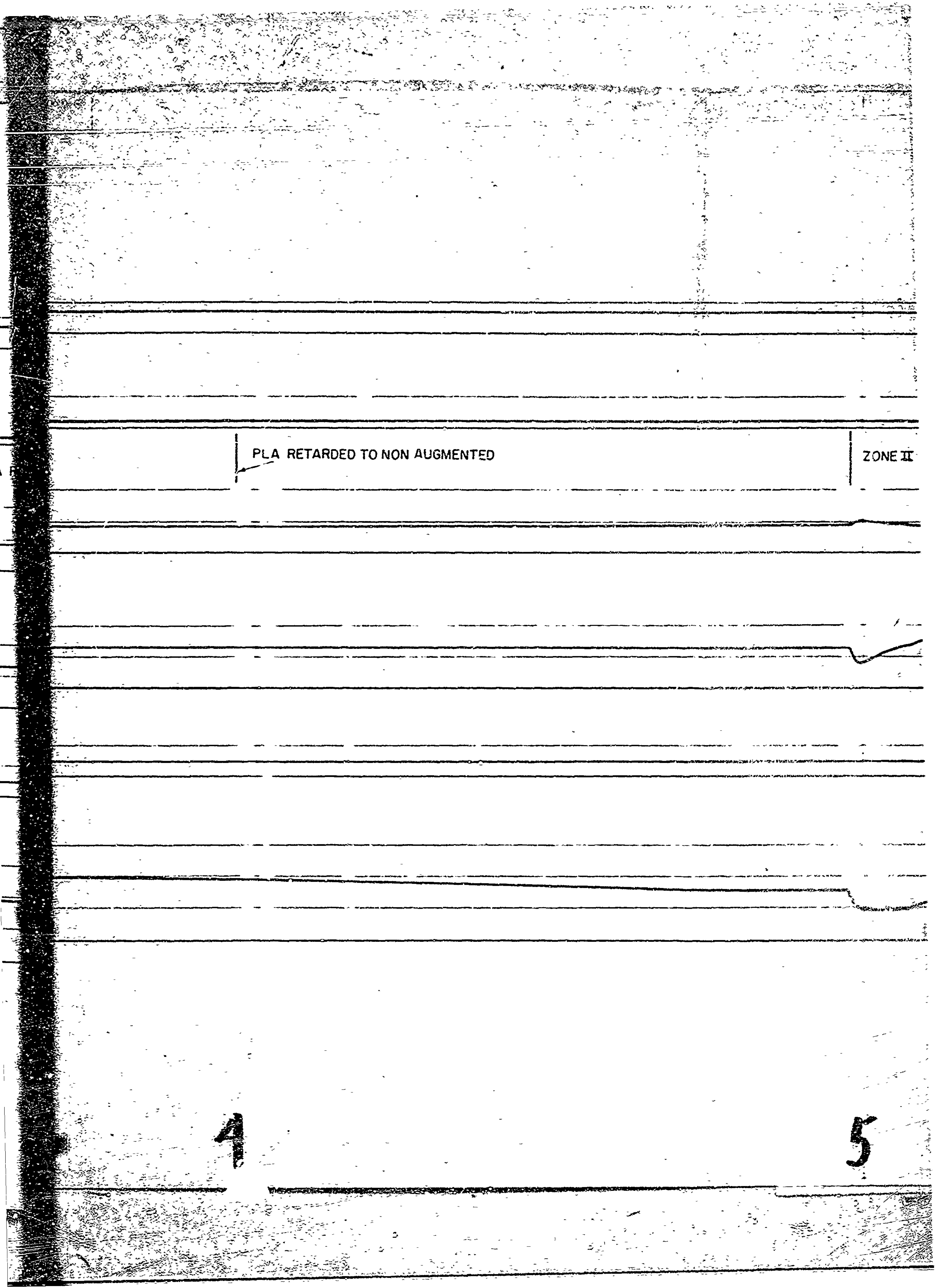
PLA RETARDED TO NON AUGMENTED
ZONE II
4
5

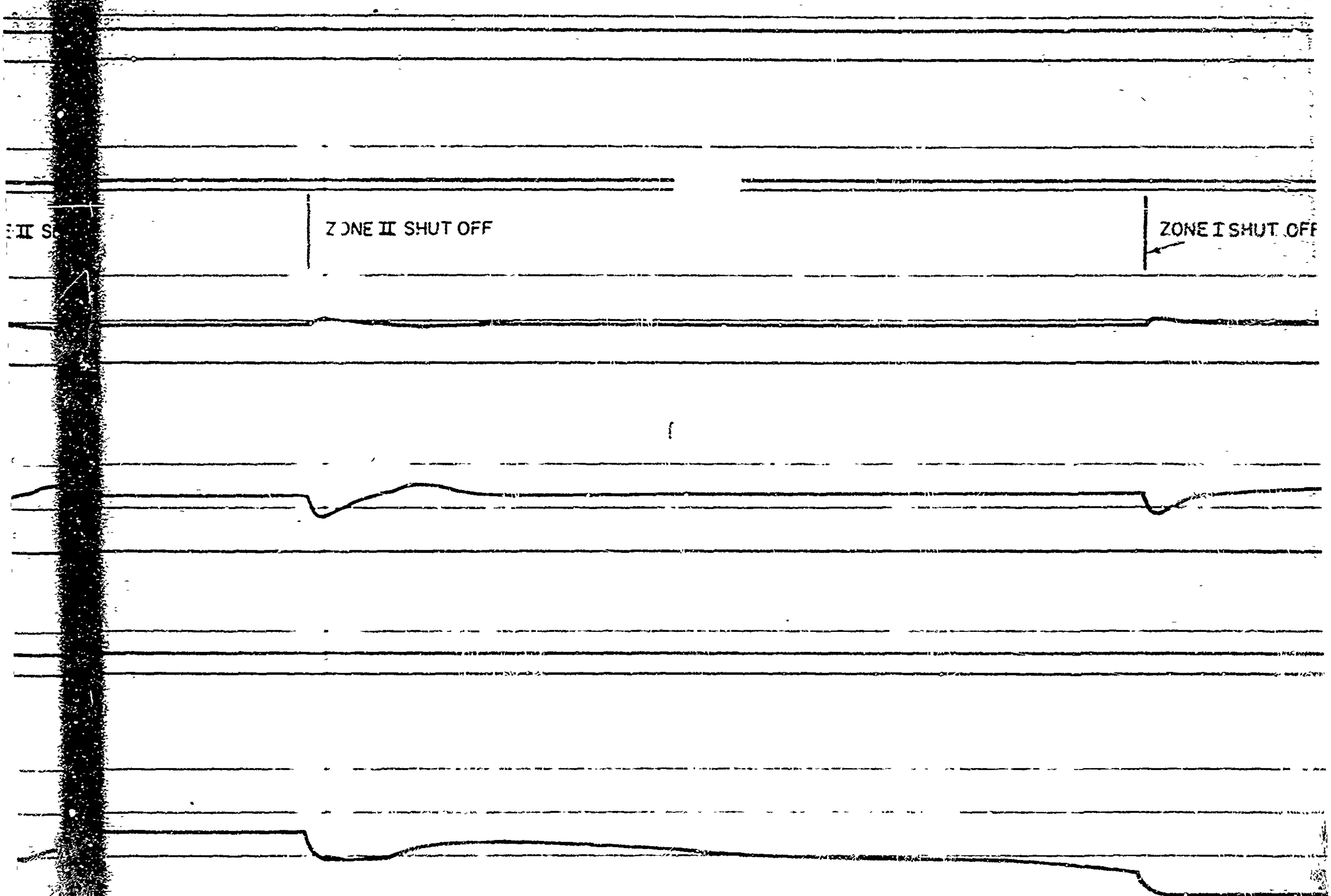

ANALOG COMPUTER TRACES OF STF219 ENGINE OPE
75,000 FEET, MACH 3.0 WITH MAXIMUM THRUST WIT
OUT AUGMENTATION.

Figure 10-21

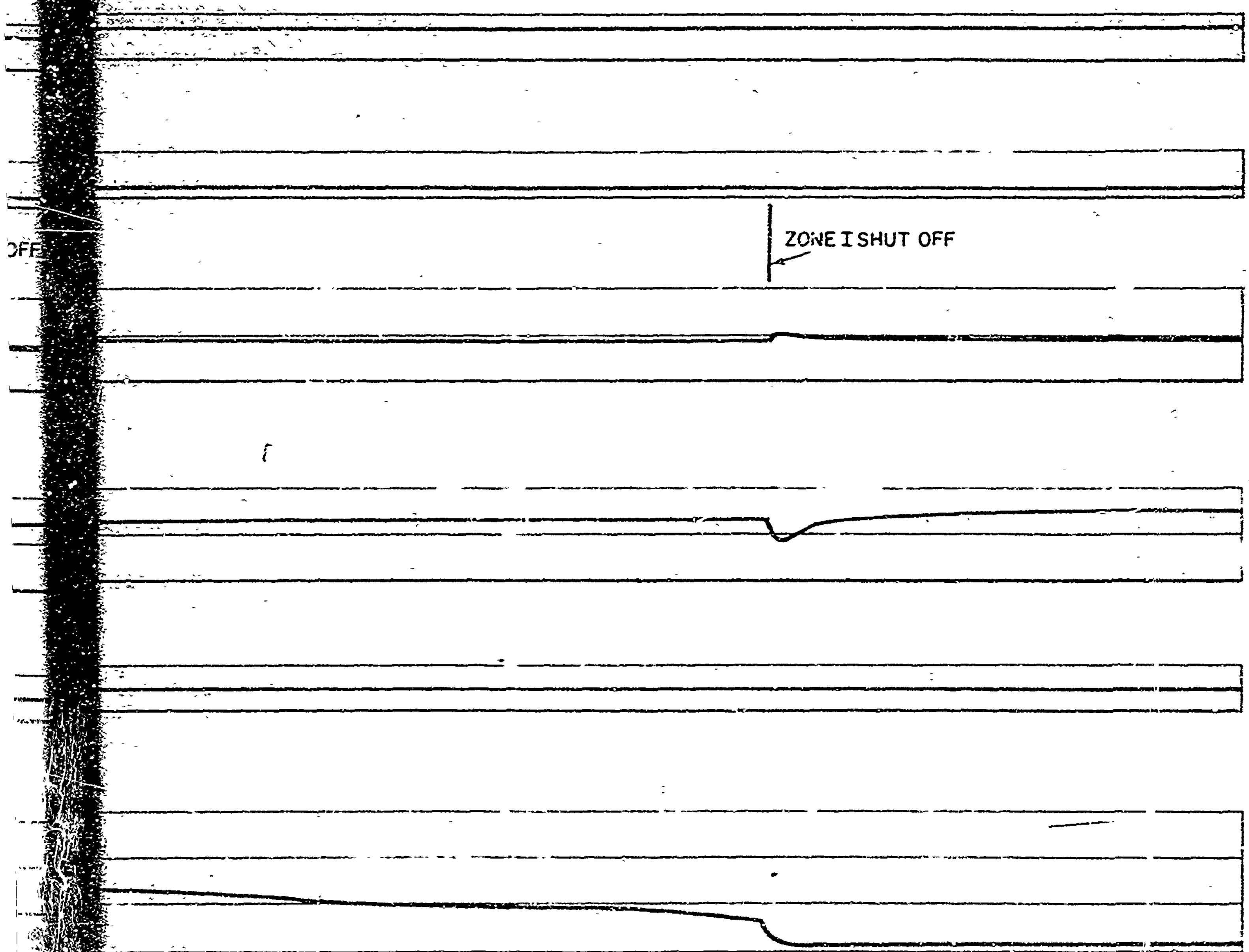

ANALOG COMPUTER TRACES OF STF219 ENGINE OPERATING AT 75,000 FEET, MACH 3.0 WITH MAXIMUM THRUST WITH AND WITHOUT AUGMENTATION.

Figure 10-21

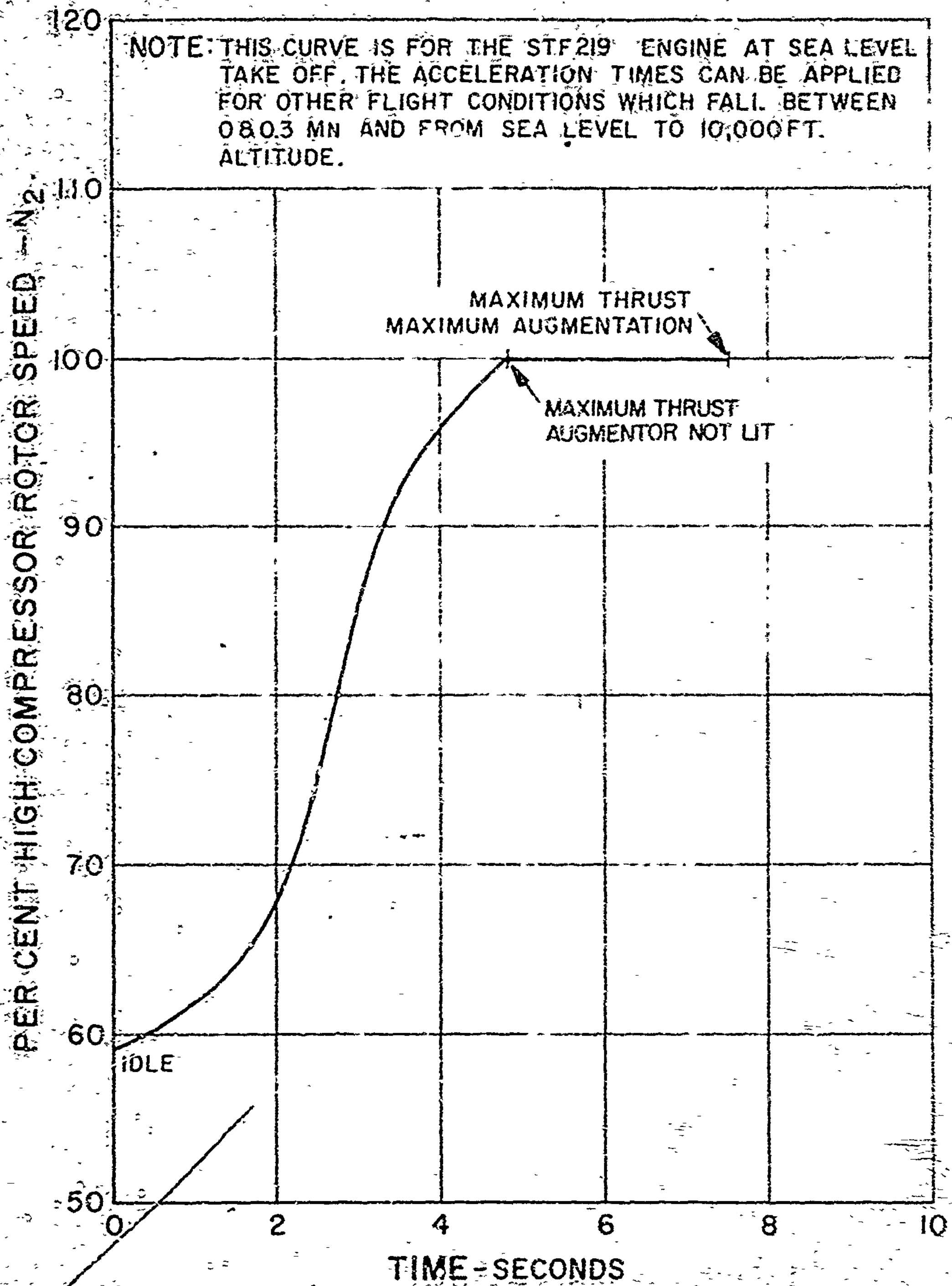

ESTIMATED ACCELERATION TIME FROM IDLE THRUST TO MAXIMUM THRUST FOR SST STF219 ENGINE

Figure 10-22

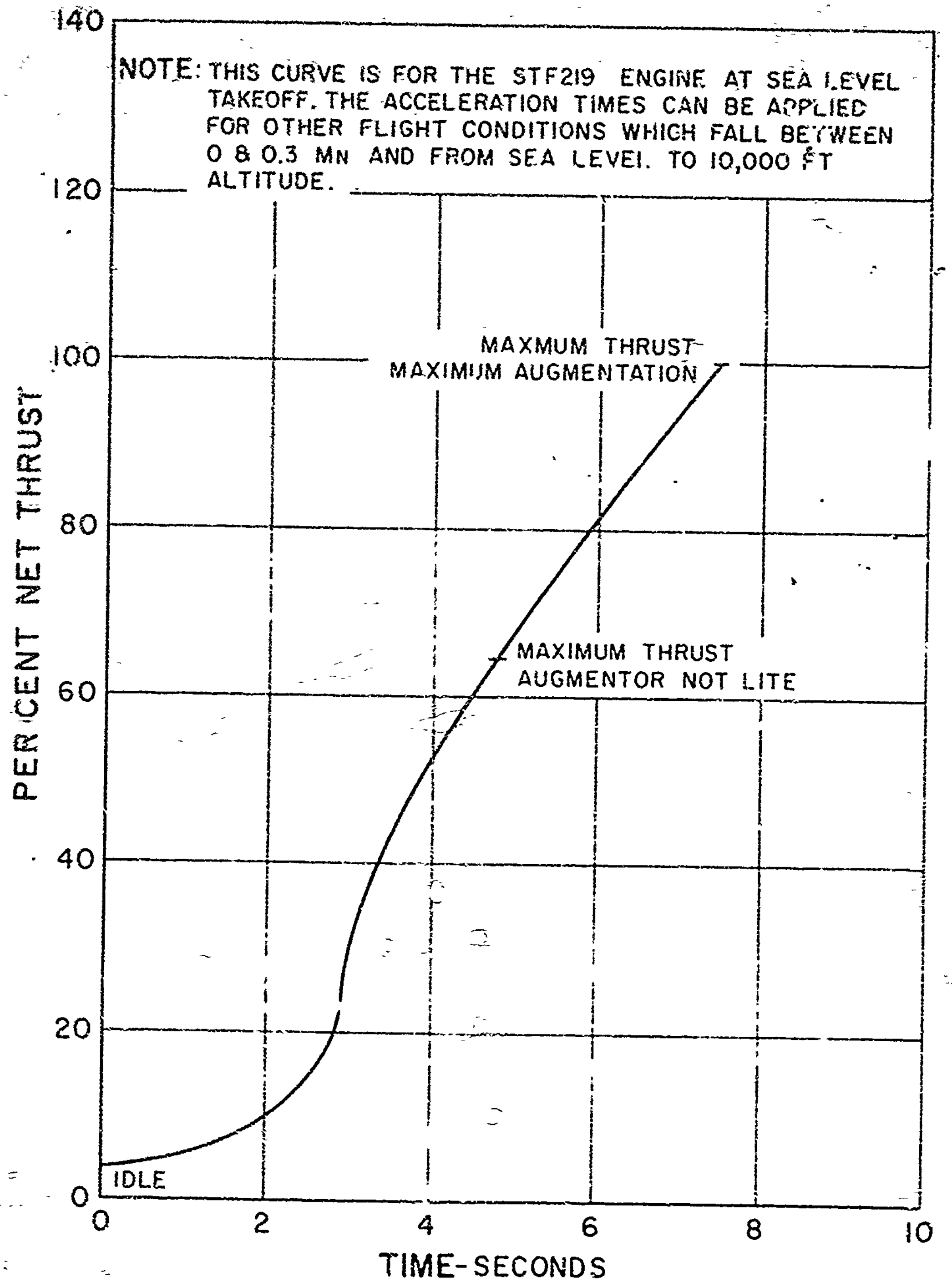

ESTIMATED ACCELERATION TIME FROM IDLE ROTOR SPEED TO MAXIMUM ROTOR SPEED FOR SST STF219 ENGINE

Figure 10-23

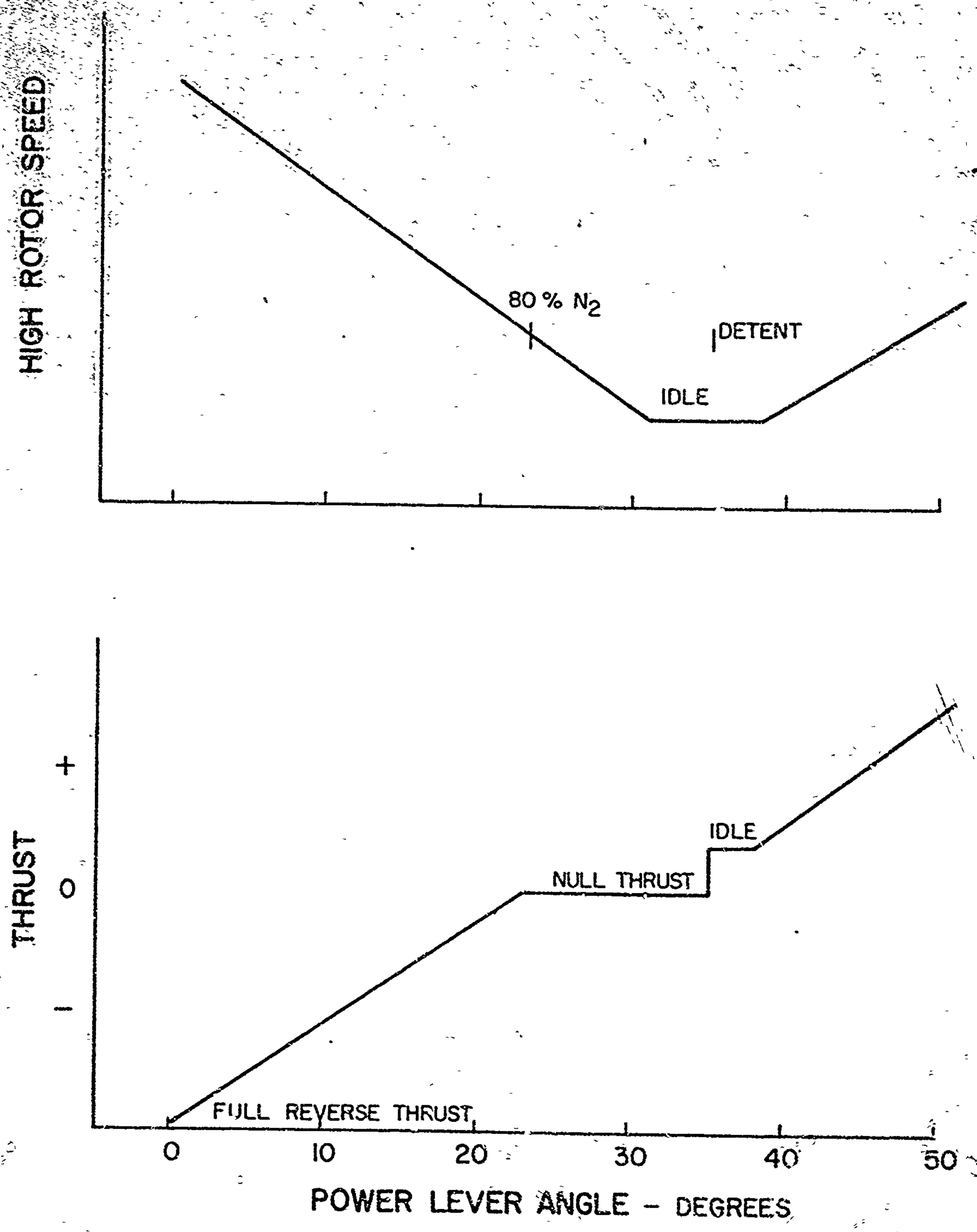

ILLUSTRATION OF POWER LEVER OPERATION IN REVERSE MODE

Figure 10-24

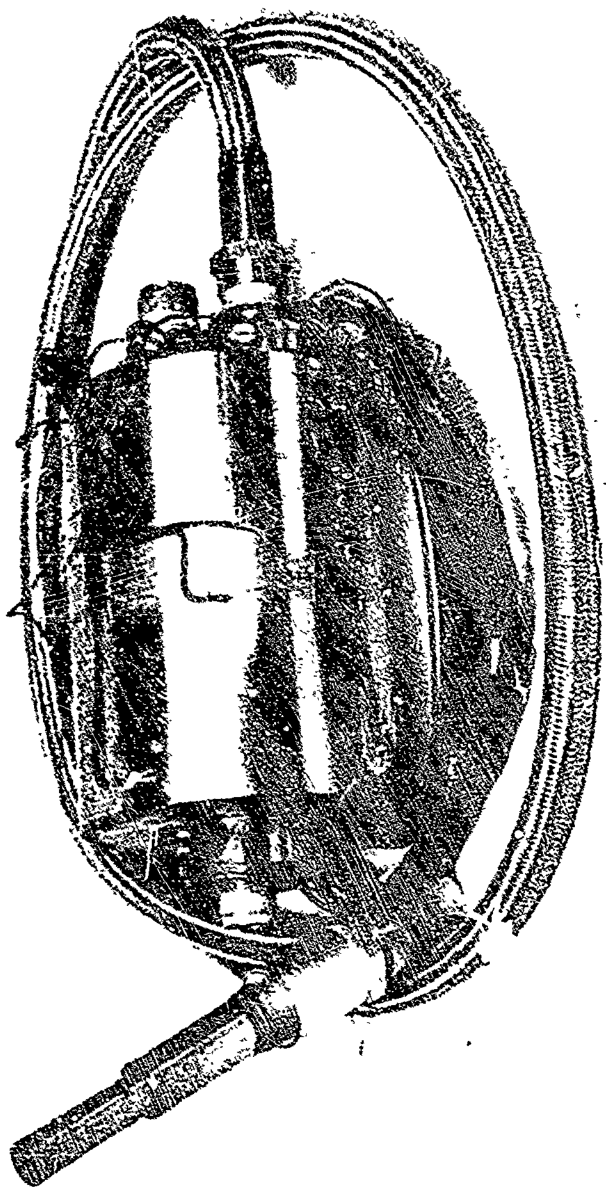

LOW-TENSION PERIPHERALLY COOLED EXCITER

Figure 10-25

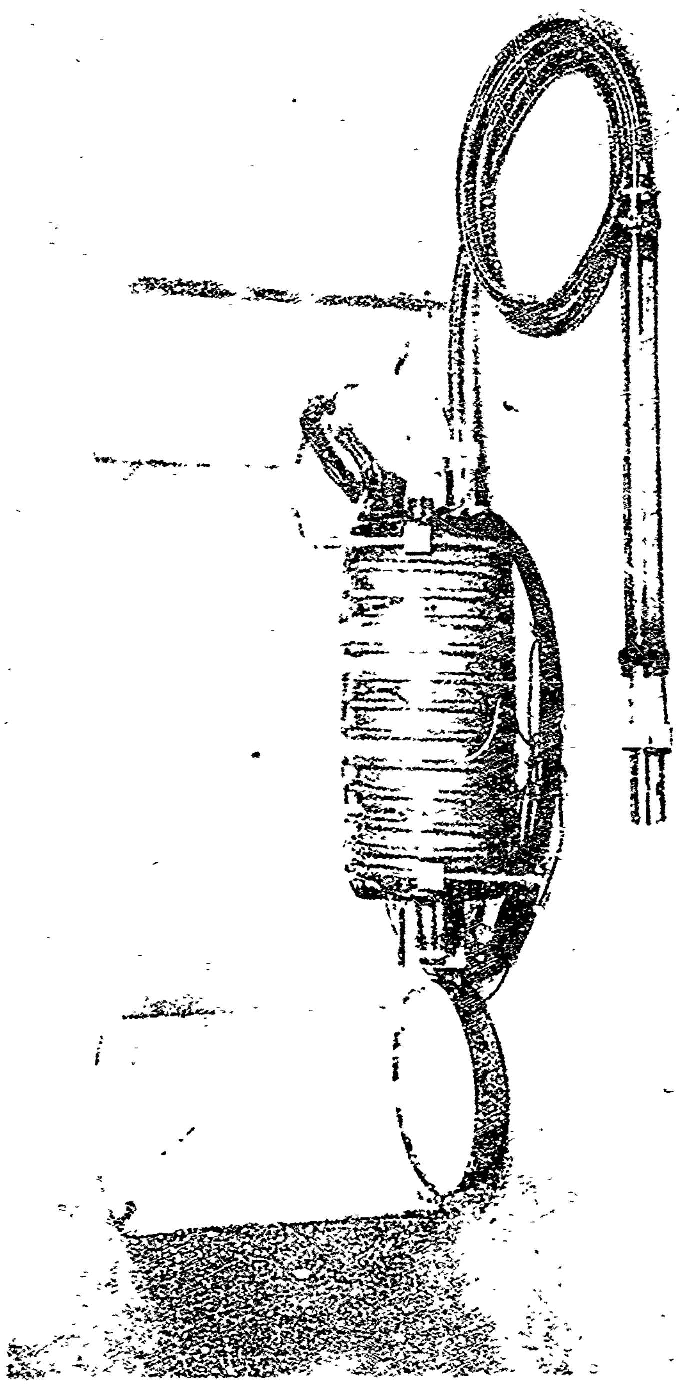

LOW-TENSION SPIRAL-WRAPPED COOLED EXCITER

Figure 10-26

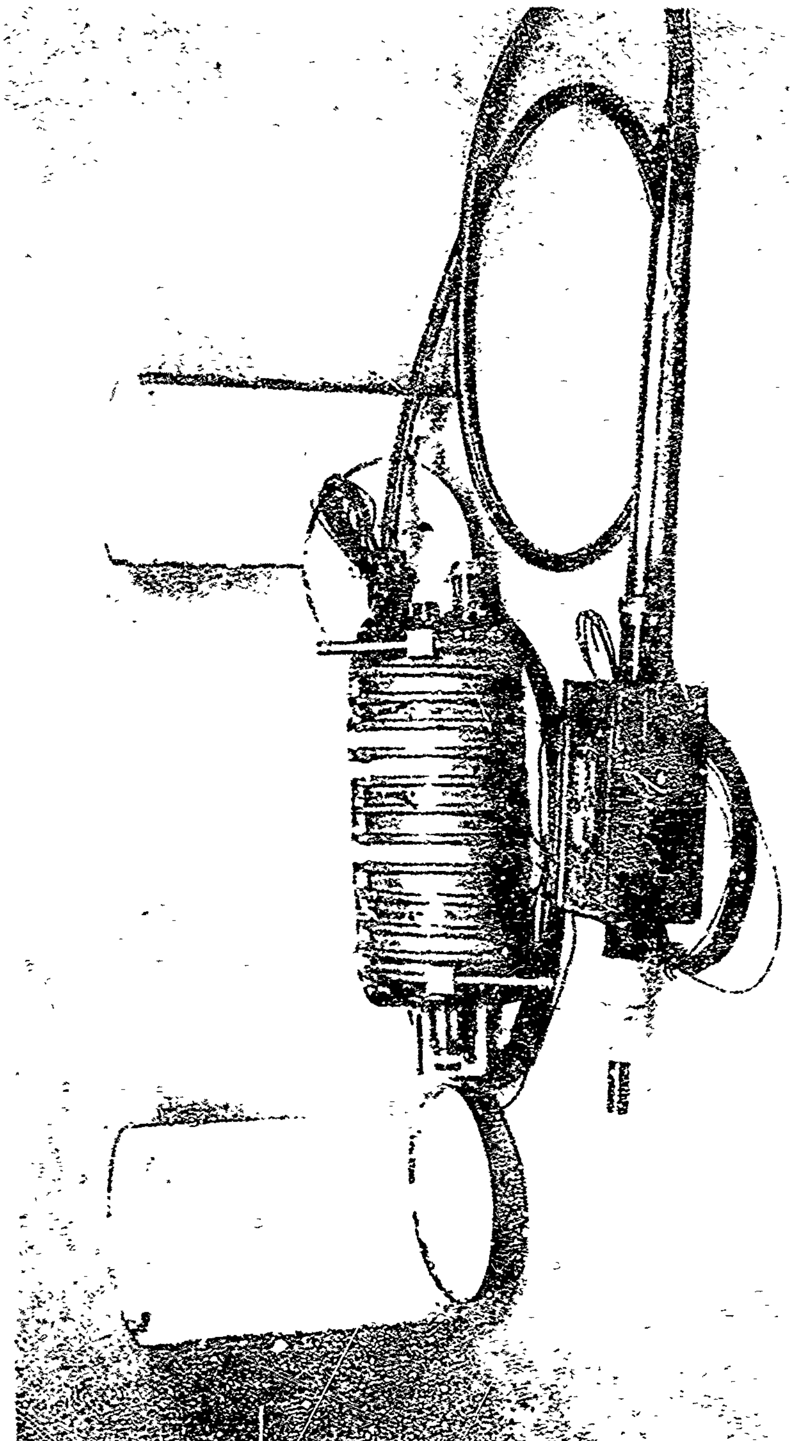

XP-43605

HIGH-TENSION SPIRAL-WRAPPED COOLED EXCITER

Figure 10-27

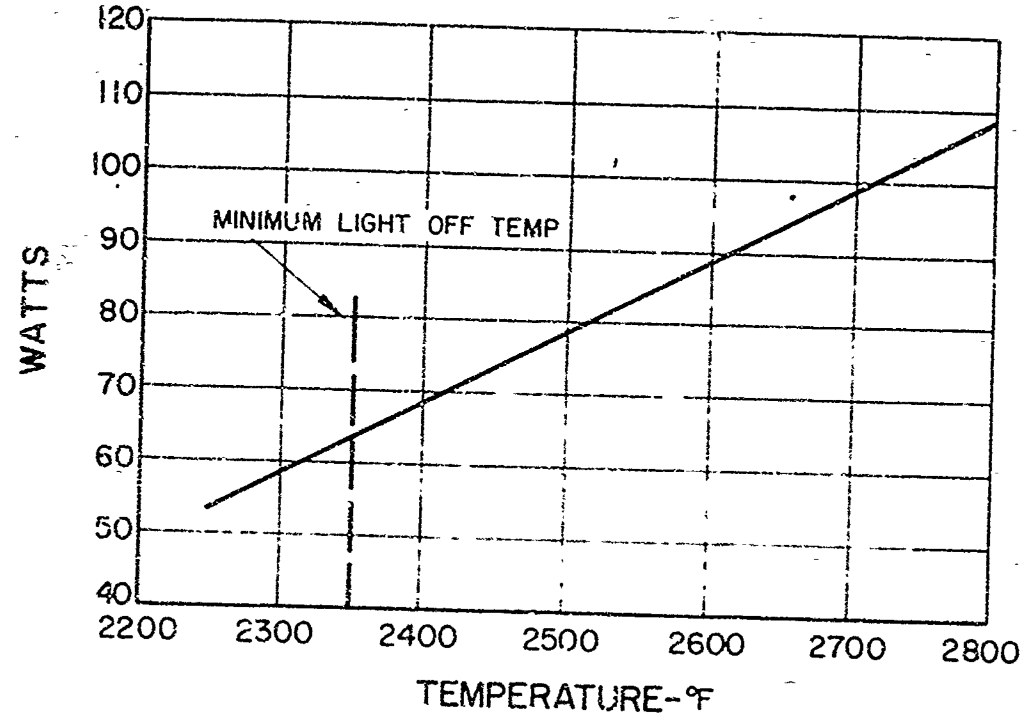

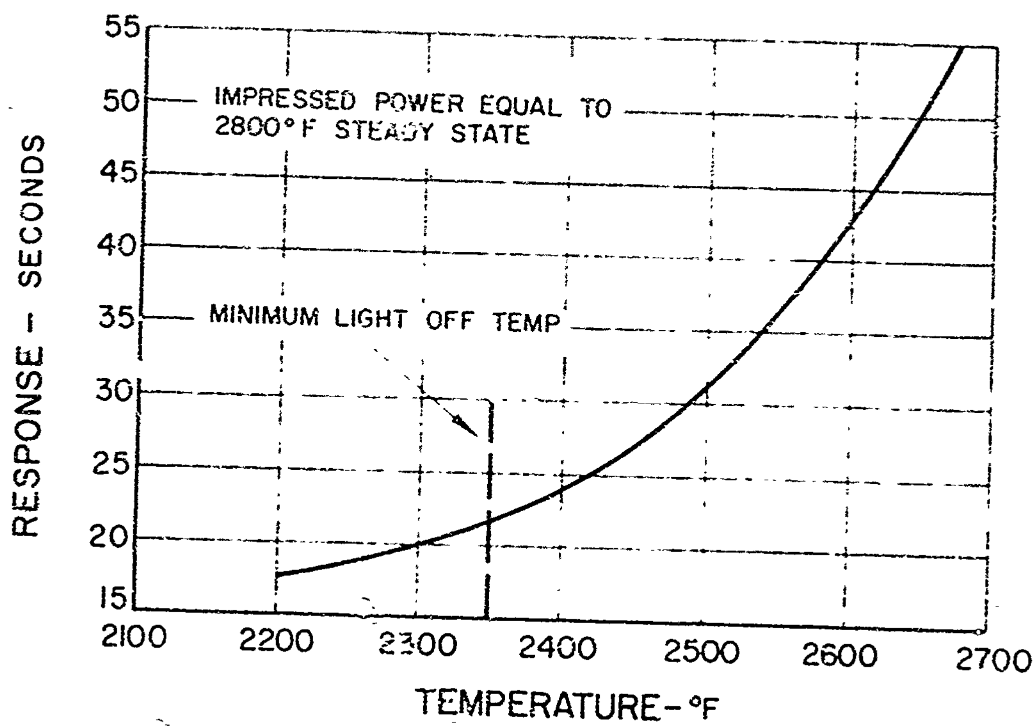

TEST RESULTS FOR GLOW PLUG IGNITER

Figure 10-28

APPENDIX 10-A

PWA Purchase Specification 819D
PWA Purchase Specification 858
PWA Purchase Specification 859
PWA Purchase Specification 860

Date: 28 February 1964
Rev. A: 22 April 1964
Rev. B: 26 June 1964
Rev. C: 1 October 1964
Rev. D: 13 October 1964

1. SCOPE

This specification establishes the engineering requirements for the fuel and area control used on a typical SST engine.

2. DESCRIPTION

2.1 The control system shall consist of a hydro-mechanical system operating to:

1. control engine speed between idle and maximum gas generator power.
2. schedule main engine fuel flow within desired limits during transient operation.
3. sequence the scheduled duct burner fuel flow, supplied from an air driven turbopump, over the operating envelope between augmentation cut-off and maximum augmentation, to two individual fuel manifolds.
4. position the exhaust nozzle area to maintain the desired engine operating condition.

3. APPLICABLE PUBLICATIONS

3.1 The applicable specifications and standards listed in ANA Bulletin No. 343n shall form a part of this specification to the extent specified herein.

3.2 The following specifications and publications shall form a part of this specification to the extent specified herein.

PWA PMC - 9041	Test Fluid
PWA 522D	Fuel
PWA-PS-720-A	Vendor Responsibilities

4. REQUIREMENTS

4.1 General Requirements

4.1.1 Materials and Processes - Materials and processes used in the manufacture of the fuel controls shall be of high quality and suitable for the purpose. Materials specifications shall conform to applicable specifications listed in ANA Bulletin No. 343n. When vendor specifications are used for material or processes which affect performance or durability of the finished product, such specifications shall be subject to release to the government. The use of non-governmental specifications shall not constitute waiver of government inspection.

4.1.1.1 Dissimilar Metals - The use of dissimilar metals in contact, as defined on MS 33586A shall be avoided wherever practicable.

4.1.1.2 Use of AMS 5610, 5620, 5621, 5630, 5631, and 5632 Materials - The use of the subject heat treatable stainless steels or equivalents is prohibited unless agreed upon in writing by PWA Engineering.

4.1.1.3 Use of Copper or Copper Alloys - The use of copper or copper alloys in areas exposed to fuel is prohibited.

4.1.2 Standard Parts - AN or MS standard parts, selected from those listed in ANA Bulletin No. 343n, shall be used unless it is determined that they are unsuitable for the purpose. They shall be identified by their standard part numbers.

4.1.3 Protective Treatments and Coatings - Protective treatment and coatings shall be in accordance with applicable specifications listed in ANA Bulletin No. 343n. With the exception of the areas listed below, all parts not in constant contact with fuel shall be corrosion resistant or suitably protected.

(1) Working surfaces

(2) Threads

(3) Drive pad faces

4.1.4 Screw Threads - All conventional straight screw threads shall conform to the requirements of MIL-S-8879 except paragraph 3.12. These include threads on standard hardware bolts and nuts, tapped holes receiving standard items, nuts for use on studs, and threads for non-standard parts where a new thread size is being incorporated in a new design or redesign and where tooling is not already available. These requirements need not apply to electrical connectors, ignition harness, thermocouple harness, interference fit threads, either thread end of studs, fluid fittings, fluid fitting bosses, tube coupling nuts, ground or cut threads, threads of non-standard items where similar parts with the same thread are already designed and tooling is already available, and helical inserts including tapped holes for same where it has been determined that the inserts will accept a MIL-S-8879 external thread.

4.1.5 Data Plate - A data plate shall be attached to the fuel control and shall include the following information:

(1) Manufacturer's name and trade-mark

(2) Manufacturer's part list number

(3) Manufacturer's part number

(4) Control serial number

4.1.5.1 Serialization - Serial numbers of controls procured under this specification shall not duplicate serial numbers of other similar components supplied by the vendor to PWA. A sufficiently large block of serial numbers shall be assigned to the basic control model to cover anticipated production. The use of letters in serial identification shall be avoided.

4.2 Test Requirements

4.2.1 Qualification Tests - Approval as a type of fuel control procured under this specification for a prototype engine shall be contingent upon satisfactory completion of [illegible] hour preliminary flight rating test in accordance with MIL-E-5156C. Approval as a type of fuel control procured under this specification for a production engine shall be contingent upon satisfactory completion of a 150-hour engine qualification test in accordance with MIL-E-5009B and satisfactory completion of a component qualification test as specified in paragraph 4.2. The component qualification test procedure shall be approved in writing by PWA before initiation of the tests. The vendor shall be required to include, as a part of his normal development program, a series of abbreviated tests to determine the extent of compliance with these requirements prior to starting the official component qualification test.

4.2.1.1 Reports - Reports of the fuel control qualification tests under this specification shall be attested to by an appropriate government representative and shall include at least the items mentioned in MIL-E-5009B, paragraph 4.1.2.1. Twelve copies of this report shall be supplied to the Engineering Department of Pratt & Whitney Aircraft for transmittal to the government.

4.2.1.2 Shipment of Production Units Prior to Approval - In the event that production units are shipped prior to satisfactory completion of the appropriate qualification testing, the vendor shall be responsible for retrofitting these units with all engineering changes required to duplicate the unit which satisfactorily completes the appropriate qualification test, except those changes which in the opinion of the cognizant PWA project engineer were not required to pass the appropriate qualification test. These exceptions are to be designated by the PWA project engineer's written approval.

The acceptance of limited quantities of production units may not be contingent upon completion of the appropriate qualification tests as specified in paragraph 4.2.1.

4.2.2 Acceptance Test - Prior to delivery, each fuel control procured under this specification shall be subjected to an acceptance test as specified in section 5.3.

4.3 Design Requirements

4.3.1 Power Lever - The control systems described by this specification are to be constructed as a single unit. A single power lever shall be provided for the purpose of operating throughout the range from maximum engine thrust through idle to full reverse thrust. A functional representation of power lever operation is shown on figure 1. The gas generator power setting shall be determined by the position of the power lever. As the power lever is advanced to initiate augmentation the gas generator is reset to the cruise power level and during the modulation range of augmentation, the gas generator power level is maintained constant. As the power lever is advanced to maximum augmentation, the gas generator is reset to the maximum power level.

The regime of gas generator controlled variables with PLA shall be as specified on figure 2. The regime of duct controlled variables with PLA shall be as specified on figures 9 and 10.

Power lever torque shall not exceed 10 inch-pounds throughout the entire operating range from engine off to maximum thrust position. If this requires a power boost servo, failure of the servo should not result in more than 25 inch-pounds torque. The power lever shall not move when placed in the operating range with the engine running unless external torque is applied. Movement of the power lever throughout the operating range shall be free of abrupt changes in actuating torque, and maximum permissible variation shall not exceed 5.0 inch-pounds.

Means for adjusting the angular position of the power lever with respect to the shaft in increments of no more than one (1) degree shall be provided.

4.3.2 Shut-Off Lever - The shut-off lever shall perform the following functions (Figure 22):

1) Operate a fuel shut off valve

2) Provide for recirculation of the pump outlet flow when the lever is in the off position and the engine windmilling.

3) Provide a position for minimum fuel flow reset

4) Provide a position to actuate the windmilling brake.

4.3.2.1 Shut-off lever torque shall not exceed 10 inch pounds throughout the entire operating range between minimum lever position and maximum lever position. The shut-off lever shall not move when placed in the operating range with the engine running unless external torque is applied, and shall not move when placed in the fuel shut off position. Movement of the shut-off lever throughout the engine operating range shall be free of abrupt changes in actuating torque, and maximum permissible variation shall not exceed 5.0 inch pounds.

Means for adjusting the angular position of the shut-off lever with respect to the shaft, in increments of no more than one (1) degree, shall be provided.

4.3.3 External Lever Stops - The control shall incorporate stops which are capable of withstanding a static torque of 300 in-lbs., without damage or deformation on all external levers.

4.3.4 Fuel Shut-Off Valves

4.3.4.1 Main Fuel Meter - The main fuel meter shall incorporate a fuel shut-off valve, operated as a function of shut-off lever angle, which will stop the fuel flow from the control discharge. Consideration shall be given to the incorporation of a mechanical shut-off valve to act as back up for the servo-operation valve. Provision shall be made to recirculate the pump output flow to the pump interstage when the shut-off lever is in the closed position and the engine is windmilling. With a pump output of *lbs per hour of the fuels specified in paragraph [illegible], the control inlet pressure shall not be more than 95 psi above pump interstage pressure during the windmilling condition. With the shut-off lever in the off position, and a pressure drop of 50 psi across the shut-off valve, leakage from the control outlet port shall not exceed 0.5 cc per minute.

4.3.4.2 Duct Heater Meter - The duct heater meter shall incorporate a means to shut off the fuel to each zone as a function of the power lever, bounded by corrected exhaust nozzle feedback position. The [illegible] for fuel shut-off valve operation, as a function of power lever positi[illegible] shown on figure 6. Each zone will have one fuel shut-off valve. Pr[illegible] for incorporating hysteresis on the shut off valve selection point, not [illegible] ceed the equivalent of 2° PLA, shall be included. With the power lever [illegible] the augmentation cut-off position, leakage shall not exceed 0.5 cc per [illegible] from each valve.

4.3.5 Back Pressure Valve The main fuel meter shall incorporate means for regulating the minimum control inlet pressure to 135 psi above pump interstage pressure when the fuel shut off valve is in the open position.

4.3.6 Maneuver Loading - When mounted on the engine, the control shall be capable of withstanding without permanent deformation, failure or malfunction the flight maneuver forces specified in figure * with the forces acting at the center of gravity of the engine. Location of the control mounting pad relative to the center of gravity of the engine is shown on PWA drawing *.

4.3.7 Space Envelope - The mounting provisions, fuel connections, and limiting contours shall be coordinated with and approved by PWA. The control mounting provisions and external dimensions of the control shall not exceed the envelope shown on PWA drawings SK 75-665.

4.3.8 Control Drive Ratio - The ratio of control drive shaft speed to engine rotor speed will be [illegible] *

4.3.9 Fuel and Ambient Temperature Limits - The control shall be designed to operate satisfactorily with the fuel metering accuracies specified herein under the following conditions:

	Ambient Air Temperature Range	Fuel Temperature Range
Requirement #1	-65 to 550°F	-65 to 325°F
Requirement #2	-65 to 750°F	-65 to 325°F

*

The maximum air velocity around the control will be * feet per second.

*To be supplied

4.3.10 Mockup - A mockup of the control must be prepared and submitted to PWA for coordination of installation requirements. The mockup shall be maintained such that it will accurately define the control outline, mounting face and all engine connections. Prior to making any changes affecting the installation or envelope a mockup must be prepared or the mockup revised and submitted to PWA for coordination of installation requirements. Changes shall be the subject of separate negotiation.

4.3.11 Installation Connections - Where internal straight screw threads are provided on the fuel control for the attachment of aircraft or engine fittings, the bosses shall be in accordance with Drawing * and sufficient clearance shall be provided for installing hose nipples or flared tube fittings.

*To be supplied.

4.3.11.1 Water and Vapor Vent Connections - Provisions shall be made to incorporate a vapor vent connection at a location in the control body which will insure the purging of trapped air. Provisions shall also be made to permit drainage of water from the control body and from each air pressure sensing bellows chamber.

4.3.12 Pressure Taps and Ports - Pressure taps shall be provided and identified at the following points:

(1) Main fuel meter inlet upstream of filter
(2) Main fuel meter inlet downstream of filter
(3) Main fuel meter discharge
(4) Main fuel metering valve upstream
(5) Main fuel metering valve downstream
(6) Duct heater meter inlet
(7) Duct heater meter discharge at each zone
(8) Duct heater metering valve upstream at each zone
(9) Duct heater metering valve downstream at each zone
(10) Control body pressure
(11) Each servo pressure
(12) Exhaust nozzle open signal
(13) Exhaust nozzle close signal
(14) A port shall be provided to supply the augmentation ignition arming signal. This signal will be servo pressure to the igniter during augmentation and body pressure during non-augmentation.
(15) A port shall be provided for duct heater meter cooling flow discharge
(16) A port shall be provided for the minimum fuel flow reset signal *

4.3.13 Control Weight. - The weight of the complete unitized control shall not exceed 110 pounds.

4.3.14 Accessibility - All parts of the control requiring routine service checking, adjustment or replacement while on engine shall be made readily accessible. This will include maximum and idle speed adjustments, fuel density adjustment, fuel screens and filters. It will also include provisions for trimming the slope of the augmentation W_f/P_b versus power lever schedule with a single adjustment, and for trimming the desired fan total to static pressure ratio schedule. Maximum and idle speed adjustments shall be designed for use with a remote trimmer. All control bench adjustments (including pivot hole changes) shall be readily accessible either externally or through the removal of an access cover and shall not require the use of special fixtures. It would be desirable to have all the bench adjustments accessible by the removal of only one cover. If a cover is used it shall be required that the removal or installation of it will not disturb any control adjustment and will not necessitate the removal of any control subassembly.

4.3.15 Interchangeability - The control shall be designed so that it can be removed from the engine without removing the compressor inlet temperature sensing device from the engine. The temperature system shall be designed such that replacement controls can be installed on the engine and can employ the already installed temperature sensing device without adversely affecting control performance. The main fuel metering valve and the duct heater metering valves must also be replaceable without removing the control from the engine and without adversely affecting control performance. In addition, this same criteria should be used in the design of the control for the turbine driven pump and the design of the pilot valves for the exhaust nozzle actuators and the starting bleeds.

4.3.16 Fuel - The control shall be designed for use with fuels conforming to * .

4.3.16.1 Fuel Density Change - The control shall incorporate means to compensate for fuel density change due to fuel temperature change. The control shall also incorporate means to compensate for fuel density change due to a change in fuel by the use of a calibrated external adjustment.

4.3.16.2 Fuel Contamination - The control shall operate satisfactorily when using contaminated fuel to the extent of 80 grams of foreign matter per 1000 gallons.

Satisfactory operation on contaminated fuel shall mean that the contaminated fuel will not in itself precipitate a sudden control failure but may cause gradual deterioration of control performance and abnormal wear of control parts. The body pressure return connection at the control shall contain means to prevent back wash of contaminated fuel into the control servos if the discharge side of the servos are not protected by screens. This foreign material shall be considered to consist of not less than 68 percent SiO_2 and shall have a particle-size analysis as follows:

*To be supplied.

Particle Size Microns	Percent of Total
0-5	39 ± 2 by weight
5-10	18 ± 3 by weight
10-20	16 ± 3 by weight
20-40	18 ± 3 by weight
over 40	9 ± 3 by weight
Through a 200-mesh screen	100 by weight

4.3.16.3 Fuel Filtration - A suitable inlet filter for both main and duct fuel meters must be provided which will retain contamination of the size that would otherwise cause control malfunctioning. The filter shall be of the bypass type and must be readily accessible for inspection and cleaning. The following additional items shall also be made part of the filter design.

(a) The bypass system must prevent entrance of the accumulated contaminant into the control during bypassing conditions.

(b) The fit of the various parts of the filter as well as the fit of the filter in the housing must be compatible with the degree of filtration desired.

(c) A means shall be provided to prevent incorrect installation of the filter elements.

(d) The filter shall be designed to prevent accumulated dirt from being left in the control when the filter is removed.

(e) The filter cover shall be identified by raised letters or colors to avoid removal of the wrong cover.

(f) Practical means of removing inspectable filters shall be considered to eliminate the need of special tools.

All filters and screens shall be designed to pass fuel of the specified contamination at the maximum rate for at least 20 hours without requiring cleaning.

4.3.17 Leakage - Fuel leakage to the overboard drain connection (if such is required) shall not exceed 1/2 cc per minute under any operating condition. No other fuel leakage is permissible.

Particle Size Microns	Percent of Total
0- 5	39 ± 2 by weight
5-10	18 ± 3 by weight
10-20	16 ± 3 by weight
20-40	18 ± 3 by weight
over 40	9 ± 3 by weight
Through a 200-mesh screen	100 by weight

4.3.16.3 Fuel Filtration - A suitable inlet filter for both main and duct fuel meters must be provided which will retain contamination of the size that would otherwise cause control malfunctioning. The filter shall be of the bypass type and must be readily accessible for inspection and cleaning. The following additional items shall also be made part of the filter design.

(a) The bypass system must prevent entrance of the accumulated contaminant into the control during bypassing conditions.

(b) The fit of the various parts of the filter as well as the fit of the filter in the housing must be compatible with the degree of filtration desired.

(c) A means shall be provided to prevent incorrect installation of the filter elements.

(d) The filter shall be designed to prevent accumulated dirt from being left in the control when the filter is removed.

(e) The filter cover shall be identified by raised letters or colors to avoid removal of the wrong cover.

(f) Practical means of removing inspectable filters shall be considered to eliminate the need of special tools.

All filters and screens shall be designed to pass fuel of the specified contamination at the maximum rate for at least 20 hours without requiring cleaning.

4.3.17 Leakage - Fuel leakage to the overboard drain connection (if such is required) shall not exceed 1/2 cc per minute under any operating condition. No other fuel leakage is permissible.

4.3.18 Fuel Pressures

4.3.18.1 Static Pressures - The control shall meter to the accuracy specified herein with pump interstage pressure from 0 to 400 psig, and with main fuel meter and duct heater meter discharge pressures in the ranges shown on figures 17, 18 & 19.

4.3.18.2 Transient Pressures - All parts of the control shall be designed to withstand a possible interstage pressure surge up to 400 psig. All parts shall be capable of withstanding a metered fuel pressure surge of 500 psi above the normal maximum working pressure.

4.3.18.3 Maximum Pressures - The maximum normal working pressure will be 800 psig for the main fuel meter section, 1400 psig for the duct heater meter sections and 1700 psig for the exhaust nozzle control section. The control shall be capable of withstanding without fracture or permanent deformation, the following pressures acting singly or in conjunction:

Main Fuel Meter Discharge Pressure	0-2100 psig
Duct Heater Meter Discharge Pressure	0-2100 psig
Return Pressure	0-400 psig
Exhaust Nozzle Control Section	0-3000 psig

Tests to demonstrate this requirement shall be subject to approval by PWA, and shall be repeated when changes or process modifications are incorporated which, in the opinion of P&WA, might adversely affect control strength. Burst pressure tests must be performed on a development unit to destruction.

4.3.18.4 Fuel Pressure Drop - The fuel pressure drop from main fuel meter inlet to main fuel meter discharge shall not exceed 100 psi when metered flow is 28500 lbs/hr of * fuel. The pressure loss across the duct heater meter from fuel inlet to fuel outlet for each zone shall not exceed 126 psi when the fuel flow for each zone is the following:

Zone I - 41,000 lbs/hr.
Zone II - 45,000 lbs/hr.

*To be supplied.

4.3.18.5 With the exhaust nozzle in full transient, the control valve must handle 50 gpm with a pressure loss not to exceed 250 psi with supply pressure 1500 psi above drain pressure. The drain pressure will be a minimum of 0 psig and a maximum of 400 psig. With the pilot valve in the null position cooling flow of 3.8 gpm will be supplied to the nozzle actuators and the pilot valve leakage to drain pressure shall not exceed 1.3 gpm

4.3.19 Reliability Analysis - The vendor shall provide three copies of a reliability analysis of the control based upon a single failure concept. This analysis shall be submitted to P&WA for review prior to approval of the design for manufacture of experimental units.

4.3.20 Environmental Requirements - The electrical section (if any) of the control shall be explosion proof and fireproof to the extent that it will not support combustion.

4.3.21 Control Bypass Requirements - All servo leakage return flow must pass to the fuel pump interstage and shall not exceed 1300 pph at the engine starting condition. The main fuel meter shall be capable of scheduling to the desired accuracy with the fuel pump output up to 36000 pph in excess of the engine requirements and with a minimum pressure drop of 135 psi across the bypass valve ports. The main fuel meter shall also provide suitable metering characteristics and be capable of metering to the desired accuracy with control bypass flow as low as 200 pph at any metered flow level.

4.3.22 Independent Concept - The unitized control system requires that any failure of the duct heater control system or exhaust nozzle control system must not affect operation of the main fuel control system.

4.4 Performance and Operational Requirements

4.4.1 Main Fuel Meter Section

4.4.1.1 Speed Control - The engine rotor equilibrium speed shall be controlled from full reverse through idle to maximum engine power through a speed sensitive permanent droop mechanical governor varying fuel flow per unit burner pressure between those limits described in paragraphs 4.4.1.10 and 4.4.1.11.

4.4.1.2 The specific value of engine rotor speed (N_2) desired and the corresponding required value of fuel flow per psia burner pressure (W_f/P_B) at any specific power lever angle with constant corrected engine inlet conditions of $\theta_{t2} = 1$ and $\delta_{t2} = 1$ are shown on Figure 2. The bias of engine rotor steady state speed (N_2) for any engine inlet condition (θ_{t2} and δ_{t2}) is shown on figures 4 and 5 for the maximum rated power and the cruise power respectively. *

4.4.1.3 The value of W_f/P_B maintained by the control shall conform to the specified values within ±2%.

4.4.1.4 The basic slope of the governor droop lines at the maximum rated power lever position and W_f/P_B shall be -.075 lbs/hr/psia/rpm N_2. The slope shall be maintained within ±2.5% and shall be adjustable over a range of +70% to -50%.

4.4.1.5 The slope of the governor droop line at idle power lever position shall be a minimum of -.075 lb/hr/psia/rpm N_2.

4.4.1.6 A range of adjustment of the position of the governor droop line shall be provided to allow ±5% engine rpm about the nominal idle speed setting of 4880 RPM (N_2) and to allow ±5% engine rpm about the nominal maximum rated engine rpm of 8275 RPM (N_2)

4.4.1.7 Under no condition shall the fuel control governor permit the engine to overshoot more than 5% of the selected equilibrium speed change following an increase in power lever position nor shall engine speed be allowed to exceed 101% of the maximum rated speed.

4.4.1.8 Under no condition shall the fuel control governor permit the engine to undershoot more than 10% of the selected equilibrium speed change following a decrease in power lever position.

4.4.1.9 Speed Failure Protection - In the event that failures prevent the control from sensing engine rotor speed (N_2) the main fuel meter shall schedule by means of positive forces within the control the values shown at zero rpm (N_2) on figure 20.

4.4.1.10 Acceleration Fuel Flow Limitation - Limitation of fuel flow metered by the control during an acceleration shall be accomplished by scheduling fuel flow per unit burner pressure (W_f/P_B) as a function of engine rotor speed (N_2), biased by engine inlet temperature (T_{T2}), to match engine operating requirements as shown on figure 20.

4.4.1.10.1 The operating range of the scheduling variables shall be as follows:

N_2	500 to 9000 rpm
T_{T2}	-60°F to 770°F
P_B	5.0 to 250 psia
P_{T2}	2.5 to 44.0 psia

4.4.1.10.2 Accuracy of acceleration fuel flow limitation shall be held within +0, -4%.

4.4.1.10.3 The relationship between acceleration fuel flow and the scheduling variables, N_2, P_B and T_{T2} shall be readily modified by adjustment or by replacement of not more than two parts without impairment of any other control function.

4.4.1.11 Minimum Fuel Flow Limitation - Limitation of the minimum fuel flow metered by the control during deceleration or steady state shall be accomplished by scheduling from burner pressure (P_B) as shown on Figure 21.

4.4.1.11.1 Minimum fuel flow shall be effective from an N_2 of 500 rpm to an N_2 of 9000 rpm under all operational conditions.

4.4.1.11.2 Accuracy of minimum fuel flow limitations shall be maintained within ±4%.

4.4.1.11.3 The flat portion of the minimum flow curve shall be adjustable over a range of 300 to 650 pounds per hour.

4.4.1.12 Minimum Fuel Flow Reset - There shall be a provision to reset minimum fuel flow to 25% of the value stated in paragraph 4.4.1.11.3. Selection of minimum fuel flow reset will be dependent on three factors:

1) High Rotor Speed must be above 50% N_2.

2) The fuel flow shut off lever must be in the minimum fuel flow reset position.

3) The power lever must be in the idle position

If anyone of these factors is not present the minimum fuel flow will remain at the value stated in paragraph 4.4.1.11.3.

When minimum fuel flow reset is actuated the control must send a hydraulic signal to an external port.

4.4.1.13 Approach Speed Reset. - Provisions shall be made to incorporate an approach speed reset on engine set speed. (Reference 4.4.1.2). The input shall be by an external lever with a total travel of ± 40 degrees. The range of reset shall be as shown on Figure 3.

4.4.2 Duct Heater Fuel Metering Section

4.4.2.1 The control shall schedule fuel flow per unit burner pressure independently to each burning zone as a function of power lever angle during steady state as shown on figure 6.

4.4.2.2 The fuel flow per unit burner pressure (W_f/P_B) schedule for zone I at 81 degrees PLA shall be biased by engine inlet conditions, θ_{T2} and δ_{T2}, as shown on figure 7. The W_f/P_B schedule for zone I at 102.5 degrees PLA shall be biased as shown on figure 8. The W_f/P_B schedule for zone II shall be biased as shown on figure 9.

4.4.2.3 There shall be an adjustable minimum fuel flow stop provided for each zone. The nominal minimum fuel flow for Zone I and Zone II is stated on figure 6.

4.4.2.4 The operational range of the scheduling variables shall be as follows:

PLA	31° to 128°
T_{T2}	-60°F to +770°F
P_b	[illegible] to 250 psia
P_{T2}	2.5 to 44 psia

4.4.2.5 The control shall schedule fuel flow within ± 2.0% of the defined fuel flow schedule.

4.4.2.6 Non Duct Heating Cooling Flow - During the non duct heating mode of operation the control must allow fuel to flow from the duct fuel turbo-pump through the duct heater meter and discharge to a port for external transfer to the main fuel pump inlet. This cooling fuel shall flow at the rate of 1000 to 1500 pph and discharge into pressures of from 0 to 50 psig.

4.4.3 Exhaust Nozzle Control Section

4.4.3.1 The desired value of fan discharge total pressure minus fan discharge static pressure divided by fan discharge static pressure, $(P_{T3}-P_{S3})/P_{S3}$, shall be scheduled as a function of fan inlet total temperature (T_{T2}) and engine rotor speed (N_2) as shown on figure 14 for operation below cruising mach numbers. The schedule of $(P_{T3}-P_{S3})/P_{S3}$ for operation during cruising mach number shall be scheduled as a function of fan inlet total temperature (T_{T2}), engine rotor speed and flight mach number as shown on figure 15. The threshold for employing figure 15 shall be $M_N = 2.0$.

4.4.3.2 The prescheduled duct area control parameter $(P_{T3} - P_{S3})/(P_{S3})$ will be maintained by sensing the actual value of $(P_{T3}-P_{S3})/(P_{S3})$ and using the error through a proportional plus integral gain system to vary, with limited authority, the nozzle area about the nominal value set by the PLA.

4.4.3.3 Provisions shall be made to reset $(P_{T3}-P_{S3})/P_{S3}$ as a function of an external lever position. The signal to the external lever will be supplied by the airframe. The amount of reset will be .02 psi/psi maximum. *

4.4.3.4 The exhaust nozzle area shall be nominally scheduled as a function of PLA as shown in figure 10 for constant engine inlet condition of $\theta_{T2} = 1.0$ and $\delta_{T2} = 1.0$. Figure 11, 12, and 13 are resultant curves. They show, respectively, how the exhaust nozzle area will vary with θ_{T2} and δ_{T2} during specific conditions of non-duct heating, max-augmentation, and min-augmentation when the prescheduled duct area control parameter, $(P_{T3}-P_{S3})/(P_{S3})$, is maintained *

[illegible].5 Th[illegible] operation[illegible] range of scheduling parameters shall be [illegible]s:

[illegible]	2.5 to 60 psia
[illegible]	2.5 to 44 psia
[illegible]	-60°F to 770°F
[illegible]A	81° to 128°
	500 to 9000 rpm
$\frac{P_{T3}-P_{S3}}{P_{S3}}$	.03 to .12 psi *
$P_{T3}-P_{S3}$	.36 to 6.1 psi
M_N	1.7 to 3.2

4.4.3.5.1 The Mach number signal will be supplied by the airframe to a lever on the control housing

4.4.3.6 The desired value of steady state $(P_{T3}-P_{S3})/(P_{S3})$ shall be maintained within ±4.0% for all flight conditions. Transient accuracy shall be maintained within ±2.0% of the steady state value including that period of operation when individual zone fuel manifolds are filling. A larger error will be allowed at the ignition and shut off points of an individual zone. In the event of a failure in the exhaust nozzle area feedback system the control shall require the nozzle to open, and cut off augmentation fuel flow.

4.4.4 Servos and Signal Amplifiers

All servos operating from the scheduling variables shall be critically damped and shall reach their new steady state position in not more than 1.0 second following step inputs calling for their full range of travel except the rotor speed servo which shall reach its new steady state position in .5 second. For small excursion step inputs the servos shall reach their new steady state position in not more than 0.25 seconds. The output force of all servos shall be a minimum of 25 pounds. These requirements shall apply to all servos unless otherwise agreed upon in writing by Pratt & Whitney Aircraft.

4.4.5 Auxiliary Functions

4.4.5.1 Initiation of fuel flow to the duct heater will be accomplished by advancing the power lever to 81 to 83 degrees. Retardation of the power lever below 80 to 82 degrees shall shut-off the fuel flow to the duct heater, but not until the duct exhaust nozzle area has closed to its minimum duct heating value. Initiation can be accomplished only upon receipt of the duct heater arming signal.

4.4.5.2 Duct Heater Arming Signal - A duct heater arming signal will operate as a function of engine rotor corrected speed ($N_2/\sqrt{\theta_{T2}}$) to preclude duct heating until the gas generator has reached a minimum power setting.

4.4.5.3 Duct Heater Blowout Protection - The control shall incorporate an override mechanism to automatically reset the exhaust nozzle to its non burning schedule in the event of duct heater blowout. This will be indicated by an increase of 40.0% in the actual value of $(P_{T3}-P_{S3})/(P_{S3})$. Upon removal of the $(P_{T3}-P_{S3})/(P_{S3})$ error the blowout signal shall be removed and the non-burning schedules to the duct heater shall be maintained. It will be necessary for the power lever to be retarded below 80 degrees to recycle the control.

4.4.5.4 Light Off Signal - At the selection of any augmentation zone, as indicated by motion of the power lever, the exhaust nozzle must be set and maintained in a position compatible with the predetermined lighting schedule. This lighting schedule of $(P_{T3}-P_{S3})/P_{S3}$ is shown as a function of N and θ_{T2} on figure 15. This light off schedule shall be selected prior to each zone light and terminated after the zone has been lit. Termination of this schedule will be indicated by a 5% decrease in the value of $(P_{T3}-P_{S3})/(P_{S3})$ after the zone has been lit.

4.4.5.5 Air Induction Control Signal - The control shall provide a signal to the air induction control prior to the initiation of each augmentation zone. Details of this system shall be coordinated with PWA and the manufacturer of the inlet control and the airframe manufacturer.

4.4.5.6 Compressor Bleed Valve Control - The control system is to provide a scheduled operation of the compressor bleed valves as a function of $N_2/\sqrt{\theta_{T2}}$ as shown on figure * . The bleed valve actuator operates on 1500 psig supply pressure above drain pressure for operation. The drain is 0-400 psig. The control mechanism to provide the high pressure supply shall not exceed a pressure drop of 300 psig with an actuator flow of 1000 lbs/hr. during bleeds open or bleeds closed operation. *

4.4.5.7 Duct Fuel Turbopump Control

The duct fuel turbopump control is required to vary the turbopump air throttle valve to maintain a coarse metering head for the duct heater meter.

4.4.5.8 Duct Heater Thermostatic Valve Signal - The thermostatic valve is to allow the duct heater meter to receive high temperature fuel from the main fuel meter bypass system. A high pressure signal shall be provided to open the valve when augmentation fuel flow is greater than or equal to 6000 ± 500 lbs/hr.

4.4.6 The fuel flows specified in all the preceding paragraphs should be scaled by the factors 64/60 and 70/60.

* To be supplied at a later date.

5. INSPECTION AND TEST PROCEDURE

5.1 General - The fuel control shall be subject to inspection by authorized representatives of the customer, who shall be given all reasonable facilities to determine conformance with this specification. Unless otherwise specifically authorized, all tests (except the engine qualification test) shall be conducted at the vendor's plant.

5.1.1 Accuracy of Data - All test apparatus shall be acceptable to the customer at the vendor's plant and shall be such as to insure that reported data shall have a static accuracy within 2% of the value obtained at the maximum value except fuel flow shall be accurate within 1%, simulated burner pressure (P_b) shall be accurate within 1/2%, and speed shall be accurate within 1/4% of the maximum value. All instruments and equipment shall be calibrated at frequent intervals to insure that this degree of accuracy is maintained.

5.1.2 Control Position - During all tests the fuel control shall be mounted as installed on the engine insofar as practicable. The position of the control when installed on the engine is with the power lever shaft horizontal and to the right as the control is viewed from the anti-drive end of the control.

5.2 Qualification Test

5.2.1 General Inspection - Prior to the test, all parts and assemblies of the fuel control shall be inspected to determine conformance to the vendor's parts list and all requirements of the contract and specifications under which they were built. Dimensional measurements of all details subject to wear shall be recorded before and after completion of the qualification test. At no time during the test shall any part of the fuel control be removed, disassembled or adjusted without prior approval of the customer.

5.2.2 Leakage - During the qualification test, there shall be no traces of external fluid leakage other than a maximum allowable leakage of 10 drops per minute from the overboard drain connection.

5.2.3 Qualification Tests Instrumentation - Sufficient instrumentation shall be provided to indicate that the performance of each element of the control remains within service limits throughout the test. Functional checks shall be performed at the end of each test or group of tests and at other times at the option of the vendor.

5.2.4 Fuel Control Calibrations - Prior to and upon completion of the fuel control qualification tests, the control shall be completely recalibrated. The results of these calibrations shall demonstrate that the unit has not changed its calibration beyond allowable service limits. The same type fluid shall be used during both calibrations.

5.2.5 Operational Test - To be specified at a later time.

5.3 Acceptance Test

5.3.1 General - Each fuel control procured under this specification shall be subjected to acceptance tests established by the vendor to determine that each unit will meet the functional requirements of this specification. The test procedures and limits shall require prior approval in writing and shall be subject to change by the customer. Each deviation from the test schedules and limits shall require approval by the customer.

5.3.2 Proof Pressure Test - Each fuel control procured under this specification shall be subjected to a proof pressure test before delivery. During the proof pressure test, external fluid leakage (other than a maximum allowable leakage of 10 drops per minute from the overboard drain connection) is not acceptable. The proof pressure test shall consist of subjecting the fuel control the following conditions while the control is in operation for a period of at least three minutes at each condition.

	Control Discharge Pressure	Body Return Pressure
Condition a.	1100 psig	183 psig
Condition b.	1100 psig	0-5 psig

5.3.3 Inspection - Fuel controls shall be inspected for conformance with the vendor's part list currently released to production by initial release or revised by subsequent engineering change.

5.3.4 Data - The vendor shall supply one copy of the acceptance test data of each fuel control procured under this specification. The acceptance test data shall be delivered to the customer not later than the date on which the control is received.

6. VENDOR RESPONSIBILITIES

6.1 Preparation for Storage - The fuel control shall be prepared for storage prior to shipment in a manner acceptable to the customer.

6.2 The requirements of the customer specification are applicable to the fuel control covered by this specification except this requirement shall not apply to experimental purchase orders.

6.3 Prior to acceptance of the qualification test on the control the vendor shall be responsible for making changes and supplying hardware for correcting deficiencies found in the development units. If a change of requirements is made, costs arising from such changes will be subject to separate negotiations. In order to support the development units, the vendor shall maintain or shall be able to obtain in a reasonable time spare parts for procurement by the customer.

6.4 The vendor shall give full support to the development program by providing an adequate engineering development effort which shall include bench development and endurance tests on controls to insure satisfactory operation of the control at the customer's facility both on the bench and engine to the requirements listed in this specification. An outline of the vendor's proposed development program shall be forwarded to the customer prior to the issuance of any purchase orders for units.

6.5 The vendor shall be responsible for retrofitting of all experimental units with all engineering changes required to duplicate the unit which satisfactorily completes the appropriate qualification tests, except those changes which in the opinion of the cognizant Pratt & Whitney Aircraft project engineer were not required to pass the appropriate qualification tests. These exceptions are to be designated by the Pratt & Whitney Aircraft project engineer's written approval. Delivery schedule of retrofit parts must be in accordance with engine development schedule.

6.6 Drawings. - The vendor shall supply one reproducible copy of all drawings pertaining to the control. Drawings shall also be supplied providing design information for special tools, fixtures, fittings, and adapters which will be required during development testing or field use.

PPS A19

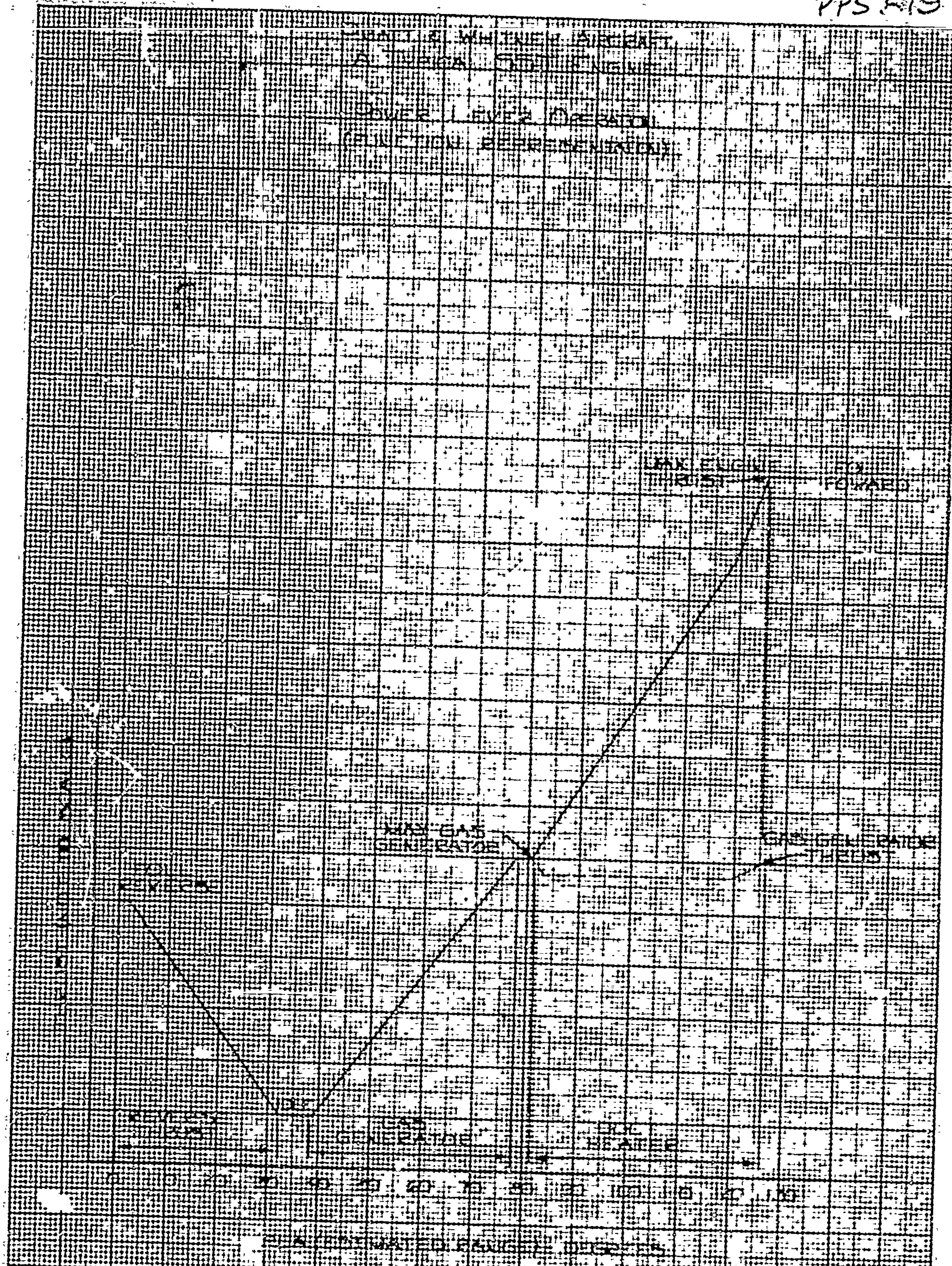

FIGURE 1

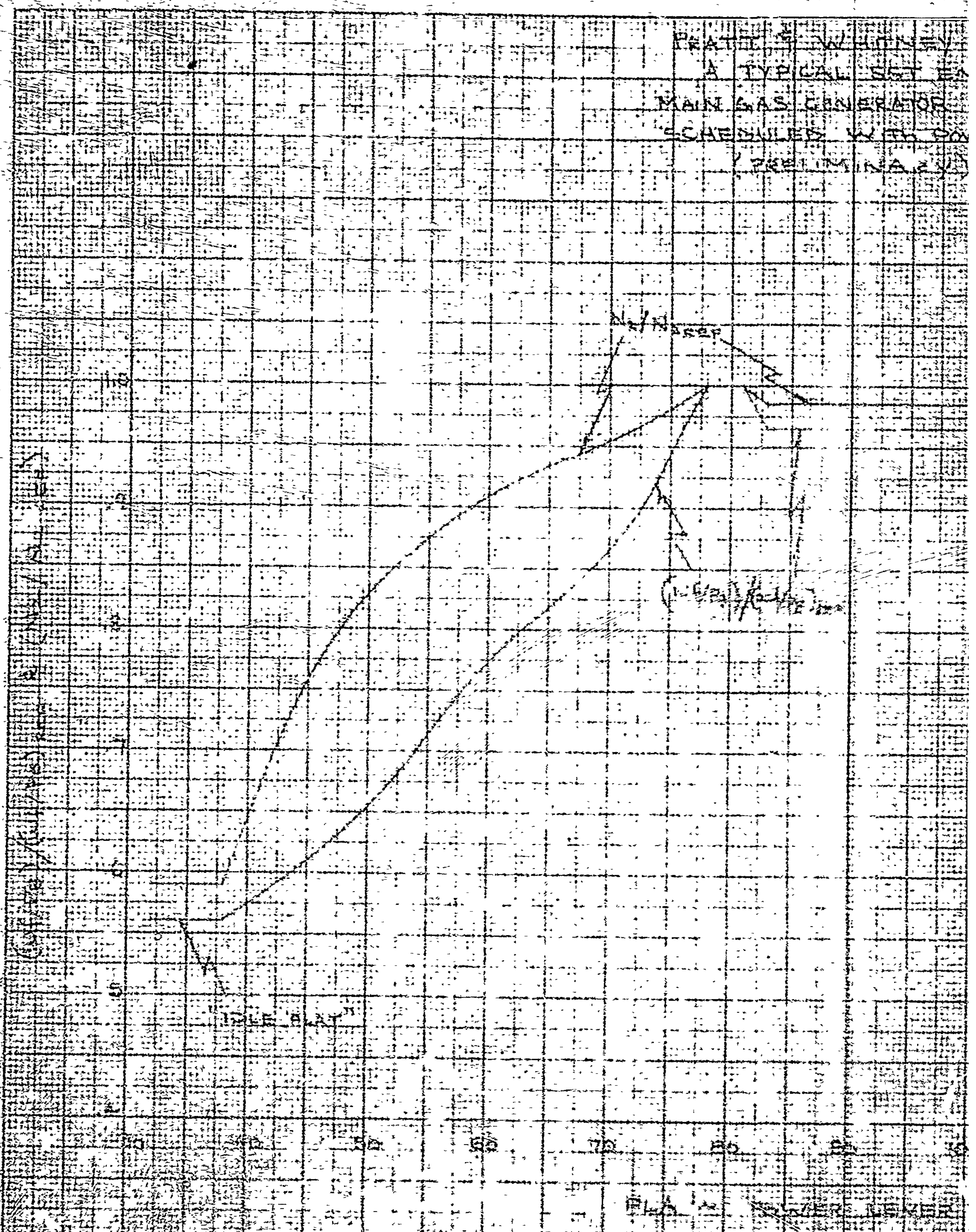
PRATT & WHITNEY
A TYPICAL SST
MAIN GAS GENERATOR
SCHEDULED
(PRELIMINARY)
IDLE FLAT
30
40
50
60
70
80
90
PLA ~ POWER LEVER

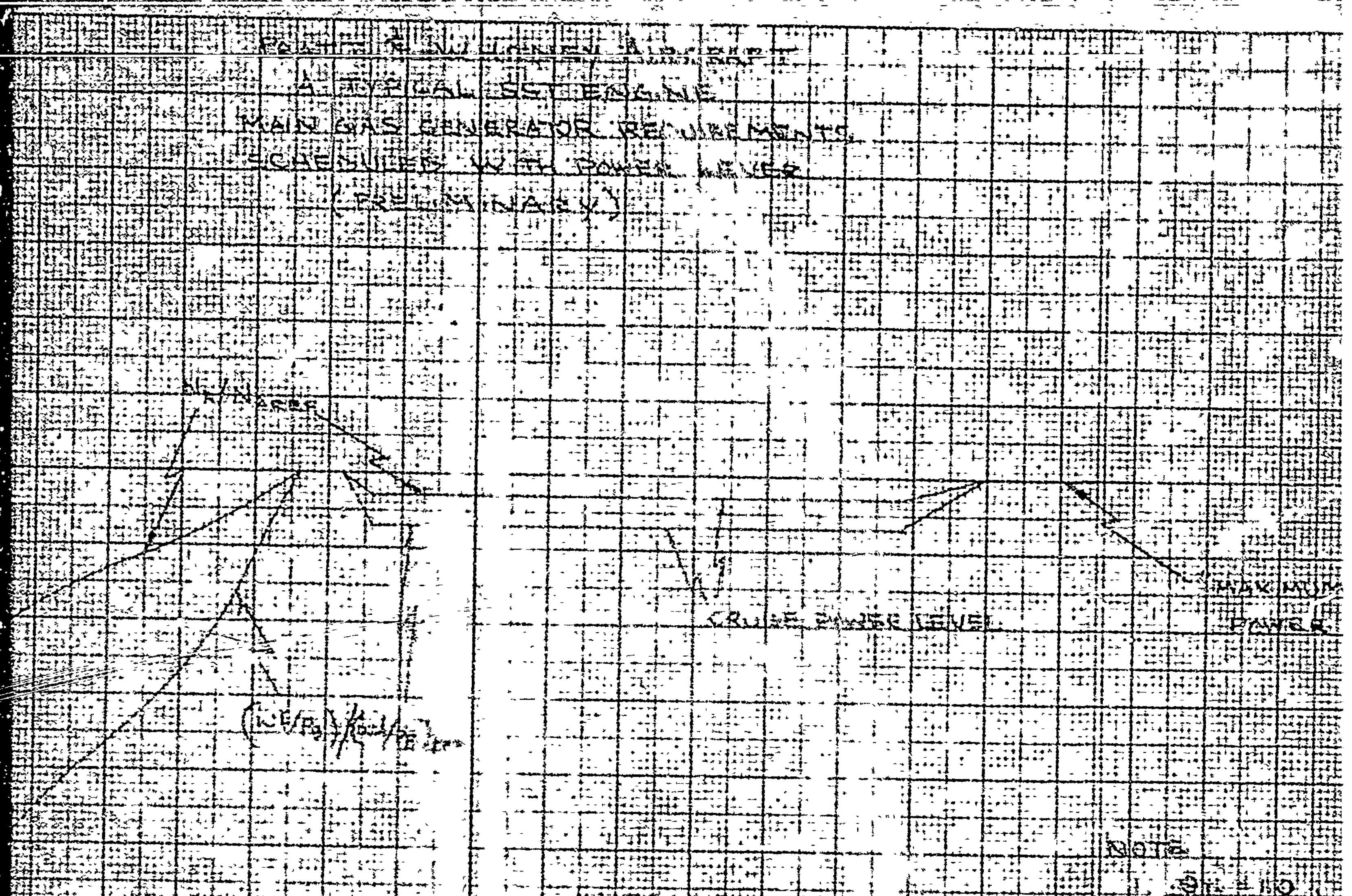
A TYPICAL SST ENGINE
MAIN GAS GENERATOR REQUIREMENTS
SCHEDULED WITH POWER LEVER
(PRELIMINARY)
CRUISE POWER LEVEL
NOTE
70
80
100
120
130
140
PLA ~ POWER LEVER ANGLE ~ DEGREES

1

2

PPS 819

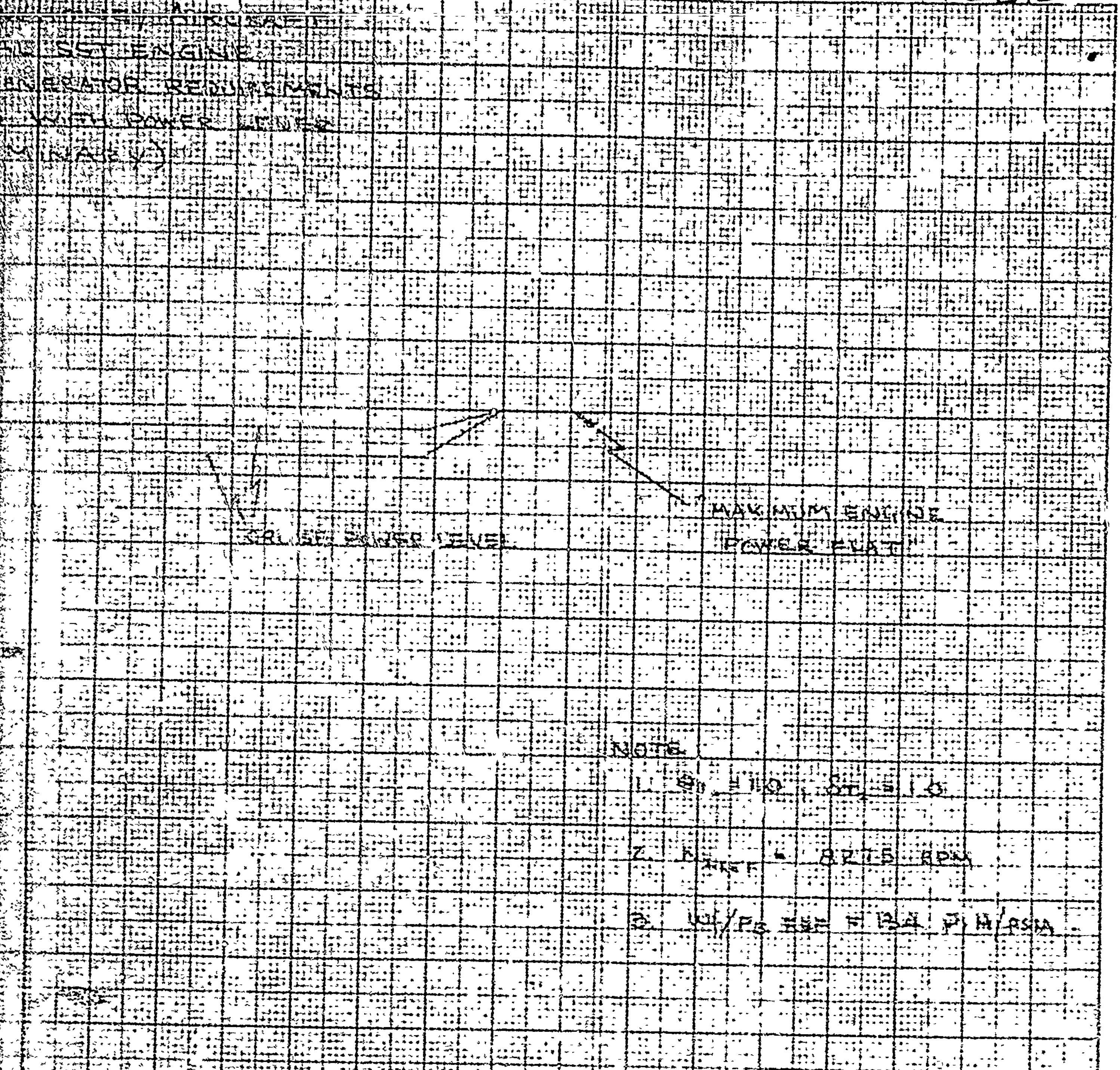

FIGURE 2

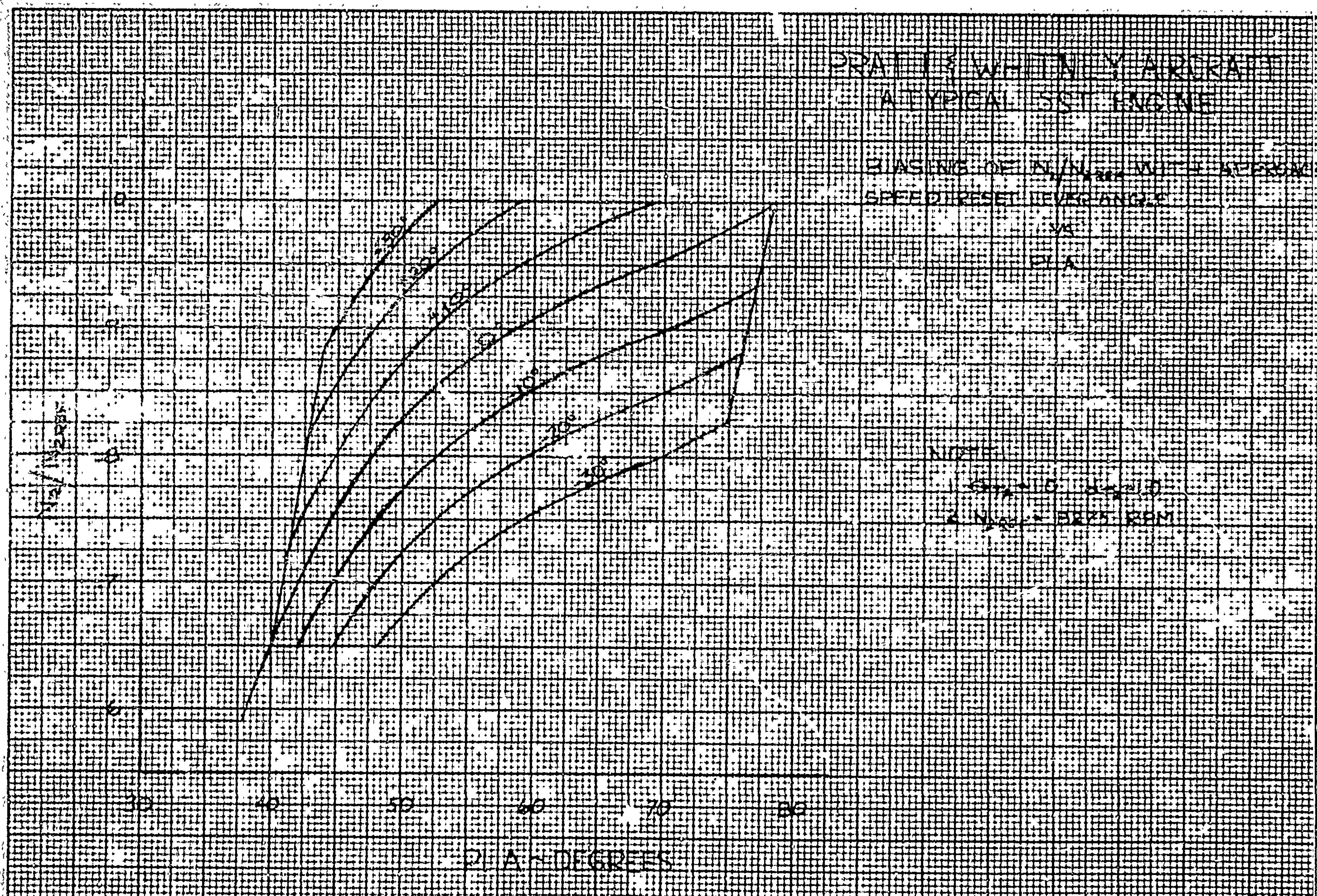
PRATT & WHITNEY AIRCRAFT
A TYPICAL SST ENGINE
SPEED RESET LEVER ANGLE
vs
PLA
NOTE
10
9
8
7
6
30
40
50
60
70
80
PLA ~ DEGREES

FIGURE 3

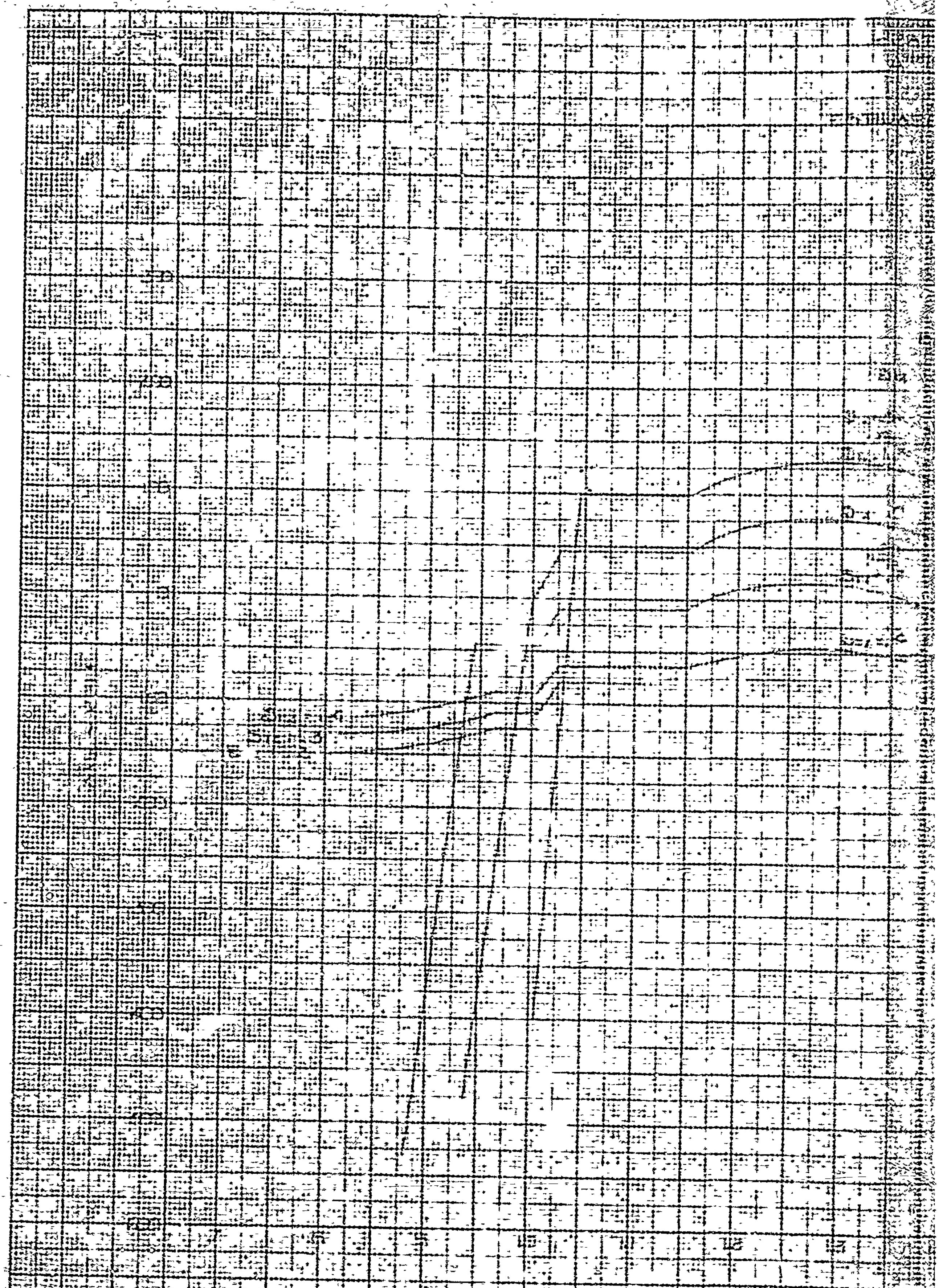

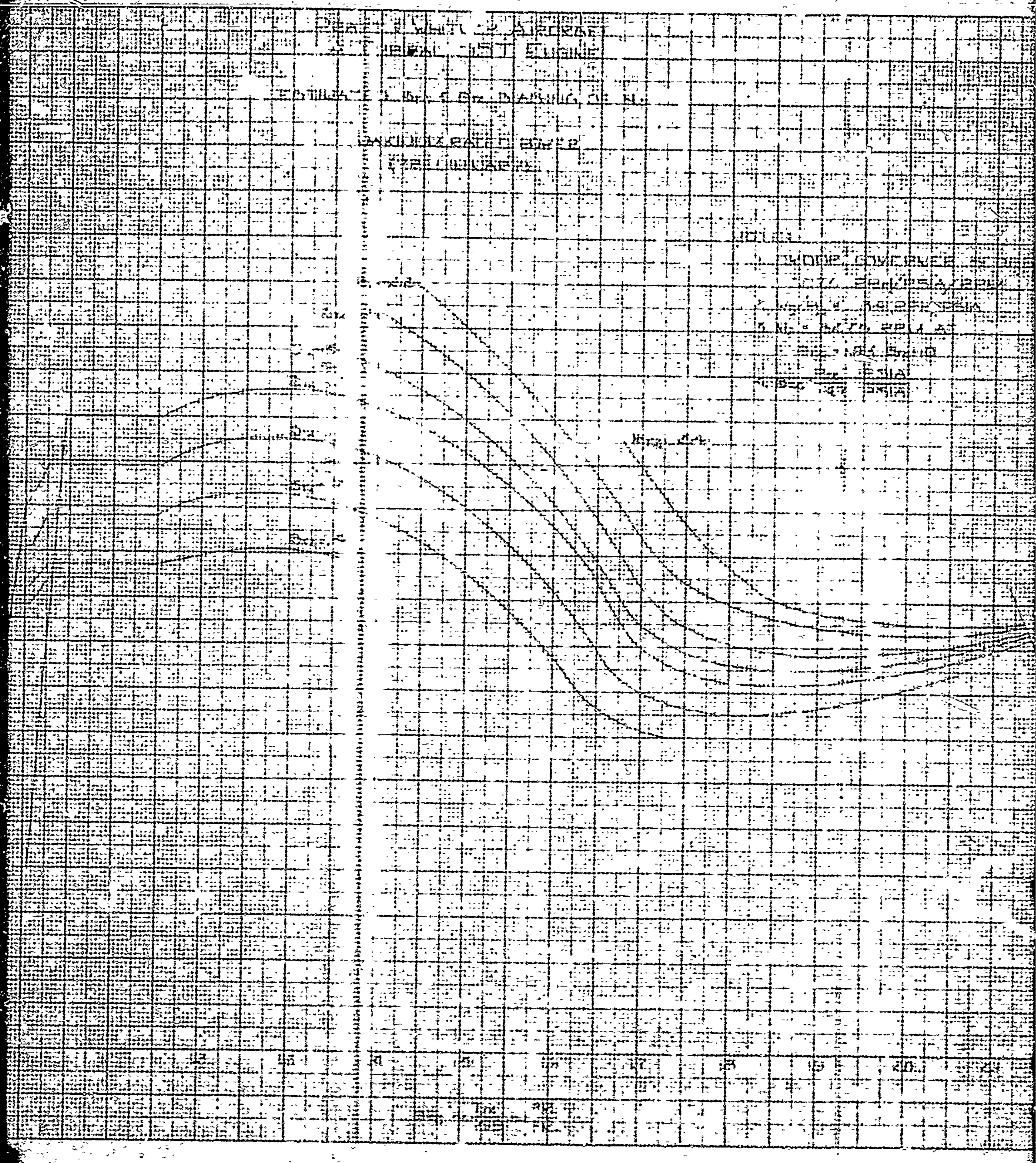

1

2

PPS 819

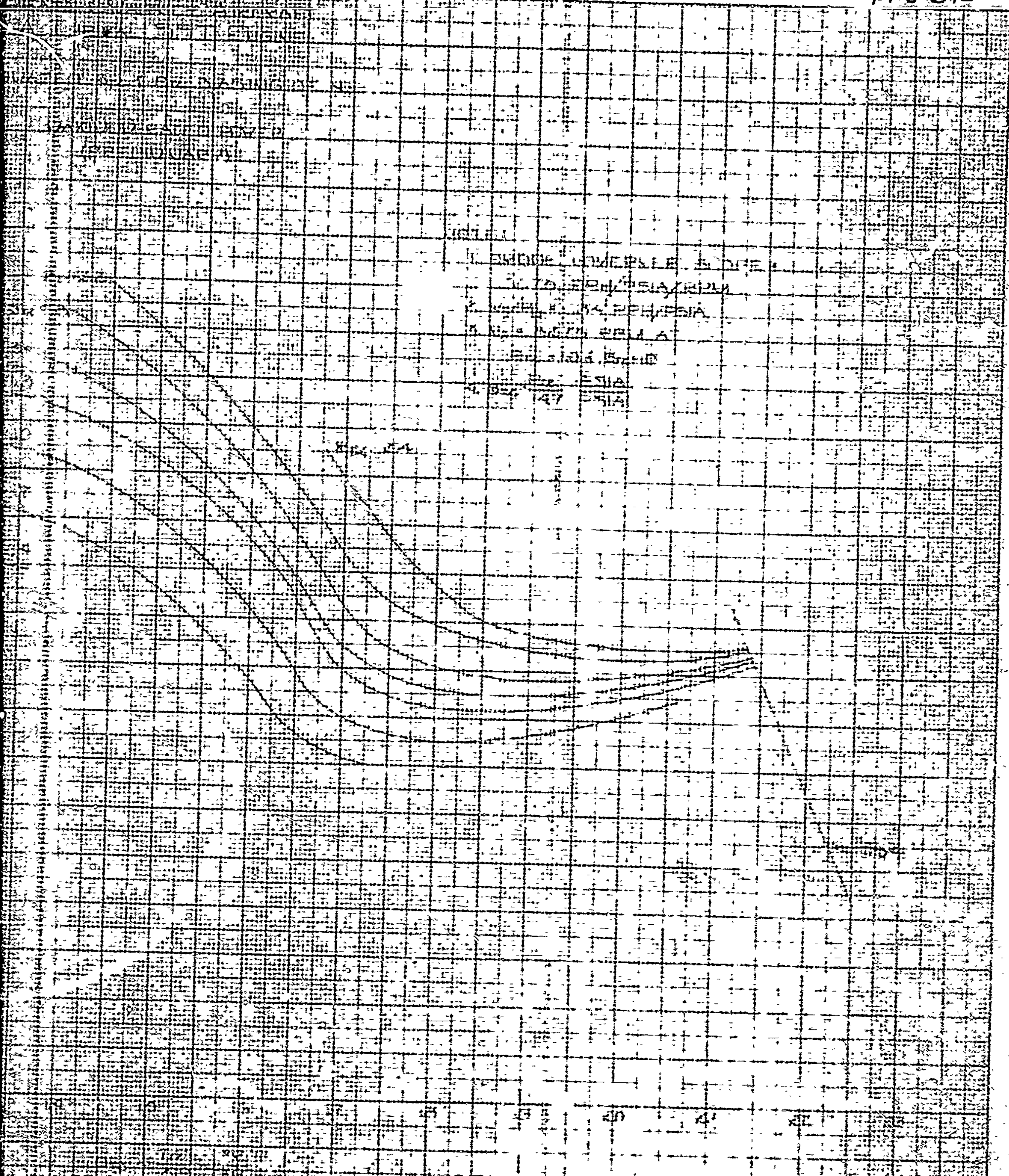

FIGURE 4

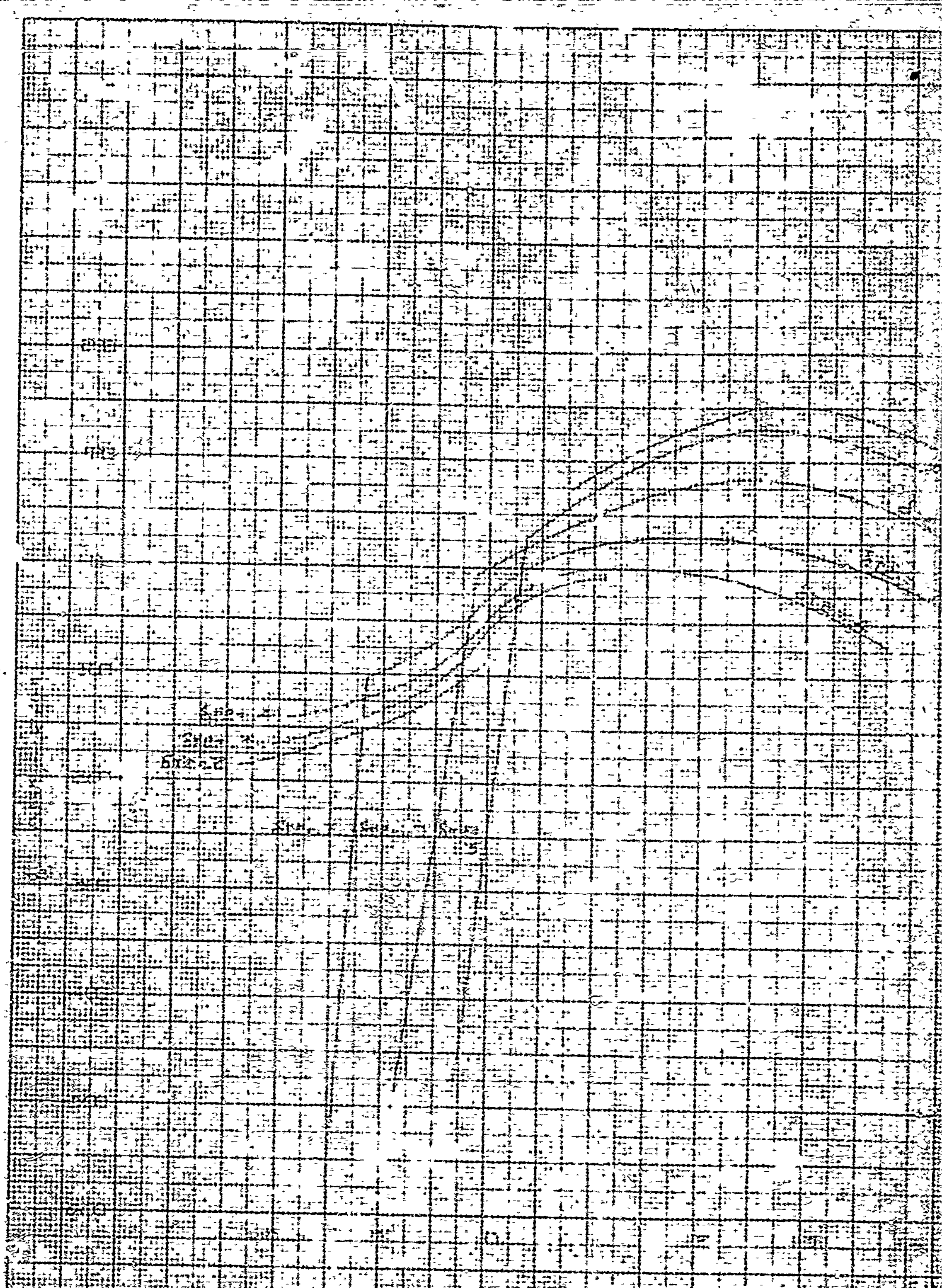

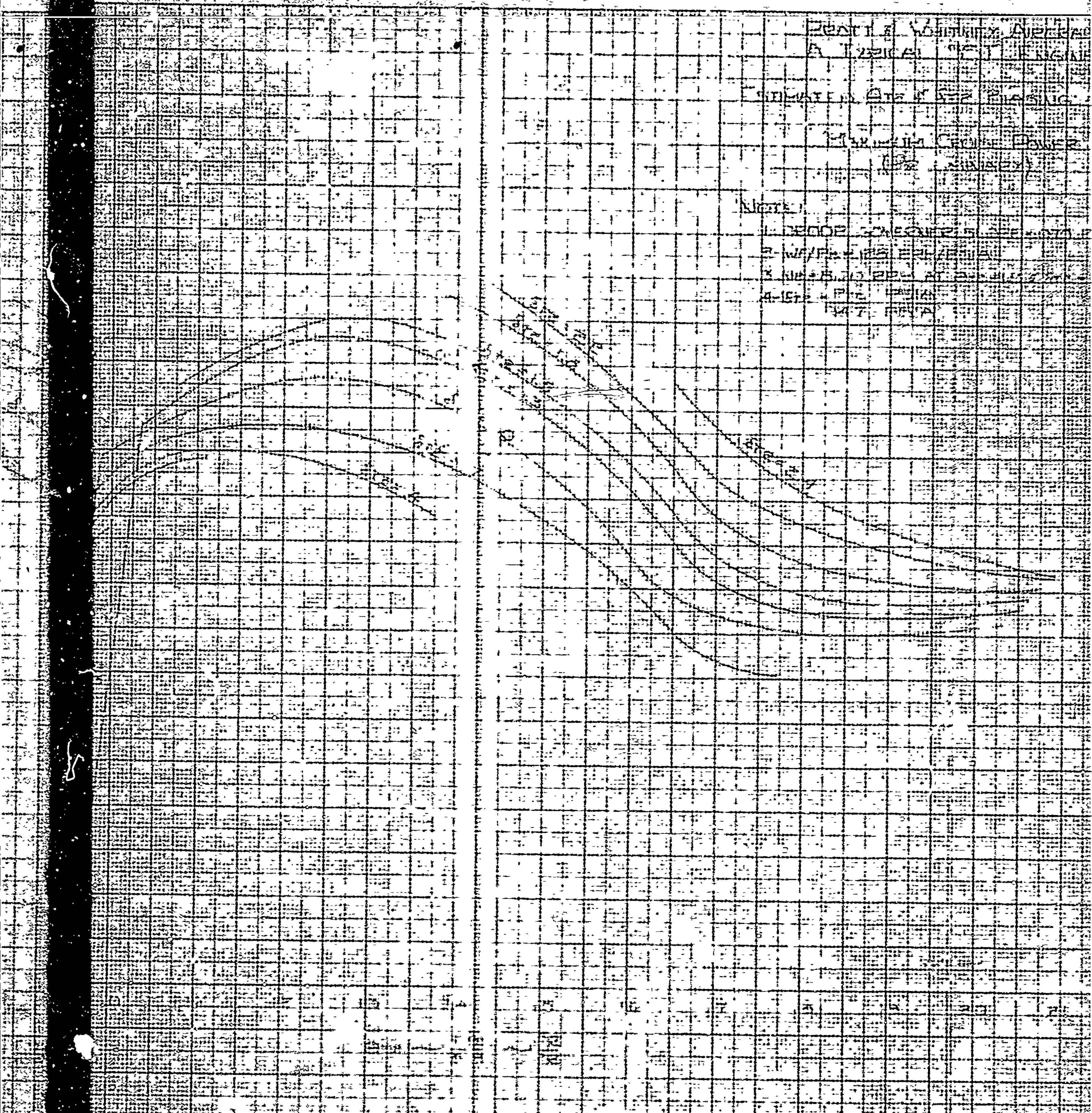

1 2

PPS 819

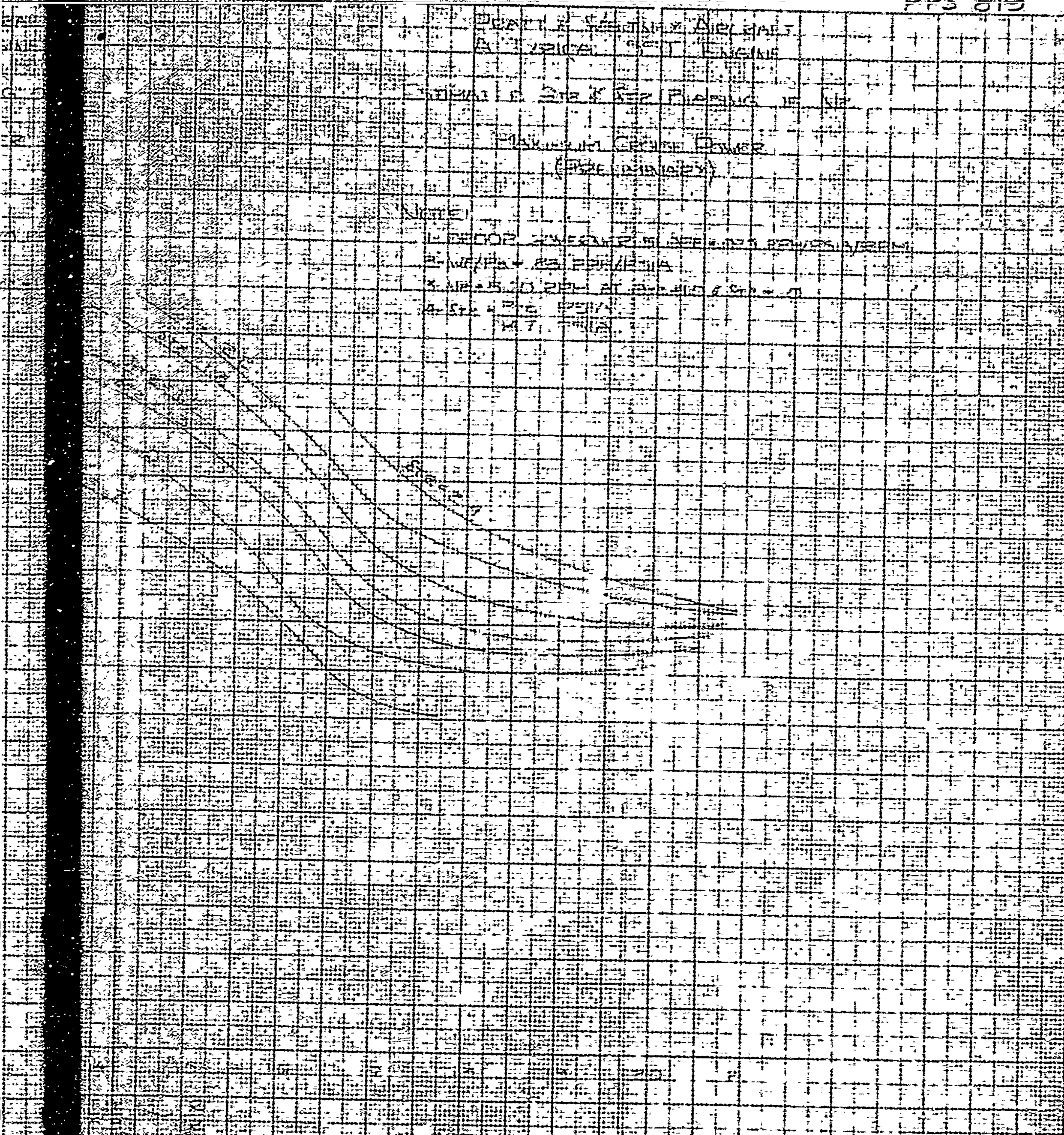

2

FIGURE 5

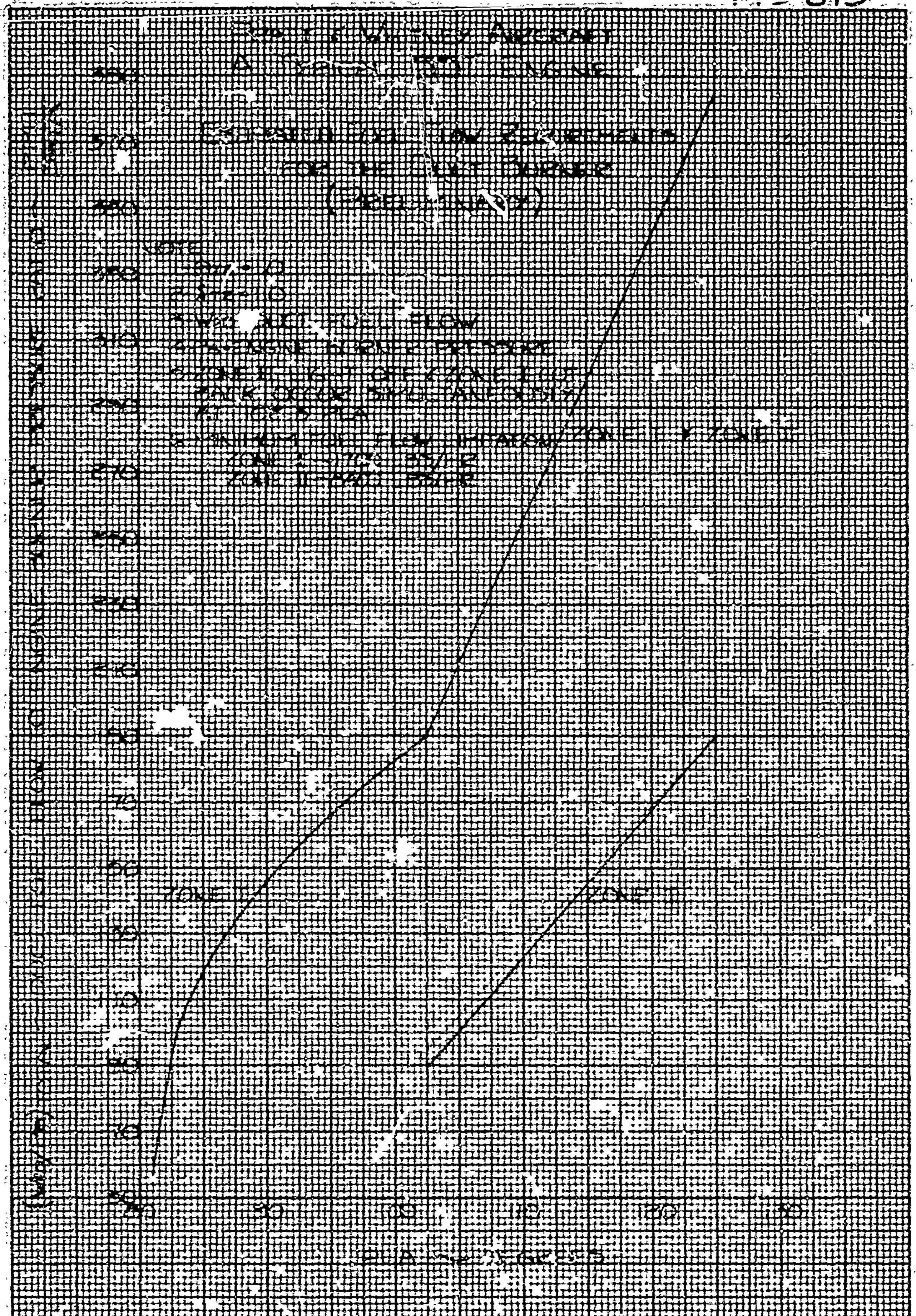

FIGURE 6

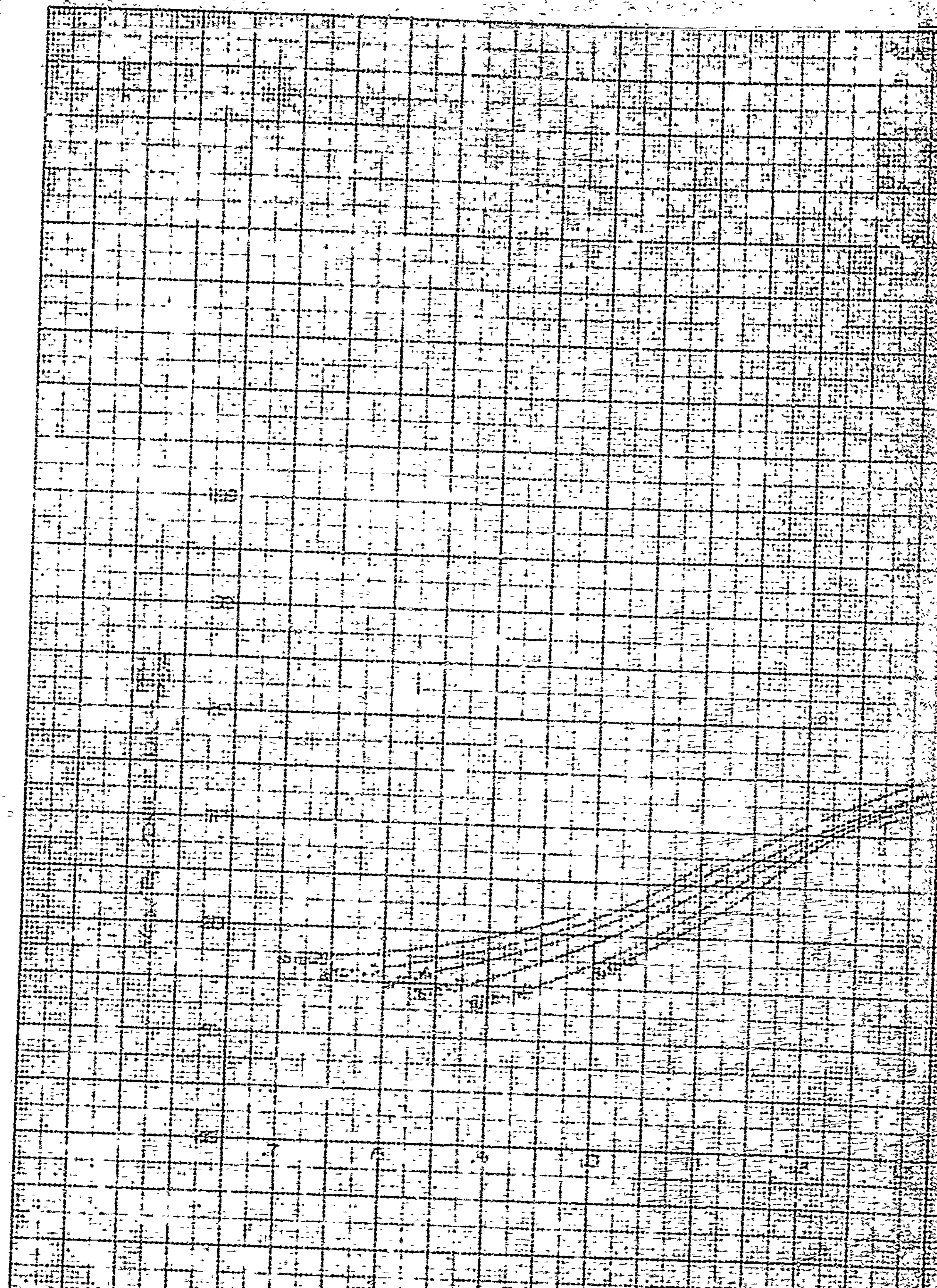

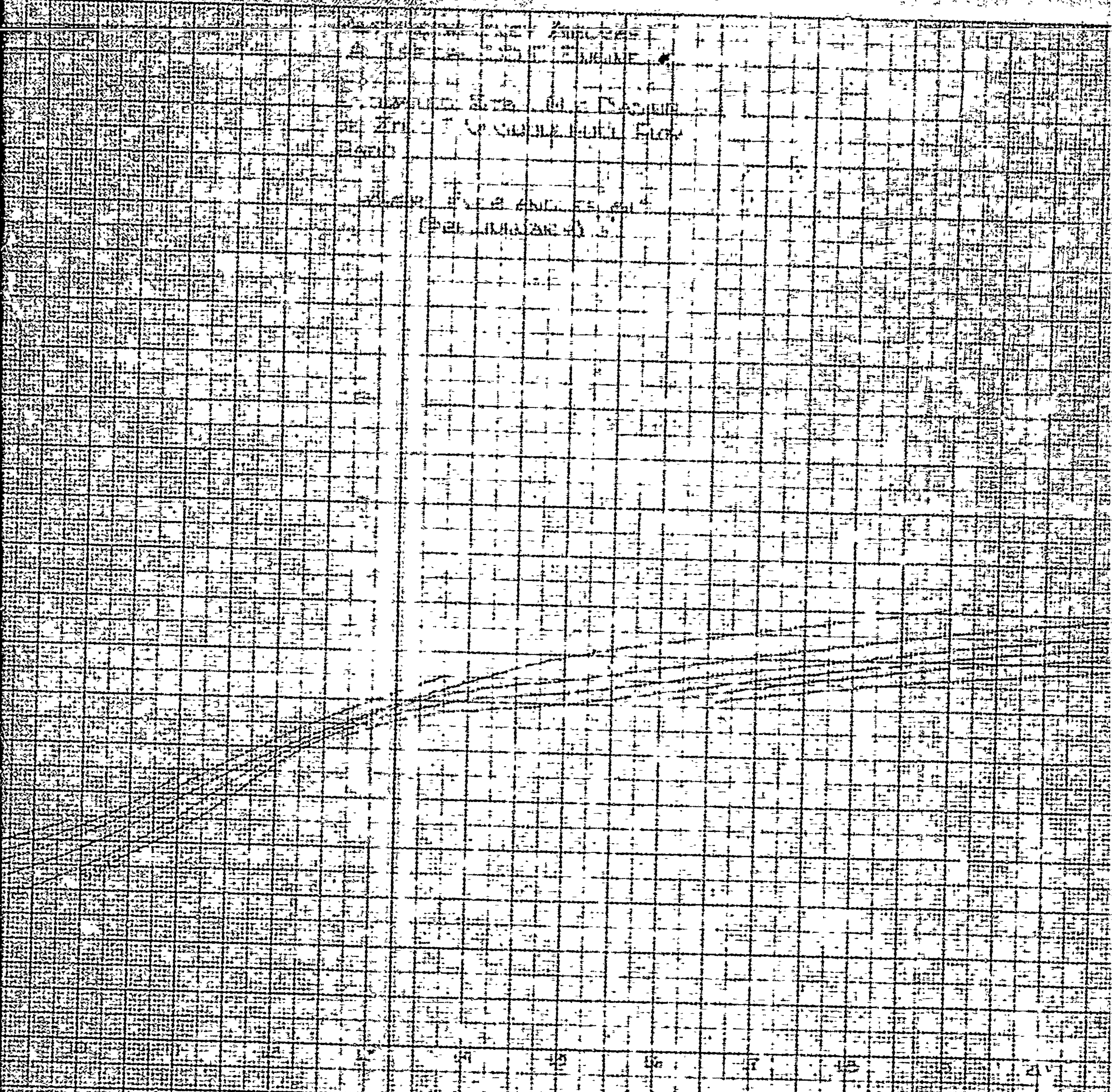

PPS 819

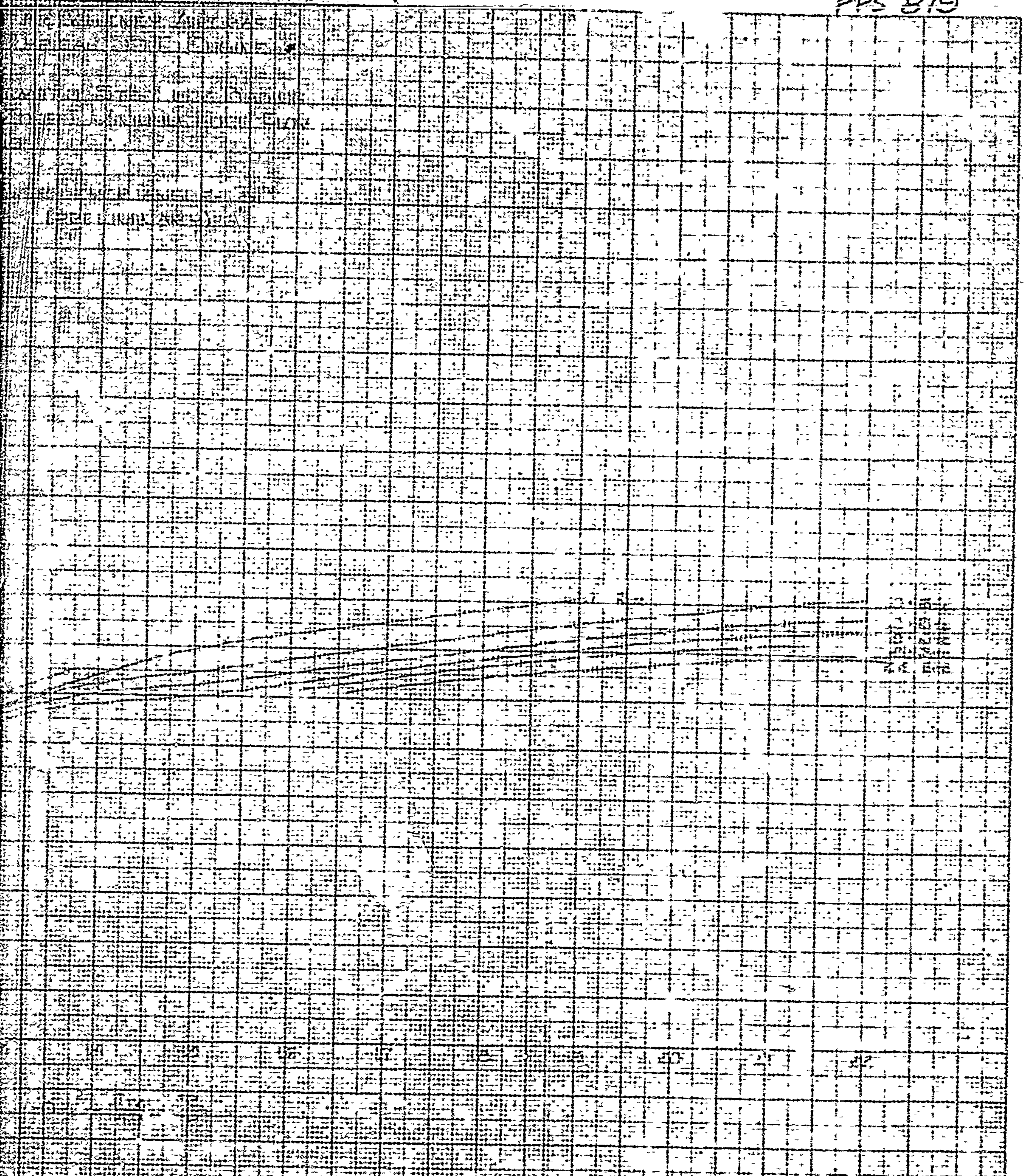

FIGURE 7

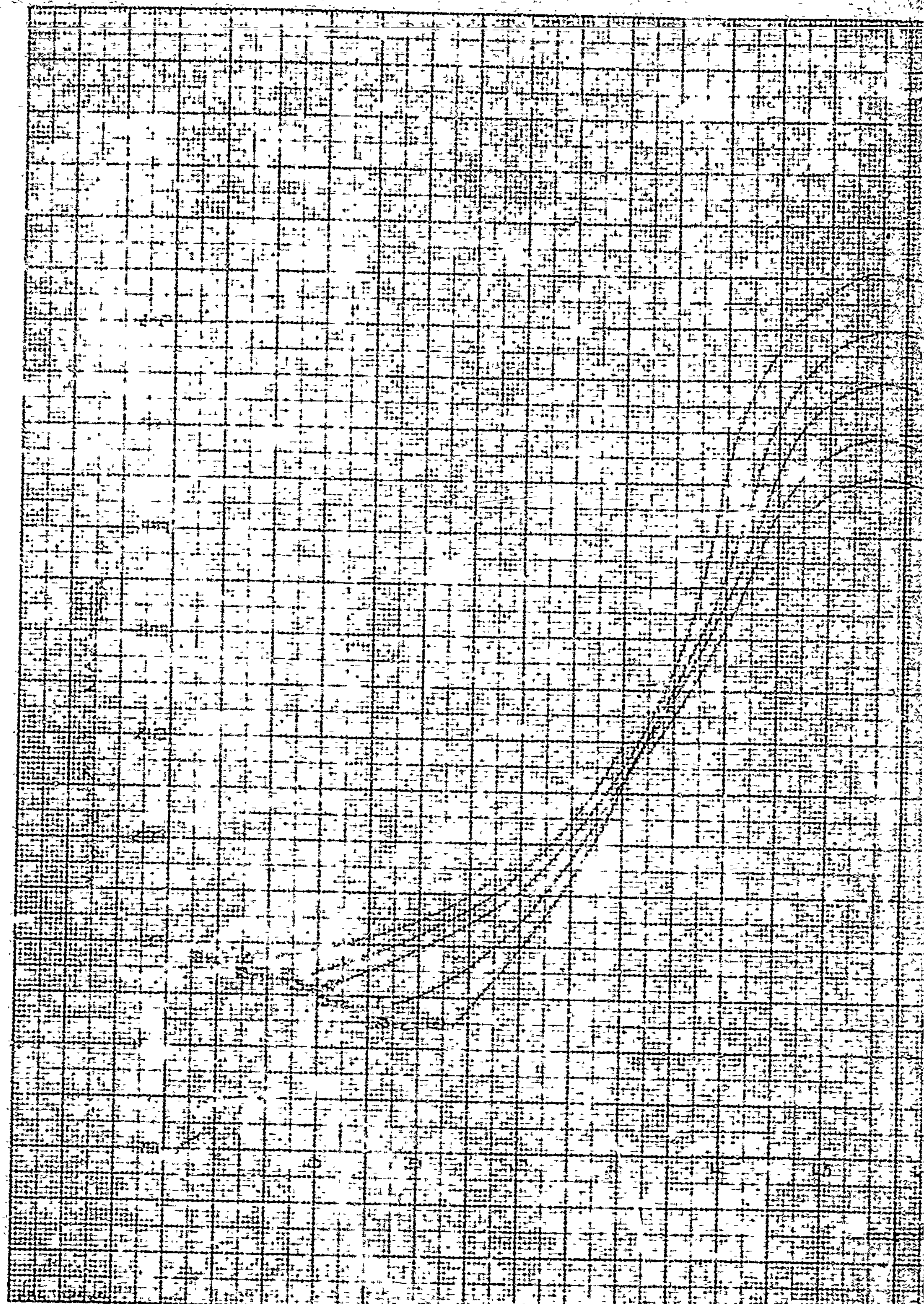

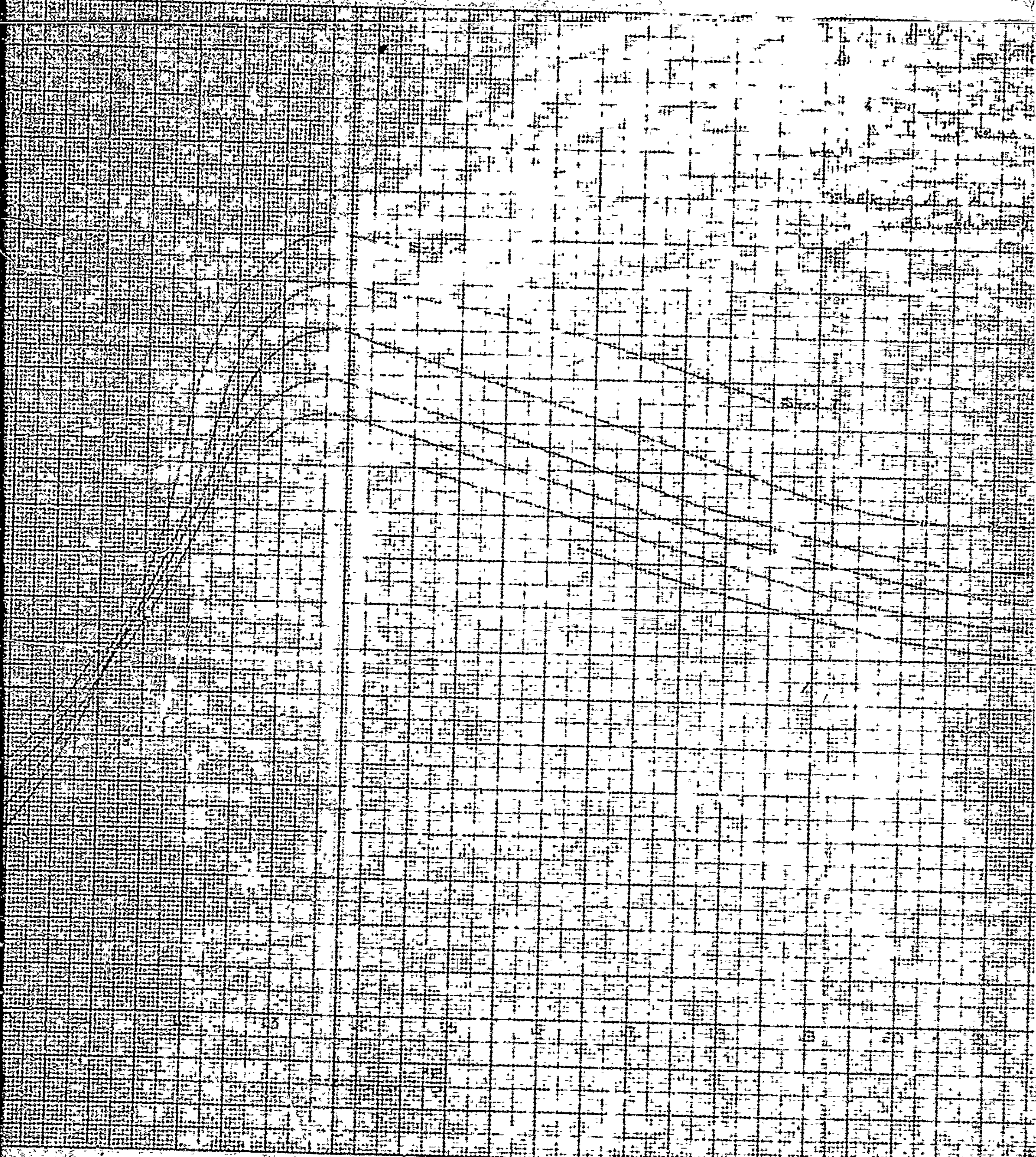

1 2

PPS 819

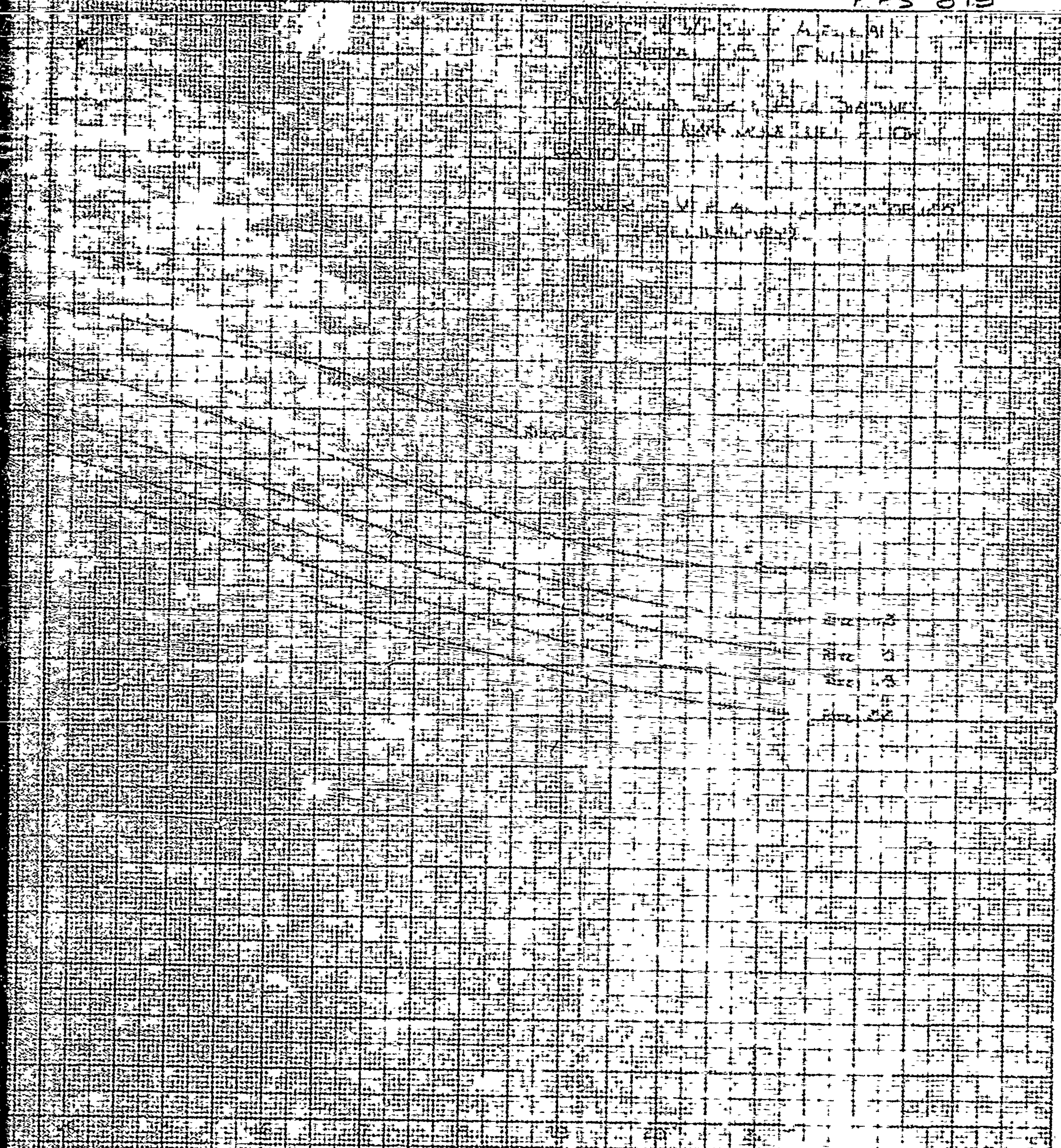

2 FIGURE 8 3

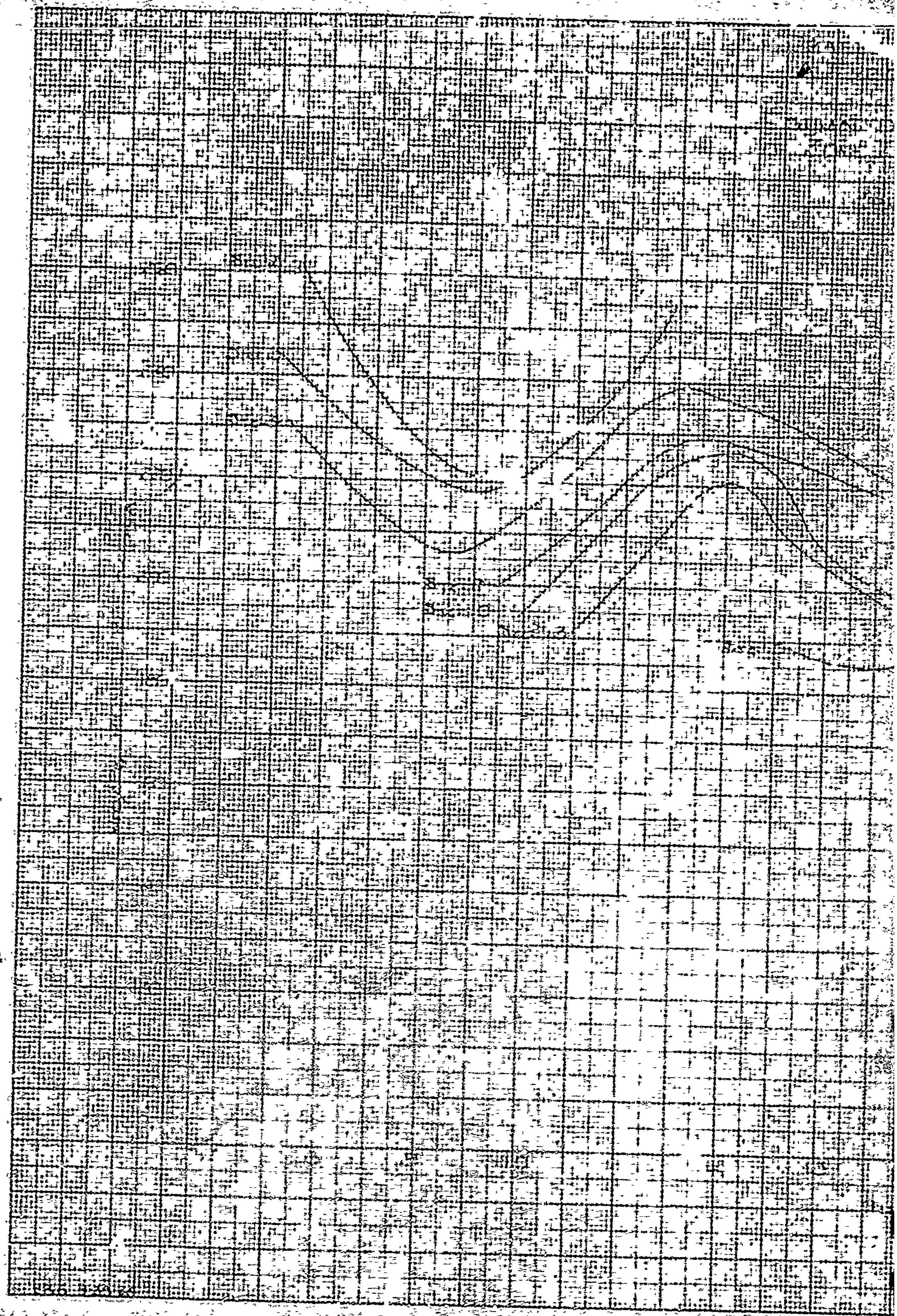

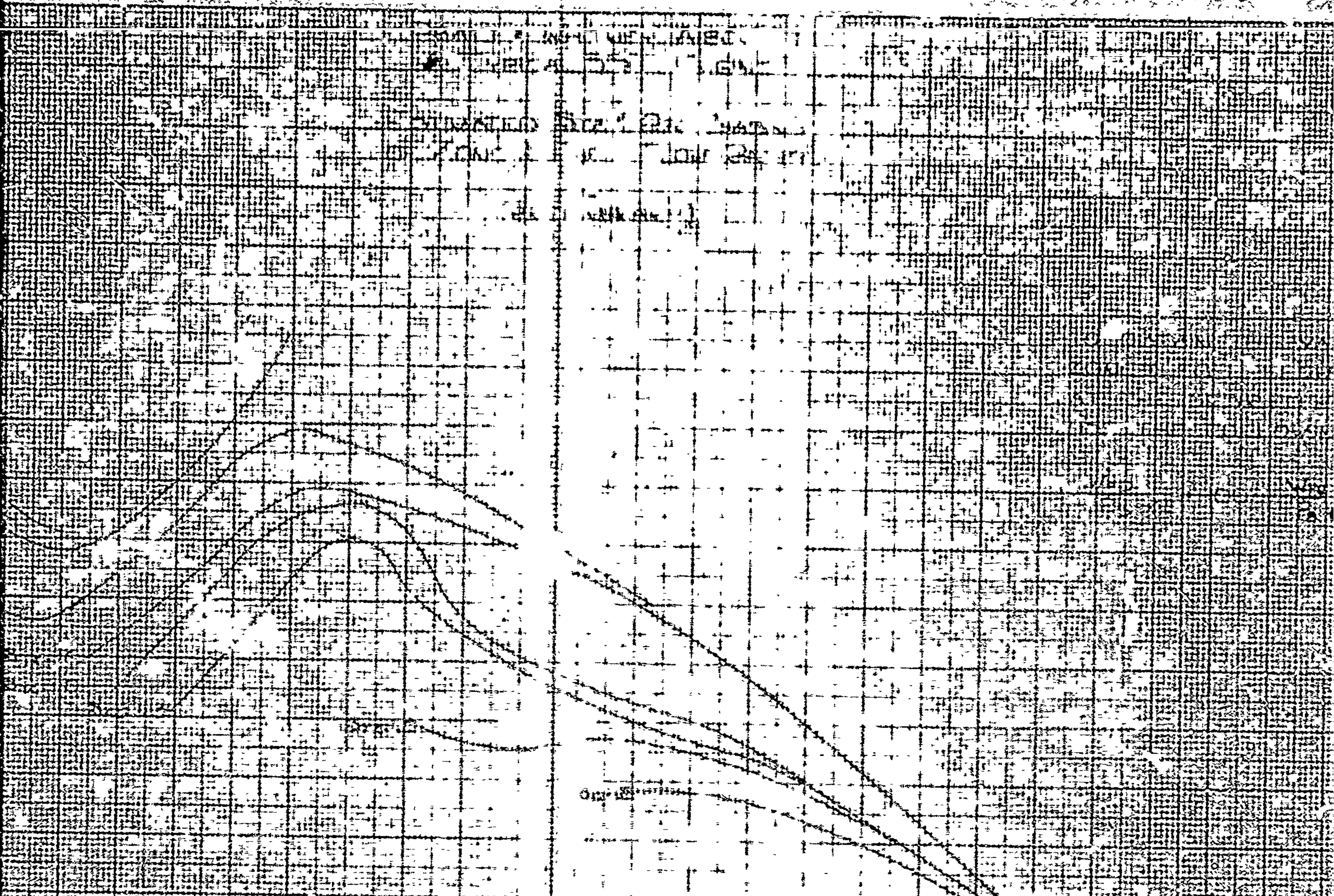

1 2

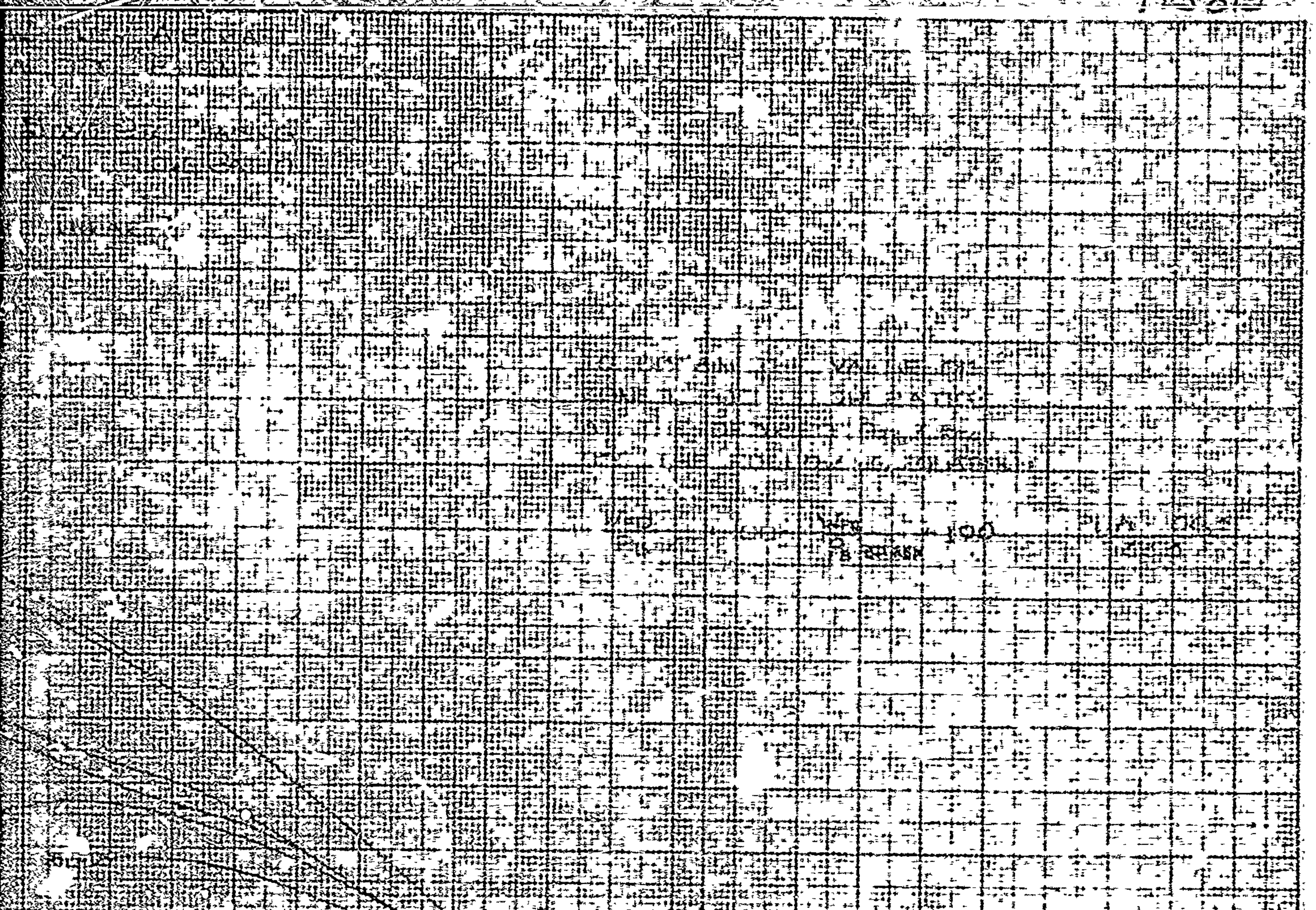

FIGURE 9

2 3

PPS 819

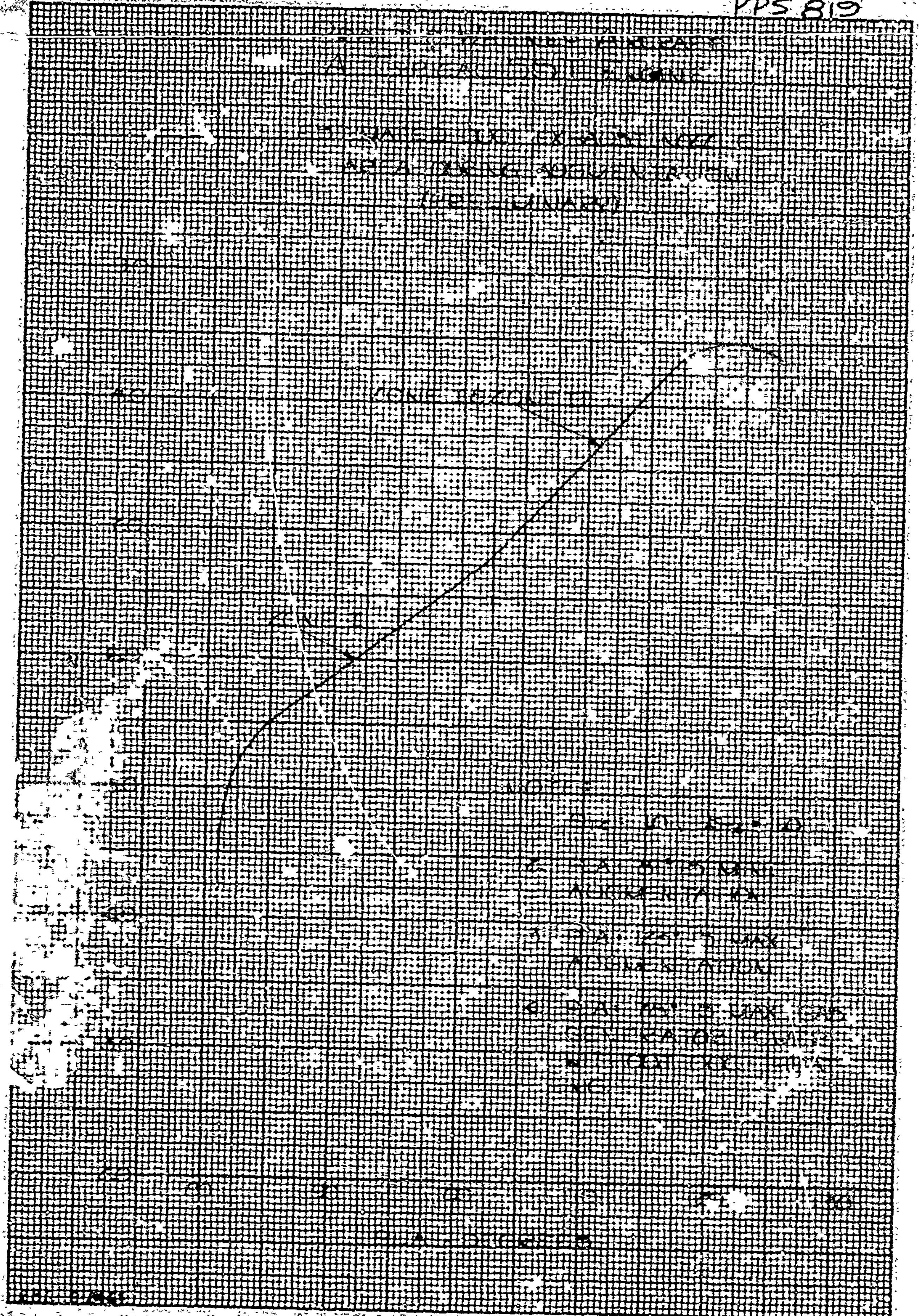

FIGURE 10

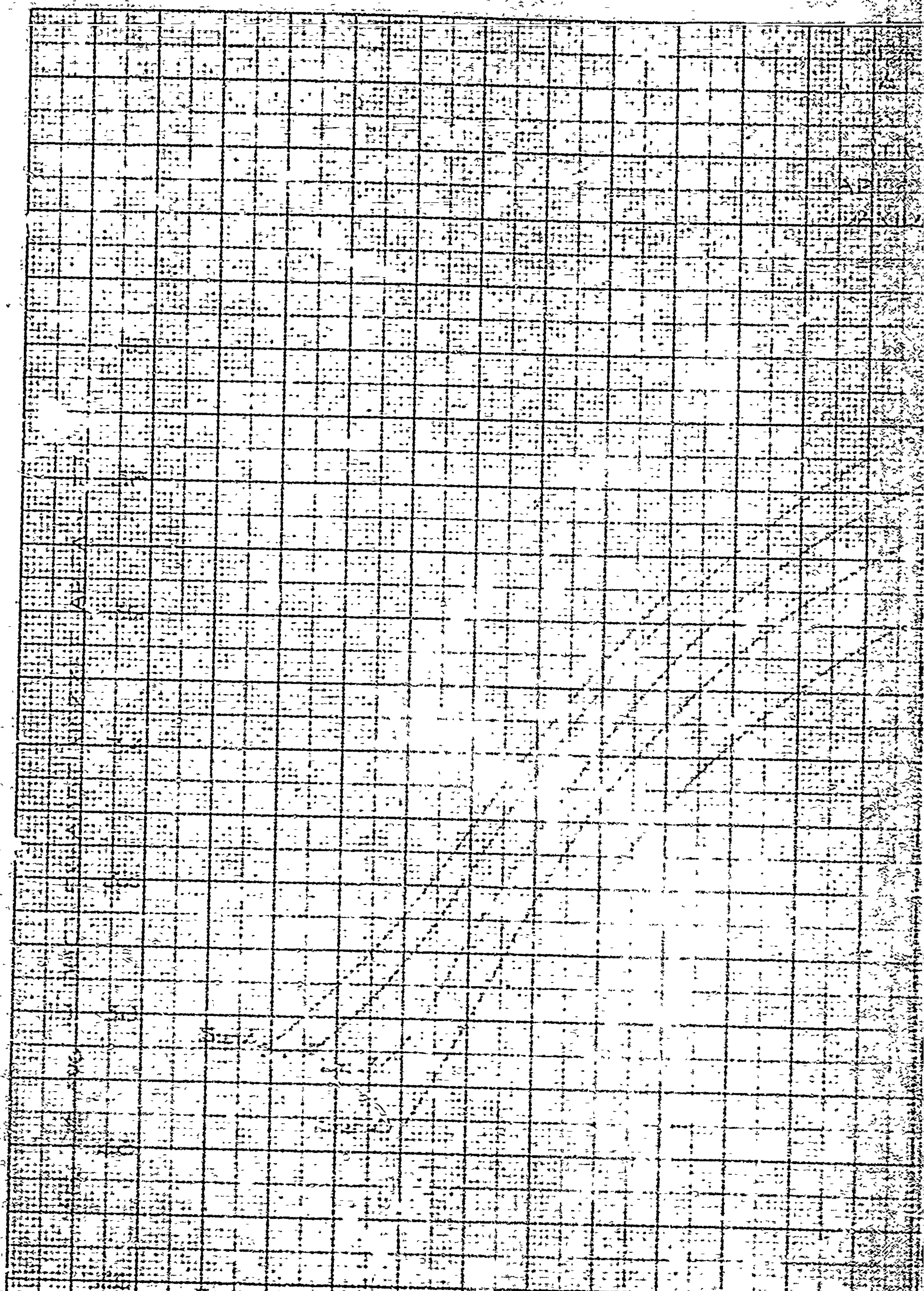

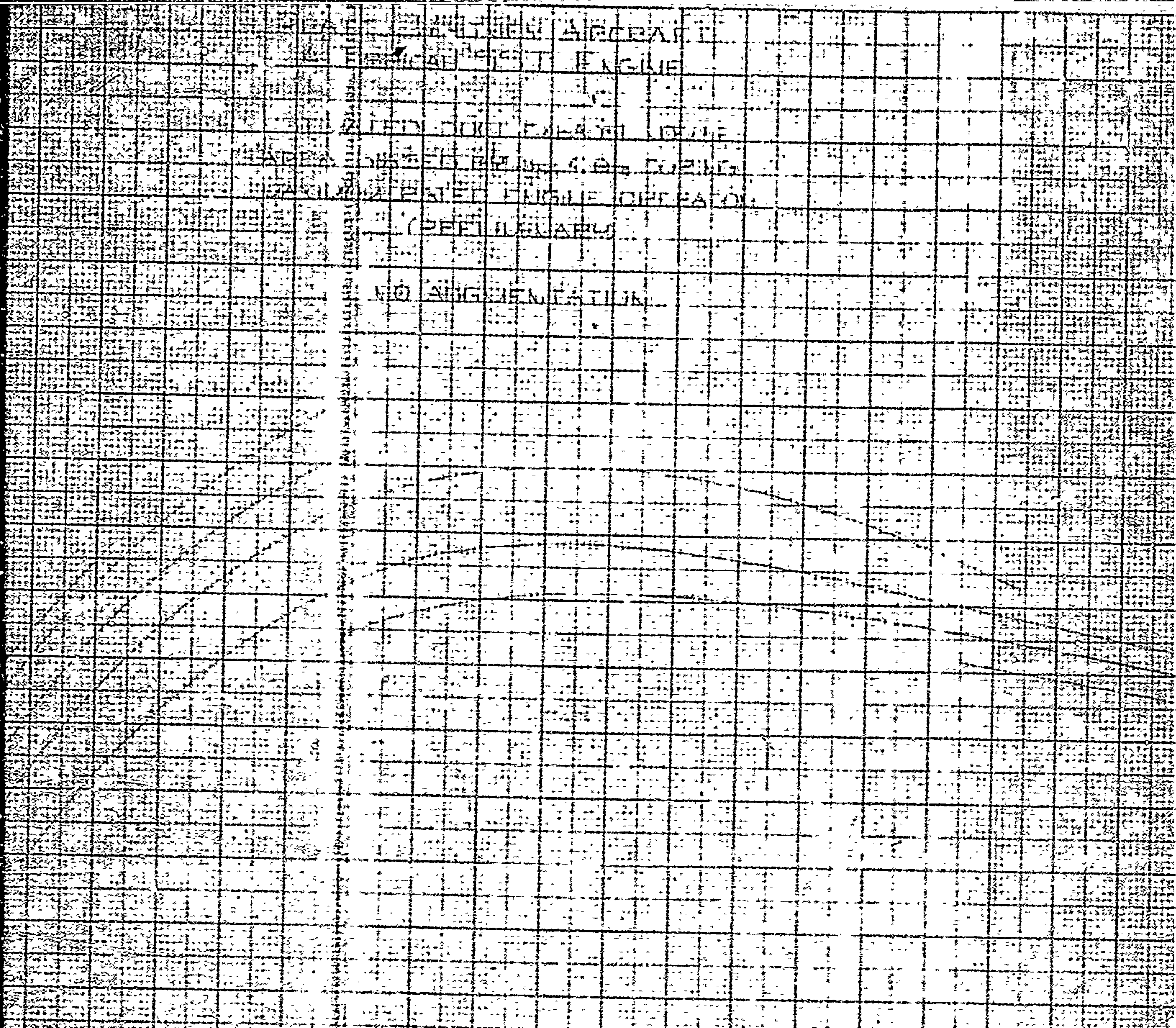
PRATT & WHITNEY AIRCRAFT
TYPICAL SST ENGINE
(PRELIMINARY)
NO AUGMENTATION

PPS 819

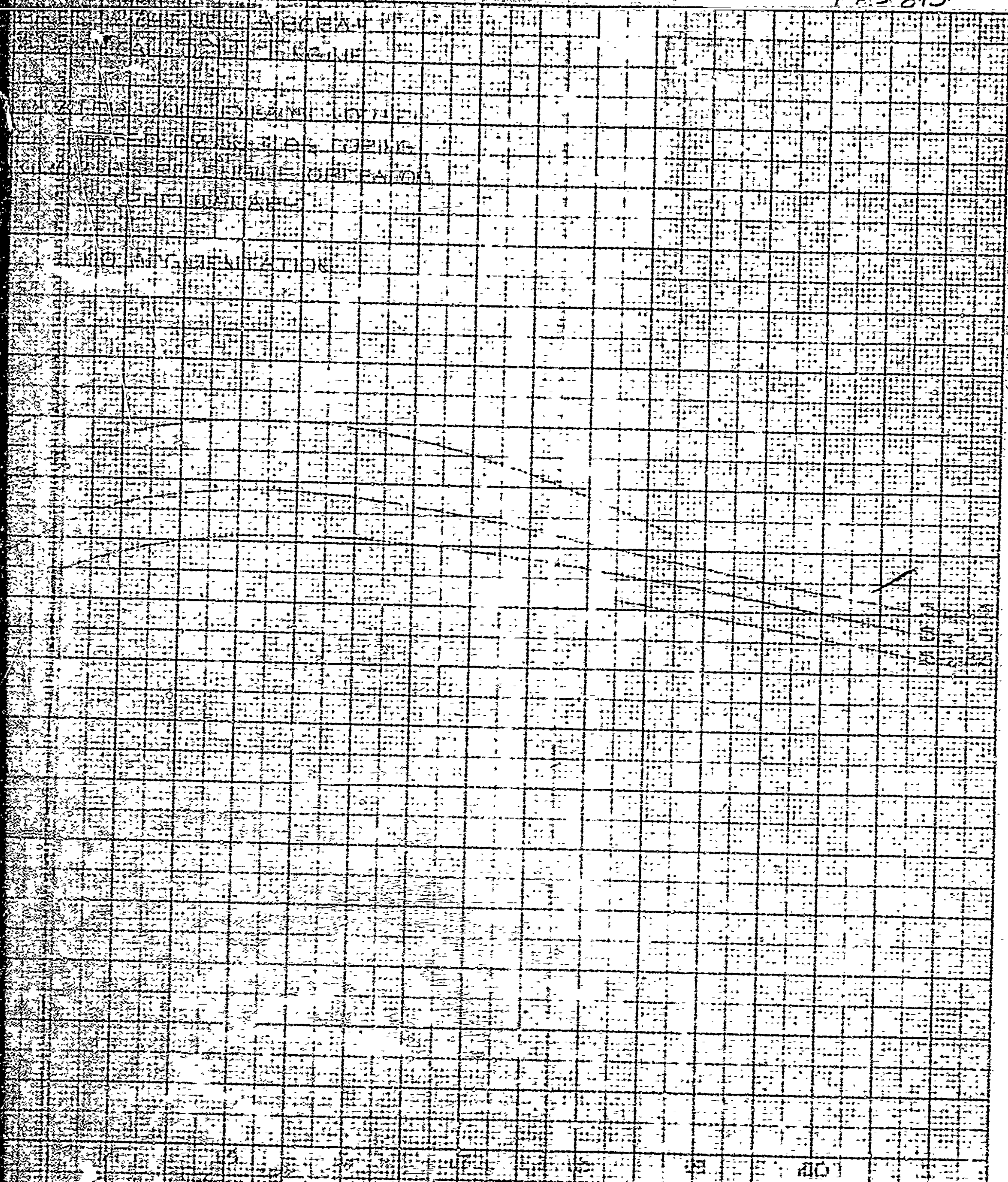

2 FIGURE 3

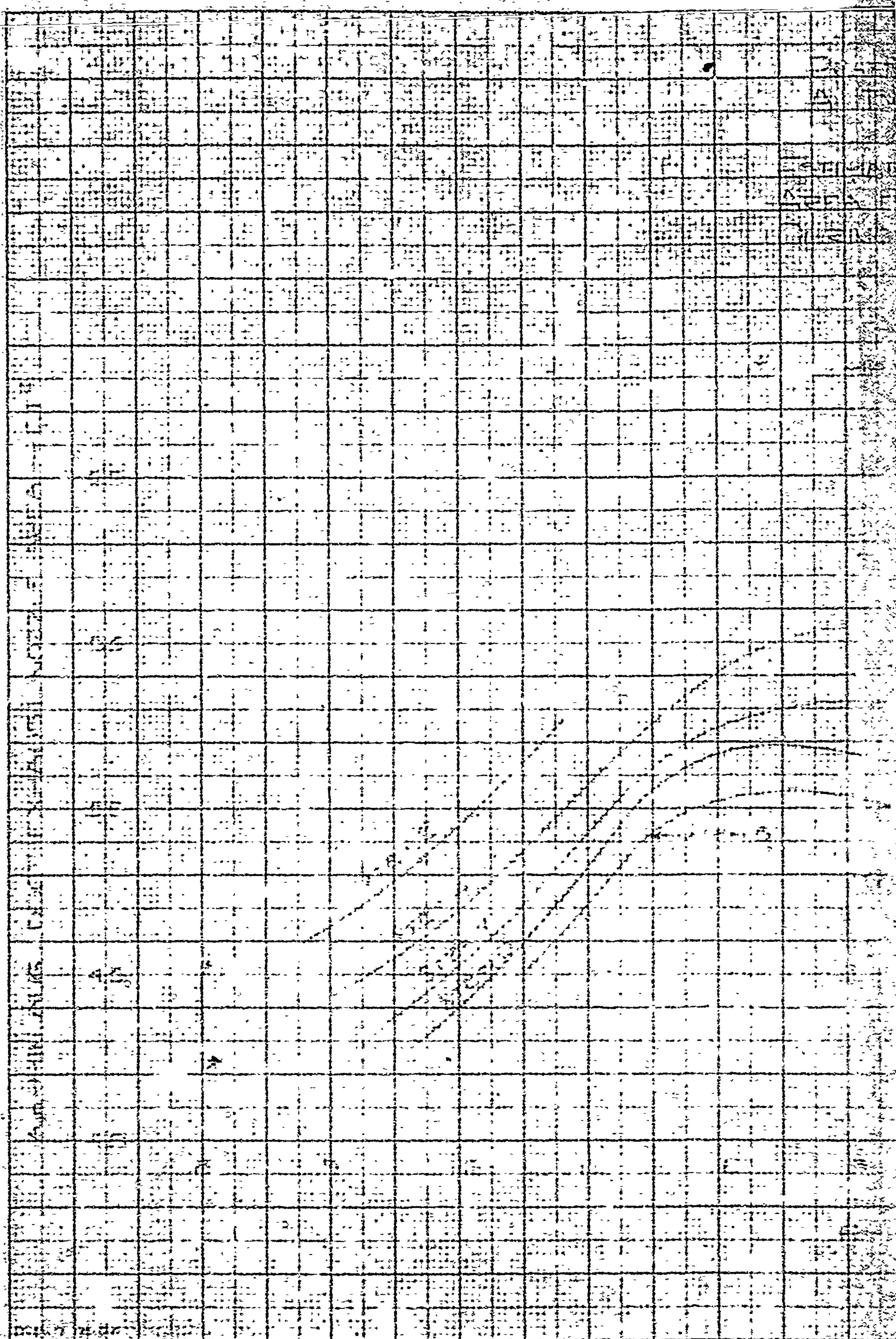

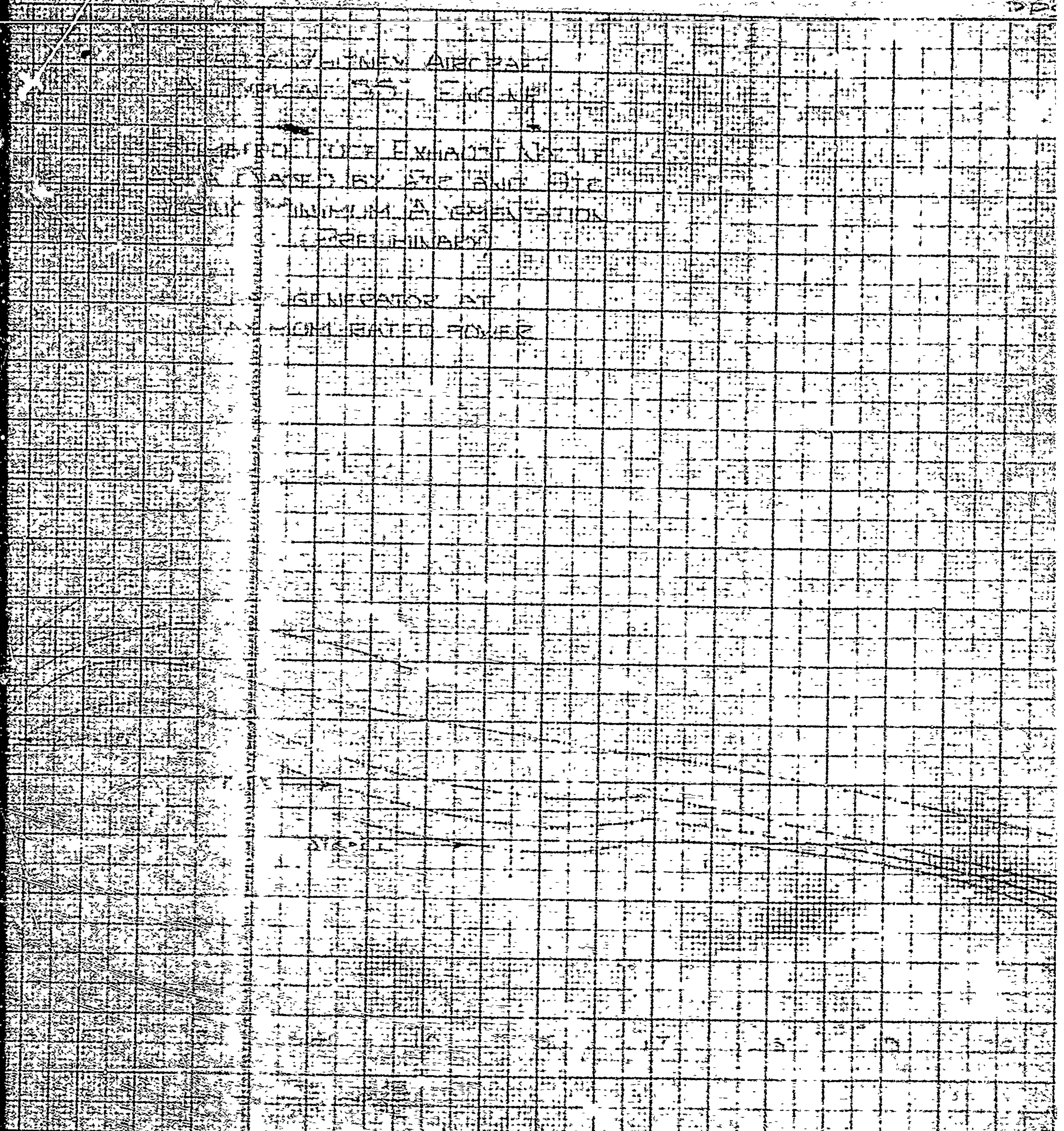
WHITNEY AIRCRAFT
ENGINE
EXHAUST NOZZLE
PRELIMINARY
GENERATOR AT
RATED POWER

2

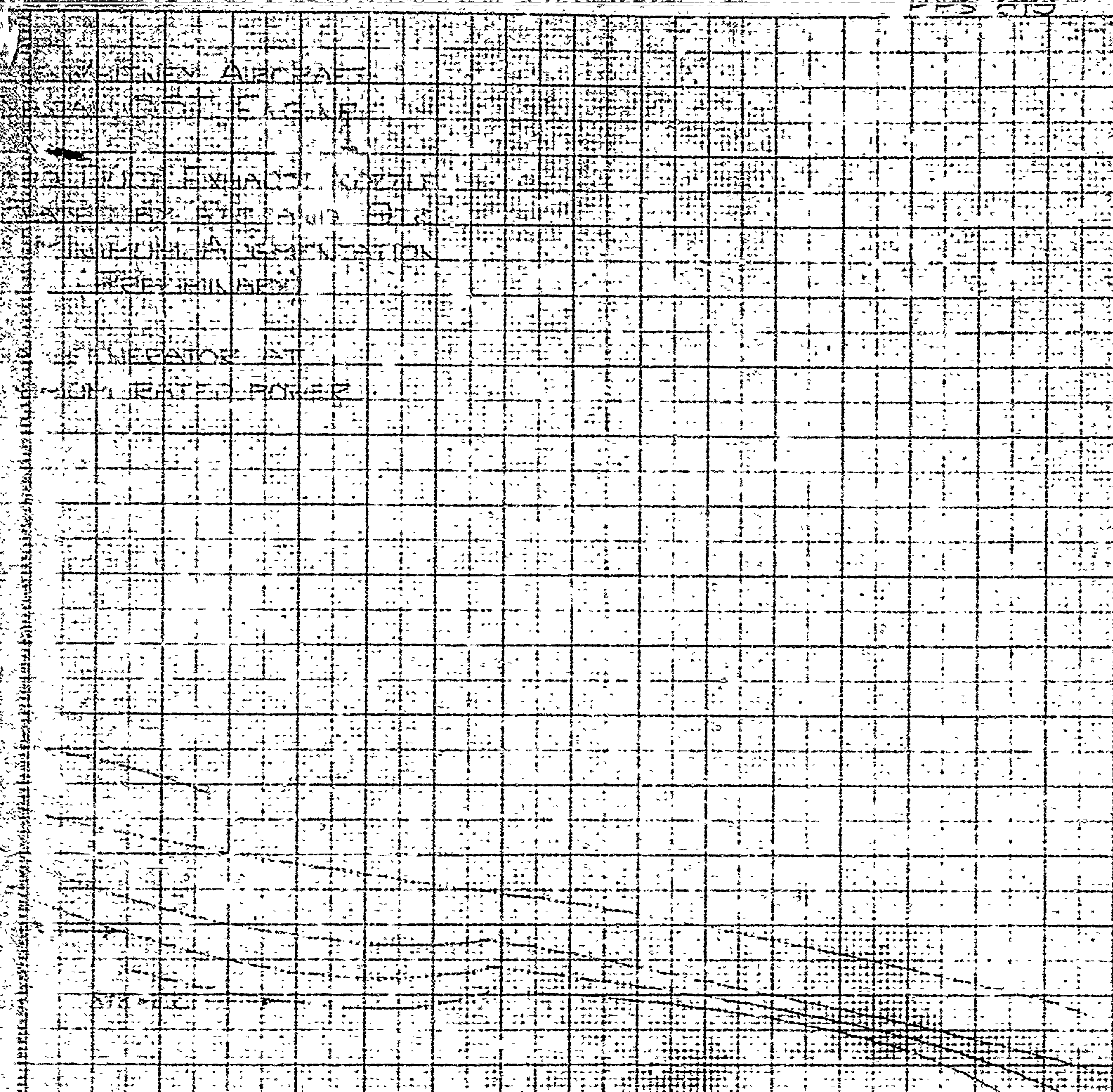

2 FIGURE 2 3

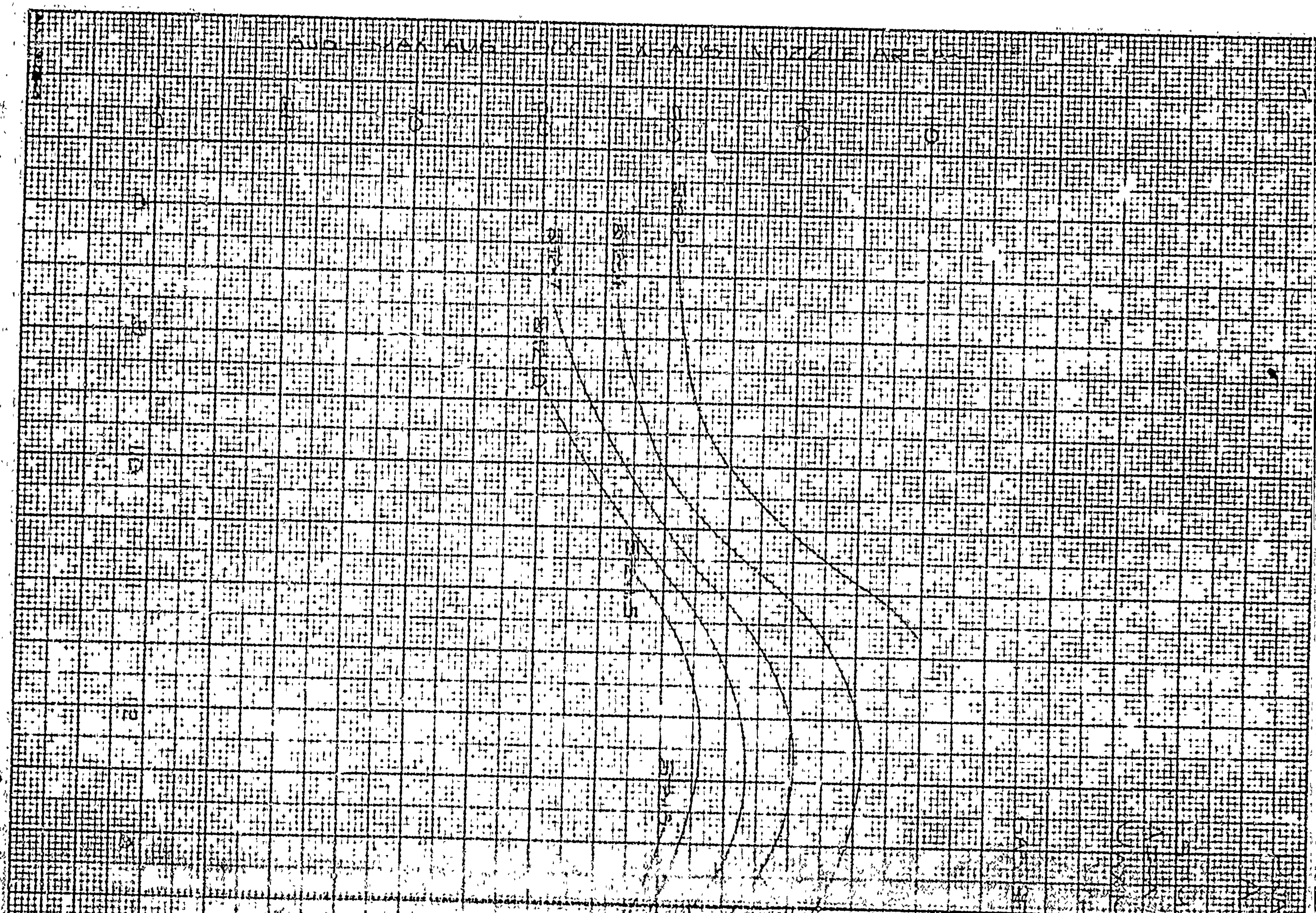

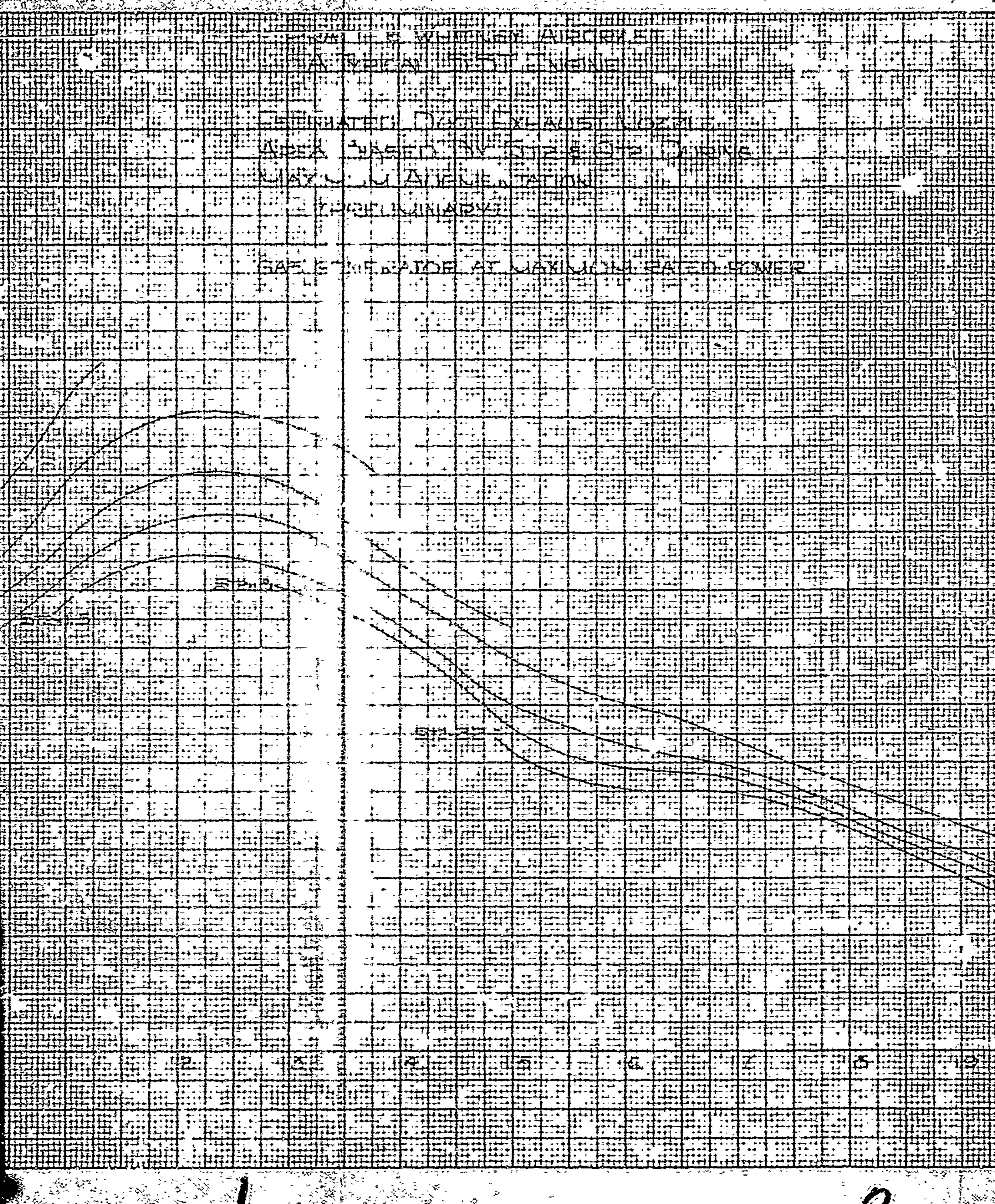
WHITNEY AIRCRAFT
A TYPICAL ENGINE
ESTIMATED EXHAUST
AREA DURING
PRELIMINARY
AT MAXIMUM RATED POWER

1

2

PPS 819

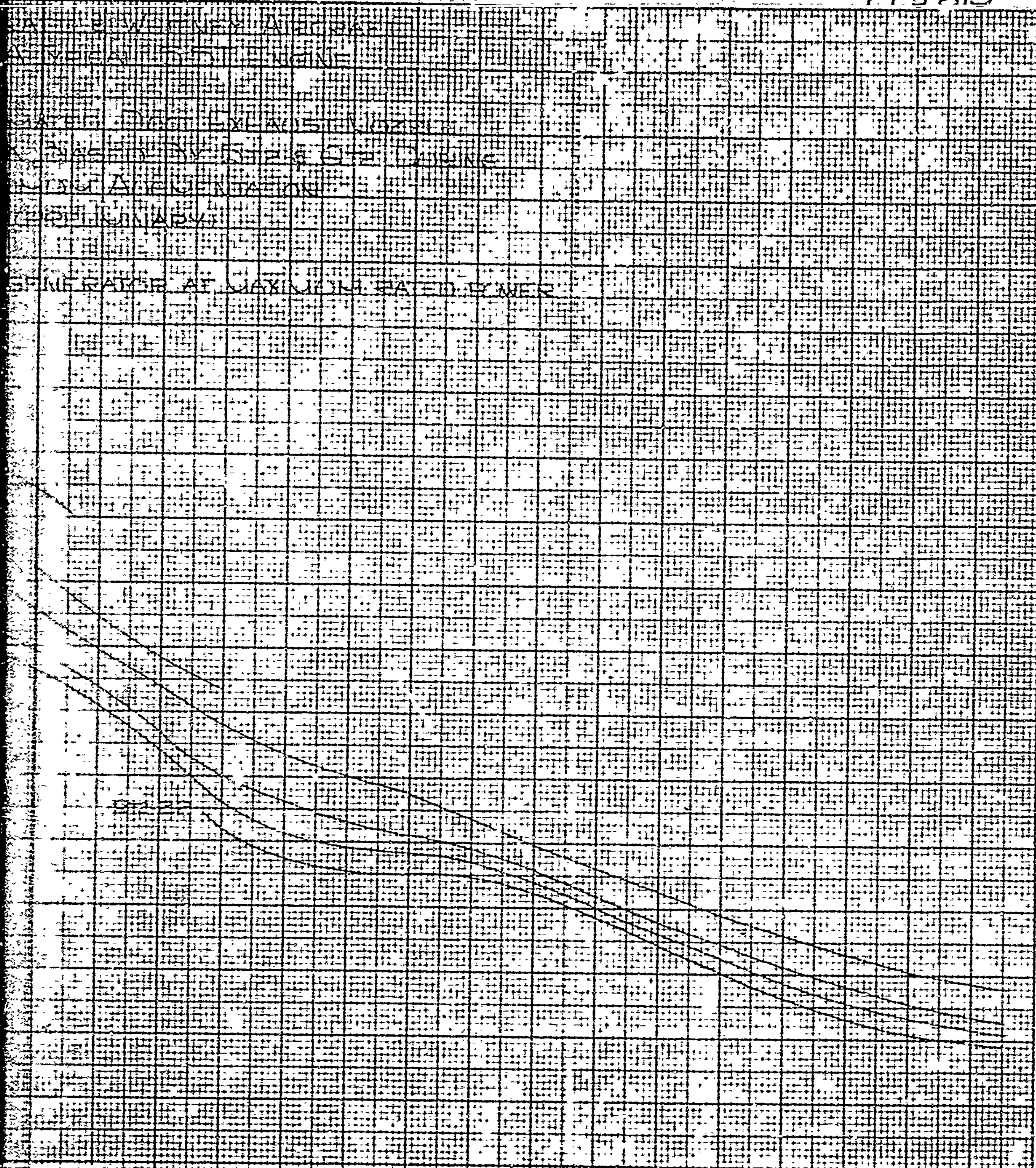

2

FIGURE 13

3

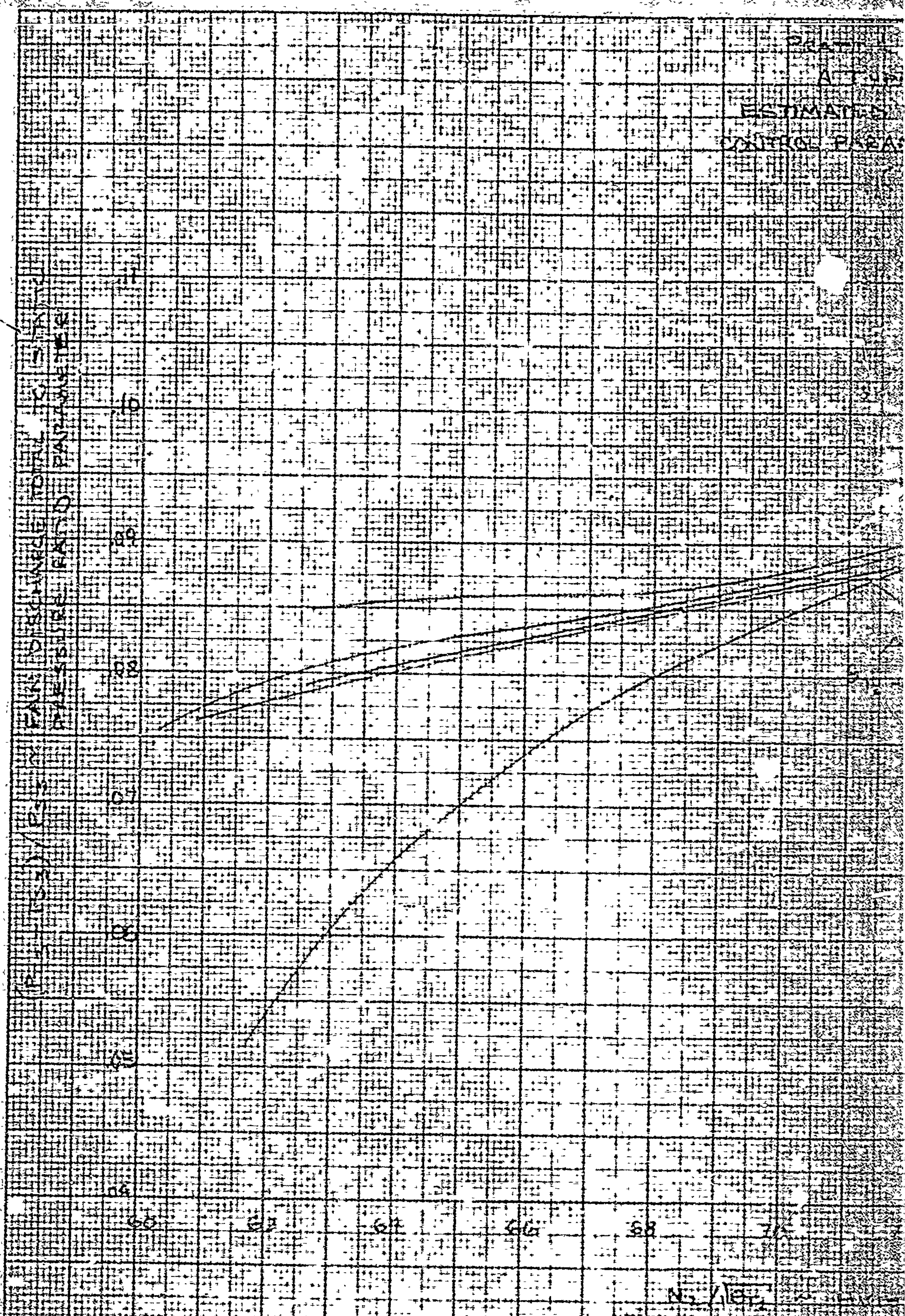

ESTIMATED
CONTROL PARA
(P...)/P... FAN DISCHARGE TOTAL ... STATIC
PRESSURE RATIO PARAMETER
.11
.10
.09
.08
.07
.06
.05
.04
60
62
64
66
68
70
$N_1/\sqrt{\theta_{T2}}$

PRATT & WHITNEY AIRCRAFT
A TYPICAL SST ENGINE
ESTIMATED BIAS OF THE DUCT AREA
CONTROL PARAMETER BELOW CRUISING MACH NUMBERS
(PRELIMINARY)

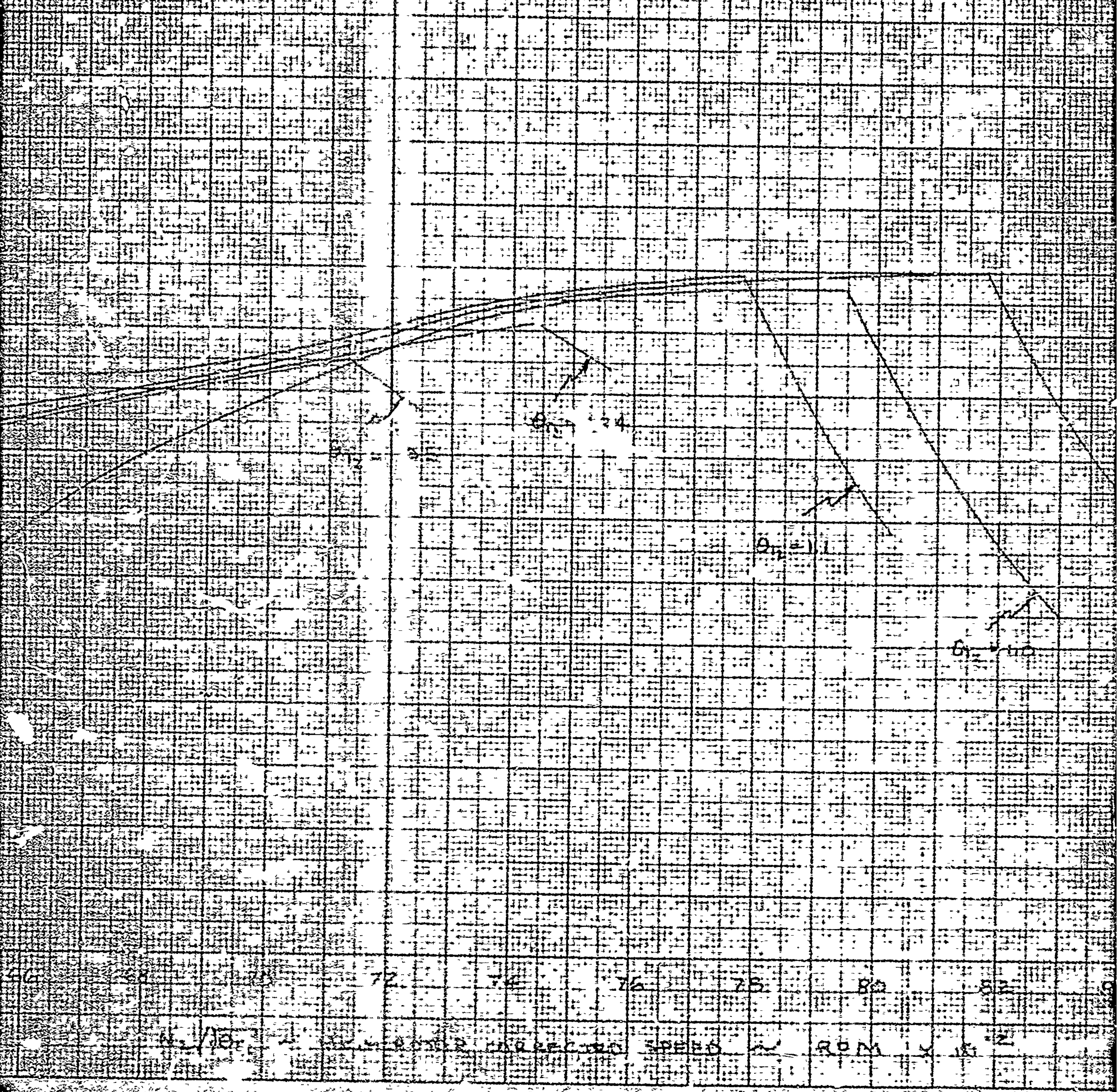

1

2

PPS 819

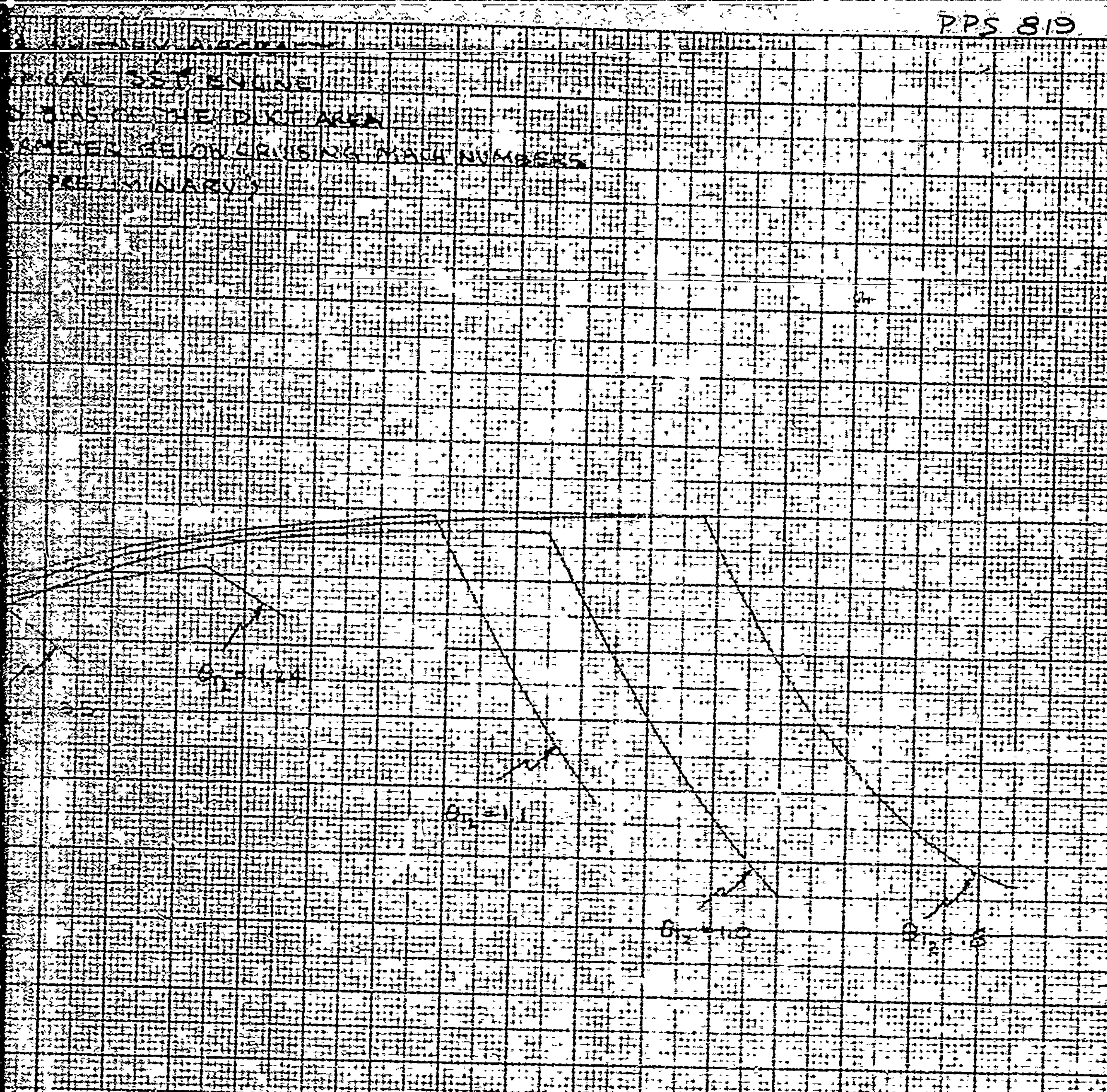

FIGURE 14

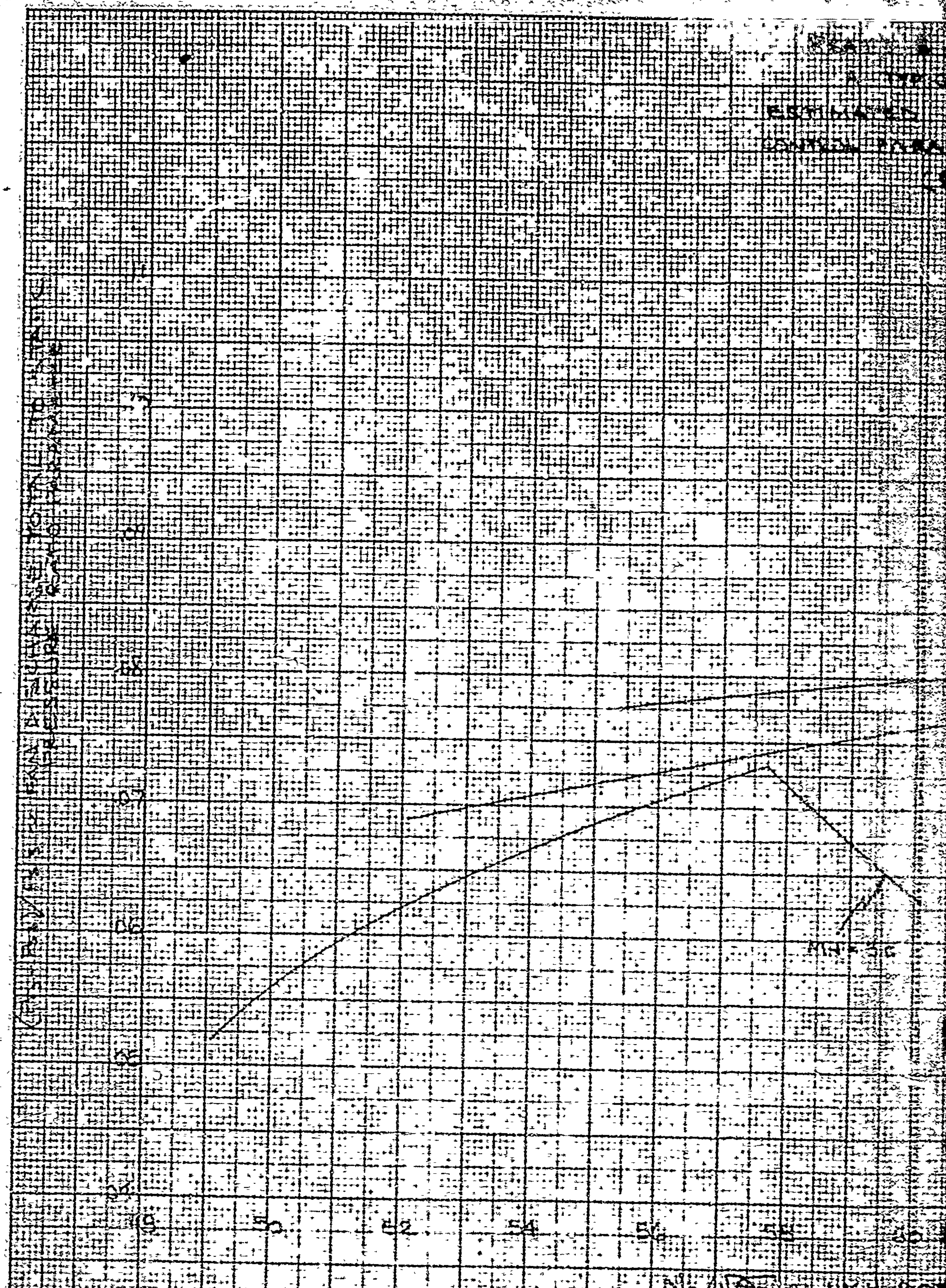

PRATT & WHITNEY AIRCRAFT
A TYPICAL SST ENGINE
ESTIMATED BIAS OF THE DUCT AREA
CONTROL PARAMETER DURING CRUISING MACH NUMBERS
(PRELIMINARY)

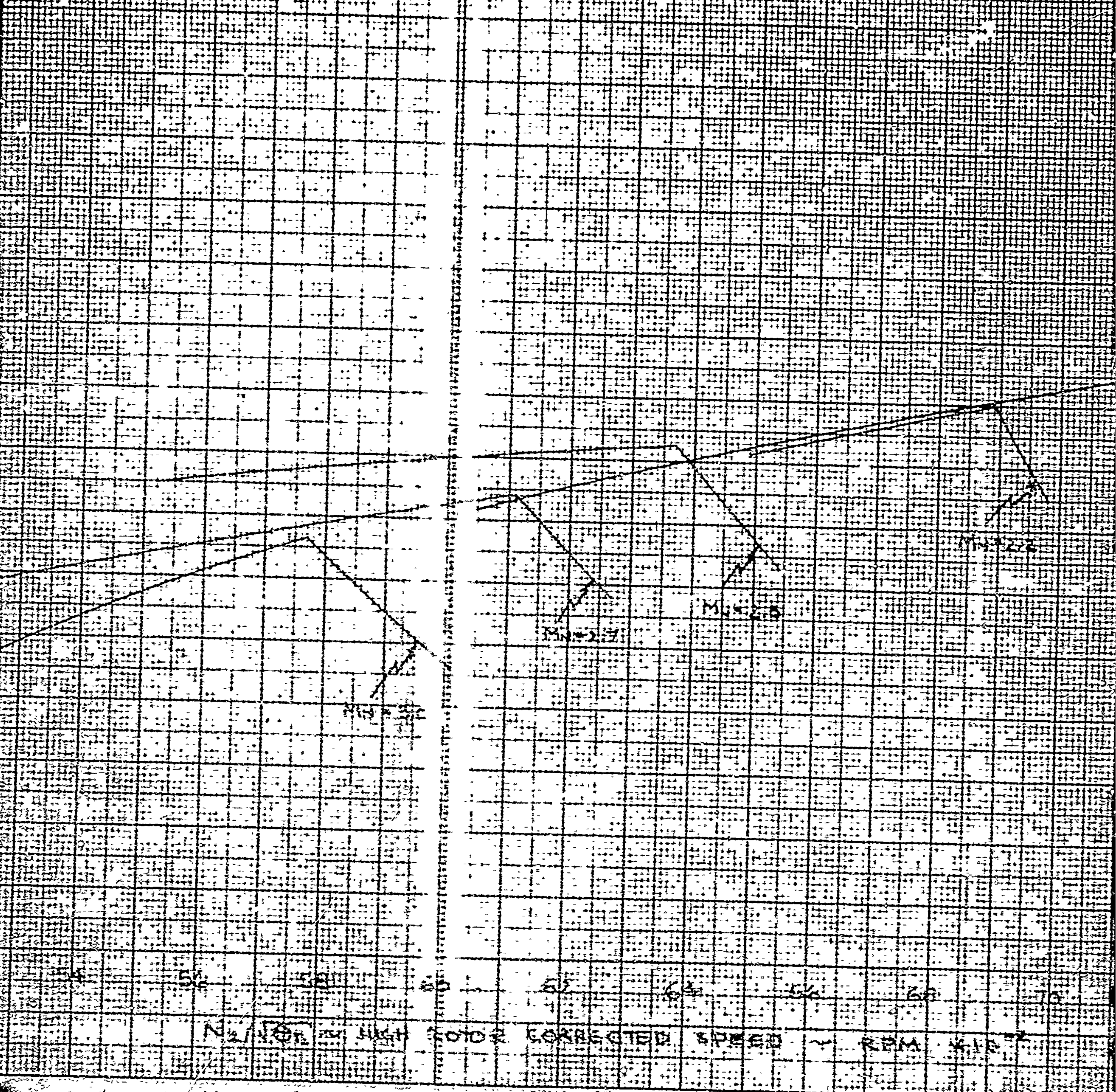

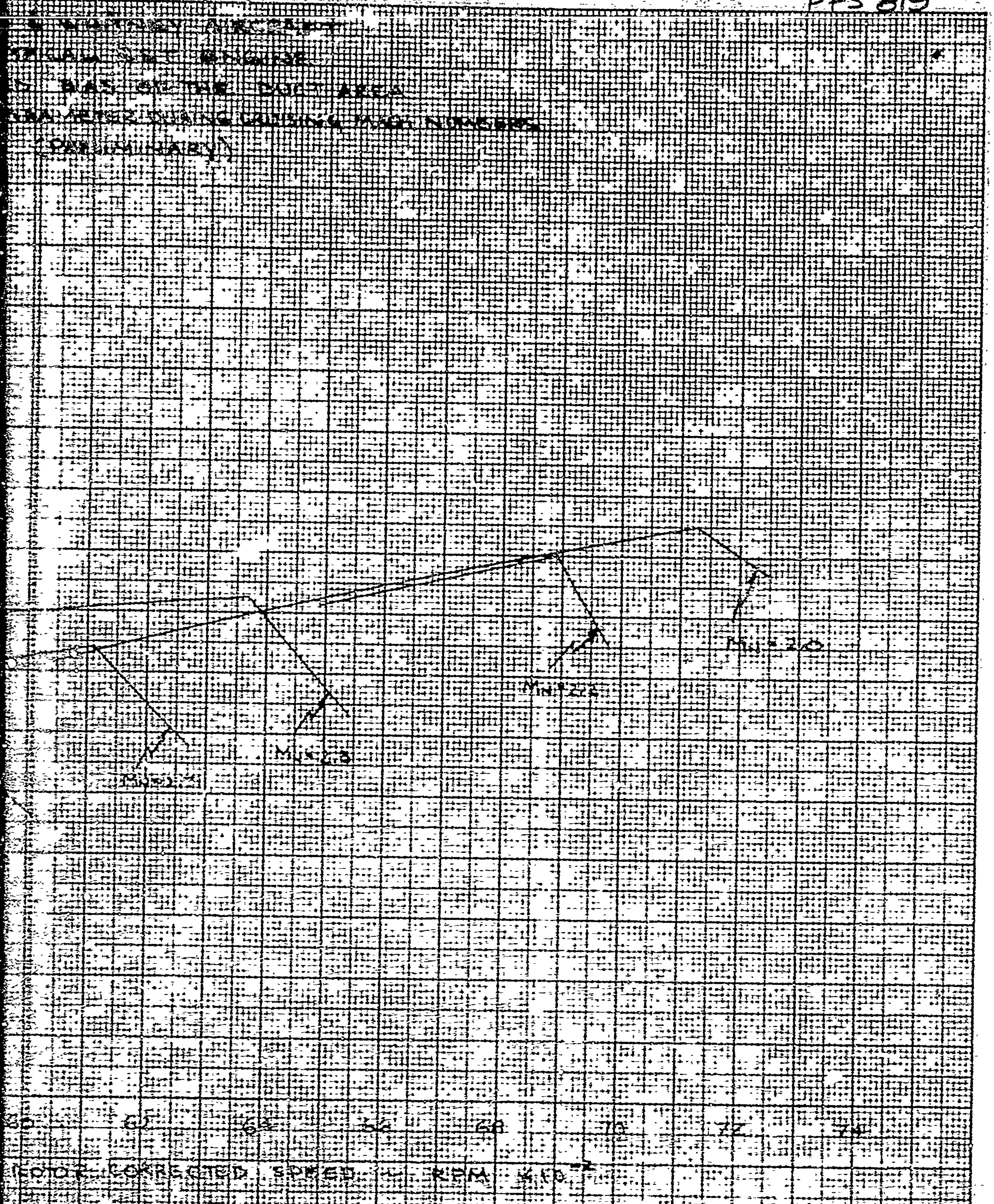
(PRELIMINARY)
MN = 2.8
MN = 2.2
MN = 2.0
60
62
64
66
68
70
72
74
ROTOR CORRECTED SPEED — RPM × 10⁻³

FIGURE 15

2 3

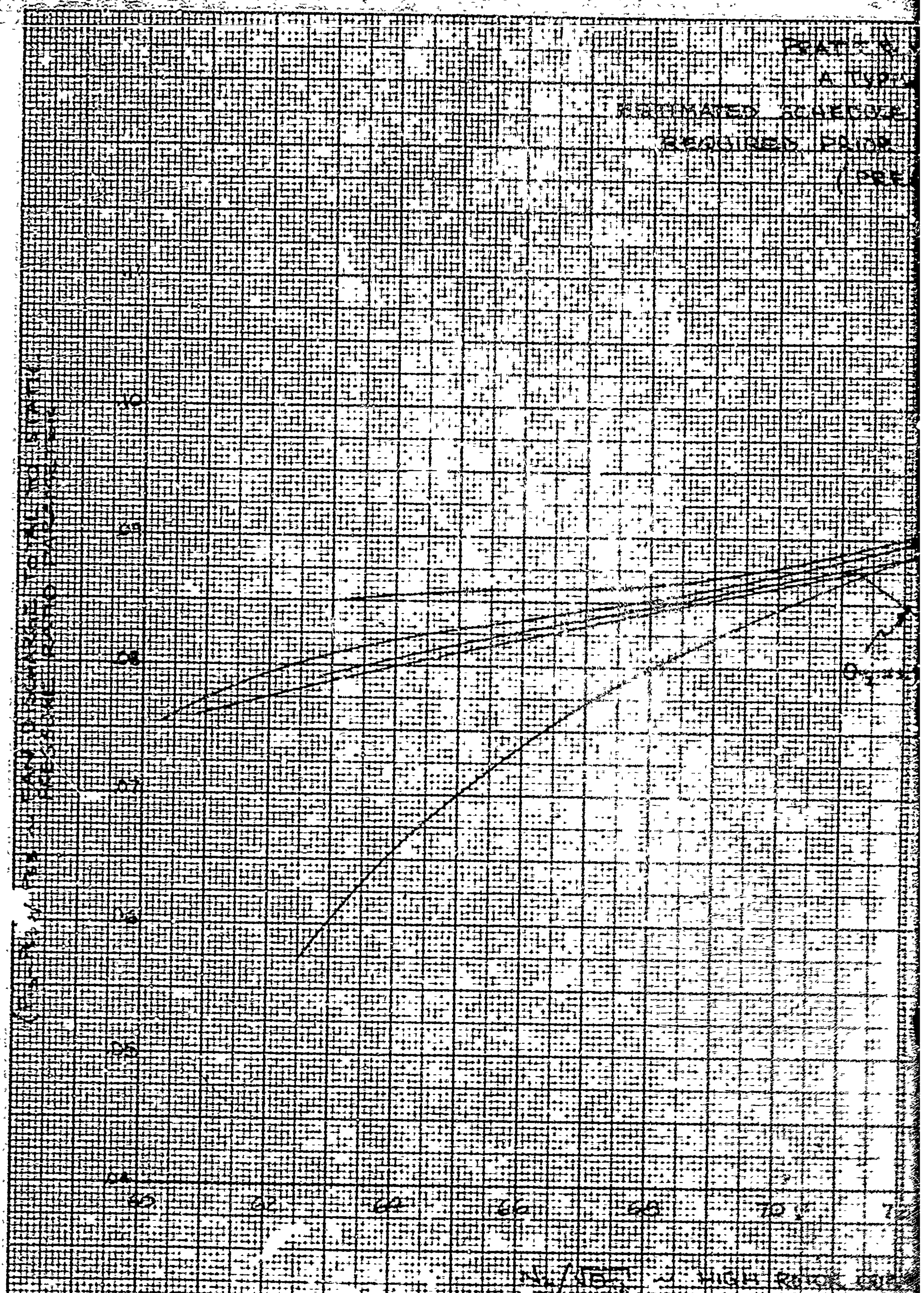

60
62
64
66
68
70

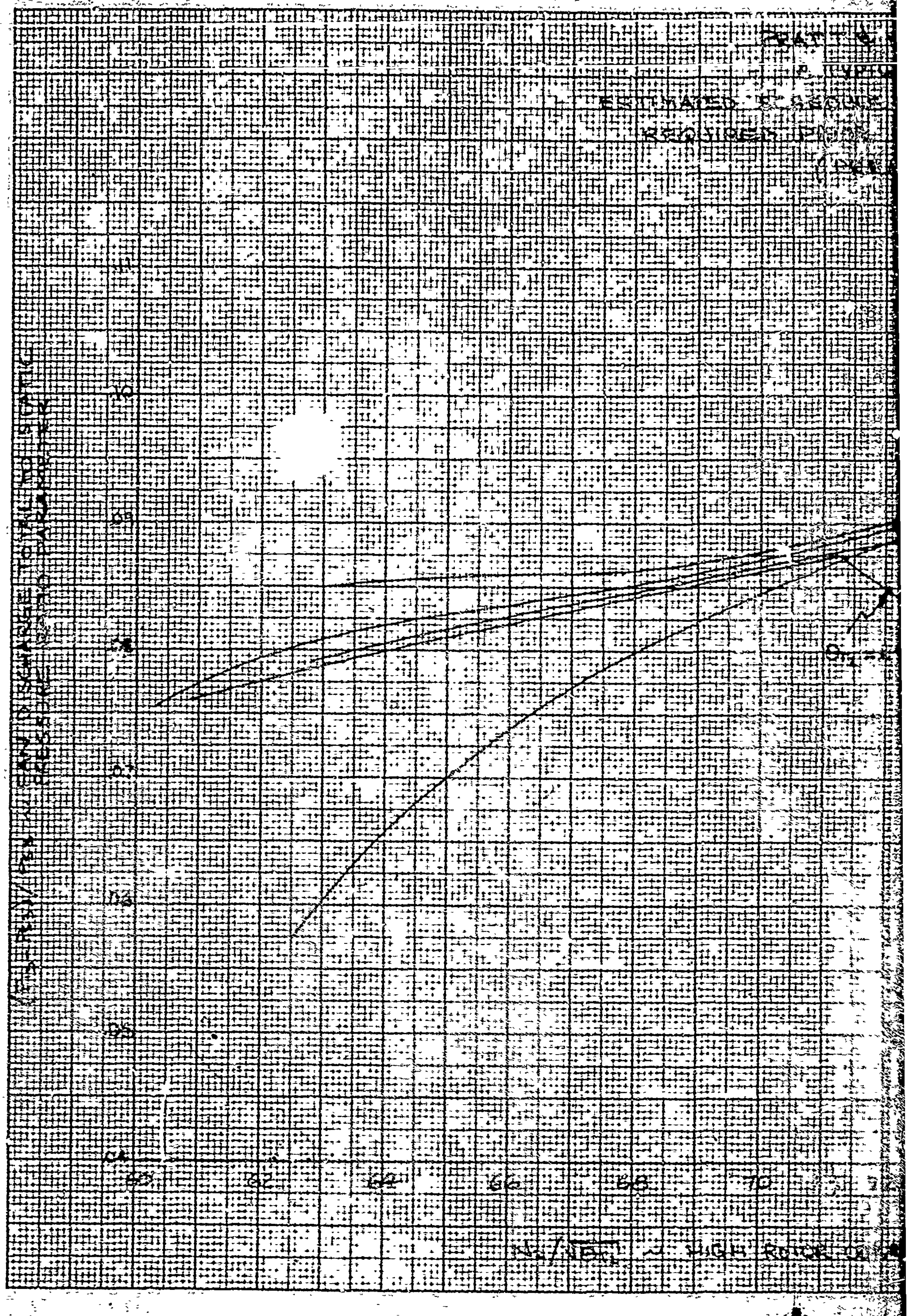
60
62
64
66
68
70

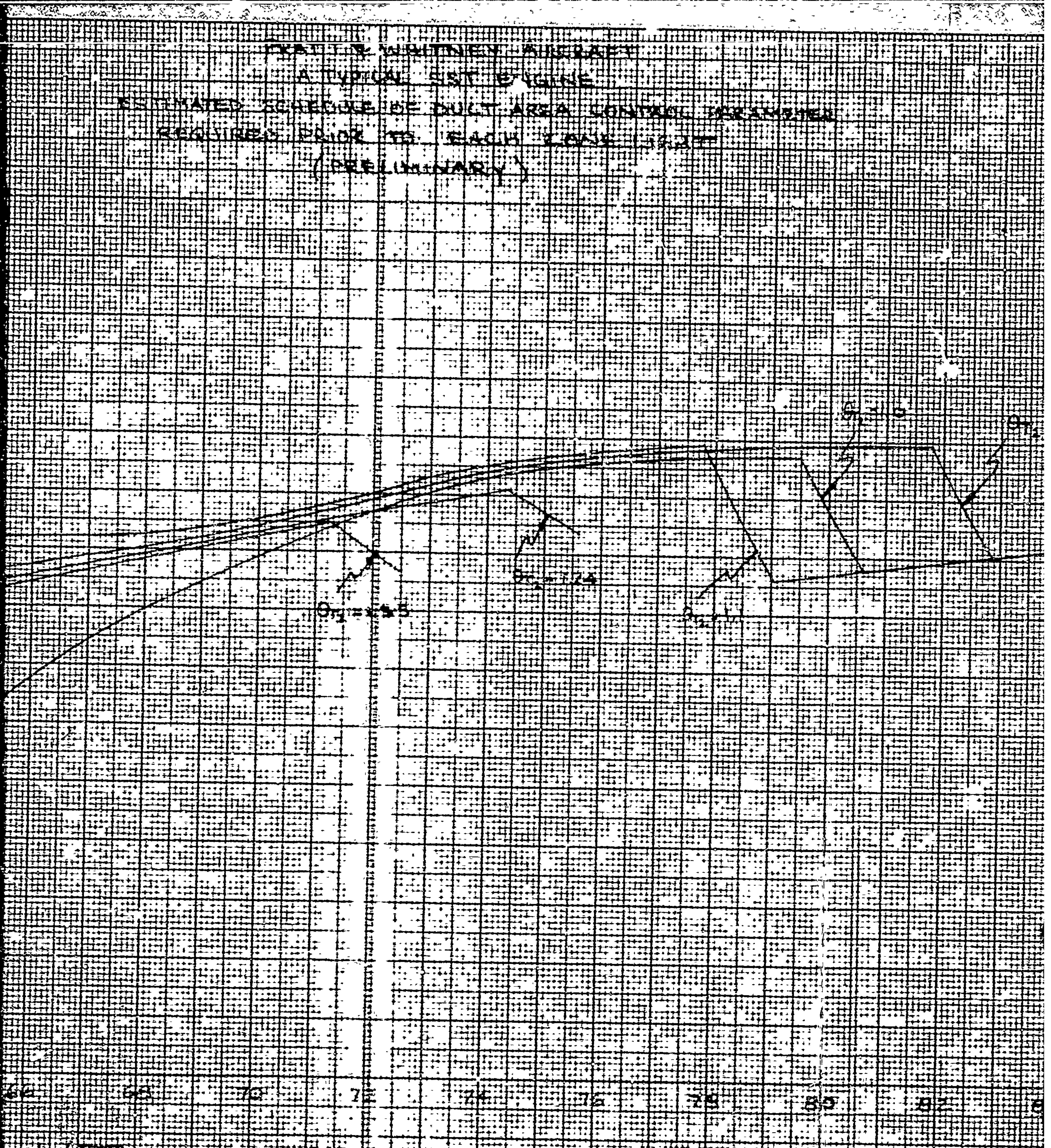
PRATT & WHITNEY AIRCRAFT
A TYPICAL SST ENGINE
ESTIMATED SCHEDULE OF DUCT AREA CONTROL PARAMETER
REQUIRED PRIOR TO EACH
(PRELIMINARY)
66
68
70
72
74
76
78
80
82
HIGH ROTOR CORRECTED SPEED ~ RPM

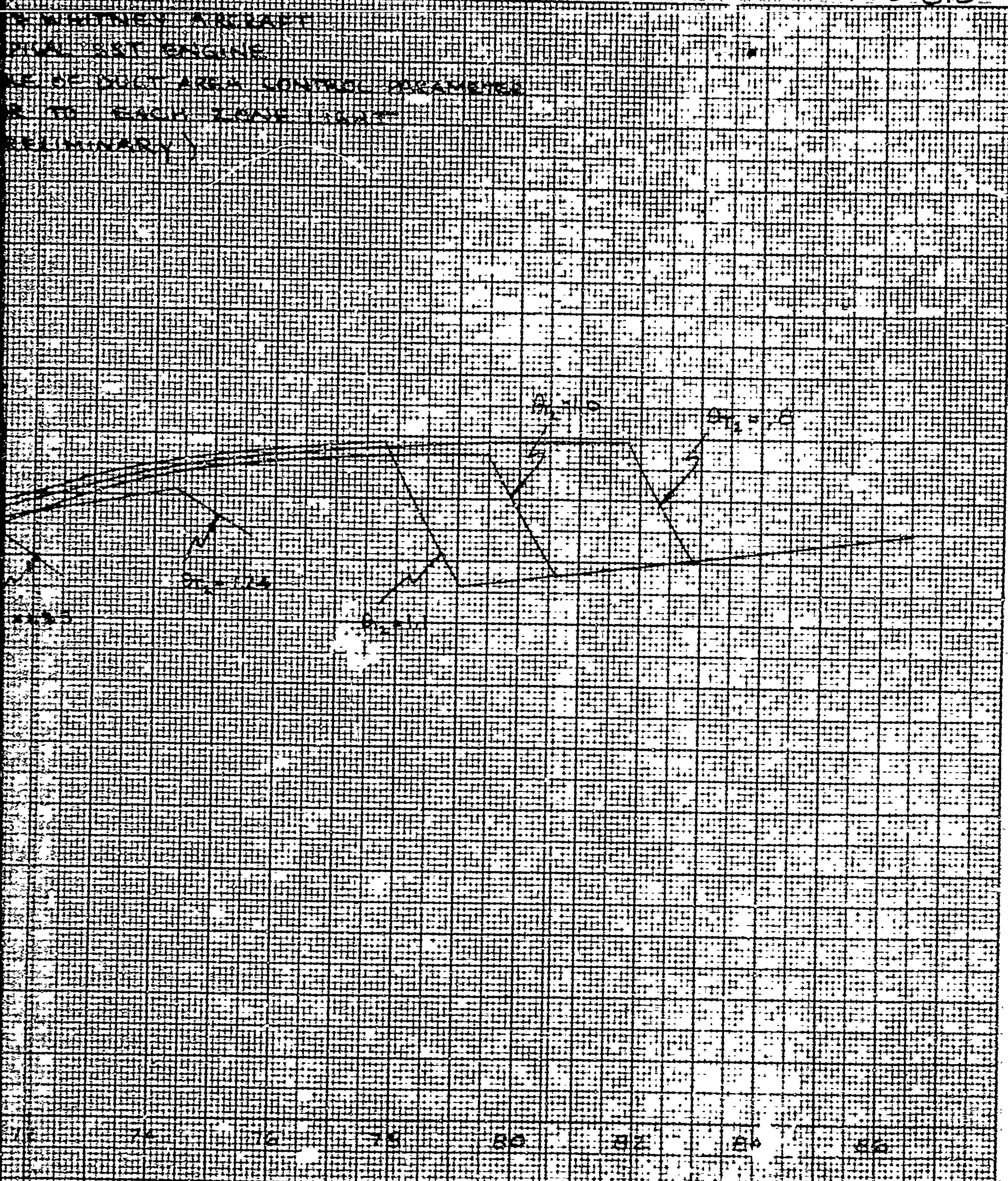

FIGURE 16.

2 3

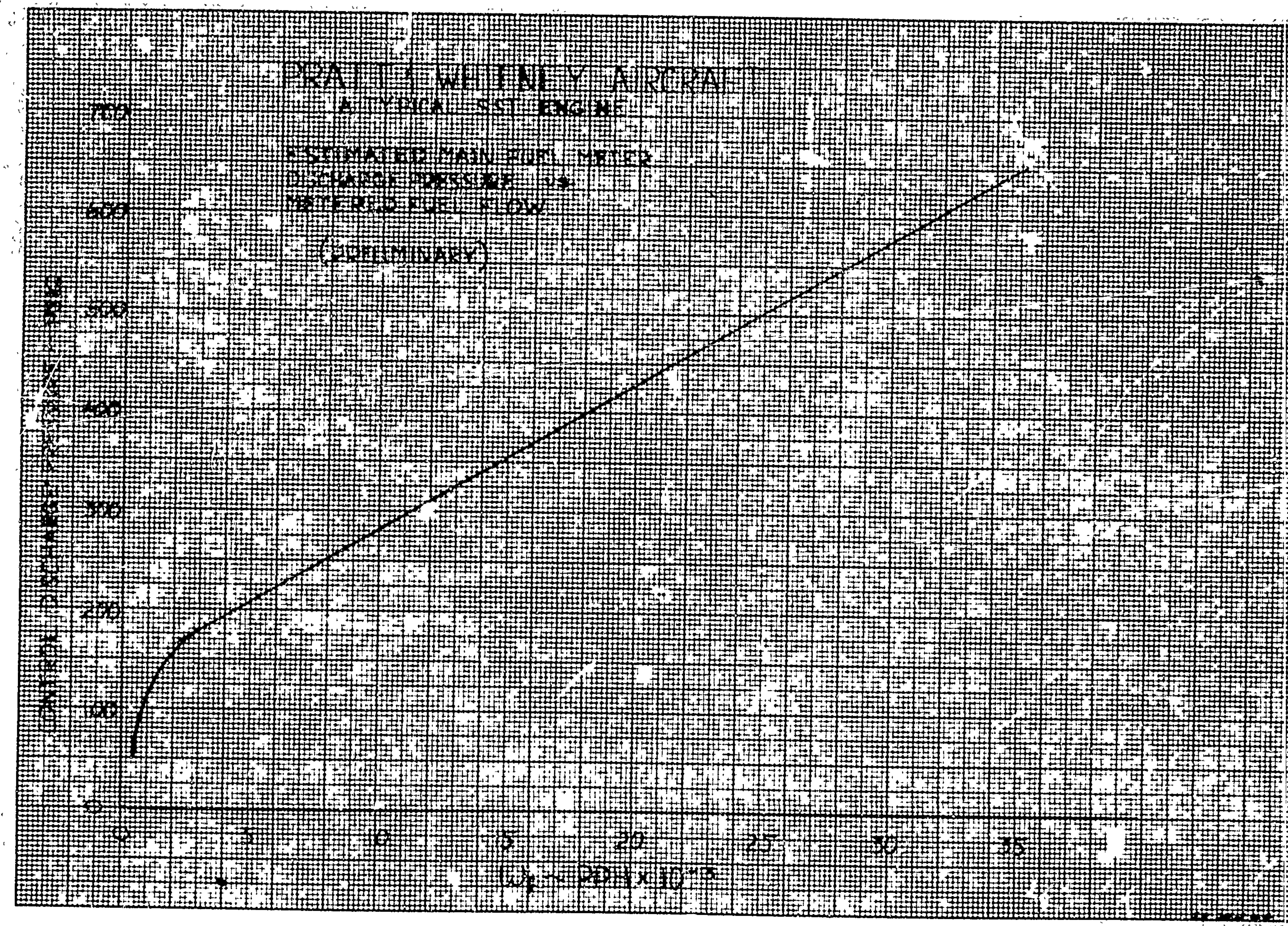

PPS 819

FIGURE 17

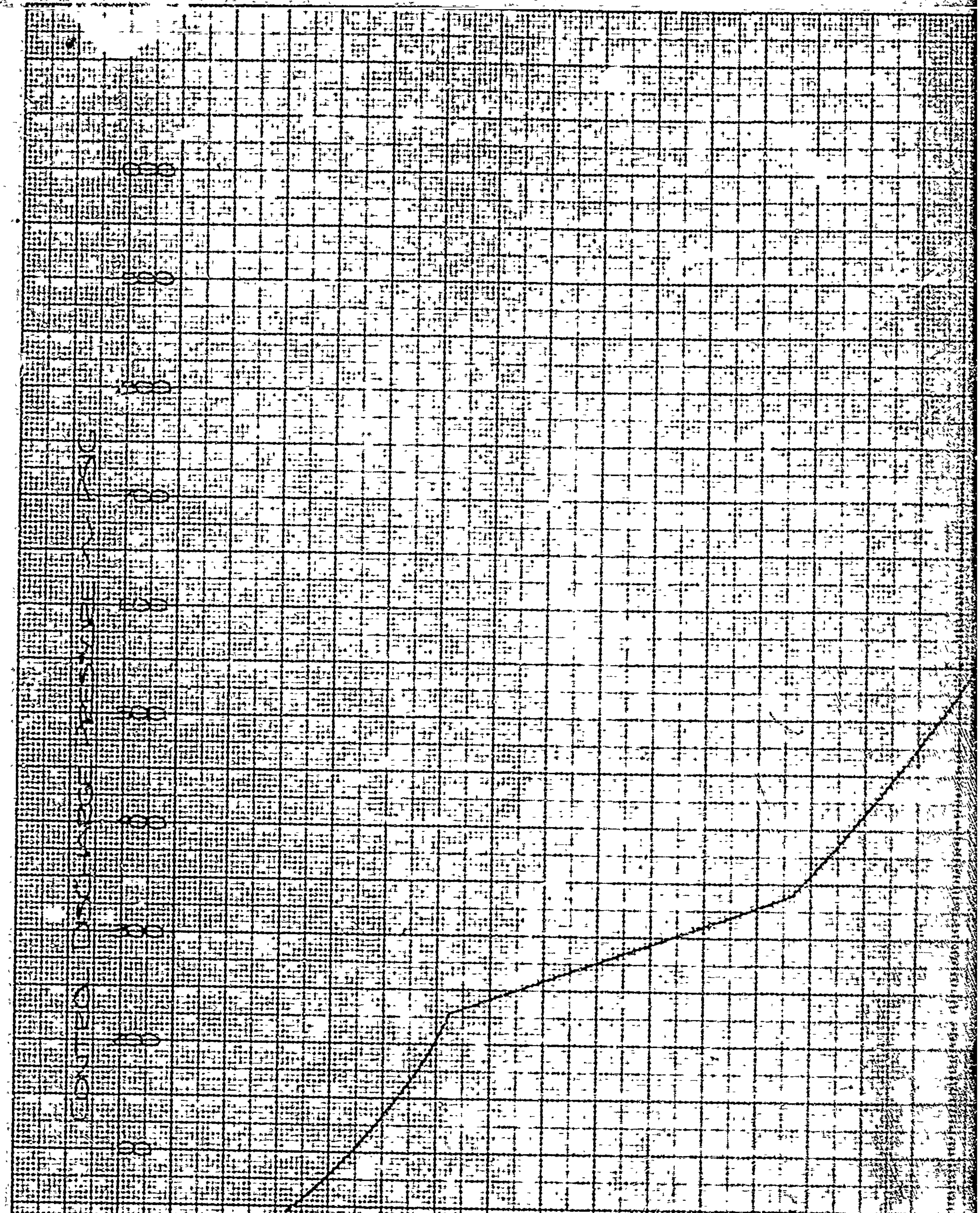
ZONE I METERS FUEL

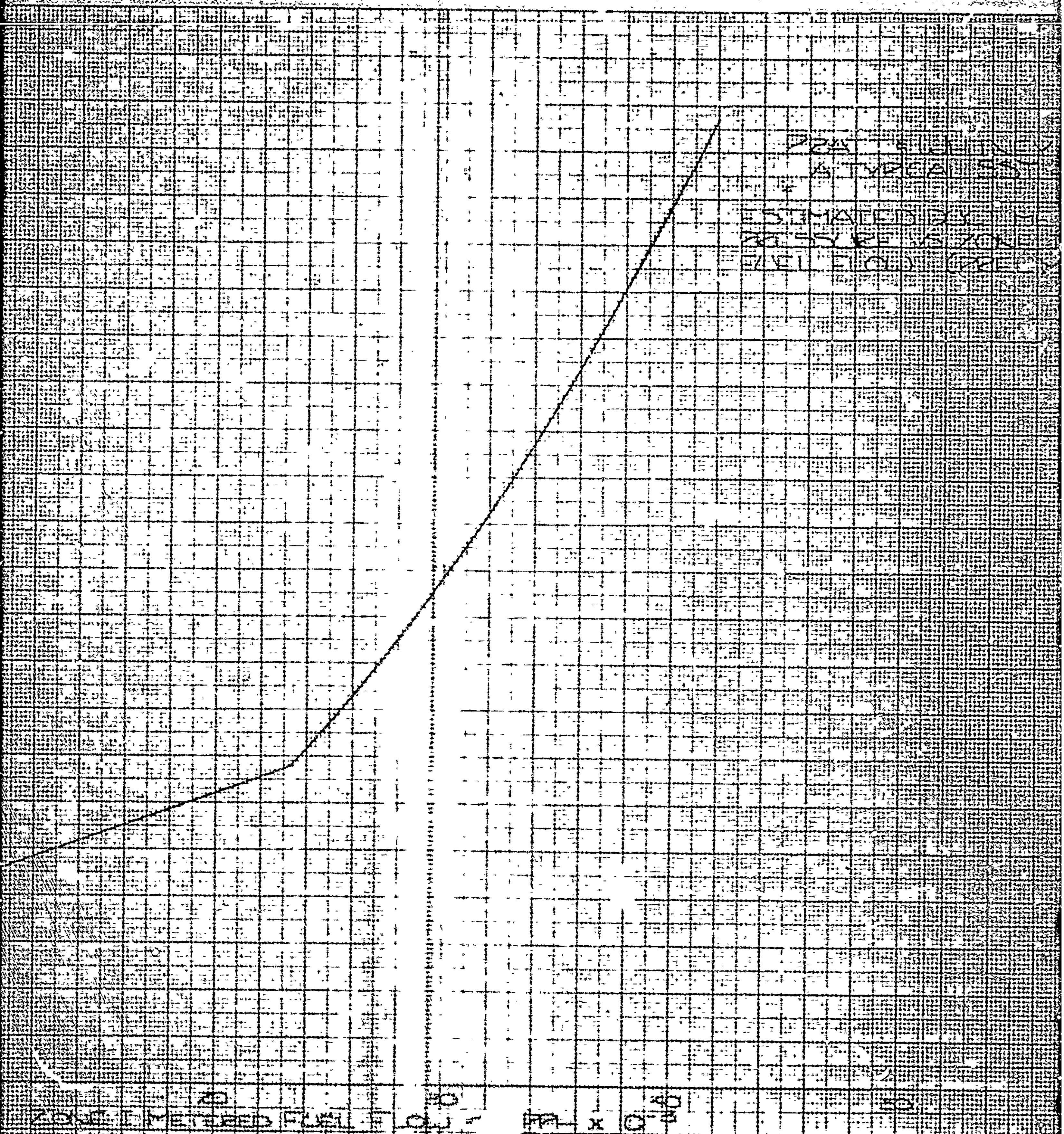

1

2

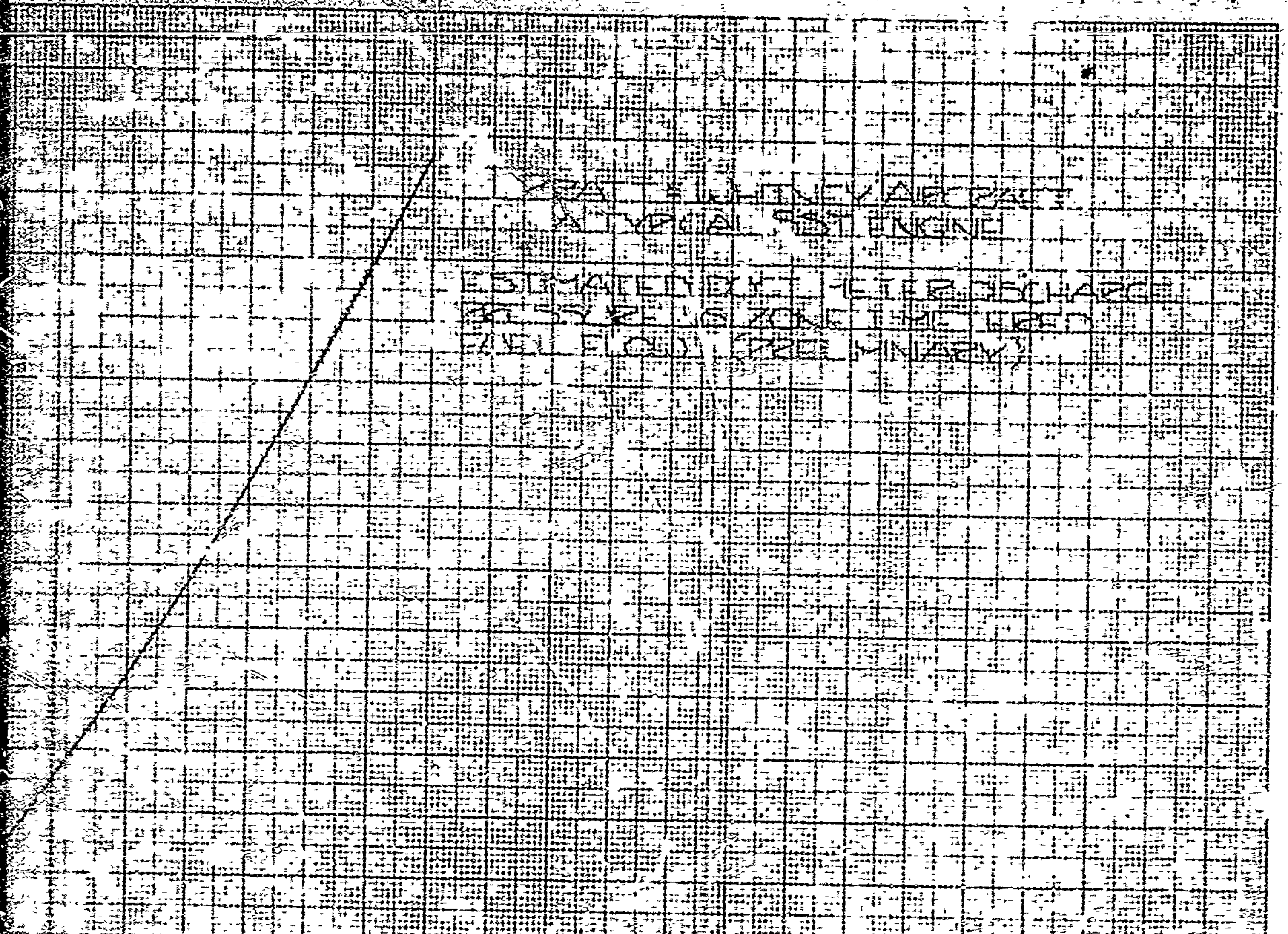

2 FIGURE 13 3

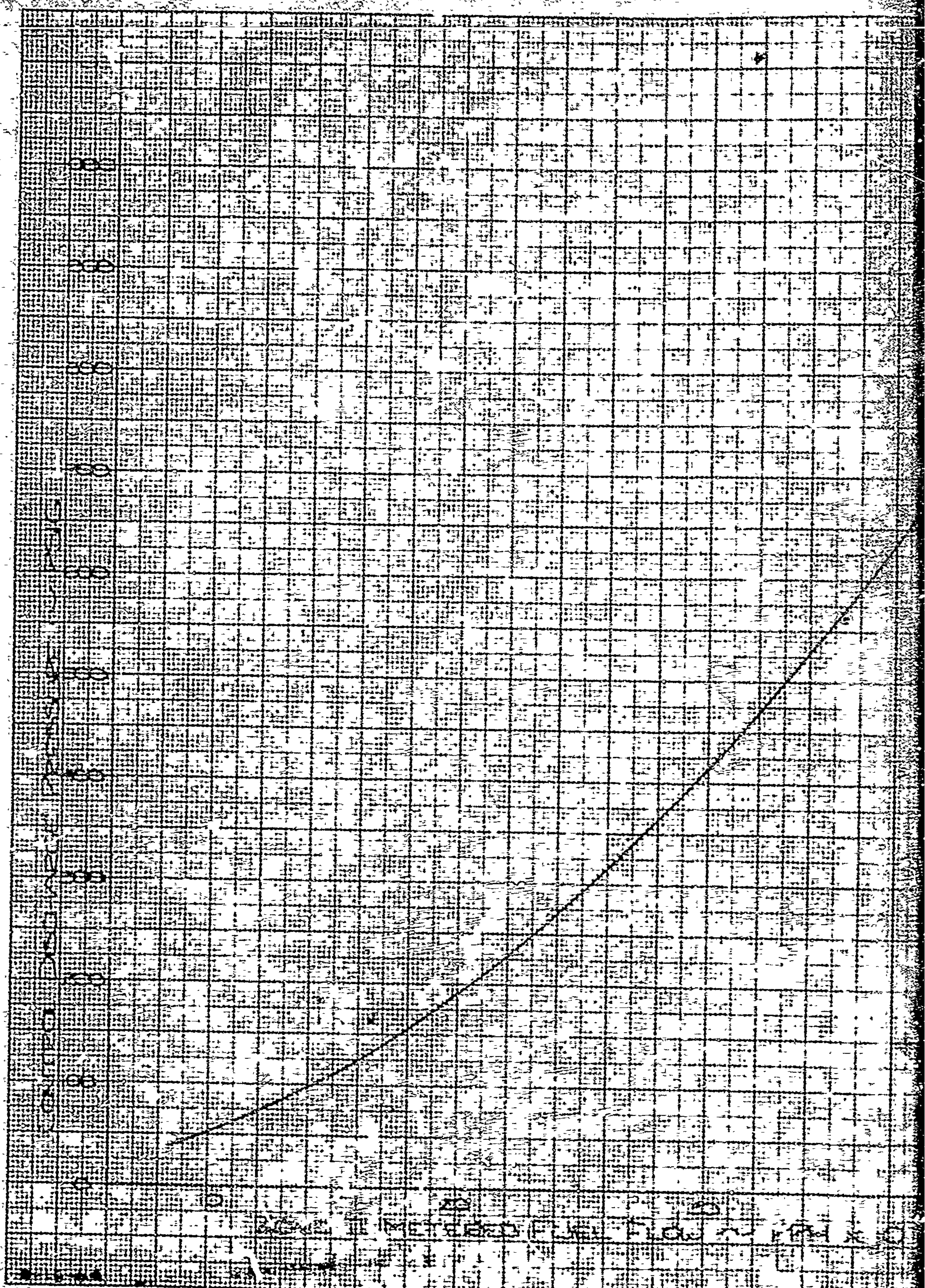

METERED FUEL FLOW ~ PPH x

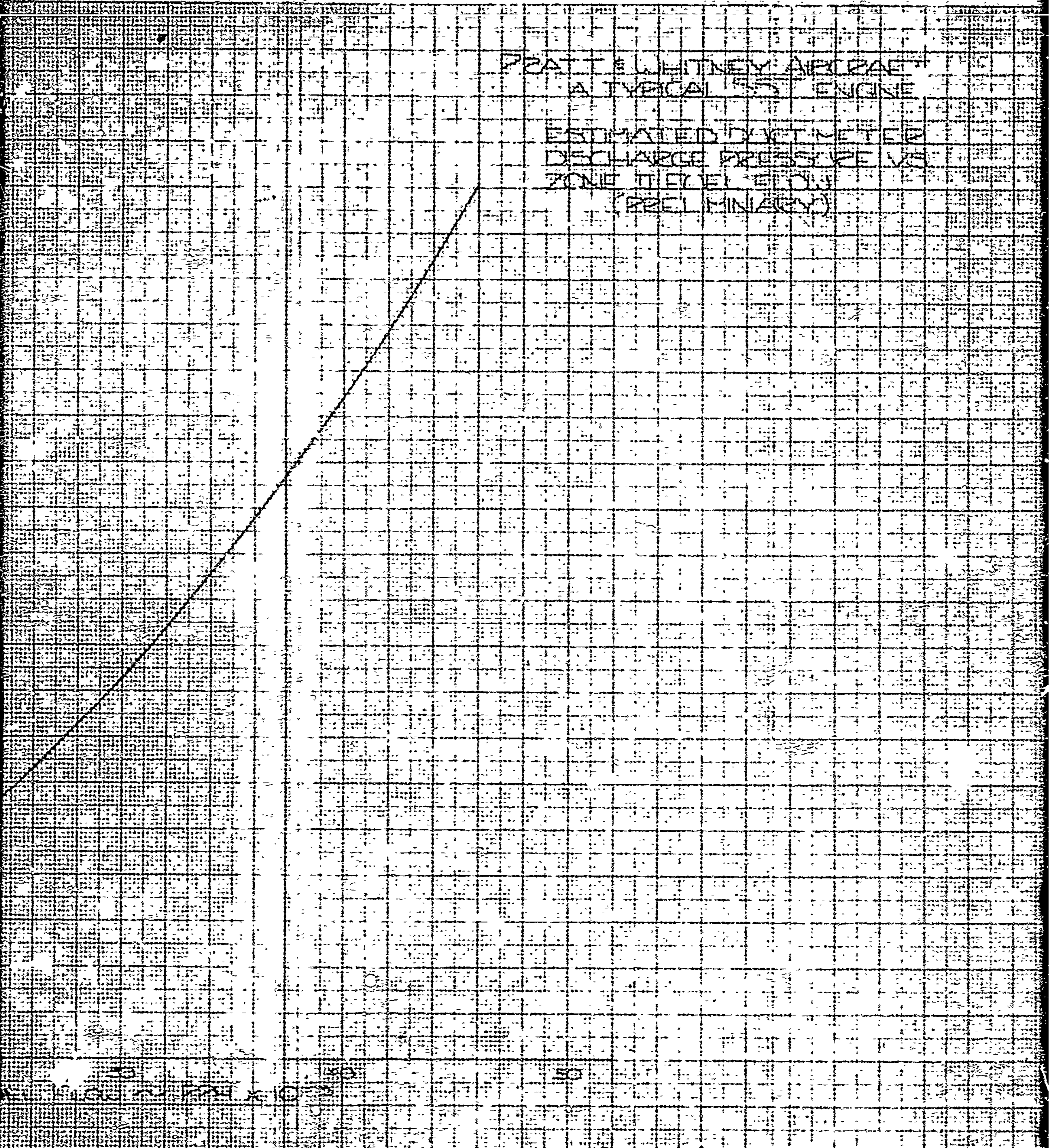
PRATT & WHITNEY AIRCRAFT
A TYPICAL ENGINE
ESTIMATED DUCT METER
DISCHARGE PRESSURE VS
ZONE II FUEL FLOW
(PRELIMINARY)
50
PPH x 10

1 2 FIGURE 19

PPS 819

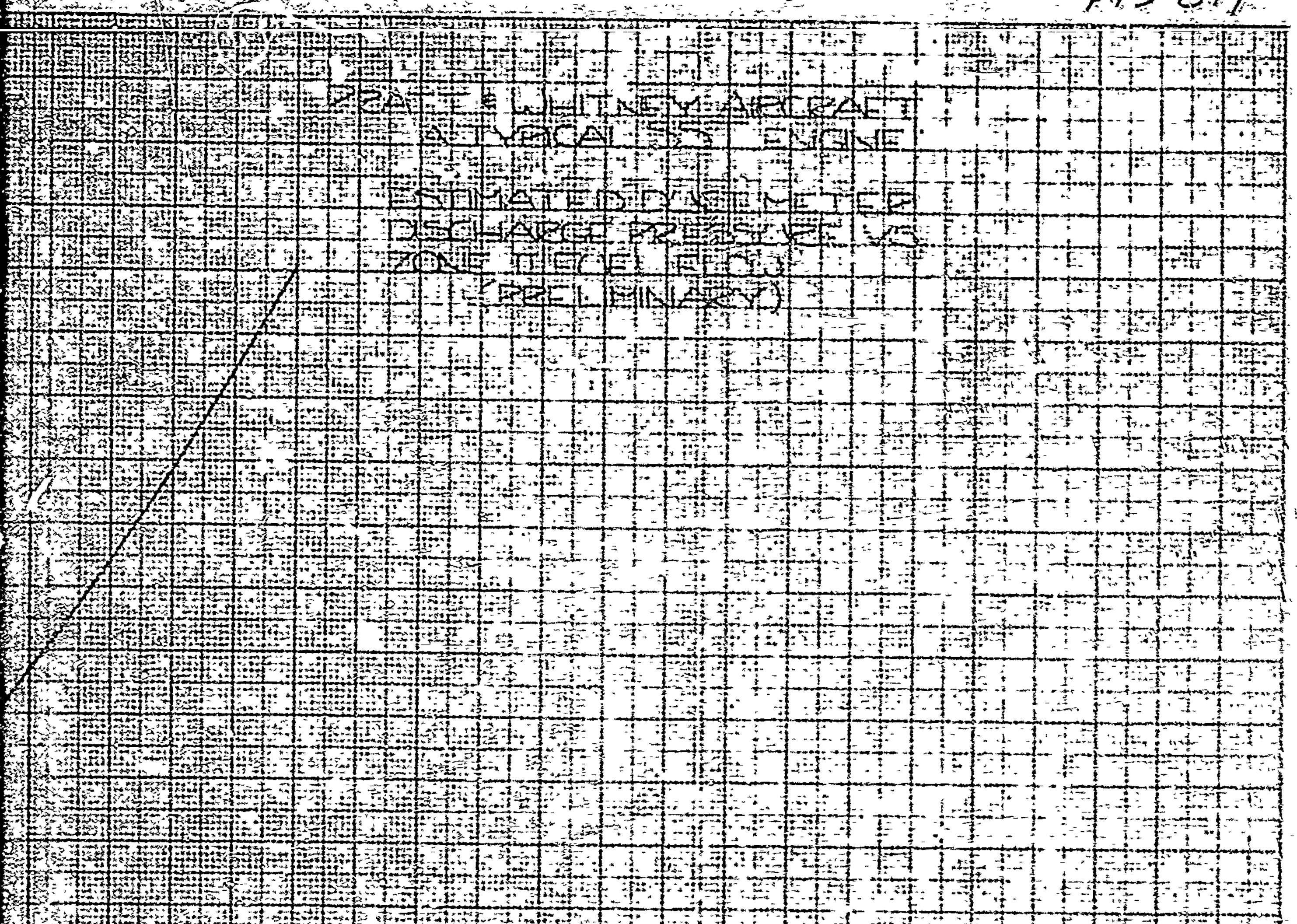

2 FIGURE 19 3

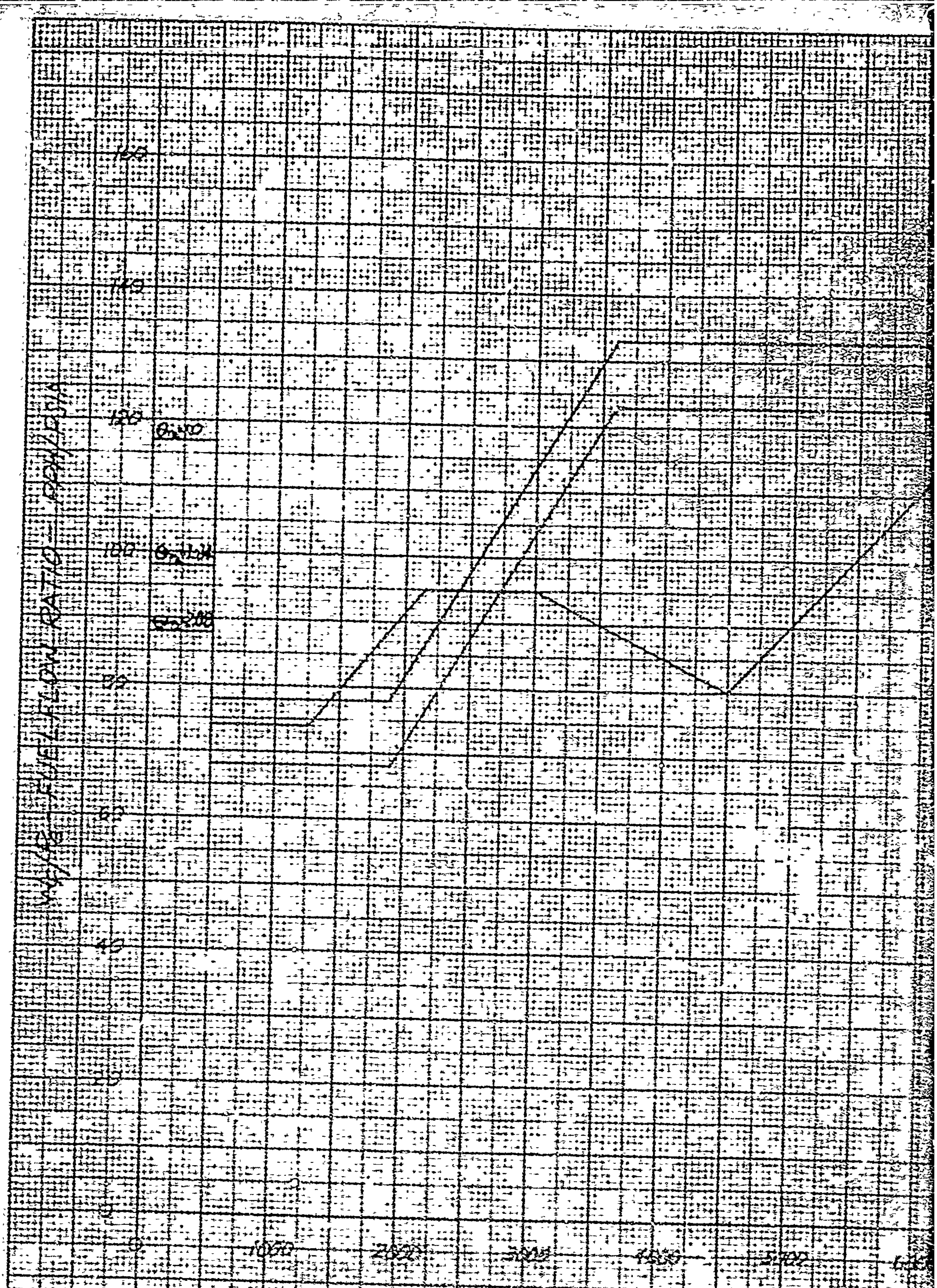

FUEL FLOW RATIO
120
100
80
60
40
20
0
1000
2000
4000
5000
ENGINE HIGH ROTOR

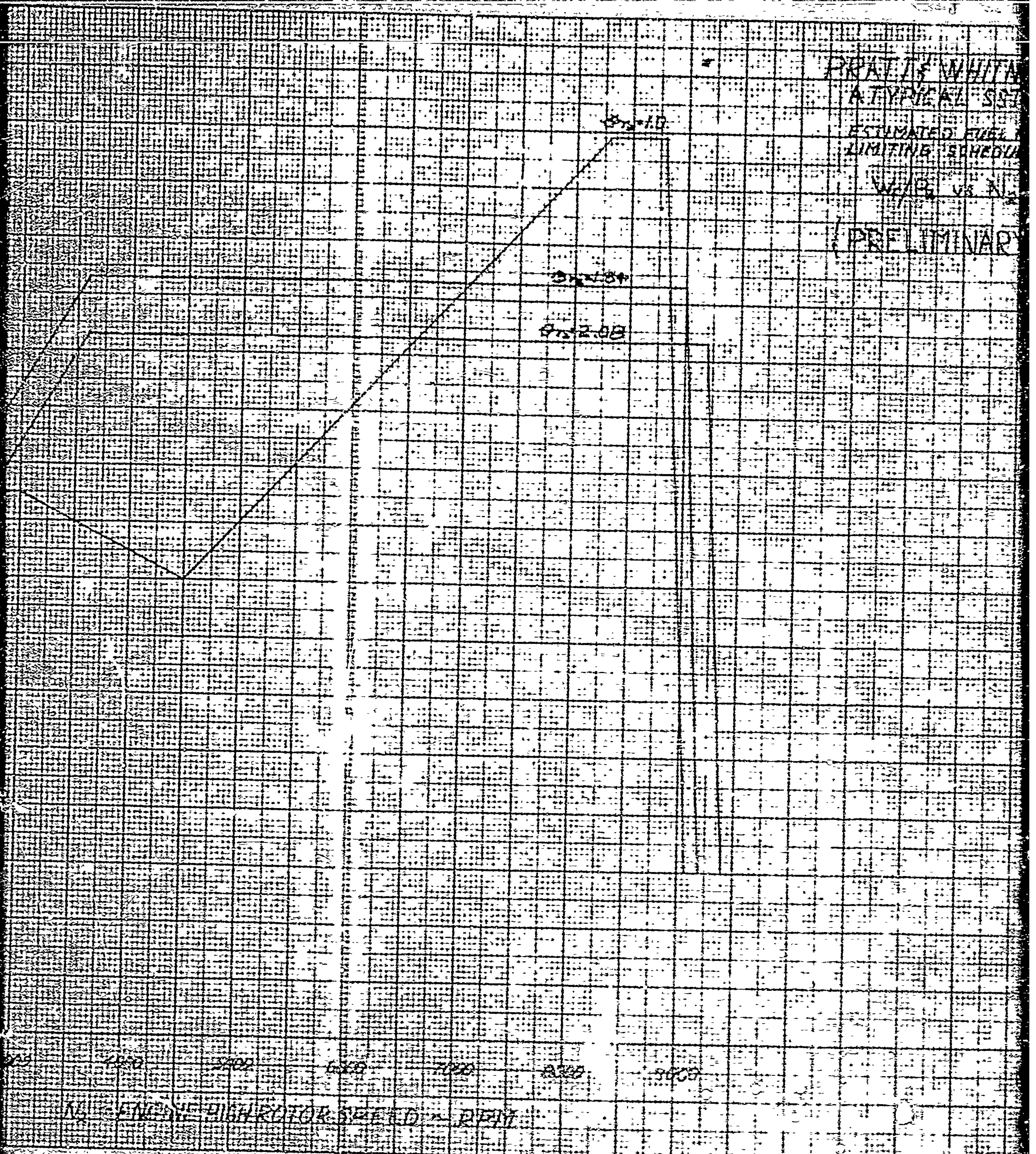
PRATT & WHITN
A TYPICAL SST
ESTIMATED FUEL
LIMITING SCHEDU
PRELIMINARY
ENGINE HIGH ROTOR SPEED ~ RPM

1

2

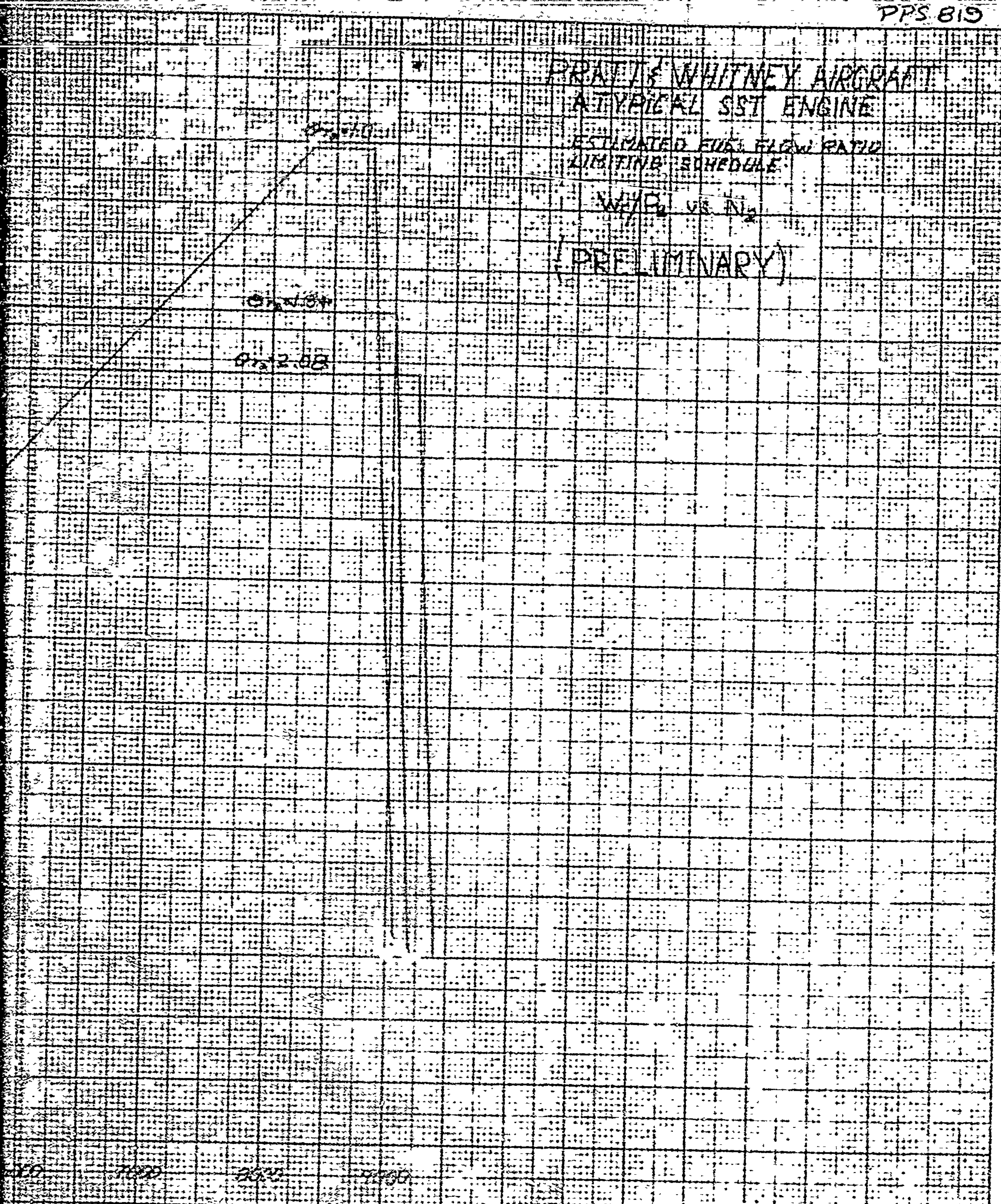
PRATT & WHITNEY AIRCRAFT
A TYPICAL SST ENGINE
ESTIMATED FUEL FLOW RATIO
LIMITING SCHEDULE
Wf/P2 vs. N2
(PRELIMINARY)
θT2 = 2.08
SPEED – RPM

FIGURE 20

PPS 819

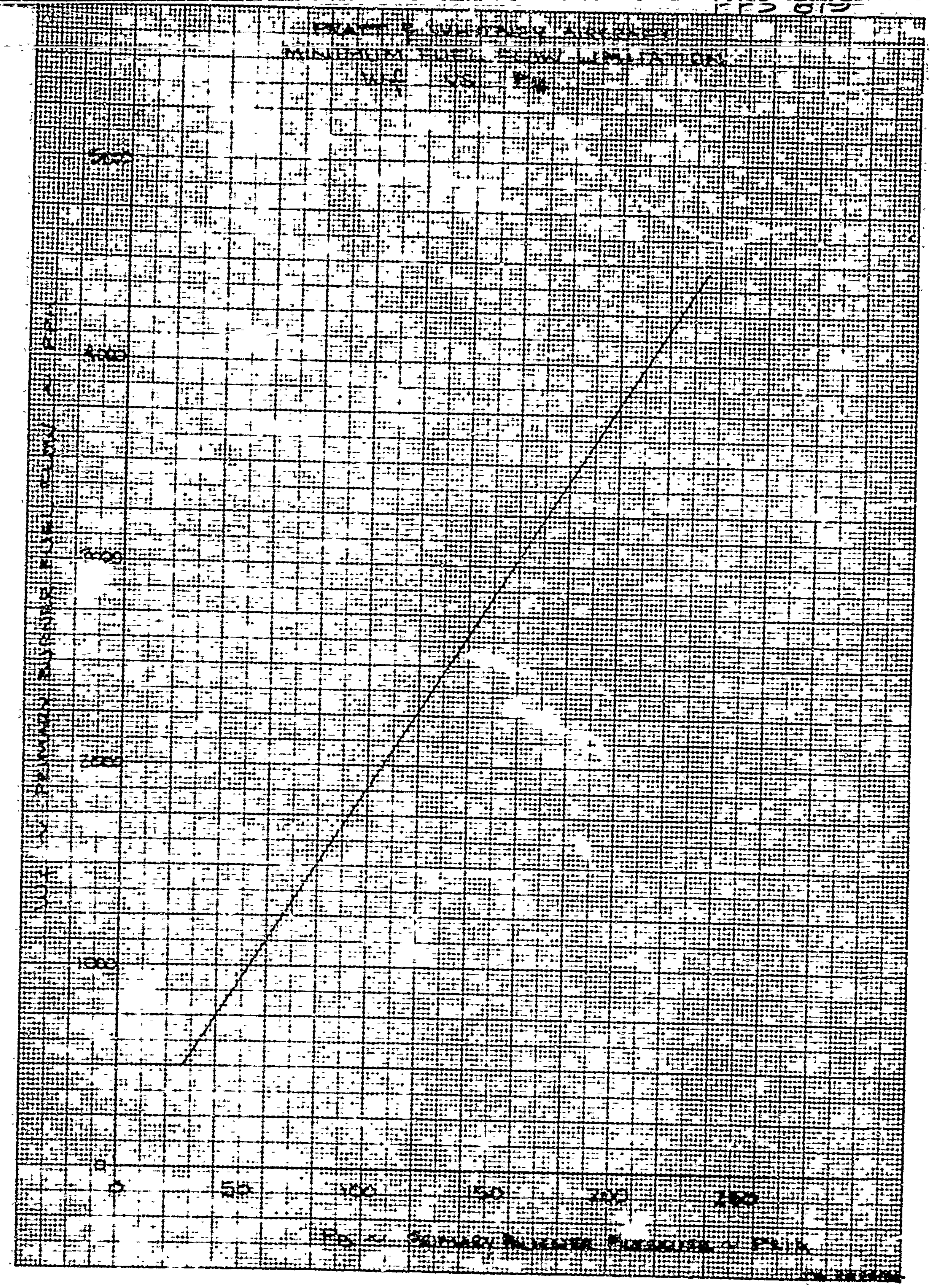

FIGURE 21

PPS 819

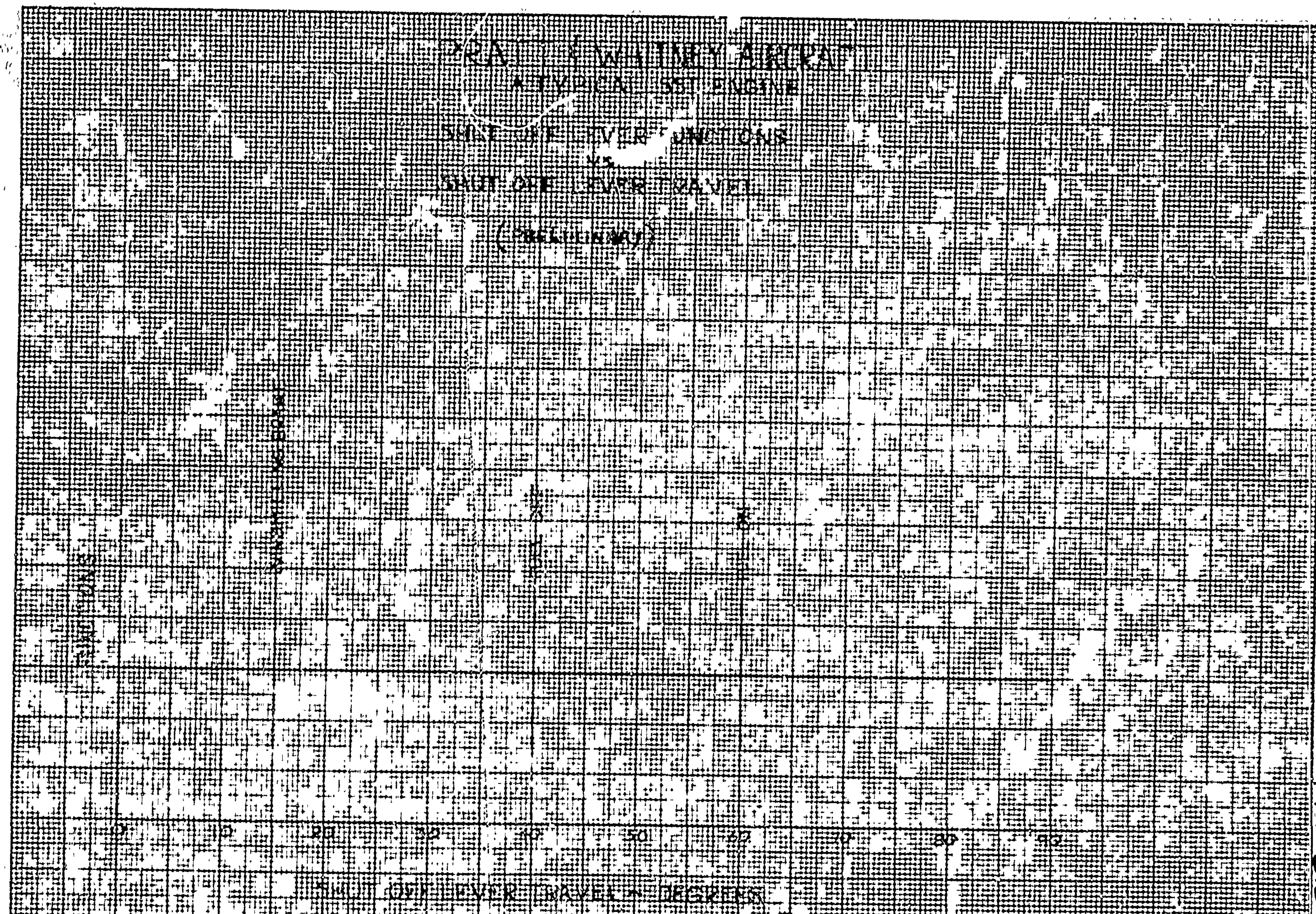

FIGURE 22

Date: 6 October 1964

1. SCOPE

1.1 This specification established requirements for an engine-driven fuel pump for a typical SST engine.

2. DESCRIPTION

2.1 The pump shall consist of a single hgih pressure stage fed by a single centrifugal stage.

3. APPLICABLE PUBLICATIONS

3.1 The applicable specifications and standard listed in ANA Bulletin No. 343n shall form a part of this specification to the extent specified herein.

3.2 The following specifications and publications shall form a part of this specification to the extent specified herein:

PWA PS-720A	Vendor Responsibilities
PWA PMC-9041	Test Fluid

4. REQUIREMENTS

4.1 General Requirements

4.1.1 Materials and Processes - Materials and processes used in the manufacture of the fuel pumps shall be of high quality and suitable for the purpose. Material specifications shall conform to applicable specifications listed in ANA Bulletin No. 343n. When vendor specifications are used for materials or processes which affect performance or durability of the finished product, such specifications shall be subject to release to the government. The use of non-government specifications shall not constitute waiver of government inspection.

4.1.2 Dissimilar Metals - The use of dissimilar metals in contact as defined on Drawing MS 33586A shall be avoided wherever practicable.

4.1.3 Use of AMS 5610, 5620, 5621, 5630, 5631, and 5632 Materials - The use of the subject heat treatable stainless steels or equivalents is prohibited unless agreed upon in writing by PWA Engineering.

4.1.4 Screw Threads - All conventional straight screw threads shall conform to the requirements of MIL-S-8879 except paragraph 3.12. These include threads on standard hardware bolts and nuts, tapped holes receiving standard items, nuts for use on studs, and threads for non-standard parts where a new thread size is being incorporated in a new design or re-design and where tooling is not already available. These requirements need not apply to electrical connectors, ignition harness, thermocouple harness, interference fit threads, either thread end of studs, fluid fittings, fluid fitting bosses, tube coupling nuts, ground or cut threads, threads of non-standard items where similar parts with the same thread are already designed and tooling is already available, and helical inserts including tapped holes for same where it has been determined that the inserts will accept a MIL-S-8879 external thread.

4.1.5 Standard Parts - AN or MS standard parts, selected from those listed in ANA Bulletin No. 343n shall be used unless it is determined that they are unsuitable for the purpose. They shall be identified by their standard part numbers.

4.1.6 Protective Treatments and Coatings. - Protective treatment and coatings shall be in accordance with applicable specifications listed in ANA Bulletin 343n with the exception of the areas listed below. All parts not in constant contact with fluid shall be corrosion resistant or suitably protected.

(1) Working surfaces
(2) Threads
(3) Mounting surfaces

4.1.7 Serialization. - Serial numbers of fuel pumps procured under the specification shall not duplicate serial numbers of similar components supplied by the manufacturer to Pratt & Whitney Aircraft. A sufficiently large block of serial numbers shall be assigned to the basic pump to cover anticipated production. The use of letters in serial identification shall be avoided.

4.1.8 Data Plate. - A data plate shall be attached to the fuel pump in a location which is visible when mounted on the engine and shall include the following information:

a) Manufacturer's Name
b) Manufacturer's parts list number
c) Manufacturer's parts number
d) Manufacturer's serial number

4.2 Test Requirements

4.2.1 Qualification Tests. - Approval as a type of fuel pump procured under this specification for a prototype engine shall be contingent upon satisfactory completion of a 60 hour preliminary flight rating test in accordance with MIL-E-5156C. Approval as a type of fuel pump procured under this specification for a production engine shall be contingent upon satisfactory completion of a 150-hour engine qualification test in accordance with MIL-E-5009B and satisfactory completion of a component qualification test as specified in paragraph 5.2. The component qualification test procedure shall be approved in writing by PWA before initiation of the tests. The vendor shall be required to include, as a part of his normal development program, a series of abbreviated tests to determine the extent of compliance with these requirements prior to starting the official component qualification test.

4.2.1.1 Reports. - Reports of the pump qualification tests under this specification shall be attested to by an appropriate government representative and shall include at least the items mentioned in MIL-E-5009B, paragraph 3.1.2.1. Twelve copies of this report shall be supplied to the Engineering Department of Pratt & Whitney Aircraft for transmittal to the government.

4.2.1.2 Shipment of Production Units Prior to Approval - In the event that production units are shipped prior to satisfactory completion of the appropriate qualification testing, the vendor shall be responsible for retrofitting these units with all engineering changes required to duplicate the unit which satisfactorily completes the appropriate qualification test, except those changes which in the opinion of the cognizant Pratt & Whitney Aircraft project engineer were not required to pass the appropriate qualification test. These exceptions are to be designated by the Pratt & Whitney Aircraft project engineer's written approval.

The acceptance of limited quantities of production units may not be contingent upon completion of the appropriate qualification tests as specified in paragraph 4.2.1.

4.2.2 Acceptance Test. - Prior to delivery each fuel pump procured under this specification shall be subjected to an acceptance test as specified in paragraph 5.4.

4.3 Design Requirements. - This section establishes design requirements for a typical SST engine fuel pump and should not be construed as inspection requirements for production pumps. It may also be noted that requirements for two installations are specified herein. If not specifically stated the requirement shall apply to both installations.

4.3.1 General. - The following design features shall apply:

a) All relief and bypass valves shall be designed and located such that free water will not be trapped in any manner which will affect normal pump operation.

b) The use of slotted head screws will not be permitted.

c) The use of snap rings as stressed retainers is discouraged and will not be allowed in critical locations where failures of the snap ring can result in performance loss. A review with PWA Engineering of each design location utilizing a snap ring is required and is subject to PWA approval.

4.3.2 Fuel. - The pump shall operate satisfactorily throughout the complete engine operating range for steady state and transient operating conditions when using fuel conforming to specification MIL-J-5624E, Grades JP-4 and JP-5 having any of the variations in characteristics permitted by specification MIL-J-5624E for these grades. The pump shall also operate satisfactorily under all operating conditions when the absolute fuel pressure at the fuel inlet connection is a minimum of 5.0 psi above the vapor pressure of the fuel used, except that there shall not be a drop between ambient tank pressure and fuel inlet pressure in excess of 3.0 psi. The maximum fuel inlet pressure shall be 50 psig. The pump shall also function satisfactorily throughout its complete operating range when using grade JP-4 fuel with the addition of an anti-icing fluid conforming to MIL-I-27686 at a concentration between 0.13 and 0.15% by volume. The pump shall also function satisfactorily with a fuel that has a true vapor pressure that does not exceed 0.5 psi at 175°F and 2.5 psi at 250°F.

4.3.2.1 Fuel Contamination - The pump shall function satisfactorily when using fuel contaminated to the extent of 80 grams of foreign matter per 1000 gallons. Satisfactory operation on contaminated fuel shall mean that the contaminated fuel will not itself precipitate a sudden pump failure but may cause gradual deterioration of pump performance and abnormal wear of pump parts. This foreign matter shall be considered to consist of not less than 68 per cent SiO_2 and shall have a particle-size analysis as follows.

Particle Size Microns	Per cent of Total
0-5	39 ± 2 by weight
5-10	18 ± 3 by weight
10-20	16 ± 3 by weight
20-40	18 ± 3 by weight
Over 40	9 ± 3 by weight
Through a 200 mesh screen	100 by weight

4.3.3 Fuel filtration

4.3.3.1A (Applicable for installation A only) - A 10 micron fuel filter shall be provided at the discharge of the centrifugal stage to protect the high pressure stage and other fuel system components. To protect against blockage, a means of by-passing the filter shall be incorporated. This by-pass shall limit the filter pressure drop to 19-21 psi under all flow conditions. The return flow from the fuel control shall enter the pump downstream of the filter. The 10 micron filter element(s) shall be accessible for removal from the bottom of the engine.

4.3.3.1B (Applicable for installation B only) - Outlet and return ports shall be provided beween the boost stage discharge and the inlet of the high pressure stage in order that boost stage discharge flow may be divered to a remotely mounted fuel filter having a 10 micron rating. This remote filter will be supplied by Pratt & Whitney Aircraft. The pump shall incorporate means of bypassing the filter to protect against blockage. This bypass shall start to open when the filter differential reaches 19-21 psi. Maximum pressure drop through this bypass shall not exceed twice the opening differential under any flow condition. The

return flow from the fuel control to the pump shall enter the pump downstream of the filter.

4.3.4 Fuel Heating

4.3.4.1A (Applicable for installation A only) There shall be no provisions for fuel heater ports.

4.3.4.1B (Applicable for installation B only)

It is possible that fuel heating may be required by the engine system. In this event, the flow path between the boost stage discharge and high pressure stage inlet connections, noted in paragraph 4.3.3.1B, will also include a fuel heater in series with the filter. Maximum pressure loss through the heat exchanger under normal conditions at rated flow is estimated to be 10 psi. The pump must be capable of withstanding changes in high pressure stage inlet temperature of 100 degrees in a 10 second period with pump inlet temperatures remaining essentially constant.

4.3.5 Discharge Vent Connection. - A connection must be supplied at the discharge of the high pressure stage to permit recirculation to the aircraft tanks through a restriction to be incorporated as a permanent part of all pumps procured under this specification. The size of the restriction and the configuration of the external connection must be coordinated with PWA Engineering. A closure suitable for flight will be required for this connection.

4.3.6 Fuel and Ambient Temperature Limits. - The pump shall be designed to operate satisfactorily with the following surrounding ambient air temperature and fuel inlet temperatures:

	Ambient Air Temp.	Inlet Fuel Temp.	Interstage Fuel Temp.
Installation A	-65 to 550°F	-65** to 250°F	-65** to 325°F
Installation B	-65 to 750°F	-65** to 250°F	-65** to 325°F

** This applies for MIL-J-5624 Grade JP-4 Fuel only. when using MIL-J-5624 Grade JP-5 the applicable temperature would correspond to a fuel viscosity of 12 centistokes.

4.3.7 Pressure Relief Valve. - A non-servoed type pressure relief valve shall be provided to limit the pressure rise across the high pressure stage. This valve shall be designed to begin relieving at 1100 psi rise and shall be capable of passing the full output of the pump with a maximum rise of 1200 psi. This valve setting shall be adjustable over a range of ±100 psi.

4.3.8 Maximum Pressure. - The fuel pump shall be capable of withstanding, without fracture or permanent deformation, 2100 psig static pressure on the high pressure side of the pump, 650 psig on the interstage and 250 psig on the inlet portion of the pump. Tests to demonstrate this requirement shall be subject to approval by the cognizant PWA project engineer, and shall be repeated when changes or process modifications are incorporated which, in the opinion of the PWA project engineer, might adversely affect pump strength. Burst pressure tests must be performed on a development unit to destruction.

4.3.9 Centrifugal Boost Stage - The pump shall contain a valve to bypass pump inlet fuel directly to high pressure stage inlet in the event of failure of the boost stage. This valve and associated passages shall be designed to keep pressure losses below 1 psi at the maximum flow condition. The bypass valve shall also incorporate provisions to prevent inadvertent opening under transient surge conditions that can occur when aircraft boost pressure is applied to pump inlet with a dry fuel pump. In addition, the boost stage performance characteristics shall be such as to provide for the maximum possible boost stage pressure rise over the full flow range of the fuel pump.

4.3.10 Hydraulic Pump Connection

4.3.10.1A (Applicable for installation A only)
Provision shall be made for a hydraulic pump supply port downstream of the filter. The return flow from the hydraulic pump shall enter the pump, downstream of the supply port.

4.3.10.B (Not applicable in installation B)

4.3.11 Pressure Taps. - Pressure taps shall be provided at the following points through the pump:

(a) Inlet to centrifugal stage

(b) Discharge of centrifugal stage immediately upstream of filter connection

(c) Immediately downstream of filter connection

(d) pump discharge

The pressure taps described in items (a) and (d) should be made accessible from the bottom of the pump

4.3.12 Drive Shaft Seal. - Drive shaft seal leakage from the drain provided shall not exceed 10 drops per minute under any operating conditions.

4.3.13 Lubrication. - The pump shall incorporate a means for lubrication of the drive spline from the engine oil system.

4.3.15 Maneuver Loading. - When mounted on the engine as shown in Figure 1, the pump shall be capable of withstanding, without permanent deformation or failure, the flight maneuver forces specified in paragraph 3.14 of MIL-E-5007B with the forces acting at the center of gravity of the engine.

4.3.16 Pump Weight. - The weight of the complete pump shall not exceed 35 lbs.

4.3.17 Reliability Analysis - The vendor shall provide three (3) copies of a reliability analysis of the fuel pump based upon a single failure concept. This analysis shall be submitted to Pratt & Whitney Aircraft for review prior to approval of the design for manufacture of experimental units.

4.3.18 One pump is required per engine. The mounting provisions, fuel connections and limiting contours shall be coordinated with and approved by the PWA Engineering Department. The pump will rotate* when viewing the drive pad end of the pump. The ratio of pump drive shaft speed to high pressure rotor speed will be .568 N_2.

4.3.19 Accessibility. - All parts of the pump requiring routine service checking or replacement while on the engine shall be made readily accessible.

4.3.20 Mockup. - A mockup of the fuel pump shall be provided prior to the delivery of the first experimental pump, and shall be maintained such that it accurately defines the outline, pump mounting pad and all connections. Prior to making any changes affecting the installation of envelope a mockup must be prepared or the existing mockup revised and submitted to PWA Engineering Department for coordination of installation requirements.

4.3.21 Installation Connections. - Where internal straight screw threads are provided on the pump for the attachment of aircraft or engine fittings, the bosses shall be in accordance with Drawing AND 10049, Revision 1, and sufficient clearance shall be provided for installing hose nipples or flared tube fittings. The overboard drain connection must be located such that it is at the bottom of the pump when mounted on the engine.

*To be supplied at a later date

4.4 Performance. - The pump performance shall meet the following requirements:

Condition	Installation A, I	Installation B, I
Fuel	MIL-J-5624E Grade JP-5**	MIL-J-5624E Grade JP-5**
Fuel Temperature	75 to 85 F	75 to 85°F
Pump Inlet Pressure	13.5 psia Maximum	13.5 psia Maximum
Pump Speed	4700 RPM	4700 RPM
Pump Discharge Flow	88.3 GPM (Min) 93.3 GPM (Max)	96.6 GPM (Min) 101.6 GPM (Max)
Pump Discharge Pressure	750 PSIG	800 PSIG
Pressure Over Fuel in Tank	14.7 PSIA	14.7 PSIA

Condition	Installation A, II	Installation B. II
Fuel	MIL-J-5624E Grade JP-5*	MIL-J-5624E Grade JP-5**
Fuel Temperature	75 to 85°F	75 to 85°F
Pump Inlet Pressure	13.5 psia Maximum	13.5 psia Maximum
Pump Speed	1070 RPM	1025 RPM
Pump Discharge Flow	8.[illegible] GPM (Min)	7.9 GPM (Min)
Fluid Discharge Pressure	150 PSIG Gear Stage Rise	150 PSIG Gear Stage Rise
Pressure Over Fuel in Tank	14.7 PSIA	14.7 PSIA

Condition	Installation A, III	Installation B, III
Fuel	MIL-J-5624E Grade JP-5**	MIL-J-5624E Grade JP-5**
Fuel Temperature	100°F Minimum	100°F Minimum
Pump Inlet Pressure	7.4 in Hg abs (.45 V/L)	7.4 in Hg abs (.45V/L)
Pump speed	4715 RPM	4715 RPM
Fluid flow	65.2 GPM	71.3 GPM
Bypass flow	Pump capacity less 65.2 GPM	Pump capacity less 71.3 GPM
Pressure over fuel in tank	23.98 in Hg abs	23.98 in Hg abs
Pump Discharge Pressure	650 PSIG	700 PSIG

4.4 Performance. - The pump performance shall meet the following requirements:

Condition	Installation A, I	Installation B, I
Fuel	MIL-J-5624E Grade JP-5**	MIL-J-5624E Grade JP-5**
Fuel Temperature	75 to 85°F	75 to 85°F
Pump Inlet Pressure	13.5 psia Maximum	13.5 psia Maximum
Pump Speed	4700 RPM	4700 RPM
Pump Discharge Flow	88.3 GPM (Min)	96.6 GPM (Min)
	93.3 GPM (Max)	101.6 GPM (Max)
Pump Discharge Pressure	750 PSIG	800 PSIG
Pressure Over Fuel in Tank	14.7 PSIA	14.7 PSIA

Condition	Installation A, II	Installation B, II
Fuel	MIL-J-5624E Grade JP-5*	MIL-J-5624E Grade JP-5**
Fuel Temperature	75 to 85°F	75 to 85°F
Pump Inlet Pressure	13.5 psia Maximum	13.5 psia Maximum
Pump Speed	1070 RPM	1025 RPM
Pump Discharge Flow	8.0 GPM (Min)	7.9 GPM (Min)
Fluid Discharge Pressure	150 PSIG Gear Stage Rise	150 PSIG Gear Stage Rise
Pressure Over Fuel in Tank	14.7 PSIA	14.7 PSIA

Condition	Installation A, III	Installation B, III
Fuel	MIL-J-5624E Grade JP-5**	MIL-J-5624E Grade JP-5**
Fuel Temperature	100°F Minimum	100°F Minimum
Pump Inlet Pressure	7.4 in Hg abs (.45 V/L)	7.4 in Hg abs (.45 V/L)
Pump speed	4715 RPM	4715 RPM
Fluid flow	65.2 GPM	71.3 GPM
Bypass flow	Pump capacity less 65.2 GPM	Pump capacity less 71.3 GPM
Pressure over fuel in tank	23.98 in Hg abs	23.98 in Hg abs
Pump Discharge Pressure	650 PSIG	700 PSIG

Condition	Installation A, IV	Installation B, IV
Fuel	MIL-J-5624 Grade JP-5**	MIL-J-5624 Grade JP-5**
Fuel Temperature	110°F Minimum	110°F Minimum
Pump Inlet Pressure	2.75 In Hg abs (0.45 V/L)	2.75 In Hg abs (0.45 V/L)
Pump Speed	4630 RPM	4630 RPM
Fluid Flow	39.7 GPM	43.4 GPM
Bypass Flow	Pump Capacity Less 39.7 GPM	Pump Capcity Less 43.4 GPM
Pressure Over Fuel In Tank	8.88 In Hg abs	8.88 In Hg abs
Pump Discharge Pressure	500 PSIG	525 PSIG

Condition	Installation A, V	Installation B, V
Fuel	MIL-J-5624 E Grade JP-5**	MIL-J-5624E Grade JP-5**
Fuel Temperature	220 F	240°F
Pump Inlet Pressure	True V. P. + 5.0 PSI (Weathered Fuel)	True V. P. + 5.0 psi (Weathered Fuel)
Pump Speed	4630 RPM	4630 RPM
Fluid Flow	41.7 GPM	45.7 GPM
Bypass Flow	Pump Capacity less 41.7 GPM	Pump capacity less 45.7 GPM
Pump Discharge Pressure	500 PSIG	525 PSIG
Fuel Tank Pressure	8.88 In Hg ABS	8.88 In Hg ABS

Condition	Installation A, VI	Installation B, VI
Fuel	MIL-J-5624E Grade JP-5**	MIL-J-5624E Grade JP-5**
Fuel Temperature	100°F Minimum	100°F Minimum
Pump Inlet Pressure	11.1 In Hg abs	11.1 In Hg abs
Pump Speed	1420 RPM	1420 RPM
Fluid Flow	4.6 GPM	5.0 GPM
Pump Discharge Pressure	250 PSIG	250 PSIG
Fuel Tank Pressure	11.1 In Hg abs	11.1 In Hg abs

Condition	Installation A, VII	Installation B, VII
Fuel	MIL-J-5624E Grade JP-5**	MIL-J-5624E Grade JP-5**
Fuel Inlet Temperature	250°F	250°F
Fuel Temperature at Bypass Return	325°F	325°F
Pump Inlet Pressure	0.7 In Hg abs - Weathered Fuel (.45 V/L)	0.7 In Hg abs Weathered Fuel (.45 V/L)
Pump Speed	4900	4900
Fluid Flow	19.6 GPM	21.5 GPM
Bypass Flow	Pump Capacity less 19.6 GPM	Pump Capacity less 21.5 GPM
Pump Discharge Pressure	350 PSIG	350 PSIG
Fuel Tank Pressure	1.04 In Hg abs	1.04 In Hg abs

** The fuel shall have a true vapor pressure which is not less than 0.5 psi at 175°F and 2.5 psi at 250°F

VIII

The pump shall be capable of priming itself when subjected to a dry life of 4 foot at an inlet pressure of 9 in. Hg. ABS.

5. INSPECTION AND TEST PROCEDURES

5.1 General. - The fuel pumps under this specification shall be subject to inspection by authorized representatives of the government and Pratt & Whitney Aircraft, both of whom shall be given all reasonable facilities to determine conformance with this specification. Unless otherwise specifically authorized, all tests, except the engine qualification test, shall be conducted at the vendor's plant.

5.1.1 Pump Position - During all tests, the fuel pump shall be mounted as installed on the engine insofar as practicable.

5.2 Preliminary Flight Rating Test:

5.2.1 Altitude Proof Test - The fuel pump to be used for this test shall be inspected for conformance to the vendor's parts list prior to assembly. The pump shall then be subjected to an acceptance test in accordance with paragraph 6.4 of this specification. Following the acceptance test, the fuel pump shall be operated for five (5) hours at the conditions specified in paragraph 6.2.1.1. There shall be no evidence of external leakage during the altitude proof test except 10 drops per minute or less at the drain provided. Upon completion of this altitude proof test, the pump shall again be subjected to the acceptance test specified in paragraph 6.4 and shall subsequently be disassembled for inspection of detail parts. This calibration and inspection shall reveal the pump performance to remain within allowable service limits and all detail parts to be suitable for continued service utilization.

5.2.1.1 Altitude Proof Test Condition -

Condition	Condition A	Condition B
Fuel	MIL-J-5624E Grade JP-5	MIL-J-5624E Grade JP-5
Fuel Temperature	100°F Minimum	100°F Minimum
Pump Speed	4770 RPM	4770 RPM
Fuel Pressure at Pump Inlet	7.5 In Hg abs	7.5 In Hg abs
Fluid Flow	67.2 GPM	73.5 GPM
By-Pass Flow	Pump Capacity less 67.2 GPM	Pump Capacity Less 67.2 GPM
Pump Discharge Pressure	725 PSIG	775 PSIG
Fuel Tank Pressure	23.98 In Hg abs	23.98 In Hg abs

During the course of this proof test, a vapor liquid ratio of 0.45 or greater shall be imposed on the pump at the inlet.

5.3 Qualification Test

5.3.1 Requirements. - Approval as a type of fuel pump procured under this specification for a prototype engine shall be contingent upon satisfactory completion of a 60 hour preliminary flight rating test in accordance with MIL E-5150C and satisfactory completion of an altitude proof test in accordance with paragraph 6.2 of this specification. Approval as a type of fuel pump for a production engine shall be contingent upon satisfactory completion of the 150-hour engine qualification test in accordance with MIL-E-5009B, section 1.2, and satisfactory completion of the component qualification tests in accordance with MIL-E-5009B, Section 4.3, as modified below. The component qualification test procedure shall be approved in writing by Pratt & Whitney Aircraft before initiation of the tests.

5.3.2 Non-Conforming Component - In the event that production units are shipped prior to satisfactory completion of the component qualification testing, the vendor shall be responsible for retrofitting these units with all engineering changes required to duplicate the unit which satisfactorily complete the component qualification test specified herein, except those changes which in the opinion of the cognizant PWA project engineer were not required to pass the qualification test. These exceptions are to be designated by the PWA project engineer's written approval. The acceptance of limited quantities of production units may not be contingent upon completion of the qualification tests specified in paragraph 5.3.1.

5.3.3 General Inspection - Prior to the tests, all parts and assemblies of the pump shall be inspected to determine if they conform to the vendor's part list and all requirements of the contract and specifications under which they were built including a dimensional inspection. At no time during the test shall any part of the pump be removed, disassembled, or adjusted without prior approval of the cognizant Pratt & Whitney Aircraft project engineer and the government inspector.

5.3.4 Leakage. - During qualification tests, there shall be no traces of external fluid leakage other than that permitted by paragraph 4.3.12 above.

5.3.5 Qualification Test Instrumentation - Sufficient instrumentation shall be provided to indicate that the performance of each element of the pump remains within service limits throughout the test. Functional checks shall be performed at the end of each test or group of tests and at other times at the option of the vendor.

5.3.6 Fuel Pump Qualification Test - The vendor shall comply with the qualification test requirements listed below and the tests shall be conducted in the order listed. Prior to starting the test, the vendor shall submit a detailed outline of the component test schedule for approval by the cognizant PWA engineer to show conformance with this purchase specification.

5.3.6.1 Fuel Pump Calibration - Prior to and upon completion of the fuel pump qualification tests, the fuel pump shall be completely calibrated. The results of these calibrations shall demonstrate that the unit has not changed its calibration beyond allowable service limits. The same type fluid shall be used during both calibrations.

5.3.6.2 Accelerated Aging - *

5.3.6.3 High Temperature - *

5.3.6.4 Room Temperature Endurance - *

5.3.6.5 Low Temperature - *

5.3.6.6 Fuel pump cavitation - *

5.3.6.7 Operation of the High Pressure Relief Valve *

5.3.6.8 Recalibration - *

5.3.6.9 Teardown Inspection - *

*To be supplied at a later date.

5.3.6.10 Contamination Test Without Micronic Filter - *

5.3.6.11 Recalibration and Inspection - *

*To be supplied at a later date.

5.3.7 Reports - Reports of pump qualification tests under this specification shall be attested to by an appropriate government representative and shall contain, essentially, the following items:

1. Title page
2. Abstract
3. List of Illustrations
4. Summary
5. Conclusions and Recommendations
6. Description (General description of the pump and detailed description of novel features)
7. Method of Test (General description of test equipment and procedure)
8. Record of Test (Chronological history of all events in connection with all of the testing)
9. Analysis of Results (A complete discussion of all phases of the test, such as probably reasons for failure, unusual wear, and analysis of general operation)
10. Calibration and Recalibration data. Suitable curves defining the pump performance before and after the qualification test shall be provided.

11. Data. Copies of all original data sheets shall be submitted upon request. Tabulated data shall be sufficient to ascertain compliance with the qualification test requirements of the specification and shall include at least the following:

Type and serial number of pump

Date and time of day

Total endurance time and number of functional cycles

Fuel (type, actual specific gravity, and viscosity)

Barometer reading

Ambient temperature

Fuel inlet temperature

Pump inlet pressure

Pump discharge pressure

12. Photographs showing general pump condition and details of all failures and unusual wear conditions.

5.3.7.1 Number of Copies - Twelve copies of the pump qualification report shall be provided for transmittal to the government by Pratt & Whitney Aircraft.

5.4 Acceptance Test - Each pump shall be subjected to an acceptance test performed by the vendor to determine that the pump will meet the functional requirements established by this specification. The acceptance test schedule and calibration limits and changes thereto shall require written approval by the cognizant Pratt & Whitney Aircraft project engineer.

5.4.1 Pump Inspection. - Fuel pumps shall be inspected for conformance with the vendor's parts list currently released to production by initial release or revised by subsequent engineering change.

5.4.2 Pressure Test - All pump assemblies or component castings, covers, and enclosures of the pump shall be subject to 1650 psi on the high pressure side or system and 150 psi on the inlet or interstage portion without fracture or permanent deformation.

5.4.3 Data - The vendor shall supply one copy of the acceptance test data of each pump procured under this specification.

5.4.4 Delivery - The vendor shall be responsible for delivery of acceptance test data for each pump to the purchaser not later than the data on which the pump is received.

6. VENDOR RESPONSIBILITIES

6.1 Preparation for Storage - The fuel pump shall be prepared for storage prior to shipment in a manner acceptable to PWA

6.2 Prior to acceptance of the qualification test on the pump the vendor shall beresponsible for making changes and supplying hardware for correcting deficiencies found in the development units. If a change of requirements is made, costs arising from such changes will be subject to separate negotiations. In order to support the development units, the vendor shall maintain or shall be able to obtain in a reasonable time spare parts for procurement by PWA.

6.3 The vendor shall give full support to the development program by providing an adequate engineering development effort which shall include bench development and endurance tests on pumps to insure satisfactory operation of the pump at PWA both on the bench and engine to the requirements listed in this specification. An outline of the vendor's proposed development program shall be forwarded to PWA prior to the issuance of any purchase orders for units.

6.4 The vendor shall be responsible for retrofitting of all experimental units with all engineering changes required to duplicate the unit which satisfactorily completes the appropriate qualification tests, except those changes which in the opinion of the cognizant Pratt & Whitney Aircraft project engineer were not required to pass the appropriate qualification tests. These exceptions are to be designated by the Pratt & Whitney Aircraft project engineer's written approval. Delivery schedule of retrofit parts must be in accordance with engine development schedule.

6.5 Drawings. - The vendor shall supply one reproducible copy of all drawings pertaining to the pump. Drawings shall also be supplied providing design information for special tools, fixtures, fittings and adapters which will be required during development testing or field use.

6.6 Reliability Analysis - The vendor shall provide three copies of a reliability analysis of the fuel pump based upon a single failure concept. This analysis shall be submitted to PWA for review prior to approval of the design for manufacture of experimental units.

Date: 6 October 1964

1. SCOPE

1.1 This specification establishes requirements for an engine driven hydraulic pump to be used on a typical SST engine.

2. DESCRIPTION

2.1 The pump shall be engine driven and be capable of pumping the required volume of hydraulic fluid at the required pressure throughout the engine operating envelope.

3. APPLICABLE PUBLICATIONS

3.1 The applicable specifications and standards listed in ANA Bulletin No. 343n shall form a part of this specification to the extent specified herein.

3.2 The following specifications and publications shall form a part of this specification to the extent specified herein.

PWA PMC-9041	Test Fluid
PWA-PS-720A	Vendor Responsibilities

4. REQUIREMENTS

4.1 General Requirements

4.1.1 Materials and Processes. - Materials and processes used in the manufacture of this pump shall be of high quality suitable for the purpose, and shall conform to applicable specifications listed in ANA Bulletin No. 343n. When vendor specifications are used for material or processes which affect performance or durability of the finished product, such specifications shall be subject to release to the government. The use of non-governmental specifications shall not constitute waiver of government inspection.

4.1.1.1 Dissimilar Metals. - The use of dissimilar metals in contact, as defined on Drawing MS 33586A shall be avoided wherever practicable.

4.1.1.2 Use of AMS 5610, 5620, 5621, 5630, 5631, and 5632 Materials. - The use of the subject heat treatable stainless steels or equivalents is prohibited unless agreed upon in writing by PWA Engineering.

4.1.2 Standard [illegible] ts - AN or MS standard parts, selected from those listed in ANA Bulletin No. 343n, shall be used unless it is determined that they are unsuitable for the purpose. They shall be identified by their standard part numbers.

4.1.3 Protective Treatments and Coatings. - Protective treatments and coatings shall be in accordance with applicable specifications listed in ANA Bulletin No. 343n. With the exception of the areas listed below, all parts not in constant contact with oil shall be either corrosion-resistant or suitably protected.

1. Working surfaces
2. Threads
3. Drive pad faces

4.1.4 Screw Threads. - All conventional straight screw threads shall conform to the requirements of MIL-S-8879 except paragraph 3.12. These include threads on standard hardware bolts and nuts, tapped holes receiving standard items, nuts for use on studs, and threads for non-standard parts where a new thread size is being incorporated in a new design or redesign and where tooling is not already available. These requirements need not apply to electrical connectors, ignition harness, thermocouple harness, interference fit threads, either thread end of studs, fluid fittings, fluid fitting bosses, tube coupling nuts, ground or cut threads, threads of non-standard items where similar parts with the same thread are already designed and tooling is already available, and helical inserts including tapped holes for same where it has been determined that the inserts will accept a MIL-S-8879 external thread."

4.1.5 Serialization - Serial numbers of pumps procured under this specification shall not duplicate serial numbers of other similar components supplied by the vendor to Pratt & Whitney Aircraft. A sufficiently large block of serial numbers shall be assigned to the basic control model to cover anticipated production. The use of letters in serial identification shall be avoided.

4.1.6 Data Plate - A data plate shall be attached to the pump and shall include the following information:

(1) Manufacturer's name and trade-mark
(2) Manufacturer's part list number
(3) Manufacturer's part number
(4) Control serial number

4.2 Test Requirements

4.2.1 Qualification Test. - Approval as a type of hydraulic pump for a prototype engine shall be contingent upon satisfactory completion of a Preliminary Flight Rating Engine test in accordance with MIL-E-5156C and upon satisfactory completion of a 5 hour altitude proof test specified in

paragraph 5.2 of this purchase specification. Approval as a type of hydraulic pump for a production engine procured under this specification shall be contingent upon satisfactory completion of a 150-hour engine qualification test in accordance with MIL-E-5009B and satisfactory completion of a component qualification test specified in paragraph 5.2 of this specification. The component qualification test procedure shall be approved in writing by Pratt & Whitney Aircraft before initiation of the tests.

4.2.1.1 Reports. - Reports of the hydraulic pump qualification tests under this specification shall be attested to by an appropriate government representative and shall include at least the items mentioned in paragraph 5.2.5 of this specification. Twelve copies of this report shall be supplied to the Engineering Department of Pratt & Whitney Aircraft for transmittal to the government.

4.2.1.2 Shipment of Production Units Prior to Approval. - In the event that production units are shipped prior to satisfactory testing, the vendor shall be responsible for retrofitting these units with all engineering changes required to duplicate the unit which satisfactorily completes the component qualification test, except those changes which in the opinion of the cognizant PWA project engineer were not required to pass the qualification test. These exceptions are to be designated by the PWA project engineer's written approval. The acceptance of limited quantities of production units may not be contingent upon completion of the qualification tests as specified in paragraph 4.2.1.

4.2.2 Acceptance Test. - Prior to delivery, each hydraulic pump procured under this specification shall be subjected to an acceptance test as specified in paragraph 5.4.

4.3 Design Requirements - This section establishes design requirements for the hydraulic pump and should not be construed as inspection requirements for production pumps.

4.3.1 General - The following design features shall apply:

4.3.1.1 All relief bypass and check valves shall be designed and located such that free water will not be trapped in any manner which will affect normal pump operation.

4.3.1.2 The use of slotted head screws will not be permitted.

4.3.1.3 The use of copper or copper alloys in areas exposed to fuel is prohibited.

4.3.1.4 The use of snap rings as stressed retainers is discouraged and will not be allowed in critical locations where failure of the snap

ring can result in a performance loss. A review with Pratt & Whitney Aircraft Engineering of each design location utilizing a snap ring is required and is subject to Pratt & Whitney Aircraft approval.

4.3.2 Fuel - The pump shall operate satisfactorily throughout the complete engine operating range for steady state and transient operating conditions when using fuels conforming to specification MIL-J-5624E, Grades JP-4 and JP-5 aving any of the variations in characteristics permitted by specification MIL-J-5624E for these grades. The pump shall operate satisfactorily under all operating conditions when the absolute fuel pressure at the fuel inlet connection is from a minimum of 10 psi above the vapor pressure of the fuel used to 165 psia with a V/L ratio of zero. The pump shall also function satisfactorily throughout its complete operating range when using Grade JP-4 fuel with the addition of an anti-icing fluid conforming to MIL-I-27686 at a concentration between 0.13 and 0.15% by volume.

4.3.2.1 Fuel Contamination - The pump shall function satisfactorily when using fuel contaminated to the extent of 80 grams of foreign matter per 1000 gallons. Satisfactory operation on contaminated fuel shall mean that the contaminated fuel will not in itself precipitate a sudden pump failure but may cause gradual deterioration of pump performance and abnormal wear of pump parts. This foreign matter shall be considered to consist of not less than 68% SiO_2 and shall have a particle-size analysis as follows:

Particle Size Microns	Percent of Total
0 - 5	39±2 by weight
5 - 10	18±3 by weight
10 - 20	16±3 by weight
20 - 40	18±3 by weight
Over 40	9±3 by weight
Through a 200-mesh screen	100 by weight

4.3.2.2 Fuel Filtration - Fuel filtered through a filter having a 10 micron rating will be provided by Pratt & Whitney Aircraft at the inlet to the hydraulic pump.

4.3.3 Fuel and Ambient Temperature Limits - The pump shall be designed to operate satisfactorily with the following surrounding ambient air temperature and fuel inlet temperatures:

	Ambient Air Temperature	Inlet Fuel Temperature
Requirement A	-65 to 550°F	-65** to 300°F
Requirement B	-65 to 750°F	-65** to 320°F

** - This applies for MIL-J-5624 Grade JP-4 Fuel only, when using MIL-J-5624 Grade JP-5 the applicable temperature would correspond to a fuel viscosity of 12 centistokes.

4.3.4 Maximum Pressure - The pump shall be capable of withstanding without fracture or permanent deformation a surge pressure 3000 psi above the normal working pressure of 1500 ± 100 psig. The inlet portion of the pump must be capable of withstanding 400 psig without permanent deformation. Tests to demonstrate this requirement shall be subject to the approval of the c ;nizant Pratt & Whitney Aircraft project engineer, and shall be repeated when changes or process modifications are incorporated which, in opinion of the Pratt & Whitney Aircraft project engineer, might adversely affect pump strength. Burst pressure tests must be performed on one development unit to destruction.

4.3.5 Drive Shaft Seal Leakage - Drive shaft seal leakage from the drain provided shall not exceed 10 drops per minute under any operating conditions.

4.3.6 Pump Weight - The weight of the complete pump shall not exceed 50.0 pounds.

4.3.7 Pressure Taps - External pressure taps shall be provided at the following points through the pump:

a. Pump centrifugal stage discharge
b. Pump discharge before outlet check valve
c. Pump discharge after outlet check valve

4.3.8 Temperature Rise - The fluid temperature rise from pump inlet to pump discharge must not exceed 20°F at flow conditions of 6.0 gpm or above.

4.3.9 Maneuver Loading - When mounted on the engine as shown in Figure 1, the pump shall be capable of withstanding, without permanent deformation or failure, the flight maneuver forces specified in paragraph 3.14 of MIL-E-5007B, with the forces acting at the center of gravity of the engine.

4.3.10 Lubrication - The pump shall incorporate provisions for lubrication of the drive spline from the engine oil system.

4.3.11 One pump is required per engine. The mounting provisions, fuel connections and limiting contours shall be coordinated with and approved by the Pratt & Whitney Aircraft Engineering Department. The ratio of pump drive shaft speed to high pressure rotor speed will be .5680 N_2.

4.3.12 Accessibility - All parts of the pump requiring routine service checking or replacement while on the engine shall be readily accessible.

4.3.13 Mockup - A fuel pump mockup, which shall accurately define the outline, pump mounting pad, and all connections, shall be provided prior to the delivery of the first experimental pump. Prior to making any changes affecting the installation or envelope a mockup must be prepared or the mockup revised and submitted to Pratt & Whitney Aircraft Engineering Department for coordination of installation requirements. Changes shall be the subject of separate negotiations.

4.3.14 Installation Connections - Where internal straight screw threads are provided on the pump for the attachment of aircraft or engine fittings, the bosses shall be in accordance with Drawing AND 10049, Revision 1; and sufficient clearance shall be provided for installing hose nipples or flared tube fittings.

4.3.15 Reliability Analysis - The vendor shall provide three copies of a reliability analysis of the fuel pump based upon a single failure concept. This analysis shall be submitted to Pratt & Whitney Aircraft for review prior to approval of the design for manufacture of experimental units.

4.4 Performance and Operational Requirements - The pump performance shall be adequate to meet the following requirements.

Condition I

Fuel	MIL-J-5624E, Grade JP-4
Fuel Temperature	300°F
Pump inlet pressure	165 psia
Pump speed	4700 RPM
Pump discharge flow	50 gpm (min) 52 gpm (max)
Pump discharge pressure	1500 ± 100 psig

Condition II

Fuel	MIL-J-5624E, Grade JP-4
Fuel Temperature	75-85°F
Pump inlet pressure	20 psig
Pump speed	2500 RPM
Pump discharge flow	26 gpm (min)
Pump discharge pressure	1500 ± 100 psig

5. INSPECTION AND TEST PROCEDURES

5.1 General - the fuel pumps under this specification shall be subject to inspection by authorized representatives of the government and Pratt & Whitney Aircraft, who shall be given all reasonable facilities to determine conformance with this specification. Unless otherwise specifically authorized, all tests, except the engine qualification test, shall be conducted at the vendor's plant.

5.1.1 Pump Positions - During all tests listed below, the fuel pump shall be mounted as installed on the engine insofar as practicable.

5.2 Altitude Proof Test - The fuel pump to be used for this test shall be inspected for conformance to the vendor's parts list prior to assembly. The pump shall then be subjected to an acceptance test in accordance with paragraph 5.4 of this specification. Following the acceptance test, the fuel pump shall be operated for five (5) hours at the conditions specified in paragraph 5.2.1. There shall be no evidence of external leakage during the altitude proof test except 10 drops per minute or less at the drain provided. Upon completion of the altitude proof test, the pump shall again be subjected to the acceptance test specified in paragraph 5.4 and shall subsequently be disassembled for inspection of detail parts. This calibration and inspection shall reveal the pump performance to remain within allowable service limits and all detail parts to be suitable for continued service utilization.

5.2.1 Altitude Proof Test Conditions

Fuel	MIL-J-5161E, Grade 1
Fuel Temperature	100°F min.
Pump speed	4770 RPM
Fuel Pressure at Pump Inlet	10 psi above true vapor pressure of fuel
Pump Discharge Flow	50 gpm
Pump Discharge Pressure	1500 psig
Fuel Tank Pressure	Sea level

5.3 Qualification Test

5.3.1 General Inspection - Prior to the test, all parts and assemblies of the pump shall be inspected to determine if they conform to the vendor's parts list and all requirements of the contract and specifications under which they were built including a dimensional inspection. At no time during the test shall any part of the pump be removed, disassembled or adjusted without prior approval of the cognizant Pratt & Whitney Aircraft project engineer and the government inspector.

5.3.2 Leakage - During qualification tests, there shall be no traces of external fluid leakage other than that permitted by paragraph 4.3.5

5.3.3 Fuel Pump Calibration - Prior to and upon completion of the fuel pump qualification tests, the fuel pump shall be completely calibrated and shall indicate that the unit has not changed its calibration beyond allowable service limits. The same type fluid shall be used during both calibrations.

5.3.3.1 Qualification Test Instrumentation - Sufficient instrumentation shall be provided to indicate that the performance of all elements of the pump remain within service limits throughout the test. Functional checks shall be performed at the end of each test or group of tests and at other times at the option of the vendor.

5.3.4 Fuel Pump Qualification Test - The vendor shall comply with the qualification test requirements listed below and the test shall be conducted in the order listed. Prior to starting the test, the vendor shall submit a detailed outline of the component test schedule for approval by the cognizant Pratt & Whitney Aircraft engineer to show conformance with MIL-E-5009B and this purchase specification.

5.3.4.1 Accelerated Aging - *

5.3.4.2 High Temperature - *

5.3.4.3 Room Temperature Endurance - *

5.3.4.4 Low Temperature - *

5.3.4.5 Fuel Pump Cavitation - *

5.3.4.6 Recalibration - *

5.3.4.7 Teardown Inspection - *

* To be supplied at a latter date.

5.3.5 Reports - Reports of pump qualification tests under this specification shall be attested to by an appropriate government representative and shall contain, essentially, the following items:

1. Title page
2. Abstract
3. List of Illustrations
4. Summary
5. Conclusions and Recommendations
6. Description (General description of the pump and detailed description of novel features)
7. Method of Test (General description of test equipment and procedure)
8. Record of Test (Chronological history of all events in connection with all of the testing)
9. Analysis of Results (a complete discussion of all phases of the test, such as probable reasons for failure, unusual wear, and analysis of general operation)
10. Calibration and recalibration data. Suitable curves defining the pump performance before and after the qualification test shall be provided.
11. Data copies of all original data sheets shall be submitted upon request. Tabulated data shall be sufficient to ascertain compliance with the qualification test requirements of the specification and shall include at least the following:

    Type and serial number of pump
    Date and time of day
    Total endurance time and number of functional cycles
    Fuel (type, actual specific gravity, and viscosity)
    Barometer reading
    Ambient Temperature
    Fuel inlet temperature
    Pump inlet temperature
    Pump discharge pressure
12. Photographs showing general pump condition and details of all failures and unusual wear conditions.

5.4 Acceptance Test - Each pump shall be subjected to an acceptance test performed by the vendor to determine that each pump will meet the functional requirements established by this specification. The acceptance test schedule and calibration limits and changes thereto shall require written approval by the cognizant Pratt & Whitney Aircraft project engineer.

5.4.1 Pump Inspection - Fuel pumps shall be inspected for conformance with the vendor's parts list currently released to production by initial release or revised by subsequent engineering change.

5.4.2 Pressure Test - All pump assemblies or component castings, covers, and enclosures of the pump shall be subject to 3500 psi on the high pressure side of the system and 250 psi on the inlet portion without fracture or permanent deformation.

5.4.3 Data - The vendor shall supply one copy of the acceptance test data of each pump procured under this specification.

5.4.4 Delivery - The vendor shall be responsible for delivery of acceptance test data to the purchaser not later than the date on which the material is received.

6. VENDOR RESPONSIBILITIES

6.1 At the request of Pratt & Whitney Aircraft Engineering the vendor shall supply three copies of a reliability analysis report of the hydraulic pump based on a single failure concept.

6.2 Prior to acceptance of the qualification test on the pump, the vendor shall be responsible for making changes and supplying hardware for correcting deficiencies found in the development units. If a change of requirements is made, costs arising from such changes will be subject to separate negotiations. In order to support the development units, the vendor shall maintain or shall be able to obtain in a reasonable time spare parts for procurement by Pratt & Whitney Aircraft.

6.3 The vendor shall give full support to the development program by providing an adequate engineering development effort which shall include bench development and endurance tests on pumps to insure satisfactory operation of the pump at Pratt & Whitney Aircraft both on the bench and engine to the requirements listed in this specification. An outline of the vendor's proposed development program shall be forwarded to Pratt & Whitney Aircraft prior to the issuance of any purchase orders for units.

6.4 Drawings - The vendor shall supply one reproducible copy of all drawings pertaining to the pump. These drawings shall also provide design information for special tools, fittings and adapters that will be required during development testing or field use.

6.5 The vendor shall be responsible for retrofitting of all experimental units with all engineering changes required to duplicate the unit which satisfactorily completes the appropriate qualification tests, except those changes which in the opinion of the cognizant Pratt & Whitney Aircraft project engineer were not required to pass the appropriate qualification test. These exceptions are to be designated by the Pratt & Whitney Aircraft project engineer's written approval. Delivery schedule of retrofit parts must be in accordance with engine development schedule.

6.6 Preparation for Storage - The fuel pump shall be prepared for storage prior to shipment in a manner acceptable to the purchaser.

PRELIMINARY

Pratt & Whitney Aircraft Date: 2? October 1964

1. SCOPE

This specification establishes the requirements for a duct heater turbopump used on a typical SST engine.

2. DESCRIPTION

The duct heater fuel pump consists of a dual element centrifugal unit driven by an auxiliary air turbine.

The air turbine is supplied with a controlled amount of bleed air flow taken from the engine high compressor discharge. The air flow to the turbine is controlled through a butterfly valve such that a predetermined pump discharge pressure is maintained. During non-duct heating a small amount of bleed air is provided to drive the turbine and provide a low fuel flow to circulate through the pump and the duct heater fuel control. The turbopump shall use engine fuel for bearing and seal cooling during all operating conditions.

3. APPLICABLE PUBLICATIONS

3.1 The applicable specifications and standards listed in ANA Bulletin 343n shall form a part of this specification to the extent specified herein.

3.2 The following specifications and publications shall form a part of this specification to the extent specified herein.

PWA-PS-320-A	Vendor Responsibilities
PWA 522-D	Fuel
PMC 9041	Calibrating Fuel

3.3 All applicable curves drawings, approvals of test programs, specifications, mission cycle requirements, etc., referenced in this specification, shall be supplied the vendor by a letter or letters of transmittal from the cognizant P&WA project engineer.

4. REQUIREMENTS

4.1 General Requirements

4.1.1 Materials and Processes - Materials and processes used in the manufacture of this turbometer shall be of high quality and suitable for the purpose. Material specification shall conform to the applicable specification listed in ANA Bulletin 343n. P&WA must be advised what materials are being used so that fuel compatibility tests may be conducted.

4.1.1.1 Dissimilar Metals - The use of dissimilar metals in contact, as defined on Drawing MS-33586A shall be avoided wherever possible.

4.1.1.2 Use of AMS 5610, 5620, 5621, 5630, 5631, and 5632 Materials. - The use of the subject heat treatable stainless steels or equivalents is prohibited unless agreed upon in writing by P&WA Engineering.

4.1.2 Standard Parts - AN or MS standard parts, selected from those listed in ANA Bulletin 343n, shall be used unless it is determined that they are unsuitable for the purpose. They shall be identified by their standard part numbers.

4.1.3 Protective Treatments and Coatings. -Protective treatment and coatings shall be in accordance with applicable specifications listed in ANA Bulletin 343n with the exception of the areas listed below. All parts not in constant contact with fluid shall be corrosion resistant or suitably protected.

1) working surfaces
2) threads
3) mounting surfaces

4.1.4 Serialization - Serial numbers of turbopumps procured under this specification shall not duplicate serial numbers of other similar components supplied by the manufacturer to Pratt & Whitney Aircraft. A sufficiently large block of serial numbers shall be assigned to the basic pump to cover anticipated production. The use of letters in serial identification shall be avoided.

4.1.5 Data Plate - A data plate shall be attached to the turbopump in a location which is visible when mounted on the engine and shall include the following information:

a. Manufacturer's name
b. Manufacturer's parts list number
c. Manufacturer's part number
d. Manufacturer's serial number

4.1.6 Screw Threads. - All conventional straight screw threads shall conform to the requirements of MIL-S 8879 except paragraph 3.12. These include threads on standard hardware bolts and nuts, tapped holes receiving standard items, nuts for use on studs, and threads for non-standard parts where a new thread size is being incorporated in a new design or redesign and where tooling is not already available. These requirements need not apply to electrical connectors, ignition harness, thermocouple harness, interference fit threads, either thread end of studs, fluid fittings, fluid fitting bosses, tube coupling nuts, ground or cut threads, threads of non-standard items where similar parts with the same thread are already designed and tooling is already available, and helical inserts including tapped holes for same where it has been determined that the inserts will accept a MIL-S-8879 external thread.

4.2 Test Requirements

4.2.1 Qualification Test. - Approval as a type of duct heater turbopump for a prototype engine shall be contingent upon satisfactory completion of a Preliminary Flight Rating Engine Test in accordance with MIL-E-5156C and upon satisfactory completion of a 5-hour altitude proof test specified in paragraph 5.2 of this purchase specification. Approval as a type of duct heater turbopump for a production engine procured under this specification shall be contingent upon satisfactory completion of the 150-hour engine qualification test in accordance with MIL-E-5009B and satisfactory completion of a component qualification test specified in paragraph 5.3 of this purchase specification. The component qualification test procedure shall be approved in writing by Pratt & Whitney Aircraft before initiation of the tests.

4.2.1.1 Reports. - Reports of the duct heater turbopump qualification tests under this specification shall be attested to by an appropriate government representative and shall include at least the items mentioned in paragraph 5.3.5 of this specification. Twelve copies of this report shall be supplied to the Engineering Department of Pratt & Whitney Aircraft for transmittal to the government.

4.2.1.2 Shipment of Production Units Prior to Approval. - In the event that production units are shipped prior to satisfactory completion of the component qualification testing, the vendor shall be responsible for retrofitting these units with all engineering changes required to duplicate the unit which satisfactorily completes the component qualification test, except those changes which in the opinion of the cognizant PWA project engineer were not required to pass the qualification test. These exceptions are to be designated by the PWA project engineer's written approval. The acceptance of limited quantities of production units may not be contingent upon completion of the qualification tests as specified in paragraph 4.2.1.

4.2.2 Acceptance Test. - Prior to delivery, each unit procured under this specification shall be subjected to an acceptance test as specified in paragraph 5.4.

4.3 <u>Design Requirements.</u> - This section establishes design requirements for the duct heater turbopump and should not be construed as inspection requirements for production pumps.

It may also be noted that requirements for two installations are specified herein. If not specifically stated the requirement shall apply to both installations.

4.3.1 <u>General.</u> - The following design features shall apply:

4.3.1.1 All relief, by-pass and check valves shall be designed and located such that free water will not be trapped in any manner which will affect normal pump operation.

4.3.1.2 The use of slotted head screws will not be permitted.

4.3.1.3 The use of copper or copper alloys in areas exposed to fuel is prohibited.

4.3.1.4 The use of snap rings as stressed retainers is discouraged and will not be allowed in critical locations where failure of the snap ring can result in a performance loss. A review with PWA Engineering, of each design location utilizing a snap ring is required and is subject to PWA approval.

4.3.2 <u>Fuel.</u> - The unit shall operate satisfactorily throughout the complete engine operating range for steady state and transient operating conditions when using fuels conforming to specification MIL-J-5624E, Grades JP-4 and JP-5, having any of the variations in characteristics permitted by specification MIL-J-5624E for these grades. The unit shall operate satisfactorily under all operating conditions when the absolute fuel pressure at the fuel inlet connection varies from a minimum of 5.0 psi above the vapor pressure of the fuel used to 50 psig with a V/L ratio of zero. The pump shall also function satisfactorily throughout its complete operating range when using grade JP-4 fuel with the addition of an anti-icing fluid conforming to MIL-I-27686 at a concentration between 0.13 and 0.15% by volume. The unit shall function satisfactorily with a fuel that has a true vapor pressure that does not exceed 0.5 psi at 175°F and 2.5 psi at 250°F.

4.3.2.1 Fuel contamination. - The unit shall be designed to operate satisfactorily on fuel containing 80 grams of foreign matter per 1,000 gallons. Satisfactory operation on contaminated fuel shall mean that the contaminated fuel will not in itself precipitate a sudden pump failure but may cause gradual deterioration of pump performance and abnormal wear of pump parts. The foreign matter shall be considered to consist of not less than 68 percent SiO_2 and shall have a particle-size analysis as follows:

Particle Size Microns	Per Cent of Total
0-5	39 ± 2 by weight
5-10	18 ± 3 by weight
10-20	16 ± 3 by weight
20-40	18 ± 3 by weight
Over 40	9 ± 3 by weight
Through a 200-mesh screen	100 by weight

4.3.3 Fuel & Ambient Temperature Limits - The unit shall be designed to operate satisfactorily with the following fuel inlet temperatures and ambient air temperatures:

	Ambient Air Temp.	Fuel Inlet Temp.
Installation A	-65 to 550°F	-65** to 250°F
Installation B	-65 to 750°F	-65** to 250°F

** - This applies for MIL-J-5624 Grade JP-4 fuel only; when using MIL-J-5624 Grade JP-5 the applicable temperature would correspond to a fuel viscosity of 12 centistokes.

4.3.4 Maximum Pressure. - The maximum normal operating pressure of the unit will be 1150 psig. Therefore, the unit shall be capable of withstanding without fracture or permanent deformation 2100 psig static pressure on the high pressure side of the unit and 250 psig on the inlet portion of the unit. Tests to demonstrate this requirement shall be subject to the approval of the cognizant PWA project engineer, and shall be repeated when changes or process modifications are incorporated which in the opinion of the PWA project engineer, might adversely affect pump strength. Burst pressure tests must be performed on one development unit to destruction.

4.3.5 Seals

4.3.5.1 It is required that all fuel-to-air seals shall reliably perform their function. No visible leakage on static seals is permissible.

4.3.5.2 All rotating or sliding shafts which require fuel-to-air seals must be provided with double seals with an interseal drain to overboard. The sealing capability of the outer seal must be no less than that of the inner seal at pressure differentials up to 40 psi. An exception to this may be the pump turbine air to overboard seal which may be a control gap type seal. All leakage past the primary seal will either be discharged to the overboard drain or to the turbine exhaust at pressure differentials up to 10 psi with maximum leakage to the turbine exhaust of 3 fluid oz/minute.

4.3.6 Fluid Leakage. - There shall be no external fuel leakage from the unit throughout the specified operating range under normal operating conditions. Leakage shall not exceed 10 drops per minute per seal and leakage from the pump overboard drain shall not exceed 40 drops per minute. Fuel leakage to ambient past the outer seal in dynamic seal applications shall not exceed 8 drops/min per seal with a minimum of 40 psig fuel pressure applied to the overboard drain except for the pump turbine air to overboard seal which will have a minimum of 10 psig fuel pressure applied across the seal and a maximum leakage of 3 fluid oz. minute into turbine air.

4.3.7 Unit Weight. - The weight of the complete turbopump shall not exceed 45 pounds for a 10,000 hour casting life expectancy.

4.3.8 Pressure Taps. - External pressure taps shall be provided at the following points through the pump.

a. Inlet to first centrifugal stage

b. Pump discharge

4.3.9 Speed Sensing. - Provisions shall be made to sense pump turbine speed. The location and design of the sensing provision shall be agreed upon by the purchaser and vendor.

4.3.10 Turbopump Air Vent - Provisions shall be incorporated to vent air trapped in the turbopump permitting normal operation.

4.3.11 Signal Lines - From 50 to 300 pph fuel flow shall exist at all times in fuel pressure signal line which pass through ambient air.

4.3.12 Maneuver Loading. - When mounted on the engine as shown in * , the unit shall be capable of withstanding, without permanent deformation or failure, the flight maneuver forces specified in paragraph 3.14 of MIL-E-5007B with the forces acting at the center of gravity of the engine.

4.3.13 Lubrication. - The unit shall incorporate provisions for lubrication of the drive shaft bearings from the engine fuel system.

4.3.14 Installation and Service

4.3.14.1 One unit is required per engine. The mounting provisions, fuel connections and limiting contours shall be coordinated with and approved by the PWA Engineering Department.

4.3.14.2 Accessibility. - All parts of the unit requiring routine service checking or replacement while on the engine shall be made readily accessible.

*To be supplied at a lat r date.

4.3.14.3 Mockup. - A mockup of the unit shall be provided prior to the delivery of the first experimental unit and maintained, which shall accurately define the outline, pump-mounting pad, all connections and the control mounting pad. Prior to making any changes affecting the installation or envelope a mockup must be prepared or the mockup revised and submitted to PWA Engineering Department for coordination of installation requirements. Changes shall be the subject of separate negotiation.

4.3.14.4 Installation Connections. - Where internal straight screw threads are provided on the unit for the attachment of aircraft or engine fittings, the bosses shall be in accordance with Drawing AND 10049, Revision 1; and sufficient clearance shall be provided for installing hose nipples or flared tube fittings.

4.3.15 Functional

4.3.15.1 Turbine

4.3.15.1.1 The turbine shall be designed to drive a dual element centrifugal pump defined by the P&WA design information with air supplied to the turbopump inlet at a maximum enthalpy defined by the pressure-temperature relationships given in the applicable P&WA curves.

4.3.15.1.2 With no fuel supplied to the pump inlet, the turbine shall be aerodynamically limited to a speed 120% of corrected turbine design speed. Fuel will be supplied to the bearings to demonstrate this requirement.

4.3.15.1.3 The turbine shall develop the required power with less than 1.5% of the engine airflow defined by the P&WA curves. Exceptions must be agreed upon in writing with P&WA engineering.

4.3.15.1.3.1 The turbine airflow will be controlled by a butterfly valve at the turbine inlet. This butterfly valve will be positioned by the pump speed controller as a function of required fuel metering section pressure drop.

4.3.15.1.3.2 In order to fully describe the pressure ratio across the turbine, the turbine discharge will be directed to ambient air pressure which is a function of air supply conditions defined by the applicable P&WA curves.

4.3.15.2 Pump

4.3.15.2.1 The centrifugal pump, defined by the applicable P&WA design information, is based on a suction specific speed necessary to provide the flows in paragraph 4.4.

4.3.15.3 Bearings

4.3.15.3.1 The lubricant shall be engine fuel supplied from the pump. The vendor shall establish the required flow to return the fuel to the system with a maximum temperature at the pump discharge of 380°F. No more than 600 pph of fuel shall be used for lubrication of bearings.

4.3.16 Reliability Analysis. - The vendor shall provide three copies of a reliability analysis of the fuel pump based upon a single failure concept. This analysis shall be submitted to Pratt & Whitney Aircraft for review prior to approval of the design for manufacture of experimental units.

4.4 Performance & Operation Requirements. - The unit performance shall be adequate to meet the following requirements for either installation:

Condition	Installation A, I	Installation B, I
Fuel	MIL-J-5624E Grade JP-5**	MIL-J-5624E Grade JP-5**
Fuel Temperature	75 to 85°F	75 to 85°F
Pump Inlet Pressure	13.5 psia max	13.5 psia max
Speed	As Required	As Required
Pump Discharge Flow	244.5 GPM	267.4 GPM
Pressure Over Fuel in Tank	14.7 PSIA	14.7 PSIA
Pump Discharge Pressure	1150 PSIG Min	1150 PSIG Min
Butterfly Valve Inlet Temperature	645°F	645°F
Butterfly Valve Inlet Pressure	190 PSIA	190 PSIA

Condition	Installation A, II	Installation B, II
Fuel	MIL-J-5624E Grade JP-5**	MIL-J-5624E Grade JP-5**
Fuel Temperature	75 to 85°F	75 to 85°F
Pump Inlet Pressure	13.5 PSIA Max	13.5 PSIA Max.
Speed	As Required	As Required
Pump Discharge Flow	173.3 GPM	189.6 GPM
Pressure Over Fuel In Tank	14.7 PSIA	14.7 PSIA
Pump Discharge Pressure	1150 PSIG Min	1150 PSIG Min
Butterfly Valve Inlet Temperature	600°F	600°F
Butterfly Valve Inlet Pressure	160 PSIA	160 PSIA

Condition	Installation A, III	Installation B, III
Fuel	MIL-J-5624 Grade JP-5**	MIL-J-5624E Grade JP-5**
Fuel Temperature	75 to 85°F	75 to 85°F
Pump Inlet Pressure	13.5 PSIA Max	13.5 PSIA Max
Speed	As Required	As Required
Pump Discharge Flow	4.1 GPM	4.1 GPM
Pressure Over Fuel In Tank	14.7 PSIA	14.7 PSIA
Pump Discharge Pressure	150 PSIG	150 PSIG
Butterfly Valve Inlet Temperature	600°F	600°F
Butterfly Valve Inlet Pressure	160 PSIA	160 PSIA

Condition	Installation A, IV	Installation B, IV
Fuel	MIL J-5624E Grade JP-5**	MIL-J-5624E Grade JP-5**
Fuel Temperature	110°F Min	110°F Min
Pump Inlet Pressure	2.75 In Hg abs (0.45 V/L)	2.75 In Hg abs (0.45 V/L)
Speed	As Required	As Required
Pump Discharge Flow	108.3 GPM	118.4 GPM
Pressure Over Fuel In Tank	8.88 In Hg abs	8.88 In Hg abs
Pump Discharge Pressure	800 PSIG	800 PSIG
Butterfly Valve Inlet Temperature	560°F	560°F
Butterfly Valve Inlet Pressure	85 PSIA	85 PSIA

Condition	Installation A, V	Installation B, V
Fuel	MIL-J-5624E Grade JP-5**	MIL-J-5624E Grade JP-5**
Fuel Temperature	250°F	250°F
Pump Inlet Pressure	1.1 In Hg abs (Weathered Fuel, .45 V/L)	1.1 In Hg abs (Weathered Fuel .45 V/L)
Speed	As required	As required
Pump Discharge Flow	84.8 GPM	92.7 GPM
Pressure Over Fuel in Tank	1.7 In Hg ABS	1.7 In Hg abs
Pressure Discharge Pressure	400 PSIG	400 PSIG
Butterfly Valve Inlet Temperature	870°F	870°F
Butterfly Valve Inlet Pressure	55 PSIA	55 PSIA

Condition	Installation VI, A	Installation VI, B
Fuel	MIL-J-5624E Grade JP-5**	MIL-J-5624E Grade JP-5**
Fuel Temperature	250°F	250°F
Pump Inlet Pressure	0.7 In Hg abs (Weathered Fuel, .45 V/L)	0.7 In Hg abs (Weathered Fuel, .45 V/L
Speed	As required	As required
Pump Discharge Flow	21.0 GPM	22.9 GPM
Pressure Over Fuel in Tank	1.03 In Hg abs	1.03 In Hg abs
Pump Discharge Pressure	350 PSIG	350 PSIG
Butterfly Valve Inlet Temperature	1030°F	1030°F
Butterfly Valve Inlet Pressure	50 PSIA	50 PSIA

** The fuel shall have a true vapor pressure which is not less than 0. 5 PSI at 175°F and 2. 5 PSI at 250°F

5. INSPECTION AND TEST PROCEDURES

5. 1 General. - The unit shall be subject to inspection by authorized representatives of P&WA, who shall be given all reasonable facilities to determine conformance with this specification. Unless otherwise specifically authorized, all tests, except the engine suitability test, shall be conducted at the vendor's plant.

5. 1. 1 Test Position - The unit must be tested while mounted in a position which is the same as its normal position on the engine.

5. 2 Altitude Proof Test. - The unit to be used for this test shall be inspected for conformance to the vendor's parts list prior to assembly. The unit shall then be subjected to an acceptance test in accordance with paragraph 5. 4 of this specification. Following the acceptance test, the unit shall be operated for five (5) hours at the conditions specified in paragraph 5. 2. 1. There shall be no evidence of external leakage during the altitude proof test except 10 drops per minute or less at the drain provided. Upon completion of the altitude proof test, the unit shall again be subjected to the acceptance test specified in paragraph 5. 4 and shall subsequently be disassembled for inspection of detail parts. This calibration and inspection shall reveal the unit performance to remain within allowable service limits and all detail parts to be suitable for continued service utilization.

5. 2. 1 Altitude Proof Test Conditions

Condition	Installation A	Installation B
Fuel	MIL-J-5624E Grade JP-5	MIL-J-5624E Grade JP-5
Fuel Temperature	100°F Min	100°F Min
Pump Inlet Pressure	7. 5 In Hg abs (. 45 V/L)	7. 5 In Hg abs (. 45 V/L)
Speed	As required	As required
Pump Discharge Flow	188. 0 GPM	205. 7 GPM
Pressure Over Fuel In Tank	23. 98 In Hg	23. 98 In Hg
Pump Discharge Pressure	1150 PSIG	1150 PSIG
Butterfly Valve Inlet Temperature	635°F	635°F
Butterfly Valve Inlet Pressure	165 PISA	165 PSIA

5.3 Qualification Test

5.3.1 General Inspection. - Prior to the tests, all parts and assemblies of the unit shall be inspected to determine if they conform to the vendor's parts list and all requirements of the contract and specifications under which they were built including a dimensional inspection. At no time during the test shall any part of the unit be removed, disassembled, or adjusted without prior approval of the cognizant Pratt & Whitney Aircraft project engineer and the government inspector.

5.3.2 Leakage. - During qualification tests, there shall be no traces of external fluid leakage other than that permitted by paragraph 4.3.6 above.

5.3.3 Unit Calibration. - Prior to and upon completion of the unit qualification tests, the turbopump shall be completely calibrated and shall indicate that the unit has not changed its calibration beyond allowable service limits. The same type fluid shall be used during both calibrations.

5.3.3.1 Qualification Test Instrumentation. - Sufficient instrumentation shall be provided to indicate that the performance of all elements of the unit remains within service limits throughout the test. Functional check shall be performed at the end of each test or group of tests and at other times at the option of the vendor.

5.3.4 Unit Qualification Test. - The vendor shall comply with the qualification test requirements listed below and the test shall be conducted in the order listed. Prior to starting the test, the vendor shall submit a detailed outline of the component test schedule for approval by the cognizant PWA Engineer to show conformance with MIL-E-5009B and this purchase specification.

5.3.4.1 Accelerated Aging. - *

5.3.4.2 High Temperature. - *

5.3.4.3 Room Temperature Endurance. - *

5.3.4.4 Low Temperature - *

5.3.4.5 Turbopump Cavitation - *

5.3.4.6 Recalibration - *

5.3.4.7 Teardown Inspection - *

*To be supplied at a later date.

5.3.5 Reports. - Reports of unit qualification tests under this specification shall be attested to by an appropriate government representative and shall contain, essentially, the following items:

1. Title Page
2. Abstract
3. List of illustrations
4. Summary
5. Conclusions and recommendations
6. Description (General description of the unit and detailed description of novel features)
7. Method of test (general description of test equipment and procedure)
8. Record of test (chronological history of all events in connection with all of the testing)
9. Analysis of results (A complete discussion of all phases of the test, such as probable reasons for failure, unusual wear, and analysis of general operation)

10. Calibration and recalibration data. Suitable curves defining the unit performance before and after the qualification test shall be provided.

11. Data. Copies of all original data sheets shall be submitted upon request. Tabulated data shall be sufficient to ascertain compliance with the qualification test requirements of the specification and shall include at least the following:

Type and serial number of unit
Date and time of day
Total endurance time and number of functional cycles
Fuel (type, actual specific gravity, & viscosity)
Barometer reading
Ambient temperature
Fuel Inlet temperature
Pump Inlet pressure
Pump discharge pressure

12. Photographs showing general unit condition and details of all failures and unusual wear conditions.

5.4 Acceptance Test. - Each unit shall be subjected to an acceptance test performed by the vendor to determine that each unit will meet the functional requirements established by this specification. The acceptance test schedule and calibration limits and changes thereto shall require written approval by the cognizant PRATT & WHITNEY AIRCRAFT project engineer.

5.4.1 Unit Inspection. - Units shall be inspected for conformance with the vendor's parts list currently released to production by initial release or revised by subsequent engineering change.

5.4.2 Pressure Test. - All unit assemblies or component castings, covers and enclosures of the unit shall be subject to 1750 psi on the high pressure side of the system and 250 psi on the inlet or interstage portion without fracture or permanent deformation. The turbine section shall be subjected to 500 psi without fracture or permanent deformation.

5.4.3 Data. - The vendor shall supply one copy of the acceptance test data of each unit procured under this specification.

5.4.4 Delivery. - The vendor shall be responsible for delivery of acceptance test data to the purchaser not later than the date on which the material is received.

6. VENDOR RESPONSIBILITIES

6.1 At the request of PWA Engineering, the vendor shall supply three copies of a reliability analysis report of the unit based on a single failure concep

6.2 Prior to acceptance of the qualification test on the unit the vendor shall be responsible for making changes and supplying hardware for correcting deficiencies found in the development units. If a change of requirements is made, costs arising from such changes will be subject to separate negotiations. In order to support the development units the vendor shall maintain or shall be able to obtain in a reasonable time, spare parts for procurement by PWA.

6.3 The vendor shall give full support to the development program by providing an adequate engineering development effort which shall include bench development and endurance tests on pumps to insure satisfactory operation of the unit at PWA both on the bench and engine to the requirements listed in this specification. An outline of the vendor's proposed development program shall be forwarded to PWA prior to the issuance of any purchase orders for units.

6.4 The vendor shall be responsible for retrofitting of all experimental units with all engineering changes required to duplicate the unit which satisfactorily completes the appropriate qualification tests, except those changes which in the opinion of the cognizant Pratt & Whitney Aircraft project engineer were not required to pass the appropriate qualification tests. These exceptions are to be designated by the Pratt & Whitney Aircraft project engineer's written approval. Delivery schedule of retrofit parts must be in accordance with engine development schedule.

6.5 Drawings. - The vendor shall supply one reproducible copy of all drawings pertaining to the unit. These drawings shall also provide design information for special tools, fittings and adapters that will be required during development testing or field use.

6.6 Preparation for Storage. - The unit shall be prepared for storage, prior to shipment, in a manner acceptable to the purchaser.

BEARINGS & SEALS

BEARINGS & SEALS

ITEM 11 - BEARING AND SEAL DEVELOPMENT

OBJECTIVE

This item of the contract required Pratt & Whitney Aircraft to conduct testing and determine the suitability of bearings and seals designed for the SST engine application. The objectives of the bearing test program were to study the performance and fatigue characteristics of candidate bearings and bearing materials, and to determine the effect of applied loads, temperature environments, and lubricants on bearing life expectancy. The data will be used to finalize the bearing materials selection and bearing compartment design for optimum performance and long life. The objective of the seal development program was to determine the seal design parameters necessary for reliable operation and long life at SST operating conditions.

A. BEARING DEVELOPMENT

1. INTRODUCTION

The first of the bearing development programs scheduled under the Phase IIA contract involved the continuation of endurance testing to determine the fatigue life and suitability of M-50 and WD-65 bearing materials. The endurance program had been initiated under a previous one-year contract; however, the anticipated number of test hours were run without producing any fatigue failures, and as a result, only figures indicating a minimum B-10 life* could be determined.

T e prime reason for the fatigue testing of full-scale bearings under si. ulated SST operating conditions is to establish the expected life of the material. This in turn dictates the useful life of the bearings. An equally important output of this testing is the reliability factor of the overall bearing for long time maximum-condition operation. Several factors, discussed below, have become evident in these programs and will require further evaluation in future programs.

* B-10 life is the life expectancy of 90% of the items in a series of test bearings.

The intent of this program was to increase the number of test hours on the bearings run in the first year program in an attempt to obtain actual fatigue failures for use in accurately determining B-10 life rather than using a minimum value which must be used when no failures are realized.

A second phase of the bearing program was to obtain a performance evaluation of main shaft thrust bearings which approximate the size to be used in the SST engine. The data obtained during test of these bearings will be significant to the early establishment of performance changes from predicted data.

2. DESCRIPTION

a. Components

The bearing design selec r fatigue failure testing was an angular-contact, ball-th ype reflecting an advanced state-of-the-art for high-temperatu e, aircraft-quality bearings. The bearing materials, either M-50 or WD-65, were also chosen on the basis of advanced technology. The M-50 material is currently in production and is stabilized for operating temperature up to 600°F, with the possibility of development to 800°F. The WD-65 material is a candidate bearing steel developed by the Crucible Steel Company under contract to the Air Force for application in oil temperatures to 800°F. A typical bearing used in the test program is shown in Figure 11-1. A description of the two bearings tested in this program is presented below:

Type: ABEC #7 duplexed angular contact, ball thrust bearing.

Material:

a) Balls and Races - CVM M-50 (PWA 725) steel melted by the consumable electrode vacuum melt procedure and stabilized for 600°F.

b) Balls and Races - WD-65 steel melted by the consumable electrode vacuum melt process and stabilized for 800°F

c) Retainer - both bearings - one piece, machined, AMS 6415 steel with .001 - .002 silver plate.

Geometry: a) 125 mm bore x 190 mm OD x 32.5 mm width, split inner-race construction. Twenty-one 0.8125 inch diameter balls. Contact angle of 23.0 to 27.0 degrees.

b) 205 mm bore x 315 mm OD x 46 mm width, split inner race construction. Twenty 1.3125 inch diameter balls. Contact angle of 23.5° to 26.5°.

Load Capacity: a) 21,000 pounds for a single bearing as calculated by the AFBMA (Anti-Friction Bearing Manufacturers Association) Standard Method. This is the load for a 10 percent life of 10^6 cycles or revolutions of the inner race.

b) 45,400 pounds for a single bearing as calculated by the AFBMA (Anti-Friction Bearing Manufacturers Association) Standard Method.

b. Rig

The rig used for bearing endurance evaluation was designed to simulate conditions of speed, thrust load and temperatures at levels representative of actual operation in an SST engine. A schematic diagram of the rig is shown in Figure 11-2. The major components of the rig include a drive shaft, a hydraulic piston load cylinder, front and rear bearing housings, a thrust ring, front and rear covers and an exterior case.

The desired load was applied to the bearings through a hydraulic load cylinder built into the rear cover. When pressurized, the piston applied load to both bearings, one opposing the other, through the strain-gaged thrust ring. The rear housing was free to move forward and load the front bearing against the stationary front housing.

Bearing lubrication was accomplished by directing a jet of oil at rotating scoops which feed the oil to the split in the bearing inner races through axial grooves in the hubs. This method duplicated the engine design. The oil was drained from the rig through a series of holes located at the bottom of the bearing cavity.

The rig used for calibration testing of bearings in this program is shown in Figure 11-3.

c. Facility

The test facility used for bearing endurance evaluation is shown in Figure 11-4. The rig was driven in this stand by a variable speed electric motor through a step-up 7.1 ratio gearbox to obtain the desired speed range. Coupling of the rig and gearbox by means of a quill shaft to accommodate any misalignment.

Thermocouples were installed in the oil-in and the oil-out lines and on the bearing races to monitor temperatures. Accelerometers were mounted in the horizontal and vertical plane on both end covers to monitor for bearing failures. The read outs for these units were calibrated to record a fatigue failure at full-scale deflection. Pressure gauges, speed counters, and other instrumentation normally associated with a test facility were used as required.

Strain gages were installed in the bearing outer races for the calibration tests in order to determine the ball pass frequency of the bearings which inturn would indicate when the bearing was in a skidding condition. The bearings were lubricated with PWA 521-A oil at 250°F using a conventional steam heat exchanger.

Heating of the bearing lubricant was accomplished with a rotating drum-type oil heater, as shown in Figure 11-5. The heater supplied the required quantity of PWA-524 oil to the rig test machine at 500°F without subjecting the oil to high localized temperature; however, due to a malfunction, immersed rod heater units were used for oil heating during the latter part of the test program.

3. METHOD OF TEST

The method used to induce bearing fatigue failure consisted of running the bearings at 12,000 rpm with a thrust load of 5900 pounds using PWA-524 oil at an average oil-in temperature of 500°F. The 5900 pound thrust level was established by assuming a 10 percent life of 100 hours and then calculating the corresponding load by AFBMA formula. The rig speed was established at a relatively high level to account for the use of test bearings which had a smaller diameter than that of the SST engine bearing. The oil temperature was established at 500°F as an approximation of the peak expected bulk oil temperature in the SST engine. The end product of the test methodology was a number which designated the ratio of the test bearing life to the bearing life predicted by the AFBMA method.

The two major readings recorded during the endurance test program were bearing race temperature and accelerometer readings. The race temperatures were monitored to protect against possible overtemperaturing due to oil starvation or other cause. As noted previously, the accelerometers were calibrated to indicate a bearing fatigue failure.

The method used to evaluate the performance of the main shaft duplex thrust bearings under various engine operating conditions consisted of varying the factors of load, speed, and oil flow over a wide range. Testing in this manner allowed data to be generated on race temperatures, heat rejection and scavenge oil flows as a function of the load, speed, and oil flow variables. Data on the bearing skidding characteristics was also obtained. These bearings were lubricated with PWA 521A oil so that a direct correlation of performance could be made with present advanced engine main shaft thrust bearing data.

The major pieces of data recorded during this testing included bearing race temperatures, speed, load, cage speed, oil flows, and oil temperatures.

4. TEST RESULTS

During a previous SST contract, bearings made from M-50 material were subjected to a complete calibration to establish feasibility and performance baselines. Analysis of the bearing endurance data indicated a fatigue life 1.94 times the predicted life based on the assumption that 10 percent of the bearings were ready to fail; however, this value was considered conservative since no actual fatigue failures were incurred during the testing. The lack of a clearly defined fatigue failure necessitated the use of a minimum rather than actual life.

Six M-50 material bearings were endurance tested for 1202.0 additional hours under the Phase II-A contract, again without any fatigue failures. Because of the method of establishing Weibull distribution, the additional running time did not substantially increase the statistical fatigue life of the subject bearings. However, as shown on Figure 11-6, the added time gives further indication that the life expectancy of the bearings will be higher than the predicted life. Further testing, especially the occurrence of a fatigue failure in the remaining six bearings, will strengthen the statistical probabilities. The endurance test times accumulated on M-50 material bearings are tabulated below:

Serial Number	Total Hours	Remarks
4-1	96	Running
4-2	96	Running
6-1	58	Misaligned
6-2	58	Misaligned
7-1	100	Stopped
7-2	100	Stopped
8-1	104	Stopped
8-2	104	Stopped
18-1	455	Stopped
18-2	455	Stopped
19-1	100	Stopped
19-2	100	Stopped
21-1	246	Stopped
21-2	246	Stopped
Total	2318	

A previous SST contract also covered the test evaluation of main thrust bearings made from WD-65 material. This endurance program was conducted under the same speed and load conditions used for test of M-50 bearings; however, several test suspensions were encountered due to low oil flows, resulting in an unrealistic B-10 life, according to the Weibull distribution, of 62 hours. The effect of lubricant difficulties on the bearings is shown in Figures 11-7 through 11-9. These problems were alleviated by the establishment of a 100-hour operating time limit on the lubricant and by increasing flow to the test bearings. The testing was completed without an actual fatigue failure of the WD-65 bearings.

Eight WD-65 bearings were endurance tested for 1406 additional hours under the Phase II-A contractual program. Figure 11-10 shows the results of the endurance testing at the end of the previous year contract along with further test results obtained during the current Phase II-A test. The highest predicted B-10 life of 193 hours, based on testing of the last eight bearings, is considered conservative in that no failures occurred. The endurance test times accumulated on WD-65 bearings are tabulated below:

Serial Number	Hours	Remarks
G1-1	388	Stopped
G1-2	390	Stopped
G2-1	34.5	Cage Failure
G2-2	34.5	Cage Wear
G3-1	225	Stopped
G3-2	166.5	Cage Wear
G4-1	30	Cage Wear
G4-2	418	Stopped
G5-1	34	Cage Wear
G5-2	34	Cage Wear
G6-1	76.5	Ball and Cage Wear
G6-2	76.5	Ball and Cage Wear
G8-1	49.5	Cage Wear
G8-2	326	Stopped
G9-1	265	Stopped
G9-2	265	Stopped
	Total 2813	

The calibration tests on these bearings were completed without incident. The curves shown in Figures 11-11 and 12 are typical of the results obtained for the bearing pair with respect to race temperatures and cage speed.

Examination of the bearings at the completion of the calibration allowed the following observations to be made:

- The general condition of both bearings and the inter-bearing baffle was good.
- A cage land riding surface of one bearing appeared worn to a greater degree in one cage section.
- The ball retention by the cages appeared to be adequate.
- The bearing oil grooves were generally clean.

5. DISCUSSION OF RESULTS

The accumulation of more than 5100 hours of endurance testing on M-50 and WD-65 material main shaft bearings has increased the confidence level in the feasibility of operating these bearings at high speeds and loads using a high-temperature lubricant. The

testing has established that serious consideration may be given to the use of these bearings in an SST engine with the expectation that after additional development the bearing durability will be commensurate with those in present production engines. The endurance programs have also indicated the necessity for an adequate fail-safe type lubrication system, operable with an oil or at a temperature level without producing sludge or causing oxidation of the lubricant.

Tests on a duplex set of large thrust bearings has yielded an insight into possible problems involved in operating a bearing of this size. Should a major problem develop with these bearings, its cause would originate in the cage, particularily in the balance requirements for this design. This reasoning is based upon the fact that uneven wear was discovered on the cage inner land riding surfaces during a post test inspection - indicating a balance problem with this cage.

Although further testing is necessary, data from the first calibration appears to show agreement with predicted values for bearing heat rejection and skidding tendencies.

6. RECOMMENDATIONS

As the result of the bearing development testing noted above, this Contractor recommends:

- Continuation of endurance testing until actual B-10 bearing lives are determined,
- Improvement of lubrication to provide longer sludge-free operation,
- Development of fail-safe systems for lubrication of bearings,
- Continuation of cage development work to obtain a reliable retainer which will be tolerant of sludge and low oil flow, and
- Continuation of development work on bearing designs to obtain optimum geometric features for actual bearing designs.
- Further evaluation of cage balance requirements.

B. BEARING MATERIALS

1. INTRODUCTION

An investigation of the ball fatigue life of bearing materials, as affected by the choice of lubricants and solvents, was undertaken under this contract to determine the penalties incurred by the use of present mid-temperature range lubricants. The investigation was considered significant to the SST engine as a method of isolating the most-promising candidate oils.

2. DESCRIPTION

a. Components

The testing was conducted with half-inch diameter CVM M-50 material balls. The fatigue life of these balls in MIL-L-7808D oil was used as a standard.

b. Rig

The ball fatigue rig, as shown in Figure 11-13, is a machine in which a single ball of material can be run under closely monitored conditions. The test ball was held between two races by a flat-plate bronze cage and loaded through the upper race by a hydraulic load piston on top of the rig. Figure 11-14 is a schematic of the rig. The rig was driven at approximately 7600 rpm by an electric motor through a belt and pulley. Lubricating oil is supplied in excess to each contact point between races and ball. The oil-in temperature was held at 300°F.

c. Facilities

A total of five rigs, as shown in Figure 11-15, were utilized for this program. To facilitate identical operating conditions, the rigs have common load and lubricating systems.

3. METHOD OF TEST

For each test, a batch of 15 balls were run until failure or 20 hours, whichever occurred first. Each rig had an accelerometer used as a failure indicator to shut off the rig when a predetermined vibration level was reached. The number of cycles for each ball was computed and plotted on a Weibull curve to give a B-10 life, which is the life expectancy of 90% of the balls in any given batch.

4. TEST RESULTS

To date, MIL-L-7808D, Mobil Jet 2, Texaco SATO 5180, and PWA 524 (Polyphenyl ether Skylube 600) have been tested at 300°F. The B-10 lives were: 15.7×10^6 cycles for the MIL-L-7808D, 13.6×10^6 cycles for the Mobil Jet 2, 2.95×10^6 cycles for the Texaco SATO 5180, and 7.3×10^6 cycles for the PWA 524. Figures 11-16 through 11-19 show the Weibull plots of these runs.

The running time required to test these four oils was as follows: 180 hours for MIL-L-7808D, 213 3/4 hours for the Mobil Jet 2, 124.9 hours for the Texaco SATO 5180, and 124.6 hours for the PWA 524.

5. DISCUSSION OF RESULTS

The Texaco SATO 5180 lubricant is definitely inferior to the standard MIL-L-7808D lubricant. There is no significant difference in the Mobil Jet 2 and MIL-L-7808D lubricant when the normal 90% confidence level is established. PWA 524 lubricant is somewhat lower in life than the standard. It should be noted here, though that 300°F represents the higher limit of operation of the type II oils, whereas the PWA 524 can be operated to at least 600°F. The significance here is that there are no appreciable fatigue life penalties incurred with the use of PWA 524 oil.

6. RECOMMENDATIONS

The data indicates that the Texaco SATO 5180 lubricant is inferior to other type II oils and its use should be discontinued. If temperature levels for the lubricant cannot be lowered sufficiently to permit the use of type II lubricants, PWA 524 can be used without a materials fatigue life penalty ratio.

C. SEAL DEVELOPMENT

1. INTRODUCTION

Programs were run prior to the Phase II-A contract to establish the feasibility of using face type seals in an SST engine application. As reported in reports PWA 2222 and 2353, these seals operate well and have reasonably low wear rates; thereby definitely establishing the feasibility of these seals for the SST.

The testing during Phase IIA was directed at completing the evaluation of alternate high temperature seal materials and designs and establishing low-pressure seal performance for normal engine operation using seal pressurizing schemes.

Bellows seals are of interest for an SST engine application because of the elimination of secondary seal leakage. This factor is important in improving lubricant life from the standpoint of oxidation and fire resistance. If an inert system were considered for the SST, extremely low leakage would be necessary to make the seal practical from consideration of inerting gas storage and usage rate.

2. DESCRIPTION

a. Component

The seals tested in this program were the face type with PO3XHT carbon sealing surfaces. The first four builds used a seal assembly with piston ring secondary seals and coil springs for statically loading the seal against the mating surface. Builds 5 and 6 were run with a bellows type seal in which the bellows formed the secondary seal and also provided the necessary static loading.

The seal plates were the flame plated oil cooled type. The first form tests used the wet face type plate in which the cooling oil is led directly to the sealing interface for cooling and to provide the necessary oil film to create a hydrodynamic bearing. The last two builds used a dry face type seal plate in which the oil is led directly through the seal plate for cooling only.

Figure 11-20 shows both types of seal used in this program.

b. Rig

The rig used for this program was designed so that simulated SST engine environmental and operating conditions could be imposed on the seal. The component parts of the rig are shown in Figure 11-21. Instrumentation necessary for recording pressures and temperatures was installed in the rig in the appropriate areas.

c. Facility

The rig mounted in the test stand is shown in Figure 11-22. This stand had the equipment necessary to supply an adequate quantity of oil and air to the rig at the proper temperatures and pressures.

The air was heated by a hot wire heater to a 1600°F limit. A calrod boost heater raised the temperature of the oil, as it came from the first-stage steam heater, from 300 to 500°F. The oil used was PWA 524. The rig was driven by an automobile engine through a 12:1 ratio step-up gearbox. The rig instrumentation was furnished as a part of the stand or supplied as special equipment.

3. METHOD OF TEST

The method of testing for the Phase IIA program consisted primarily of establishing initial seal performance by running several check points and comparing seal leakage with baseline data. Once the seal performance was established, the endurance program was started, and readings were taken at regular intervals to monitor air temperature, pressure, and leakage; and oil temperature, pressure, and flow. All other readings normally associated with a test program were also monitored.

The endurance conditions run for first, second, third and fifth tests are shown below.

Speed	12,500 RPM
Air Pressure	150 psig
Air Temperature	900°F minimum
Oil Temperature	500°F

For the fourth and sixth tests, the test conditions were reduced to values noted below to simulate environmental conditions which will exist in a fan discharge pressurized seal compartment. The conditions for these tests were as follows.

Speed	12,500 RPM
Air Pressure	40 psig
Air Temperature	800°F
Oil Temperature	400°F

4. TEST RESULTS

Six tests were run during this program in which variations in operating conditions and alternate high temperature carbons were evaluated. The results of these tests are tabulated below; results of seal tests completed during the Phase II contract are also listed for comparison.

Phase IIA Results

Build	Type	Carbon	Lip Width Inch	Total Time (hours)	Max. Press. psi	Wear (mils/100 hours)	Remarks
1	Wet Face	PO3XHT	.200	11.00	150	Excess	Unstable
2	Wet Face	PO3XHT	.150	8.25	150	363	
3	Wet Face	PO3XHT	.150	15.75	150	253	
4	Wet Face	PO3XHT	.150	102.00	40	29.7	
5	Bellows Dry Face	PO3XHT	.150	16.75	150	47.2	
6	Bellows Dry Face	PO3XHT	.150	64.5	40	79.5	

Phase II Results

Build	Type	Carbon	Lip Width Inch	Total Time (hours)	Max. Press. psi	Wear (mils/100 hours)	Remarks
1	Wet Face	CDJ-83	.150	29.5	150	27	
2	Dry Face	CDJ-83	.150	28.5	50	27	
3	Wet Face	CDJ-83	.150	100	150	3.1	
4	Combination	CDJ-83	.150	0	---	---	Would not seal
5	Metal to Metal	---	.150	3.5	50	Excess	High rubbing friction
6	Bellows	2490	.150	3.5	50	Excess	Seal Overloaded
7	Combination	CDJ-83	.150	0	---	---	Would not seal
8	Wet Face	CDJ-83	.150	28.5	150	10	
9	Wet Face	CDJ-83	.150	25	150	14	

The general trend of the data indicates a significant difference in wear rates based on the material used. Apparently, the PO3XHT carbon experienced some difficulty when running with PWA 524 oil at 500°F which CDJ-83 carbon did not. A comparison of the above tables indicates that wear rates were significantly higher with seals using PO3XHT carbon, regardless of operating conditions.

5. DISCUSSION OF RESULTS

The tests conducted during Phase IIA contributed to the general SST development program by establishing that the present wet face seal designed in this program is satisfactory for use in the early development phase of an SST engine. A factor which may be contributing to the higher wear rate noted in PO3XHT carbon is that it is somewhat more porous than CDJ-83. As a result, oil may be oxidizing in the asperities, causing wear. The carbons used in these tests were sent to the Materials Development Laboratory to determine whether oxidized oil or other substances exist in the carbon structure. Programs are being set up using prepared specimens which may be useful in making a more positive analysis.

The possibility of oil oxidation was discernable only as a result of the progress made in overcoming the sludge and coking problems encountered during a previous study contract.

The significant drop in wear rate of the carbon at the lower pressure levels in the wet face seal indicates a definite advantage can be realized by incorporating pressurized and vented seal assemblies.

In the dry face seal, the wear rates are high and therefore the variation in wear at the two pressure levels must be considered inconclusive. There are definite indications that optimization of the seal balance and spring load (for the operating conditions and the lubricant) are critical factors towards obtaining a reliable long-life seal. Improper seating forces can either destroy the air film between the seal and seal plate and cause hard rubbing and high wear, or allow the seal to float away from the seal plate and permit high leakage rates.

The significant decrease in wear rate of the seal at 40 psig compared to 150 psig suggests that a decrease in wear rate can also be expected with seals having CDJ-83 carbon. Variations in seal performance between tests also suggest that secondary variables have a more significant effect on the seals at the SST operating conditions than in current advanced engine seal applications.

6. RECOMMENDATIONS

The test results point out the necessity for a continued seal development program in which all the aspects of geometric variations, materials combinations, cooling and lubricants are investigated. New and advanced sealing concepts must also be studied along with methods of achieving minimum leakage seals for use in inert gas systems.

Long-time endurance runs are required on all potential seals for use in an SST engine in order to establish durability, reliability, and potential time between overhaul.

D. RING SEAL DESIGN

1. INTRODUCTION

The reason for this work is to develop a ring seal design that will perform satisfactorily at higher rubbing speeds required in the SST engine. The higher rubbing speeds are a result of larger diameters and higher rpm. The geometry must be such that the seal will fit in the allowable space, and the wear rates obtained under conditions of higher pressure and temperature must be low enough to insure long life.

2. DESCRIPTION

a. Component

The component tested was a carbon ring seal with geometric and design variations as shown in Figures 11-23 and 11-24.

Two seal types are being evaluated, the radial groove type and the circular groove type. The seal plates, against which the seals mated, were of Haynes Stellite 6B alloy of three-quarter inch thickness to provide a heat sink. The rubbing faces of the seal plates were ground and lapped to a 2 light-band flatness. Figures 11-25 and 11-26 show the seal components and shaft stackup.

b. Test Rig

The rig used for the test evaluation of the ring seals is shown schematically in Figure 11-27. Two seals were mounted back to back on the rotating shaft between lapped seal plates. The stationary seal liner

was chrome plated on the ID rubbing surfaces. Two seals were tested to eliminate thrust forces due to pressure loading in the rig. For this program, two rigs and four interchangeable shafts were used for efficient operations.

c. Facility

The test stand used in this program was equipped with all the necessary equipment and instrumentation for running up to three independent rigs simultaneously. Power was provided by 15 hp electric motors at 1750 rpm through variable speed pulleys. The pulleys were connected to a 5 to 1 ratio gearbox and the rigs were mounted on the gearboxes. Air at pressures up to 120 psig was used for the rigs: necessary oil systems and fire extinguishing equipment were mounted in the stand. See Figure 11-28.

Air pressure, air temperatures and rig rpm were controlled from a console mounted in front of the stand. See Figure 11-29. Oil pressures and temperatures, breather temperatures and rotometers flows were read and recorded.

3. METHOD OF TEST

The test program consisted of operating the seals at 200, 250, and 275 ft/sec speed levels at 40 and 60 psig using air at ambient temperatures.

Each test was scheduled for five hours. A test was terminated prior to that time if the breather (air out) temperature reached 400°F or if there was more than a 15 percent increase in seal leakage between each step. The seal was considered to have failed if there was a sudden increase in seal leakage or if the leakage rate reached 100 percent on the stand flowmeters. High seal leakage or seal temperatures were avoided because of the fire hazard.

Each of the test ring seals were precisely measured axially and radially prior to and after test. The difference in measurements was multiplied by 20 to give wear in mils/100 hours.

4. TEST RESULTS

Three-hundred hours of test time were accumulated on the four ring seal designs as follows:

Type	Size	Points Run	Test Hours
Circular groove	Six-Inch	15	50
Circular groove	Eight-Inch	16	57.1
Radial groove	Six-Inch	18	85.25
Radial groove	Eight-Inch	23	107.0

The results of the testing, as applicable to each of the four seal designs, are tabulated in Figure 30 through 34.

5. CONCLUSIONS

The conclusions made on the basis of the above testing were as follows:

- The circular groove design was inherently weak, Many tests were prematurely ended because of broken seals. In many other cases seals were found to be broken when the rig was disassembled. In nearly all cases the seals broke radially at points where the circular grooves meet the ID of the seal. Because of repeated failures the circular groove design seal was considered unacceptable for future consideration and the program terminated.

- The radial groove design performs well but certain limitations are apparent.

  a. The 0.200 inch radial width seals have too little rubbing surface. Many seals of this width either broke or had very high wear rates (to over 1000 mils/100 hours).

  b. The 0.800 inch radial width seals wore very little. This was more evident in the eight-inch than the six-inch design.

  c. Tests to optimize seal width show only a slight increase in wear as seal width was decreased. However, 0.400 inch radial width is probably a practical minimum.

6. RECOMMENDATIONS

It is recommended.

- That future designs of seals for this application be of the radial groove type.

- That testing of radial groove seals to continued to complete the planned statistical program. On its completion the effect of sealing lip width and the number and size of face grooves can be fully evaluated.

- That the minimum radial width of the seals should be not less than 0.400 inches. Further testing at more rigorous conditions should be undertaken to determine whether 0.400 inches is adequate or should be increased.

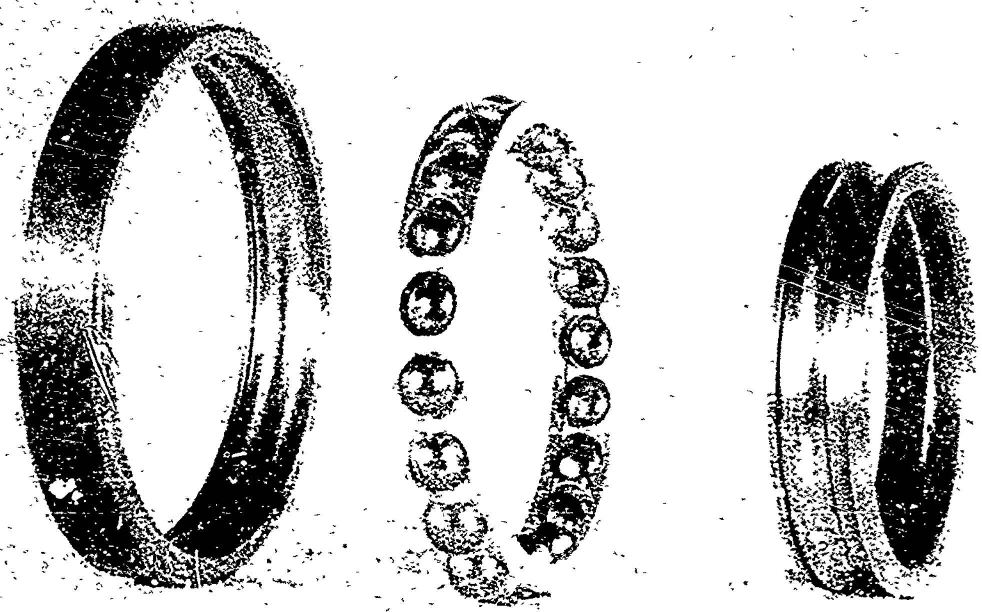

TYPICAL ANGULAR-CONTACT THRUST BEARING USED FOR ENDURANCE EVALUATION TEST UNDER SIMULATED SST ENGINE CONDITIONS

Figure II-1

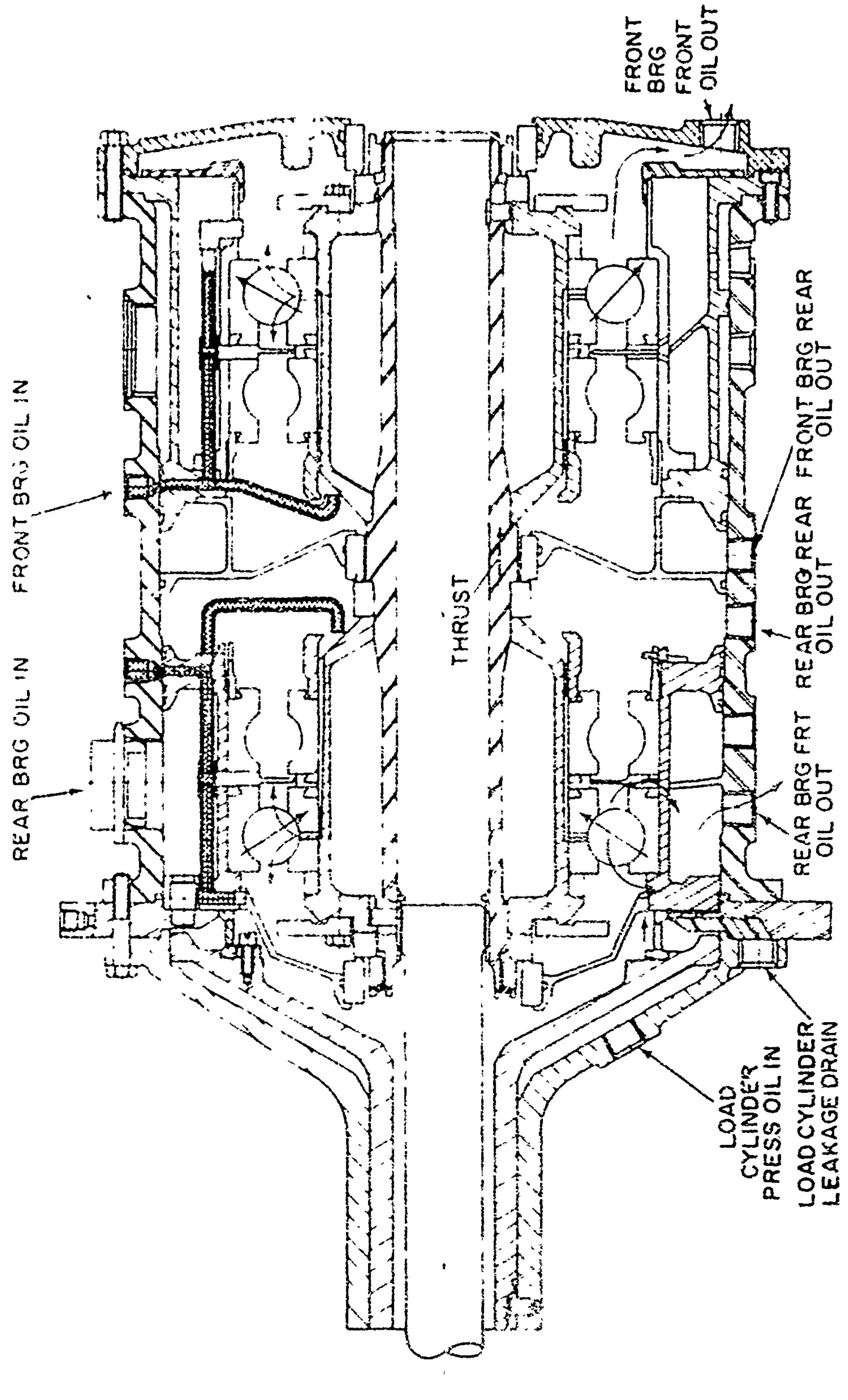

SCHEMATIC DIAGRAM OF THRUST BEARING TEST RIG

Figure II-2

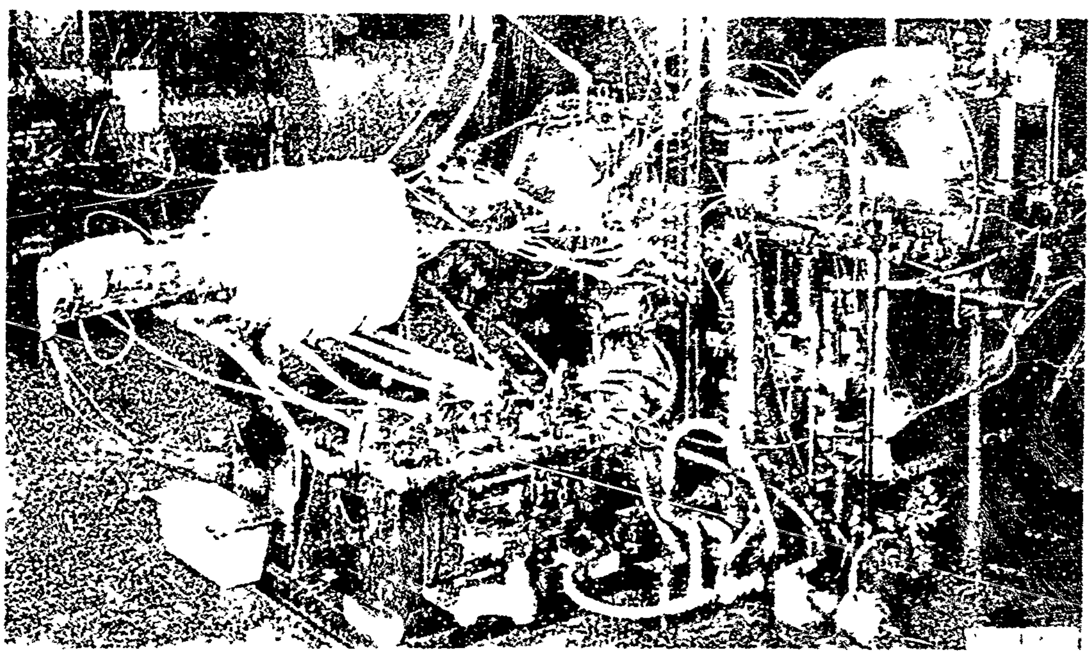

BEARING CALIBRATION RIG

Figure II-3

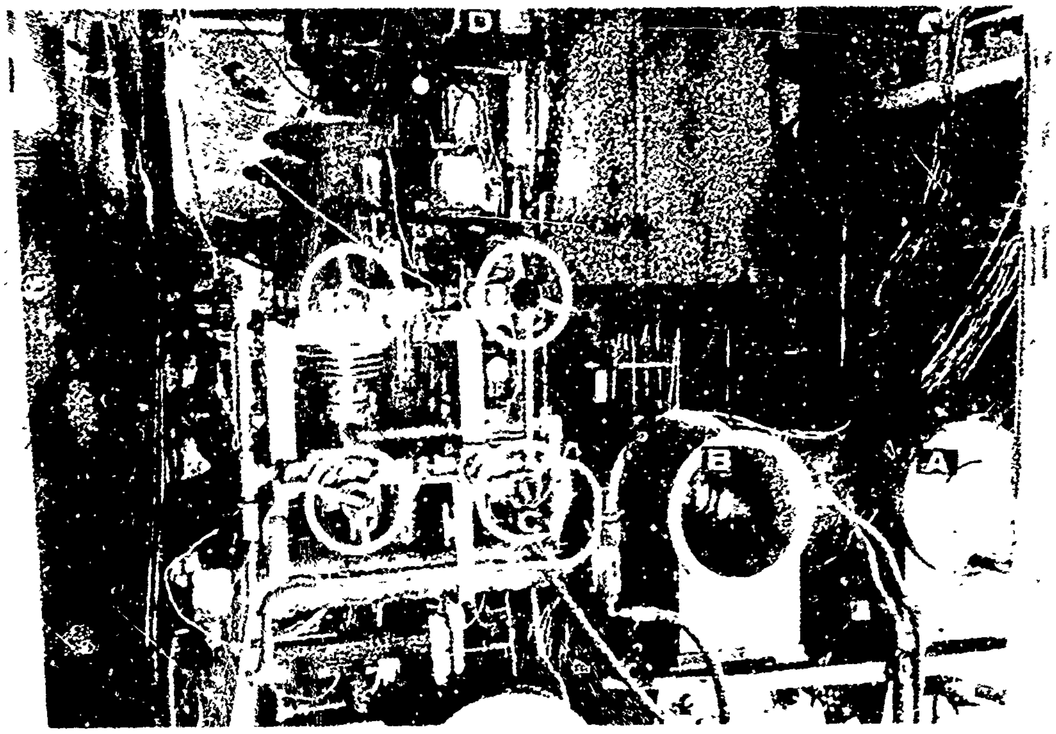

THRUST BEARING TEST RIG INSTALLATION INCLUDING (A) RIG IN STAND FOR OPERATION, (B) RIG HOUSING WITH BEARINGS REMOVED, (C) FILTER CONTROL VALVES, (D) FLOWRATERS

Figure 11-4

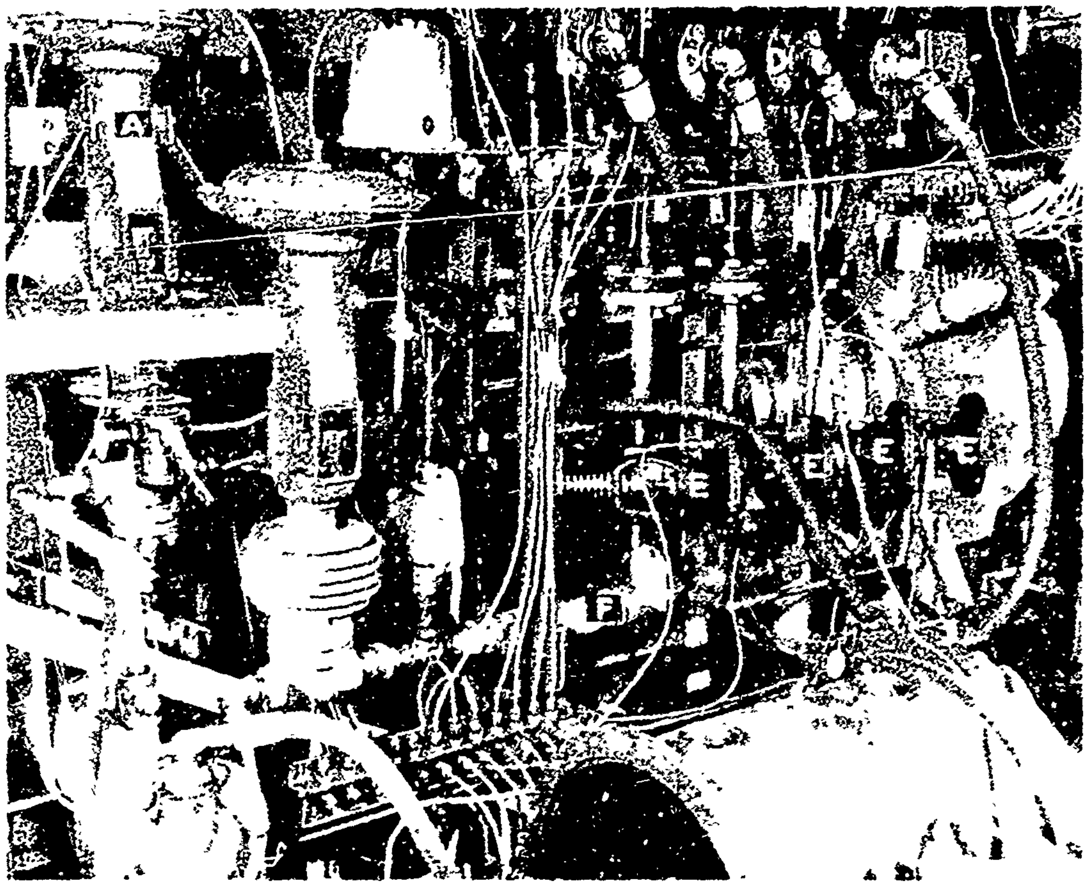

ROTATING DRUM OIL HEATER INSTALLATION INCLUDING (A) MIXING VALVE, (B) RADIATOR, (C) MANIFOLD PRESS. CONTROL VALVE, (D) FLOW INDICATORS, (E) REMOTE FLOW CONTROL VALVE, (F) MANIFOLD, (G) OIL HEATER

Figure 11-5

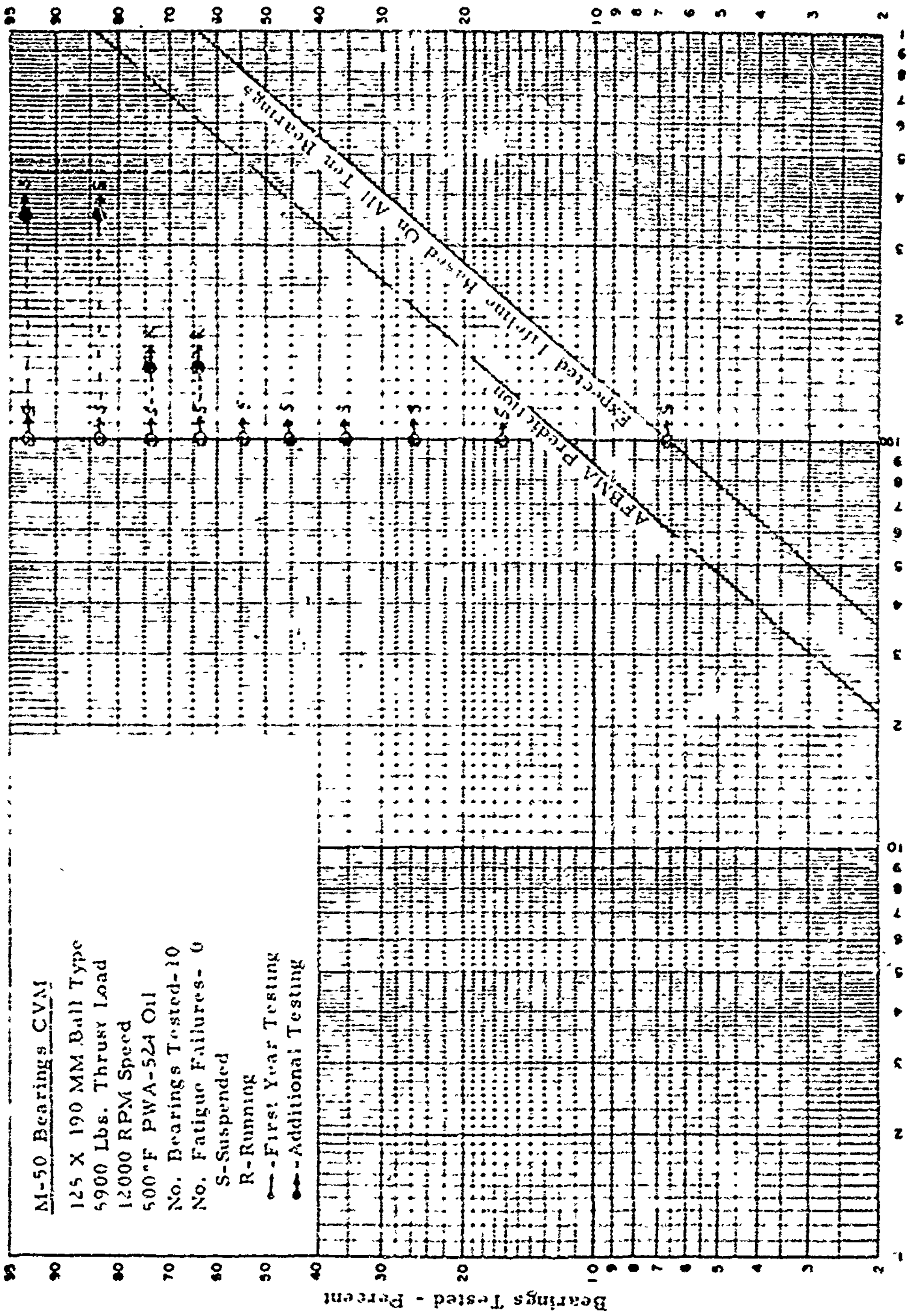

WEIBULL DISTRIBUTION OF M-50 BEARING TEST RESULTS

Figure 11-6

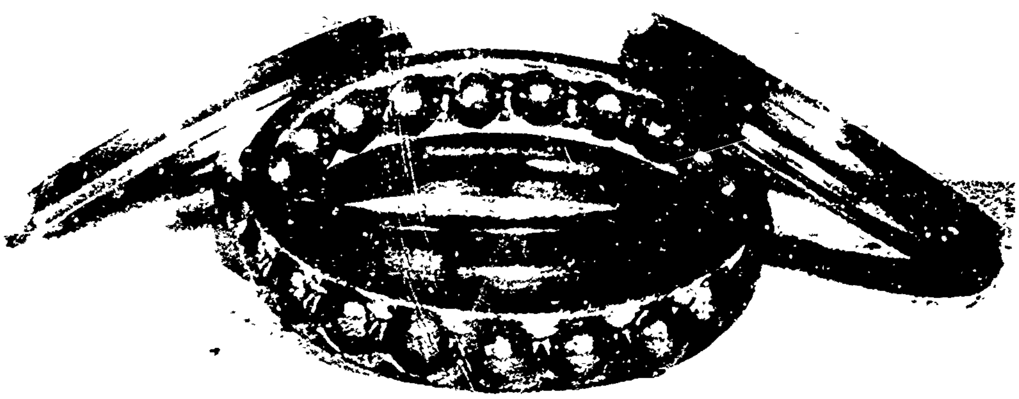

THRUST BEARING AFTER 265 HOURS OF ENDURANCE TEST IN 500°F PWA-524 LUBRICANT

Figure 11-7

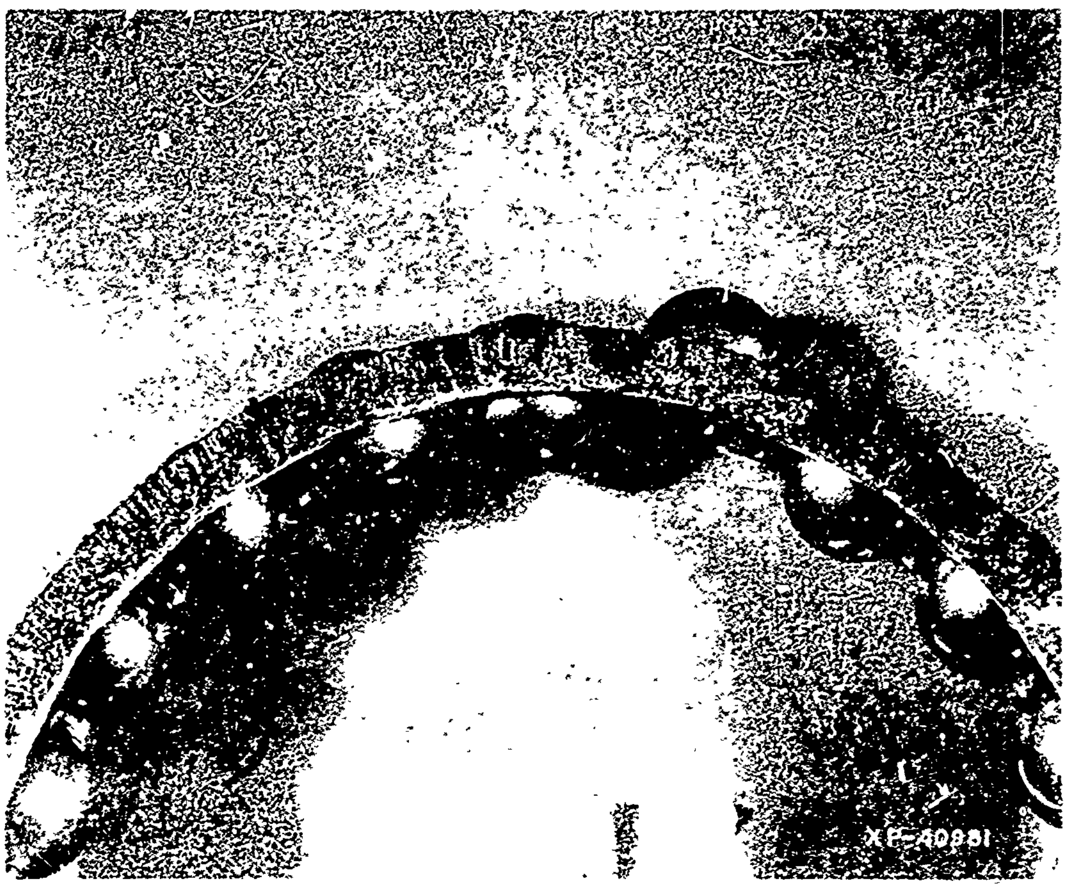

CAGE FROM THRUST BEARING SHOWING DEPOSITS AFTER 2[illegible]5 HOURS OF ENDURANCE TEST WITH 500°F PWA-524 LUBRICANT

Figure II-8

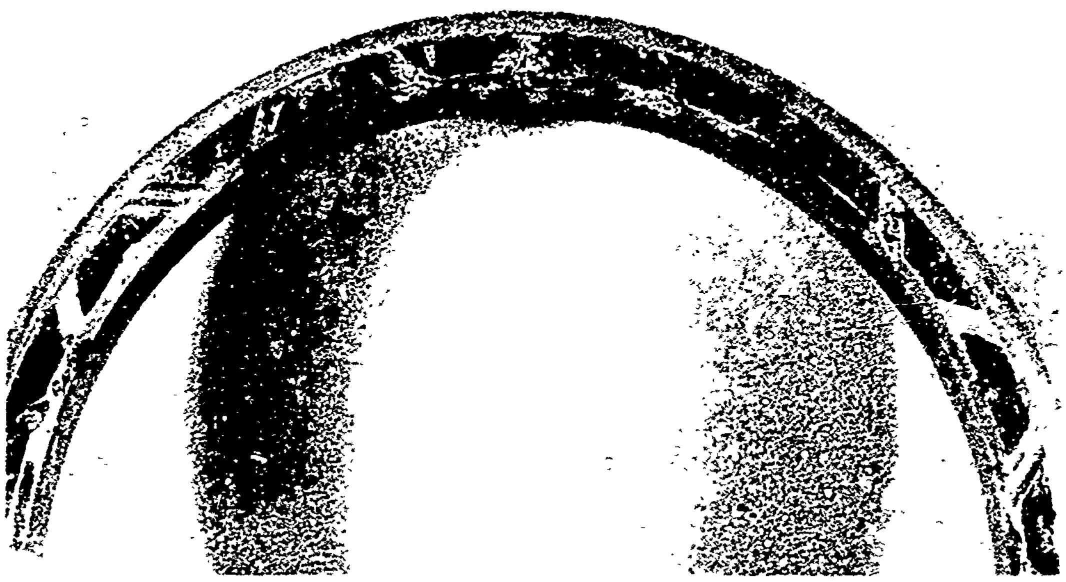

THRUST BEARING INNER RACE SHOWING PLUGGED OIL GROOVES AFTER 265 HOURS OF ENDURANCE TEST WITH 500°F PWA-524 LUBRICANT

Figure II-9

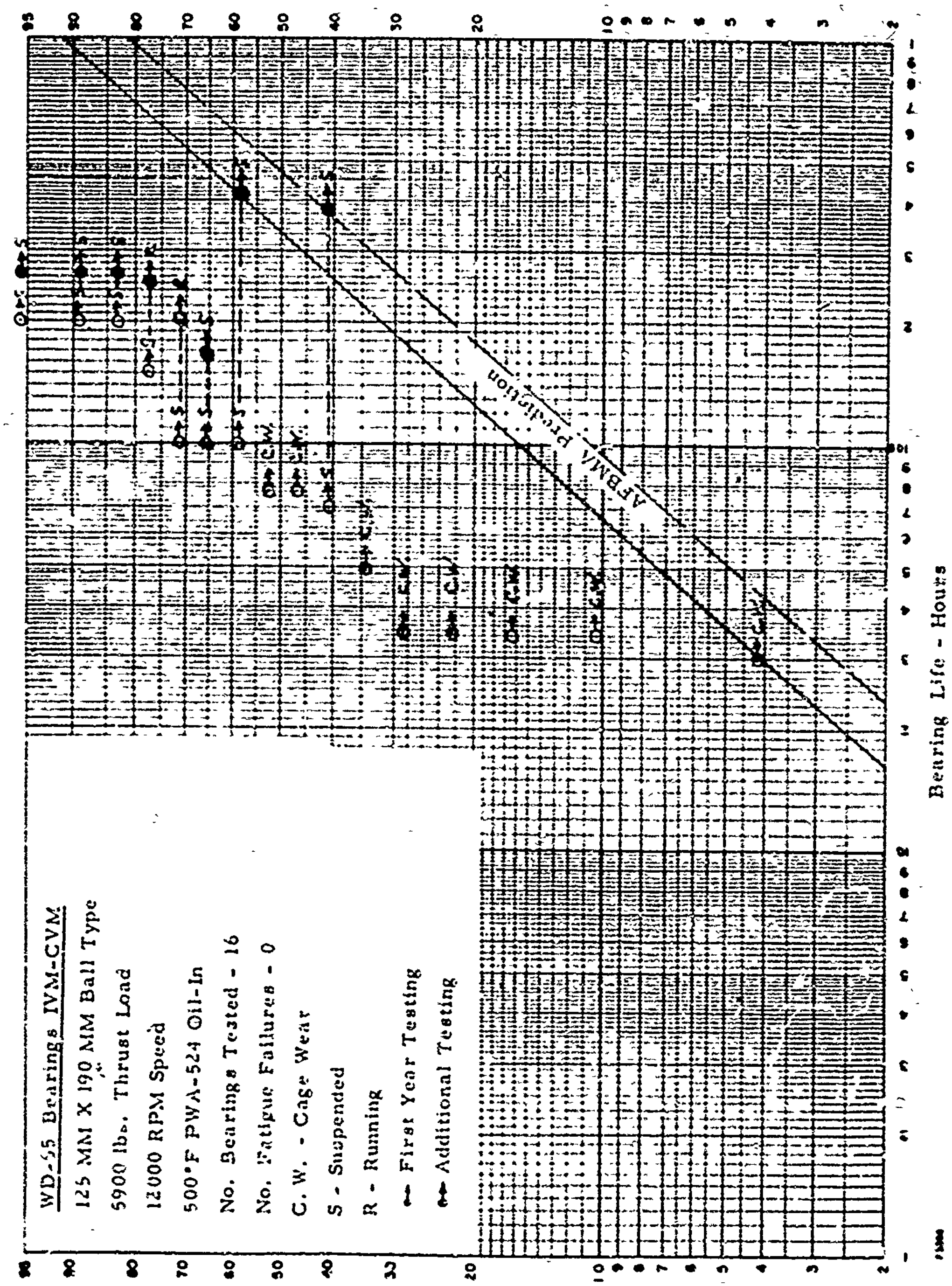

WEIBULL DISTRIBUTION OF WD-65 BEARING TEST RESULTS

Figure 11-10

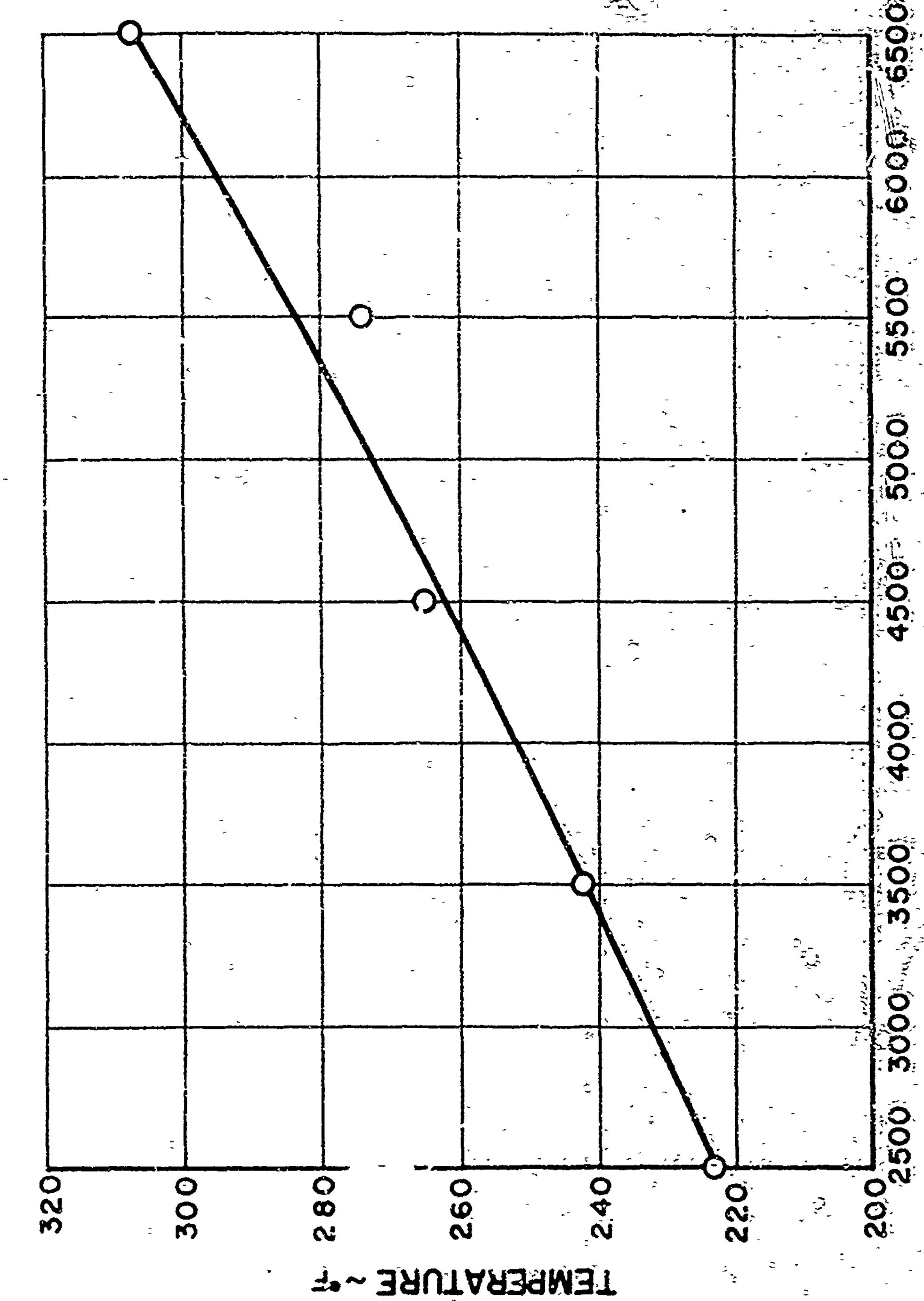

OUTER RACE TEMPERATURES
AS A FUNCTION OF SPEED

Figure 11-11

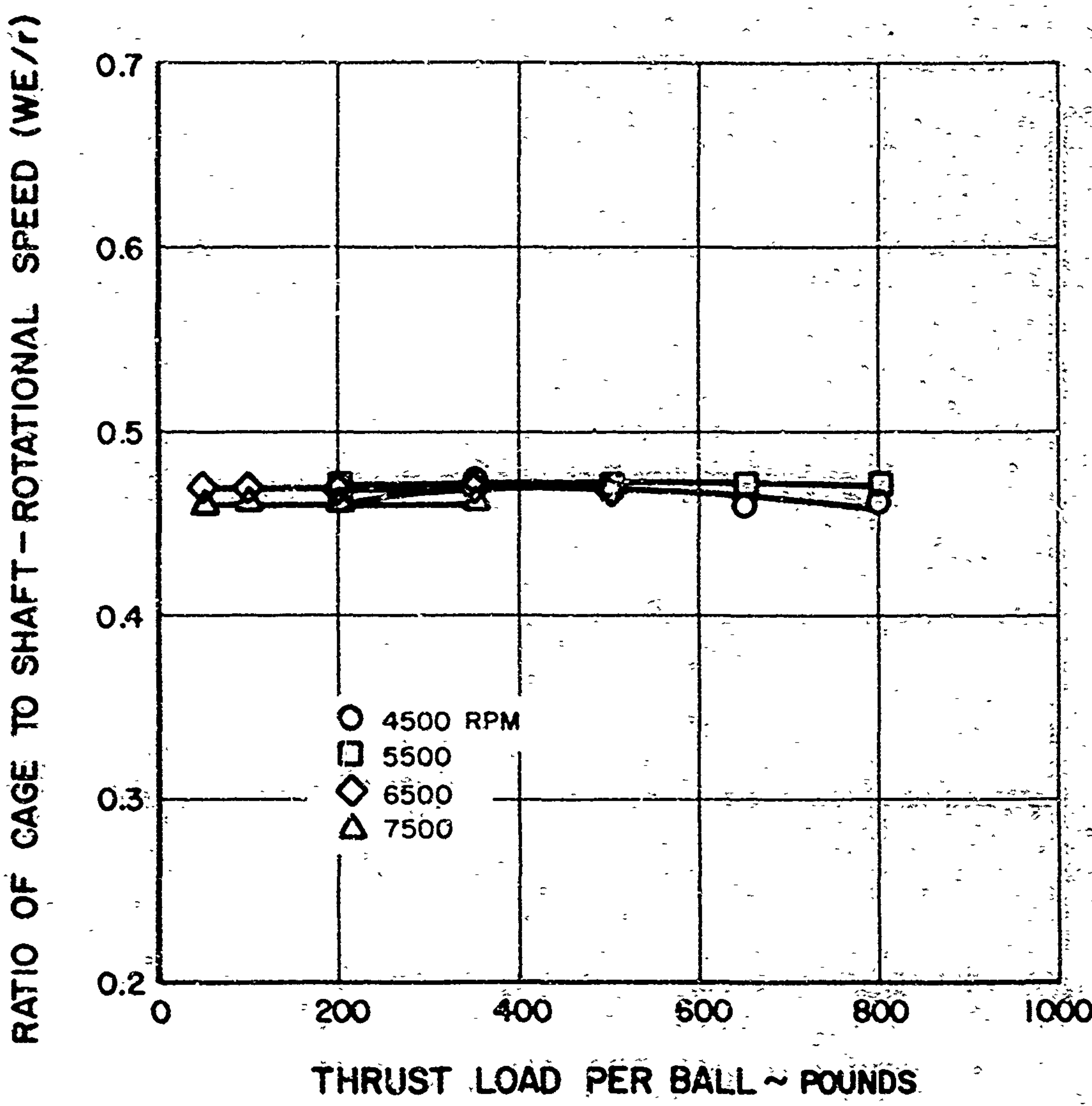

EFFECT OF THRUST LOAD
PER BALL ON CAGE SPEED

Figure 11-12

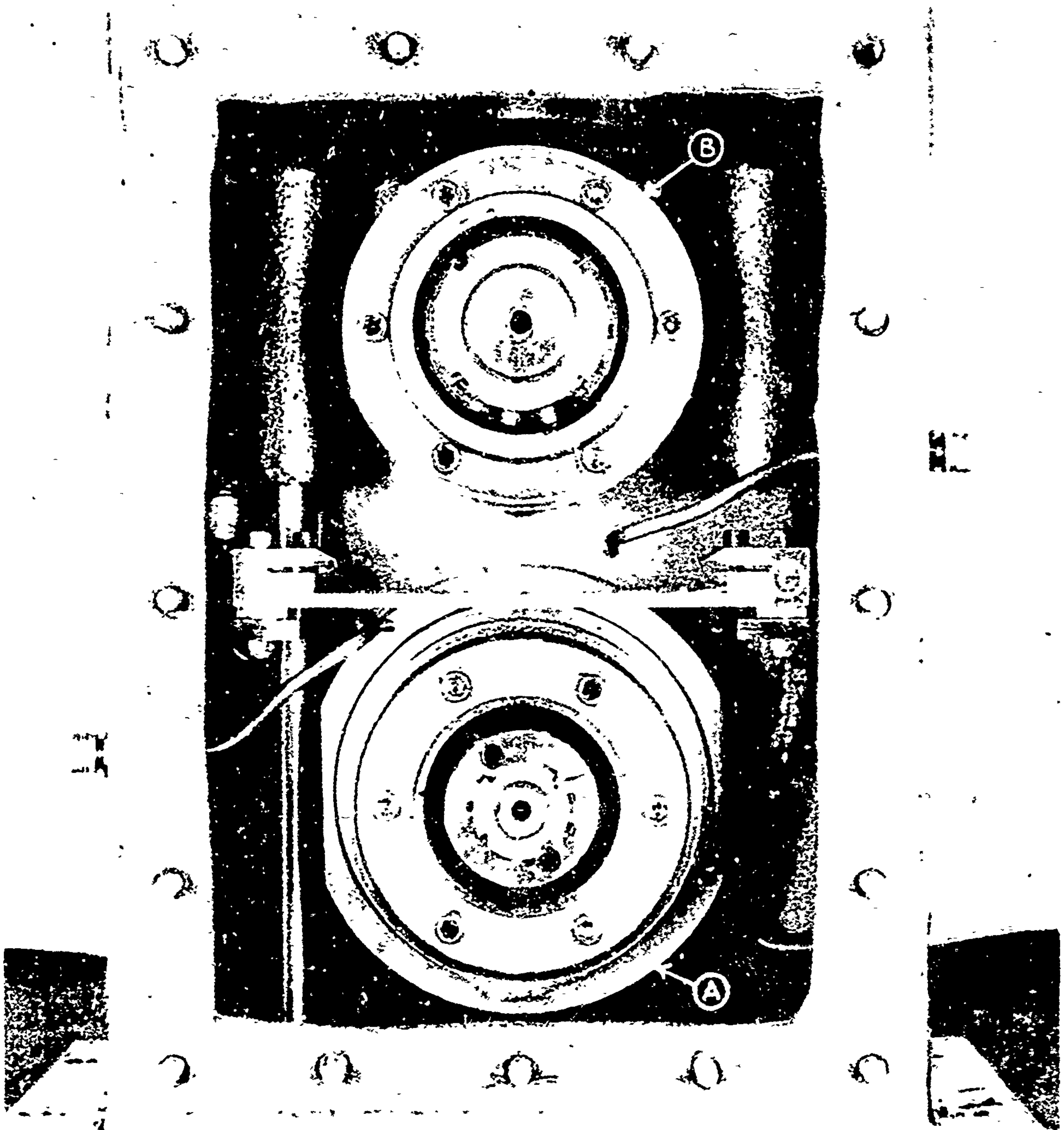

XP-17155

SINGLE-BALL FATIGUE TEST RIG SHOWING (A) LOWER RACE, (B) UPPER RACE IN UP POSITION, (C) CAGE HOLDER

Figure 11-13

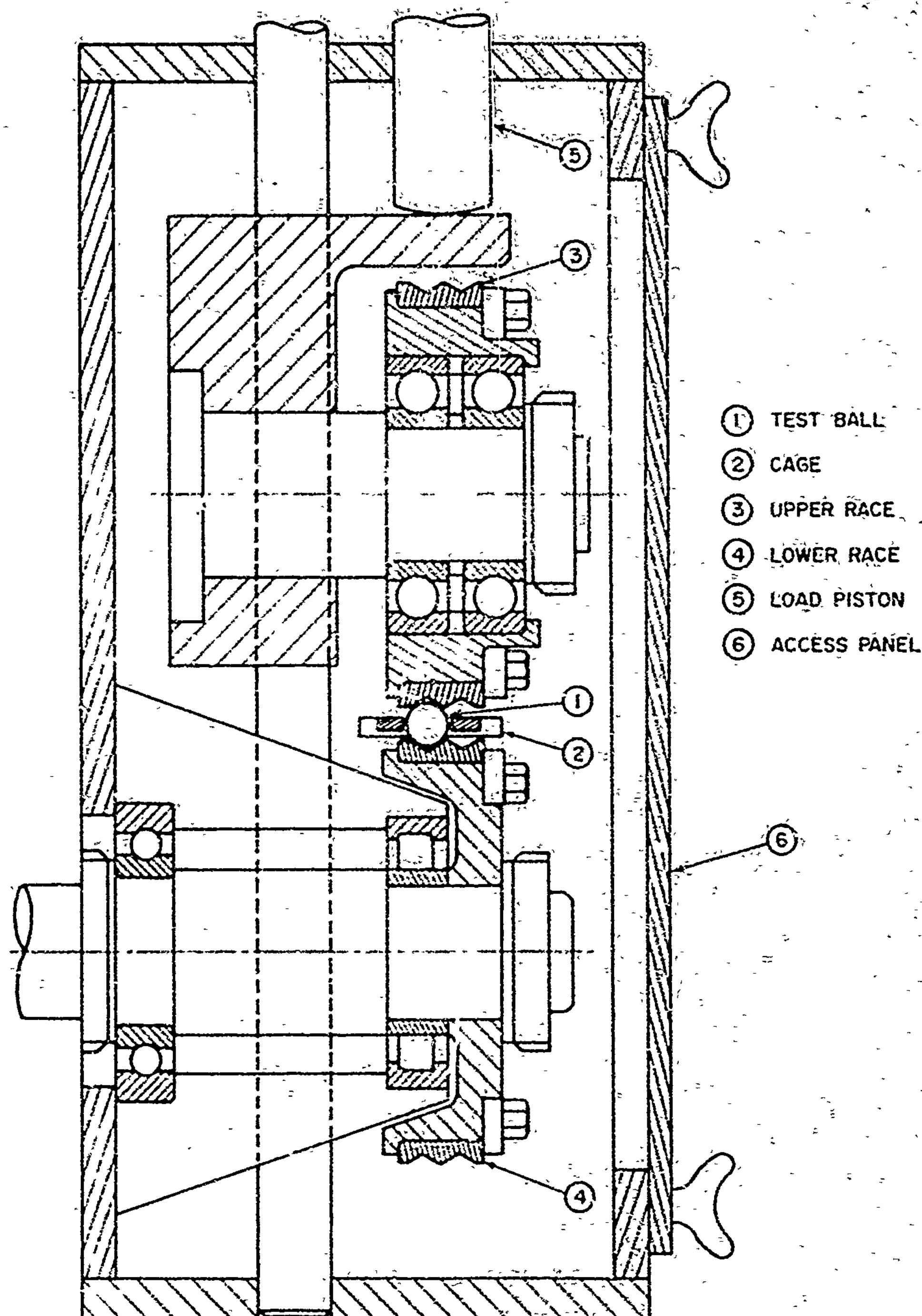

SCHEMATIC DIAGRAM OF SINGLE-BALL FATIGUE TEST RIG

Figure 11-14

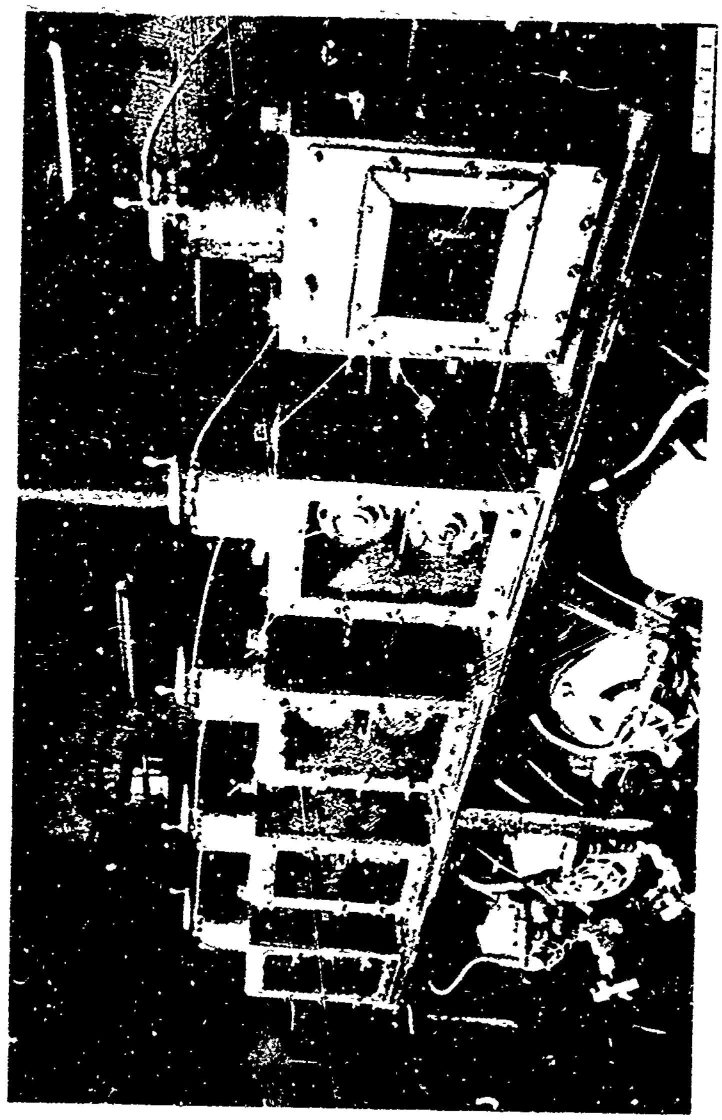

INSTALLATION OF RIGS INCLUDING (LEFT TO RIGHT) FOUR SINGLE-BALL FATIGUE RIGS AND HIGH-TEMPERATURE OIL RIG (A).

Figure 11-15

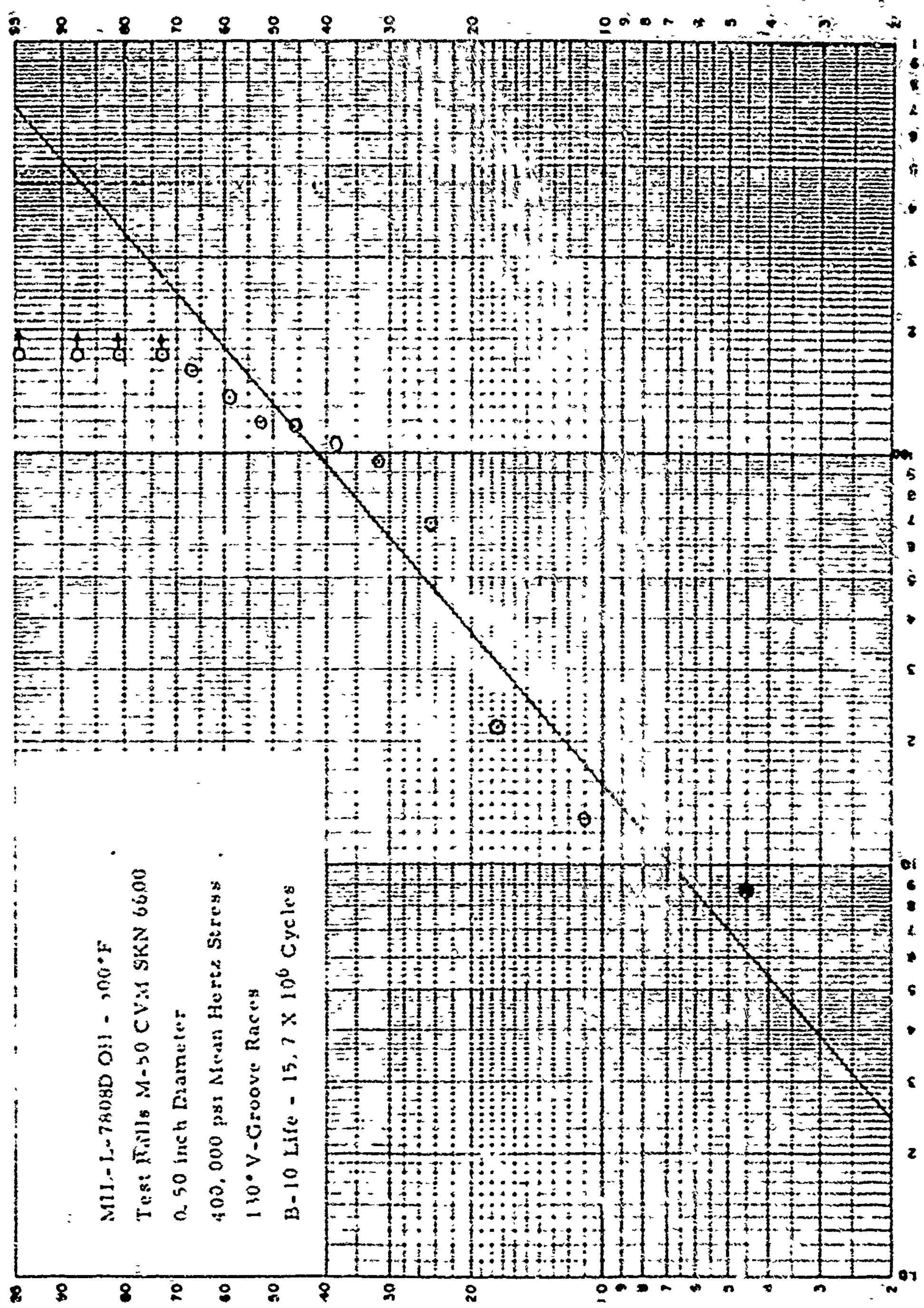

WEIBULL DISTRIBUTION OF BALL TEST IN MIL-L-7808D OIL

Figure 11-16

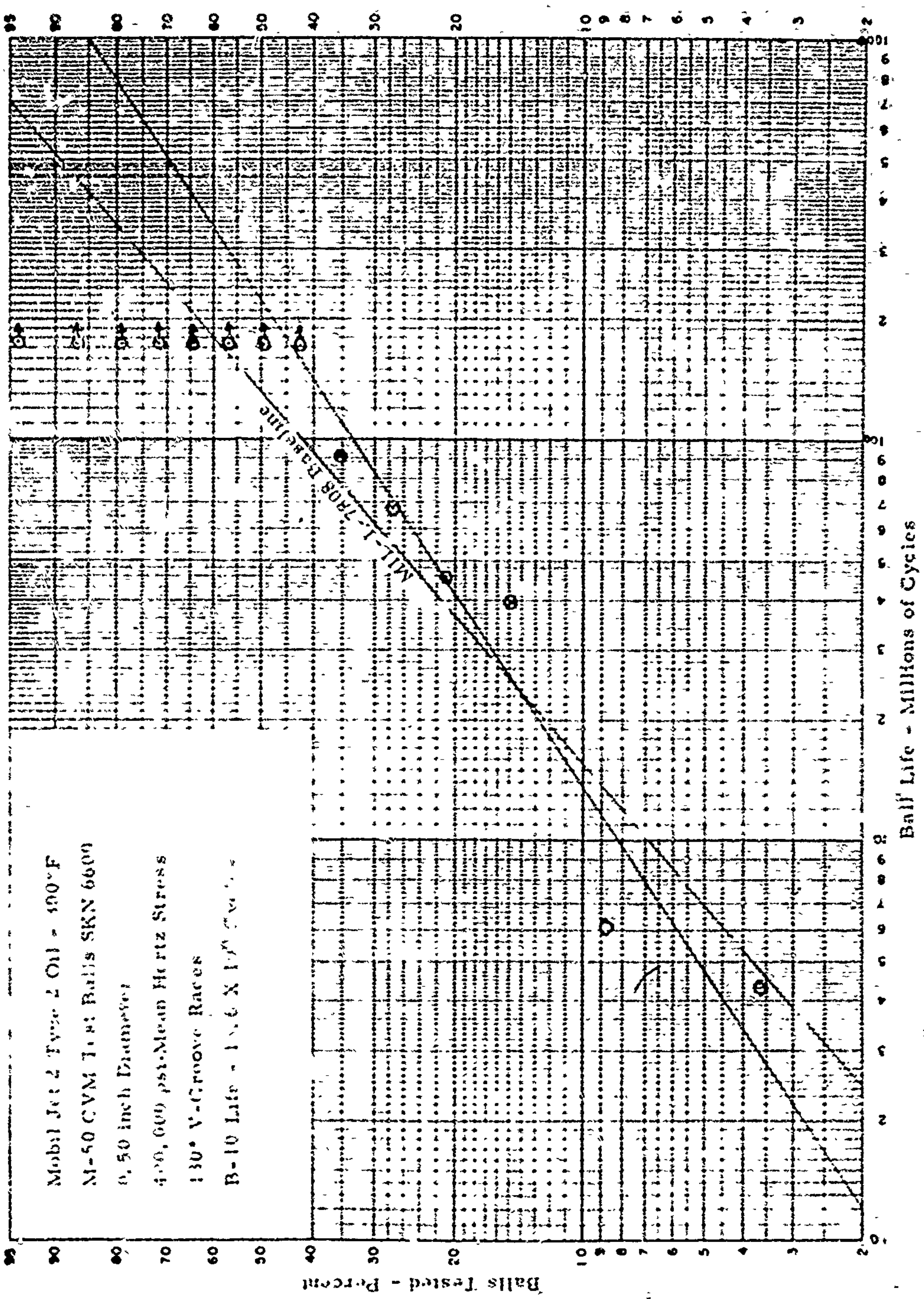

WEIBULL DISTRIBUTION OF BALL TEST IN TYPE II OIL

Figure II-17

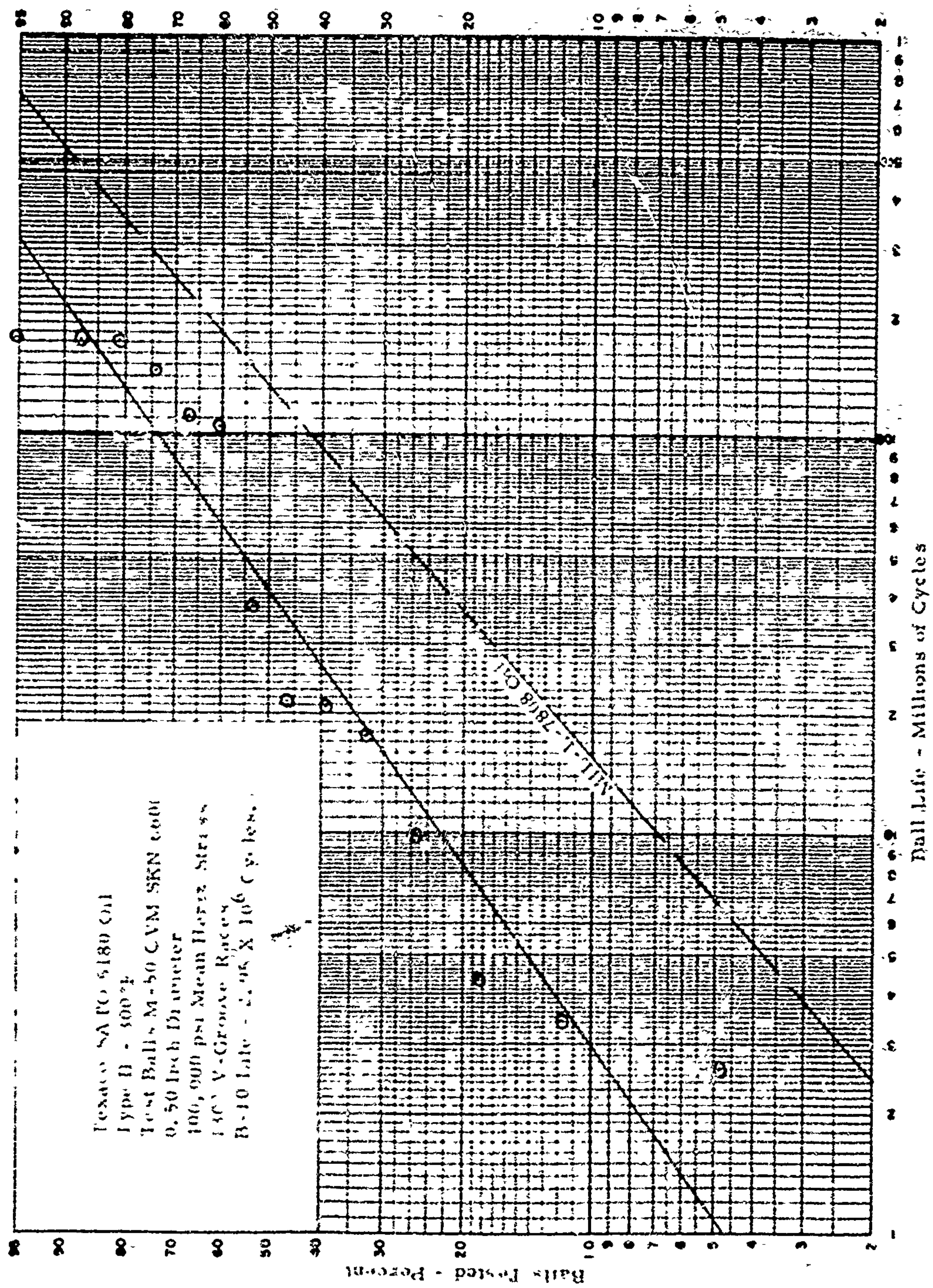

WEIBULL DISTRIBUTION OF BALL
TEST IN SATO 5180 OIL

Figure 11-18

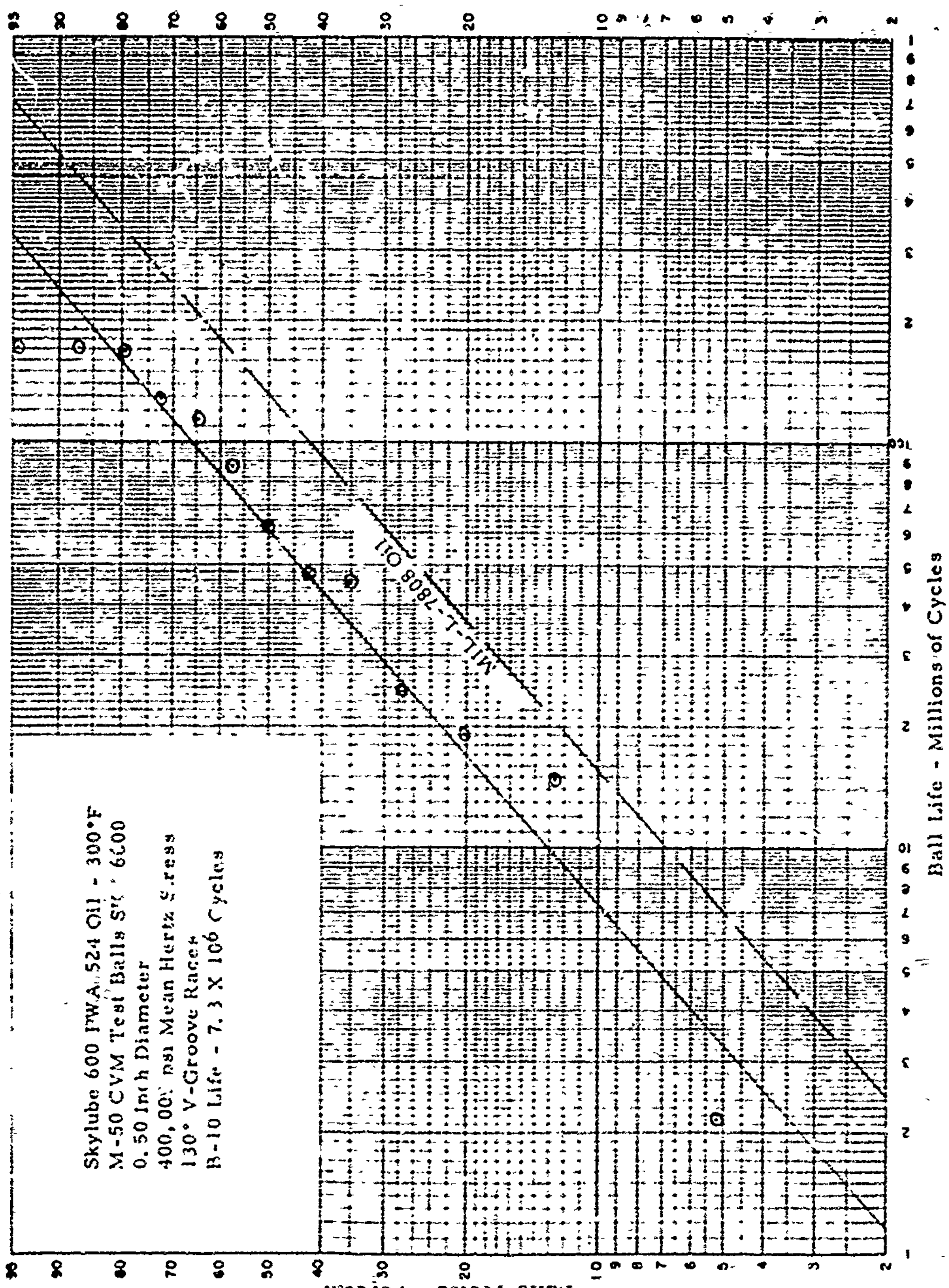

WEIBULL DISTRIBUTION OF BALL TEST IN
PWA-524 OIL

Figure 11-19

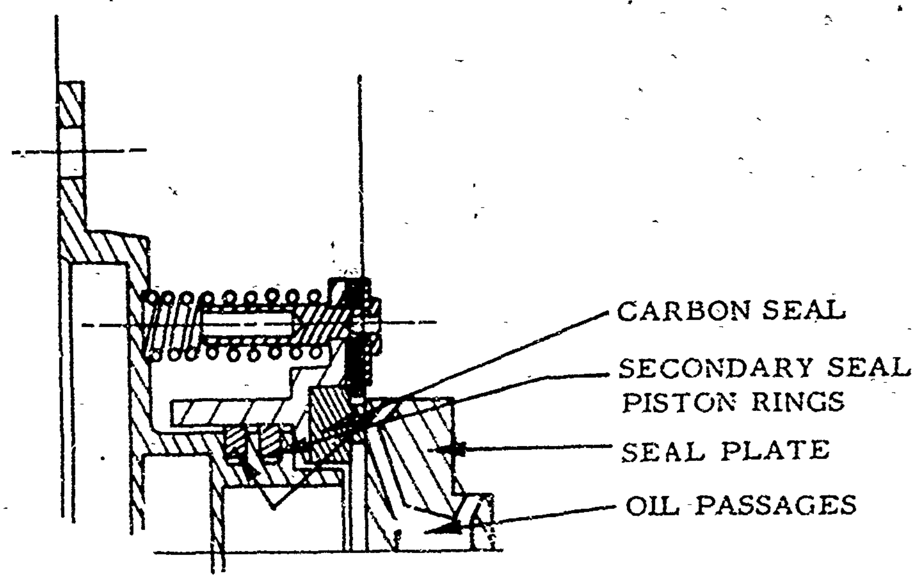

WET-FACE SEAL

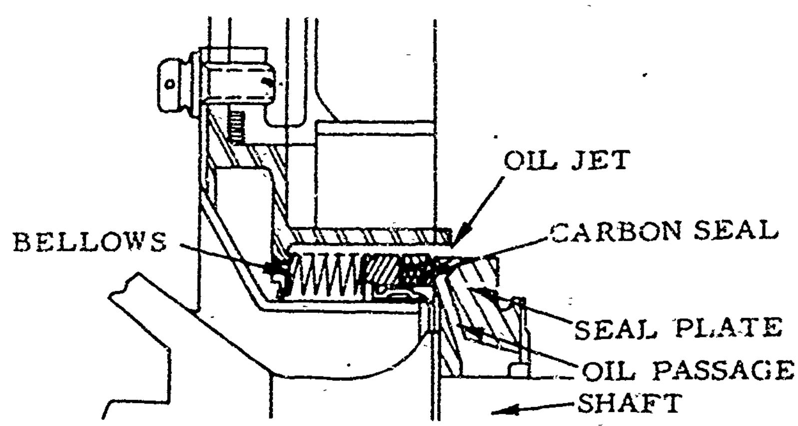

BELLOWS-TYPE WET-FACE SEAL

SCHEMATIC DIAGRAMS OF FACE-TYPE OIL SEALS

Figure 11-20

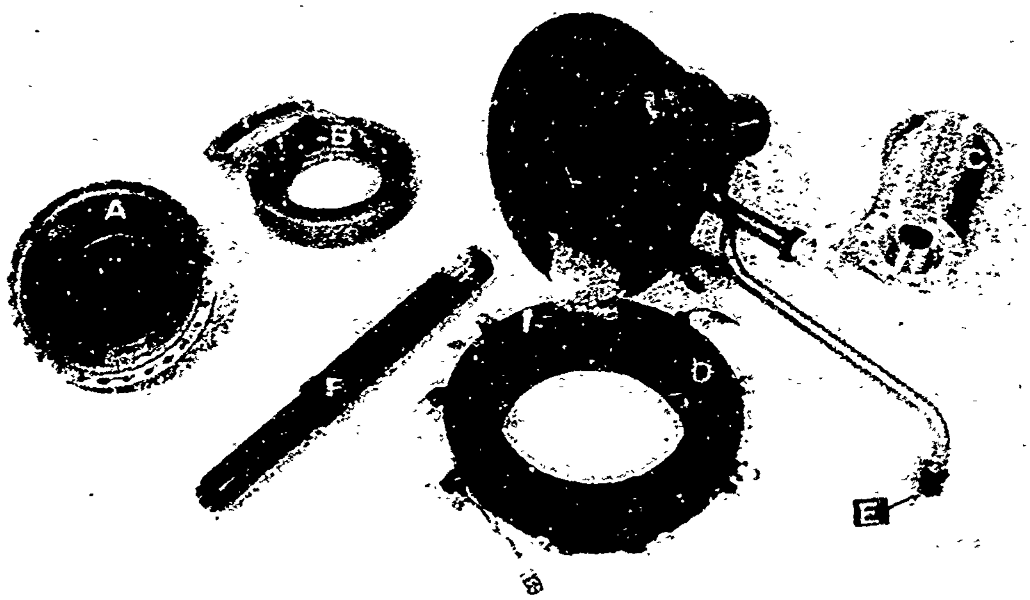

XP-31680

COMPONENT PARTS OF OIL SEAL TESTING RIG INCLUDING (A) FRONT COVER, (B) RIG BEARING, (C) HUB, (D) OIL JET TO SEAL PLATE, (E) BREATHER MANIFOLD, (F) SHAFT.

Figure 11-21

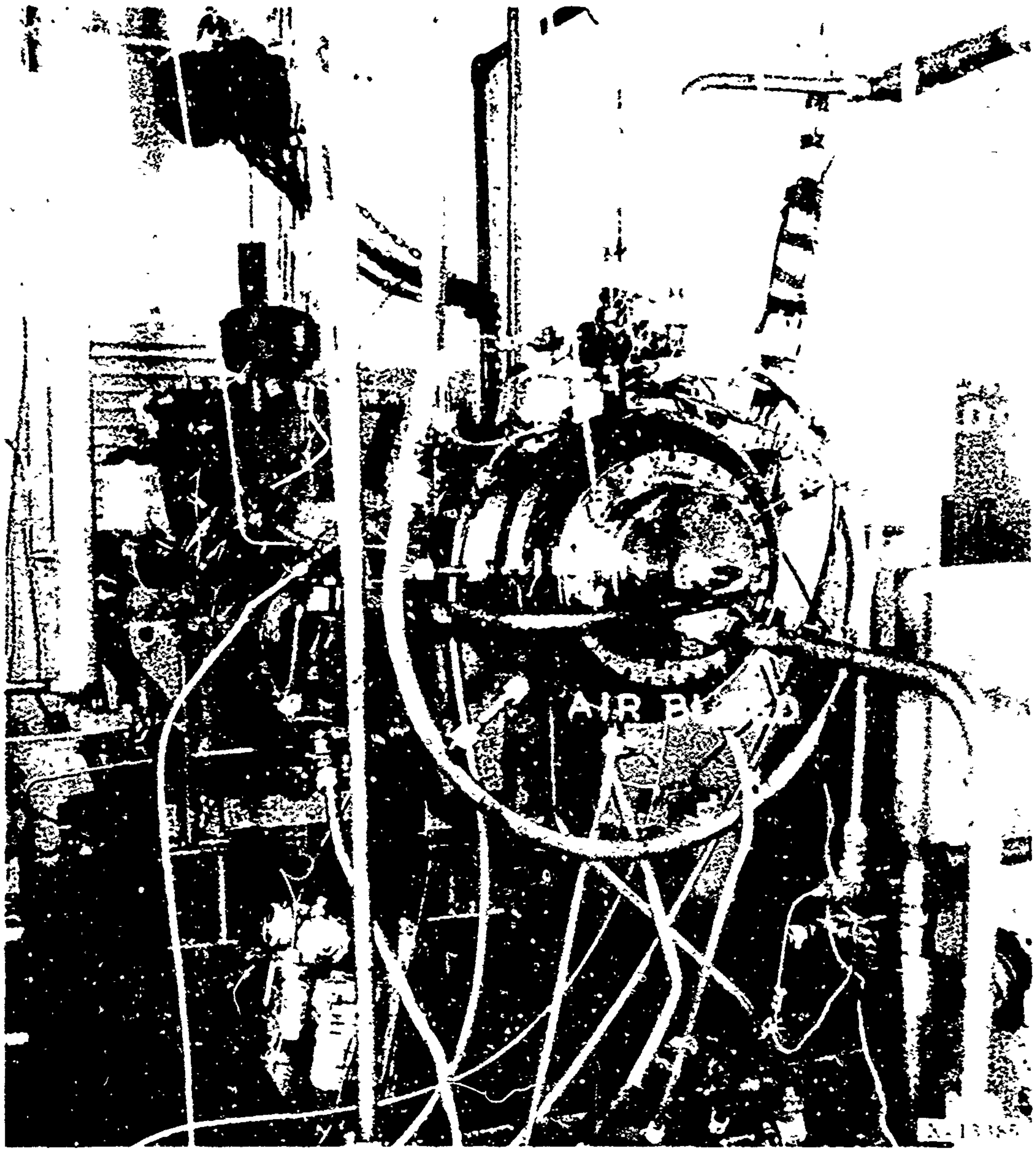

FACE SEAL HIGH-TEMPERATURE TEST RIG
INSTALLATION

Figure 11-22

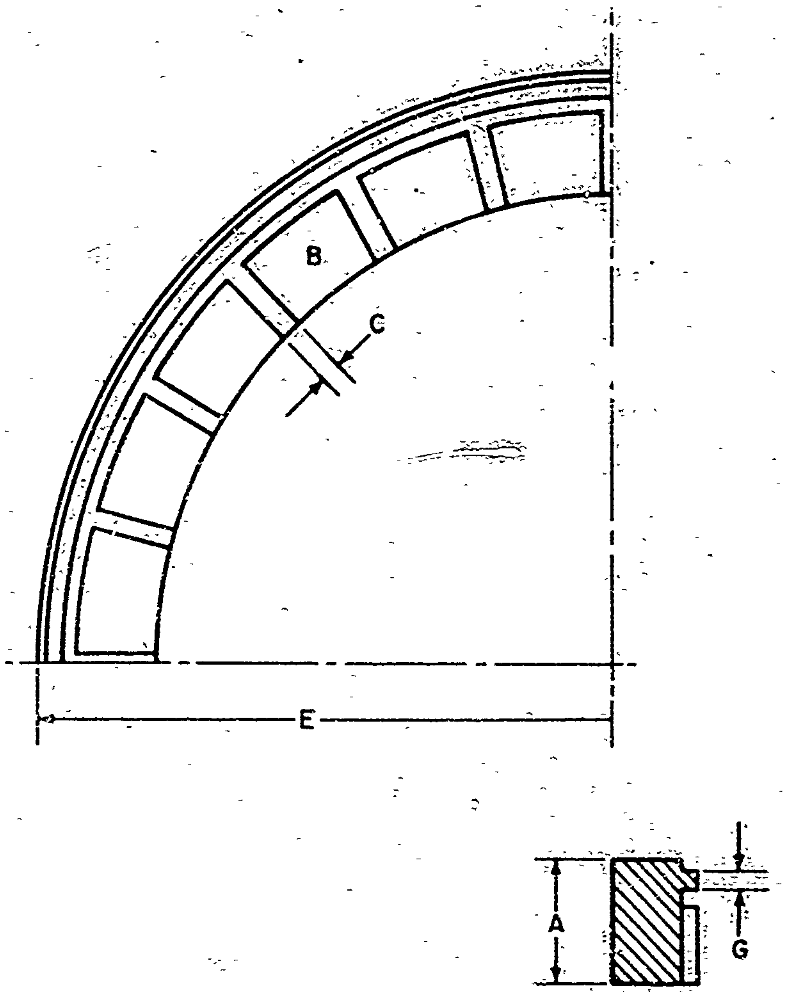

VARIABLES AND LEVELS

A – THICKNESS: 0.2, 0.8 INCH
B – NO. OF PADS PER INCH OF DIA : 4, 6
C – GROOVE WIDTH: 0.155, 0.200 INCH
E – OUTSIDE DIA: 6, 8 INCHES
G – LIP WIDTH: 0.025, 0.050 INCH

RADIAL GROOVE TYPE RING SEAL DESIGN

Figure II-23

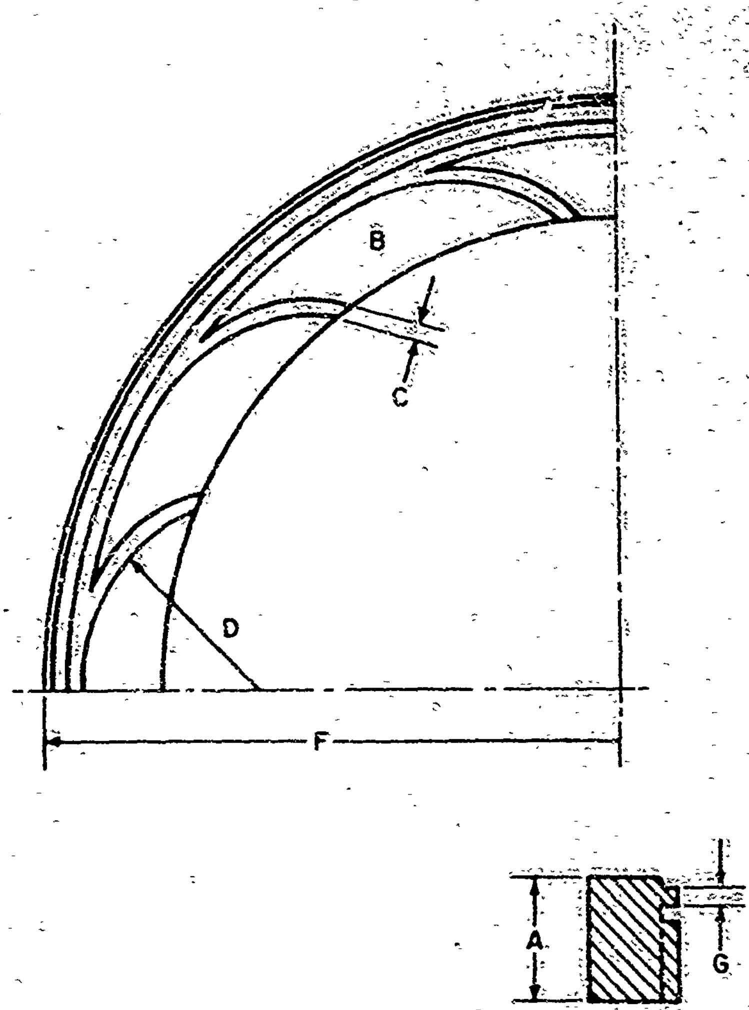

VARIABLES AND LEVELS

A – THICKNESS: 0.2, 0.8 INCH
B – NO. OF PADS PER INCH OF DIA: 3, 4
C – GROOVE WIDTH: 0.025, 0.050 INCH
D – GROOVE RADIUS: 1.00, 2.00 INCHES
F – OUTSIDE DIA: 6, 8 INCHES
G – LIP WIDTH: 0.025, 0.050 INCH

CIRCULAR GROOVE TYPE RING SEAL DESIGN

Figure 11-24

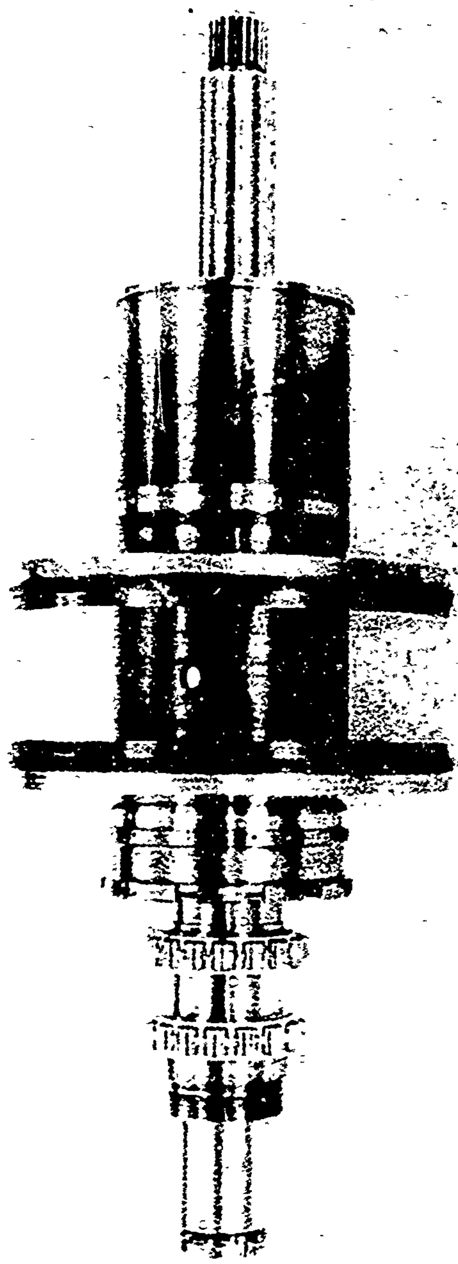

XP-43337

RING SEAL DESIGN TEST SHAFT INCLUDING (1) BACK-UP PLATE, (2) RING SEAL AND (3) SEAL PLATE

Figure 11-25

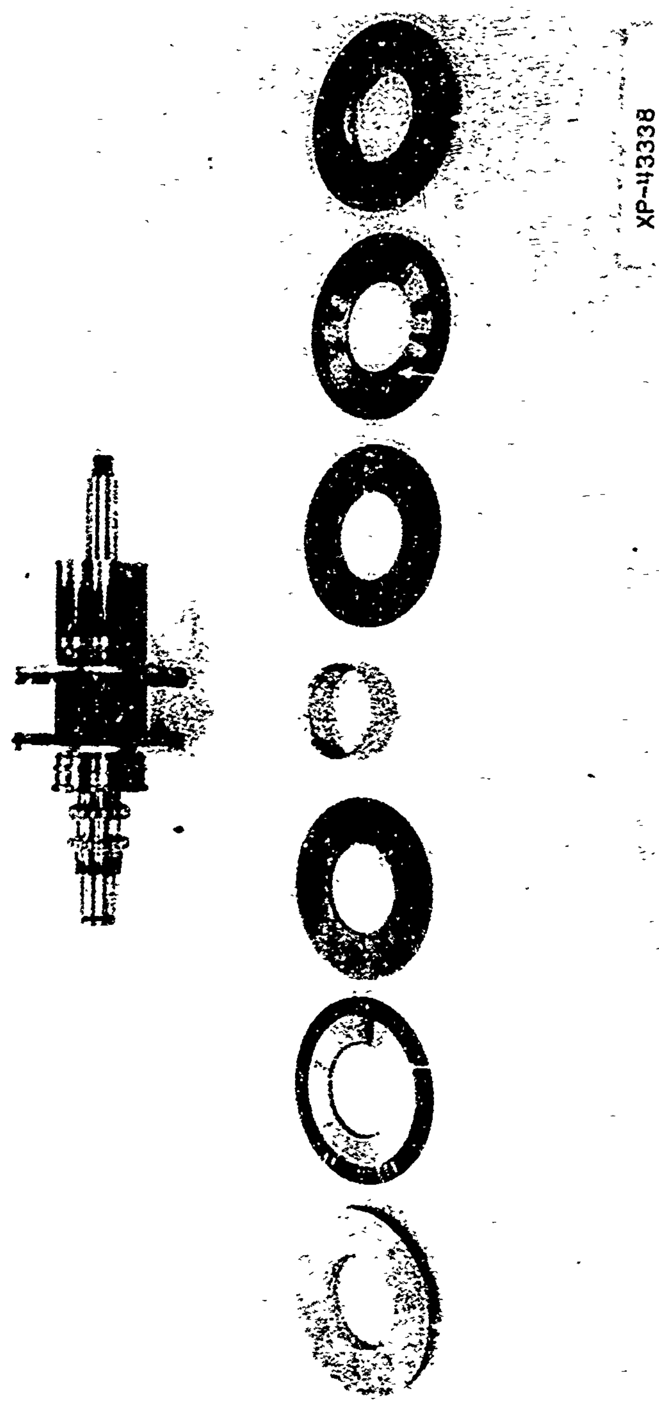

RING SEAL TEST SHAFT STACK-UP INCLUDING
(1) SEAL PLATE, (2) RING SEAL, (3) SPACER,
(4) BACK-UP PLATE, AND (5) SPACER.

Figure 11-26

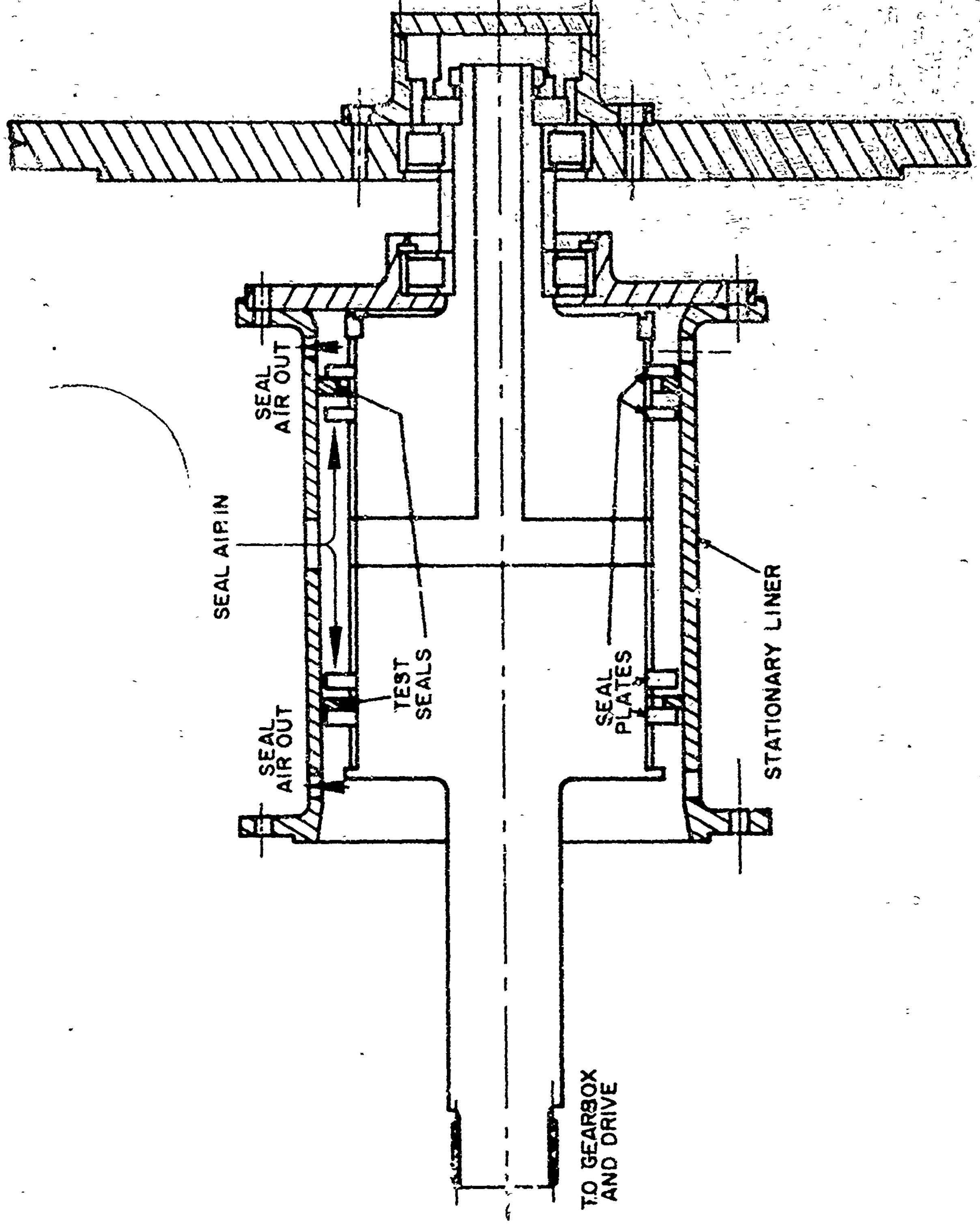

SCHEMATIC DIAGRAM OF SEAL MATERIAL EVALUATION TEST RIG

Figure 11-27

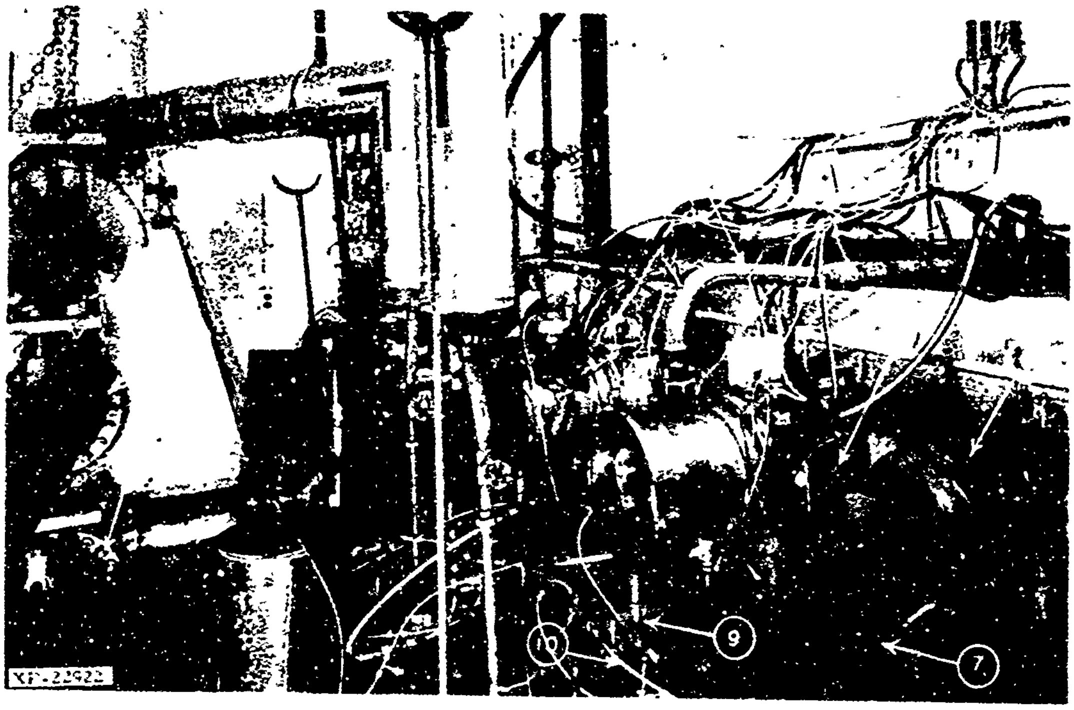

INSTALLATION OF RING SEAL TEST RIG INCLUDING (1) AIR HEATERS, (2) HIGH PRESSURE AIR LINES, (3) STAND BREATHER LINE, (4) THERMOCOUPLE CONDUIT, (5) RIG BREATHER, (6) DRIVE MOTORS (THREE 15 HP), (7) GEARBOX OIL DRAIN, (8) TWO-SPEED GEARBOXES, (9) RIG DRAIN, (10) RIG OIL SUPPLY MANIFOLD

Figure 11-28

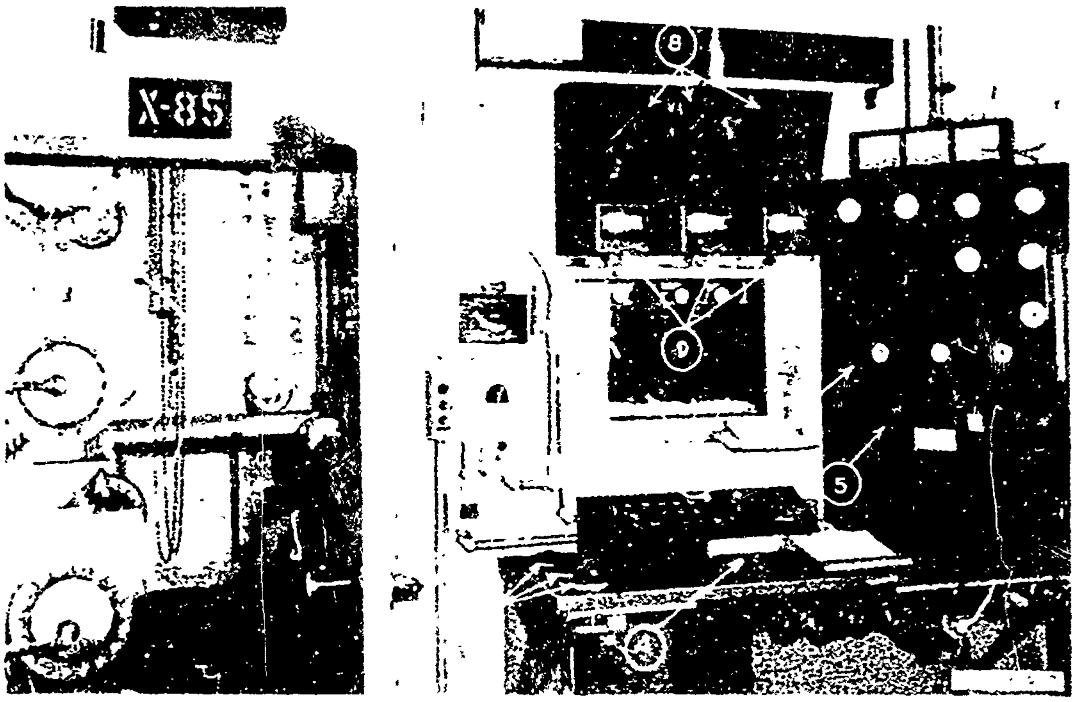

TYPICAL RIG TEST CONTROL STAND INCLUDING (1) AIR HEATER, (2) FIRE CONTROL, (3) POWER STATION TO CONTROL HEATER, (4) LEWIS SWITCH, (5) POTENTIOMETER, (6) PRESSURE GAUGES, (7) ROTOMETERS (8) PRESSURE GAGES, (9) HEATER TEMPERATURE CONTROLS

Figure II-29

RING SEAL TEST DATA

Six-inch Ring Seal Design - Circular Grooves

Seal Plate - Stellite 6B

Temperature - Ambient

Carbon - CDJ-83

Test Point	Press. psig	Speed rpm	Test Time hours	Front Wear (mils/100	Rear Wear hours)
1	60	10,510	1.0	Broke	Broke
2	40	7,640	5.0	6.0	20.0
3	40	9,550	5.0	28.0	22.0
4	40	11,460	4.5	Broke	Broke
5	60	7,640	5.0	84.0	82.0
6	60	9,550	0.5	Broke	Broke
7	40	9,550	5.0	14.0	22.0
8	60	10,510	0.4	Broke	Broke
9	60	9,550	5.0	92.0	146.0
10	40	10,510	0.5	Broke	Broke
11	60	7,640	5.0	1050.0	1050.0
12	60	9,550	2.8	Broke	Broke
13	60	7,640	0.3	Broke	Broke
4	40	10,510	5.0	Broke	Broke
					214.0
7	40	9,550	5.0	24.0	Broke
					202.0

Figure 11-30

RING SEAL TEST DATA

Eight-inch Ring Seal Design - Circular Grooves

Seal Plate - Stellite 6P Temperature - Ambient

Carbon - CDJ-83

Test Point	Press.	Speed	Test Time	Front Wear (mils/100	Rear Wear hours)
14	40	7,150	5.0	Broke 36.0	Broke 42.0
15	60	7,150	3.0	Broke	Broke
18	40	5,730	5.0	Broke 32.0	28.0
21	60	7,150	5.0	Broke 102.0	Broke 92.0
24	60	5,730	5.0	Broke 60.0	Broke 720.0
16	60	5,730	2.0	Broke	Broke
17	40	7,150	5.0	624.0	1878.0
19	40	5,730	5.0	56.0	58.0
20	40	7,150	5.0	160.0	868.0
22	60	5,730	5.0	156.0	1056.0
23	40	7,870	1.25	Excessive	Missing
25	60	7,870	25	Broke	Broke
26	60	7,870	0.5	Broke	Broke
44	40	7,870	0.1	Excessive	Excessive
42	40	7,870	5.0	4.0	426.0
14	40	7,150	5.0	152.0	344.0

Figure 11-31

RING SEAL TEST DATA

Eight-inch Ring Seal Design - Radial Groove

Seal Plate - Stellite 6B — Temperature - Ambient

Carbon - CDJ-83

Test Point	Press.	Speed	Test Time	Front Wear (mils/100 hours)	Rear Wear (mils/100 hours)
2	40	9,540	5.0	78.0	124.0
4	40	7,640	5.0	2.0	8.0
6	40	9,540	5.0	650.0	232.0
7	60	7,640	5.0	4.0	56.0
8	60	9,540	5.0	74.0	102.0
3	40	10,490	5.0	28.0	82.0
10	60	10,490	5.0	387.0	118.0
11	60	10,490	5.0	70.0	140.0
24	40	10,490	5.0	64.0	2.0
26	60	10,490	5.0	50.0	104.0
28	40	10,490	5.0	4.0	2.0
29	40	9,540	5.0	2.0	2.0
24	40	10,490	5.0	90.0	164.0
8	60	9,540	0.25	Broke	Broke
7	60	7,640	5.0	4.0	4.0
4	40	7,640	5.0	0.0	26.0
24	40	10,490	5.0	92.0	4.0
27	40	9,540	5.0	64.0	14.0

Figure 11-32

RING SEAL TEST DATA

Eight-inch Ring Seal Design - Radial Grooves

Seal Plate - Stellite 6B

Temperature - Ambient

Carbon - CDJ-83

Test Point	Press.	Speed	Test Time	Front Wear (mils/100 hours)	Rear Wear (mils/100 hours)
15	40	7,870	5.0	440.0	1466.0
17	40	7,870	2.5	Broke	Broke
19	60	5,730	5.0	0.0	6.0
21	80	8,600	10 min.	Excessive	Missing
36	60	5,730	5.0	0.0	2.0
12	40	7,870	5.0	2.0	2.0
35	40	7,150	5.0	340.0	1214.0
39	60	5,730	5.0	2.0	0.0
40	60	7,870	5.0	54.0	50.0
42	60	5,730	5.0	34.0	0.0
12	40	7,870	5.0	0.0	0.0
36	60	5,730	5.0	0.0	6.0
39	60	5,730	5.0	2.0	2.0
41	60	7,150	5.0	16.0	66.0
44	40	7,150	4.5	16.0	Missing

Figure 11-33

RING SEAL TEST DATA

Eight-inch Ring Seal Design - Radial Grooves
Radial Width Optimization

Seal Plate - Stellite 6B

Carbon - CDJ-83

Temperature-Ambient

Pressure - 60 psig

Speed - 5730 rpm (200 ft./sec.)

Test Point	Radial Width Inches	Test Time Hours	Front Wear (Mils/100	Rear Wear hours)
19*	.800	5.0	0.0	6.0
39*	.800	5.0	2.0	0.0
39*	.800	5.0	2.0	2.0
45	.600	5.0	8.0	2.0
45	.600	5.0	2.0	0.0
46	.500	5.0	12.0	8.0
46	.500	5.0	12.0	4.0
46	.500	5.0	4.0	4.0
47	.400	5.0	16.0	16.0
47	.400	5.0	2.0	2.0
48	.200	5.0	60.0	434.0

*These points also listed in Figure 11-33.

Figure 11-34

FUELS & LUBRICANTS

ITEM 12 - FUELS

OBJECTIVE

This item of the contract required that Pratt & Whitney Aircraft continue work with major oil companies to investigate fuels suitable for use in the engine of a supersonic transport aircraft.

The goal of this program was to obtain a satisfactory compromise between engine design parameters and engine fuel delivery temperatures and to establish the capability of, or the improvement required to make jet "A" kerosene satisfy the requirements for economical supersonic transport operation.

A. INTRODUCTION

Pratt & Whitney Aircraft has continued to work with the major oil companies during Phase II-A to investigate fuels suitable for use in the engine of the supersonic transport airplane. This work has included (1) a survey of current Jet A aviation kerosene fuels used domestically, (2) an investigation of the effect of dissolved oxygen on fuel thermal stability and (3) a further definition of the environment to which the fuel will be subjected in a supersonic transport airplane and powerplant. These investigations were undertaken to determine if fuels of current Jet A quality would be satisfactory for the supersonic transport powerplant and to support the selection of a fuel of suitable quality at a cost equivalent to current Jet A fuel.

B. JET FUEL SURVEY

Commercial jet aircraft presently operate with three types of fuel which are described in Specification ASTM D-1655 as Jet A, Jet A-1 and Jet B. While each of these fuels is procured under a number of specifications issued by the airlines and the engine manufacturers, the technical requirements for each fuel type are comparable.

Jet A fuel is a kerosene type with -40°F freezing point. It is used predominately where operations do not expose fuel to extremely low temperatures as a result of cold soaking either in flight or on the ground. Because most domestic flights are of short duration, this fuel is used at most secondary air terminals.

Jet A-1 is similar to Jet A except for a -58°F freezing point required for long flights in cold climate areas such as the North Atlantic. This fuel is consequently stocked at major international air terminals and is also used on cross-continent flights in the U. S. As a consequence, this fuel represents a large percentage of the aviation kerosene used domestically.

Jet B is a JP-4 type fuel used mainly in overseas flights where it can afford lower fuel costs because of the existing domestic tax structure. This fuel was not considered suitable for SST applications and, therefore, the fuel survey was limited to Jet A and Jet A-1 type fuels.

Previous studies have shown that, while Jet A kerosene generally had sufficiently low volatility and vapor pressure characteristics to be usable in supersonic transport applications, its thermal stability was not adequate as presently defined by existing specifications. According to these, Jet A must have a minimum thermal stability level of 300°F preheater temperature/400°F filter temperature (300/400) when tested in the ASTM-CFR Fuel Coker, ASTM Method D-1660. While all existing Jet A and Jet A-1 fuels are manufactured to this minimum, it is known that some fuels can have considerably higher thermal stability as a result of differing crude source, composition, refining methods and "built-in" margins because of coker test reproducibility.

To determine the thermal stability margins presently existing in today's aviation kerosene fuels and to further define the fuels as presently used, a survey of domestic fuel sources was made. To assure that this sampling would be statistically valid, yet within budgetary limitations, it was limited to thirteen major oil companies who produce and supply about eighty-seven percent of the aviation kerosene. Twelve petroleum companies responded by providing one drum of each Jet A or Jet A-1 fuel presently being produced for airline accounts. In addition, a two drum quantity of each fuel normally supplied to J. F. Kennedy, O'Hare, Los Angeles and San Francisco International Air Terminals was obtained. The latter fuel samples were subjected to more extensive testing as these locations represented the largest fuel volume usage. Samples were provided from refinery sources representing fuel batches currently in process of delivery or from bulk terminal areas normally supplying various airport locations.

In all, forty-nine samples of Jet A or Jet A-1 fuel were provided; sixteen of these represented the four major air terminals. The fuels were shipped directly to a contract laboratory for the following tests:

1. An inspection of each fuel sample to determine physical properties in relation to existing specifications such as ASTM D-1655.

2. A determination of the thermal stability breakpoint temperature in the ASTM-CFR Fuel Coker for each fuel.

3. A determination of thermal stability break point temperature in the CRC Research Fuel Coker with a heated reservoir. (The breakpoint temperature is the temperature at which a Code 3 deposit level is produced). Breakpoint temperatures were determined for the sixteen major air terminal samples only.

4. A determination of fuel lubricity characteristics in the Ryder Gear Machine for the 16 major air terminal samples only.

The results of these investigations are described in the four subsections which follow.

1. FUEL INSPECTION DATA

Upon receipt at the laboratory the fuels were assigned individual sample numbers. A listing of these numbers, with information on the vendor source (coded), air terminal where used and ASTM fuel type, is presented in Figure 12-1. Laboratory tests were conducted on these fuels to determine physical properties; these data are listed in Figure 12-2. Maximum, minimum and average values of these physical properties for the Jet A and Jet A-1 fuel samples are listed at the end of this table. Distillation data were also obtained on the fuel samples and are listed in Figure 12-3.

2. BREAKPOINT TEMPERATURES

ASTM-CFR Fuel Coker tests were conducted on all the fuel samples to determine breakpoint temperatures. In these tests the ASTM-CFR Fuel Coker was operated at successively higher preheater/filter temperature conditions on each sample to obtain preheater deposits bracketing a Code 3 deposit level. Testing steps were made at 25°F increments. The results of these tests are tabulated in Figure 12-4.

Tests were conducted in a CRC Research Fuel Coker on each of the sixteen major air terminal samples at fuel reservoir temperatures of ambient (approx. 75°F), 175°F and 250°F. Preheater/filter temperature levels were raised at 25°F increments until preheater deposits bracketing a Code 3 deposit level were obtained. Data derived from this survey is tabulated in Figure 12-5.

In both the ASTM and CRC Research Coker tests, a Code 3 deposit level was used to define the breakpoint temperature. Selection of the Code 3 deposit level tends to yield a breakpoint temperature which is higher than the limits established in existing specifications; these being generally Code 2 maximum. However, this approach yields more definitive breakpoints from the available data and is somewhat compensated by the fact that resulting deposits frequently went from Code 1 to Code 4 within a 25°F preheater increment. Breakpoint temperature was further interpreted as the higher preheater temperature at which a deposit of Code 3 or lower deposit code was obtained when the next higher temperature (25°F increment) yielded a deposit exceeding Code 3.

Breakpoint temperature data are summarized in Figure 12-6 for both the ASTM-CFR Fuel Coker and the CRC Research Fuel Coker. Differences in breakpoint temperatures are to be expected with these two test methods because of the differing equipment geometry and the use of a heated fuel reservoir in the CRC Research Fuel Coker test. The latter test is believed to be more indicative of the thermal performance of fuels in a supersonic airplane because it includes to some extent the type of heating fuel receives in the aircraft tanks and in the airframe fuel system prior to delivery to the engine. The distribution of preheater breakpoint temperatures in the ASTM coker are shown in Figure 12-7 and plotted in Figure 12-8. "Breakpoints" fell in the range of 275°F - 425°F and generally confirmed that a wide variation in thermal stability margins exist in current fuels. It is not yet known whether the single fuel shown as being below specification limits truly represented this possibility or whether this particular result was occasioned by sampling technique or handling of the fuel during this survey. The latter is more probable. As shown in Figure 12-8, the average fuel used at the major air terminals had a preheater breakpoint of 350°F, the average of all fuels being 350-375°F breakpoint temperature (based on preheater deposits).

Figures 12-9 and 12-10 indicate the ASTM coker preheater breakpoint temperature distribution after correcting the breakpoint data of Figures 12-7 and 12-8 for conformance to a maximum filter pressure increase of 13" Hg during the ASTM-CFR fuel coker test. In comparison to the previous distribution plot, it more nearly represents the distribution of "usable" specification fuel, although it is quite similar overall.

The distribution of CRC Research Fuel Coker preheater temperature breakpoints, based on Code 3 deposits, is tabulated in Figure 12-11 and plotted in Figures 12-12 and 12-13 for reservoir temperatures of ambient, 175°F and 250°F. These breakpoint temperature distributions differ from those of the ASTM coker for the reasons previously noted. However, the average fuel (50% level) showed a similar preheater breakpoint temperature (350-375°F).

3. EFFECT OF RESERVOIR HEATING

It was previously mentioned that the CRC Research Fuel Coker test is believed to be more indicative of fuel thermal stability requirements in a supersonic airplane because it also includes the bulk heating effect imposed by the airframe fuel tank environment and to some extent simulates airframe heat sink inputs.

The effect of such bulk heating on preheater breakpoint temperature is shown for individual fuels in Figure 12-14. Generally, the effect of bulk heating in the range of 75°F to 250°F was very flat for the survey fuels and in most cases, was within a 25°F band. This sensitivity is considered to be within the repeatable accuracy of the coker test. The flat response of the survey fuels to bulk heating was also confirmed by the distribution of breakpoints for each bulk fuel (reservoir) temperature condition as shown in Figure 12-15.

The information on fuel thermal stability, breakpoint characteristics and bulk heating effects obtained during this survey, was subsequently correlated with environmental data in order to determine what changes in the characteristics of present Jet A fuels would be necessary to permit their use in an SST application. The latter work is described in subsection C starting on page 12-7 of this report.

4. FUEL LUBRICITY

Present fuels contain trace impurities, sulfur and nitrogen compounds which are polar in nature and hence, provide some beneficial lubrica-

tion effect for fuel pumps, controls and actuating mechanisms. Serious wear problems, malfunctions, etc. in existing equipment, have not been experienced with these fuels to date because of any lubrication deficiency. However, it is anticipated that the supersonic transport powerplant, because of higher fuel temperatures, may not have adequate viscosity-derived lubricity and may further be deprived of the beneficial effects of trace impurities by the need to provide a more thermally stable fuel.

In order to determine what levels of fuel lubricity exist in present commercial aviation fuels, the sixteen fuel samples from the major international air terminals (Kennedy, O'Hare, Los Angeles and San Francisco) were tested in the Ryder Gear Machine.

The Ryder Gear Machine is universally used to determine the load-carrying ability of aviation gas turbine oils as required by several specifications. Federal Test Method Standard No. 791, Method 6508 describes the machine and method of test. The Ryder Machine employs high precision spur test gears mounted on parallel shafts and lubricated with the test fluid. Through use of meshing helical gears and a four-square loading principle, the test gears are operated under step loads for 10-minute periods. The amount of scuffing or abrasion on each test gear tooth is determined after each load application; load-carrying ability being defined as the load (lbs/inch of tooth face width) that occurs when 22 1/2 percent of the tooth face area is scuffed. The Ryder test provides high relative sliding velocities and in other investigations has been shown to be applicable to lubricity problems associated with fuel pumping and metering. In applying this test to the measurement of fuel lubricity, operation is similar to that used for oils except that the test fluid is unheated and smaller load increments are used.

Data from these tests on the load-carrying ability of the sixteen samples of fuel from the four major air terminals are shown in Figure 12-16. These tests indicated that present commercial aviation kerosene fuels had Ryder values of load carrying ability (fluid lubricity) ranging from 257 to 452 lbs/inch tooth face width with one fuel yielding 615 lbs/inch. These levels are similar to average values already determined for JP4 (250 lb/inch) and JP5 (375 lb/inch) type fuels. It can only be concluded at this time that present commercial aviation kerosene fuels have lubricity characteristics (as defined by the Ryder Gear Test) comparable to similar type hydrocarbon fuels and do not show significant variation of this property within the accuracy limitations of the Ryder test device.

No correlation could be found between fuel lubricity levels (Ryder Scuff value) and breakpoint temperature for the fuels tested. Accordingly, it may be further concluded that significant decreases in fuel lubricity are not likely to occur as a result of attaining a more thermally stable Jet A type fuel to meet the stability requirements determined in Section D of this report.

Whether these lubricity levels will be satisfactory for SST application, or impose heavier component design and development burdens can only be determined through environmental operation of SST hardware and components.

C. INVESTIGATION OF THE EFFECT OF OXYGEN CONTENT ON FUEL THERMAL STABILITY

The measurement of fuel thermal stability in the ASTM-CFR and CRC Research Fuel Coker tests is conducted with the fuel fully saturated with air at the start of each test. The equilibrium oxygen content of fuel under these conditions is about three to four percent by volume of oxygen (55-70 ppm) for most Jet A type fuels. While it is known that the complete elimination of dissolved oxygen significantly improves fuel thermal stability, present commercial aircraft do not operate with fuels having low oxygen content. However, the possibility exists that a supersonic transport cruising at high altitudes (about 60-70,000 ft.) and with normally vented fuel tanks may experience a reduction in oxygen content in the fuel with attendant fuel thermal stability benefits. In order to investigate this possibility, CRC Research Fuel Coker tests were conducted on three fuels having relatively low thermal breakpoint temperatures to determine what improvement in breakpoint temperature could result from a reduction in oxygen content. In this program CRC Research Fuel Coker tests were conducted at 175°F reservoir temperature using the following fuels:

F-1497	A West Coast Jet A-1 fuel from the same source as fuel F-1350 in the jet fuel survey which had previously shown an ASTM-CFR Coker breakpoint of 350°F.
F-1498	An East Coast Jet A-1 fuel made from Texas crude from the same source as fuel number F-1368 in the Jet Fuel Survey which previously showed a standard ASTM Coker breakpoint of 325°F.

F-1065 A MIL-J-5161E, grade JP-5 referee fuel which normally has an ASTM-CFR Coker breakpoint of 325°F.

Low breakpoint temperature fuels were selected because these were expected to show the most beneficial effects from oxygen reduction.

Breakpoint temperatures for these fuels, when fully saturated with oxygen, were initially determined at 175°F reservoir temperature in the CRC Research Coker to serve as base line data. Coker tests were then conducted with low oxygen content which was obtained by drawing a vacuum of 0.9 ± 1.0 psia on the coker reservoir prior to the start of testing. A magnetic stirrer was operated in the fuel reservoir during each test to hasten oxygen elimination. The 1.0 psia tank pressure represents a typical cruise altitude for a supersonic transport flying at Mach 2.7 cruise with open tank vents and is equivalent to equilibrium fuel oxygen content of 4 ppm (0.25% by volume). Tests with oxygen levels equivalent to 1.5 ± 0.1 psia (50,000 ft. altitude) and 8 ppm oxygen content (0.5% by volume) were also made. A Beckman Model 777 oxygen sensor, which was used to determine oxygen content, was initially installed in the fuel reservoir but was subsequently moved to a reservoir return line after the coker fuel pump. Prior to each reduced oxygen content test, the sensor probe was calibrated in air and installed in the by-pass loop.

In order to determine saturated oxygen contents for each test fuel the fuels were sent to a testing laboratory having gas liquid chromatographic equipment and gas analysis capabilities. The test fuels were air saturated at 80°F by bubbling air through them. They were subsequently degassed by a cyclic thin film vacuum technique and the gas composition analyzed in a chromatograph. The oxygen saturation values at 80°F are listed below. These are the dissolved oxygen values of the test fuels at the start of each coker test inasmuch as the test fuel was air-saturated prior to coker tests at either standard or reduced reservoir pressure conditions.

Fuel	Saturated Dissolved Oxygen Content at 80°F
F-1497	3.17% vol.
F-1065	4.13% vol.
F-1498	4.00% vol.

Test results obtained at 175°F reservoir temperature in the CRC Research Fuel Coker with saturated fuel and ambient atmospheric pressure are shown in Figure 12-17. In each case the fuel was aerated in the fuel reservoir to attain air saturation. This was done at 80°F to produce dissolved oxygen concentrations similar to those noted above. In addition, oxygen content was determined on the F1065 fuel during a test at 175-450/550 conditions. During this test dissolved oxygen content of the fuel entering the preheater section was found to be 4.13 percent at the start of the test and 3.98 percent by volume at the end of the test.

The results of research fuel coker tests conducted at a reservoir pressure of 1.0±0.1 psia (reduced fuel oxygen content) and a reservoir temperature of 175°F are shown in Figure 12-18 for the three test fuels. Typical values of dissolved fuel oxygen measured during these tests by means of a Beckman oxygen sensor probe located in the reservoir by-pass loop after the coker fuel pump are shown in Figure 12-19. A plot of the fuel oxygen content during a typical test (No. 2101) is shown in Figure 12-20. Test Nº2130 and those following were conducted with the oxygen sensor probe located in a by-pass loop prior to the fuel coker pump inlet. A review of the fuel oxygen contents shown in Figures 12-19 and 12-20 indicates that the low target value (0.25% by volume) of equilibrium fuel oxygen content associated with a reservoir or altitude pressure of 1.0±.01 psia was attained or exceeded in these tests.

The performance of the three test fuels in the research coker at both air-saturated and low-oxygen content conditions (equivalent to 1.0±0.1 psia pressure altitude) are shown in Figures 12-21 through 12-23.

As shown in Figure 12-21, the West Coast Jet A-1 fuel (F1497) had a preheater deposit breakpoint, based on Code 3 deposits of 356°F when air saturated. Under conditions of low oxygen content, preheater deposits generally remained at a Code 2 level for this fuel up to a preheater temperature of 475°F, and a definitive breakpoint could not be found for the preheater deposits. However, the 13" Hg. maximum allowable filter pressure increase permitted in current fuel specifications was exceeded under both saturated and low oxygen level tests at temperatures below and slightly above the normal 356°F breakpoint temperature.

The JP-5 referee fuel (F1065) showed a normal preheater breakpoint (using air-saturated fuel) of 400°F. As shown in Figure 12-22 reduced fuel oxygen content did not produce any significant improvement in the coker performance of this fuel in terms of preheater deposits although some slight improvement in filter pressure increase was evidenced in some tests.

The East Coast Jet A-1 fuel (F 1498) was the only one of the three test fuels showing a consistent improvement in coker performance at reduced fuel oxygen levels. Under sea level reservoir conditions with air-saturated fuel, this fuel showed a Code 3 breakpoint temperature of 381°F. At the reduced pressure conditions, a breakpoint temperature based on Code 3 deposits could not be induced up to a preheater temperature of 475°F, although a filter pressure drop of 13" Hg maximum was attained at this temperature.

The results of research fuel coker tests conducted at a reservoir pressure of 1.5 ± 0.1 psia (reduced fuel oxygen content) and a reservoir temperature of 175°F are shown in Figure 12-24 for the three test fuels. Typical values of dissolved fuel oxygen content measured during these tests by means of a Beckman oxygen sensor probe located in a reservoir return loop at the pump inlet are shown in Figure 12-25. A plot of fuel oxygen content during a typical test (No. 2149) is shown in Figure 12-26.

The performance of the three test fuels in the research fuel coker at both air saturated and low-oxygen content conditions (equivalent to 1.5 ± 0.1 psia altitude pressure) are shown in Figures 12-27 through 12-2_.

The tests conducted at the 1.5 psia reservoir condition (equivalent to 9 ppm dissolved oxygen content) demonstrated that low levels of fuel oxygen content suppress heavy "hot wall" deposits, these being not more than Code 3 level up to temperatures considerably higher than the normal air saturated coker breakpoint temperature of the fuel. However, no beneficial effect was found on filter pressure increase in the coker tests.

While it appears from these tests that fuels vary in their sensitivity to oxygen content, a reduction in dissolved oxygen generally results in less severe deposit formation. While this directional improvement might indicate that a fuel could operate at higher temperatures with very low oxygen content, the practical applications of this trend are uncertain at present, because of the indication that filter pressure increases do not follow this same trend and both these factors are equally

important in improving fuel quality. It appears that low fuel oxygen contents can only be exploited as a means of attaining high fuel temperature performance at low fuel cost, if fuels are refined especially to respond to this factor in both preheater tube deposits and filter pressure increase. The possible role of fuel additives in achieving this goal is discussed in Section E.

More extensive testing of additional fuels in the coker at conditions simulating various oxygen levels is required to obtain a greater understanding of the rate of oxygen depletion on thermal stability before advantage can be taken of this phenomenon in actual aircraft operation.

D. REVIEW OF THERMAL STABILITY REQUIREMENTS

Under the Phase II-A contract, fuel environmental temperatures in the supersonic transport aircraft and powerplant were reviewed further in order to more accurately establish thermal stability requirements. Inasmuch as previous studies have shown that the general properties and volatility characteristics of current Jet A type fuel were suitable for SST applications, the present study has concentrated on fuel thermal stability characteristics. Because of the requirement that a satisfactory SST fuel must be capable of being produced without an increase in price over that of ASTM Jet A fuel, related economic factors were also investigated.

In subsonic applications a determination of fuel thermal stability requirements is relatively uncomplicated and these requirements can be easily extrapolated from existing applications by taking into account the total engine cooling load and its effect on fuel oil cooler, fuel system and fuel manifold temperatures. The application of this approach to supersonic aircraft fuel temperatures is complicated by the prior heating which the fuel receives in the airframe components. This includes both the temperature increase in the tank fuel as a result of aerodynamic heating and the rejection of airframe heating loads to the fuel in heat exchangers prior to the delivery of fuel at the engine interface. The latter heat input is similar to that acquired by the engine fuel in absorbing oil heat rejection, but occurs at lower temperatures. In extrapolating fuel thermal stability requirements for supersonic transport applications, it is necessary to estimate and compensate for such prior heating.

A study of aircraft and engine data indicates that the maximum fuel and fuel system environmental temperatures which will be encountered

during cruise operation in the two proposed SST aircraft are as follows:

Temperature of fuel from airframe	250°F (max.)
Temperature of fuel into engine (at engine fuel manifold inlet)	325°F (max.)
Temperature of oil from engine	375°F (av.)
	425°F (max.)
Temperature of oil into engine	275°F (av.)
	350°F (max.)

The selection of fuel thermal stability requirements based on these environmental conditions was approached first as a straight-forward extrapolation from existing allowable limits. From these and from current service experience, it is known that presently available fuels meeting a 300/400/6 standard fuel coker requirement can be used at a fuel temperature of 275°F at the inlet of the engine fuel manifold. At this point the fuel has already served its role as a heat sink for oil cooling and must only face the additional heating environment of the engine manifold and similar distributing lines. Temperature rise through the manifold and fuel nozzle area is about 20°F. This increase in bulk fluid temperature has only a minor influence in determining the required level of fuel thermal stability as it will occur in the manifold and similar distribution lines mainly as a result of heat transfer from the hot walls contacting the fuel. By judicious design and taking full advantage of time-temperature relationships as they effect deposit-forming reactions, plus the use of heat shielding, it is possible to hold metal exposure temperatures at relatively low levels (400-450°F) in these portions of the system. The consideration of metal temperatures will, therefore, be temporarily neglected in this portion of the analysis as they are considered to be non-critical.

The extrapolation process is illustrated in the table below which lists the fuel thermal stability requirements with and without bulk heating for several levels of fuel temperature delivered to the engine airframe interface. In each case it was assumed that the fuel temperature rise in the engine fuel pumps, oil coolers, hydraulic systems and fuel controls is constant at 75°F.

Fuel pump inlet Temperature, °F	200	250	275	300
Engine Manifold, fuel inlet Temperature, °F	275	325	350	375

ASTM-CFR Fuel Coker Requirement (without compensation for bulk heating)	300/400	350/450	375/475	400/500
ASTM-CFR Fuel Coker Requirement Compensated for higher pump inlet temp. (bulk heating effect)	---	350/450	400/500	425/525

As previously mentioned a fuel inlet temperature at the manifold of 275°F can be attained with fuel meeting a standard coker requirement of 300/400; the corresponding engine fuel pump inlet temperature being 200°F. As shown above, each increase in pump inlet temperature will be reflected by a similar and identical temperature increase at the engine fuel manifold inlet because of the constant 75°F rise across the engine fuel system. Neglecting the prior heating history of the fuel and the effect of higher pump inlet temperatures, it is reasonable to assume that higher manifold inlet fuel temperatures will require fuels of higher thermal stability. The 300/400 base level of thermal stability has accordingly been increased by the same temperature increments. Thus, the 325°F manifold inlet temperature requires, through extrapolation alone, a fuel with 350/450 thermal stability while a manifold inlet fuel temperature 100°F above the ba[illegible] requires a fuel with 100°F higher thermal stability (400/

However, it is known that prior heating of fuel can degrade thermal stability by about 0.25-1.0°F for each degree of bulk heating. In obtaining compensated ASTM coker requirements as shown above, it was noted from the results of the jet fuel survey (Figure 12-14 and Figure 12-15) that the response of current Jet A and Jet A-1 fuels to bulk heating was quite flat over a bulk heating range of 100°F to 250°F (150°F range) and that the change in fuel breakpoint temperature over this range was in the order of 25°F for any particular fuel.

A compensating increase of 25°F was accordingly applied against the highest temperature considered (300°F pump inlet temperature). This was also applied against the 275°F pump inlet requirement as a safety factor. It was not considered necessary to apply this correction against the 250°F pump inlet requirement because of the low order of extrapolation of this condition from the existing base.

The above analysis shows that current Jet A fuels will require an ASTM-CFR Fuel Coker thermal stability of 350/450 to be satisfactory in the SST airplane and powerplant. Based on the survey of domestic fuel sources described in Section A this level of thermal stability can be met by approximately ninety percent of existing Jet A or Jet A-1 type fuels, as shown in Figure 12-8 and Figure 12-9.

The suitability of this fuel was also investigated as regards to its metal temperature breakpoint. This was accomplished by replotting the preheater deposit breakpoint temperatures determined for the survey fuels in terms of metal temperature contacting the fuel rather than the usual preheater fuel outlet temperature. Using this approach, it was found that the survey fuels had a distribution of metal temperature breakpoint (Code 3 deposit) for the standard and research fuel cokers as shown in Figure 12-30. As shown, the research coker had a similar breakpoint distribution curve for both 75°F and 175°F reservoir fuel temperature.

Accordingly, the generally higher metal breakpoint temperature shown for the ASTM coker is believed to result from mechanical differences between the cokers and not because of fuel bulk heating effects in the resear[illegible] coker.

The differences between the research and ASTM fuel cokers is further demonstrated in Figure 12-31 which shows the relationship between preheater breakpoint temperature and fuel coker metal temperatures for the survey fuels. On the basis of the relationship shown, the 350/450 standard coker fuel can be used in a system having metal temperatures in contact with fuel of 475°F. Review of the environmental fuel temperatures indicates that maximum metal temperature in the engine oil heat exchanger will be about 400°F, this temperature being within the thermal capability of a 350/450 ASTM Coker fuel. Likewise, it has previously been mentioned that other fuel system metal temperatures can be held, through design, below 450°F.

Criteria on the suitability of SST fuel requires that the fuel be current aviation kerosene of the Jet A type or a fuel of equivalent cost. Inasmuch as a technical review of SST requirements has indicated a need for a fuel having a thermal stability 50°F better than current Jet A, the economic aspects of the required fuels were analyzed.

In this analysis the results of the ASTM-CFR Coker tests conducted during the survey, described at the beginning of this section, were

examined to determine what portion of the domestic supply of Jet A type fuel could presently meet the required SST thermal stability levels. In examining the available data it was assumed that Jet A and Jet A-1 type fuels would not have different thermal stability characteristics because of slight volatility differences. Accordingly, all of the available standard coker data was examined to obtain a wider statistical coverage. Based on the current acceptable levels of preheater deposit and filter pressure increase it was found that forty out of forty-nine survey fuels or eighty-two percent of the total were acceptable as indicated in the tabulation below:

Number of fuels passing ASTM-CFR Coker Test at 350/450 Code 2 P/H deposits, max. 13"Hg. Filter pressure rise. Max.	40
Number of fuels failing	8
Marginal	1*
Number of Fuels in Survey	49

* On basis of 13.2 inches Hg. filter pressure rise

While the above data indicates that a large percentage of present commercial aviation kerosene was acceptable for SST usage, it was not known whether including a specification requirement for a fuel thermal stability of 350/450 based on ASTM coker tests would permit procurement of fuel under the "comparable price criteria." To determine this, five major oil companies were requested to submit statements indicating whether this level of Jet A thermal stability would entail increased fuel prices relative to Jet A fuel.

Replies from four of the five major producers have confirmed that fuel meeting the 350/450 thermal stability requirement can be supplied by them for SST operation in the 1970 period at no increase in price relative to fuels of ASTM Jet A quality. Three replies specifically indicated that no price differential with Jet A would result; one replied to the effect that no substantial differential would occur, while one replied that some increase in fuel costs should be expected. Pertinent excerpts from the replies received from each major oil company are quoted below:

Major Oil Co. A. "We consider it feasible to supply kerosene type turbofuel for the SST meeting a thermal stability

requirement of 350/450 in the standard coker. We anticipate that this requirement can be met at our refineries at no increase in cost over the then prevailing cost of kerosene type turbofuel meeting the requirements of ASTM Type A".

Major Oil Co. B. "....we expect improvements in refinery processes and refinery equipment which will make this quality level possible starting in 1970 at no increase in price in Jet A type fuel due only to this increase in thermal stability requirement".

Major Oil Co. C. "With regard to price of SST fuel in the 1970-1972 period, we can only advise that this will be determined by the supply and demand conditions existing at that time. However, we can state that we would not expect a substantial difference in the 1970-72 price for this fuel and the Type A fuel for subsonic aircraft, provided that quality levels are essentially the same and that more costly distribution facilities are not required to maintain SST fuel quality".

Major Oil Co. D. "...will be able to supply fuel meeting 350/450 thermal stability requirements at competitive prices beginning 1970-72". (Telegram reply)

Major Oil Co. E. "While much of (our) production of Jet A-1 meets.. the 350/450 conditions there is sizable production which will not now meet this criterion. To bring all (our) production up to this criterion would require some increase in treating costs. It is difficult to be definite about price levels this far in advance of 1970.... In any event we forsee some increase in fuel costs as compared to Jet A-1".

E. THERMAL STABILITY IMPROVEMENT WITH ADDITIVES

As a supplement to the SST Phase II-A test program on fuels, Pratt & Whitney Aircraft undertook at its own expense a series of fuel thermal stability tests, utilizing the domestic survey fuels and the SSF Modified version of the standard ASTM coker to demonstrate that fuel thermal stability could be upgraded by means of additives at no significant fuel price increase.

The SSF Modified version of the ASTM-CFR Fuel Coker was chosen because it requires only gallons of test fuel and, like the research fuel coker, operates wi ated fuel reservoir. Tests on the survey fuels were carried out at a reservoir temperature of 175°F and a flow rate and duration of 2.5 lbs/hr. and 5 hours respectively.

Breakpoint temperatures seeking a Code 3 preheater deposit level were obtained on the survey fuels to establish a non-additive base line performance. The fuels were retested after addition of a thermal stability additive at a concentration of 30 lb/1000 BBL, using DuPont JFA5 as the additive. Based on prices currently in effect for this additive, the cost of treatment was 0.05 cents/gallon; the concentration level being arbitrarily set at twice the maximum concentration currently approved for this additive.

Results of the Modified Fuel Coker tests obtained to date with and without the additive are shown in Figure 12-32. In all cases, significant improvement through complete elimination of filter pressure drop was attained by use of the additive. For some fuels, significant improvement in preheater deposit code was also obtained. However, preheater deposit code improvement was not obtained with this additive in all instances.

It is believed that these tests show the feasibility of improving the thermal stability of current Jet A fuels which are low in the quality spectrum by means of low cost additive treatments. It is also believed that this improvement by additive treatment can be made with lower treating cost than that indicated through more careful selection of additive and concentration; this being the usual line of attack at the individual refinery level.

IDENTIFICATION OF SAMPLES FOR DOMESTIC JET A AND JET A-1 FUEL SURVEY

PWA Sample No.	Vendor Code	Location Where Used	ASTM Fuel Type
1332	A	LAX, SFO	A-1
1333	B		A
1334	B		A
1335	B	JFK	A-1
1336	B	JFK	B
1337	C		A-1
1338	C		A
1339	C		A-1
1340	C		A
1341	C		A-1
1342	C		A
1343	C		A
1344	C		A
1345	C		A
1346	C	JFK	A
1347	C	JFK	A-1
1348	C	JFK	A-1
1349	C		B
1350	D	SFO	A-1
1351	D	LAX	A-1
1352	D		A-1
1353	D		A-1
1354	E		A

Figure 12-1
(Sheet 1 of 3)

IDENTIFICATION OF SAMPLES FOR DOMESTIC JET A AND JET A-1 FUEL SURVEY (Cont)

PWA Sample No.	Vendor Code	Location Where Used	ASTM Fuel Type
1355	E		A
1356	E		A
1357	E		A
1358	E		A-1
1359	E		A
1360	E	ORD	A-1
1361	E		A
1362	F		A
1363	F		A
1364	F		A
1365	F		A
1366	G		A
1367	G		B
1368	G	ORD	A-1
1369	H	JFK	A
1370	H	JFK	A
1371	J	ORD	A-1
1372	J		A-1
1373	K	JFK	A-1
1374	K		A-1
1375	K		A-1
1376	K		A-1
1377	L		A

Figure 12-1
(Sheet 2 of 3)

IDENTIFICATION OF SAMPLES FOR DOMESTIC JET A AND JET A-1 FUEL SURVEY (Cont)

PWA Sample No.	Vendor Code	Location Where Used	ASTM Fuel Type
1378	L		A-1
1379	M		A
1380	M		A
1381	M	ORD	A
1382	M	LAX	A-1
1383	M	SFO	A-1

N. B. When "Location Where Used" line is blank, fuel,is used at air-fields other than the four major international air terminals – J. F. Kennedy, New York City, (JFK), O'Hare, Chicago, (ORD), Los Angeles (LAX) and San Francisco (SFO)

Figure 12-1
(Sheet 3 of 3)

PHYSICAL PROPERTIES OF DOMESTIC JET FUEL SAMPLES

PWA Sample Number	ASTM Fuel Type	Gravity °API	Flash Point °F	Freeze Point °F	Pour Point °F	Kinematic Viscosity Centistokes at -30°F	Kinematic Viscosity Centistokes at 100°F	Aniline Point °F	Water Tolerance ml	Water Tolerance Appearance
1332	A-1	42.3	123.	-63.	-80.	7.54	1.40	57.3	0.8	1
1333	A	44.2	135.	-61.	-72.	8.70	1.48	63.0	1.	1
1334	A	44.7	141.	-56.	-58.	8.83	1.51	64.5	1.1	1
1335	A-1	42.6	143.	-62.	-66.	9.68	1.54	60.2	1.	1
1336	B	52.2	<25.	<-75.	<-100.	1.94	0.70	44.4	2.	3
1337	A-1	45.5	129.	-67.	-76.	7.76	1.40	62.6	0.8	1
1338	A	43.9	134	-60.	-69.	11.26	1.49	62.4	0.1	1
1339	A-1	44.1	129.	-69.	-75.	7.62	1.39	61.1	10.	4
1340	A	46.7	128.	-56.	-69.	9.09	1.52	63.4	0.	2
1341	A-1	51.4	131.	-74.	-87.	6.79	1.31	57.4	0.	1b
1342	A	44.8	138.	-54.	-59.	8.97	1.51	65.6	0.9	1
1343	A	45.2	131.	-58.	-63.	7.86	1.41	63.1	1.	1
1344	A	43.5	136.	-53.	-63.	10.09	1.58	65.4	0.	1
1345	A	43.8	128.	-60.	-73.	8.78	1.49	63.4	3.	4
1346	A	44.1	130.	-60.	-63.	8.90	1.50	64.6	1.	1
1347	A-1	44.1	130	-67.	-75.	7.83	1.46	62.4	1.	1
1348	A-1	45.6	123.	-72.	-83.	6.49	1.29	60.4	1.	1
1349	B	54.7	<50.	<-72.	<-100.	2.31	0.76	55.8	1.1	1b
1350	A-1	41.2	111.	-67.	-75.	8.68	1.49	57.6	1.	1
1351	A-1	40.2	104.	-67.	<-100.	8.87	1.49	57.1	4	4
1352	A-1	43.3	126.	-65.	-69.	8.29	1.42	67.4	1.	3
1353	A-1	46.7	116.	-65.	-67.	6.36	1.27	61.8	1.	4
1354	A	41.8	142.	-45.	-49.	12.70	1.80	64.8	0.5	3
1355	A	43.2	134.	-45.	-68.	9.69	1.54	63.2	1	1b
1356	A	43.7	127.	-51.	-57.	9.30	1.52	63.9	12.	4
1357	A	44.0	121.	-62.	-71.	7.37	1.37	60.6	0.7	1
1358	A-1	42.8	138.	-56.	-47.	9.65	1.55	63.1	0.5	1
1359	A	43.0	127.	-42.	-71.	8.02	1.67	66.1	4.	3
1360	A-1	45.0	124.	-60.	-67.	10.62	1.41	62.9	0.3	1
1361	A	42.1	128.	-62.	-51.	11.60	1.70	63.9	5.	4
1362	A	44.2	127.	-56.	-59.	8.76	1.57	64.7	10.	4
1363	A	46.6	119.	-54.	-67.	8.14	1.32	63.2	1.	1

Figure 12-2
(Sheet 1 of 4)

PHYSICAL PROPERTIES OF DOMESTIC JET FUEL SAMPLES (Cont'd)

PWA Sample Number	ASTM Fuel Type	Gravity °API	Flash Point °F	Freeze Point °F	Pour Point °F	Kinematic Viscosity Centistokes at -30°F	Kinematic Viscosity Centistokes at 100°F	Aniline Point °F	Water Tolerance ml	Water Tolerance Appearance
1364	A	45.0	108.	-58.	-73.	6.16	1.40	64.3	0.2	3
1365	A	44.7	119.	-54.	-55.	7.51	1.39	62.2	0.5	3
1366	A	45.4	114.	-63.	-69.	6.71	1.31	61.4	1.	1
1367	B	55.1	<30.	<-74.	<-100.	2.24	0.70	55.8	0.2	3
1368	A-1	43.2	115.	-67.	-77.	7.57	1.39	61.2	0.5	1
1369	A	44.2	131.	-49.	-51.	9.44	1.54	65.6	0.4	1
1370	A	41.5	133.	-47.	-53.	10.32	1.61	62.0	1.	1b
1371	A-1	44.3	113.	-49.	-71.	8.17	1.38	61.6	0.	1b
1372	A-1	44.2	119.	-63.	-70.	7.27	1.36	59.8	0.1	1
1373	A-1	42.2	118.	-74.	-80.	7.71	1.40	60.1	0.9	1
1374	A-1	43.9	112.	-67.	-75.	7.65	1.[illegible]8	59.2	1.	1
1375	A-1	43.1	116.	-65.	-75.	7.34	1.40	58.5	0.2	1
1376	A-1	44.0	108.	-65.	-73.	7.14	1.35	60.9	1.	2
1377	A	44.2	123	-67.	-75.	7.50	1.42	62.0	1.	1
1378	A-1	44.1	122	-65.	-77.	7.40	1.38	61.8	2.	1
1379	A	42.9	129.	-58.	-65.	9.96	1.57	63.8	1.	1
1380	A	41.4	131.	-62.	-73.	10.82	1.62	62.5	0.	2
1381	A	43.6	128.	-60.	-65.	7.80	1.41	59.9	1.	1
1382	A-1	42.7	114.	-71.	-75.	7.56	1.40	58.2	0.9	1
1383	A-1	43.8	129.	-65.	-69.	8.03	1.42	59.9	0.	1
Minimum	A	41.4	108.	-42.	-49.	6.16	1.31	59.9		
Maximum	A	46.7	142.	-67.	-75.	12.70	1.80	66.1		
Average	A	43.9	129.	-56.	-64.	9.0	1.51	63.4		
Minimum	A-1	40.2	104.	-49.	-47.	6.49	1.27	57.1		
Maximum	A-1	53.4	143.	-74.	<-100.	10.62	1.55	63.1		
Average	A-1	44.0	121.	-65.	-74.	7.91	1.40	60.3		

Figure 12-2
(Sheet 2 of 4)

PHYSICAL PROPERTIES OF DOMESTIC JET FUEL SAMPLES (Cont'd)

PWA Sample Number	ASTM Fuel Type	Sulfur Wt. %	Mercaptan Sulfur Wt. %	Corrosion 3 Hrs. at 212°F	Aromatic Vol. %	Olefin Vol. %	Smoke Point m.m.	Existent Gum mg./100ml	Net Heat of Combustion B.T.U./lb.	Luminometer Number
1332	A-1	.0101	<.0001	1a	16.2	3.6	21	3.2	18,465	46
1333	A	.0057	.0001	1b	13.1	3.1	23	1.6	18,566	46
1334	A	.0096	<.0001	1a	13.0	2.6	24	2.2	18,738	46
1335	A-1	.0106	.0001	1a	17.1	2.3	21	3.2	18,625	49
1336	B	.0196	.0063	1a	19.1	1.9	23	1.0	18,070	48
1337	A-1	.0167	.0001	1b	12.5	2.0	25	<1.0	18,501	53
1338	A	.0309	.0001	1a	12.6	2.3	24	<1.0	18,710	50
1339	A-1	.0057	.0001	1a	14.5	2.4	23	<1.0	18,622	44
1340	A	.0333	<.0001	1a	12.6	2.1	23	[illegible]	18,675	47
1341	A-1	.0086	.0001	1a	16.1	2.0	21	1.8	18,568	44
1342	A	.0248	.0001	1b	12.0	2.3	25	1.0	18,578	56
1343	A	.0141	.0001	1b	14.6	2.8	25	1.0	18,359	54
1344	A	.0190	<.0001	1b	12.1	1.5	23	1.2	18,514	57
1345	A	.0525	<.0001	1b	12.8	2.2	23	1.0	18,628	57
1346	A	.0232	<.0001	1b	12.6	2.2	24	<1.0	18,501	51
1347	A-	.0301	.0001	1b	12.9	1.3	22	1.4	18,536	56
1348	A-1	.0004	.0002	1a	[illegible]	1.8	23	2.0	18,553	56
1349	B	.0027	.0009	1a	[illegible]	1.2	28	1.4	18,191	70
1350	A-1	.0042	<.0001	1a	16.1	1.8	19	1.0	18,421	42
1351	A-1	.0070	.0002	1a	15.4	1.6	19	2.2	18,423	47
1352	A-1	.0063	.0001	1a	13.0	1.0	23	<1.0	18,496	53
1353	A-1	.0045	.0006	1a	16.0	1.0	24	<1.0	18,564	53
1354	A	.0184	<.0001	1b	16.0	1.0	21	<1.0	18,490	47
1355	A	.0062	<.0001	1b	17.5	1.5	21	<1.0	18,452	47
1356	A	.0043	<.0001	1b	13.5	2.0	23	2.2	18,584	47
1357	A	.0811	.0001	1a	[illegible]	2.0	21	1.6	18,620	47
1358	A-1	.0000	.0001	1a	13.0	1.5	21	3.4	18,725	47
1359	A	.0425	<.0001	1b	14.5	1.5	23	1.8	18,635	51
1360	A-1	.0196	.0001	1a	12.5	1.0	24	<1.0	18,585	54
1361	A	.0002	<.0001	1b	14.1	2.3	22	1.8	18,523	49
1362	A	.0182	.0002	1a	[illegible]	1.0	24	<1.0	18,644	54
1363	A	.0000	.0002	1a	13.2	3.9	25	<1.0	18,683	60

Figure 12-2
(Sheet 3 of 4)

PHYSICAL PROPERTIES OF DOMESTIC JET FUEL SAMPLES (Cont'd)

PWA Sample Number	ASTM Fuel Type	Sulfur Wt. %	Mercaptan Sulfur Wt. %	Corrosion 3 Hrs. at 212°F	Aromatic Vol. %	Olefin Vol. %	Smoke Point m.m.	Existent Gum mg./100ml	Net Heat of Combustion B.T.U./lb.	Luminometer Number
1364	A	.0029	<.0001	1b	9.9	1.9	25	1.8	18,617	57
1365	A	.0024	<.0001	1a	14.9	1.9	21	1.8	18,602	52
1366	A	.0016	.0002	1b	14.5	1.0	23	2.2	18,661	54
1367	B	.0062	.0002	1b	7.6	1.4	28	1.3	18,060	78
1368	A-1	.0005	<.0001	1a	13.0	1.0	22	<1.0	18,595	50
1369	A	.0005	.0004	1a	13.0	1.0	22	1.0	18,676	55
1370	A	.0001	<.0001	1a	15.7	1.9	20	<1.0	18,422	47
1371	A-1	.0159	<.0001	2b	15.2	1.4	23	<1.0	18,347	60
1372	A-1	.0020	.0001	1a	17.0	1.5	22	1.0	18,561	51
1373	A-1	.0040	<.0001	1a	15.5	1.0	23	1.0	18,576	49
1374	A-1	.0163	<.0001	1a	17.0	1.0	21	2.4	18,518	49
1375	A-1	.0106	.0002	1a	17.5	1.0	21	<1.0	18,553	51
1376	A-1	.0095	.0001	1a	14.5	1.0	22	<1.0	18,595	53
1377	A	.0052	<.0001	1b	14.5	1.0	23	1.0	18,585	55
1378	A-1	.0047	<.0001	1a	14.0	2.0	23	1.0	18,612	55
1379	A	.0142	.0001	1a	14.5	1.5	23	<1.0	18,578	44
1380	A	.0094	<.0001	1a	14.0	1.5	22	1.6	18,597	49
1381	A	.0095	.0004	1a	18.0	1.0	21	1.3	18,589	49
1382	A-1	.0095	<.0001	1a	17.0	1.0	21	1.8	18,590	40
1383	A-1	.0055	<.0001	1a	17.5	1.5	21	1.6	18,614	48
Minimum	A	.0000	<.0001		9.9	1.0	20	<1.0	18,359	44
Maximum	A	.0811	.0004		18.0	3.1	25	2.2	18,738	60
Average	A	.0165	.0001		13.8	1.8	23		18,587	51
Minimum	A-1	.0000	<.0001		12.5	1.0	19	<1.0	18,347	40
Maximum	A-1	.0301	.0006		17.5	3.6	25	3.4	18,725	60
Average	A-1	.0086	.0001		15.2	1.6	22		18,550	50

Figure 12-2
(Sheet 4 of 4)

DISTILLATION DATA OBTAINED ON JET A AND JET A-1 FUEL SAMPLES USED IN DOMESTIC FUEL SURVEY

PWA Sample Number	ASTM Type	IBP	5	10	20	50	90	EP	% Residue	% Loss
1332	A-1	336	358	364	374	402	472	503	1.2	1.0
1333	A	363	377	383	394	419	472	488	1.5	1.0
1334	A	369	380	385	393	417	467	503	1.5	1.5
1335	A-1	363	377	385	397	423	479	507	1.4	1.0
1335	B	199	225	237	257	289	330	358	1.0	1.3
1337	A-1	345	363	371	381	405	463	503	1.9	1.1
1338	A	356	364	374	384	414	488	526	2.5	1.0
1339	A-1	347	360	366	375	402	462	498	1.0	1.0
1340	A	339	365	375	388	420	479	497	1.0	1.0
1341	A-1	353	362	367	374	391	447	501	2.3	1.2
1342	A	350	371	380	390	418	474	504	1.1	1.4
1343	A	352	366	373	382	407	469	487	2.5	1.0
1344	A	342	382	392	406	430	470	487	2.0	1.0
1345	A	344	369	378	390	420	470	492	1.5	2.5
1346	A	342	361	368	380	417	483	508	2.0	1.0
1347	A-1	351	359	363	373	404	465	495	1.0	1.5
1348	A-1	341	351	357	367	393	449	479	1.4	1.2
1349	B	151	197	211	235	306	407	450	1.4	1.5
1350	A-1	334	346	357	375	414	490	519	2.2	0.9
1351	A-1	317	339	349	365	410	501	515	4.9	0.3
1352	A-1	345	356	364	375	408	471	483	1.8	1.0
1353	A-1	327	347	355	365	391	460	497	2.0	1.0
1354	A	378	389	399	414	442	500	517	2.0	1.5

Figure 12-3
(Sheet 1 of 3)

DISTILLATION DATA OBTAINED ON JET A AND JET A-1 FUEL SAMPLES USED IN DOMESTIC FUEL SURVEY (Cont)

PWA Sample Number	ASTM Type	IBP	5	10	20	50	90	EP	% Residue	% Loss
1355	A	360	371	382	397	428	489	510	2.0	1.5
1356	A	347	365	377	391	422	479	506	1.0	2.0
1357	A	337	351	359	369	399	475	513	1.5	1.5
1358	A-1	359	379	386	395	419	486	515	2.0	1.0
1359	A	333	369	389	409	447	491	510	1.9	1.1
1360	A-1	346	362	369	380	407	459	487	1.7	1.2
1361	A	361	387	401	416	440	487	513	1.5	2.1
1362	A	349	367	376	386	417	473	488	1.7	1.2
1363	A	339	349	355	363	395	474	509	1.5	1.5
1364	A	323	345	357	372	407	472	506	1.0	1.5
1365	A	332	356	363	375	411	471	495	1.0	2.0
1366	A	322	345	354	367	399	465	501	1.0	1.0
1367	B	161	195	207	225	263	404	475	1.4	1.6
1368	A-1	330	345	352	370	403	472	497	1.5	1.5
1369	A	359	372	381	390	426	490	518	1.5	1.0
1370	A	358	377	388	402	435	494	524	1.3	1.7
1371	A-1	334	353	362	380	408	470	493	1.5	1.5
1372	A-1	329	350	360	374	410	469	490	1.0	2.0
1373	A-1	331	350	361	372	406	475	514	1.2	1.0
1374	A-1	338	357	363	376	406	464	514	1.5	1.2
1375	A-1	330	348	360	378	406	472	512	2.0	1.0
1376	A-1	323	349	358	371	404	464	486	1.8	1.2
1377	A	343	361	371	379	401	467	515	1.1	2.0

Figure 12-3
(Sheet 2 of 3)

DISTILLATION DATA OBTAINED ON JET A AND JET A-1 FUEL SAMPLES USED IN DOMESTIC FUEL SURVEY (Cont)

PWA Sample Number	ASTM Type	IBP	5	10	20	50	90	EP	% Residue	% Loss
1378	A-1	341	358	364	373	403	481	509	1.6	1.4
1379	A	367	375	385	397	426	478	508	1.7	2.1
1380	A	342	368	379	394	432	486	508	1.5	1.0
1381	A	350	360	364	375	408	487	502	2.7	1.3
1382	A-1	341	358	364	377	409	476	500	2.0	2.0
1383	A-1	356	366	372	382	411	470	499	1.5	1.5
Minimum	A	322	345	354	363	395	465	487	1.0	1.0
Maximum	A	378	389	401	416	447	500	526	2.7	2.5
Average	A	348	367	376	389	419	479	505	1.6	1.4
Minimum	A-1	317	339	349	365	391	447	479	1.0	0.3
Maximum	A-1	363	379	386	397	423	501	519	4.9	2.0
Average	A-1	340	356	364	376	406	470	501	1.8	1.2

Figure 12-3
(Sheet 3 of 3)

SUMMARY OF TESTS TO DETERMINE BREAKPOINT TEMPERATURES OF DOMESTIC FUEL SURVEY SAMPLES IN ASTM-CFR FUEL COKER

PWA Sample Number	Temp. Conditions Preheater/Filter	Filter ΔP/Time	Tube Deposit Cold — Hot
1332	350/450	2.8/300	0 2 1 0 0 0 1 1 1 2 2 2 2
	400/500	3.8/300	1 2 1 1 1 1 1 1 1 2 4 4 3
	450/550	9.5/300	1 1 1 1 1 1 1 1 6 5 6 6 5
1333	350/450	3.2/300	1 1 1 1 1 1 1 1 1 1 1 1 1
	375/475	2.7/300	1 2 1 1 1 1 1 1 1 1 1 2 2
	400/500	2.0/300	0 1 1 0 1 0 0 1 1 1 1 1 2
	425/525	25. /224	1 1 1 1 1 1 1 1 5 5 5 5 3
1334	350/450	5.8/300	1 1 1 1 1 1 1 1 1 1 1 1 1
	375/475	0.8/300	1 1 1 1 1 1 1 1 1 1 1 2 2
	400/500	22. /300	1 1 1 1 1 1 1 1 1 1 1 1 1
	425/525	3.3/300	0 1 2 1 1 1 1 1 1 1 3 3 2
	450/550	2.3/300	1 1 1 1 1 2 3 4 4 4 6 6 3
1335	350/450	7.2/300	1 2 2 1 1 1 1 1 1 1 2 2 2
	400/500	4.5/300	2 2 1 1 1 1 1 1 1 2 3 4 4
	450/550	25. /198	0 0 0 0 0 0 0 2 6 6 6 3 3
1336	350/450	0.5/300	1 2 2 1 1 1 1 1 1 1 1 1 1
	375/475	0.1/300	1 2 1 1 1 1 1 1 1 1 1 1 1
	400/500	0.2/300	1 2 2 1 1 1 1 1 1 2 2 2 2
	425/525	0.5/300	1 1 1 1 1 1 1 1 2 3 3 3 2
1337	375/475	0.2/300	1 2 2 2 2 1 1 2 1 1 1 1 1
	400/500	8.0/300	1 2 1 1 1 1 1 1 1 1 1 2 2
	425/525	25. /175	1 2 2 2 2 2 2 2 2 3 3 3 3
1338	350/450	0.2/300	1 1 1 1 1 1 1 1 1 1 1 1 1
	375/475	0.9/300	1 1 1 1 1 1 1 2 3 3 4 4 2
1339	350/450	0.2/300	1 2 1 1 1 1 1 1 1 1 1 2 2
	375/475	0.5/300	0 1 1 1 1 1 1 1 1 1 1 2 2
	400/500	1.1/300	1 2 2 1 1 1 1 1 1 1 1 3 6
1340	350/450	0. /300	1 1 1 1 1 1 1 1 1 1 1 1 1
	375/475	0. /300	1 1 1 1 1 1 1 1 1 1 1 1 1
	400/500	0.1/300	0 1 1 1 1 1 1 1 1 1 1 3 3
1341	350/450	0. /300	1 1 1 1 1 1 1 1 1 1 1 1 1
	375/475	0.1/300	2 2 2 2 2 2 2 2 2 2 2 2 2
	400/500	0.2/300	0 2 0 0 0 0 1 1 1 2 2 2 2
	425/525	0.2/300	1 1 1 1 1 1 1 1 1 2 6 6 6

Figure 12-4
(Sheet 1 of 5)

SUMMARY OF TESTS TO DETERMINE BREAKPOINT TEMPERATURES OF DOMESTIC FUEL SURVEY SAMPLES IN ASTM-CFR FUEL COKER (Cont)

PWA Sample Number	Temp. Conditions Preheater/Filter	Filter ΔP/Time	Tube Deposit Cold												Hot
1342	350/450	0.6/300	1	2	2	1	1	1	1	1	1	1	1	2	2
	375/475	0.7/300	1	2	2	0	0	0	0	1	1	1	1	2	2
	400/500	1.9/300	1	2	1	1	1	1	1	1	5	5	5	5	5
1343	350/450	0/300	1	1	1	1	1	1	1	1	1	1	1	1	1
	375/475	0.3/300	1	2	2	1	1	1	1	1	1	1	1	1	2
	400/500	18./300	1	2	2	1	1	1	1	1	1	2	2	2	2
	425/525	25./180	1	2	1	1	1	1	2	3	4	4	4	4	3
1344	350/450	0.1/300	0	1	0	0	0	1	1	0	0	0	0	1	1
	375/475	0.2/300	1	1	1	1	1	1	1	1	1	1	1	1	1
	400/500	3.7/300	1	1	1	1	1	1	1	1	2	2	2	2	2
	425/525	25./207	1	1	1	1	1	1	1	1	2	3	6	6	4
1345	350/450	1.4/300	1	1	1	1	1	1	1	1	1	1	1	1	1
	375/475	1.3/300	.1	.1	.1	.1	.1	.1	.1	.1	.1	.1	.1	.1	.1
	400/500	13 /300	1	1	0	0	0	0	0	0	1	1	1	1	1
	425/525	25/75	0	1	1	1	1	1	2	2	3	3	3	3	3
1346	350/450	13./300	0	2	0	0	0	0	0	1	1	1	1	1	1
	375/475	22/300	1	2	2	2	2	2	2	2	2	2	2	2	2
	400/500	14/300	0	2	1	1	1	1	1	1	3	3	1	2	3
	450/550	25/145	1	2	2	1	2	2	5	6	7	7	7	7	6
1347	325/425	0.4/300	0	0	0	1	1	1	1	1	1	1	1	1	2
	350/450	14/300	1	3	3	1	1	1	1	1	2	2	2	3	3
	375/475	25/291	0	3	0	0	0	0	0	0	4	4	4	3	3
	400/500	25/107	0	2	0	0	0	0	0	0	3	3	3	3	3
	425/525	25/121	1	2	2	1	1	1	1	1	1	2	3	4	4
	450/550	25/132	.1	.2	.2	.1	.1	.1	.1	.2	.3	.3	.4	.4	.4
1348	350/450	0.3/300	1	1	1	1	1	1	1	1	1	1	1	1	1
	375/475	0.3/300	1	1	1	1	1	1	1	1	3	3	4	4	4
1349	350/450	0.1/300	0	2	2	1	2	2	2	1	1	1	2	2	2
	375/475	0.1/300	1	1	1	1	1	1	1	1	1	1	4	4	3
1350	350/450	0.2/300	0	1	1	0	0	1	2	2	2	2	2	2	2
	375/475	25/38	1	1	1	1	1	1	1	4	6	5	5	6	6
1351	350/450	0.8/300	1	2	1	1	2	2	2	2	2	2	2	2	2
	375/475	25/255	0	0	1	1	1	1	1	1	1	2	2	2	0
	400/500	25/38	0	0	1	1	1	1	1	2	3	4	4	4	3

Figure 12-4
(Sheet 2 of 5)

SUMMARY OF TESTS TO DETERMINE BREAKPOINT TEMPERATURES OF DOMESTIC FUEL SURVEY SAMPLES IN ASTM-CFR FUEL COKER (Cont)

PWA Sample Number	Temp. Conditions Preheater/Filter	Filter ΔP/Time	Tube Deposit												
			Cold												Hot
1352	325/425	0/300	1	2	2	1	1	1	1	1	1	1	2	2	1
	350/450	0/300	1	1	1	0	0	0	2	6	6	6	3	3	1
	375/475	0.2/300	1	1	1	1	1	1	1	1	1	2	5	5	3
1353	350/450	0.6/300	0	1	0	1	1	1	1	1	1	2	2	2	1
	375/475	25./104	0	1	1	0	0	1	1	2	2	3	3	3	2
1354	350/450	0.3/300	1	1	1	1	1	1	1	1	1	1	1	1	1
	375/475	0.4/300	1	1	1	1	1	1	1	1	1	1	1	3	3
	400/500	2.0/300	2	2	2	2	2	2	2	2	4	5	5	5	4
1355	350/450	0.1/300	1	1	1	1	1	1	1	1	1	2	2	2	2
	375/475	0.1/300	2	2	1	1	1	1	1	1	1	2	2	2	2
	400/500	1.6/300	1	1	1	1	1	1	3	6	6	6	5	5	6
1356	275/375	0./300	1	1	1	1	1	1	1	1	1	1	1	1	1
	300/400	0.7/300	1	1	1	1	1	1	1	1	3	3	4	3	2
	325/425	0/300	1	2	1	1	1	2	3	3	4	4	4	4	4
	350/450	0./300	0	2	2	2	2	1	2	2	2	3	4	3	4
1357	350/450	1.5/300	0	2	2	0	0	0	0	0	0	0	0	2	2
	375/475	8.8/300	1	1	1	1	1	1	1	1	1	1	1	2	2
	400/500	2.6/300	1	1	1	1	1	1	1	1	1	2	3	3	2
1358	350/450	0.7/300	1	2	2	1	1	1	1	1	1	1	1	2	2
	375/475	0.2/300	1	2	2	1	1	1	1	1	1	1	1	2	2
	400/500	0.5/300	1	2	2	1	1	1	1	1	1	1	2	2	2
	425/525	25/259	1	1	1	1	1	1	1	1	4	6	6	6	5
1359	350/450	0/300	1	1	1	1	1	1	1	2	2	2	2	2	2
	375/475	0./300	1	1	1	1	1	1	1	2	2	2	2	3	3
1360	350/450	0.9/300	0	1	1	0	0	1	1	1	1	2	2	2	2
	375/475	4.8/300	1	2	2	1	1	1	1	1	1	1	1	1	1
	400/500	25/268	1	2	1	1	1	1	2	2	2	4	4	3	3
	450/550	25/135	1	2	1	1	1	2	2	4	4	5	5	5	3
1361	350/450	0.2/300	1	1	1	1	1	2	2	1	1	1	1	1	2
	375/475	0.1/300	1	2	1	1	2	2	3	4	4	4	4	4	4
1362	350/450	11./300	1	1	1	1	1	1	1	1	1	1	1	1	1
	375/475	25/258	1	1	1	1	1	1	1	1	1	1	1	1	1
	400/500	25/192	1	1	1	1	1	1	1	2	3	6	6	6	2

Figure 12-4
(Sheet 3 of 5)

SUMMARY OF TESTS TO DETERMINE BREAKPOINT TEMPERATURES OF DOMESTIC FUEL SURVEY SAMPLES IN ASTM-CFR FUEL COKER (Cont)

PWA Sample Number	Temp. Conditions Preheater/Filter	Filter ΔP/Time	Tube Deposit Cold . Hot
1363	350/450	1.4/300	0 1 1 0 0 0 1 1 1 1 1 1 1
	375/475	1.0/300	0 2 2 1 1 1 1 1 1 1 2 2 1
	400/500	0.3/300	1 2 2 1 1 1 1 1 1 1 1 2 2
	425/525	0.1/300	1 2 2 2 2 2 2 2 3 3 4 4 3
1364	350/450	0.4/300	0 1 1 1 1 1 1 1 1 1 1 1 1
	375/475	25/219	1 2 2 1 1 1 1 1 2 2 2 2 2
	400/500	25/254	0 2 1 1 1 1 1 2 2 3 3 4 3
1365	350/450	0/300	1 2 2 2 2 1 1 1 1 1 1 2 2
	375/475	1.0/300	1 1 1 1 1 1 1 1 5 5 5 5 1
1366	325/425	1.2/300	.1 .2 .2 .2 .2 .2 .2 .1 .1 .1 .2 .2 .2
	350/450	1.2/300	1 2 2 1 1 1 1 2 2 3 2 2 3
1367	350/450	0.7/300	1 2 2 1 1 1 1 1 1 1 1 2 2
	375/475	0.7/300	1 1 1 1 0 0 0 0 1 2 2 2 1
	400/500	1.7/300	1 1 1 1 1 1 1 1 3 4 4 3 2
1368	300/400	0.4/300	0 1 0 0 0 0 0 0 0 0 0 1 1
	325/425	0.4/300	1 1 1 1 1 1 1 1 1 1 1 1 1
	350/450	1.3/300	0 1 0 0 1 2 2 4 4 4 4 3 1
	450/550	25/68	1 1 1 0 0 0 0 4 6 6 6 6 5
1369	350/450	0.2/300	1 2 1 1 1 1 2 2 2 2 2 2 2
	375/475	0.1/300	1 1 1 1 1 1 1 1 1 1 1 1 1
	400/500	0.8/300	0 0 0 0 0 0 0 2 6 7 7 4 1
	450/550	25/174	0 1 0 0 0 3 6 6 6 7 7 6 6
1370	350/450	2.2/300	2 2 2 1 1 1 1 1 2 2 1 2 2
	375/475	0.2/300	0 0 0 0 0 0 1 1 1 1 1 1 1
	400/500	25/204	1 2 1 0 0 0 0 5 6 6 6 6 3
	450/550	25/198	1 2 1 1 1 1 2 6 5 7 7 7 5
1371	350/450	7.3/300	1 1 1 1 1 1 1 1 1 1 1 2 2
	375/475	6.7/300	0 1 1 2 2 2 3 3 1 1 1 1 1
1372	350/450	0.9/300	1 1 2 2 2 2 2 2 1 [illegible] 1 2 2
	375/475	6.3/300	1 2 2 2 2 2 1 1 1 1 1 2 2
	400/500	6.1/300	0 2 1 1 1 1 0 0 0 0 1 2 3
1373	350/450	5.2/300	1 2 1 1 1 1 1 1 1 1 1 2 2
	375/475	12./300	0 2 0 0 3 3 3 0 0 0 0 0 2

Figure 12-4
(Sheet 4 of 5)

SUMMARY OF TESTS TO DETERMINE BREAKPOINT TEMPERATURES OF DOMESTIC FUEL SURVEY SAMPLES IN ASTM-CFR FUEL COKER (Cont)

PWA Sample Number	Temp. Conditions Preheater/Filter	Filter ΔP/Time	Tube Deposit Cold … Hot
1374	350/450	0.6/300	1 2 2 1 1 1 1 1 1 1 1 2 2
	375/475	3.0/300	1 2 1 1 1 1 1 1 1 1 1 2 1
	400/500	25/223	1 2 2 1 1 1 1 1 1 6 5 5 6
1375	350/450	0.7/300	1 2 2 1 1 1 1 1 1 1 1 2 2
	375/475	2.0/300	0 2 1 1 1 1 1 1 1 1 1 2 2
	400/500	22./300	1 2 2 1 1 1 1 1 1 1 1 3 3
1376	350/450	0./300	1 1 1 1 1 1 1 1 1 1 1 1 1
	375/475	0.1/300	1 1 1 1 1 1 1 1 1 1 1 1 1
	400/500	0.5/300	1 1 1 1 1 1 1 1 1 1 1 1 1
	425/525	25/167	1 1 1 1 1 1 1 2 5 6 7 7 6
1377	350/450	0.3/300	0 2 1 1 0 1 0 0 0 0 0 2 2
	375/475	3.2/300	1 2 1 1 1 1 2 2 2 2 1 2 2
	400/500	6.3/300	1 2 2 2 2 3 3 4 3 2 2 3 4
1378	325/425	25/278	1 2 2 1 1 1 1 1 1 1 1 2 2
	350/450	0.1/300	2 2 1 1 1 4 4 1 1 1 1 2 2
1379	350/450	19/300	1 1 1 1 1 1 1 1 1 1 1 1 1
	375/475	25/92	1 1 1 1 1 2 2 2 2 2 2 2 2
	400/500	25/108	0 0 0 1 1 1 1 2 3 4 5 5 4
1380	350/450	0.4/300	1 2 2 1 1 1 1 1 1 1 1 2 2
	375/475	0.6/300	1 2 1 1 1 1 1 1 1 1 1 1 2
	400/500	0.8/300	1 2 2 1 1 1 1 1 1 1 1 2 2
	425/525	13/300	0 2 1 1 1 1 1 1 3 6 6 4 4
1381	250/350	0.2/300	0 2 1 1 1 1 1 1 1 1 1 1 1
	275/375	0.1/300	1 3 3 2 1 1 1 1 2 2 2 3 3
	300/400	1.3/300	1 3 3 1 1 1 1 1 1 1 1 3 3
	325/425	2.6/300	1 3 1 1 1 1 1 1 1 1 1 3 3
	350/450	9.4/300	1 3 3 1 1 1 1 1 1 1 2 3 3
	375/475	6.1/300	.1 .5 .5 .1 .1 .1 .1 .1 .1 .1 .. 3 3
1382	350/450	2.1/300	1 2 1 1 1 1 1 1 1 2 2 2 2
	375/475	6.3/300	1 2 1 1 1 1 1 1 1 1 1 2 2
	400/500	3.8/300	1 2 2 1 1 1 2 2 2 2 3 3 3
1383	350/450	4.2/300	1 2 2 1 1 1 1 1 1 1 1 2 2
	375/475	19./300	0 2 2 0 0 0 0 0 0 1 1 2 2
	400/500	25./282	1 2 2 1 1 1 1 3 3 4 4 4 3

Figure 12-4
(Sheet 5 of 5)

SUMMARY OF TESTS TO DETERMINE BREAKPOINT TEMPERATURES OF DOMESTIC FUEL SURVEY SAMPLES IN CRC RESEARCH FUEL COKER

PWA Sample Number	Temp. Conditions RES.	Preheater/ Filter	Filter ΔP/Time	Tube Deposit Cold												Hot
1332	250	350/450	0.8/300	1	1	1	1	1	1	1	1	1	1	1	1	1
		400/500	2.9/300	0	0	1	1	1	1	2	2	2	2	2	2	2
		425/525	5.5/300	1	2	2	2	2	2	2	2	2	2	4	2	1
	175	375/475	0.8/300	2	2	2	2	2	2	2	2	2	2	2	2	2
		400/500	25/243	0	1	1	1	1	1	1	1	4	4	6	5	5
		425/525	4.1/300	0	1	2	2	2	2	2	2	2	4	4	4	4
	AMB	375/475	9.6/300	1	1	1	1	1	1	1	1	1	1	1	1	1
		400/500	25./241	1	1	1	1	1	1	1	1	1	4	6	5	6
1335	250	350/450	1.1/300	1	1	1	1	1	1	1	1	1	1	1	1	1
		400/500	0.6/300	1	1	1	1	1	1	1	1	1	1	2	2	2
		425/525	14/300	1	1	1	1	1	1	1	2	3	3	3	2	2
	175	425/525	1.2/300	1	1	1	1	1	1	1	1	1	2	2	2	2
		450/550	0.7/300	1	1	1	1	1	1	1	2	2	2	2	3	3
	AMB	400/500	1.1/300	0	1	1	1	1	1	1	1	1	1	1	1	1
		425/525	0.2/300	1	1	1	1	1	1	1	1	1	3	4	4	3
		450/550	0.5/300	1	1	1	1	1	1	1	1	3	4	3	3	3
1336	250	400/500	0.4/300	2	2	2	2	2	2	2	2	2	2	2	2	2
		425/525	0.8/300	1	1	1	1	1	1	2	2	2	3	4	4	3
	175	375/475	2.0/300	1	1	1	1	1	1	1	1	1	2	2	2	2
	175	400/500	0.4/300	1	1	1	1	1	1	1	1	2	3	5	4	5
		425/525	25./139	0	2	2	2	2	1	1	1	2	4	6	6	6
	AMB	375/475	3.1/300	1	1	1	1	1	1	1	1	1	1	1	1	1
1346	250	375/475	25/283	1	1	1	1	1	1	1	1	1	1	1	1	1
		400/500	25/228	5	5	5	5	5	6	6	2	2	1	2	2	2
		425/525	25/141	1	1	1	1	1	1	1	1	2	4	4	4	4
	175	375/475	9.5/300	1	1	1	1	1	1	1	1	1	1	1	1	1
		400/500	25/278	0	0	0	1	1	1	1	1	1	1	2	3	3
		425/525	25/185	1	1	1	1	1	1	1	1	1	6	6	6	5
	AMB	375/475	2.2/300	1	1	1	1	1	1	1	1	1	1	1	1	1
		400/500	25/250	0	0	0	0	1	1	1	1	1	2	6	6	6
1347	250	325/425	1.3/300	1	1	1	1	1	1	1	1	1	1	1	1	1
		375/475	2.2/300	1	1	1	1	1	1	1	1	1	1	1	1	1
		400/500	25/103	0	0	0	0	0	0	1	1	1	1	6	4	3
		425/525	25/107	0	1	1	1	1	1	1	1	1	6	4	5	5

Figure 12-5
(Sheet 1 of 4)

SUMMARY OF TESTS TO DETERMINE BREAKPOINT TEMPERATURES OF DOMESTIC FUEL SURVEY SAMPLES IN CRC RESEARCH FUEL COKER (Cont)

PWA Sample Number	Temp. Conditions			Tube Deposit												
	RES.	Preheater/ Filter	Filter ΔP/Time	Cold												Hot
1347	175	375/475	25/211	1	1	1	1	1	1	1	1	1	1	1	1	1
		400/500	25/155	1	1	1	1	1	1	1	1	1	3	6	6	6
	AMB	375/475	25/114	1	1	1	1	1	1	1	1	1	1	1	2	3
		400/500	25/172	0	1	1	1	1	1	1	1	1	1	3	3	4
1348	250	350/450	0.7/300	0	1	1	1	1	1	1	1	1	1	1	2	1
		375/475	25/200	1	1	1	1	1	1	1	1	2	6	6	5	6
		400/500	25./70	1	1	1	1	1	1	1	2	5	6	6	6	5
	175	350/450	0.1/300	1	1	1	2	2	2	2	2	2	2	2	2	2
		375/475	25./284	1	1	1	1	2	2	1	1	1	6	6	5	6
	AMB	325/425	0.1/300	2	2	2	2	2	2	2	2	2	2	2	2	2
		350/450	1.1/300	1	1	1	1	1	1	1	1	1	1	4	6	6
1350	250	350/450	25/145	1	1	1	1	1	1	1	1	2	2	1	1	2
		375/475	25/54	0	0	0	0	0	0	1	1	2	3	3	4	3
	175	325/425	3.3/300	1	1	1	1	1	1	1	1	1	1	2	2	2
		350/450	25/94	1	1	1	1	1	2	2	2	2	3	4	4	4
		375/475	25/64	0	1	2	2	2	2	2	3	6	6	5	6	6
	AMB	325/425	25/201	1	1	1	1	1	1	1	1	1	1	1	1	1
		350/450	25./59	1	1	1	1	1	1	1	1	2	3	6	6	6
1351	250	350/450	25./104	0	0	0	0	1	1	1	1	1	1	1	2	[illegible]
		375/475	25./32	1	1	1	1	1	1	1	1	6	6	5	6	6
	175	350/450	1.2/300	1	1	1	1	1	1	1	1	1	1	1	1	1
		375/475	25./30	1	1	1	1	1	1	1	3	5	5	5	5	5
	AMB	350/450	1.2/300	1	1	1	1	1	1	1	1	1	1	1	1	1
		375/475	25/40	1	1	1	1	1	1	1	2	6	5	5	5	5
1360	250	350/450	0.2/300	0	0	1	1	1	1	1	1	1	1	1	1	1
		400/500	1.5/300	1	1	1	1	1	2	2	2	2	2	2	2	2
		425/525	25/146	1	1	1	1	1	1	1	2	2	2	3	3	3
	175	425/525	25/214	1	1	1	1	1	1	1	1	1	2	2	2	2
		450/550	25/192	1	1	1	1	1	1	2	2	2	3	3	3	3
	AMB	425/525	7.0/300	0	0	0	1	1	1	1	1	1	2	2	2	2
		450/550	25./257	1	1	1	1	1	1	1	1	2	2	3	3	2

Figure 12-5
(Sheet 2 of 4)

SUMMARY OF TESTS TO DETERMINE BREAKPOINT TEMPERATURES OF DOMESTIC FUEL SURVEY SAMPLES IN CRC RESEARCH FUEL COKER (Cont)

PWA Sample Number	Temp. Conditions RES.	Preheater/ Filter	Filter ΔP/Time	Tube Deposit Cold												Hot
1368	250	325/425	0.3/300	1	1	1	1	1	1	1	1	1	1	1	1	1
		350/450	0.5/300	1	1	1	1	1	1	1	2	2	2	2	2	2
		375/475	25/97	0	1	1	1	1	1	1	2	5	5	5	4	4
		400/500	18./300	1	1	1	1	1	1	1	3	2	2	6	6	6
	175	350/450	0.6/300	1	1	1	2	2	1	1	1	1	1	1	2	2
		375/475	7.6/300	0	1	1	1	1	1	1	1	1	1	3	4	4
	AMB	350/450	0.5/300	0	1	1	1	2	2	2	2	2	2	2	2	2
		375/475	2.8/300	1	2	1	1	2	2	2	2	2	2	4	4	3
1369	250	350/450	0.1/300	0	0	0	0	0	0	0	1	1	1	1	1	1
		375/475	1.6/300	2	3	3	2	2	2	2	3	4	6	6	6	6
		400/500	0.4/300	0	0	0	2	2	1	1	1	3	5	6	6	6
	175	325/425	0.2/300	0	1	0	0	0	0	0	0	1	1	1	1	1
		350/450	0 /300	1	1	1	1	1	1	1	1	1	2	3	3	2
		375/475	0.8/300	1	1	1	1	1	1	1	1	6	6	6	6	4
		400/500	0.3/300	1	1	1	1	1	2	2	2	2	4	6	6	6
	AMB	350/450	1.0/300	0	0	1	1	1	1	1	1	1	1	2	2	2
		375/475	0.1/300	0	0	1	1	1	1	1	1	1	1	2	4	2
1370	250	350/450	1.3/300	1	1	1	1	1	1	1	1	1	1	1	1	1
		375/475	20/300	0	0	0	0	0	0	1	1	2	3	3	2	2
		400/500	25/240	1	1	1	1	1	1	1	1	1	1	5	5	6
	175	375/475	0.2/300	1	1	1	2	2	2	2	2	2	2	2	2	2
		400/500	0.3/300	1	1	1	2	2	2	2	2	2	2	2	3	3
	AMB	375/475	0.4/300	1	1	1	1	1	1	1	1	1	1	1	1	1
		400/500	0.5/300	1	1	1	1	1	1	1	1	1	1	1	6	6
1371	250	400/500	25./240	1	1	1	1	1	1	1	2	2	2	2	2	2
		425/525	25/192	1	1	1	1	1	1	1	1	1	2	2	2	2
		450/550	25/178	1	1	1	1	1	1	1	1	2	2	2	3	4
	175	425/525	25/190	0	2	2	2	2	2	1	1	2	1	1	1	1
		450/550	25/196	1	1	1	1	1	1	1	1	1	2	2	2	4
	AMB	425/525	25/196	0	1	1	1	1	1	1	2	2	3	3	3	3
1373	250	350/450	25./220	1	1	1	1	1	1	1	1	1	1	2	2	2
		375/475	25./147	1	1	1	1	0	0	0	1	2	2	4	4	4
		400/500	25./130	1	1	1	1	1	1	1	2	6	6	6	5	6
	175	375/475	2.9/300	1	1	1	1	1	1	1	1	1	1	2	2	2
		400/500	13./300	0	1	1	1	1	2	2	2	2	4	6	6	6
	AMB	350/450	0.2/300	1	1	1	1	1	1	1	1	1	2	2	2	2
		375/475	0.5/300	1	1	1	1	2	2	2	2	2	2	6	6	5

Figure 12-5
(Sheet 3 of 4)

SUMMARY OF TESTS TO DETERMINE BREAKPOINT TEMPERATURES OF DOMESTIC FUEL SURVEY SAMPLES IN CRC RESEARCH FUEL COKER (Cont)

PWA Sample Number	Temp. Conditions RES.	Preheater/ Filter	Filter ΔP/Time	Tube Deposit Cold ... Hot
1381	250	275/375	0.5/300	0 2 1 1 2 2 2 2 1 1 1 1 1
		300/400	0.6/300	1 2 2 2 2 2 2 2 2 2 2 2 2
		325/425	0.9/300	1 1 1 1 1 1 1 1 1 1 1 1 1
		375/475	1.8/300	0 0 0 1 1 1 1 1 1 2 2 2 2
	175	350/450	1.3/300	1 1 1 1 1 1 1 1 1 1 1 1 1
		375/475	1.8/300	1 1 1 1 1 1 1 3 1 1 1 1 2
		400/500	25/279	1 1 1 1 1 1 1 1 1 2 3 6 6
	AMB	375/475	25/202	0 1 1 1 1 1 1 1 1 1 2 5 5
1382	250	350/450	0.2/300	1 1 1 1 1 1 1 1 1 1 1 1 1
		375/475	0.5/300	1 1 1 1 1 1 1 1 1 1 1 1 1
		400/500	0.6/300	1 1 1 1 1 1 1 1 1 1 1 1 1
		425/525	0.5/300	1 1 1 1 1 1 1 1 1 1 2 3 1
	175	425/525	0.5/300	1 1 1 1 1 1 1 1 1 2 2 1 1
		450/550	1.8/300	1 1 1 1 1 1 1 1 1 6 6 6 3
	AMB	400/500	0.7/300	1 1 1 1 1 1 1 1 1 1 1 2 2
		425/525	0.4/300	1 1 1 1 1 1 1 2 2 2 3 4 4
1383	250	325/425	10/300	1 1 1 1 1 1 1 1 1 1 2 2 2
		350/450	2.7/300	2 2 2 2 2 2 2 2 2 2 3 3 3
		400/500	25/271	1 1 1 1 1 1 1 1 1 1 1 1 1
		450/550	25/201	1 1 1 1 1 0 0 0 4 4 3 3 2
	175	350/450	0.7/300	1 1 1 1 1 1 1 1 1 1 1 1 1
		375/475	6.[illegible]/300	1 1 1 1 1 1 1 1 1 1 1 1 1
		400/500	25/275	1 1 1 1 1 1 1 1 1 1 1 1 1
		450/550	25/202	1 1 1 1 1 1 2 2 5 6 6 6 4
	AMB	425/525	25/103	1 1 1 1 1 1 1 1 1 4 6 5 4

Figure 12-5
(Sheet 4 of 4)

SUMMARY OF BREAKPOINT TEMPERATURES OF DOMESTIC FUEL SURVEY SAMPLES BASED ON CODE 3 PREHEATER DEPOSITS

PWA Sample Number	ASTM-CFR Coker Breakpoint Temp. - °F	CRC Research Coker Breakpoint Temp. - °F Ambient Reservoir	175°F Reservoir	250°F Reservoir
1332	375	375	375	400
1333	400			
1334	425			
1335	375	400	450	425
1337	400			
1338	350			
1339	375			
1340	400			
1341	400			
1342	375			
1343	400			
1344	400			
1345	425			
1346	400	375	400	375
1347	350	375	375	375
1348	350	325	350	350
1350	350	325	325	350
1351	375	350	350	350
1352	325			
1353	375			
1354	375			
1355	375			
1356	275			
1357	375			
1358	400			
1359	375			
1360	375	450	450	425
1361	350			
1362	375			
1363	400			
1364	375			
1365	350			

Figure 12-6
(Sheet 1 of 2)

SUMMARY OF BREAKPOINT TEMPERATURES OF DOMESTIC FUEL SURVEY SAMPLES BASED ON CODE 3 PREHEATER DEPOSITS (Cont)

PWA Sample Number	ASTM-CFR Coker Breakpoint Temp. - °F	CRC Research Coker Breakpoint Temp. - °F Ambient Reservoir	175°F Reservoir	250°F Reservoir
1366	350			
1368	325	350	350	350
1369	375		350	350
1370	375	375	400	375
1371	375	425	425	425
1372	400			
1373	375	350	375	350
1374	375			
1375	400			
1376	400			
1377	375			
1378	325			
1379	375			
1380	400			
1381	350		375	375
1382	400		425	425
1383	375		400	350

Figure 12-6
(Sheet 2 of 2)

DISTRIBUTION OF PREHEATER BREAKPOINT TEMPERATURES
AS DETERMINED IN ASTM-CFR FUEL COKER

	All Fuels in Survey			JFK, O'Hare, LAX SFO Only		
Breakpoint Temp. - °F	No.	%	Cumulative %	No.	%	Cumulative %
275	1	2.0	2.0			
300	0	0	2.0			
325	3	6.1	8.1	1	6.2	6.2
350	8	16.3	24.4	4	25.0	31.2
375	21	42.9	67.3	9	56.3	87.5
400	14	28.6	95.9	2	12.5	100.0
425	2	4.1	100.0			
	49	100.0		16	100.0	

Figure 12-7

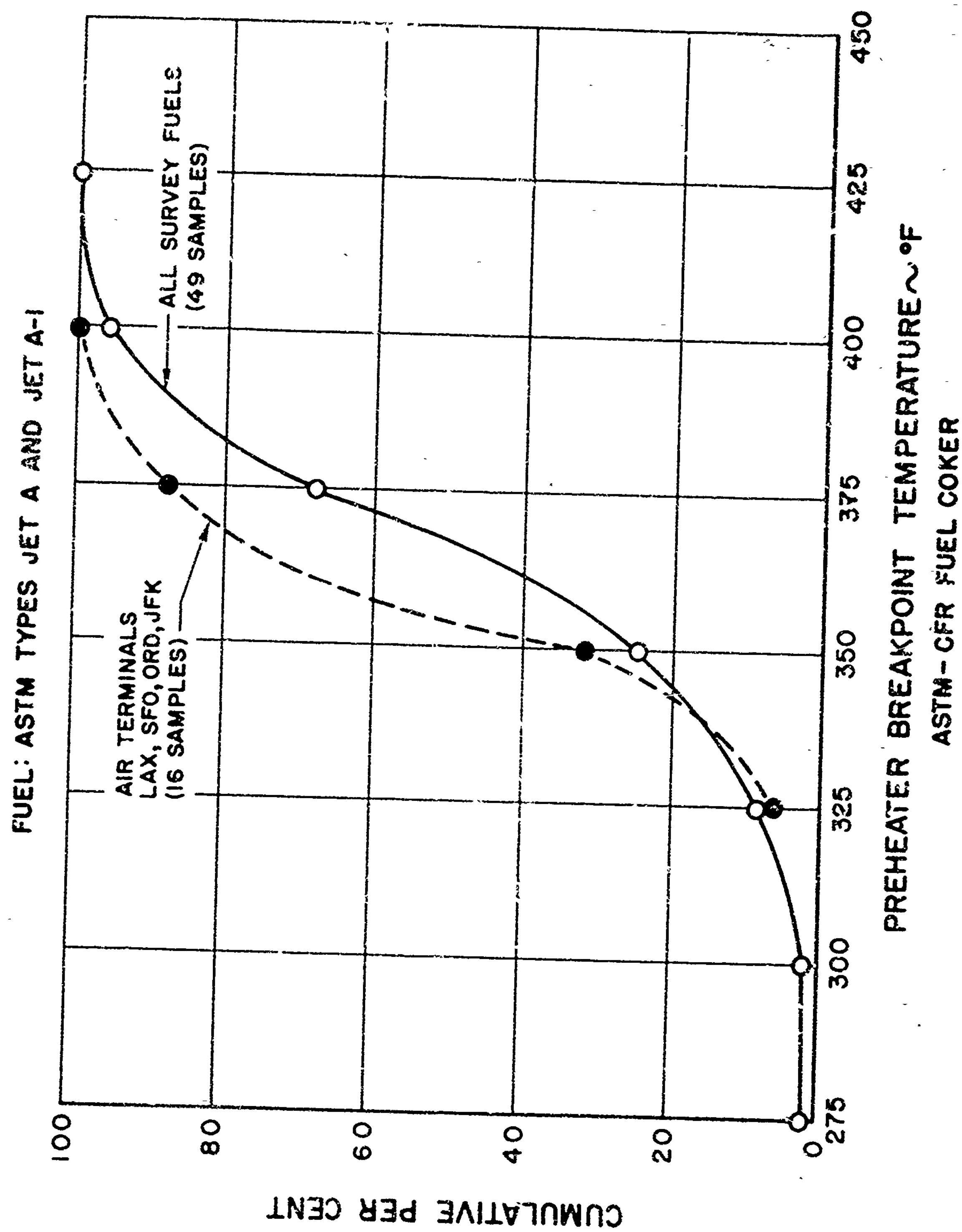

PREHEATER BREAKPOINT TEMPERATURE DISTRIBUTION
ASTM-CFR FUEL COKER

Figure 12-8

DOMESTIC JET FUEL SURVEY

ASTM-CFR FUEL COKER
P/H BREAKPOINT TEMP. DISTRIBUTION

Corrected for ΔP (Code 3)*

Temperature	No. of Fuels	%	Cumulative %
275	1	2.1	2.1
300	1	2.1	4.2
325	3	6.1	10.3
350	14	28.5	38.8
375	16	32.6	71.4
400	13	26.5	97.9
425	1	2.1	100.0
	49	100.0	

*Based on Code 3 P/H deposit max. provided ΔP <13" Hg max. Otherwise next lowest 25F increment passing ΔP requirement and Code 3 max.

Figure 12-9

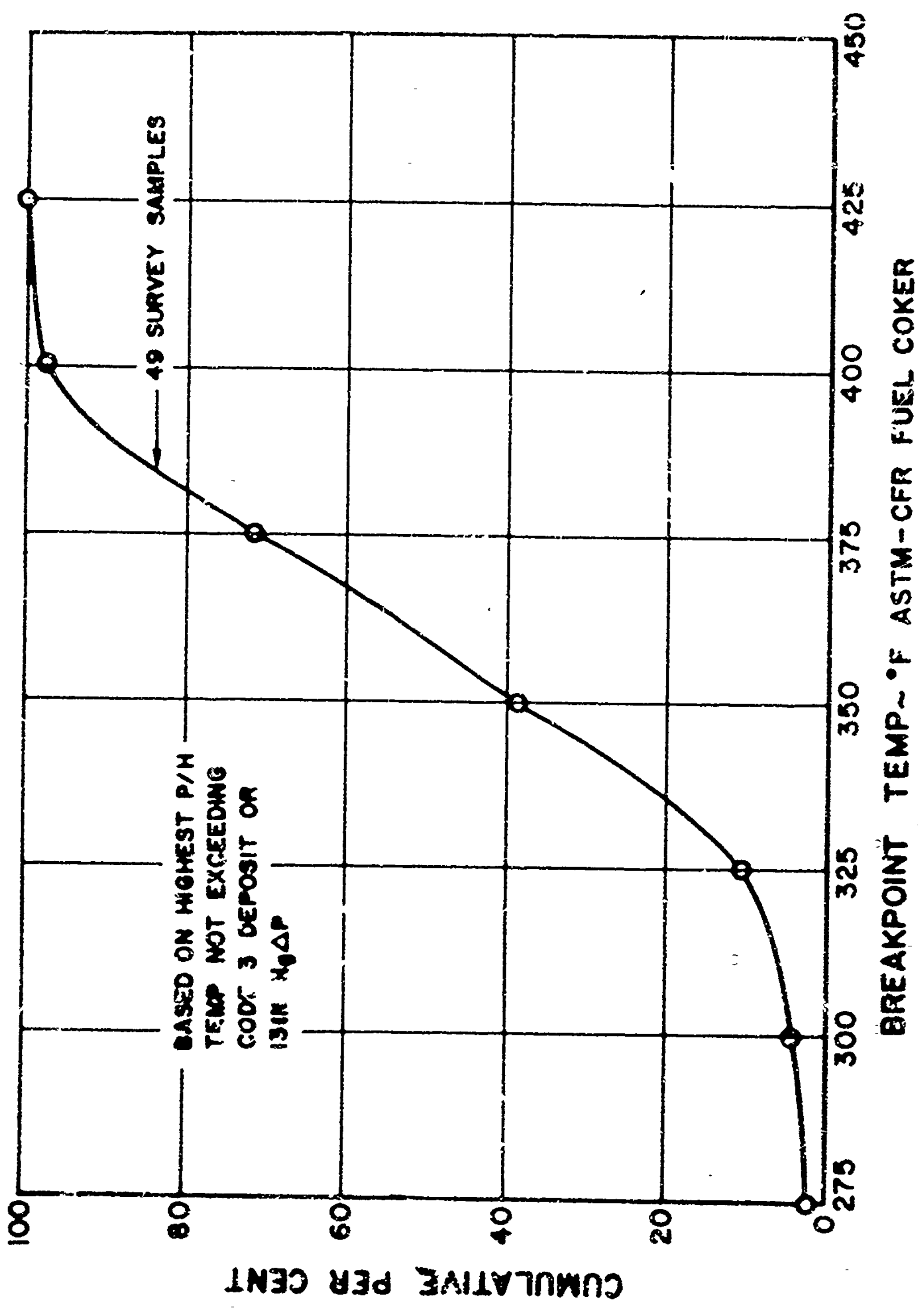

PREHEATER BREAKPOINT DISTRIBUTION
OF SURVEY FUELS

Figure 12-10

DOMESTIC JET FUEL SURVEY

BREAKPOINT TEMPERATURE DISTRIBUTION IN TESTS WITH
CRC RESEARCH FUEL COKER

	Amb. Reservoir			175°F Reservoir			250°F Reservoir		
Breakpoint Temp. - °F	No.	%	Cumulative %	No.	%	Cumulative %	No.	%	Cumulative %
325	2	16.8	16.8	1	6.2	6.2			
350	3	25.0	41.8	4	25.0	31.2	7	43.8	43.8
375	4	33.3	75.1	4	25.0	56.2	4	25.0	68.8
400	1	8.3	83.4	3	18.8	75.0	1	6.2	75.0
425	1	8.3	91.7	2	12.5	87.5	4	25.0	100.0
450	1	8.3	100.0	2	12.5	100.0			
	12	100.0		16	100.0		16	100.0	

Figure 12-F1

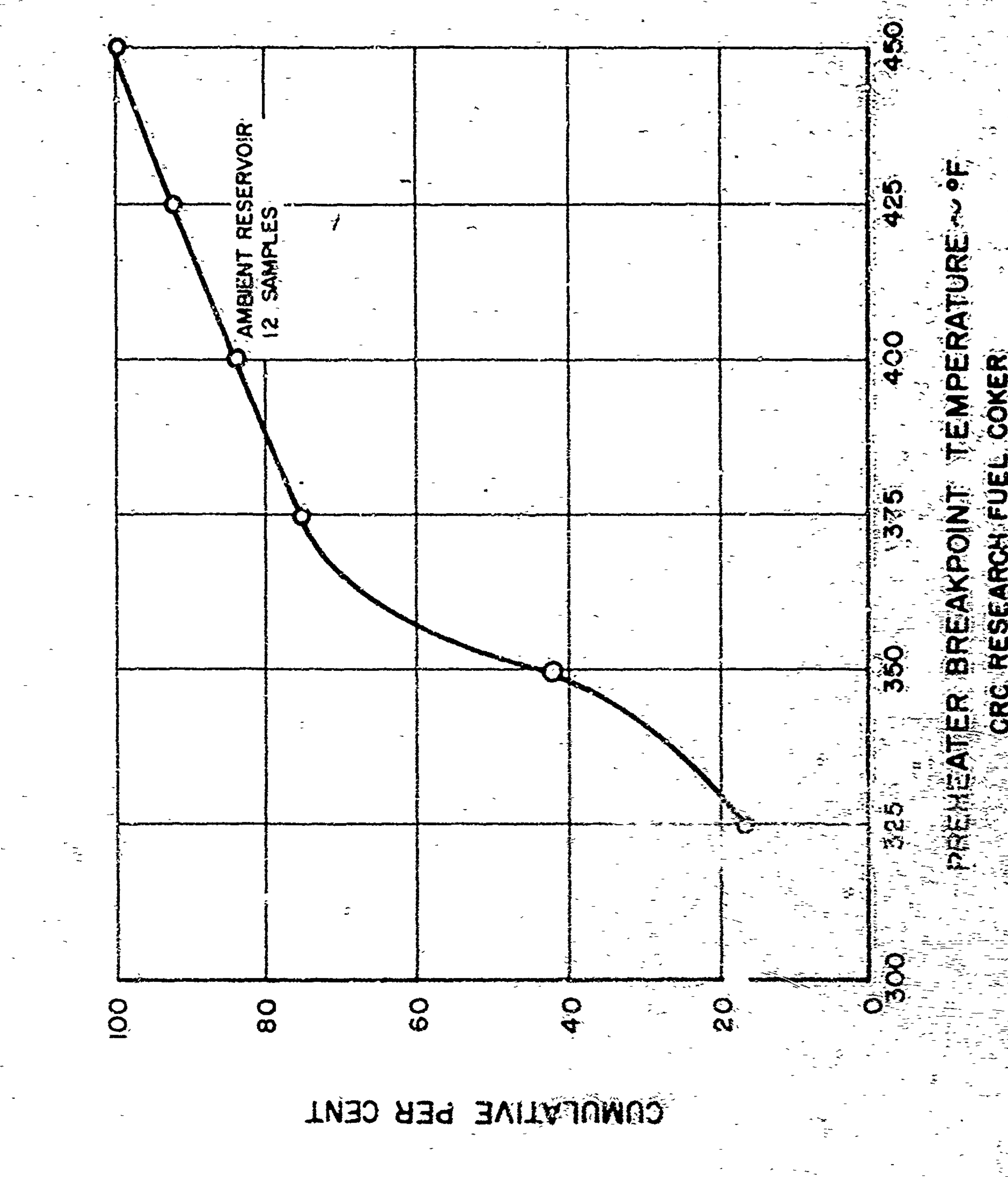

PREHEATER BREAKPOINT TEMPERATURE DISTRIBUTION
CRC RESEARCH FUEL COKER (11 SAMPLES)

Figure 12-12

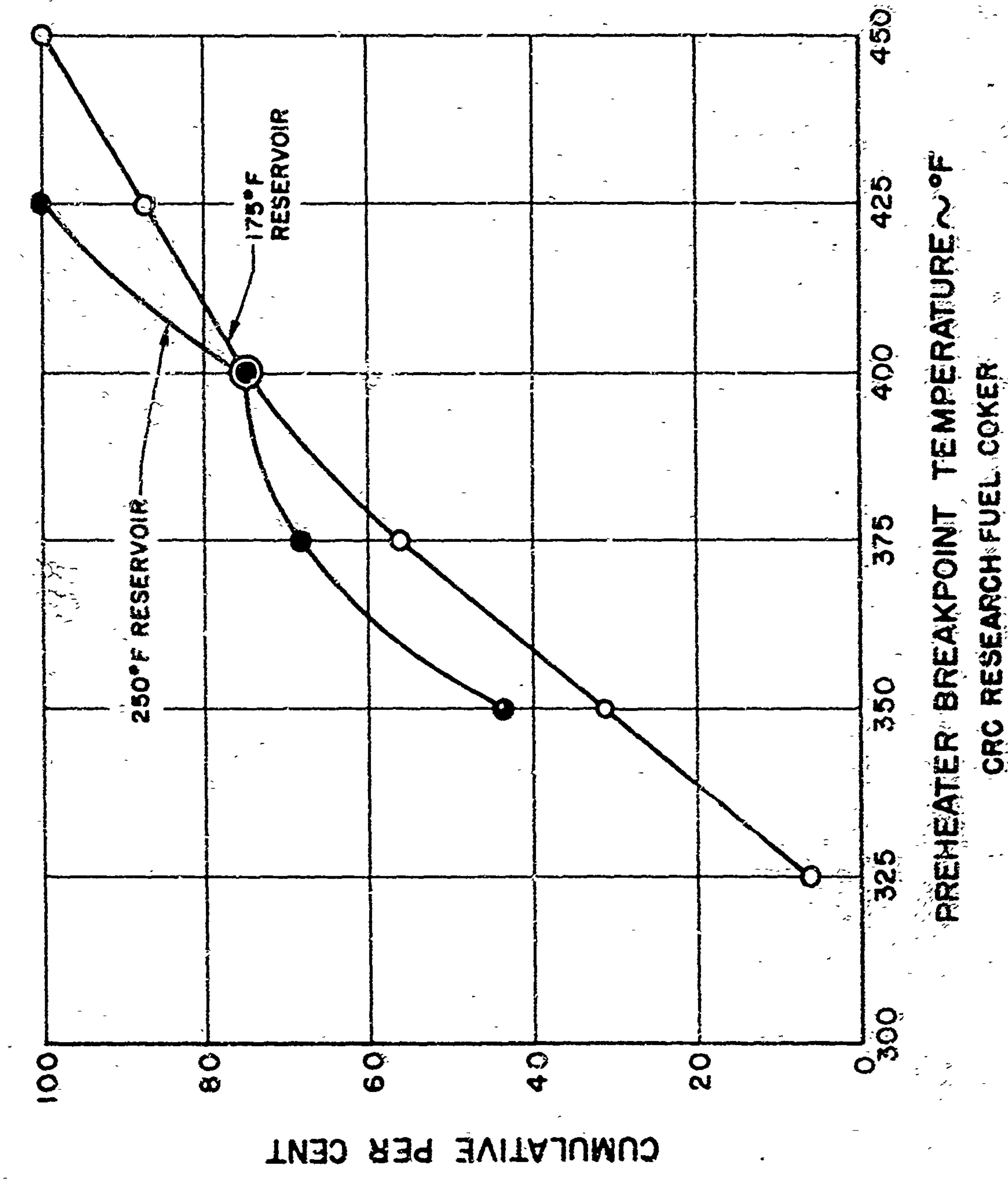

PREHEATER BREAKPOINT TEMPERATURE DISTRIBUTION
CRC RESEARCH FUEL COKER (16 SAMPLES)

Figure 12-13

FUEL SAMPLES
FROM MAJOR AIR TERMINALS

12 SAMPLES

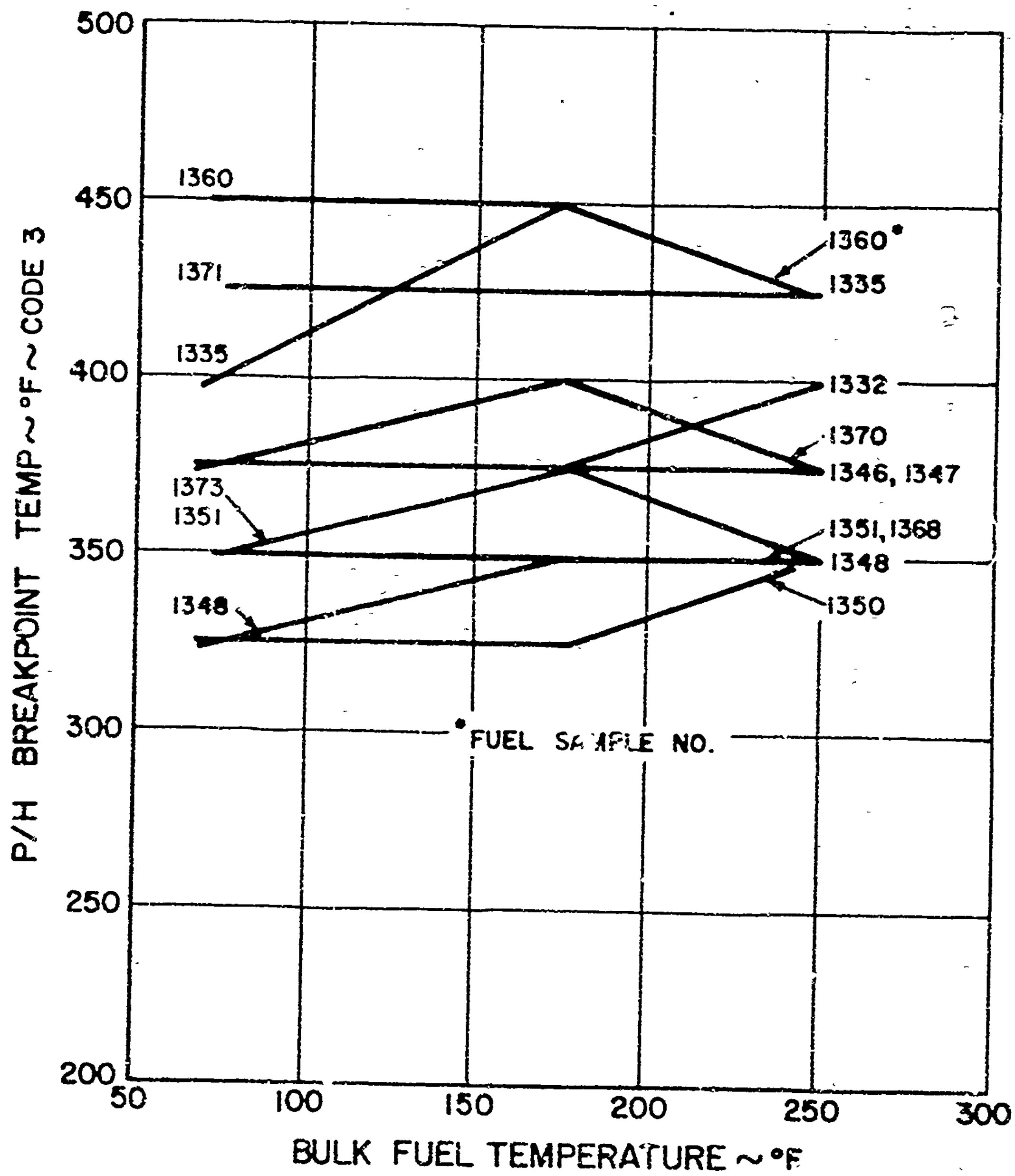

EFFECT OF RESERVOIR FUEL HEATING ON PREHEATER BREAKPOINT TEMPERATURE IN CRC RESEARCH FUEL COKER

Figure 12-14

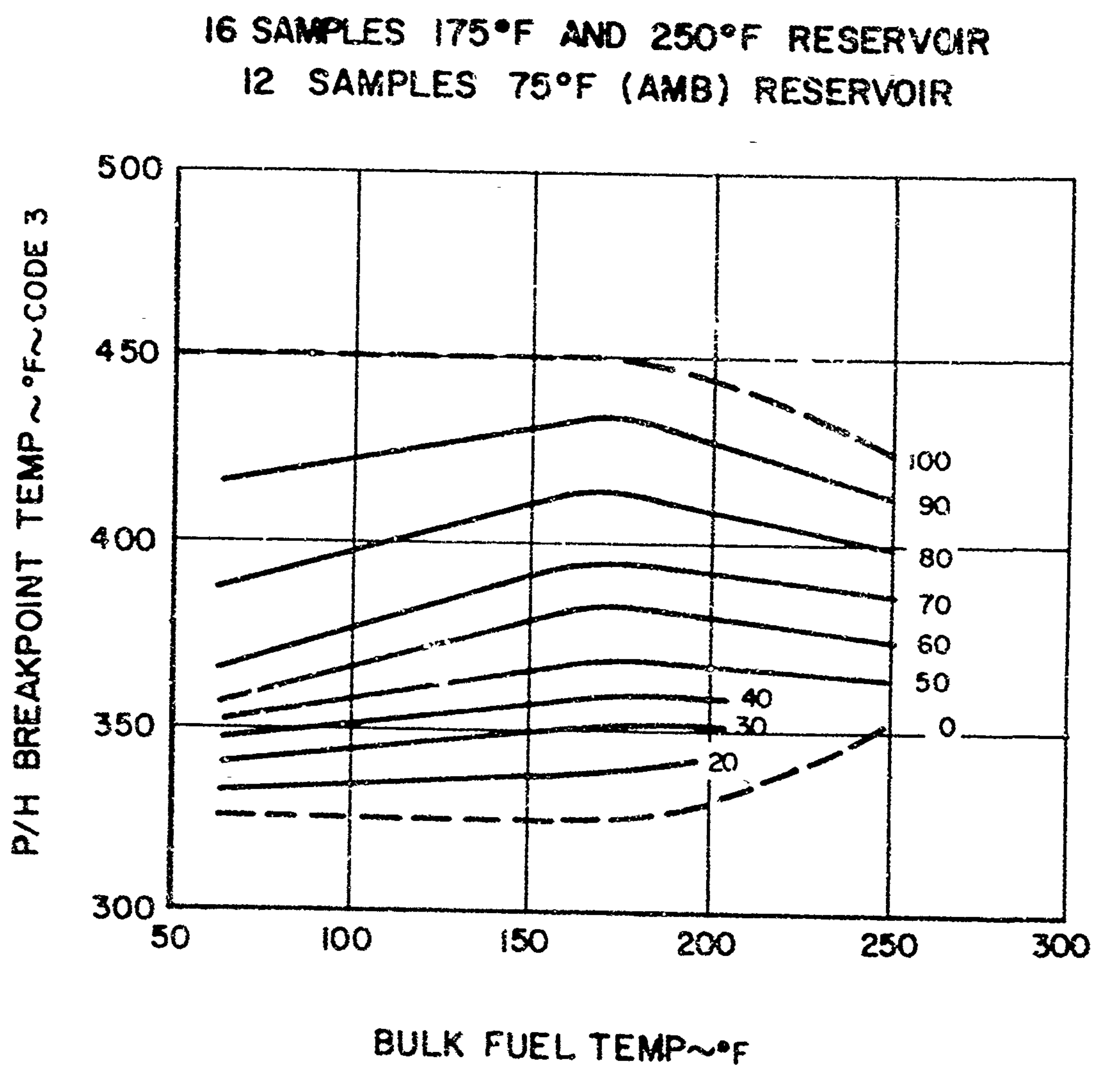

BREAKPOINT PROFILE DISTRIBUTION OF SURVEY FUELS

Figure 12-15

LUBRICITY VALUES OF DOMESTIC SURVEY FUELS

Fuel Sample Number	Ryder Gear Load Carrying Ability, lb/inch "A"-side	"B"-side	Average
F1332	646	585	615
1335	250	432	341
1346	402	503	452
1347	465	353	409
1348	582	258	420
1350	227	394	310
1351	298	246	272
1360	446	409	427
1368	466	331	398
1369	233	286	259
1370	423	482	452
1371	328	290	309
1373	325	229	277
1381	162	353	257
1382	330	286	308
1383	313	328	320
Minimum (lb/in.)			257
Average (lb/in.)			364
Maximum (lb/in.)			615

Figure 12-16

CRC RESEARCH FUEL COKER TESTS FOR DETERMINATION OF PREHEATER BREAKPOINT TEMPERATURE STANDARD RESERVOIR CONFIGURATION

Fuel	Test Number	Condition Res. - P/F	Max P/H Code	Filter ΔP/Minutes	P/H Tube Deposits Cold — Hot
F1497	2072	175-350/450	2	7.1/300	1 2 2 2 2 2 2 2 2 2 2 2 2
F1497	2075	175-375/475	6	25/196	1 1 1 1 1 1 1 1 1 2 5 6 5
F1497	2098	175-350/450	2	25/260	2 2 2 2 2 2 2 2 2 2 2 2 2
F1065	2079	175-350/450	2	6.1/300	1 1 1 1 1 2 2 2 2 2 2 2 2
F1065	2080	175-375/475	2	24/300	1 1 1 1 1 1 1 2 2 2 2 2 2
F1065	2084	175-400/500	3	25/257	1 1 1 1 1 1 1 1 1 2 3 3 3
F1065	2131	175-450/550	3	25/53	1 1 1 1 1 1 1 3 3 3 3 3 3
F1065	2114	175-425/525	6	25/94	1 1 1 1 1 1 2 3 6 3 3 3 3
F1498	2076	175-350/450	2	0.7/300	2 2 2 2 2 2 2 2 2 2 2 2 2
F1498	2077	175-375/475	2	1.2/300	2 2 2 2 2 2 2 2 2 2 2 2 2
F1498	2078	175-400/500	6	25/186	1 2 2 1 1 1 1 1 3 6 5 5 6

Figure 12-17

RESEARCH FUEL COKER TESTS FOR DETERMINATION OF PREHEATER BREAKPOINT TEMPERATURE

Reduced Fuel Oxygen Content
1.0 ±0.1 Psia Reservoir Pressure

Fuel	Test Number	Condition Res. - P/F	Max P/H Code	Filter ΔP/Minutes	P/H Tube Deposit Cold												Hot
F1497	2096	175-350/450	2	25/229	1	1	1	1	1	1	1	1	2	2	2	2	2
F1497	2094	175-375/475	3	25/120	1	1	1	1	2	2	3	3	3	3	3	3	3
F1497	2097	175-375/475	2	25/126	1	1	1	1	1	1	1	2	2	2	2	2	2
F1497	2102	175-375/475	2	25/142	1	1	1	1	1	1	1	2	2	2	2	2	1
F1497	2101	175-400/500	2	17.7/300	1	1	1	1	1	1	1	1	1	1	1	1	2
F1497	2103	175-425/525	3	25/147	1	1	1	1	1	1	2	2	2	3	3	3	2
F1497	2113	175-450/550	2	7.4/300	1	1	2	2	1	2	2	2	2	1	1	1	1
F1497	2115	175-475/575	2	10.5/300	1	1	1	1	1	2	2	2	2	2	2	2	2
F1497	2134	175-350/450	2	25/289	1	1	1	2	2	2	2	1	1	1	1	1	1
F1497	2135	175-375/475	2	25/281	1	1	1	2	2	1	1	2	2	2	2	2	2
F1497	2136	175-400/500	3	14.5/300	1	1	2	1	1	1	1	1	1	3	3	3	3
F1497	2137	175-500/600	3	14.7/300	1	1	3	2	1	2	2	2	3	3	2	1	1
F1065	2106	175-375/475	2	7.6/300	1	1	1	1	1	1	1	1	2	2	2	2	2
F1065	2108	175-375/475	3	23/300	1	1	1	1	1	1	1	2	2	3	3	3	2
F1065	2104	175-400/500	4	23.2/300	1	1	1	1	1	1	1	4	4	4	4	4	3
F1065	2107	175-400/500	3	11.4/300	1	1	1	1	1	2	2	2	2	2	3	3	3
F1065	2099	175-425/525	3	13.5/300	1	1	1	1	1	2	2	3	3	3	3	3	3
F1065	2130*	175-450/550	4	25/107	0	1	1	1	1	1	1	3	4	4	3	2	2

* Test Aborted at 210 Minutes.

Figure 12-18
(Sheet 1 of 2)

RESEARCH FUEL COKER TESTS FOR DETERMINATION OF PREHEATER BREAKPOINT TEMPERATURE (Cont)

Reduced Fuel Oxygen Content
1.0±0.1 Psia Reservoir Pressure

Fuel	Test Number	Condition Res. - P/F	Max P/H Code	Filter ΔP/Minutes	P/H Tube Deposit Cold — Hot
F1065	2131*	175-450/550	3	25/53	1 1 1 1 1 1 1 3 3 3 3 3 3
F1065	2132	175-450/550	3	25/94	1 1 1 1 1 1 2 3 3 3 3 3 2
F1065	2133	175-375/475	3	3.0/300	1 1 1 1 1 1 1 1 1 2 3 3 3
F1498	2109	175-400/500	2	5.0/300	1 1 1 1 1 1 2 2 2 2 2 2 2
F1498	2110	175-425/525	2	3.8/300	1 1 1 1 1 1 1 2 2 2 2 2 2
F1498	2112	175-450/550	2	2.4/300	1 1 1 1 1 1 2 2 2 2 2 2 2
F1498	2116	175-475/575	1	15.3/300	1 1 1 1 1 1 1 1 1 1 1 1 1
F1498	2111	175-425/525	2	6.3/300	1 1 1 1 1 1 1 2 2 2 2 2 2
F1498	2147	175-375/475	1	0.7/300	1 1 1 1 1 1 1 1 1 1 1 1 1
F1498	2148	175-500/600	2	1.2/300	0 0 0 1 1 1 2 2 2 1 1 1 1

* Air Saturated and Standard Reservoir Pressure

Figure 12-18
(Sheet 2 of 2)

MEASURED FUEL OXYGEN CONTENT DURING RESEARCH FUEL COKER TESTS AT 175F RESERVOIR TEMPERATURE
1.0±0.1 PSIA RESERVOIR PRESSURE

Test Number	2101	2103	2104	2107	2112	2113
Fuel Number	1497	1497	1065	1065	1498	1497
Condition, P/F	400/500	425/525	400/500	400/500	450/550	450/550
Meter Calib. %(1)	19	20	20	20	21	20
Fuel Oxygen Content, %(2)						
Reservoir heater on	0.40		0.53	0.28	0.74	0.47
Start test, 0 minutes	0.33	0.36	0.39	0.18	0.15	0.27
30 minutes	0.21	0.27	0.41	0.16	0.09	0.18
60 minutes	0.16	0.38	0.31	0.12	0.13	0.17
90 minutes	0.09	0.35	0.31	0.11	0.16	0.17
120 minutes	0.07	0.30	0.62	0.09	0.17	0.17
150 minutes	0.07	0.33	0.45	0.08	0.20	0.18
180 minutes	0.06	0.30	0.54	0.08	0.21	0.21
210 minutes	0.06	0.25	0.49	0.07	0.22	0.21
240 minutes	0.06	0.15	0.46	0.06	0.22	0.21
270 minutes	0.06	0.19	0.39	0.06	0.23	0.21
End test, 300 minutes	0.06	0.19	0.34	0.05	0.23	0.22
Average O_2 Content (0-300 min)	0.11	0.28	0.43	0.09	0.18	0.20

Note (1) Calibration indicates percent oxygen in air obtained by sensor probe during calibration prior to each test. This reading equivalent to fuel oxygen content when air saturated.

(2) Based on fuels having 80°F saturated oxygen content as follows: F1497, 3.17% v; F1065, 4.13% v; F1498, 4.00% v.

Figure 12-19
(Sheet 1 of 5)

MEASURED FUEL OXYGEN CONTENT DURING RESEARCH FUEL COKER TESTS AT 175°F RESERVOIR TEMPERATURE (Cont)
1.0±0.1 PSIA RESERVOIR PRESSURE

Test Number	2115	2116	2102	2106	2108	2109
Fuel Number	1497	1498	1497	1065	1065	1498
Condition, P/F	475/575	475/575	375/475	375/475	375/475	400/500
Meter Calib., % (1)	20	20	19	20	20	20
Fuel Oxygen Content, % (2)						
Reservoir heater on	0.29	0.36	0.21	-	0.52	-
Start test, 0 minutes	0.21	0.09	0.19	0.21	0.39	0.18
30 minutes	0.12	0.04	0.17	0.10	0.31	0.06
60 minutes	0.09	0.04	0.16	0.08	0.31	0.05
90 minutes	0.09	0.03	0.15	0.08	0.2[illegible]	0.05
120 minutes	0.08	0.04	0.13	0.07	0.22	0.05
150 minutes	0.08	0.04	0.11	0.08	0.20	0.06
180 minutes	0.08	0.04	0.08	0.08	0.18	0.06
210 minutes	0.08	0.04	0.07	0.07	0.15	0.06
240 minutes	0.07	0.03	0.04	0.07	0.13	0.07
270 minutes	0.07	0.03	0.04	0.07	0.11	0.07
300 minutes	0.07	0.03	0.04	-	0.11	0.07
Average O_2 Content during Coker Test	0.09	0.04	0.11	0.09	0.22	0.07

Note (1) Meter reading for air calibration and air satured fuel prior to test.

(2) O_2 Content based on: F-1497 = 3.17% v O_2 content sat. at 80°F
F-1498 = 4.00% v O_2 content sat. at 80°F
F-1065 = 4.13% v O_2 content sat. at 80°F

Figure 12-19
(Sheet 2 of 5)

MEASURED FUEL OXYGEN CONTENT DURING RESEARCH FUEL COKER TESTS AT 175F RESERVOIR TEMPERATURE (Cont)
1.0±0.1 PSIA RESERVOIR PRESSURE

Test Number	2110	2111	21[illegible]0	2131*	2132
Fuel Number	1498	1498	1065	1065	1065
Condition, P/F	425/ 525	425/ 525	450/ 550	450/ 550	450
Meter Calib., %(1)	20	20	20	20	20
Fuel Oxygen Content, %(2)					
Reservoir heater on	0.44	0.37	0.58		
Start test, 0 minutes	0.20	0.30	0.31	4.05	0.17
30 minutes	0.09	0.10	0.17	4.05	0.12
60 minutes	0.08	0.12	0.12	4.00	0.10
90 minutes	0.08	0.14	0.10	4.00	0.09
120 minutes	0.08	0.15	0.10	3.96	0.08
150 minutes	0.08	0.17	0.13	3.90	0.08
180 minutes	0.08	0.17	0.10	3.92	0.08
210 minutes	0.08	0.17	0.10	3.90	0.08
240 minutes	0.08	0.17	test aborted	3.90	0.08
270 minutes	0.08	0.17		3.90	0.08
End test, 300 minutes	0.08	0.19		3.90	0.08
Average O_2 Content (0-300 min)	0.09	0.17		3.95	0.09

Note (1) Meter reading for air calibration and air saturated fuel prior to test.
(2) Based on fuels having 80°F saturated oxygen content as follows: F1497, 3.17%v; F1065, 4.13%v; F1498, 4.00%v.

*Standard reservoir pressure and air saturated fuel.

Figure 12-19
(Sheet 3 of 5)

MEASURED FUEL OXYGEN CONTENT DURING RESEARCH FUEL COKER TESTS AT 175F RESERVOIR TEMPERATURE (Cont)
1.0±0.1 PSIA RESERVOIR PRESSURE

Test Number	2133	2094	2096	2097	2099
Fuel Number	1065	1497	1497	1497	1065
Condition, P/F	375/ 475	375/ 475	350/ 450	375/ 475	425/ 525
Meter Calib., % (1)	20	17	Out	Out	Out
Fuel Oxygen Content, % (2)					
Reservoir heater on	-	0.52	Out	Out	Out
Start test, 0 minutes	1.00	0.35	Out	Out	Out
30 minutes	0.60	Out	Out	Out	Out
60 minutes	0.53	Out	Out	Out	Out
90 minutes	0.48	Out	Out	Out	Out
120 minutes	0.40	Out	Out	Out	Out
150 minutes	0.40	Out	Out	Out	Out
180 minutes	0.40	Out	Out	Out	Out
210 minutes	0.40	Out	Out	Out	Out
240 minutes	0.40	Out	Out	Out	Out
270 minutes	0.39	Out	Out	Out	Out
End test, 300 minutes	0.39	Out	Out	Out	Out
Average O_2 Content (0-300 min)	0.49	-	-	-	-

Note (1) Meter reading for air calibration and air saturated fuel prior to test.

(2) Based on fuels having 80°F saturated oxygen content as follows: F1497, 3.17%v; F1065, 4.13%v; F1498, 4.00%v.

Figure 12-19
(Sheet 4 of 5)

MEASURED FUEL OXYGEN CONTENT DURING RESEARCH FUEL COKER TESTS AT 175F RESERVOIR TEMPERATURE (CONT'D)
1.0±0.1 PSIA RESERVOIR PRESSURE

Test Number	2134	2135	2136	2137	2147	2148
Fuel Number	1497	1497	1497	1497	1498	1498
Condition, P/F	350/ 450	375/ 475	400/ 500	500/ 600	375/ 475	500/ 600
Meter Calib. % (1)	20	20	20	20	20	20
Fuel Oxygen Content, % (2)						
Reservoir Heater on	-	0.59	0.62	0.84	0.72	0.45
Start Test, 0 minutes	0.25	0.21	0.29	0.44	0.18	0.14
30 minutes	0.14	0.15	0.17	0.43	0.07	0.04
60 minutes	0.10	0.10	0.08	0.42	0.06	0.04
90 minutes	0.08	0.08	0.07	0.41	0.05	0.03
120 minutes	0.08	0.07	0.07	0.41	0.05	0.03
150 minutes	0.08	0.07	0.07	0.41	0.09	0.03
180 minutes	0.08	0.07	0.07	0.41	0.06	0.03
210 minutes	0.07	0.07	0.07	0.41	0.05	0.03
240 minutes	0.07	0.07	0.07	0.41	0.04	0.03
270 minutes	0.07	0.07	0.07	0.41	0.04	0.03
End Test 300 minutes	0.07	0.07	0.07	0.41	0.04	0.05
Average O_2 Content (0-300 min.)	0.09	0.08	0.10	0.41	0.06	0.04

Note (1) Meter reading for air calibration and air saturated fuel prior to test.

(2) Based on fuels having 80°F saturated oxygen content as follows: F1497, 3.17%v; F1065, 4.13%v; F1498, 4.00%v.

Figure 12-19
(Sheet 5 of 5)

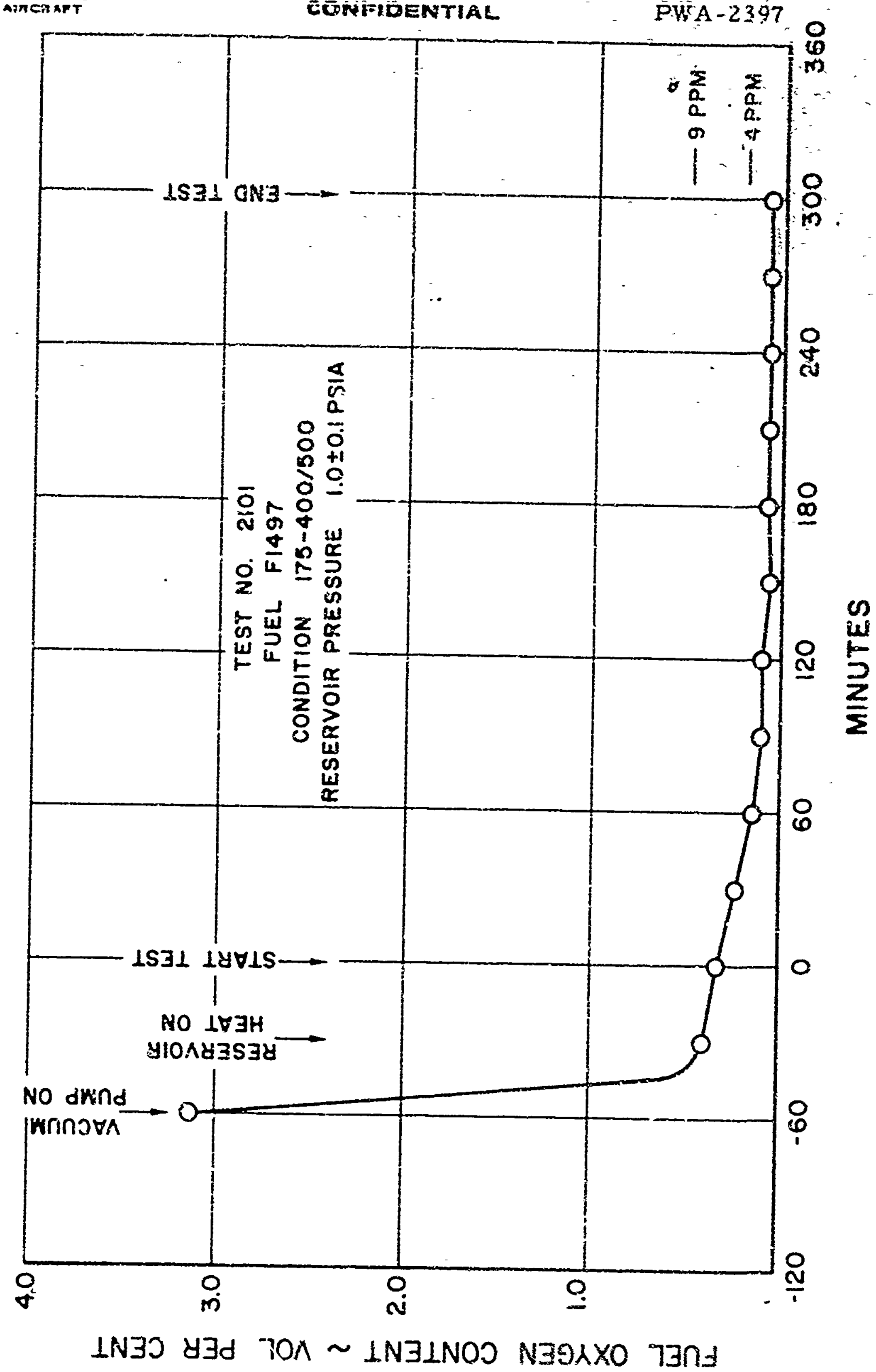

TYPICAL FUEL OXYGEN CONTENT DURING
RESEARCH FUEL COKER TEST AT LOW PRESSURE CONDITIONS

Figure 12-20

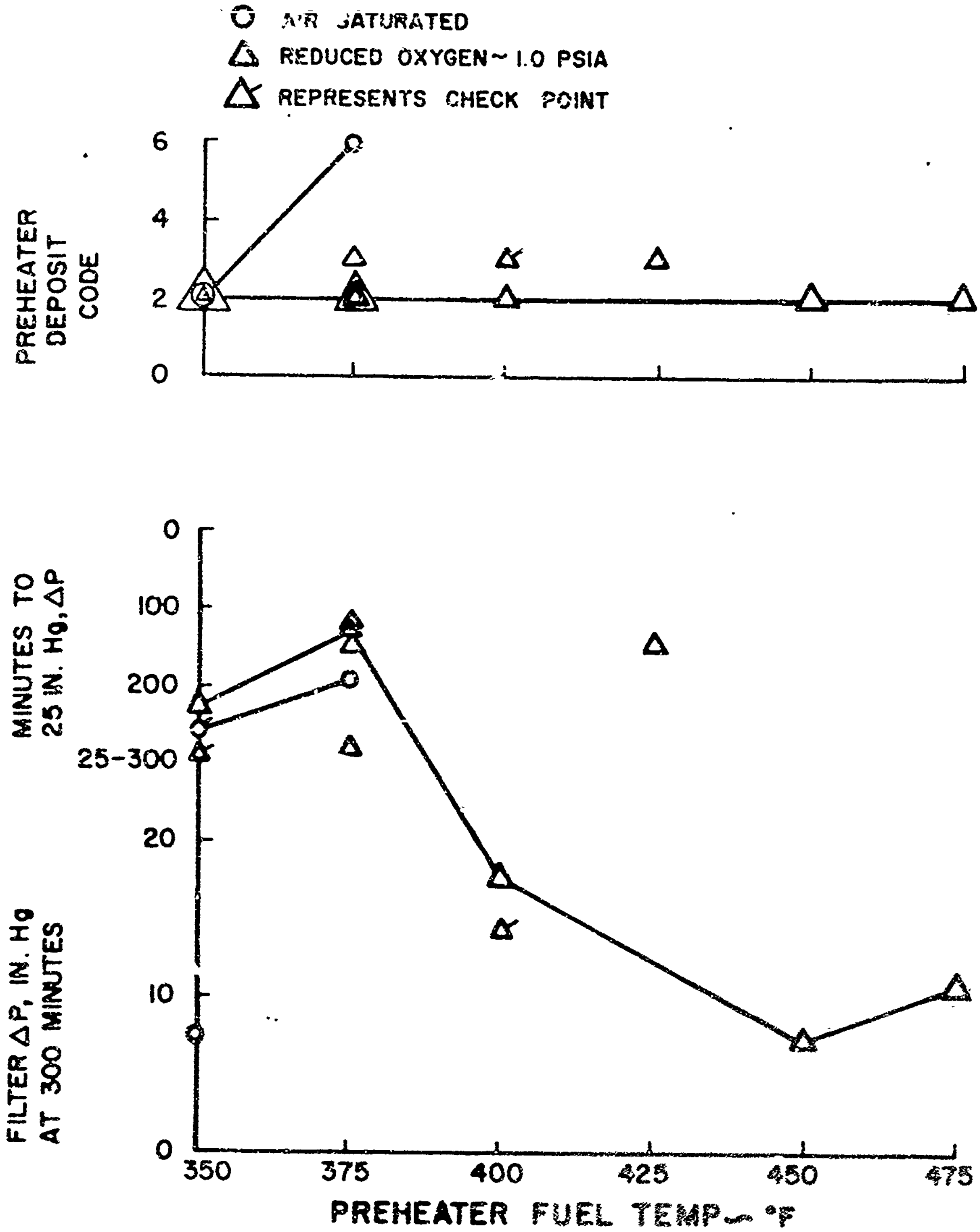

THERMAL STABILITY CHARACTERISTICS OF WEST COAST JET A-1 FUEL NO. F-1497 IN CRC RESEARCH FUEL COKER AT 175°F RESERVOIR TEMPERATURE

Figure 12-21

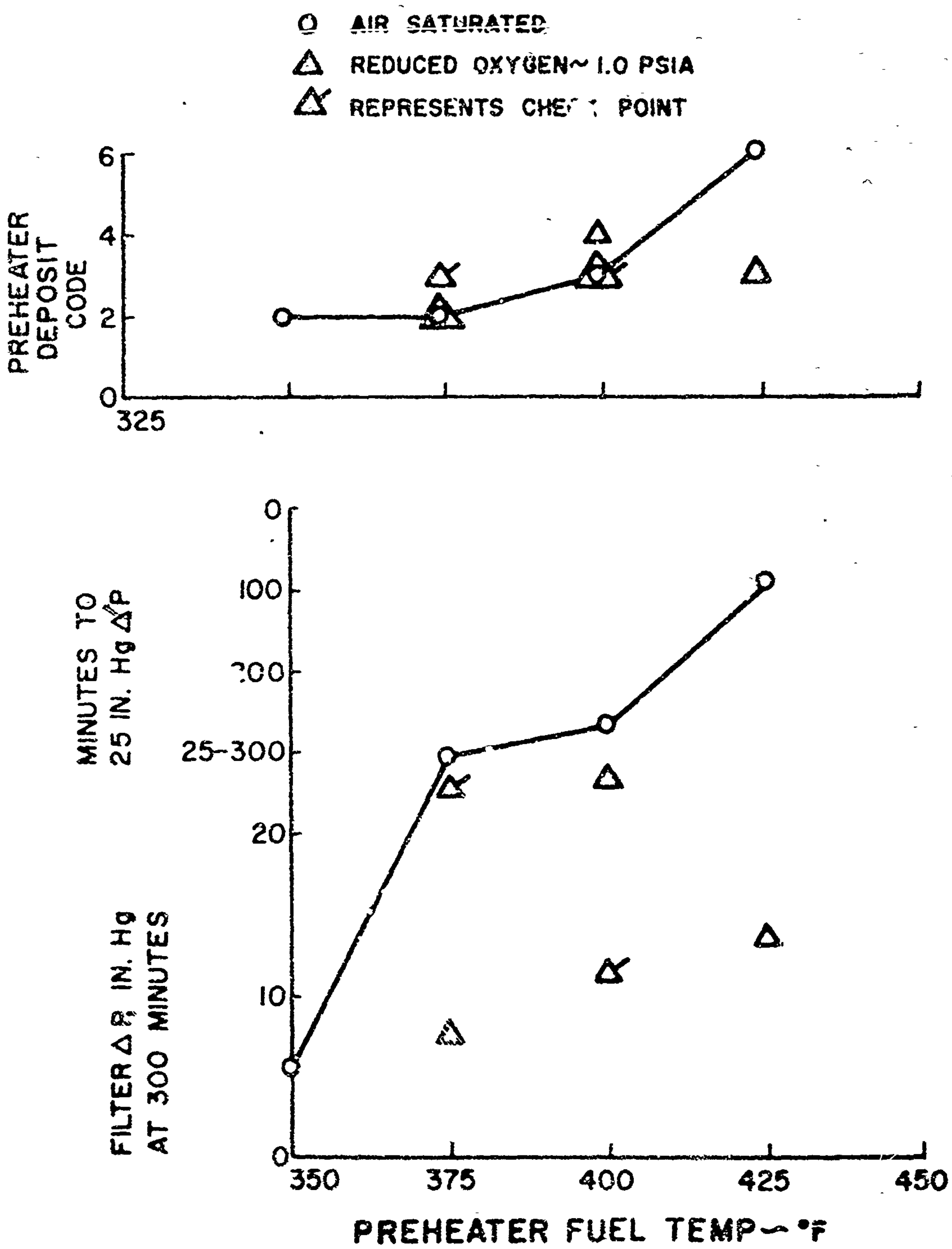

THERMAL STABILITY CHARACTERISTICS OF
JP-5 REFEREE FUEL NO. F1065
IN CRC RESEARCH FUEL COKER AT
175°F RESERVOIR TEMPERATURE

Figure 12-22

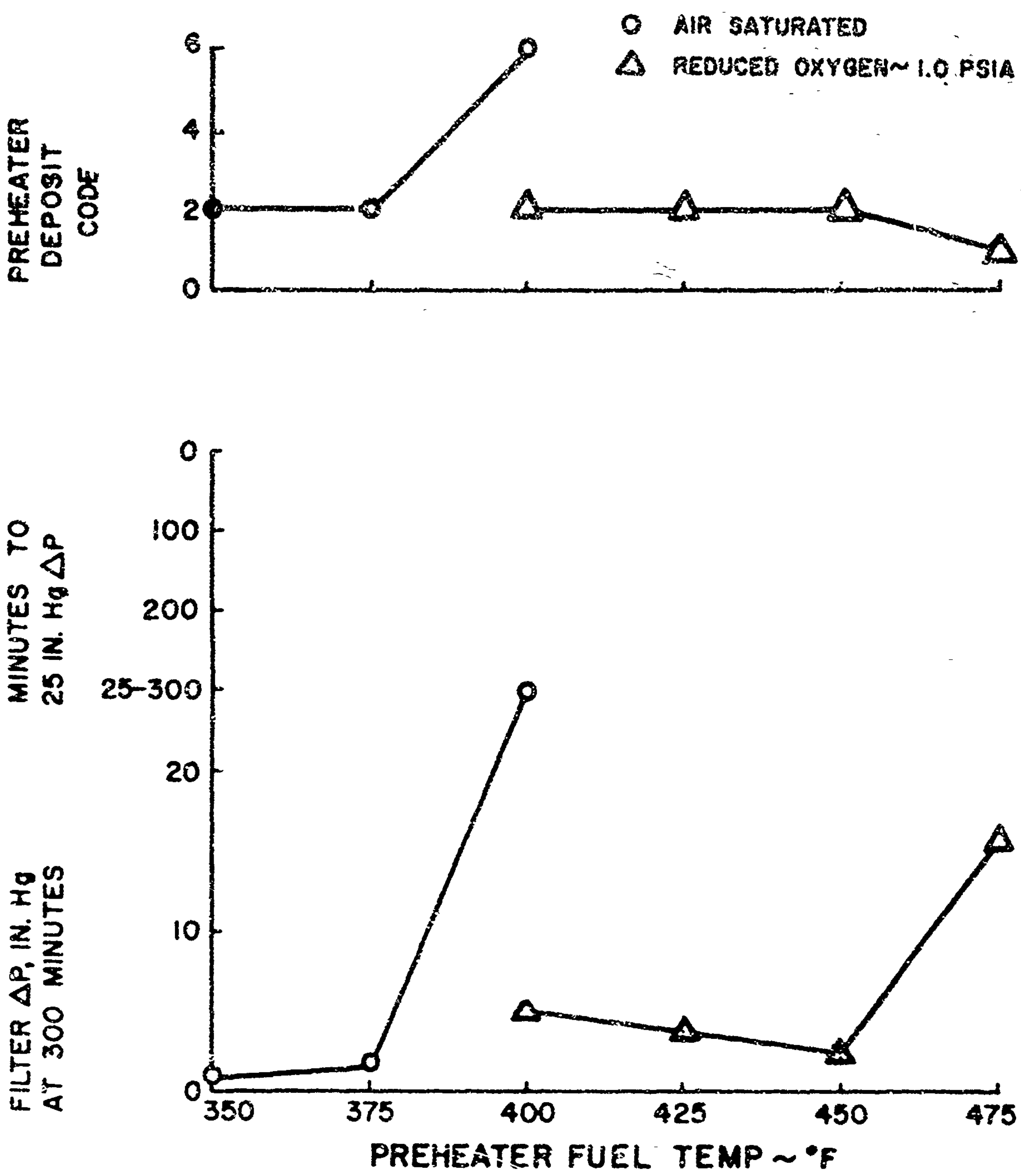

THERMAL STABILITY CHARACTERISTICS OF
EAST COAST JET A-1 FUEL NO. F-1498
IN CRC RESEARCH FUEL COKER AT
175°F RESERVOIR TEMPERATURE

Figure 12-23

RESEARCH FUEL COKER TESTS FOR DETERMINATION OF PREHEATER BREAKPOINT TEMPERATURE

Reduced Fuel Oxygen Content
1.0±0.1 Psia Reservoir Pressure

Fuel	Test Number	Condition Res. - P/F	Max P/H Code	Filter P/Minutes	P/H Deposit Code Cold ... Hot
F1497	2169	175-325/425	2	8.2/300	0 0 0 0 2 1 1 1 1 1 1 1 1
F1497	2166	175-350/450	2	25/249	0 0 0 1 1 1 1 1 1 1 1 2 2
F1497	2149	175-375/475	2	25/246	1 1 1 2 2 1 1 1 1 2 2 2 2
F1497	2150	175-400/500	2	25/176	1 1 2 2 1 1 1 1 2 2 2 2 1
F1497	2151	175-425/525	3	25/226	0 0 3 2 0 0 1 2 2 3 3 2 1
F1497	2163	175-450/550	3	25/180	1 1 1 2 2 2 2 3 3 3 3 2 2
F1065	2167	175-350/450	1	1.9/300	1 1 1 1 1 1 1 1 1 1 1 1 1
F1065	2161	175-375/475	2	25/220	1 1 1 1 1 1 1 1 1 2 2 2 1
F1065	2160	175-400/500	3	25/271	0 0 0 0 1 1 1 1 2 2 2 3 2
F1065	2158	175-425/525	8	25/37	1 1 1 1 1 3 3 5 8 8 8 3 3
F1065	2159	175-425/525	3	25/211	0 0 0 0 0 1 1 1 2 3 3 3 3
F1498	2164	175-350/450	2	0.6/300	0 0 0 0 1 1 1 1 1 1 2 2 2
F1498	2157	175-375/475	2	15.1/300	1 1 1 1 1 1 1 1 2 2 2 2 2
F1498	2156	175-400/500	3	25/115	1 1 1 1 1 1 2 3 3 3 3 3 3
F1498	2165	175-425/525	3	25/268	1 1 1 1 1 1 1 2 2 3 3 3 3
F1498	2168	175-450/550	3	22.5/300	0 1 1 1 1 1 2 2 2 2 3 3 3
F1498	2170	175-475/575	2	4.8/300	1 1 1 1 1 1 2 2 2 2 2 2 2

Figure 12-24
(Sheet 1 of 1)

MEASURED FUEL OXYGEN CONTENT DURING RESEARCH FUEL COKER TESTS AT 175F RESERVOIR TEMPERATURE
1.5 PSIA RESERVOIR PRESSURE

Test Number	2149	2150	2151	2156	2157	2158
Fuel Number	1497	1497	1497	1498	1498	1065
Condition, P/F	375/ 475	400/ 500	425/ 525	400/ 500	375/ 475	425/ 525
Meter Calib. % (1)	20	20	20	20	20	20
Fuel Oxygen Content, % (2)						
Reservoir Heater on	0.71	0.46	0.87	0.88	0.77	0.93
Start Test, 0 minutes	0.41	0.40	0.53	0.50	0.38	0.56
30 minutes	0.36	0.30	0.26	0.24	0.26	0.48
60 minutes	0.32	0.29	0.23	0.22	0.20	0.41
90 minutes	0.29	0.25	0.21	0.22	0.18	0.37
120 minutes	0.26	0.24	0.19	0.22	0.18	0.33
150 minutes	0.24	0.21	0.18	0.22	0.18	0.31
180 minutes	0.22	0.19	0.17	0.21	0.18	0.29
210 minutes	0.21	0.18	0.17	0.21	0.17	0.27
240 minutes	0.20	0.18	0.17	0.23	0.17	0.27
270 minutes	0.20	0.18	0.17	0.29	0.17	0.27
End Test 300 minutes	0.20	0.18	0.17	0.22	0.17	0.27
Average O_2 Content (0-300 min.)	0.26	0.24	0.22	0.25	0.20	0.35

Note (1) Meter reading for air calibration and air saturated fuel prior to test.

(2) Based on fuels having 80°F saturated oxygen content as follows: F1497, 3.17%v; F1065, 4.13%v; F1498, 4.00%v.

Figure 12-25
(Sheet 1 of 3)

MEASURED FUEL OXYGEN CONTENT DURING RESEARCH FUEL COKER TESTS AT 175F RESERVOIR TEMPERATURE 1.5 PSIA RESERVOIR PRESSURE

Test Number	2159	2160	2161	2163	2164	2165
Fuel Number	1065	1065	1065	1497	1498	1498
Condition, P/F	425/ 525	400/ 500	375/ 475	450/ 550	350/ 450	425/ 525
Meter Calib. %(1)	20	20	20	20	20	20
Fuel Oxygen Content, % (2)						
Reservoir Heat on	1.34	0.93	0.93	0.90	1.25	1.00
Start Test, 0 minutes	0.60	0.76	0.72	0.57	0.43	0.44
30 minutes	0.50	0.46	0.43	0.41	0.29	0.32
60 minutes	0.44	0.40	0.35	0.35	0.20	0.24
90 minutes	0.39	0.36	0.32	0.32	0.19	0.20
120 minutes	0.34	0.31	0.29	0.24	0.17	0.18
150 minutes	0.31	0.28	0.27	0.22	0.17	0.17
180 minutes	0.31	0.27	0.27	0.20	0.17	0.17
210 minutes	0.30	0.26	0.27	0.19	0.16	0.17
240 minutes	0.30	0.25	0.26	0.17	0.14	0.17
270 minutes	0.30	0.25	0.26	0.17	0.17	0.17
End Test 300 minutes	0.30	0.25	0.26	0.17	0.15	0.17
Average O_2 Content (0-300 min.)	0.37	0.35	0.34	0.27	0.20	0.22

Note (1) Meter reading for air calibration and air saturated fuel prior to test.

(2) Based on fuels having 80°F saturated oxygen content as follows: F1497, 3.17% v; F1065, 4.13% v.; F1498, 4.00%v.

Figure 12-25
(Sheet 2 of 3)

MEASURED FUEL OXYGEN CONTENT DURING RESEARCH FUEL COKER TESTS AT 175F RESERVOIR TEMPERATURE 1.5 PSIA RESERVOIR PRESSURE

Test Number		2166	2167	2168	2169	2170
Fuel Number		1497	1065	1498	1497	1498
Condition, P/F		350/ 450	350/ 450	450/ 550	325/ 425	475/ 575
Meter Calib. % (1)		20	20	20	20	20
Fuel Oxygen Content, % (2)						
Reservoir Heat On		0.90	0.74	1.00	0.90	0.74
Start Test	0 minutes	0.55	0.47	0.46	0.46	0.35
	30 minutes	0.40	0.37	0.33	0.35	0.15
	60 minutes	0.33	0.29	0.26	0.31	0.11
	90 minutes	0.29	0.26	0.20	0.28	0.10
	120 minutes	0.2[illegible]	0.23	0.18	0.24	0.10
	150 minutes	0.2[illegible]	0.22	0.18	0.22	0.10
	180 minutes	0.25	0.22	0.18	0.20	0.10
	210 minutes	0.22	0.22	0.18	0.19	0.10
	240 minutes	0.21	0.22	0.18	0.19	0.10
	270 minutes	0.21	0.22	0.18	0.19	0.10
End Test	300 minutes	0.20	0.22	0.18	0.19	0.11
Average O_2 Content (0-300 min.)		0.29	0.27	0.23	0.26	0.13

Note (1) Meter reading for air calibration and air saturated fuel prior to test.
(2) Based on fuels having 80°F saturated oxygen content as follows: F1497, 3.17% v.; F1065, 4.13% v.; F1498, 4.00% v.

Figure 12-25
(Sheet 3 of 3)

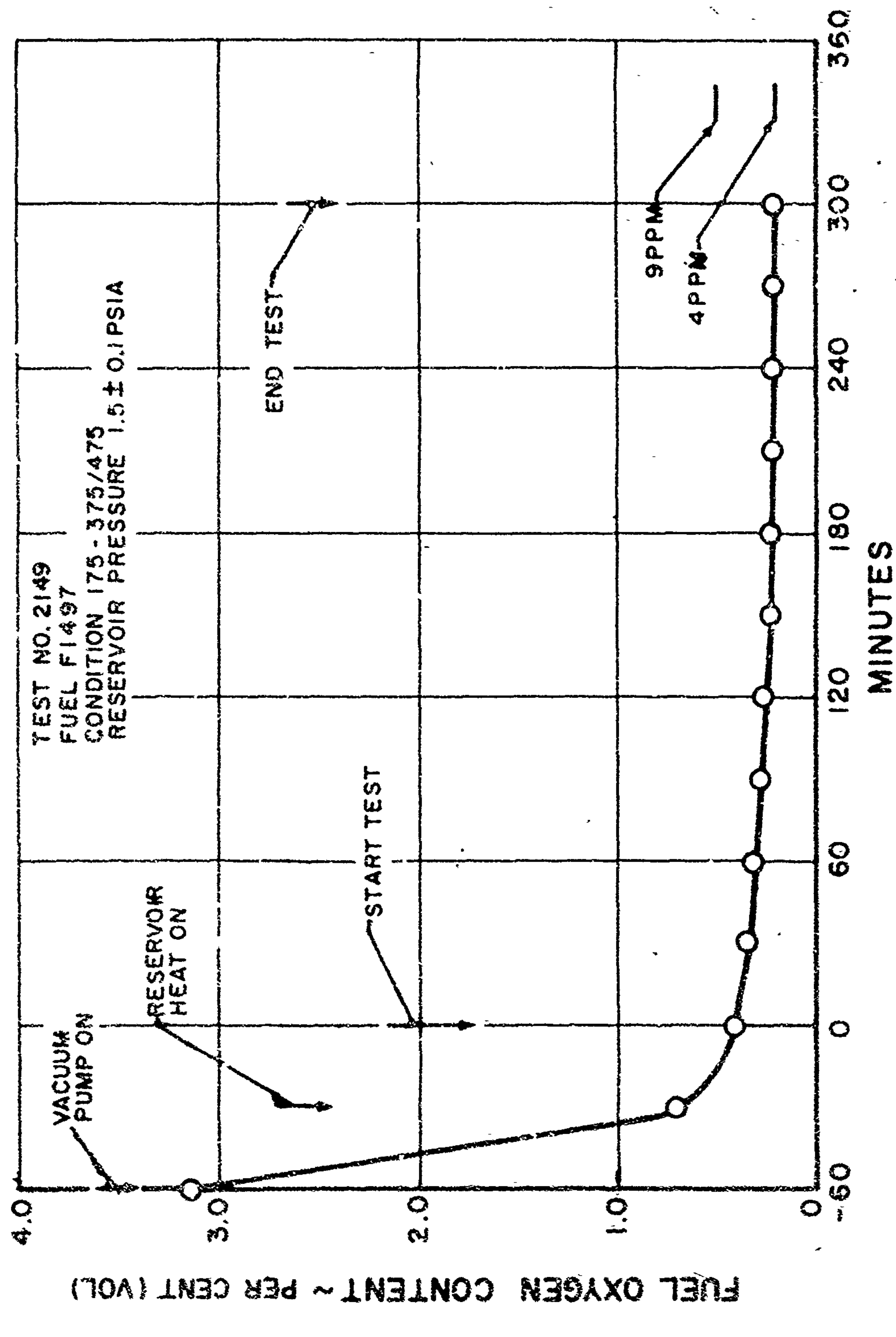

TYPICAL FUEL OXYGEN CONTENT DURING RESEARCH FUEL COKER TEST AT LOW PRESSURE CONDITIONS

FIGURE 12-26

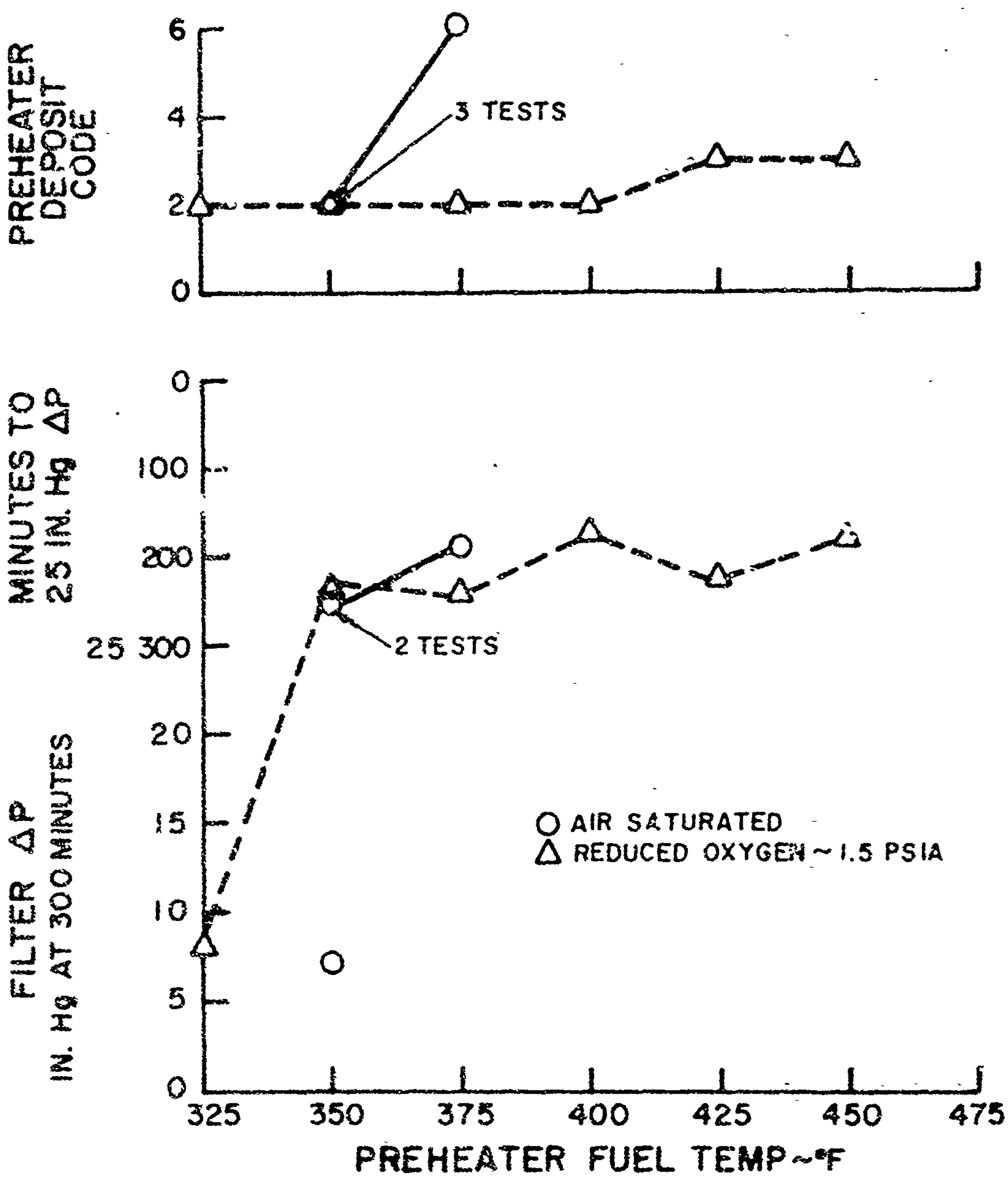

THERMAL STABILITY CHARACTERISTICS OF WEST COAST JET A FUEL NO. F1497 IN CRC RESEARCH FUEL COKER AT 175°F RESERVOIR TEMPERATURE

FIGURE 12-27

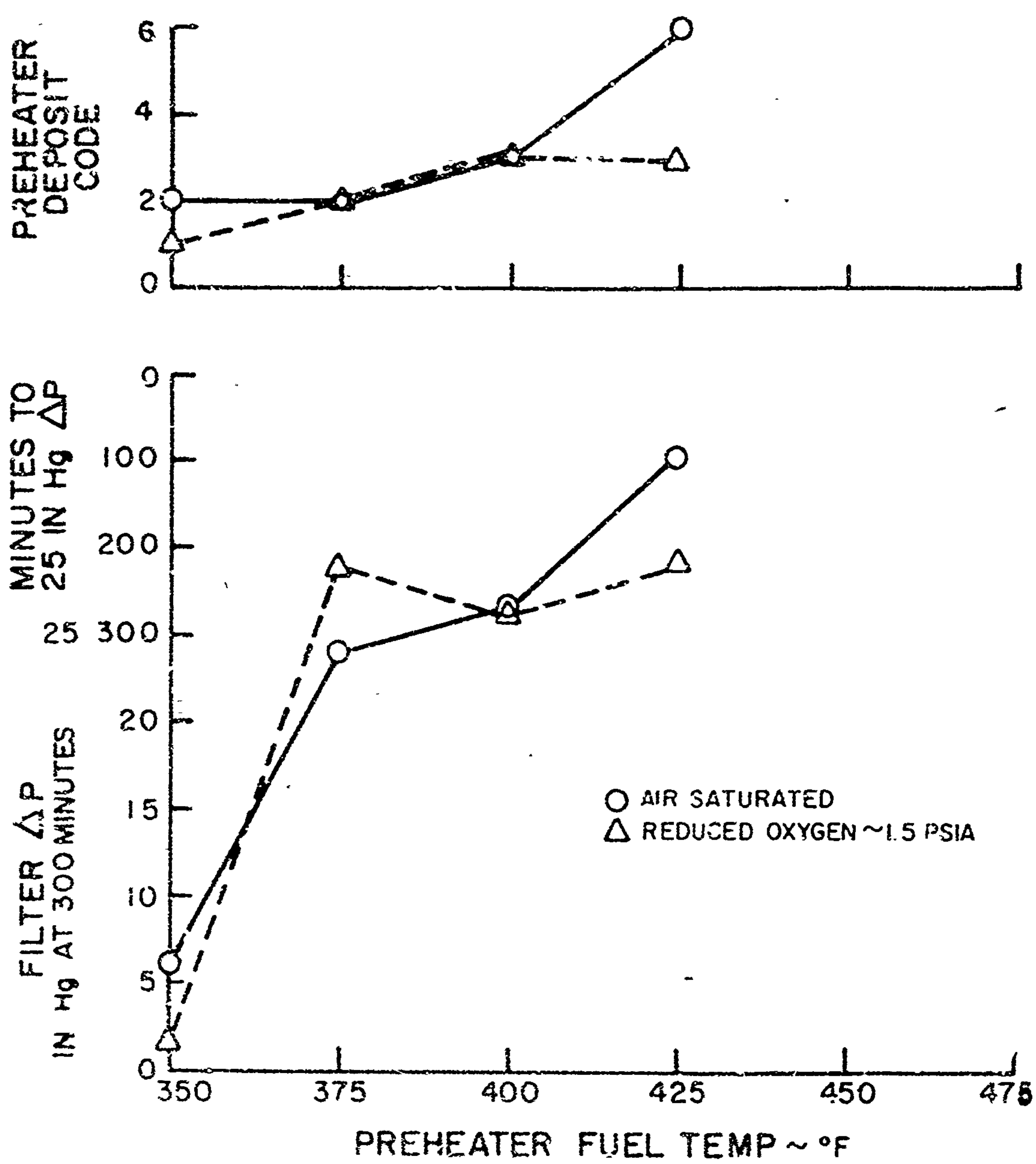

THERMAL STABILITY CHARACTERISTICS OF JP-5 REFEREE FUEL NO. F1065 IN CRC RESEARCH FUEL COKER AT 175F RESERVOIR TEMPERATURE

FIGURE 12-28

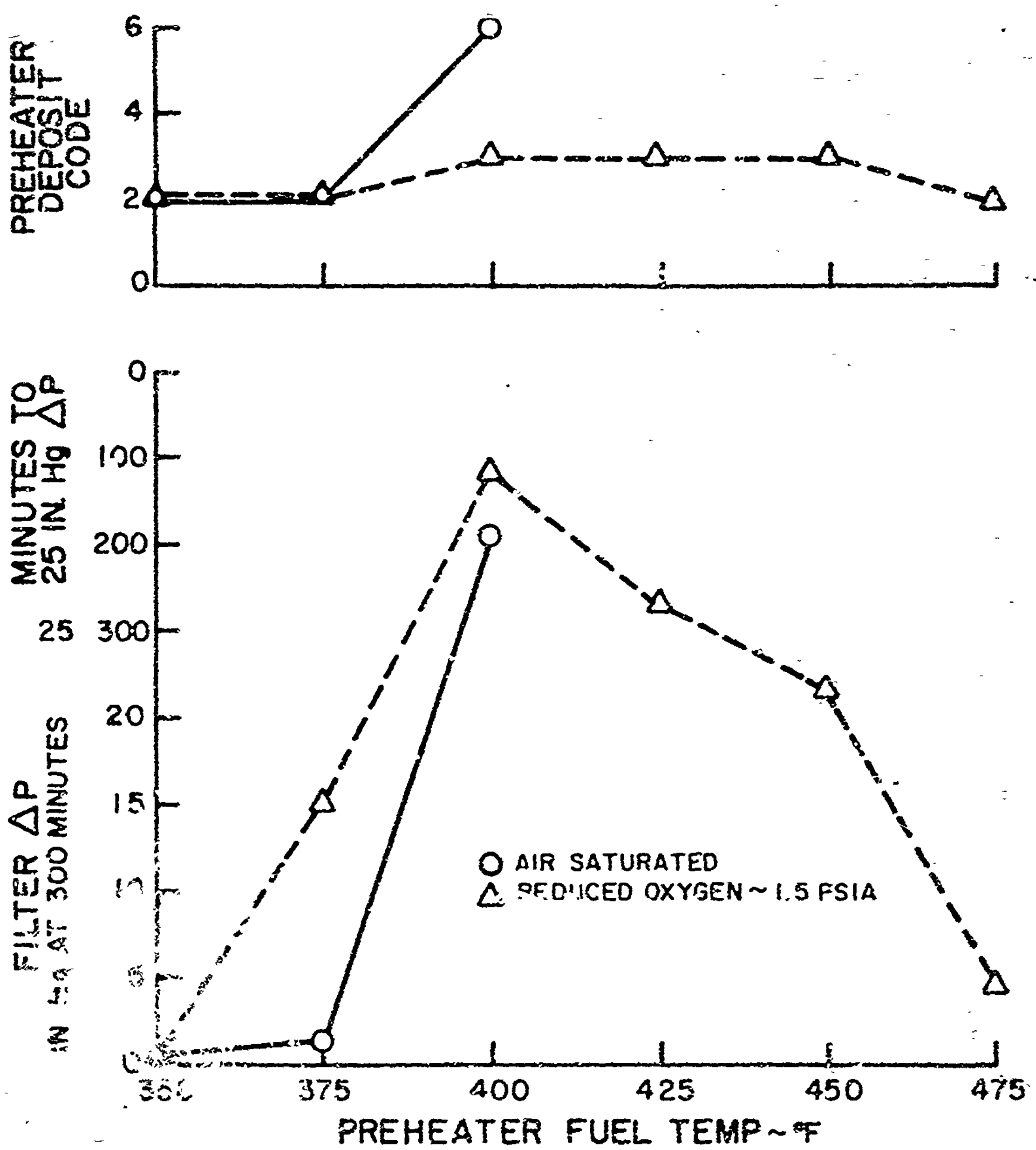

THERMAL STABILITY CHARACTERISTICS OF EAST COAST JET A-1 FUEL NO. F1498 IN RESEARCH FUEL COKER AT 175F RESERVOIR TEMPERATURE

FIGURE 12-29

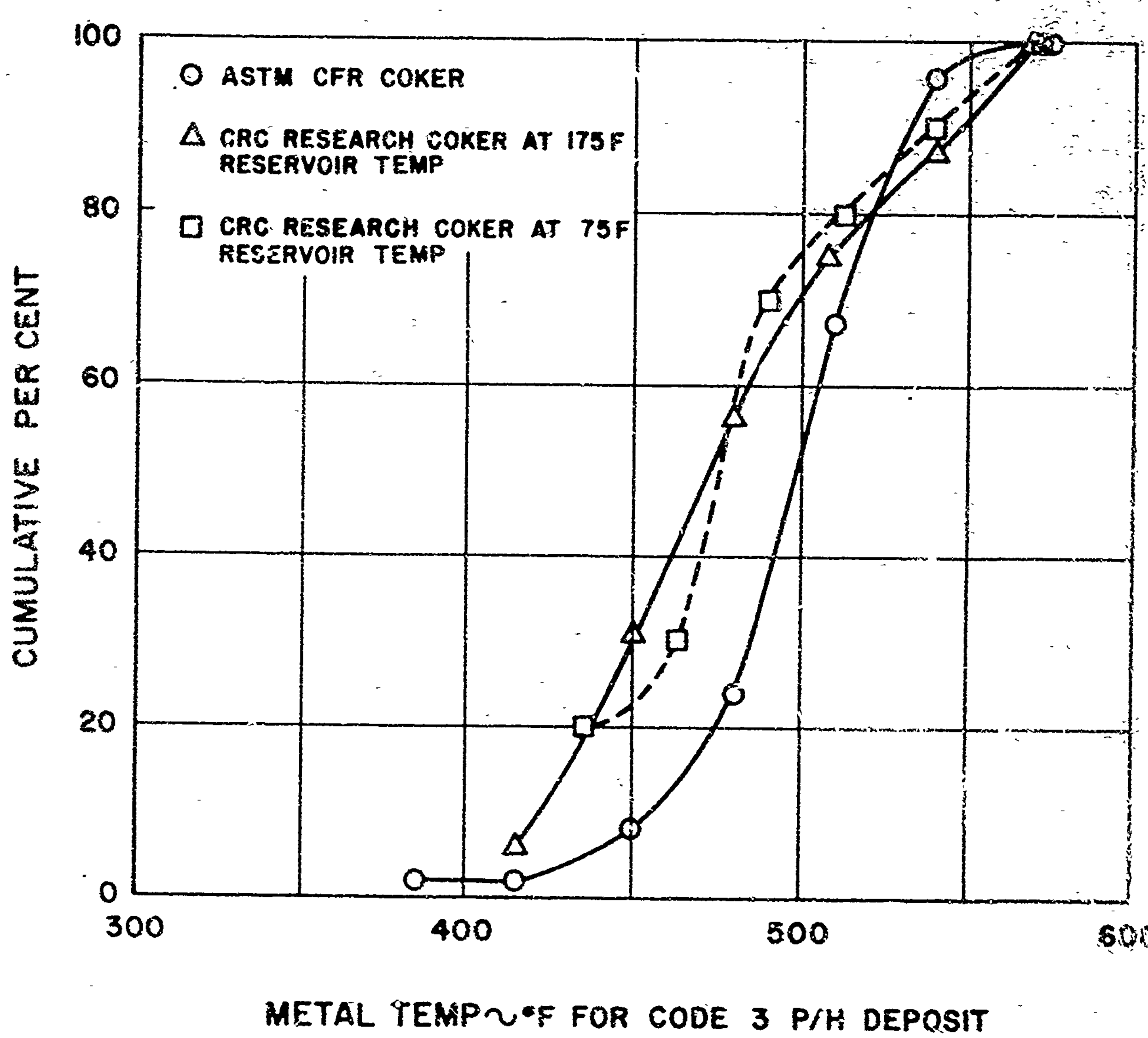

BREAKPOINT DISTRIBUTION OF SURVEY FUELS IN TERMS OF COKER METAL TEMPERATURES

Figure 12-30

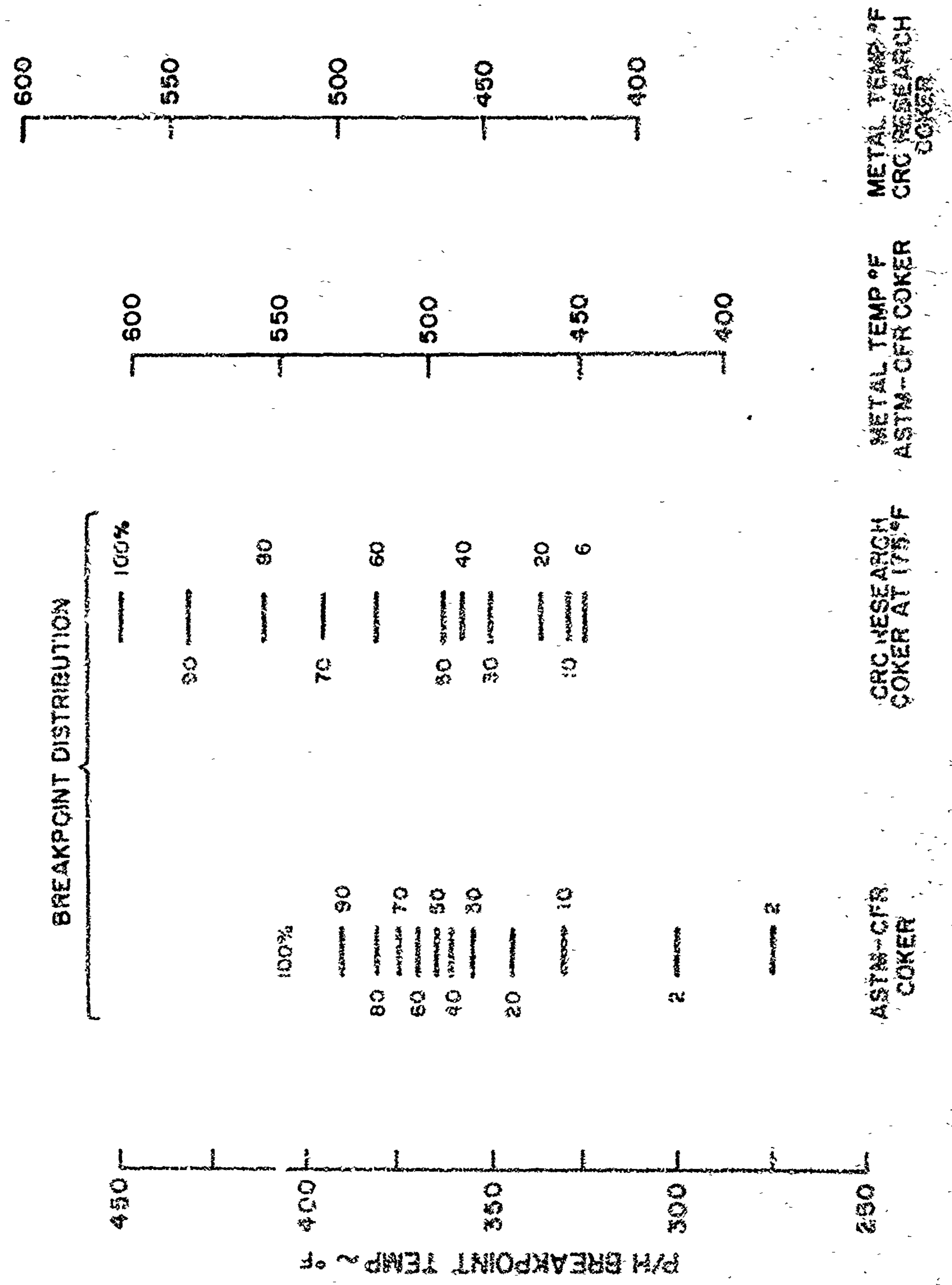

BREAKPOINT DISTRIBUTION OF SURVEY FUELS IN ASTM RESEARCH COKER AS RELATED TO METAL TEMPERATURE

Figure 12-31

EFFECT OF ADDITIVE ON FUEL THERMAL STABILITY
MODIFIED (SSF VERSION) FUEL COKER TEST
175F RESERVOIR

				WITH ADDITIVE*	
TEST FUEL	TEST CONDITION P/F	P/H CODE	FILTER P/TIME	P/H CODE	FILTER P/TIME
F1350	325/425	1	25/259	-	-
	350/450	3	25/104	2	0/300
	375/475	2	1.7/300	2	0/300
	375/475	-	-	2	0/300
	400/500	-	-	2	0/300
	475/575	-	-	6	0/300
F1368	375/475	2	1.7/300		
	400/500	2	25/23[illegible]	2	0.1/300
	425/525	5	25/206	4	0/300
F1348	350/450	1	25/294		
	375/475	3	25/77	3	0/300
F1351	325/425	1	0.3/300	-	-
	350/450	3	25/215	-	-
	375/475	3	25/85	1	0/300
	400/500	-	-	2	0/300
	425/525	-	-	6	0/300
F1373	350/450	2	4.7/300		
	375/475	3	25/175		
	400/500	4	25/117	2	0/300
	425/525			4	0/300

*30 lb/MB DuPont JFA5

Figure 12-32
(Sheet 1 of 2)

EFFECT OF ADDITIVE ON FUEL THERMAL STABILITY
MODIFIED (SSF VERSION) FUEL COKER TEST (Cont'd)
175F RESERVOIR

Test Fuel	Test Condition P/F	P/H Code	Filter P/Time	With Additive * P/H Code	With Additive * Filter P/Time
F1332	400/500	2	5.5/300	2	0/300
	425/525	4	1.2/300	5	0.1/300
F1346	375/475	1	25/289	2	0.1/300
	400/500	3	25/187	4	0/300
	425/525	4	1.9/300	4	0/300
F1371	375/475	-	-	3	0.3/300
	400/500	2	25/244	3	0/300
	425/525	4	25/214	3	0/300
F1335	350/450	-	-	1	0/300
	375/475	-	-	3	0/300
	400/500	2	0/300	3	0/300
	425/525	3	0.2/300	4	0/300
	450/550	3	0/300	-	-
	475/575	3	0/300	-	-
F1382	375/475	-	-	2	0/300
	400/500	-	-	3	0/300
	425/525	-	-	3	0/300
	450/550	2	0.2/300	3	0/300
	475/575	3	0.1/300	4	0.3/300

* 30 lb/MB DuPont JFA5

Figure 12-32
(Sheet 2 of 2)

ITEM 13 - LUBRICANTS

OBJECTIVE

The goal of this program is to obtain the most favorable compromise between engine design parameters, environments, and lubricant capability to satisfy the requirements for safe, economical operation of a supersonic transport powerplant.

A. INTRODUCTION

Because metal fatigue is a critical problem in extended engine operation and there are indications that lubricant composition and temperature levels have significant effect on the rolling contact fatigue life of steels, it is necessary to determine and evaluate the effect of selected lubricants on the rolling contact fatigue life of gear materials at temperature levels expected to be encountered in supersonic aircraft engines.

In order to assure that the most recent lubricant requirements are being disseminated to potential lubricant suppliers, analytical studies to determine the environmental conditions which will be imposed on the lubricant were made in conjunction with continuing design studies using the latest fuel delivery temperature information furnished by the airframe contractor.

B. LUBRICANT ENVIRONMENT

Because the predominant factor governing many temperatures throughout the oil system is the temperature of the fuel delivered to the engine fuel system, the current predicted temperature data and environmental conditions are based upon the temperature of the fuel delivered from the airframe as shown in Figure 13-1. As this figure indicates, the fuel temperature rises sharply to a peak of 250°F during descent and then rapidly declines, approaching 200°F. Any increase in the fuel temperatures shown in Figure 13-1will result in changes in the expected lubricant system temper-

ature pattern; large temperature increases could conceivably require a lubricant with properties superior to those evaluated in this contract period. In addition, supplemental cooling utilizing unscheduled fuel flow returned to the fuel tanks is necessary to prevent excessive temperature levels in the lubrication system during descent from the flight cruise condition. Therefore, the environmental conditions must be considered as estimates.

During this contract period, additional studies were conducted of the lubricant environment. These environmental conditions are outlined below:

1. TEMPERATURE

Lubricant temperatures during a typical flight spectrum are shown in Figure 13-2. In addition, bearing temperatures are expected to reach a maximum steady-state level of 400°F at the end of the cruise, and may possibly approach 500°F during the descent portion of the flight. Local compartment wall hot spots are not expected to exceed 600°F.

2. OIL TANK CAPACITY

6 gallons nominal oil

4 gallons usable oil

3. AIR CONTACTING OIL

Flow - 0.06 lbs/sec/seal; 0.4 lb/sec/seal with seal failure

Temperature - 630°F max. at Mach 3.0

4. BEARINGS

a. Materials

Races, rollers, balls - PWA 724 CVM or AMS 6490

Cages - AMS 6415, silver-plated per AMS 2410

b. Types

Angular Contact-Split Inner Race, Single Bearing, ABEC #7 Tolerances:

170 x 260 x 42 mm at 6100 rpm and 200 x 300 x 51 mm at 8250 rpm.

Roller - Preloaded, 200 x 300 x 38 mm at 8250 rpm.

5. ALLOYS IN LUBRICATING SYSTEM

Tank - AMS 5510, 5645

Oil Filter - AMS 5362, 5640

Fuel-Oil Cooler - AMS 5362, 5571, 5646

Scavenge Pumps - AMS 5362, 5640, PWA 724

Piping - AMS 5570, 5571, 5645, [illegible]

Bearing Compartments - AMS 5062, 5613, 5616, 5688, 6322, 6323, 7310; PWA 724

6. GEARS

Hertz Stress - 92,000 psi starting, 71,000 psi steady-state

Material - PWA 724 heat-treated

7. ELASTOMERS

None in lubricating system

8. LUBRICANT VISOCITY

Lubricating system does not impose any restrictions on oil viscosity.

9. LUBRICANT VOLATILITY

Volatility requirements of the lubricating system are compatible with the volatility characteristics of MIL-L-23699 lubricants.

C. GEAR PITTING TESTS

Gear pitting fatigue tests which were initiated during the previous contract period, were continued through this contract period using a MIL-L-23699 lubricant (L-919) and AMS 6260 carburized test gears. These steady-state gear pitting fatigue tests were conducted in Ryder Gear Machines at lubricant temperature of 250, 300, 325, 350 and 375°F and at Hertz stresses ranging up to 260,000 psi; the Hertz stresses were kept at high levels to accumulate a maximum of data in the shortest possible time interval. Other test parameters such as test oil flow rate and rate of stress application were maintained at constant levels. Figure 13-3 demonstrates gear pitting fatigue data obtained during this contract period as well as during the previous contract period; supplemental data from other sources was also used in the preparation of the graph.

The equipment used to conduct the gear pitting fatigue tests was the Ryder Gear Machine and the Erdco Universal Drive Test Stand as described in Federal Test Method Standard No. 791a, Method 6508. The High Temperature Erdco Bearing Rig described in the previous contract report numbered PWA-2353, was used to evaluate the deposit-forming and degradation characteristics of the MIL-L-23699 lubricant (L-919) at conditions simulating supersonic flight. Lubricant samples were withdrawn from the oil tank at the beginning and end of each test cycle to determine viscosity and neutralization number. Make-up oil was added to the tank when the tank level was reduced to a predetermined quantity; a procedure resulting in a test which is more severe than one where the make-up oil would be added after each test cycle.

In addition to the gear pitting fatigue program, a MIL-L-23699 lubricant (L-919) was evaluated in the High Temperature Erdco Bearing Rig at temperature profiles shown in Figure 13-2. The temperature profiles are quite similar to those shown in Figure IX-15 of report number PWA-2353 from the previous contract period but represent a lubricant environment more severe than that expected in the supersonic transport powerplant.

D. DISCUSSION

The selection of a lubricant for use in the supersonic transport powerplant is based primarily upon the lubricant's ability to withstand the oxidative and thermal stresses encountered in the lubricant system environment. The lubricant must also demonstrate satisfactory lubrication

characteristics such as: effect on metal rolling contact fatigue, volatility, carbon seal wear rates, gear load-carrying ability and corrosive tendencies in oxidizing atmospheres. During the current and previous contract periods, these characteristics were evaluated in tests covering a large range of operational severities utilizing the most recent lubrication system environmental parameters. During this contract period, effort was primarily concentrated upon rolling contact fatigue.

Due to the nature of fatigue testing, the data is presented as bands rather than lines. It is quite evident that further testing is necessary to positively establish the slope of the curve before extrapolating to the fatigue life to be expected at lubricant temperatures in the 400-450°F range. It is estimated that approximately 1500 hours of testing at 400°F will be necessary to establish a reliable projected fatigue life of gears at that temperature level.

Figure 13-4 is a summary of the cyclic bearing test run with temperature schedules as shown in Figure 13-2. Although this test was more severe than the predicted supersonic transport engine-operational conditions, the data indicated that the lubricant will satisfactorily withstand the thermal and oxidative stresses imposed on it by the predicted lubricant environment.

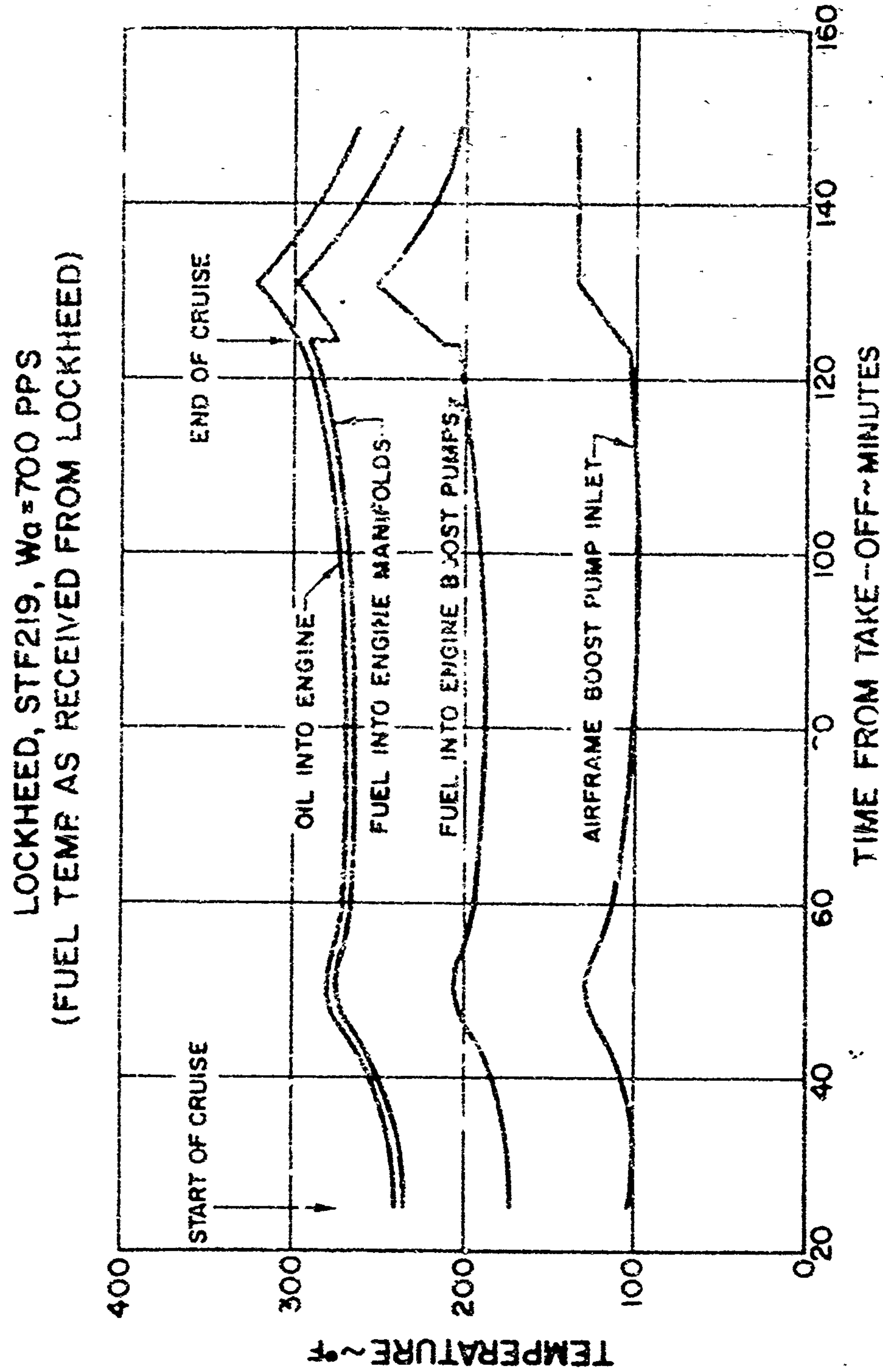

ESTIMATED FUEL AND OIL TEMPERATURES VERSUS MISSION TIME

Figure 13-1

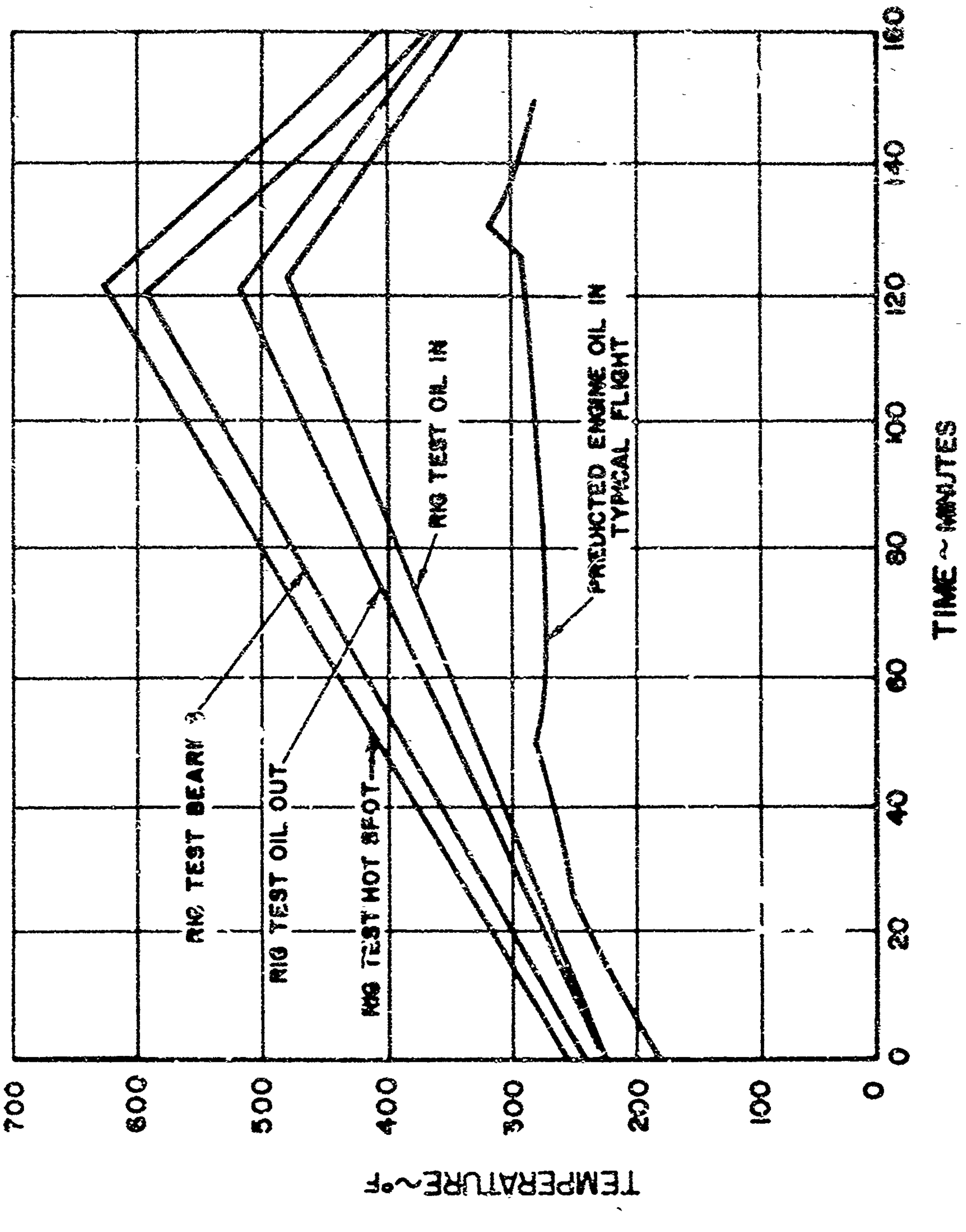

LUBRICANT TEST ENVIRONMENT

Figure 13-2

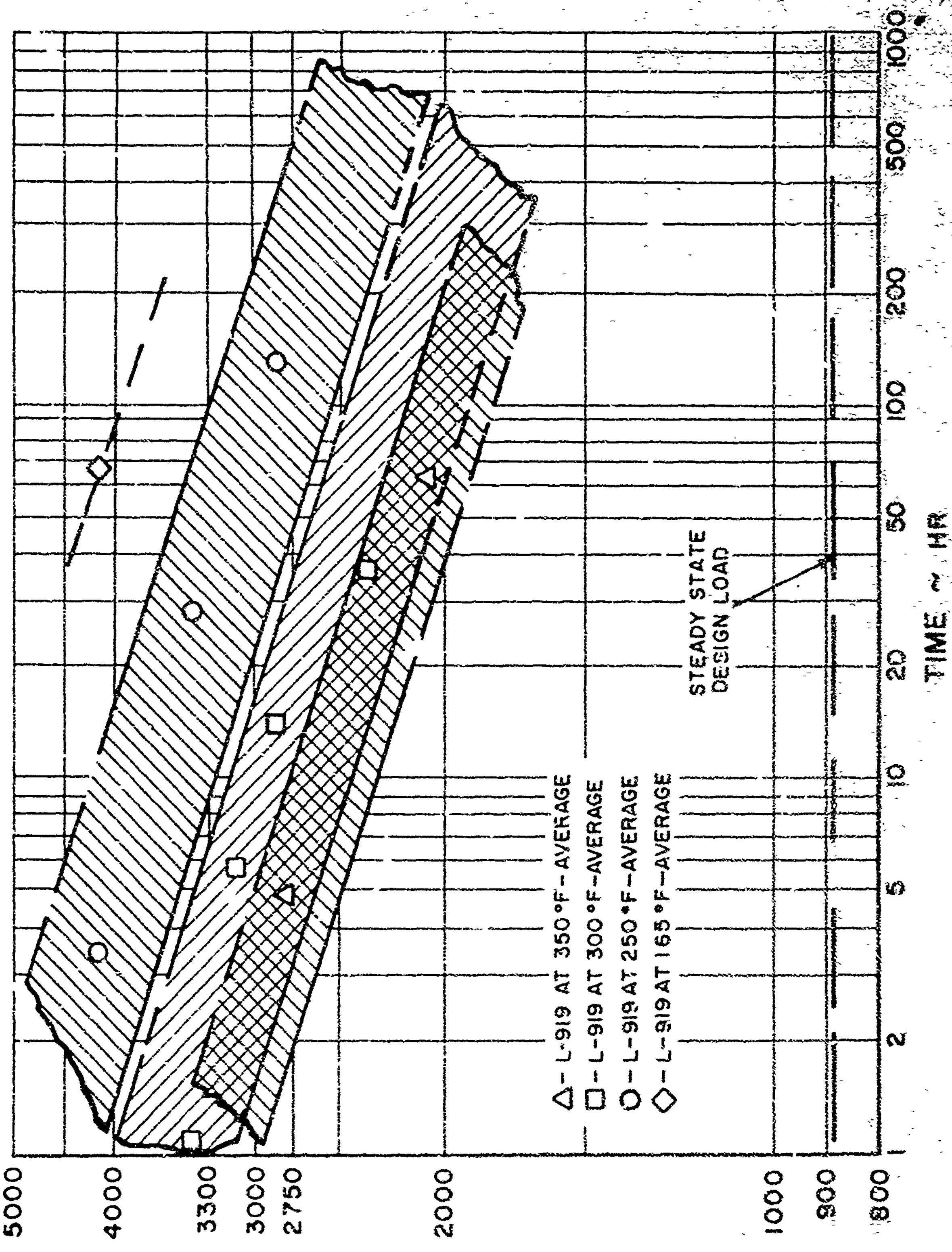

GEAR PITTING FATIGUE LIFE IN RYDER GEAR MACHINE

Figure 13-3

Test Data Summary For L-919 Lubricant

In The High Temperature Erdco Bearing Rig

Lubricant	MIL-L-23699 (L-919)
Test Schedule Type	Cyclic
Schedule Figure No.	13-2
Test Duration	23 cycles
Total Test Time	72.15 hours
Oil Consumption	39.3 cc/hr.
Make-up oil	3540 cc
Consumption	49.0 cc/hr.
Condensate Collected	800 cc; 670 cc oil, 130 cc H_2O
Viscosity Increase	25 centistokes
Percent at 100°F	100% approximately
Neutralization Number	
Before	0.00
After	2.50

Figure 13-4

INLETS

ITEM 14 - INLETS

OBJECTIVE

To conduct investigations in cooperation with each airframe contractor aimed at determining engine-inlet compatibility. Steady state performance and flow distortion over typical engine-aircraft flight conditions as well as transient inlet conditions were considered.

A. ENGINE-INLET COMPATIBILITY

1. INTRODUCTION

The goal of this program was to arrive at an inlet-engine combination which will satisfy all steady state and transient performance requirements for the safe and economical operation of a supersonic transport. During the Phase II-A contract period Pratt & Whitney Aircraft worked continually with both the Boeing Company and the Lockheed California Company to ensure engine-inlet compatibility for the supersonic transport. Pratt & Whitney Aircraft, upon request, reviewed its experience in solving engine-inlet compatibility problems in numerous subsonic and supersonic aircraft, including the B-52, F-100, F-101, F-102, F-105, F-106, and F8U-1.

Distortion data received from the aircraft companies were converted into detailed distortion contour maps and radial distortion plots for comparison with Pratt & Whitney Aircraft specifications, and for studies to investigate the effect of these distortion levels on compressor operation.

2. DISCUSSION

a. The Boeing Company Inlet

The Boeing inlet design for the supersonic transport is an axisymmetric, pod mounted, external-internal compression type. It utilizes an adjustable centerbody to vary contraction ratio with flight Mach number, which also accomplishes the required airflow variations. A constant area throat and throat boundary layer bleed help to stabilize the normal shock and minimize distortion. Cowl bypasses are utilized for airflow matching. Both inboard and outboard inlets are located in the compression field area of the wing.

The test data from the Boeing Company at Mach 1.1, where the engine corrected airflow is a maximum, indicated a radial distortion pattern that is within the distortion limits set by Pratt & Whitney Aircraft. This was indicated for the case when the inlet bypasses were open, as well as when the bypass doors were closed.

No data at simulated aircraft angles of attack at subsonic speed have been received but the straightening effect of the wing, coupled with the favorable diffuser passage shape, are expected to greatly reduce the angle of attack effects.

Minimizing the radial distortion at both walls during supersonic acceleration, and particularly at supersonic cruise is essential.

The initial Mach 2.5 distortion data received from Boeing early in the program exhibited radial distortion profiles which appeared to exceed those for penalty free engine operation. At that time Boeing's subsonic diffuser shape was not finalized and supporting struts not included. Pratt & Whitney Aircraft and the Boeing Company discussed this problem in considerable detail and the latter embarked on an extensive test program, varying diffuser length and shape, incorporating vortex generators, and testing various strut arrangements. The results of these tests were extremely encouraging. Vortex generators at the ID wall induced considerable mixing and reduced local ID gradients as shown in Figure 14-1. These tests indicate that inlet radial distortion can be appreciably reduced through mechanical and aerodynamic tailoring.

The size, shape, number, and axial location of the inlet struts affect compressor operation because generated wakes may excite a particular blade natural frequency. In addition, if the wakes generate large local depressions, compressor stall margin may be affected. For this reason a detailed discussion was held with Boeing concerning the various trade factors involved and Boeing tested a number of strut configurations. The results of these tests indicated that although the distribution of total pressure is changed somewhat by the struts the overall distortion level is about the same.

The landing gear on the Boeing supersonic transport airplane is so located that its traverse from a fully retracted to a fully extended position allows it to pass in front of the inlet. The Boeing Company conducted a series of tests with a simulated landing gear in the various positions it would assume in its travel in front of the inlet at speeds of 100, 125,

and 150 knots. When compared with results for the gear stowed, the distortion remained essentially unchanged, thus indicating no significant effect due to the landing gear.

b. The Lockheed California Company Inlet

The Lockheed Inlet for the supersonic transport is a self-starting two dimensional pod-mounted configuration incorporating both external and internal compression. A double vertical compression ramp bisects the inlet through to the compressor face. Throat boundary layer bleed and a constant area throat are used to help stabilize the normal shock and reduce distortion. The double ramps collapse as flight Mach number is reduced so that at transonic and subsonic speeds a continuous, gently diverging passage is formed. Transition f[illegible] rectangular to a bifurcated annulus shape is accomplished appro[illegible]ely one engine diameter upstream of the engine inlet.

All four inlet pods are located in the shock field of the wing so at supersonic speeds the approach angles of attack or yaw to the inlet are very small, thus essentially eliminating the large circumferential distortion effects normally caused by large angles of attack. At subsonic speeds and straightening effect of the wing will act to reduce angle of attack effects.

All two dimensional inlets exhibit some degree of circumferential distortion, even with no angle of attack. However, careful design can keep this to a minimum. The distortion data received from Lockheed at the Mach 3.0 cruise condition indicated that reasonable levels of circumferential and radial distortion existed. The collapsed ramps at subsonic and transonic flight speeds should appreciably reduce the effects of diffuser turning encountered in many supersonic inlet designs.

c. General

The work conducted by Pratt & Whitney Aircraft in cooperation with the Boeing Company and the Lockheed California Company on inlet-engine control response to airflow transients resulting from duct burner light off or gas generator transients is reported in the inlet control section, Item 10 of this report.

3. CONCLUSIONS

It is not possible to predict with absolute certainty the tolerance of an engine to inlet distortion, or even the final inlet distortion itself until the two are tested together. The Pratt & Whitney Aircraft specification for inlet distortion was revised to reflect an increased overall allowable inlet distortion. Allowable distortion within the overall tolerance is subject to future negotiation based on actual engine/inlet experience.

The Boeing inlet proposed for the supersonic transport, as understood by Pratt & Whitney Aircraft at this time, meets the overall distortion requirements at the critical flight conditions set forth by Pratt & Whitney Aircraft.

The Lockheed California Company also has a sound approach and is currently engaged in an extensive wind tunnel program. The inlet has a favorable location on the aircraft, sufficient length, boundary layer bleed, and favorable diffuser contours that should yield acceptable distortion profiles throughout the range of operation.

The experience of both airframe manufacturers and Pratt & Whitney Aircraft in mutually solving engine-inlet compatibility problems, coupled with the sound inlet design approaches taken by both companies assures a compatible system for the Supersonic Transport. The levels of distortion demonstrated by the airframe companies to date are very close to the levels specified by Pratt & Whitney Aircraft for this early time phase in the program. As in any normal development program, problems will be solved as they arise through mutual cooperation. Every effort will be made to make the engine as distortion tolerant as possible while the airframe companies will continue to reduce inlet flow distortion. Both inlet and engine may require additional tailoring when they are tested together.

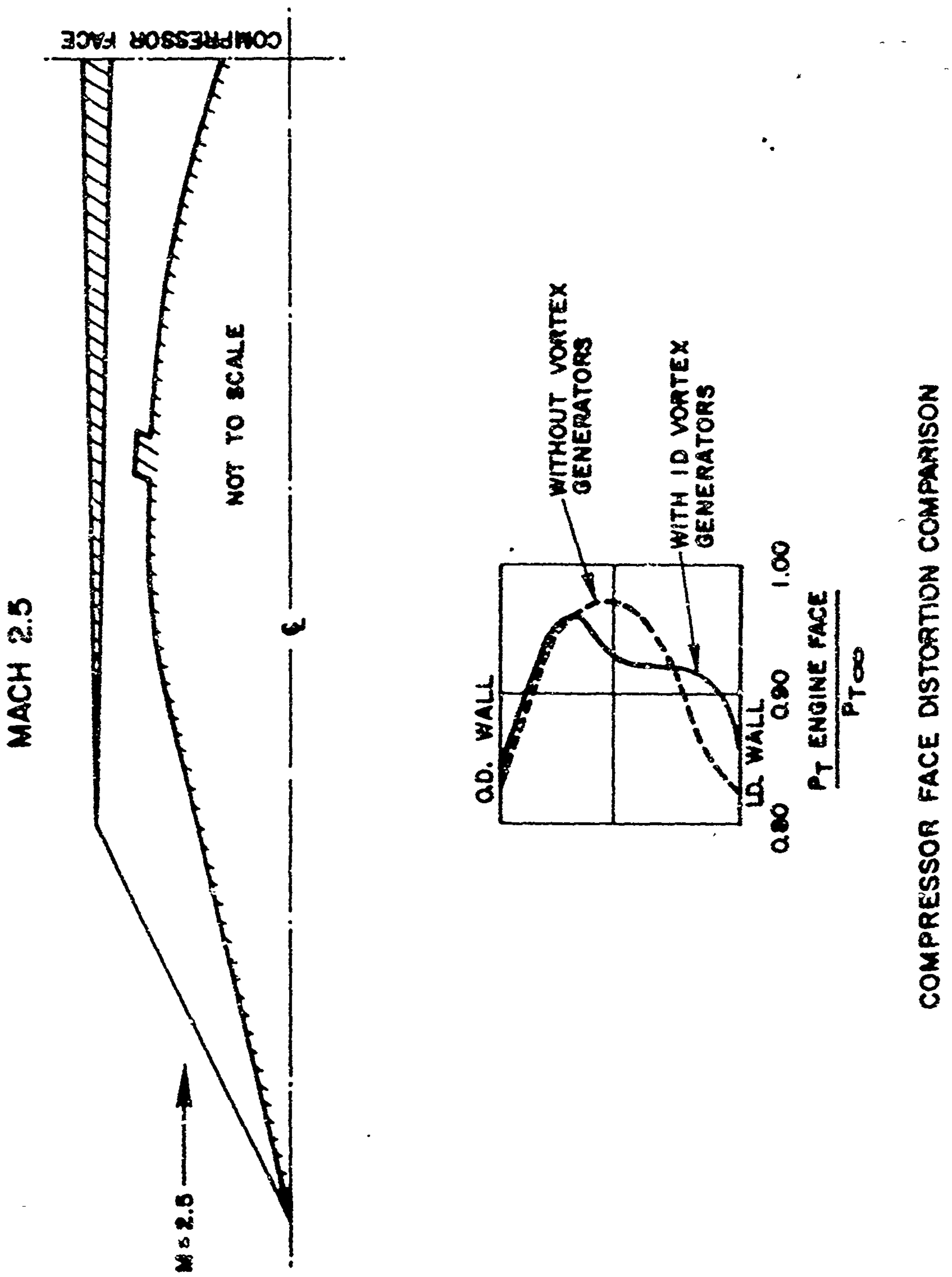

EFFECT OF VORTEX GENERATORS ON BOEING INLET DISTORTION (MACH 2.5)

Figure 14-1

ITEM 15 - MATERIALS AND MANUFACTURING TECHNIQUES

OBJECTIVE

The over-all goal of the various programs which were undertaken under Item 15 of the Contract Work Statement was the development of such information about materials and coatings as would enable selection of those with optimum characteristics for use in the design of a satisfactory SST power plant.

A. INTRODUCTION

The progress made on programs under Item 15 of the Contract Work Statement is presented herein under two main category headings: Compressor Materials and Turbine Materials. Under the first, the characteristics of various potential compressor-disk materials, as determined by such methods as combined stress-fatigue testing, rotating-beam fatigue testing, low-cycle-fatigue testing, and cyclic-tension testing, are discussed as the initial topic. These characteristics include long-time creep and fatigue at realistic temperatures, and notch sensitivity factor. As a second topic under Compressor Materials, the results of testing conducted to determine the susceptibility to salt corrosion of several potential blade materials are reported. A third topic deals with testing to determine the containment characteristics of candidate materials for compressor blading.

Under the second main category heading, Turbine Materials, are discussed the results of long-time creep testing of potential turbine-component materials. This program has been formulated for the conduct of fundamental thermal-fatigue studies of such materials, long-time erosion-bar testing of base-metal coating systems, and the results of electron metallographic and X-ray studies.

B. COMPRESSOR MATERIALS

1. DISK MATERIAL EVALUATIONS

Initial creep and mechanical-property evaluation testing was conducted using specimens of IMI 679 titanium alloy. The specimens were machined from a disk which had been forged from that alloy.

Parts of this disk had been furnished to Wyman-Gordon and Titanium Metals for their test evaluations. A disk section was heat-treated at 1650°F for one hour and air cooled. It was then reheated to 925°F, held there for twenty-four hours, and air-cooled. This procedure had been followed for the disk sections furnished to Wyman-Gordon and Titanium Metals.

The creep specimens were machined tangentially from the disk rim and were tested at temperatures and stresses designed to produce 0.1 per cent creep in 1000 hours and also in 3000 hours. All of the specimens tested by this Contractor were found to creep rapidly. They attained 0.1 per cent creep in approximately ten per cent of the estimated time. Post-test examination of the specimens revealed their microstructures to be similar to that of the original as-forged disk material, rather than that of properly heat-treated material from the same forging. The principal difference between the microstructures was the lesser amount of primary alpha structure in the properly heat-treated specimens. It was suspected that the material from which the Contractor-tested specimens had been fabricated had failed to reach the specified 1650°F solution temperature in the heat-treatment process. Further laboratory investigations are continuing.

The creep data obtained by Wyman-Gordon and Titanium Metals on IMI 679 compressor-disk forging sections were not sufficient to enable a quantitative analysis to be made. However, those data did indicate that IMI 679 material was comparable to PWA 1203 material in creep strength and superior to the latter material in yield strength.

In addition to the work on IMI 679 titanium-alloy material which has been mentioned, tests were conducted on PWA 1007 nickel-base-alloy material. Specimens of two heats of the latter material were tested for creep, stress-rupture, and tensile properties. The results obtained are presented in Figures 15-1 through 15-3. At temperatures above 1200°F, it was found that PWA 1007 material showed greater creep strength than had been found for PWA 1003 and PWA 1010 materials, as reference to Figures 15-4 through 15-6 indicates.

In a second phase of the work statement which is related to compressor-disk materials, fatigue properties of PWA 1007 disk-forging material (Heat Code No. XF1R) were investigated in a number of ways. The disk which was involved in this series

of test programs differed in microstructure from previously evaluated disks of PWA 1007 material, primarily in that its grain size was more uniform (although not optimum). Combined stress-fatigue properties of specimens from Heat Code No. XFIR were determined at 1000°F and for steady-stress values of 25, 47.5, and 85 ksi. A notch-sensitivity factor (K_t) of 1.5 was used and the cyclic range covered was extended from 10^5 through 10^7. The test results are tabulated in Figure 15-7. The combined-stress fatigue strengths of the specimens, at the different steady-stress levels, were found to be generally higher than those obtained from prior testing of PWA 1007 material of other heats. These strengths were nearly as high as those which had been obtained for PWA 1010 (Inco 718) material. The greater fatigue strength which had been found for the latter material was attributed to its lower solution-heat-treat temperature, which produces a finer grain size, and to its higher yield strength at 1000°F, at which temperature both of the materials are yield-limited. Data points which were obtained from the testing of PWA 1007 and PWA 1010 material appear in Figures 15-8 through 15-10.

In a third phase of the program to evaluate compressor disk materials, rotating-beam fatigue tests were conducted at 1000°F on smooth and on notched specimens of PWA 1007 material. Notch-factor values of 1.5 and 3.0 were used and the cyclic range from 10^5 through 10^7 was explored. The results appear in Figure 15-11. The data are presented in plotted form in Figures 15-12 through 15-14. Smooth specimens showed slightly higher fatigue strength than those from other PWA 1007 disks, which had been previously evaluated. The data for notched fatigue strength, although showing considerable scatter, appeared to be comparable to that of previously obtained data on other specimens.

In another phase of the program, low-cycle fatigue tests were conducted on specimens of PWA 1007 material in the cyclic range from 10^3 to 10^5 and for notch factors of 2.0 and 3.0. Results are indicated in tabular form in Figure 15-15. Smooth specimens demonstrated substantially greater fatigue strength values than those used in present design practice (see Figure 15-16). As can be seen by reference to Figure 15-17, notch-specimen life approached design values as the notch factor increased. Improved smooth-bar life, accompanied by virtually unaffected notched-bar life, was considered to be the result of improved grain-size control.

Cyclic-tension fatigue testing was conducted on the PWA 1007 specimens, using a notch factor of 2.3, a cyclic range to 10^3, and temperature values of 1200°F and 1350°F. Results are shown in Figure 15-18 (tabulated) and in Figures 15-19 and 15-20 (plotted). It was found that at 1350°F, rim-tangential and web-radial specimens had similar ultimate tensile strengths, but that the latter were slightly lower than those indicated by the average of data obtained from earlier testing of other specimens of the same material. The stresses which were required in order to produce fatigue failure of a specimen closely approximated those obtained from previous testing of other PWA 1007 specimens. They exceeded those based on typical PWA 1010 and PWA 1003 data. At a temperature of 1200°F, radial specimens from the disk web showed low-cycle, tensile-fatigue properties which were nearly identical to those revealed by data from prior testing.

Finally, with reference to other investigations involving compressor disks, long-time-creep properties were, and currently are still being, studied, using specimens of several potential materials, including PWA 1003 (Inco 901) and PWA 1010 (Inco 718), nickel-base alloys, and AMS 4928, PWA 1202, and PWA 1203, titanium alloys. The heat-treatments and the compositions of these materials are tabulated in Figure 15-21. All materials used in this program phase conformed to their respective specification requirements, except for PWA 1010, which had a slightly low columbium content.

Figures 15-22 through 15-26 are plots of the actual data obtained from the test program, and also the estimated data. All the data shown are, of course, preliminary in nature and are subject to revision as test work proceeds. The temperatures at which the testing was conducted were selected so as to include the range wherein the materials were creep-limited, but not to exceed the useful range of each alloy.

Figures 15-27 through 15-28 present the estimated stress for 0.1 per cent creep in 1000, 3000, and 5000 hours for the materials under study. The estimates were based on testing which was in process when this report material was prepared. As of that time, no instabilities of the materials had been indicated by those tests which had been completed. Review of the creep data revealed that, for a 0.1 per cent creep in 5000 hours, PWA 1010 material has stress capability essentially equal to PWA 1003 material at temperatures of 1150°F and 1200°F, and that PWA 1007

material was superior to PWA 1003 material at temperatures exceeding 1200°F. The titanium alloys showed even wider separation than the nickel-based alloys. At 850°F, the only common temperature used, PWA 1203 material was superior to PWA 1202 material and was vastly superior to AMS 4928 material. At 950°F, the creep properties of PWA 1202 and PWA 1203 appeared to be similar.

The tensile properties of the several compressor-disk materials are shown in Figures 15-29 through 15-33. The current test program calls for tensile testing of specimens at the same temperatures as those at which the creep testing is being conducted.

2. DISK AND BLADE MATERIAL EVALUATIONS - SALT CORROSION

The Contractor's pre-Contract experience had been that the stress-corrosion testing of PWA 1202 and AMS 4928 titanium-alloy, salt-coated specimens under static conditions revealed both alloys to be subject to stress-corrosion cracking, particularly PWA 1202 material. In work under this contract, it was desired to determine possible differences between the materials when the latter were tested under dynamic moving-air conditions. The dynamic conditions would more closely simulate actual engine conditions. A dynamic test rig which would expose material specimens to a moving airstream with ingested salt water was therefore constructed. This rig, the fabrication and set-up of which consumed the major portion of the Contract period, consists of a four-station, rotating-specimen holder which can accommodate either smooth specimens or simulated-blade-root specimens. The specimens are torqued to the desired stress levels between cantilever plates fabricated from AMS 4928 titanium alloy. They are then subjected to an airstream into which salt spray is continuously injected. The airstream temperature can be controlled with ± 20°F of a desired level.

In initial testing using the rig described in the previous paragraph, a set of four simulated-blade-root specimens and a set of four modified creep specimens, both machined from 1.25-inch-diameter barstock in accordance with the data given in Figure 15-34, were subjected to a stream of air and salt spray (continuous) for one hundred hours, with the airstream being at a temperature of 700°F and the levels of stress in the specimens at 30,000 and 40,000 psi. At the conclusion of the 100-hour run, the specimens were examined. It was found that salt had collected heavily - to a maximum of three-eighths inch - on the surfaces. The salt could be removed by a hot-water rinse. It is possible that the

build-up of salt at the gage sections of the specimens served to retard failure. Tests have been scheduled during which salt spray is to be injected into the airstream impinging on the specimens, for one-half hour every ten-hour period until one-hundred hours have been accumulated. This may more closely approximate realistic moving-air conditions.

Post-test analysis was conducted on the smooth-bar modified creep specimens. Although the torquing stresses in the specimens had initially been set at 30,000 and 40,000 psi, as previously stated, some relaxation in the stresses in the specimens made from AMS 4928 material was noted, the post-test values being 23,500 and 31,500 psi. There was no measurable relaxation of the stresses in the specimens made from PWA 1202 material. Tensile tests revealed stress-corrosion cracks in the gage sections of the PWA 1202 specimens; no such cracks were observed in the AMS 4928 specimens, although the rig-testing stress and temperature conditions should have been severe enough to cause such cracking in still air. Figure 15-35 compares the stresses required in order to produce stress-corrosion cracking and 0.1 per cent creep for PWA 1202 and AMS 4928 materials.

In the case of PWA 1202 material, the stress necessary to produce stress-corrosion cracking is much less than that required for producing 0.1 per cent creep. thus, stress-corrosion cracking is the limiting design parameter for this material. As stated, PWA 1202 specimens did not creep under the test conditions and therefore did not relax to a lower stress. Figure 15-36 lists the post-exposure tensile-test results for each specimen. The reduced tensile ductility found for PWA 1202 specimens was attributed to the presence of stress-corrosion cracks.

3. CASE MATERIAL EVALUATIONS - CONTAINMENT

One of the conclusions reached by the Contractor as a result of its spin-pit test programs dealing with engine components is that different construction materials have different capabilities for absorbing the kinetic energy

of high-velocity objects, such as failed compressor blades impacting the compressor case. The program under this contract with respect to this subject matter, had as its objective the screening of eleven compressor-case materials as to their respective abilities to withstand impact damage when at compressor-operating temperatures. The effects of hardness and thickness of some of the materials on impact-damage extent were also to be investigated. The initial phase of the program was to consist of ballistic tests. When these were completed, it was planned to subject two of the more promising materials to spin-pit testing, so that their containment characteristics under conditions more closely simulating those of engine operation might be evaluated.

The ballistic testing consisted of firing bullets at increasing velocities at one-foot-square test panels of the materials being evaluated until a velocity designated as the "containment velocity" was reached. "Containment velocity" is defined as the velocity at which a bullet fired at a plate just penetrates the latter. Penetration must be with so little residual energy that the bullet fails to penetrate a thin aluminum indicator panel behind the test plate.

The muzzle velocity, as measured by an electric chronometer, is used in deriving the kinetic energy of the bullet. The latter, when divided by the weight of the test panel, yields a number known as the "containment factor".

The spin-pit containment testing consisted of inducing a compressor-blade failure by notching the root of the blade and increasing the rotational speed of the disk until blade failure occurred. Failures were induced at increasing disk rotational velocities until a blade fragment barely penetrated a ring which encircled the blades in the manner of a compressor case. As in the ballistic testing, the containment factor is described as the kinetic energy of the blade divided by the weight of the ring, the latter being fabricated from the material undergoing test evaluation.

It should be pointed out that, because the weight of an engine's protective structure is a crucial factor in its selection, it was taken into account in evaluating the results obtained from the ballistic and spin-pit tests.

The results of the ballistic testing conducted at room temperature, at 500°F, and at 600°F are tabulated in Figure 15-37. The materials for which results are presented are listed in the order of descending containment factors as determined by the room temperature test program.

Testing of two thicknesses of the same material demonstrated that, with one exception, the containment factors obtained were within 12 per cent of each other. The exception was PWA-1030 material for which the containment factor for 0.116-inch thick material was more than 20 per cent lower than that for 0.070-inch thick material. For PWA-1030 material, therefore, the results are tabulated separately, whereas, for the other materials, the average of the two values is tabulated.

An analysis was conducted to determine the effect of temperature on the containment factor. The results indicated that the containment factor decreases with increasing temperature for all materials, although the rate of decrease is lower for titanium alloys and age hardenable AMS 5542 and PWA 1030 alloys than for the other materials tested. The martensitic stainless steels (AMS 5504 and AMS 5508) in the hardened condition exhibited good containment factors at room temperature, but the factors dropped by 27 per cent between room temperature and 800°F. For the austenitic stainless steels (AMS 5515 and AMS 5524) the decrease was as high as 40 per cent. Hence, although the martensitic alloys look much better than the age hardenable corrosion-resistant materials at room temperature, their superiority vanishes at 800°F where the containment factors of the martensitic alloys drops off but that of the age hardenable materials remains high.

The effect of hardness on the containment factor was investigated by ballistic testing with two martensitic stainless steels and two age hardenable alloys in a hard condition (Rc 38 to 45) and in a soft condition (Rc 20 to 28). The hardened martensitic specimens had the highest containment factor of the materials tested. However, the softer specimens of the age hardenable materials demonstrated higher containment factors than hardened specimens of the same materials.

The ballistic test program was conducted to inexpensively screen candidate containment materials in preparation for spin testing the more promising materials. Examination of the room-temperature test results indicates that PWA 1202 (Ti-8Al-1Mo-1V) is by far the best material tested. Alternate materials are AMS 5504, PWA 1030, AMS 5508, and AMS 4910 in that order.

Because of the short duration of the contract, spin testing was commenced with the more promising materials before the ballistic program was completed. Spin tests were conducted on AMS 5504, AMS 4910, and PWA 1202. The weights of cases made of these materials relative to a case made of AMS 5524 are shown below.

Material	Relative Weight
AMS 4910	0.70
PWA 1202	0.77
AMS 5504	0.95
AMS 5524	1.00

Additional testing conducted with higher blade-failure velocities would be required to realize the full potential of PWA 1202 material indicated by the ballistic tests. It has not been determined why ballistic testing indicated that AMS 5504 material was superior to AMS 4910, whereas spin testing indicated the reverse Further testing and consideration of the manner in which the specimen weights are factored into the results may resolve this inconsistency.

C. TURBINE MATERIALS

1. LONG-TIME CREEP TESTING

Testing of PWA 658 and PWA 659 cast, nickel-base alloys in a temperature range from 1500°F to 2000°F had reached the status shown in the tabulation in Figure 15-38. The specification-required and the actual chemical compositions of the creep specimens used in the program are listed in Figure 15-39. All specimens, except that of PWA 658 material which was tested at 1500°F, were tested in the coated conditions using a diffused aluminum-base coating (PWA 47). The PWA 658 material, however, was exposed to the temperatures produced during the coating procedure, but was not coated.

The times to creep one per cent, shown in Figure 15-40, were, with six exceptions, estimated. From the results obtained, it appeared that PWA 659 material had greater creep resistance than PWA 658 material in the temperature range shown in the Figure. PWA 659 material, when its creep properties were compared to those of other nickel-base alloys in the heat-treated condition as determined by

the Contractor, was found to have the greatest creep strength, based on stress for one per cent creep in 1000 hours or in 5000 hours in a temperature range from 1500°F to 2000°F. The heat treatments and densities of the nickel-base alloys investigated in the creep studies appear in Figure 15-41, and the plotted results used in the comparison are shown in Figures 15-42 and 15-43. The following is a list of tested materials in descending order of creep strength: PWA 659, PWA 663, PWA 658, PWA 689, and PWA 655. PWA 689 material exhibited greater creep strength than did PWA 655 material in the temperature range from 1500°F to 1700°F, but the reverse was true at 1800°F.

2. PROGRAMS FOR FUNDAMENTAL THERMAL-FATIGUE STUDIES

Emphasis in this program was placed on the design and construction of a strain-cycling rig. The design features and manner of operation of the rig will be discussed briefly.

The strain-cycling rig is a hydraulically operated device for cyclic axial loading of hollow, cylindrical specimens between desired deflection (strain) limits. It consists of a rigid, symmetrical frame, with a master loading piston centered in one end-housing. Two smaller driving pistons, connected to either side of the master loading cylinder, move the master loading piston. These driving pistons are actuated by an adjustable wobble plate, with the result that one is retracting while the other is extending and forcing oil into the cavity on its side of the master loading piston, thus producing sinusoidal motion. The cyclic rate can be altered by changing the speed of the electric-drive motor.

Specimens are heated by induction and testing is conducted at constant temperature. The latter is maintained by thermopile and optical devices, and thermocouples welded to specimen shoulders are monitored as a precaution against specimen overheating.

Test load is measured by a bridge-wired load-cell device located in the piston rod directly attached to the specimen. An extensometer mounted in the center of the hollow specimen is attached to a linear, variable, differential transformer and provides strain measurements. The outputs of the load-cell device and the transformer are plotted on individual recorders and on an X - Y plotter.

The test program was drawn up to include cyclic testing, stress-strain curve determination, and impact testing. The program is presented in Figure 15-44 and the specimens tested are shown in Figure 15-45. The data obtained appear in Figures 15-46 and 15-47

3. LONG-TIME EROSION-BAR TESTING

Long-time erosion-bar testing was initiated to evaluate several base metal-coating systems. The testing is being conducted in a burner-test rig capable of accommodating seven or eight rotating specimens at temperatures ranging from 1450°F to 2300°F. Test specimens rotate in an environment consisting of the products of combustion of JP-5 fuel. When this report was prepared, the several base metal-coating systems listed in Figure 15-48 had been erosion tested at 1830°F metal temperature for 1050 to 1100 hours. Inspection of the specimens at that time did not disclose any evidence of coating distress.

4. ELECTRON-MICROSCOPY AND PHASE-IDENTIFICATION STUDIES

Several materials having potential applicability to turbine components for the SST engine were studied with reference to their characteristics after long exposures to high temperatures. One group of studies involved electron metallography and phase identification; the other, X-ray diffraction and fluorescence. The materials investigated in both groups of studies were PWA 658, PWA 659, and PWA 663 (cast, nickel-base alloys), and PWA 689 (wrought, nickel-base alloy).

For the electron-metallographic and phase-identification studies, all specimens were in the heat-treated condition and had been exposed for long-times at temperatures ranging from 1500°F to 2000°F, except for a few specimens, which had been heat-treated but not exposed so that they might serve as reference pieces in the studies. The specimens are identified as to heat number, heat treatment, exposure temperature, and exposure time in the tabulation in Figure 15-49.

All of the alloys examined exhibited a fine, secondary, gamma-prime precipitate in the heat-treated, but unexposed, condition. This precipitate coarsened with exposures at 1800°F, 1900°F, and 2000°F. Sigma phase was observed in PWA 658 specimens after exposure at 1500°F, and in PWA 689 specimens after exposures at 1500°F, and 1600°F. Small needle-shaped carbides, identified as M_6C, were evident in PWA 663 specimens, without pre-examination aging at 1600°F for fifty hours, after exposure at 1600°F. Larger needle-shaped carbides were evident in PWA 663 specimens, both with and without pre-examination aging, after exposure at 1800°F. Large carbide needles, identified as M_6C carbide, were also found in PWA 659 specimens after their exposures

at 1900°F and 2000°F. Coarsening of gamma prime in PWA 663, PWA 658, and PWA 659 specimens was observed after their exposure at 1600°F. The coarsening became more evident, especially in the grain-boundary areas, after exposure at higher temperatures. Small carbide particles in these widened grain boundaries appeared to form sub-boundaries. PWA 689 material appeared to have the narrowest grain boundaries of the alloys examined after exposures at 1400°F and 1700°F.

The results of the X-ray-diffraction and X-ray-fluorescence studies conducted on the large-particle and small-particle residues from the digested alloy specimens are tabulated in Figures 15-50 and 15-51. No M_6C was found to be present in PWA 658. The MC in this alloy became less dominant with increasing exposure temperature, whereas the amount of $M_{23}C_6$ appeared to increase with increasing exposure temperature. PWA 658 alloy exposed to 2000°F showed a large amount of MC and a small amount of $M_{23}C_6$. After the exposures at the lower temperatures (1500°F and 1600°F), there was found to be more $M_{23}C_6$ in the small-particle residue than in the large-particle residue. $M_{23}C_6$ was more dominant in PWA 658 alloy than in PWA 659 or PWA 663 alloys. Sigma phase was found in PWA 658 after exposure at 1500°F, as previously stated; however, it did not appear after exposures at 1600°F and 1700°F.

PWA 659 alloy exhibited no M_6C after exposures below 1700°F. The amount of this carbide phase increased rapidly above 1800°F and became more dominant in the large-particle, rather than the small-particle, residue. In general, the dominance of MC decreased with increasing exposure temperatures. Above an exposure temperature of 1800°F, the relative amount of $M_{23}C_6$ phase decreased. The specimen exposed at 1900°F for 1674.6 hours showed a very dominant M_6C phase; however, in the specimen exposed at 1900°F for 536 hours, MC was the dominant phase. No large carbide needles were noted in the specimen with the shorter exposure times; such needles were observed in the specimen with the longer exposure times. The nickel and cobalt contents of the residues increased with increasing exposure temperature, becoming quite high for 1900°F and 2000°F.

PWA 663 alloy showed decreasing dominance of MC with increasing exposure temperature in the large-particle residue, whereas MC reached maximum dominance at exposure temperatures of 1600°F and 1700°F in the small-particle residue. The MC phase was more dominant in the small-particle, rather than in the large-particle, residues

after exposure at 2000°F. The studies indicated increasing M_6C-phase dominance with increasing exposure temperature in the large-particle residues; they showed a maximum of M_6C phase at exposure temperatures of 1700°F and 1800°F in the small-particle residues. A small amount of $M_{23}C_6$ was observed after exposures below 1900°F but not at 1900°F or 2000°F. M_3B_2 phase was found after all exposures in both types of residues. In the large-particle residue, the molybdenum content was lower after exposures at 1500°F and 1600°F. In both large-particle and small-particle residues, titanium content decreased with increasing exposure temperature, whereas nickel and cobalt contents reached their maxima after exposure at 1700°F.

With reference to PWA 689 alloy, no M_6C was found after exposure of the specimen at 1400°F. M_3B_2 boride was observed after all exposures.

In summary, sigma phase was found in PWA 658 alloy after about 1000 hours at 1500°F and in PWA 689 alloy after about 1000 hours at 1500°F and at 1600°F. Borides, M_3B_2, were found in PWA 658, PWA 663, and PWA 689 alloys after exposure. Neither sigma nor boride phases were observed in PWA 659 alloy. After the higher temperature exposure, most of the PWA 659 residues were M_6C carbide. Of the four alloys investigated, PWA 659 and PWA 663 alloys appeared, on the basis of completed work, to be the most resistant to gamma-prime coarsening and grain-boundary widening, and the most stable in the temperature range in which the evaluations were made.

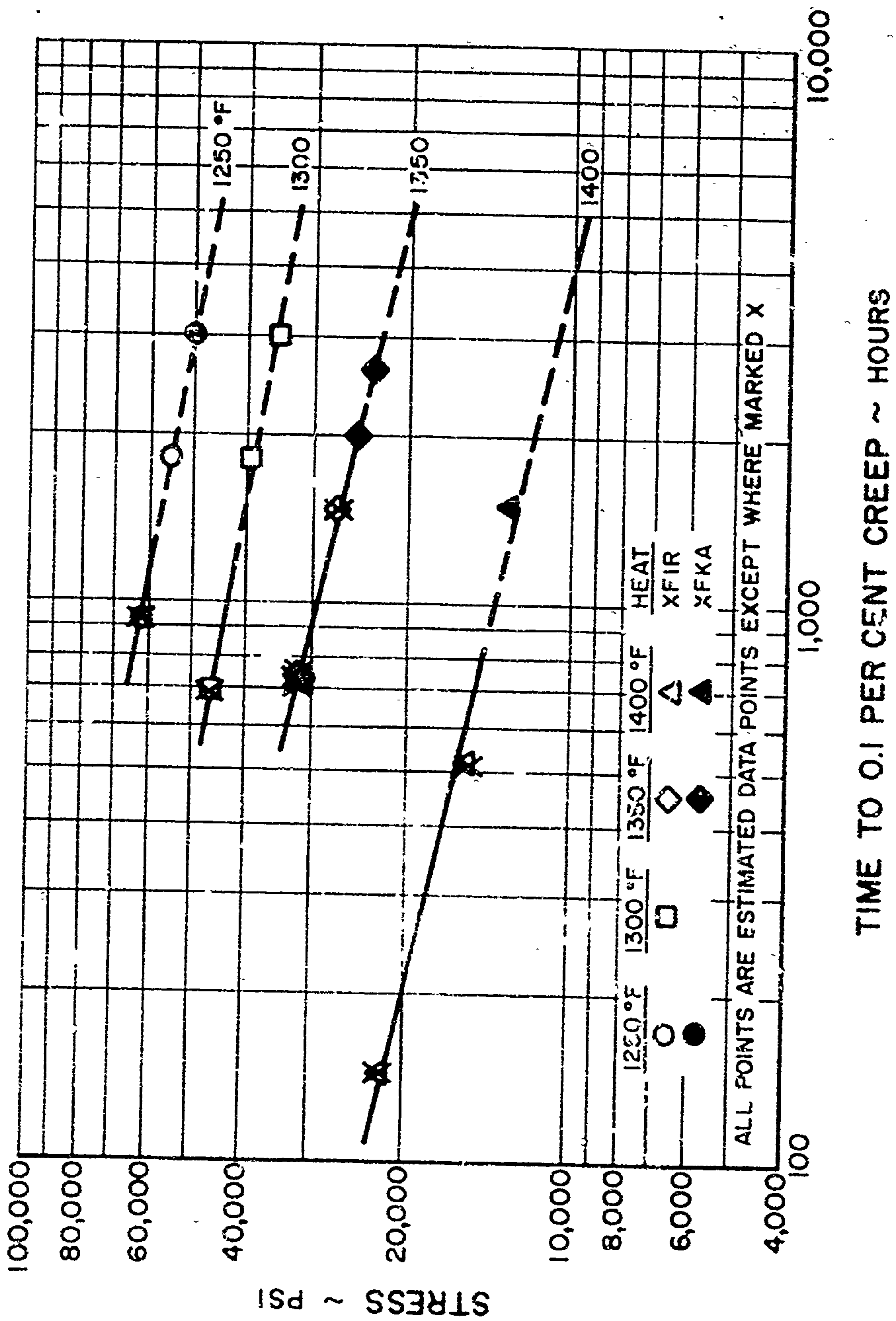

CREEP PROPERTIES OF PWA 1007 NICKEL-BASE ALLOY, HEATS XFIR AND XFKA

Figure 15-1

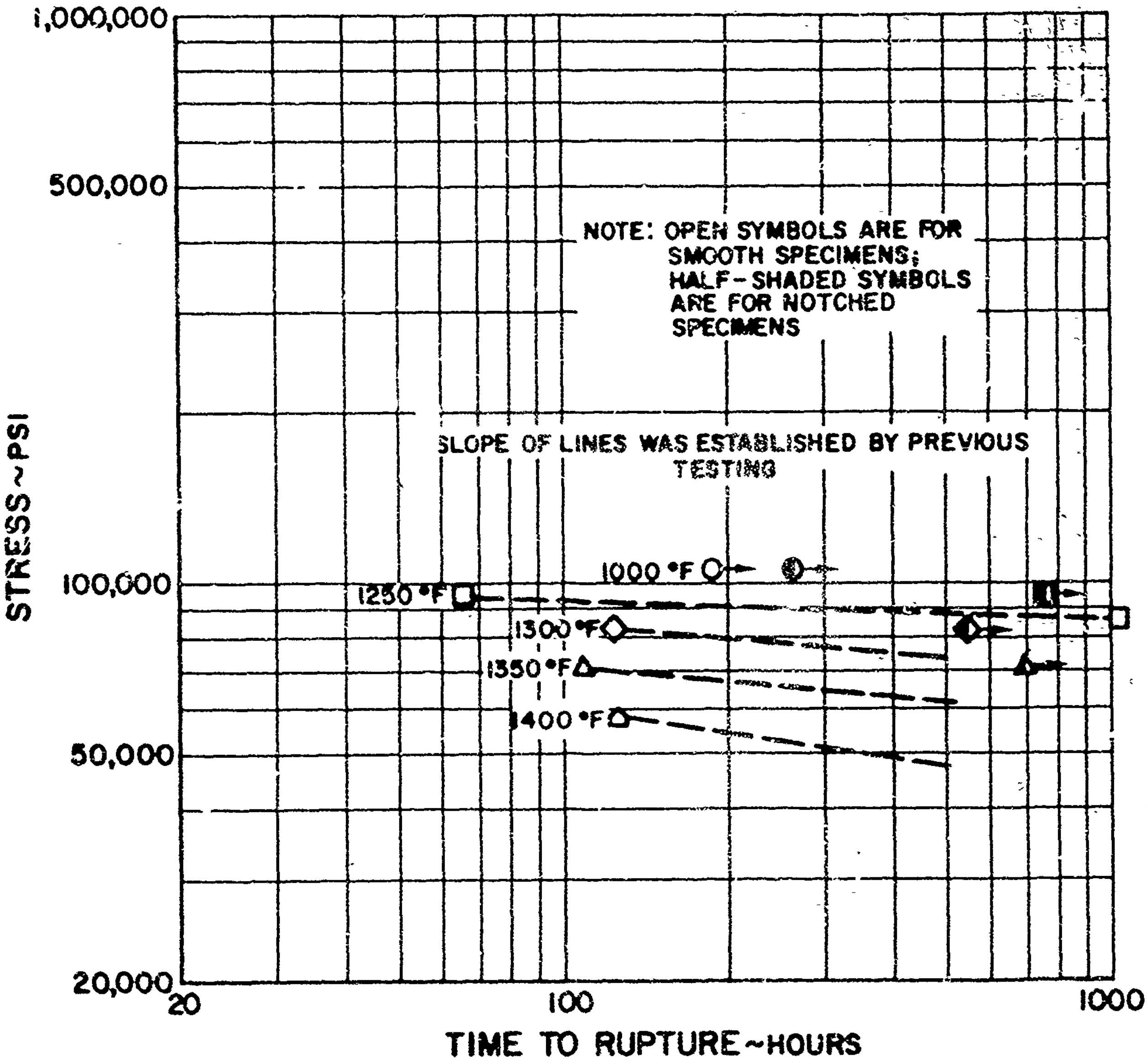

STRESS-RUPTURE PROPERTIES OF PWA 1007 NICKEL-BASE ALLOY, HEATS XFIR AND XFKA

Figure 15-2

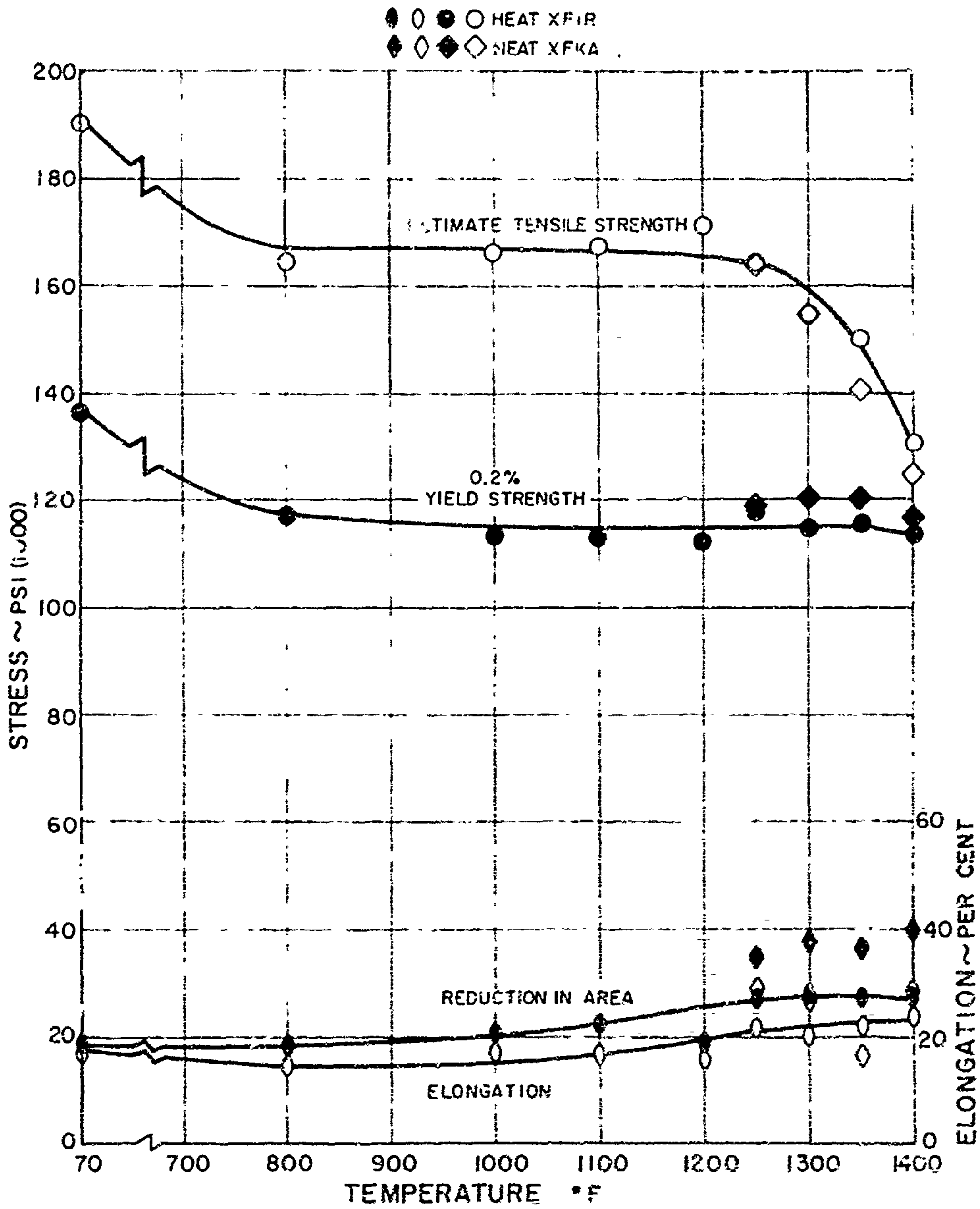

TENSILE PROPERTIES OF PWA 1007 NICKEL-BASE ALLOY

Figure 15-3

Material	Heat	Temp. (°F)	Stress (psi)	Time to 0.1% Creep (hrs)
PWA 1003	ABET	1150	80,000	*1000
	ABBK	1150	66,000	*2800
	ABBK	1150	66,000	*2800
	ABET	1150	[illegible]0,000	*3500
	ABBK	1200	60,000	*2400
	ABET	1200	56,000	*1500
	ABET	1200	52,000	*2000
	ABBK	1250	45,000	26
	ABET	1250	45,000	*1000
	ABET	1250	40,000	*3000
	ABBK	1250	36,500	*3450
	ABET	1300	32,000	*2000
	ABET	1300	27,000	*2500
PWA 1007	XFKA	1250	62,500	950
	XFIR	1250	55,000	*1800
	XFKA	1250	50,000	*3000
	XFIR	1300	46,000	695
	XFIR	1300	39,500	*1800
	XFIR	1300	35,000	*3000
	XFIR	1350	32,000	735

*Time for 0.1% creep estimated from test in process when this tabulation prepared.

CREEP PROPERTIES OF PWA 1003, PWA 1007, PWA 1010, PWA 1202, PWA 1203 AND AMS 4928 ALLOYS

Figure 15-4 Sheet 1 of 3

Material	Heat	Temp. (°F)	Stress (psi)	Time to 0.1% Creep (hrs)
PWA 1007 (Cont)	XFKA	1350	32,000	735
	XFIR	1350	27,000	*1460
	XFKA	1350	25,000	*2000
	XFKA	1350	23,500	*2600
	XFIR	1400	22,000	142
	XFIR	1400	1[illegible] 500	520
	XFKA	1400	13,000	*1500
PWA 1010	CGNJ	1150	72,000	*1000
	CGNJ	1150	68,000	*1900
	CGNJ	1200	56,000	*1000
	CGNJ	1200	51,000	*2400
	CGNJ	1250	34,000	1100
	CGNJ	1250	23,500	*2900
	CGNJ	1300	20,000	950
	CGNJ	1300	13,000	*3200
PWA 1202	WSTL	750	52,000	1045
	WSTL	750	49,000	*3100
	WSTL	850	50,000	42
	WSTL	850	33,000	850
	WSTL	850	27,500	*2700

*Time for 0.1% creep estimated from test in process when this tabulation prepared.

CREEP PROPERTIES OF PWA 1003, PWA 1007, PWA 1010, PWA 1202, PWA 1203 AND AMS 4928 ALLOYS

Figure 15-4 Sheet 2 of 3

Material	Heat	Temp. (°F)	Stress (psi)	Time to 0.1% Creep (hrs)
PWA 1202 (Cont)	WSTL	950	15,500	1360
	WSTL	950	12,000	*3400
PWA 1203	WEKY	850	47,000	1025
	WEKY	850	37,000	*3100
	WEKY	950	17,500	885
	WEKY	950	12,500	*2800
	WEKY	1050	5,100	930
	WEKY	1050	3,700	*2800
AMS 4928	WLGM	650	60,000	240
	WLGM	650	50,000	510
	WLGM	650	41,000	*2000
	WLGM	750	27,000	180
	WLGM	750	22,000	445
	WLGM	750	18,500	*2000
	WLGM	850	12,000	205
	WLGM	850	9,600	380
	WLGM	850	7,900	*645

*Time for 0.1% creep estimated from test in process when this tabulation prepared.

CREEP PROPERTIES OF PWA 1003, PWA 1007, PWA 1010, PWA 1202, PWA 1203 AND AMS 4929 ALLOYS

Figure 15-4 Sheet 3 of 3

	Temp. (°F)	Stress for 1000 Hrs (psi)	Stress for 3000 Hrs (psi)	Stress for 5000 Hrs (psi)
PWA 1003	1150	60,000	64,000	58,000
	1200	61,000	48,000	42,000
	1250	45,000	39,000	36,000
	1300	39,000	27,000	22,500
PWA 1007	1250	62,000	50,000	46,000
	1300	43,000	35,000	32,000
	1350	30,000	23,000	20,000
	1400	14,[illegible]00	10,500	9,400
PWA 1010	1150	72,000	65,000	62,000
	1200	56,000	50,000	48,000
	1250	35,000	23,000	19,000
	1300	1[illegible],500	13,500	11,000
PWA 1202	750	52,000	49,000	48,000
	850	32,000	27,000	26,000
	950	17,000	12,500	10,500
PWA 1203	850	45,000	37,000	33,000
	950	17,000	12,500	10,500
	1050	5,200	3,600	3,000
AMS 4928	650	43,000	33,000	34,000
	750	19,000	14,000	13,500
	850	6,700	4,300	3,800

ESTIMATED STRESSES TO PRODUCE 0.1% CREEP IN PWA 1003, PWA 1007, PWA 1010, PWA 1202, PWA 1203, AND AMS 4928 ALLOYS

Figure 15-5

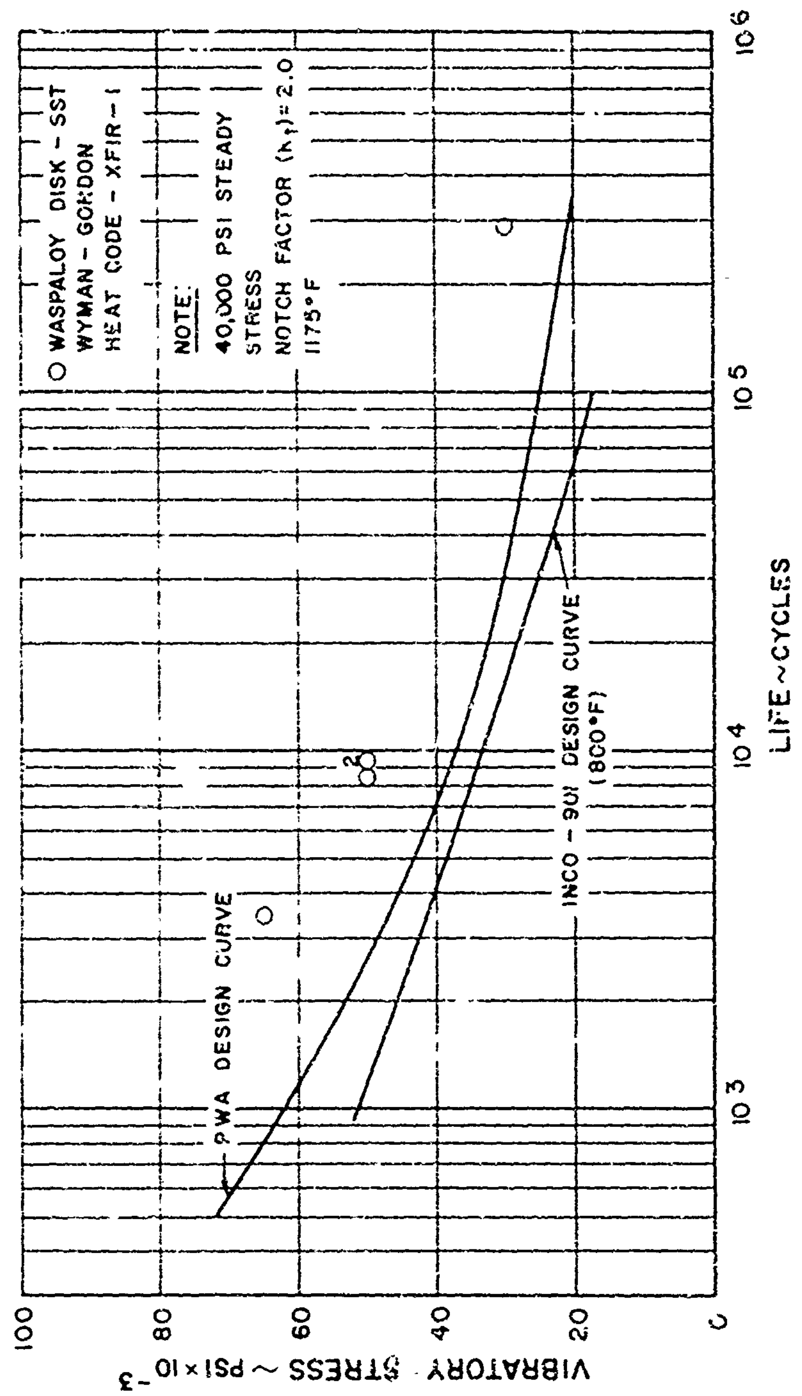

LOW-CYCLE FATIGUE NOTCHED TEST RESULTS FOR PWA 1007 NICKEL-BASE ALLOY

Figure 15-6

Notch Factor	Temp. (°F)	Imposed Steady Stress (psi)	Imposed Vibratory Stress (psi)	Cycles to Failure
1.5	1000	47,500	55,000	4.88×10^6
			55,000	4.7×10^5
			55,000	2.1×10^7
			70,000	3.2×10^4
			70,000	3.4×10^4
			70,000	6.3×10^4
			60,000	5.58×10^5
			60,000	1.27×10^6
			60,000	1.5×10^6
1.5	1000	55,000	45,000	1.6×10^7
			45,000	1.38×10^5
			45,000	1.2×10^7
			45,000	1.0×10^6
			47,500	1.55×10^7
			47,500	6.0×10^5
			47,500	5.1×10^5
			50,000	9.9×10^5
			50,000	7.9×10^5
			50,000	4.2×10^5
			60,000	1.2×10^5
			60,000	7.3×10^4
			60,000	3.6×10^4

COMBINED-LOAD TEST DATA FOR PWA 1007 NICKEL-BASE ALLOY

Figure 15-7 Sheet 1 of 2

Notch Factor	Temp. (°F)	Imposed Steady Stress (psi)	Imposed Vibratory Stress (psi)	Cycles to Failure
1.5	1000	25,000	60,000	6.2×10^5
			60,000	2.7×10^6
			70,000	6.48×10^4
			70,000	1.8×10^5
			70,000	3.1×10^5

COMBINED-LOAD TEST DATA FOR PWA 1007 NICKEL-BASE ALLOY

Figure 15-7 Sheet 2 of 2

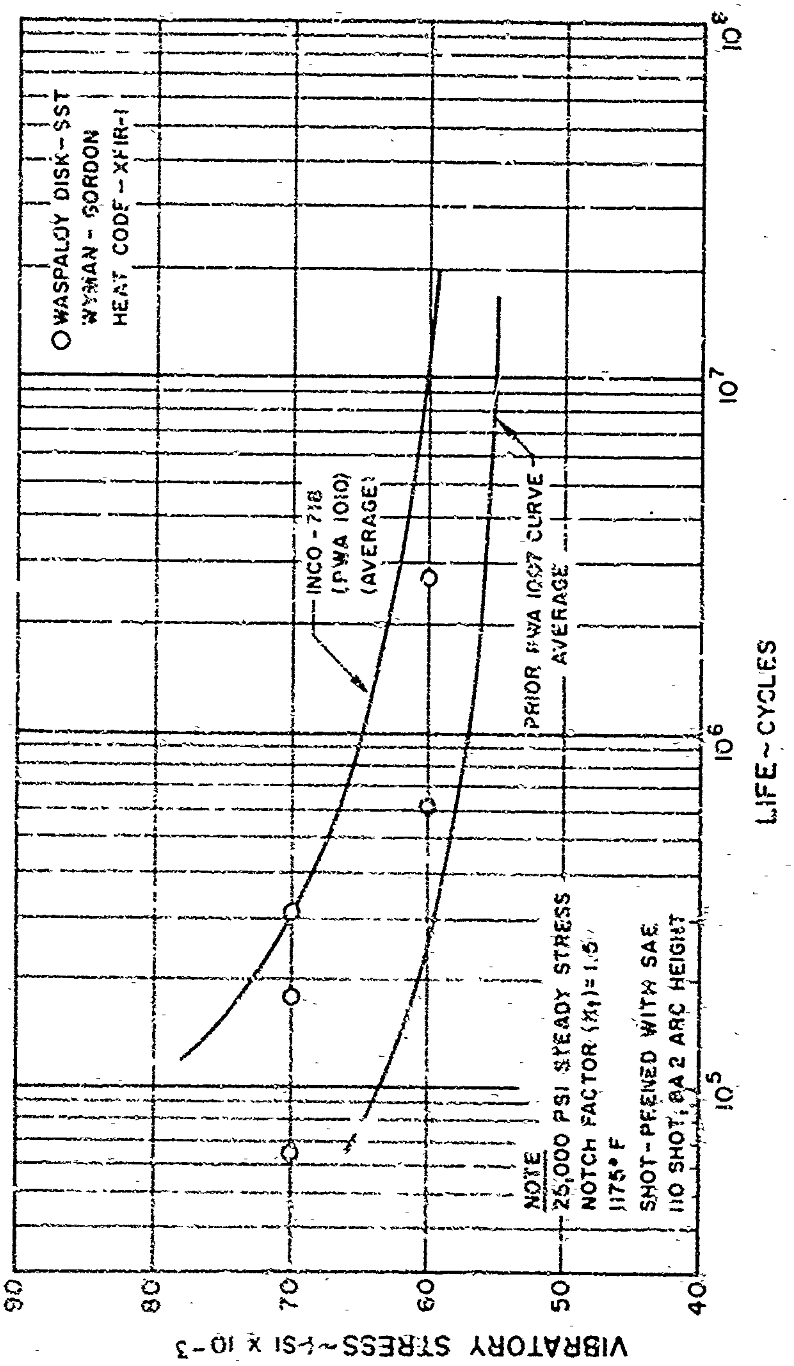

COMBINED-LOAD NOTCHED TEST RESULTS FOR PWA 1007 AND PWA 1010 NICKEL-BASE ALLOYS

Figure 15-8

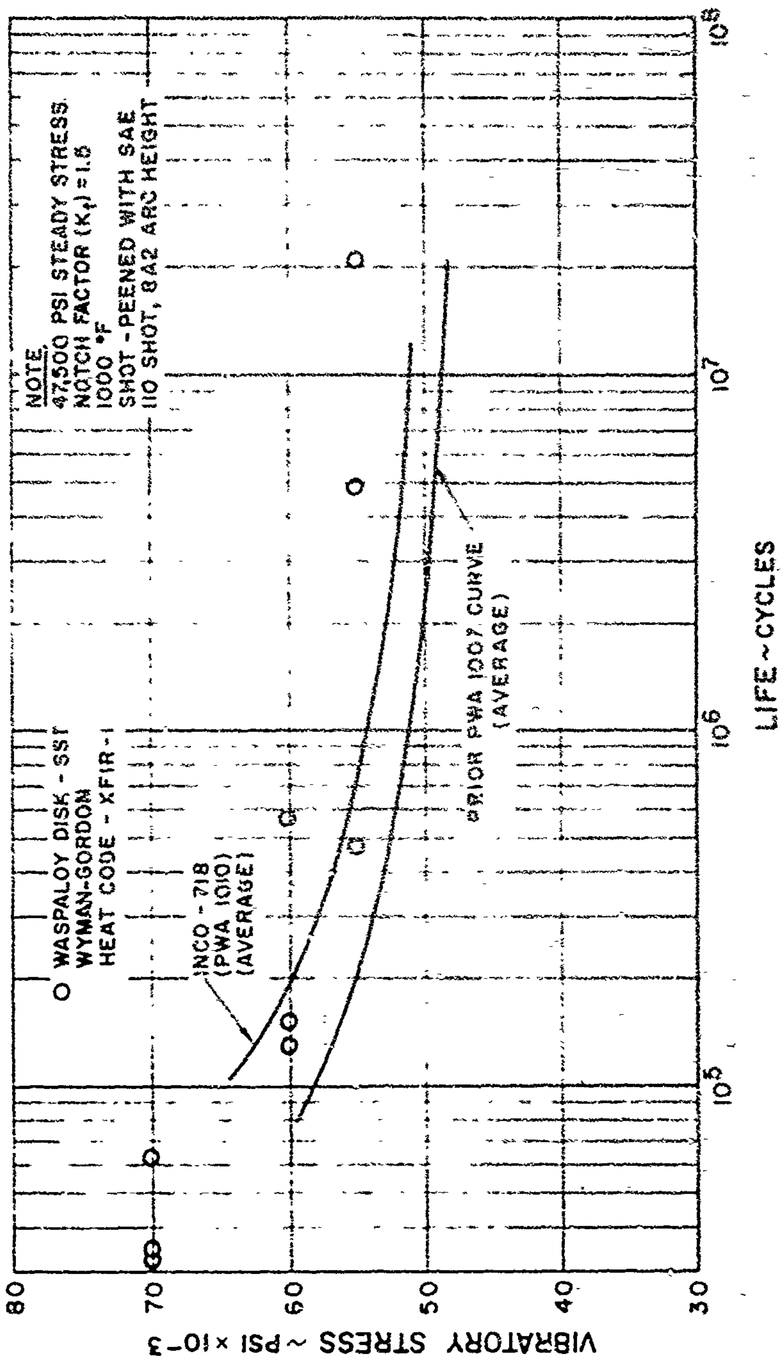

COMBINED-LOAD NOTCHED TEST RESULTS FOR PWA 1007 AND PWA 1010 NICKEL-BASE ALLOYS

Figure 15-9

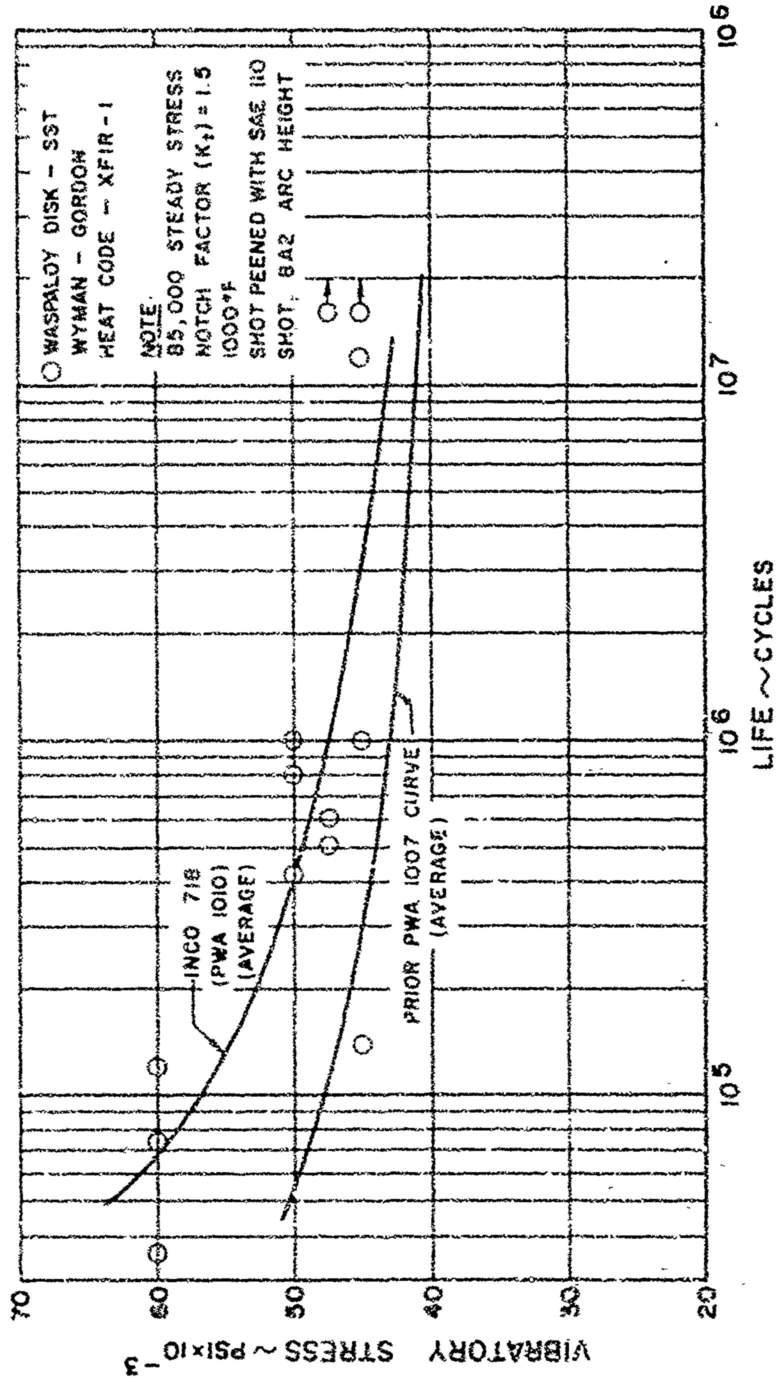

COMBINED-LOAD NOTCHED TEST RESULTS FOR PWA 1007 AND PWA 1010 NICKEL-BASE ALLOYS

Figure 15-10

Notch Factor	Temp. (°F)	Imposed Stress (psi)	Cycles to Failure	Remarks
Smooth	1000	100,000	2.48×10^5	
			2.8×10^5	
			3.07×10^5	
		80,000	5.3×10^5	
			9.5×10^5	
			1.1×10^6	
		70,000	2.5×10^6	
			8.5×10^6	
			1.2×10^7	
		65,000	2.7×10^6	
			3.2×10^6	
			7.4×10^6	
			2×10^7	
		62,500	2.8×10^6	
			3.95×10^6	
		60,000	2×10^7	No Failure
			2×10^7	No Failure
1.5	1000	60,000	1.1×10^5	
			3.3×10^5	
			5.4×10^5	
		50,000	5.2×10^5	
			5.76×10^5	
			1.97×10^7	No Failure

ROTATING BEAM TEST DATA FOR PWA 1007 NICKEL-BASE ALLOY

Figure 15-11 Sheet 1 of 2

Notch Factor	Temp. (°F)	Imposed Stress (psi)	Cycles to Failure	Remarks
1.5 (Cont)	1000 (Cont)	45,000	$1x10^7$	
			$2x10^7$	No Failure
			$2x10^7$	No Failure
		60,000	$5.6x10^4$	
			$5.7x10^4$	
			$6.5x10^4$	
			$9.9x10^4$	
			$3.3x10^5$	
3.0	1000	50,000	$2.6x10^4$	
			$8.16x10^4$	
			$4.2x10^5$	
		45,000	$6.75x10^4$	
			$6.7x10^4$	
			$8.7x10^4$	
		40,000	$1.9x10^6$	
			$1.09x10^7$	
			$2x10^7$	No Failure

ROTATING BEAM TEST DATA FOR PWA 1007 NICKEL-BASE ALLOY

Figure 15-11 Sheet 2 of 2

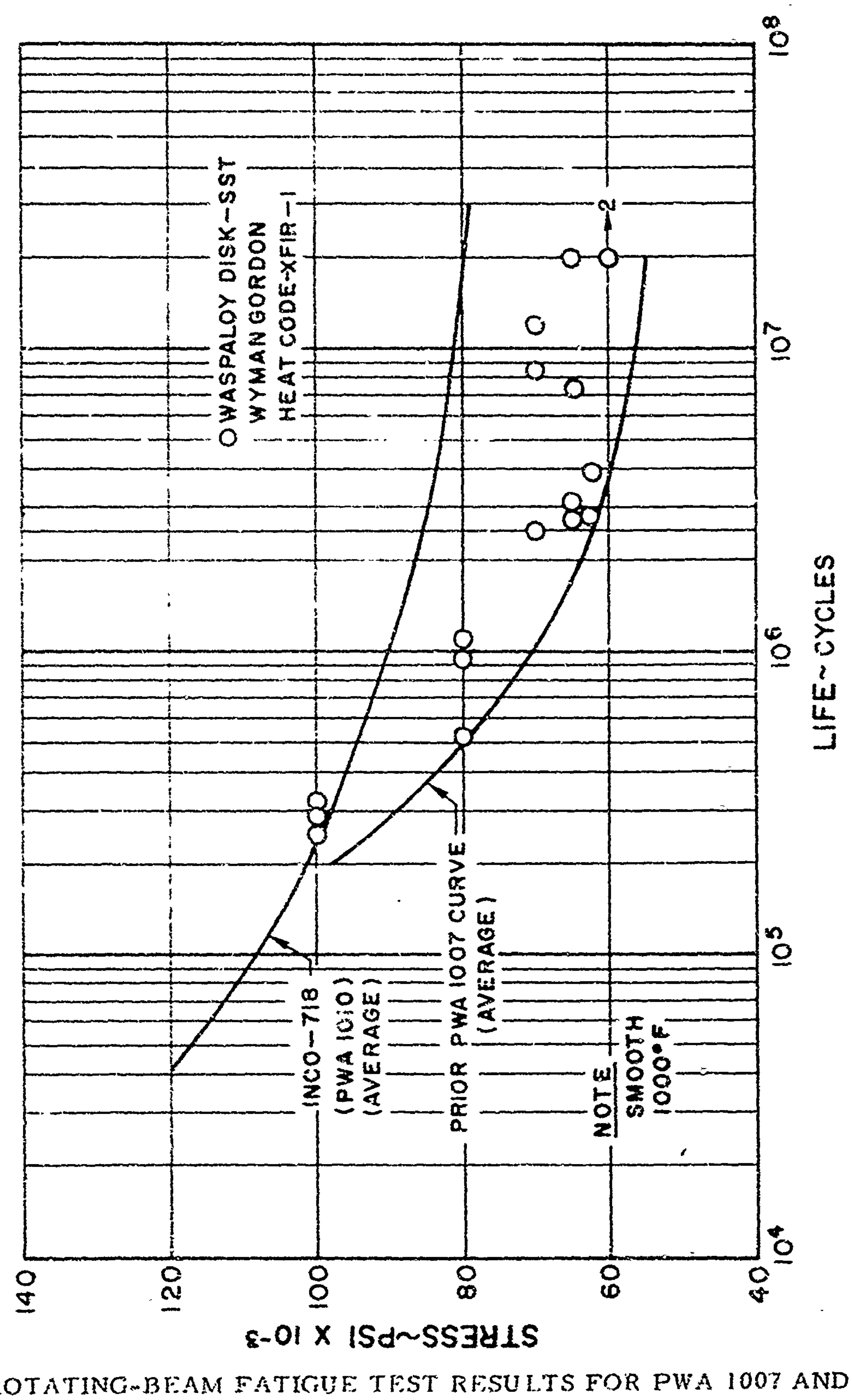

ROTATING-BEAM FATIGUE TEST RESULTS FOR PWA 1007 AND PWA 1010 NICKEL-BASE ALLOYS

Figure 15-12

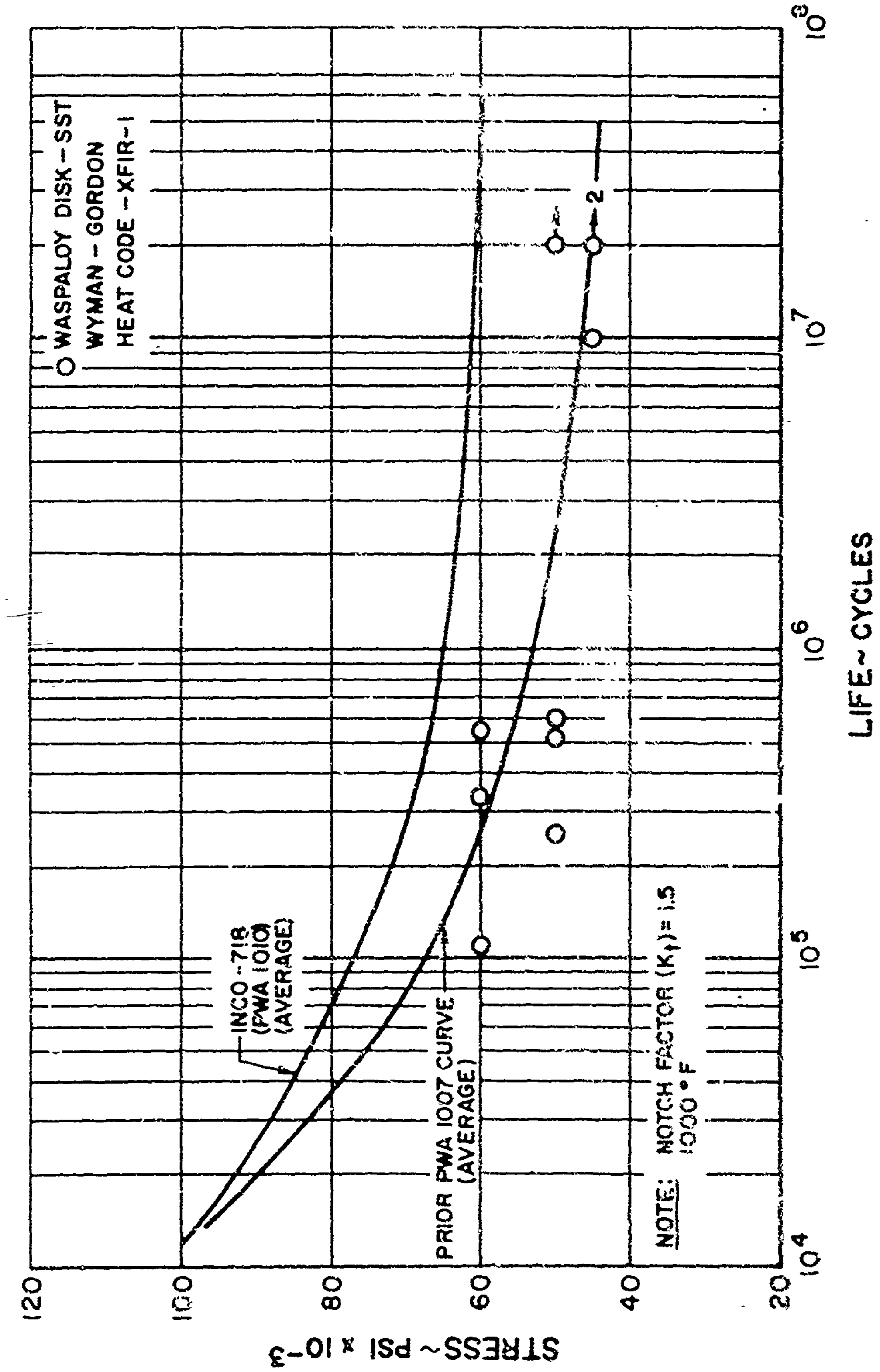

ROTATING-BEAM FATIGUE TEST RESULTS FOR PWA 1007 AND PWA 1010 NICKEL-BASE ALLOYS

Figure 15-13

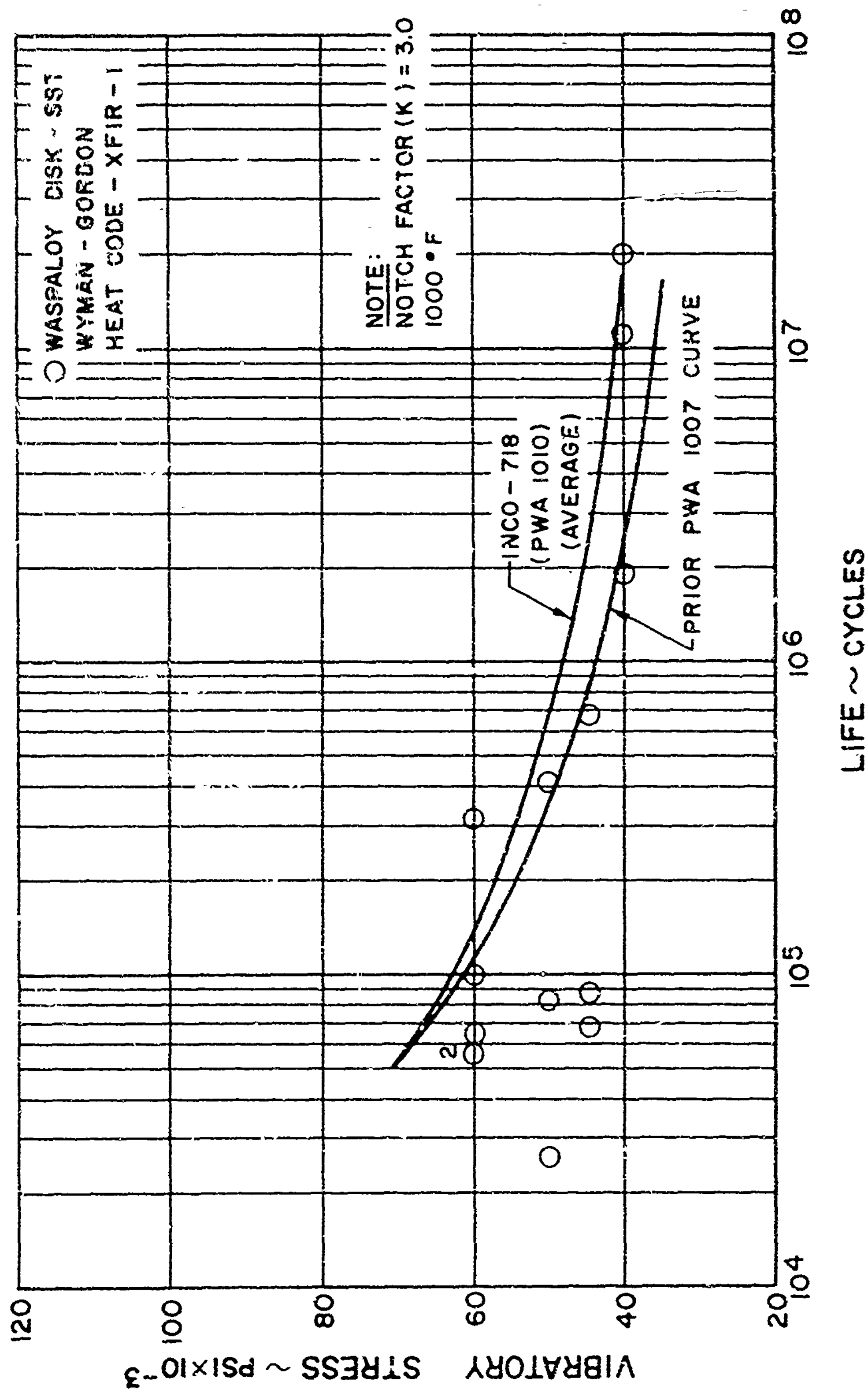

ROTATING BEAM FATIGUE TEST RESULTS FOR PWA 1007 AND PWA 1010 NICKEL-BASE ALLOYS

Figure 15-14

Notch Factor	Temp (°F)	Imposed Steady Stress (psi)	Imposed Vibratory Stress (psi)	Cycles	Remarks
			80 000	18 000	
				13 800	
				21 180	
Smooth	1175	40 000	65 000	59 000	
				178 000	
				225 000	
				367 000	
				3 000	No crack
			65,000	1 000	Crack
				5 800	Total
2.0	1175	40 000		7 000	No crack
				5 00[illegible]	Crack
				14 950	Total
			50 000	8 000	No crack
				1 000	Very faint indication
				1 000	Crack
				13 750	Total
				9 000	No crack
				1 000	Crack
				1[illegible] 390	Total
			30 000	285 000	No crack
				[illegible] 000	Crack
				305 960	Total
				7 000	No crack
				1 000	Crack
				9 310	Total
			40 000	6 000	No crack
				7 000	Crack
				9 430	Total
3.0	1175	40 000		5 000	No crack
				1 000	Crack
				10 920	Total
				15 000	No crack
				18 000	Crack
				39 900	Total
			25 000	17 000	No crack
				18 000	Crack
				41 291	Total

LOW CYCLE FATIGUE TEST DATA FOR PWA 1007 NICKEL-BASE ALLOY

Figure 15-15

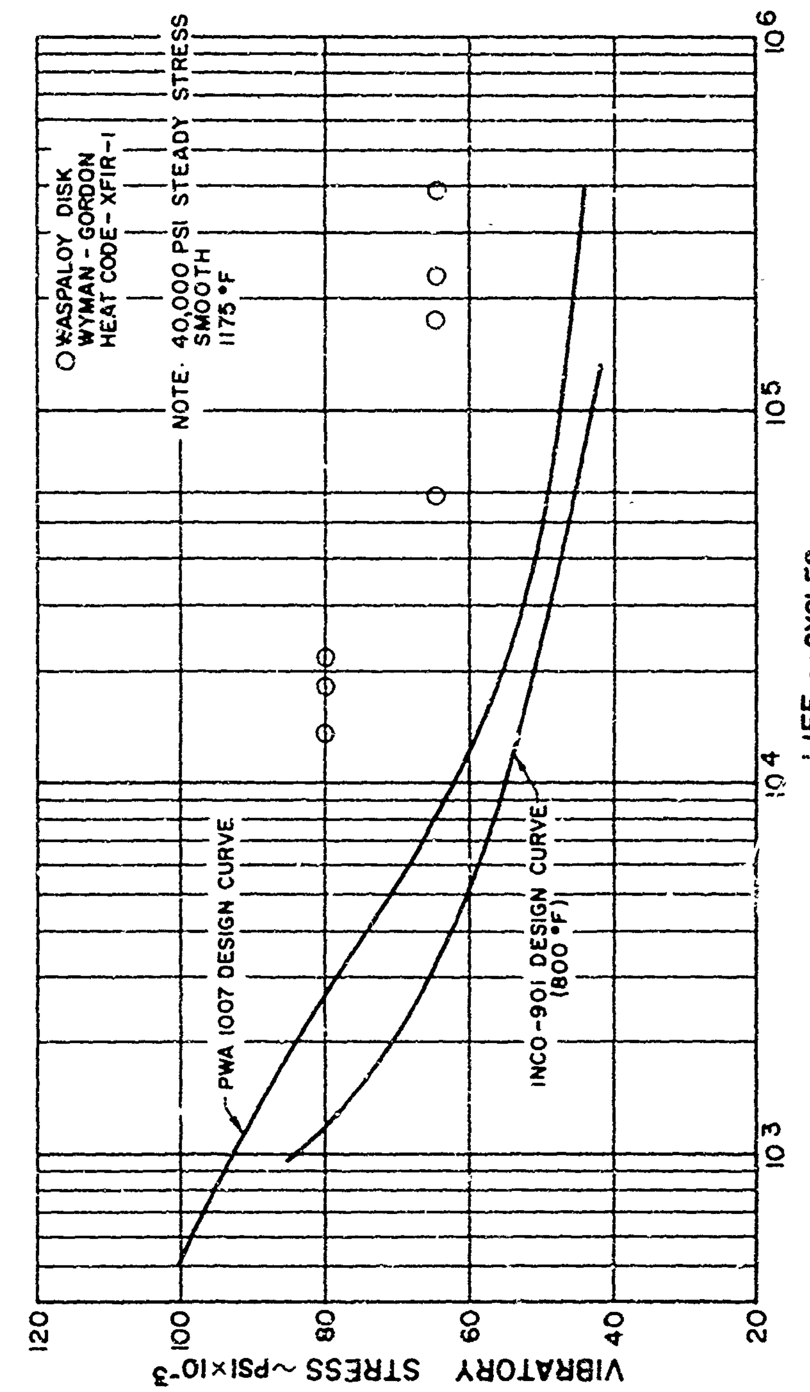

LOW CYCLE FATIGUE TEST RESULTS FOR PWA 1007 NICKEL-BASE ALLOY
Figure 15-16

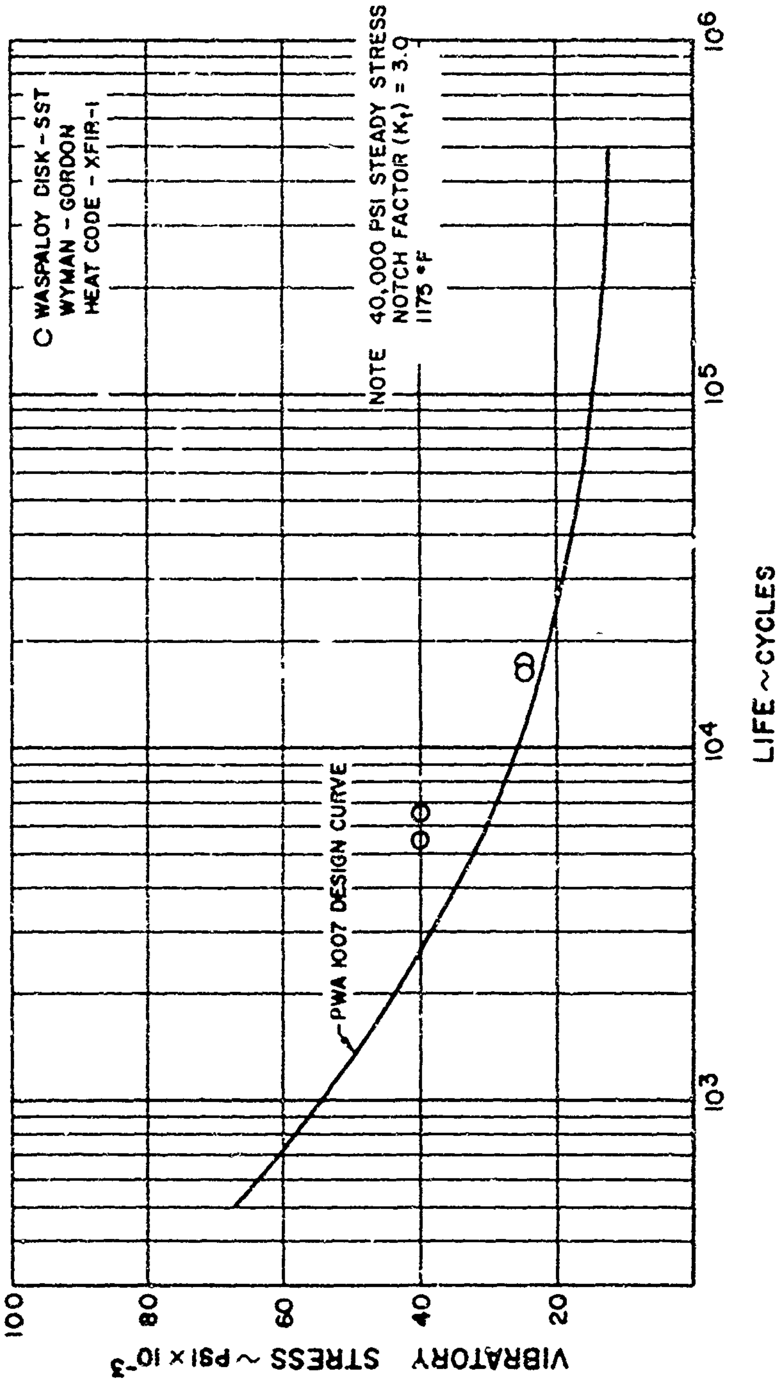

LOW CYCLE FATIGUE NOTCHED TEST RESULTS FOR PWA 1007
NICKEL-BASE ALLOY

Figure 15-17

Notch Factor	Temp. (°F)	Cut	Imposed Vibratory Stress (psi)	Cycles to Failure
2.3	1350	Radial	182,000	1/2
			179,300	1/2
			175,000	1/2
			175.000	7 1/2
			170.000	[illegible] 1/2
			170.000	[illegible]
			170.000	29
			160.000	28
			160.000	23
			160.000	30
			150.000	119
			140.000	208
			140.000	365
			140.000	367
			130.000	518
			124.000	975
			124.000	1421
			124.000	1495
			120.000	1568
			110.000	2850
			110.000	3731
		Tang	178.000	1/2
			170.930	6 1/2
			160,000	55
			150,000	107
			140.000	364
			130,000	831
	1200	Radial	173.000	1/2
			178.000	2 1/2

CYCLIC TENSION FATIGUE NOTCHED TEST DATA FOR PWA 1007 NICKEL-BASE ALLOY

Figure 15-18 Sheet 1 of 2

Notch Factor	Temp. (°F)	Cut	Imposed Vibratory Stress (psi)	Cycles to Failure
	1200	Radial	175,000	88
			165,000	238
			160,000	277
			160,000	220
			160,000	404
			155,000	456
			145,000	743
			140,000	683
			140,000	1563
			140,000	1343
			170,000	210
			170,000	228
			170,000	184
			134,000	1914
			130,000	2777
			130,000	3064
			130,000	3281

CYCLIC TENSION FATIGUE NOTCHED TEST DATA FOR PWA 1007 NICKEL-BASE ALLOY

Figure 15-18 Sheet 2 of 2

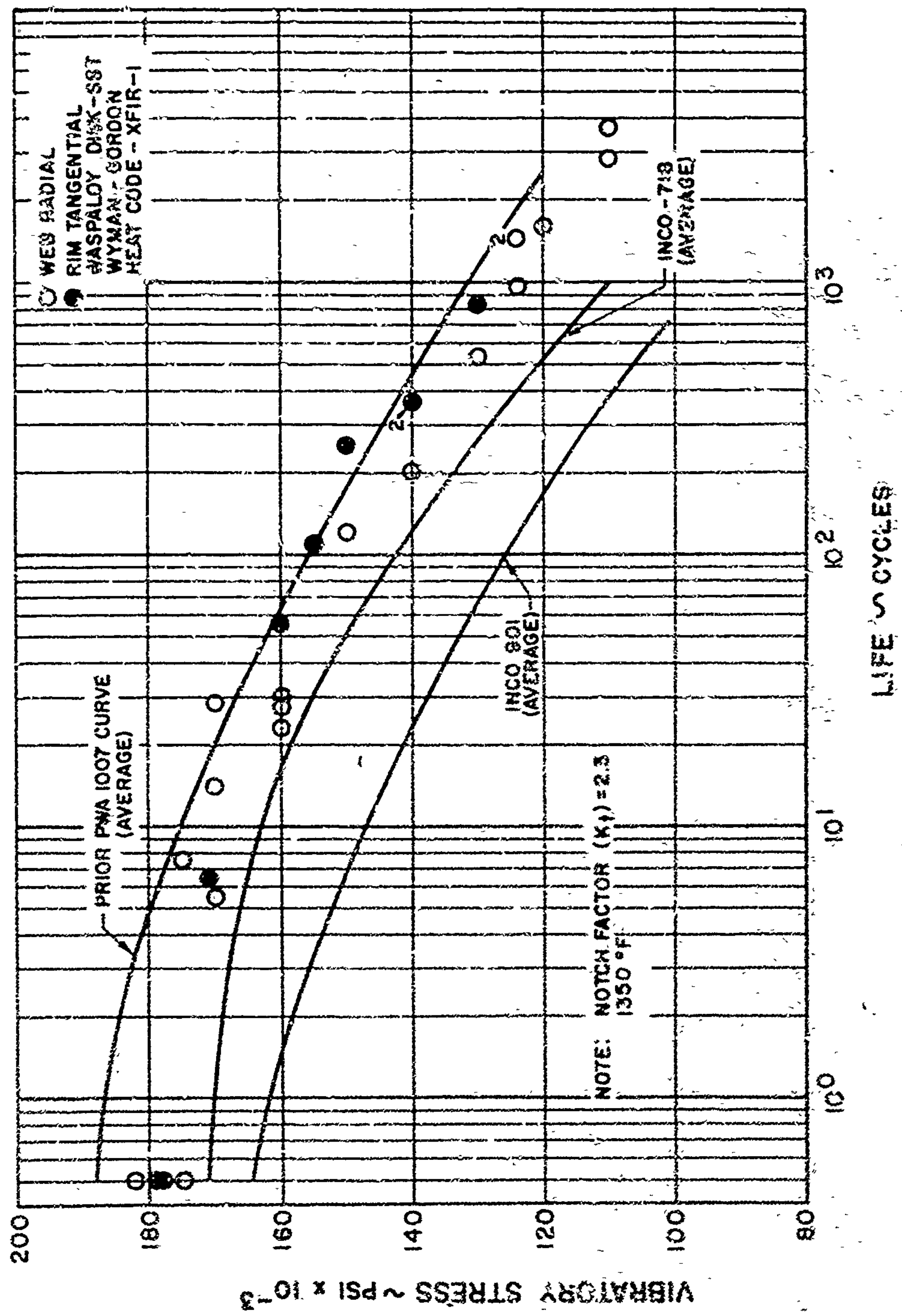

CYCLIC TENSION FATIGUE NOTCHED TEST DATA FOR PWA 1007 NICKEL-BASE ALLOY

Figure 15-19

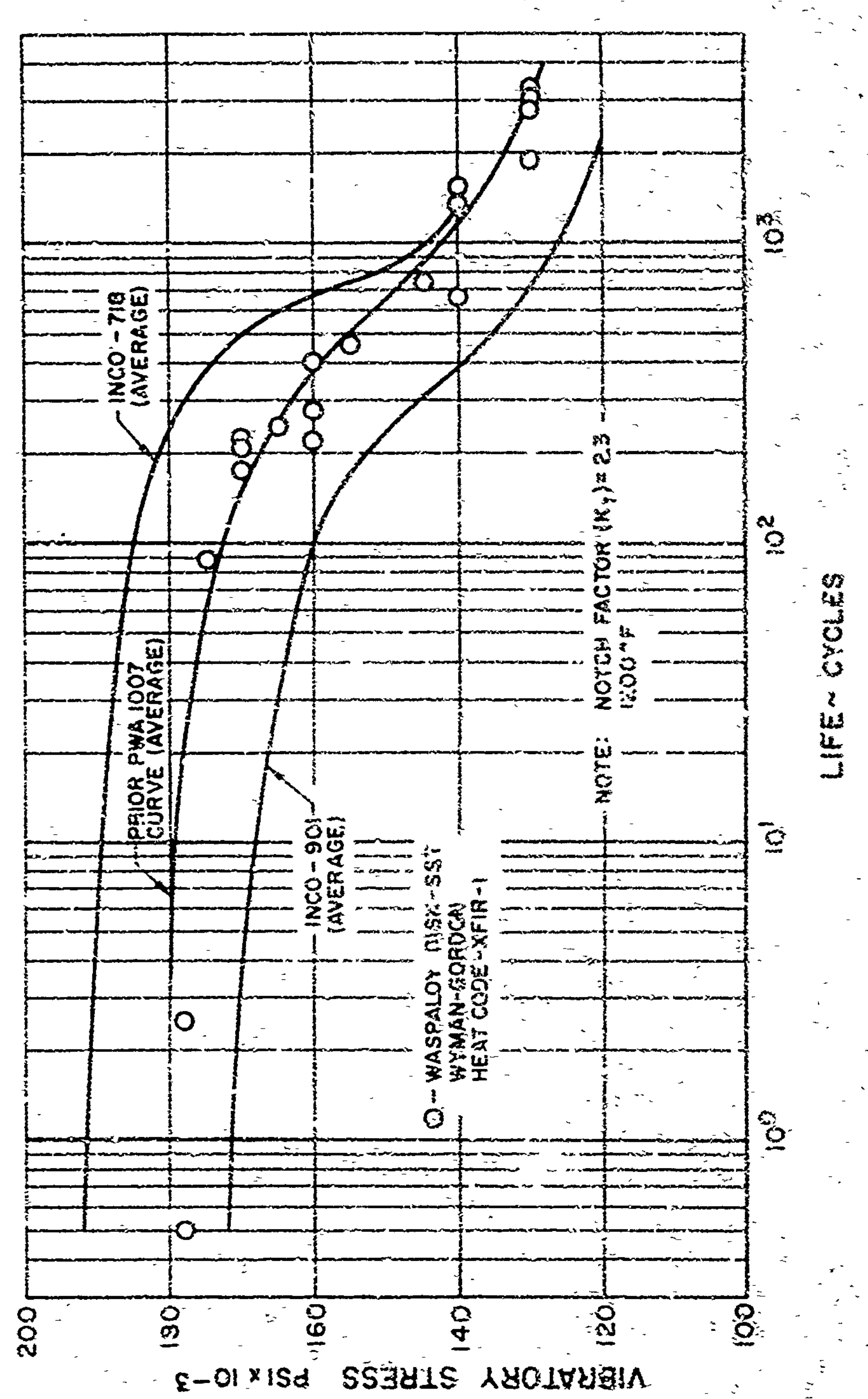

CYCLIC TENSION FATIGUE-NOTCHED TEST RESULTS FOR PWA 1007 NICKEL-BASE ALLOY

Figure 15-20

Material	Heat Code	Heat Treatment	Composition
PWA [illegible]	[illegible]	[illegible]°F(1)AC + [illegible]°F(8)FC [illegible] to 1150°F + 1150°F [illegible] (8)AC	C [illegible], Mn [illegible], Si [illegible], [illegible], Cr [illegible], Ni [illegible], Co 0.55, Cb 1.78, Ta [illegible], Mo 2.99, Ti 0.94, Al 0.14, B 0.001, Cu [illegible], Fe [illegible]
PWA [illegible]	ABPK-[illegible]		C [illegible], Mn [illegible], P [illegible], S [illegible], Cr [illegible], Ni 13.[illegible], Mo [illegible], Ti [illegible], Al [illegible], Cb [illegible], B [illegible], Co [illegible]
PWA [illegible]	[illegible]	[illegible]°F(1)WQ + [illegible]°F(1)AC + [illegible]°F(1)AC	C [illegible], Mn [illegible], [illegible], Cr [illegible], Ni 13.[illegible], Mo [illegible], Ti [illegible], Al [illegible], Cu [illegible], [illegible], Co [illegible]
PWA [illegible]	XFKA-[illegible]		C [illegible], Mn [illegible], [illegible], Cr 14.[illegible], Mo 3.36, Ti [illegible], Al 1.33, Zr .04, B 0.004, Fe 0.57, Cu 0.01, Ni Bal
PWA [illegible]	[illegible]	[illegible]°F(4)OQ + [illegible]°F(1)AC + [illegible]°F(1)AC	C [illegible], Mn [illegible], [illegible], Cr 18.7, [illegible], Mo [illegible], Ti [illegible], Al 1.60, Zr [illegible], B [illegible], Fe [illegible], Cu [illegible], Ni Bal
PWA [illegible]	[illegible]	[illegible]°F(1)OQ + [illegible]°F(8)AC	
PWA [illegible]	WERY-1	[illegible]°F(1)AC	[illegible], Fe [illegible], [illegible], [illegible], Sn 1.92, N₂ .013, Zr 5.00, Al 8.01, Ti Bal
IMI 679	DM2	1650°F(1)AC + 925°F(24)AC	C 0.022, Fe [illegible], W [illegible], Si [illegible], Mo [illegible], H_2 0.002, Zr 4.6, Sn 10.6, O_2 0.08, Al 2.4, Ti Bal.
AMS 4928	WLGM	1300°F(2)AC	C [illegible], Al 6.20, V [illegible], Fe [illegible], O 0.116, N_2 [illegible]027, H_2 0.009, Ti Bal.

HISTORY AND COMPOSITION OF MATERIALS TESTED

Figure 15-21

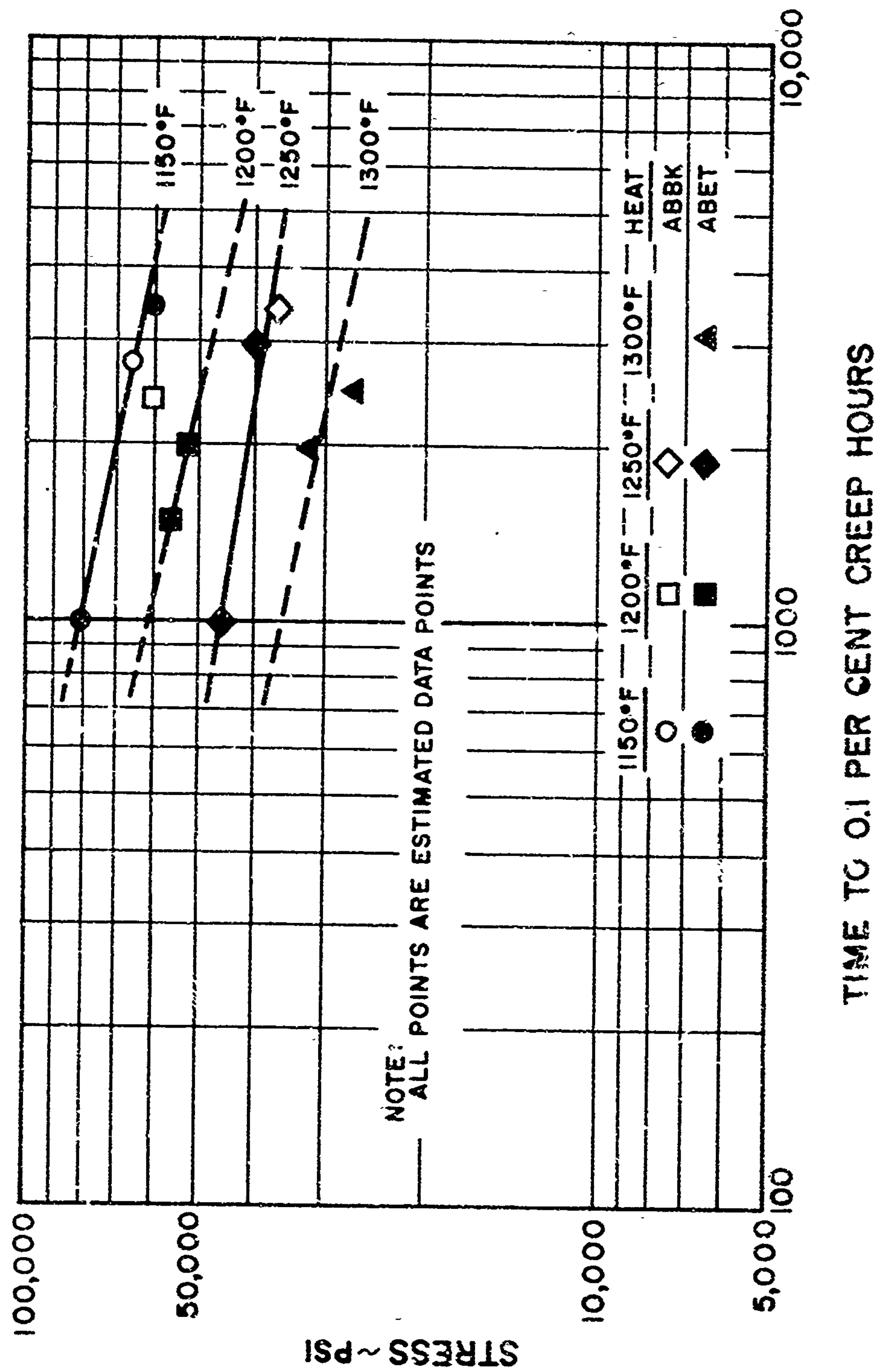

CREEP PROPERTIES OF PWA 1003 NICKEL-BASE ALLOY

Figure 15-22

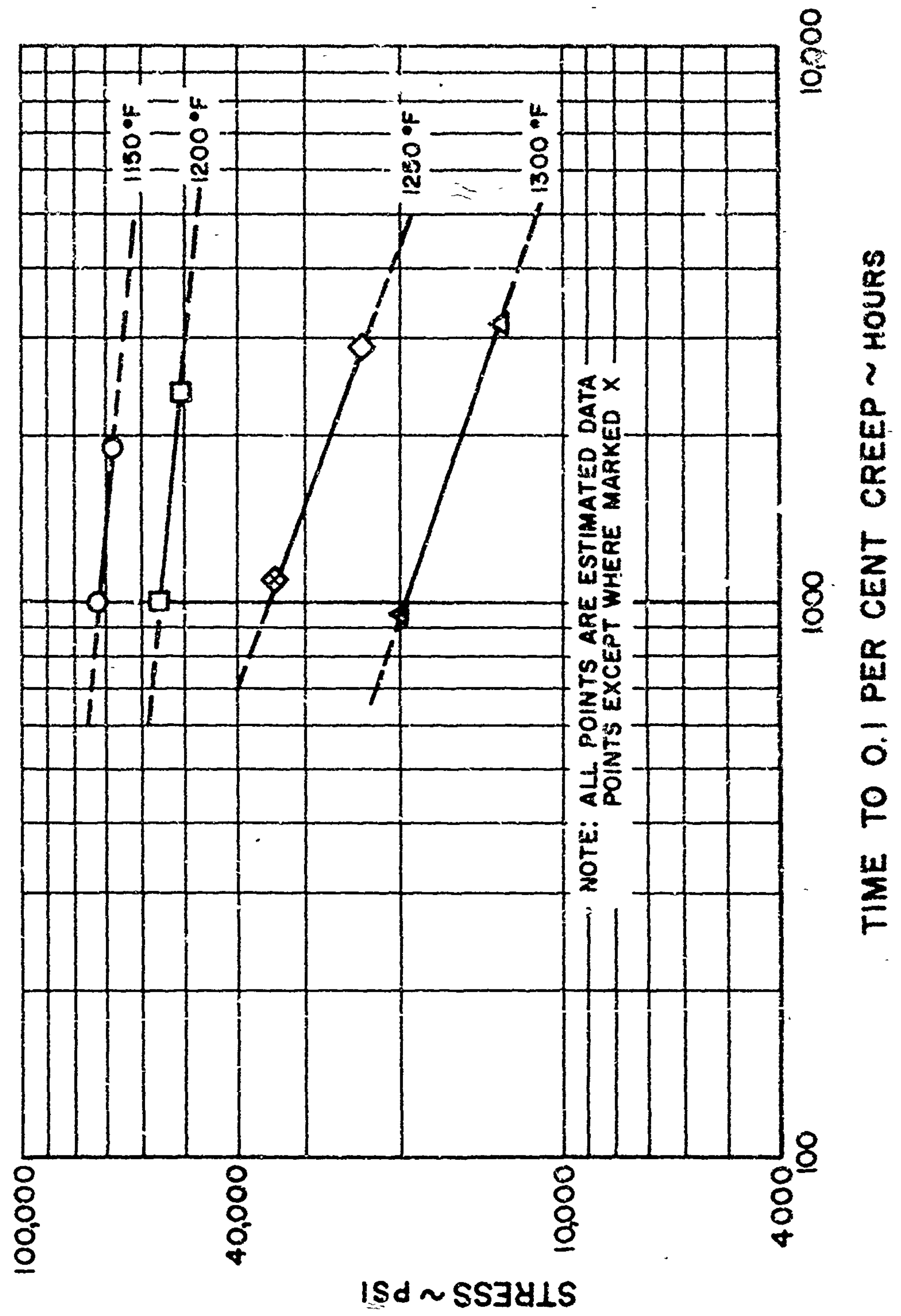

CREEP PROPERTIES OF PWA 1010 NICKEL-BASE ALLOY

Figure 15-23

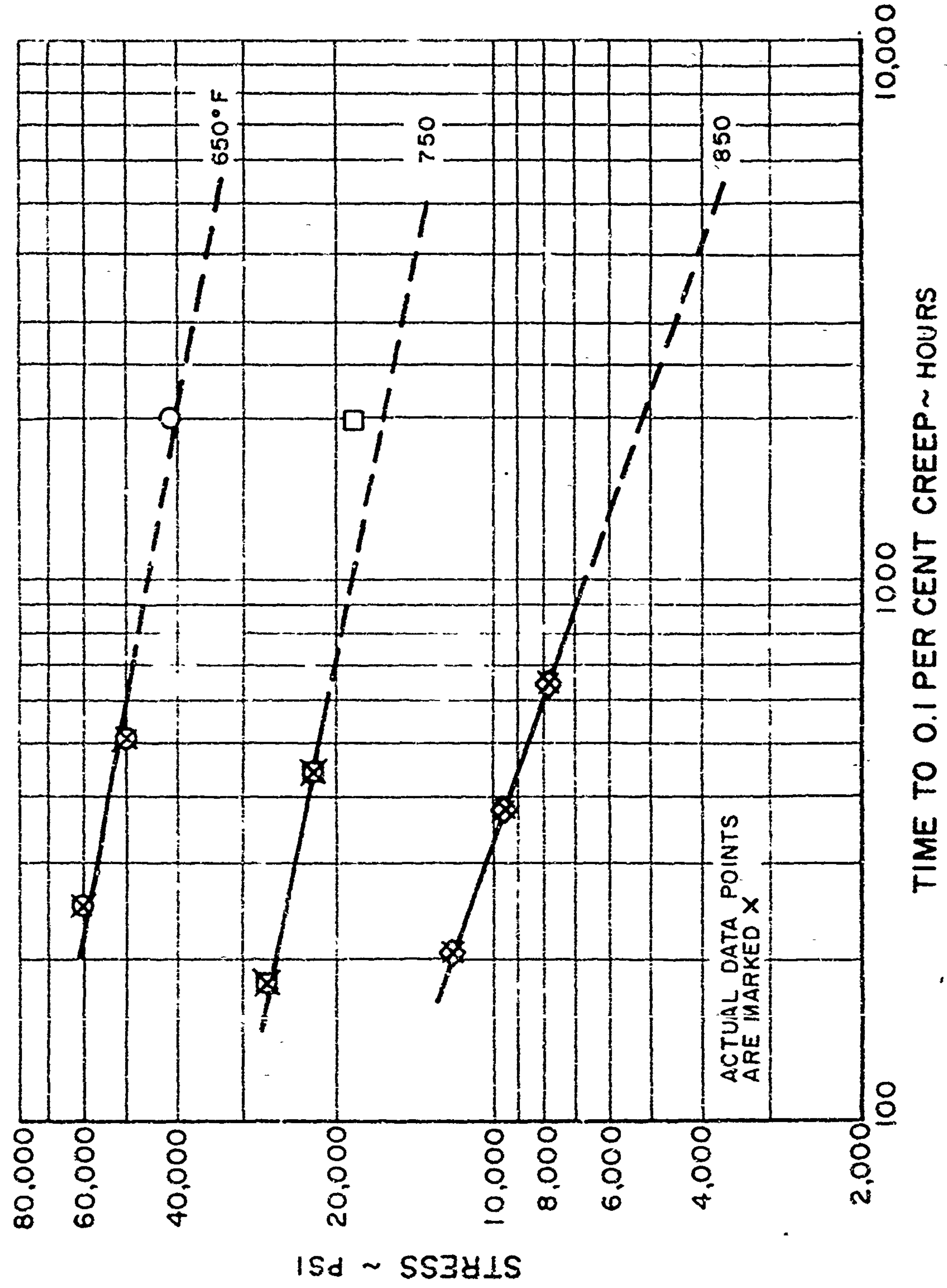

CREEP PROPERTIES OF AMS 4928 TITANIUM ALLOY

Figure 15-24

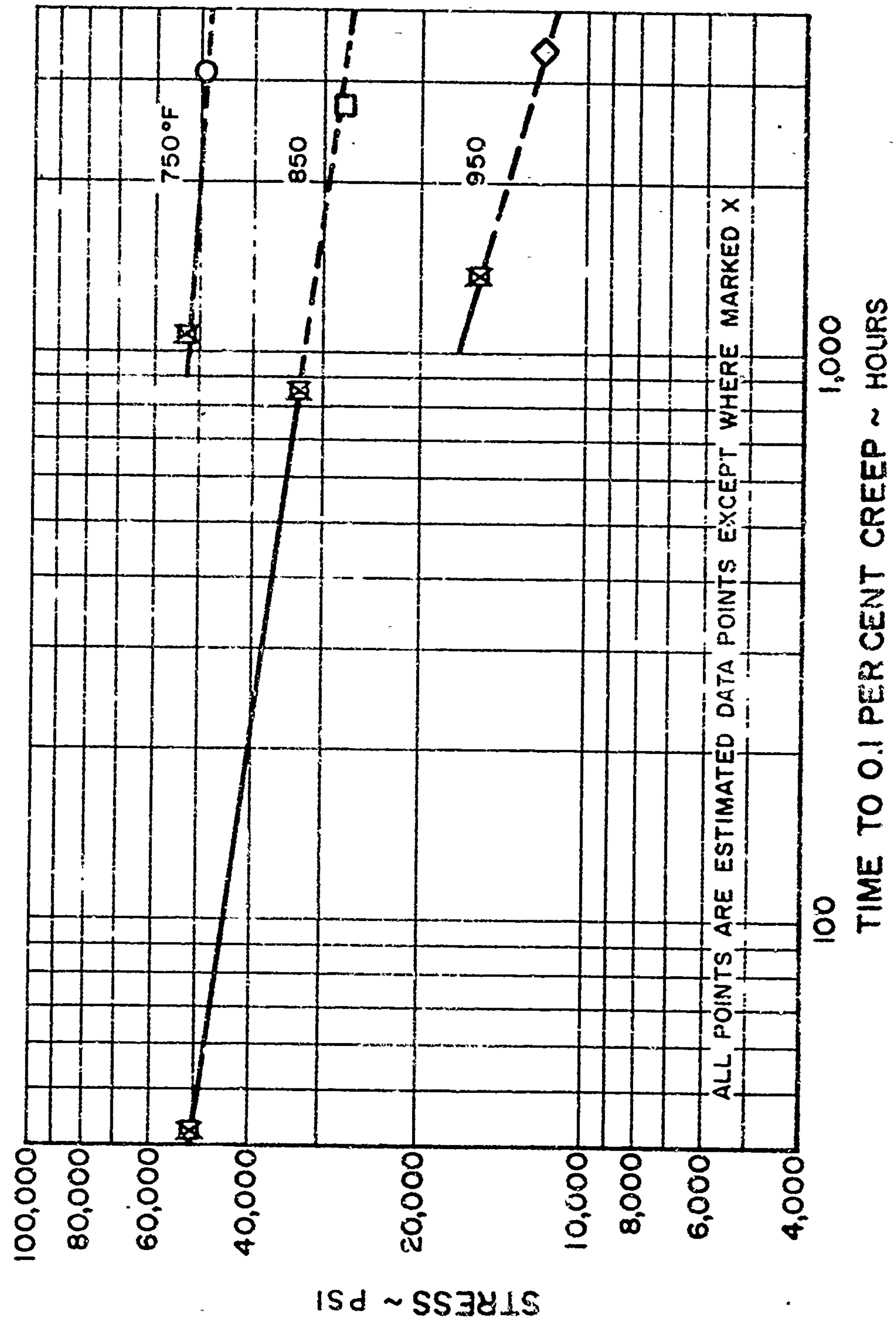

CREEP PROPERTIES OF PWA 1202 TITANIUM ALLOY

Figure 15-25

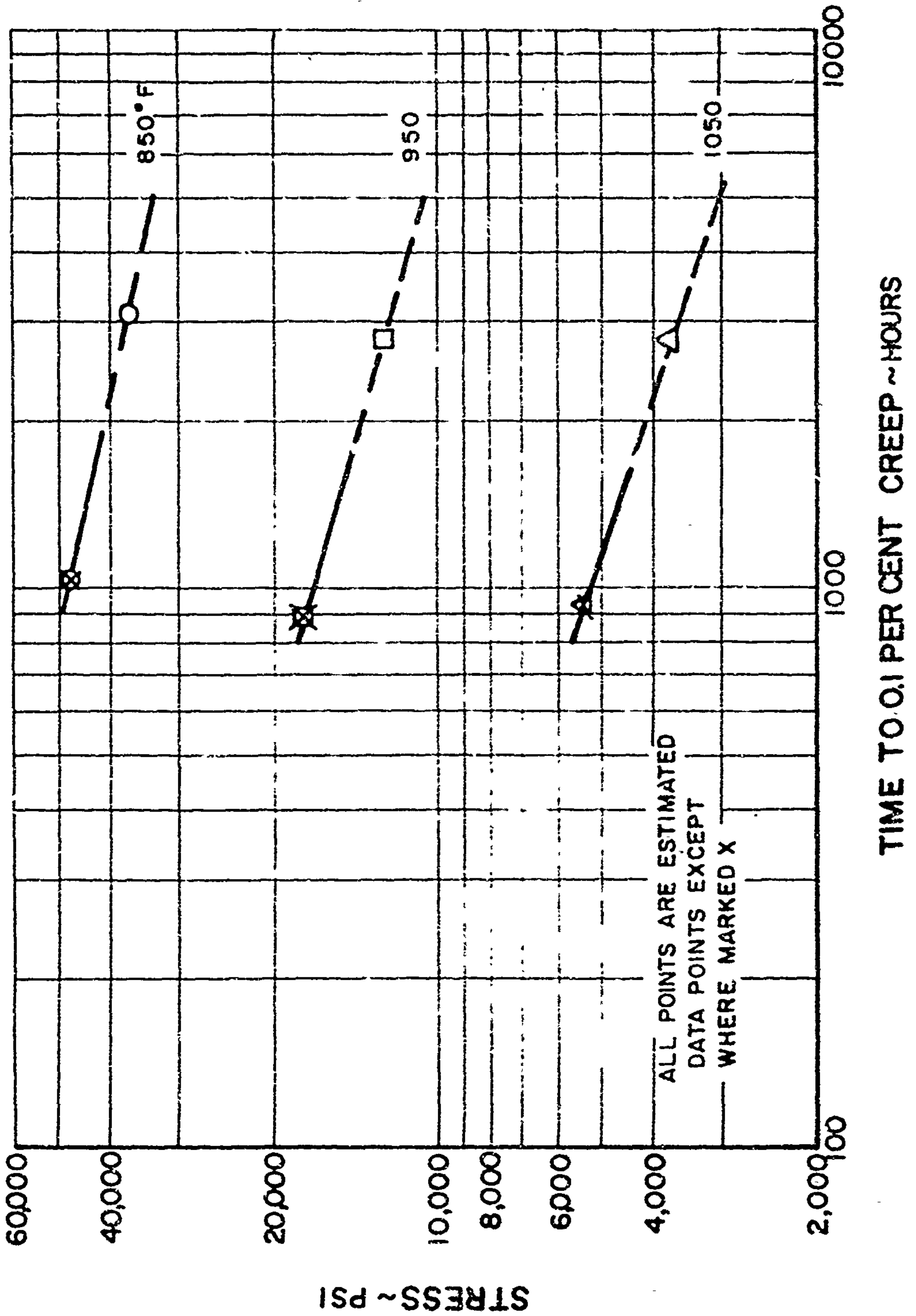

CREEP PROPERTIES OF PWA 1203 TITANIUM ALLOY

Figure 15-26

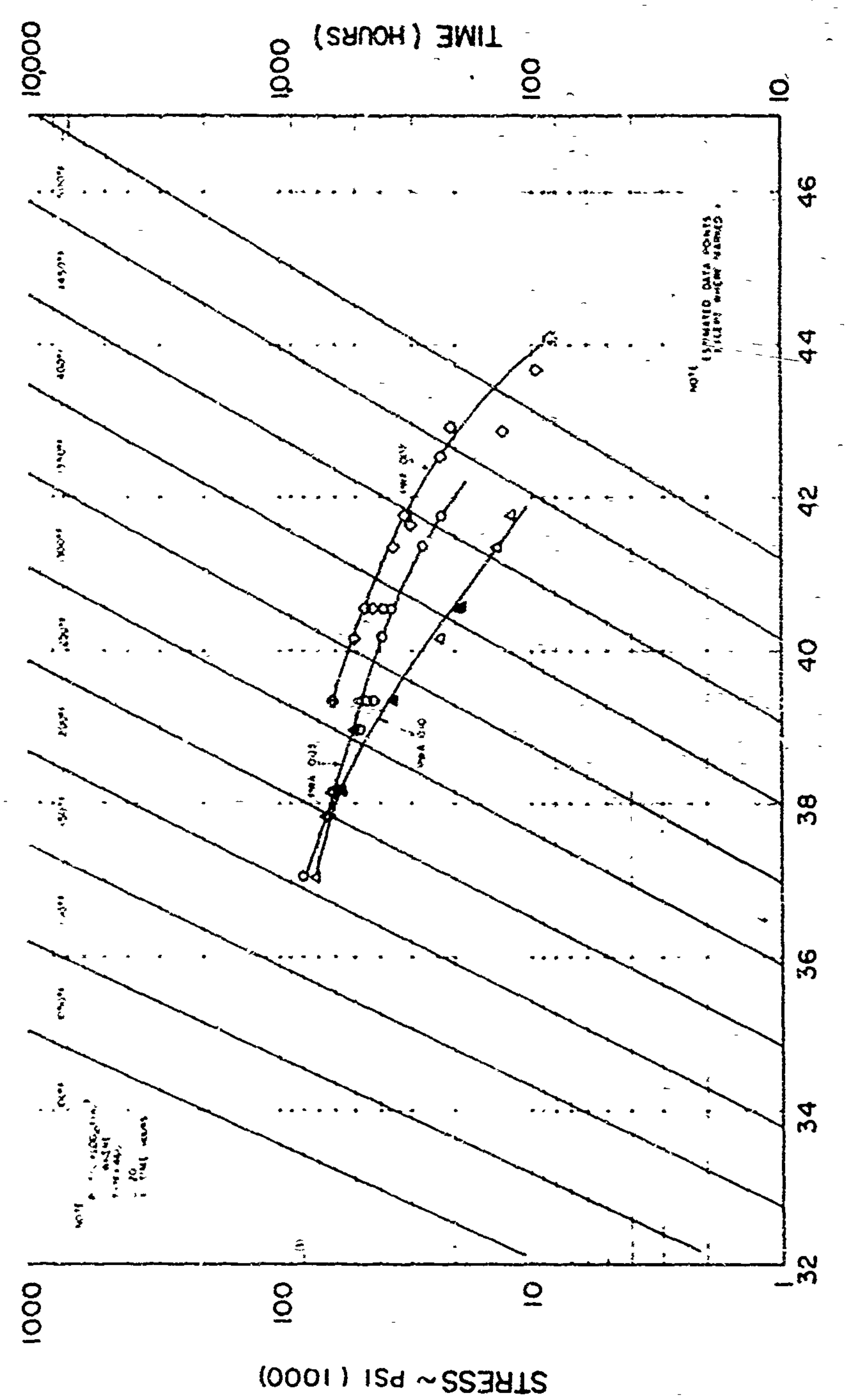

LARSON MILLER PLOT OF TIME TO 0.1% CREEP FOR NICKEL-BASE ALLOYS

Figure 15-27

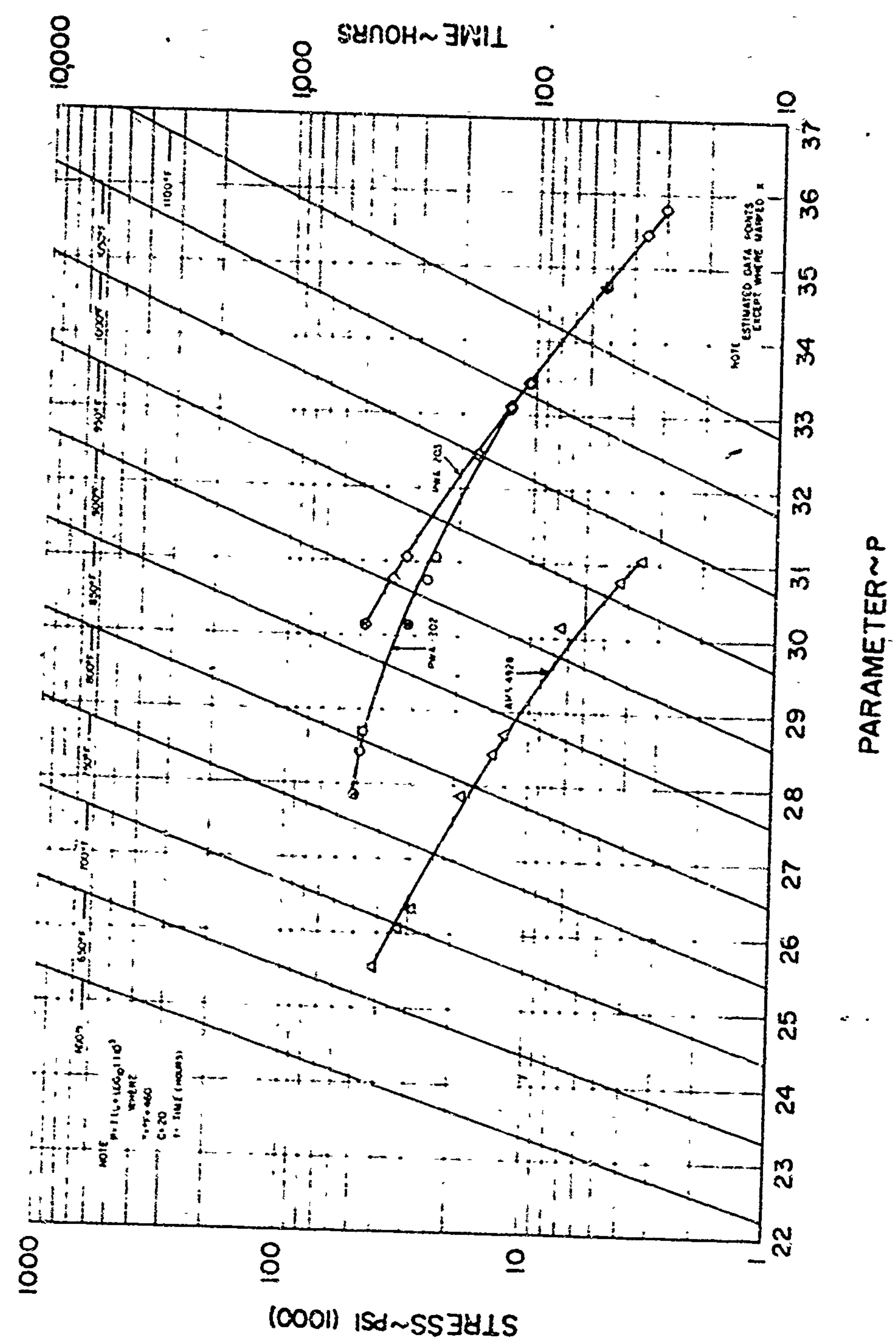

LARSON MILLER PLOT OF TIME TO 0. 1% CREEP FOR TITANIUM ALLOYS

Figure 15-28

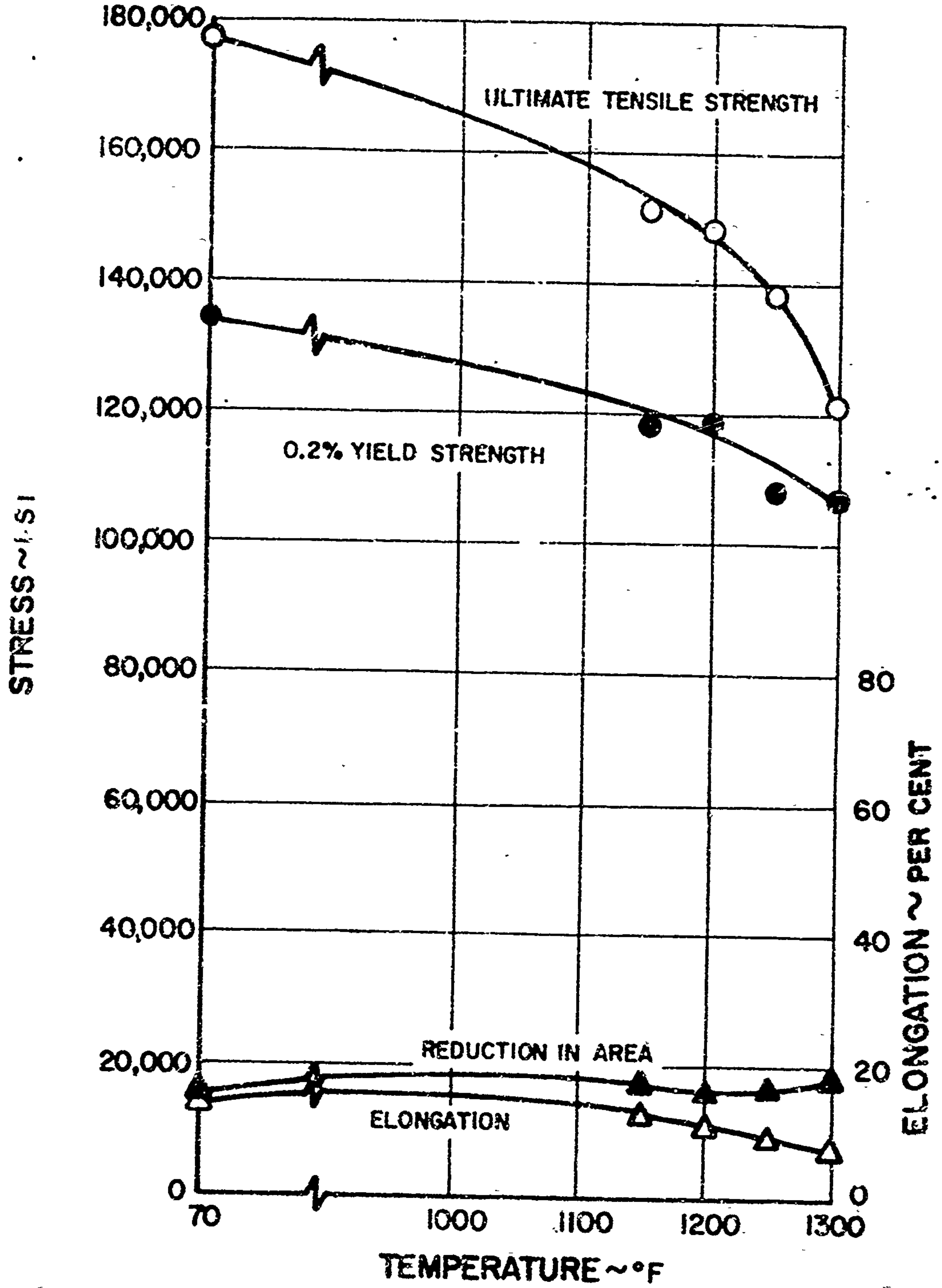

TENSILE PROPERTIES OF PWA 1003 NICKEL-BASE ALLOY HEAT ABET

Figure 15-29

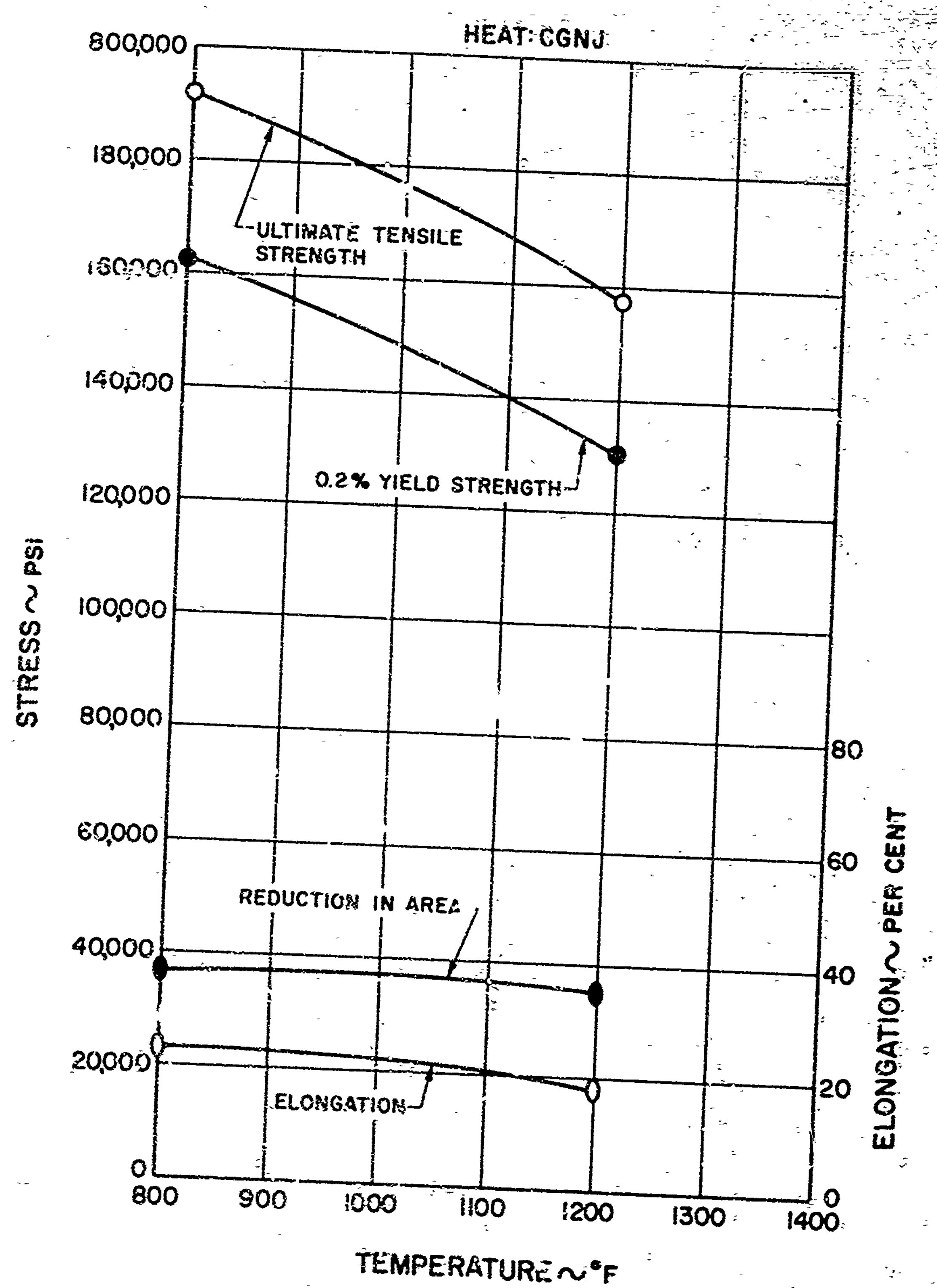

TENSILE PROPERTIES OF PWA 1010 NICKEL-BASE ALLOY HEAT CGNJ

Figure 15-30

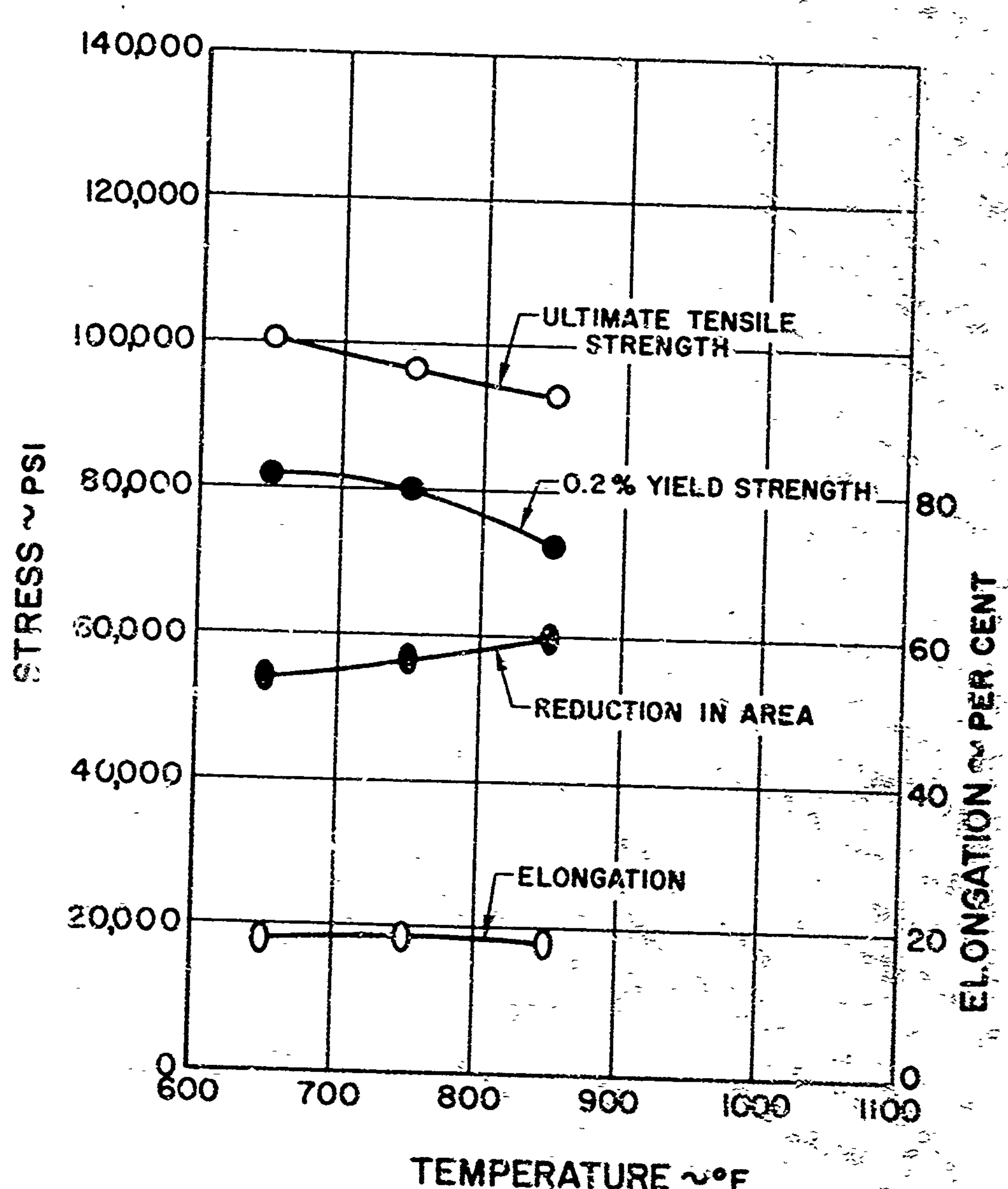

TENSILE PROPERTIES OF AMS 4928 TITANIUM-BASE ALLOY

Figure 15-31

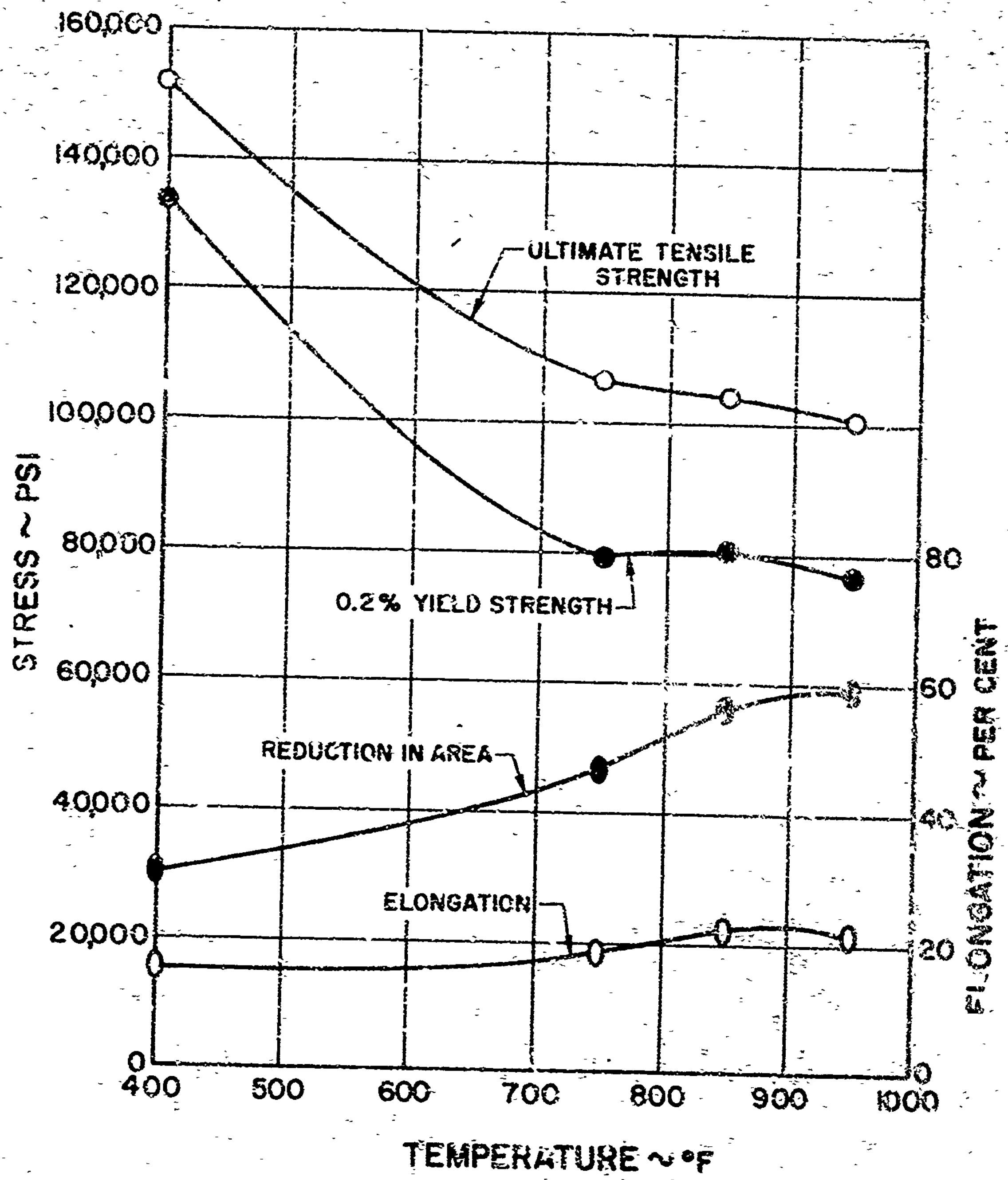

TENSILE PROPERTIES OF PWA 1202 TITANIUM-BASE ALLOY

Figure 15-32

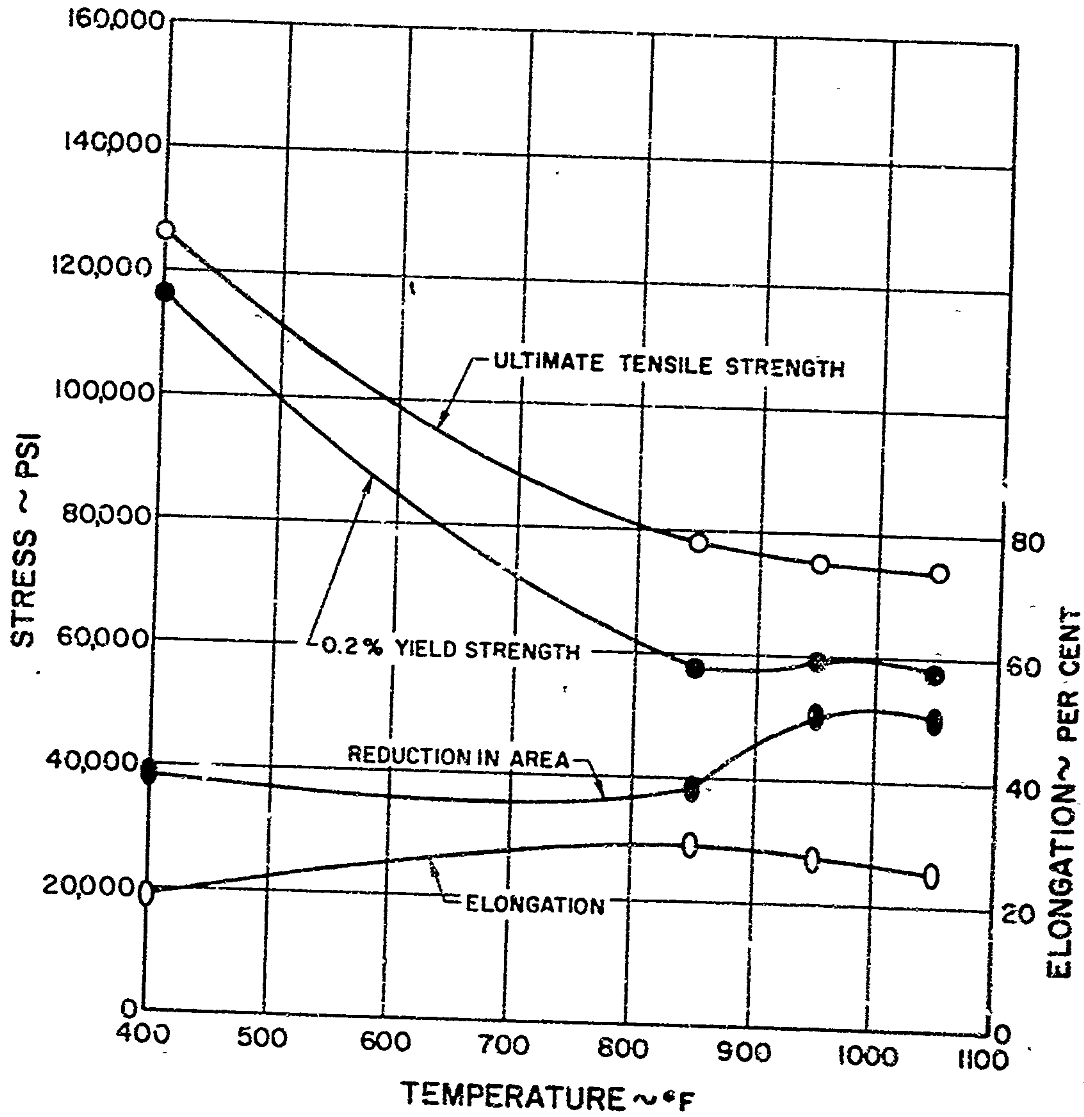

TENSILE PROPERTIES OF PWA 1203 TITANIUM-BASE ALLOY

Figure 15-33

Tensile Test (70° F)	U. T. S. (psi)	Y. S. (psi)	Elong. (%)	RA (%)	Hardness (R_c)
PWA 1202					
TMCA	157,000	150,000	17	32	34/37
MDL	158,300	142,000	15	25.4	35/36
Min. Spec.	130,000	120,000	10	20	39 max.
AMS 4928					
TMCA	132,800	123,600	13	36	33
MDL	144,700	134,300	15	40	33.0/33.5
Min. Spec.	130,000	120,000	10	25	39 max.

Composition	C	N_2	H_2	O_2	Fe	Al	V	Mo	Ti
PWA 1202									
TMCA	0.023	0.016	0.007	0.08	0.07	7.8	1.0	1.0	Rem.
MDL	0.03	0.012	0.008	0.109	<0.3	8.20	0.86	0.88	Rem.
Spec.	0.08 max.	0.05 max.	0.015 max.	0.12 max.	0.30 max.	7.30 8.50	0.75 1.25	0.75 1.25	Rem.
AMS 4928									
TMCA	0.040	0.018	0.0088		0.18	6.12	4.05	--	
MDL	0.03	0.016	0.009	0.087	<0.3	6.10	4.00	--	
Spec.	0.10 max.	0.05 max.	0.0125 max.	0.20 max.	0.30 max.	5.50 6.75	3.50 4.50	--	

ACCEPTANCE DATA FOR 1.25-INCH BAR STOCK OF PWA 1202 AND AMS 4928 TITANIUM-BASE ALLOYS

Figure 15-34

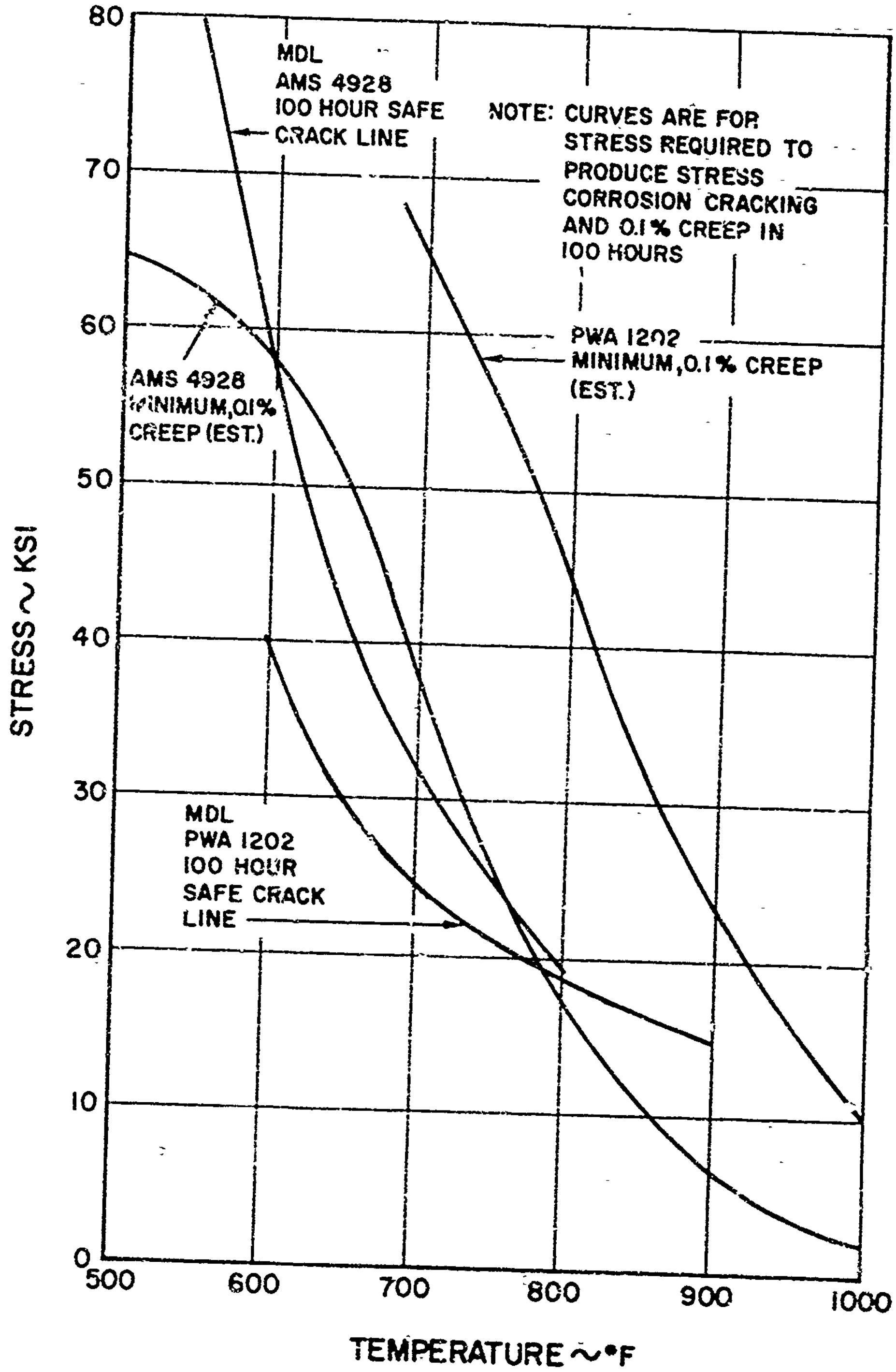

STRESS REQUIRED TO PRODUCE STRESS CORROSION CRACKING AND 0.1% CREEP IN 100 HOURS FOR PWA 1202 AND AMS 4928 TITANIUM-BASE ALLOYS

Figure 15-35

Specimen Number	Material	Temp. (°F)	Ultimate Tensile Strength (psi)	0.2% Yield Strength (psi)	0.02% Yield Strength (psi)	Elongation (Per Cent)	Reduction in Area (Per Cent)
1	AMS 4928	70	143,000	137,500	132,000	13	45
2	AMS 4928	70	142,900	136,800	130,500	12	51
3*	PWA 1202	70	144,000	136,000	123,800	5	13
4*	PWA 1202	70	143,500	137,700	123,800	3	11
5	AMS 4928	70	147,200	-	-	-	46
6	AMS 4928	70	147,800	-	-	16	47
7*	PWA 1202	70	145,400	-	-	12	39
8*	PWA 1202	70	146,500			14	29
9	AMS 4928	70	145,800	135,000	130,000	19	50
10*	AMS 4928	70	142,100	134,000	124,500	20	53
11*	PWA 1202	70	147,200	136,100	124,500	14	28
12*	PWA 1202	70	144,500	133,200	124,200	9	17
13	AMS 4928	70	144,000	136,000	134,000	17	52
14	AMS 4928	70	142,500	134,000	132,000	19	54
15*	PWA 1202	70	144,500	134,000	124,500	9	15
16*	PWA 1202	70	139,500	132,000	113,700	4	10
17*	PWA 1202	70	145,500	135,600	124,300	4	9
18**	PWA 1202	70	139,600	134,000	122,700	22	46
19**	PWA 1202	70	139,200	136,000	134,000	22	46
20**	PWA 1202	70	139,200	135,000	137,000	24	47

* Denotes Presence of Prior Cracks
** Denotes Compressive Stresses Induced in Surface of Specimen and Different Heat of Material

POST-EXPOSURE TENSILE TEST RESULTS

Figure 15-36

Material	Thickness (Inch)	Hardness Rc	Containment Factor At Room Temp.	At 500°F	At 800°F
PWA 1202 (Ti8Al-1Mo-1V)	0.125	33	201	183	178
AMS 5504 (410)	av of 0.070 and 0.110	41	167	143	116
PWA 1030 (Waspaloy)	0.070	20	165	149	144
AMS 5508 (Greek Ascolloy)	0.080	45	160	137	123
AMS 4910 (Ti-5Al-2.5Sn)	0.107	37	150	120	130
PWA 738 (18% Ni Maraging)	0.110	30	149	111	109
PWA 1203 (Ti-5Al-5Sn-5Zr)	0.086	32	142	135	127
AMS 5542 (Inconel X)	0.110	22	141	120	119
AMS 5504	av of 0.070 and 0.110	25	138	110	92
AMS 5515 (302)	0.100	R_B80	137	106	81
AMS 5542	av of 0.073 and 0 110	38	134	120	124
AMS 5524 (316)	0.110	R_B82	132	86	87
AMS 5508	0.080	28	131	108	96
PWA 1030	0.116	21	130	131	112
AMS 5536 (Hastelloy X)	0.120	14	122	112	98
PWA 1030	av of 0.070 and 0.116	42	120	126	122

CONTAINMENT PROPERTIES FOR CANDIDATE CASE MATERIALS

Figure 15-37

Alloy	Heat	Condition	Temp.(°F)	Stress(ksi)	Time to 1% Creep(Hrs)	Present Time(Hrs)	Status % Creep
PWA 658	KJS-105	2000°F(4) + 1600°F(12)	1500	45	1862	Discontinued	
PWA 658	KJS-105	PWA 47* + 1600°F(12)	1600	26	2635	Discontinued	
PWA 658	KJS-105	PWA 47* + 1600°F(12)	1700	16	**3100	2920	0.875
PWA 658	KJS-105	PWA 47* + 1600°F(12)	2000	4	984	Discontinued	
PWA 659	PA1015A	PWA 47 + 1600°F(50)	1600	33	2030	Discontinued	
PWA 659	PA1014A	PWA 47 + 1600°F(50)	1600	35	1445	Discontinued	
PWA 659	PA1014A	PWA 47 + 1600°F(50)	1700	21	**3350	1461	0.471
PWA 659	PA1014A	PWA 47 + 1600°F(50)	1700	23	**3050	1443	0.488
PWA 659	PA956A	PWA 47 + 1600°F(50)	1800	15	**1650	1439	0.798
PWA 659	PA956A	PWA 47 + 1600°F(50)	1900	8.5	** 888	Discontinued	

*Protective coating
**Estimated

CREEP PROPERTIES FOR PWA 658 AND PWA 659 CAST NICKEL-BASE ALLOYS

Figure 15-38

Material	C	Mn	[illegible]	[illegible]	Cr	[illegible]	Mo	[illegible]	[illegible]	[illegible]	Al	Al + Ti	[illegible]	B	Zr	Fe	Cu	N
PWA [illegible] Spec.	[illegible]	[illegible] max.	[illegible] max.	[illegible]	[illegible]	[illegible]	[illegible]	[illegible]	[illegible]	[illegible]	[illegible]	[illegible]	[illegible]	[illegible]	[illegible]	1.00 max.		
Heat K[illegible]	0.1[illegible]	0.0[illegible]	0.0[illegible]	[illegible]	[illegible]	[illegible]	[illegible]	[illegible]	[illegible]	[illegible]	[illegible]	[illegible]	[illegible]	[illegible]	0.08	0.42		
PWA [illegible] Spec.	[illegible]	[illegible] max.	[illegible] max.	[illegible]	[illegible]	[illegible]	[illegible]	[illegible]	[illegible]	[illegible]	[illegible]	[illegible]	[illegible]	[illegible]	0.03-0.08	1.50 max.	0.12 max.	-
Heat PA [illegible]A	0.11	[illegible]	[illegible]	[illegible]	[illegible]	[illegible]	[illegible]	[illegible]	[illegible]	[illegible]	[illegible]	[illegible]	[illegible]	0.015	0.047	0.20	0.1	0.005
Heat PA [illegible]HA	0.11	[illegible]	[illegible]	[illegible]	[illegible]	[illegible]	[illegible]	11.8	[illegible]	[illegible]	[illegible]	[illegible]	[illegible]	0.015	0.054	0.11	<0.1	0.008
Heat PA [illegible]SA	0.10	[illegible]	0.005	[illegible]	[illegible]	[illegible]	[illegible]	12.0	[illegible]	[illegible]	[illegible]	[illegible]	[illegible]	0.014	0.047	0.15	0.1	0.005

CHEMICAL COMPOSITIONS OF CREEP SPECIMENS

Figure 15-39

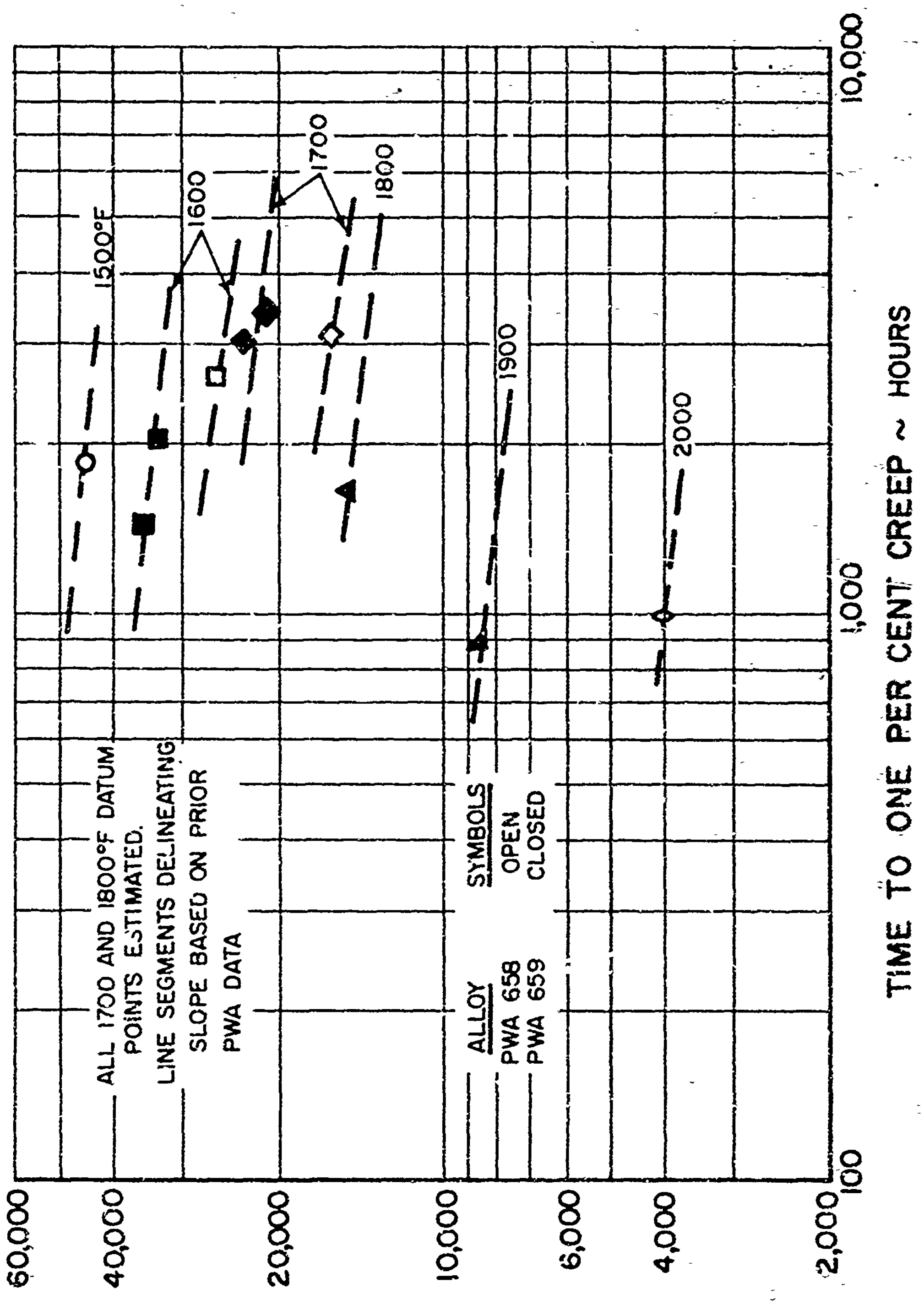

CREEP PROPERTIES OF PWA 658 AND PWA 659 CAST NICKEL-BASE ALLOYS

Figure 15-40

Alloy	Heat Treatment	Density (lb/in.^{3})
PWA 655 (Inco 713)	2000° F(4) + 1600° F(12)	0.286
PWA 658 (IN 100)	2000° F(4) + 1600° F(12)	0.282
PWA 659 (Mar-M200, SM200)	2000° F(4) + 1600° F(50)	0.308
PWA 663 (B-1900A)	2000° F(4) + 1600° F(50)	0. [illegible]
PWA 689 (U700)	2150° F(4) + 1975° F(4) + 1550° F(24) + 1400° F(16)	0. [illegible]

HEAT TREATMENTS AND DENSITIES FOR CANDIDATE ALLOYS

Figure 15-41

MATERIAL	HEAT TREATMENT
PWA 655	2000°F(4) + 1600°F(12)
PWA 658	2000°F(4) + 1600°F(12)
PWA 659	2000°F(4) + 1600°F(50)
PWA 663	2000°F(4) + 1600°F(50)
PWA 689	2150°F (4) + 1975°F(4) + 1550°F(24) + 1400°F(16)

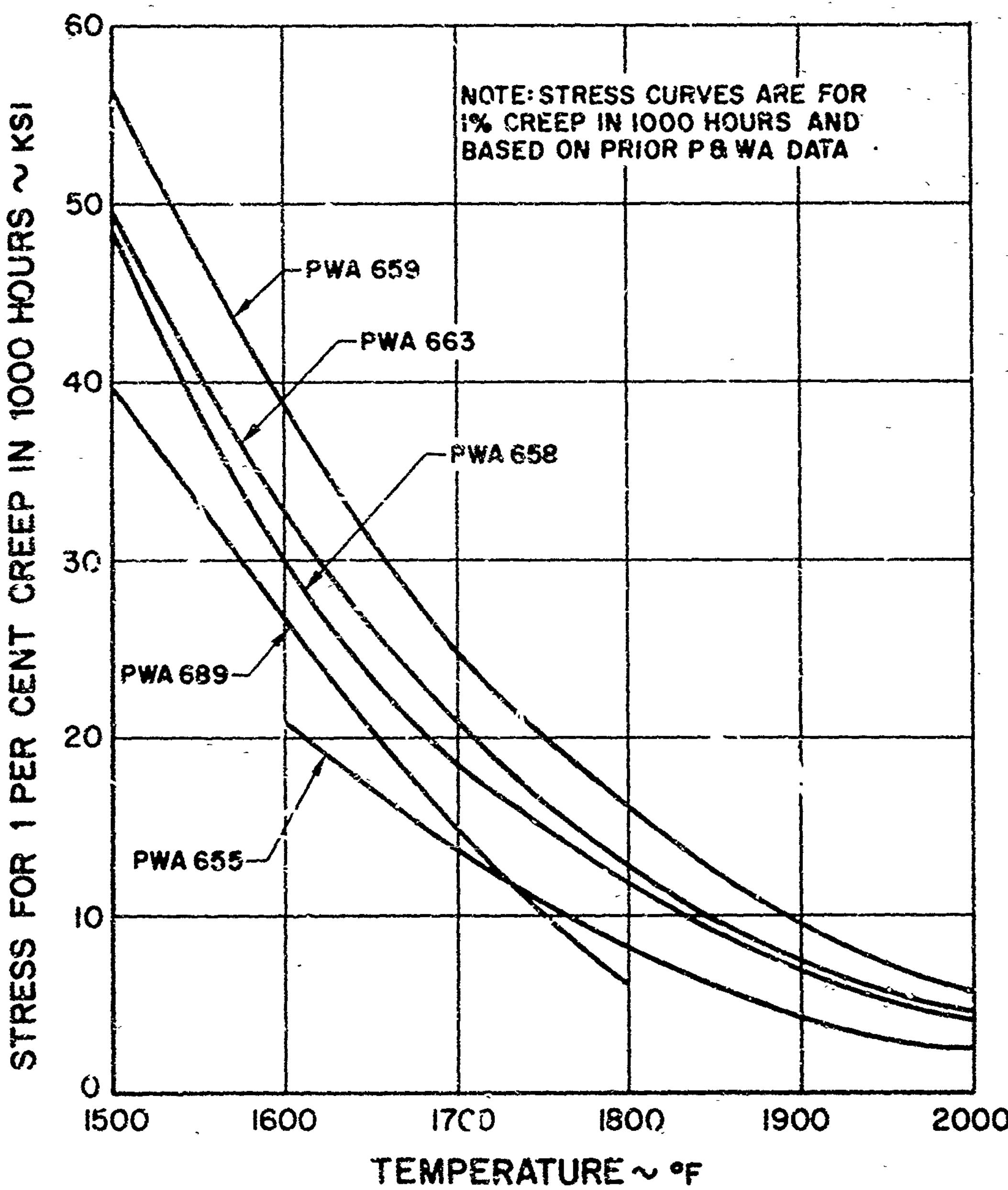

STRESS FOR 1% CREEP IN 1000 HOURS FOR HEAT-TREATED NICKEL-BASE ALLOYS

Figure 15-42

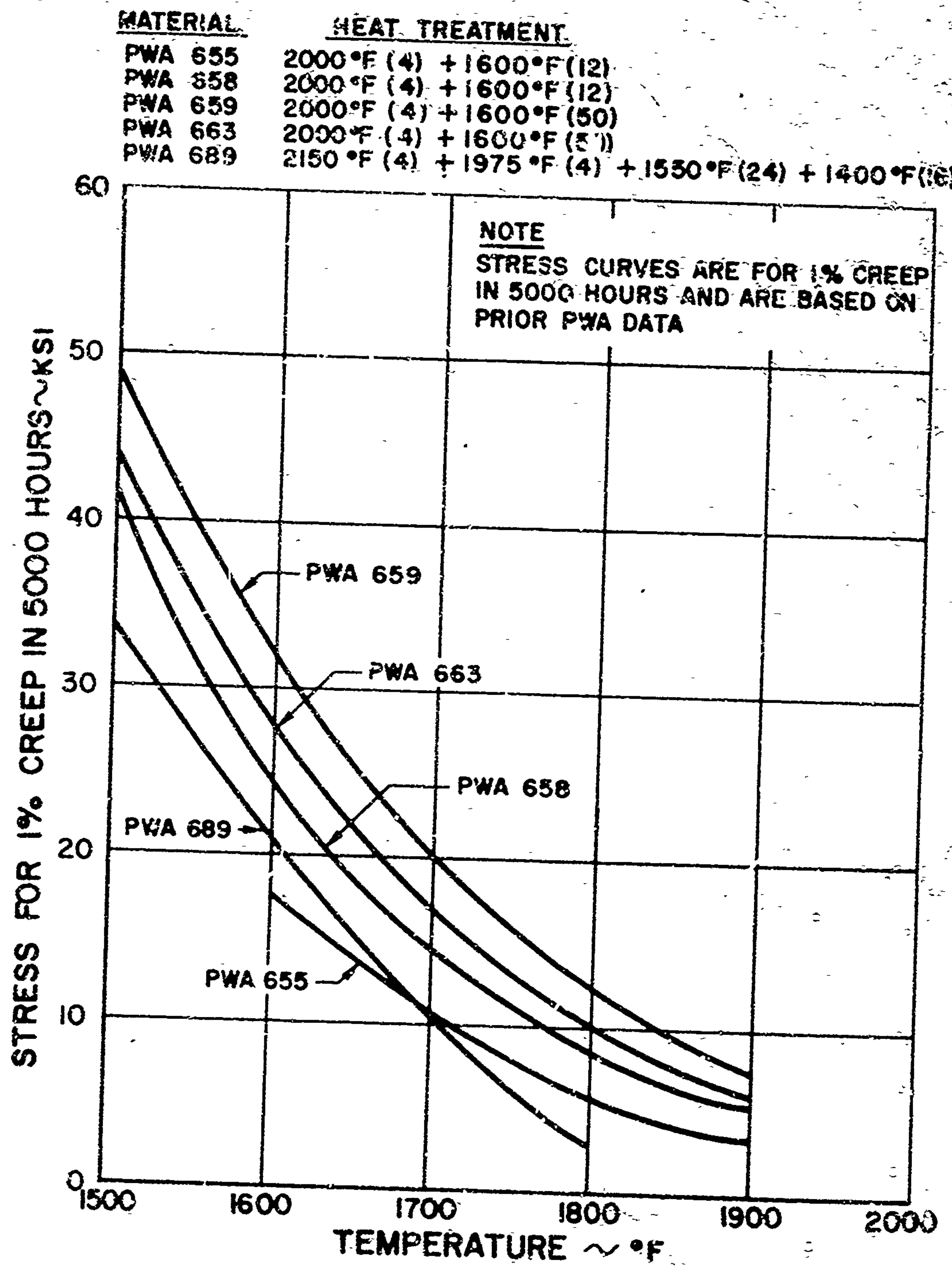

STRESS FOR 1% CREEP IN 5000 HOURS FOR HEAT-TREATED NICKEL-BASE ALLOYS

Figure 15-43

Temperature (°F)	Alloy and No. and Type of Tests			
	PWA 657	PWA 663 Fine-Grained	PWA 663 Coarse-Grained	PWA 659
1300	12C* 4T 4I	12C 4T 4I	12C 4T 4I	-- -- --
1500	12C 4T 4I	12C 4T 4I	12C 4T 4I	6C 2T 2I
1700	12C 4T 4I	12C 4T 4I	12C 4T 4I	-- -- --

*C = cyclic testing at three thermal-fatigue-life levels (10, 100, and 1000 cycles)
T = tensile test for stress-strain curve
I = impact test

THERMAL FATIGUE TEST PROGRAM

Figure 15-44

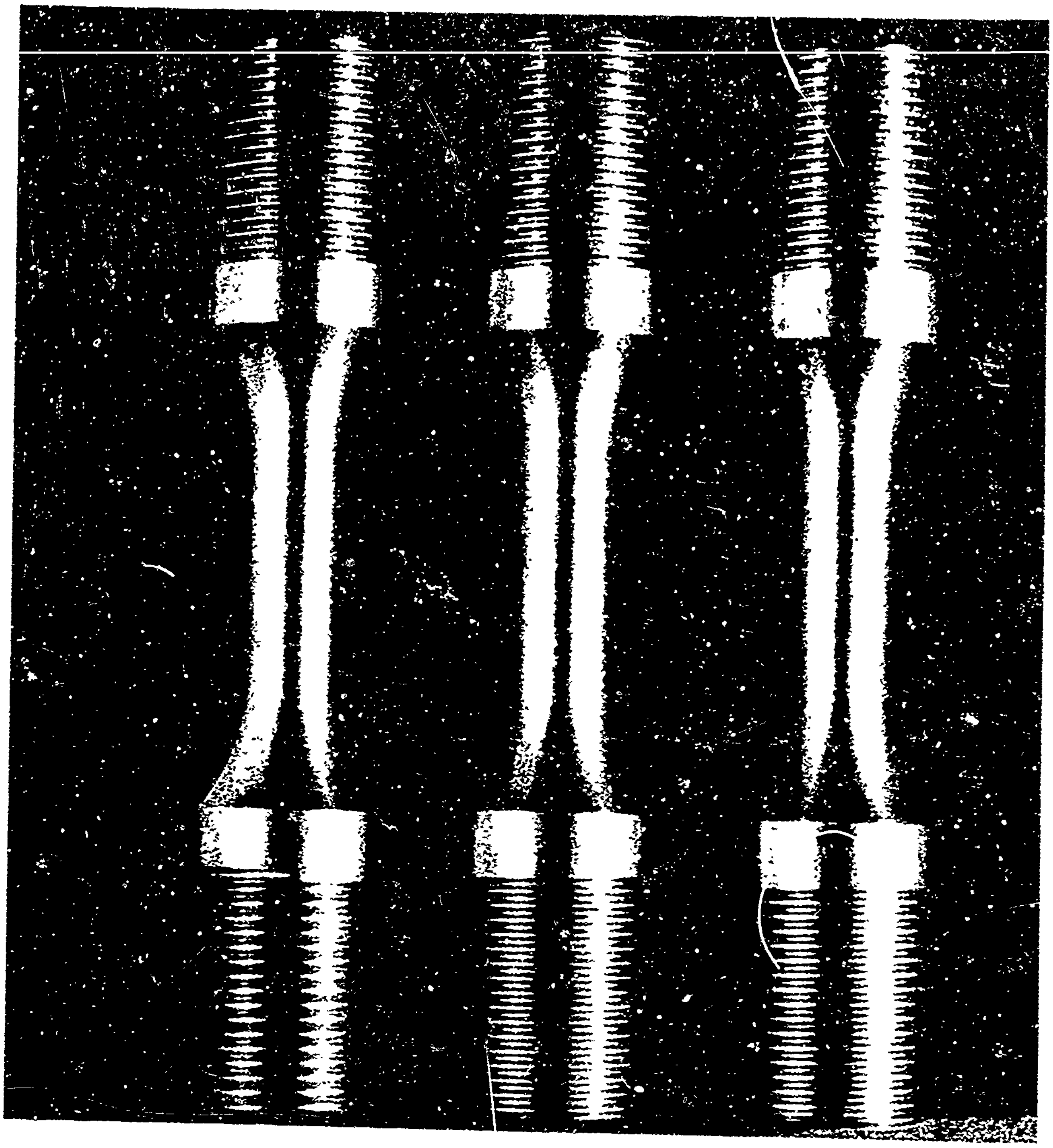

TYPICAL PWA 657, PWA 659, A[illegible] MAL FATIGUE SPECIMENS BEFORE CO[illegible] TESTING. PARALLEL GAGE SECTION IS 1" LONG WITH 0.480" OD AND 0.320" ID.

Figure 15-45

Material	Source	Heat Code	Coating	Temperature	Specimens Tested
PWA 657	PWA Foundry	- - -	none	1300F	8
PWA 663 1/32"-1/16" Grain Size	Austenal	54V3549	PWA47-14L	1700F	4
PWA 663 1/8"-1/4" Grain Size	Austenal	54V3240	PWA47-14L	1300F 1700F	9 10
PWA 659	Martin Metals	A1106	PWA47-14L	1300F	2

NOTE: Specimens tested at 1300F are coated on the outside only. Those tested at 1700F are coated on both the inside and outside

THERMAL FATIGUE DATA FOR COMPLETED SPECIMENS

Figure 15-46

Alloy	Specimen Number	Temp (°F)	Total Strain	Cycles To Failure	Grain Size (Inch)	Remarks
PWA 657	71	1300	-	-	1/8	failed on overload
	72	1300	-	1	1/8	faulty material
	73	1300	0.0159	9	1/8	
	74	1300	0.0055	30	1/8	
	75	1300	0.0075	4430	1/8	discontinued
	76	1300	0.0090	190	1/8	3400 previous cycles
	77	1300	0.0040	2735	1/8	
	78	1300	0.0080	11	1/8	
PWA 66[illegible]	31	1300	0.0074	3330	1/8 to 1/4	load increased
	31	1300	0.0167	107	1/8 to 1/4	
	32	1300	0.0077	1993	1/8 to 1/4	load increased
	32	1300	0.0134	125	1/8 to 1/4	
	33	1300	0.0115	1114	1/8 to 1/4	
	35	1300	0.0116	848	1/8 to 1/4	
	36	1300	0.0094	3296	1/8 to 1/4	
	37	1300	0.0102	3139	1/8 to 1/4	
	38	1300	0.0163	70	1/8 to 1/4	
	39	1300	0.0320	7	1/8 to 1/4	
	310	1300	0.0275	12	1/8 to 1/4	
	312	1700	0.0157	108	1/8 to 1/4	
	313	1700	0.0097	629	1/8 to 1/4	
	314	1700	0.0099	786	1/8 to 1/4	
PWA 6[illegible]3	315	1700	0.0149	121	1/8 to 1/4	
	317	1700	0.0245	28	1/8 to 1/4	
	318	1700	0.0100	1008	1/8 to 1/4	
	319	1700	0.0300	17	1/8 to 1/4	
	320	1700	0.0350	7	1/8 to 1/4	
	321	1700	0.0940	2330	1/8 to 1/4	
	322	1700	0.0380	8	1/8 to 1/4	
PWA 663	31F	1700	0.0364	6	1/32 to 1/16	
	32F	1700	0.0063	2880	1/32 to 1/16	load increased
		1700	0.0123	75	1/32 to 1/16	
	33F	1700	0.0137	110	1/32 to 1/16	
	34F	1700	0.0140	416	1/32 to 1/16	
PWA 659	91	1300	0.0177	10	1/8	
	92	1300	0.0137	209	1/8	

THERMAL FATIGUE DATA

Figure 15-47

Base Metal	Coating
PWA 653	PWA 45
PWA 657	PWA 45
PWA 658	PWA 47
PWA 658	$TaAl_3$
PWA 659	PWA 47
PWA 659	$TaAl_3$
PWA 663	PWA 47
PWA 663	$TaAl_3$

SPECIMENS BEING SUBJECTED TO EROSION TESTING

Figure 15-48

Alloy	Ident.	Heat	Heat Treatment Prior to Exposure	Temp. (°F)	Time (Hrs.)
PWA 658	81	KJS-105	2000°F(4) + 1600°F(12)	1500	1004.6
	82	KJS-103	2000°F(4) + 1600°F(12)	1500	1265.6
	83	KJS-103	2000°F(4) + 1600°F(12)	1600	1383.7
	84	KJS-105	2000°F(4) + 1600°F(12)	1600	1722.0
	85	KJS-105	2000°F(4) + 1600°F(12)	1700	1481.5
	86	KJS-105	2000 F(4) + 1600°F(12)	1800	1343.4
	87	KJS-103	2000°F(4) + 1600°F(12)	1900	543.8
	88	KJS-103	2000°F(4) + 1600°F(12)	2000	548.0
	89	KJS-105	2000°F(4) + 1600°F(12)	1900	2517.5
	810	KJS-103	2000°F(4) + 1600°F(12)	2000	910.0
	-	KJS-103	2000°F(4) + 1600°F(12)	No Exposure	
PWA 659	91	PA-992A	2000°F(4) + 1600°F(50)	1500	1795.8
	92	PA-991A	2000°F(4) + 1600°F(50)	1600	2397.6
	93	PA-991A	2000°F(4) + 1600°F(50)	1700	1915.2
	94	PA-991A	2000°F(4) + 1600°F(50)	1800	1619.8
	95	PA-991A	2000°F(4) + 1600°F(50)	1900	536.0
	96	PA-996A	2000°F(4) + 1600°F(50)	2000	1790.0
	97	PA-991A	2000°F(4) + 1600°F(50)	1900	1654.6
	98	PA-991A	2000°F(4) + 1600°F(50)	2000	1552.1
	-	PA-1014A	2000°F(4) + 1600°F(50)	No Exposure	
PWA 663	31	T-1349	2000 F(4)	1500	576.0
	32	T-1347	2000 F(4)	1600	1795.5
	33	T-1347	2000°F(4)	1700	1481.2
	34	T-1349	2000°F(4)	1800	908.2
	35	T-1348	2000°F(4)	1900	497.4
	36	T-1349	2000°F(4)	2000	806.4
	37	T-1348	2000°F(4) + 1600 °50)	1900	1450.0
	38	T-1347	2000°F(4) + 1600°(50)	1800	1000.0
	39	T-1349	2000°F(4) + 1600°F(50)	1500	436.6
	310	T-1347	2000°F(4) + 1600°F(50)	1700	1482.9
	311	T-1348	2000 F(4) + 1600°F(50)	1600	2322.5
	312	T-1349	2000°F(4) + 1600°F(50)	2000	498.0
	-	T-1443	2000°F(4)	No Exposure	
PWA 689	8918	VNWX	2150°F(4) + 1975°F(4) + 1550°F(24) + 1400°F(16)	1500	1097.5
	8918	VNWX	2150°F(4) + 1975°F(4) + 1550°F(24) + 1400°F(16)	No Exposure	
	8917	VNWX	2150°F(4) + 1975°F(4) + 1550°F(24) + 1400°F(16)	1600	1104.6
	8917	VNWX	2150°F(4) + 1975°F(4) + 1550°F(24) + 1400°F(16)	No Exposure	

SPECIMEN HEAT TREATMENTS AND EXPOSURE CONDITIONS

Figure 15-49

Ident.	Alloy	Exposure Temp. (°F)	Large-Particle Residue MC	Large-Particle Residue M_6C	Large-Particle Residue $M_{23}C_6$	Large-Particle Residue M_3B_2	Small-Particle Residue MC	Small-Particle Residue M_6C	Small-Particle Residue $M_{23}C_6$	Small-Particle Residue M_3B_2	Small-Particle Residue Sigma
81	PWA 658	1500	14		5		12		11		1
82	PWA 658	1500	8		6		9		12-1/2		1
83	PWA 658	1600	6		4		7		15		
84	PWA 658	1600	7		8		7		15		
85	PWA 658	1700	7		15		6		16	1	
86	PWA 658	1800	1		25		1/2		20		
87	PWA 658	1900	4		18		4		18		
89	PWA 658	1900	2-1/2		25		9		18		
88	PWA 658	2000	20		5		18		5		
810	PWA 658	2000	All MC				All				
91	PWA 659	1500	18		6		18		6		
92	PWA 659	1600	20		4		18		5		
93	PWA 659	1700	6		6		11	1-1/2	3-1/2		
94	PWA 659	1800	11	12	7						
95	PWA 659	1900	18	10	4						
97	PWA 659	1900	8	45	3		16	18	2-1/2	TiN	
96	PWA 659	2000	4	45	2		3	17	5		
98	PWA 659	2000	5	40	1		14	14	2-1/2	TiN	
31	PWA 663	1500	24	4	3	1-1/2	24	3	3	2	
39	PWA 663	1500	40	5	3	2-1/2	20	3	3	1-1/2	
32	PWA 663	1600	24	12	2	1-1/2	21	7-1/2	1	1-1/2	
311	PWA 663	1600	24	12	1-1/2	2	30	8	1-1/4	1-1/4	
33	PWA 663	1700	16	16	1-1/2	1-1/2	20	16		2	
310	PWA 663	1700	14	14	9	2	30	18	1/2	1-1/2	
34	PWA 663	1800	26	16	1/2	1	19	10		1/2	
38	PWA 663	1800	16	20	3-1/2	2	24	24	2	1-1/2	
35	PWA 663	1900	13	16		1	18	16		1-1/2	
36	PWA 663	2000	17	15		2-1/2	22	9		1	
312	PWA 663	2000	13	17		2	22	9		2	
8918	PWA 689	1500	2		5-1/2	2	1-1/2		5	2	
8917	PWA 689	1600	3		5	4	1/4		6	1	

X-RAY DIFFRACTION RESULTS

Figure 15-50

Ident	Alloy	Exposure Temp (°F)	Residue	Mo	Zr	Ni	Co	Fe	Cr	Ti
-	PWA 658	-	Large	9.96	1.28	1.76	1.34	0.19	2.82	5.25
			Small	8.58	1.15	0.96	0.56	0.13	2.46	4.74
81	PWA 658	1500	Large	9.73	0.96	4.29	2.69	0.20	7.68	5.38
			Small	6.14	0.61	3.01	2.37	0.39	10.70	4.67
82	PWA 658	1500	Large	9.73	1.02	3.14	3.14	0.13	9.95	4.22
			Small	7.30	0.51	3.07	2.37	0.13	13.80	2.82
83	PWA 658	1600	Large	10.24	0.77	3.39	3.90	0.13	15.10	3.0
			Small	11.40	0.51	2.69	2.75	0.15	14.30	1.46
84	PWA 658	1600	Large	10.10	0.64	4.80	5.98	0.32	15.90	2.30
			Small	6.01	0.38	3.58	3.20	0.20	15.10	1.42
85	PWA 658	1700	Large	8.06	0.77	3.65	2.43	0.13	7.42	1.23
			Small	5.12	0.38	2.82	2.05	0.13	14.60	0.82
86	PWA 658	1800	Large	11.50	0.89	4.54	3.20	0.07	33.10	0.69
			Small	1.45	0.13	2.18	1.54	0.13	13.66	0.32
87	PWA 658	1900	Large	5.89	0.38	2.11	1.50	0.10	12.30	1.14
			Small	2.62	0.06	2.02	1.34	0.10	10.50	0.61
89	PWA 658	1900	Large	9.47	0.25	2.59	1.92	0.11	16.10	1.04
			Small	3.97	0.06	2.18	1.60	0.13	12.80	1.17
88	PWA 658	2000	Large	3.86	0.25	0.82	0.45	0.06	1.28	2.94
			Small	3.14	0.13	1.15	1.12	0.13	4.22	2.08
810	PWA 658	2000	Large	3.01	0.13	0.77	0.14	0.18	0.42	2.78
			Small	1.02	0.09	0.21	0.05	0.15	0.26	1.15

Ident	Alloy	Exposure Temp (°F)	Residue	Cb	Zr	W	Ni	Co	Fe	Cr	Ti
	PWA 659	-	Large	17.50	0.89	2.82	1.38	0.12	0.06	1.15	1.31
			Small	2.21	0.51	[illegible]	0.51	0.18	0.10	0.85	0.11
91	PWA 659	1500	Large	8.74	0.89	3.84	2.18	0.38	0.26	3.71	1.02
			Small	2.45	0.25	1.28	0.98	0.40	0.12	3.20	0.36
92	PWA 659	1600	Large	7.30	1.28	2.56	2.12	0.85	0.50	2.62	1.06
			Small	2.11	0.51	1.97	0.98	0.21	0.10	1.34	0.38
93	PWA 659	1700	Large	5.64	1.15	2.94	3.71	1.22	0.08	5.76	0.52
			Small	1.60	0.38	1.62	0.80	0.32	0.1[illegible]	1.60	0.28
94	PWA 659	1800	Large 1	2.56	0.63	1.98	2.18	0.96	0.10	4.86	0.40
			Large 2	8.66	0.89	3.20	3.65	1.70	0.10	5.12	0.67
			Small	0.85	0.25	1.07	2.46	0.59	0.10	1.92	0.17
95	PWA 659	1900	Large	10.7	1.43	3.18	3.52	1.54	0	1.12	1.28
			Small	1.41	0.39	1.02	1.33	0.34	0.10	0.30	0.20
97	PWA 659	1900	Large	4.86	0.27	3.84	9.86	5.25	0.07	1.35	0.34
			Small	2.11	0.25	1.60	1.89	0.66	0.13	0.61	0.40
96	PWA 659	2000	Large	7.54	0.13	3.58	12.80	8.64	0	2.75	0.27
			Small	0.61	0.12	3.28	1.70	0.64	0.10	0.93	0.05
98	PWA 659	2000	Large	[illegible]	0.25	6.38	13.31	6.14	0	3.33	0.65
			Small	6.96	0.13	3.14	3.71	0.80	0.16	0.91	0.22

Ident	Alloy	Exposure Temp (°F)	Residue	Mo	Zr	Ni	Co	Fe	CrKβ1	CrKα TaLβ(2)	TaLβ12	Ti
	PWA 663	---	Large	9.09	1.15	6.66	1.92	0.32	0.26	1.31	0.88	0.35
			Small	3.65	0.58	2.14	0.54	0.13	0.10	0.64	0.55	0.28
31	PWA 663	1500	Large	8.70	1.10	4.13	1.54	0.07	0.70	3.58	1.82	0.58
			Small	4.48	0.77	2.30	0.93	0.10	0.61	3.26	0.93	0.48

X-RAY FLOURESCENCE RESULTS

Figure 15-51 Sheet 1 of 2

Ident	Alloy	Exposure Temp (°F)	Residue	Mo	Zr	Ni	Co	Fe	CrKβ1	CrKα TaLβ(2)	TaLβ12	Ti
39	PWA 663	1500	Large	7.81	1.16	3.61	1.47	0.10	0.67	3.46	1.41	0.58
			Small	5.25	0.90	2.18	0.90	0.13	0.54	2.69	0.93	0.45
32	PWA 663	1600	Large	7.17	.69	5.38	2.59	0.51	0.98	2.37	0.66	0.30
			Small	6.54	0.64	3.33	1.63	0.13	0.29	1.59	0.69	0.34
311	PWA 663	1600	Large	6.53	.86	3.90	1.82	0.13	0.43	2.02	0.72	0.34
			Small	3.99	0.70	2.40	1.12	0.15	0.32	1.38	0.48	0.28
33	PWA 663	170	Large	16.6	1.41	19.2	6.40	0.23	0.86	3.10	0.84	0.40
			Small	6.14	0.51	6.34	2.56	0.16	0.35	1.82	0.49	0.26
310	PWA 663	1700	Large	7.81	1.02	7.04	3.07	0.16	0.42	2.32	0.45	0.21
			Small	6.02	0.77	5.38	2.40	0.13	0.32	1.60	0.66	0.32
34	PWA 663	[illegible]	Large	17.1	1.26	14.6	5.76	0.0	0.32	2.94	0.99	0.37
			Small	2.1	0.32	2.18	0.83	0.17	0.14	1.10	0.18	0.10
38	PWA 663	1800	Large	18.7	1.26	14.3	6.53	0.56	1.34	6.02	0.61	0.22
			Small	5.89	0.25	5.31	2.30	0.10	0.48	2.30	0.29	0.14
35	PWA 663	1900	Large	19.7	1.15	15.9	5.63	0.13	0.61	2.88	0.77	0.27
			Small	4.22	0.25	4.67	1.54	0.13	0.22	0.99	0.27	0.18
36	PWA 663	2000	Large	12.5	0.64	9.34	2.82	0.07	0.29	1.6	1.04	0.36
			Small	2.50	0.26	2.24	0.67	0.13	0.13	0.54	0.40	0.22
312	PWA 663	2000	Large	17.9	0.65	11.3	3.14	0.45	0.58	2.48	0.78	0.30
			Small	5.97	0.45	3.20	1.09	0.22	0.36	1.86	0.59	0.33

Ident	Alloy	Exposure Temp (°F)	Residue	Mo	Zr	Ni	Co	Fe	Cr	Ti
8926	PWA 689	-	Large	1.66	0.13	2.45	2.30	0.58	2.53	0.83
			Small	1.60	0.13	1.22	0.61	0.06	3.46	0.94
8918	PWA 689	1500	Large	4.35	0.06	1.60	0.96	0.16	6.02	1.15
			Small	1.41	0.03	0.93	0.51	0.16	3.33	0.36
8917	PWA 689	-	Large	1.26	0.13	2.43	0.86	0.36	2.87	0.91
			Small	1.98	0.03	1.76	0.86	0.06	4.93	1.20
8917	PWA 689	1600	Large	2.50	0.13	1.60	0.96	0.13	5.89	0.67
			Small	1.18	0.03	1.12	0.56	0.13	4.54	0.24

X-RAY FLOURESCENCE RESULTS

Figure 15-51 Sheet 2 of 2

ITEM 16 - OPERATIONS AND ECONOMICS

OBJECTIVE

This item of the contract requires that Pratt & Whitney Aircraft perform the following tasks in the areas of operations and economics:

a. In conjunction with the airframe manufacturer, establish the engine configuration to ensure that the supersonic transport has the best combination of range and payload capabilities.

b. Evaluate the economic aspects of alternate engine configurations and design changes.

c. Prepare sales price and spare parts estimates for use by the Airframe Contractors and the Government in supersonic transport system economics studies. The Contractor will also conduct analyses to determine engine operating costs and their effect on the overall economics of the supersonic transport.

The goal of this program is to establish the powerplant economic factors needed to optimize the design of the SST configurations being proposed by the Airframe Contractors.

A. INTRODUCTION

The overall economics of the supersonic transport will be greatly affected by the engine. However, the engine is not an independent variable since it must be compatible with the various requirements created by the aircraft. The aerodynamic and structural capabilities of the aircraft set the goal for the engine design.

When studying the engine's contribution to aircraft direct operating costs, it is helpful to examine historical trends for factors which may affect projections to the supersonic era. Historical trends in relation to airplane capacity and the engine's portion of aircraft direct operating costs are shown in Figures 16-1 and 16-2.

One of the major reasons why transport aircraft have improved in their ability to provide economical transportation has been the increased capacity of each succeeding generation of aircraft. As improvements in the state of the art were incorporated, it became possible to build an aircraft with higher payload capabilities. Although reciprocating engine powered aircraft showed a higher dollar per hour cost for each improved aircraft, the cost per unit of payload was lower. In contrast, turbine powered aircraft lowered the cost per mile as well as increasing the units of payload. SST projections show a marked increase in dollars/mile of engine-contribution but a reasonable increase in payload capability (following the historical trend) reduces this to a level per unit of payload where this cost compares favorably with early subsonic turbine-powered aircraft. It is only reasonable to expect that, with future state of the art improvements, the engine contributions to aircraft dollar/mile costs can be reduced as well as the cost per seat mile.

With the above in mind, as well as the great increase in productivity which the SST will bring, it seems that the projected costs for the supersonic transport should be compared with subsonic transports on a cost per seat mile rather than on a cost per mile basis.

When calculations are made of the engine's contribution to aircraft direct operating costs using the STF-219 engines, the results, as shown in Figure 16-2, indicate that the SST with 200 seats is already reduced in costs per seat mile to the same level as the early actual experience of subsonic jet powered transports, and that an increase in payload capacity and/or a reduction in expense could reduce the cost to the level of the best of current aircraft. It is recognized that there

may be further improvements in the operating cost of subsonic jets which will provide an ever lower target for the SST to attain. One should remember, however, that the subsonic jet experience has been much better than estimates indicated at the time that the "go-ahead" was given for these aircraft. By the time the supersonic transport becomes operational, it can be expected that it too will be better than presently predicted.

A further examination of Figure 16-2 reveals that the engine costs associated with both the reciprocating engine powered and the subsonic jet powered aircraft have improved with further development. The supersonic transport can be expected to do this also, particularly since it will then be the most advanced transportation mode and, as such, will receive most of the development effort.

B. STUDIES TO DETERMINE OPTIMUM ENGINE CONFIGURATION

As part of the phase II-A contract effort, Pratt & Whitney Aircraft worked in cooperation with the airframe contractors on studies to determine the engine configuration which would provide the best combination of range and payload capabilities. These studies evaluated all engine cycles that had been suggested as suitable for a supersonic transport aircraft in the Mach 2.7 to 3.0 cruise range. Scaling data were provided to permit optimization of the engine to whatever size was required to provide the best aircraft characteristics from the standpoint of range /payload, block speed, takeoff and landing paths and distances, sonic boom overpressures, noise levels and overall utility and flexibility. In addition, the study evaluated the effects of engine performance, engine weight and price as these affected the performance and economics of the optimized aircraft.

In support of these studies, parametric type data were developed and provided to the airframe contractors. The information is briefly summarized below:

1. RELATIVE ENGINE PRICE

Figure 16-3 shows the estimated relative engine price excluding all development costs for the supersonic transport engine cycles which were studied in most detail by the aircraft contractors. (See Item 1 for details of the engines and their performance.) As noted, the prices were based on a 200-aircraft program at a stabilized production rate of 2.5 aircraft per month. Refer to the section on Value Engineering in Item 17 for additional details.

2. RELATIVE DEVELOPMENT COST

On the basis of studies during Phase I, it was anticipated that differences in relative development costs would be small for those engine cycles and sizes most likely to be chosen for optimized Phase II-A aircraft designs. Accordingly no detailed analysis was made of relative development cost among the various engine cycles and sizes. Airframe-contractor engine selections were based on other governing factors without requiring consideration of the expected small effect of relative development cost.

3. EFFECT OF PROGRAM SIZE

To assist the airframe contractors in assessing the effect of program size on supersonic transport economic potential, estimates were made of the effects on engine price of programs which varied from 100 to 400 aircraft. The results are presented in Figure 16-4.

4. EFFECT OF DESIGN CRUISE MACH NUMBER

To assist the airframe contractors in assessing the effects of design cruise mach number on SST economic potential, estimates were made of the effects on engine unit price excluding amortization of any engine development costs and on total engine development costs. The results are presented in Figure 16-5.

The relative development cost can be considered applicable to costs before and after aircraft certification.

5. ESTIMATED ENGINE LABOR COSTS

A comprehensive review of engine labor costs for subsonic commercial turbine engines, submitted by the airlines to the CAB, indicated that the 1960 ATA method for estimating labor man-hours per flight hour should be changed. The P&WA method outlined below uses the same parameters as the 1960 ATA method, namely engine thrust and time between overhauls (TBO) but the level of the man-hours required has been increased over the ATA method.

The specific analysis procedure followed in developing this method involved a thorough review of current airline experience with powerplant labor costs. Data was gathered from Civil Aeronautics Board form 41, using reported costs for 1962 and 1963. The accounts used were 5225.2 (labor-aircraft engines) and 5243.2 (aircraft engine repair - outside). Account 5243.2 was used for reference only and is not included in the computed engine costs.

Man-hours per flight hour were computed using a labor rate of \$3.50/man-hour. The TBO's used were averages computed over the year for which the corresponding cost data applied.

The parameters used in the 1960 ATA formula, i. e., thrust and TBO, were still basically applicable. Plotting available data against thrust yielded a wide scatter of points having no apparent relationship. In order to obtain a more meaningful set of data, any point which represented more than 30% outside repairs or less than 20,000 hours yearly aircraft fleet utilization was eliminated. Imposing this restriction yielded a much closer set of points. This data was further refined to give the curve plotted in Figure 16-6. An explanation of the use of this curve formula for calculating engine labor costs is given in Figure 16-7.

Figure 16-6 provides an estimate of quick engine change labor man-hours. For supersonic transport use it is recommended these man-hours be reduced to bare engine man-hours by dividing by 1.5. To account for the additional labor requirements of the ejector, augmentor, variable nozzle, and reverser, bare engine labor should be increased by an estimated twenty-five percent.

6. ANALYSIS OF FACTORS AFFECTING ENGINE MAINTENANCE MATERIAL COST

The following parameters were considered in setting up a system for estimating maintenance materials costs:

- Time between overhaul
- Premature engine removal rate
- Engine price
- Turbine inlet temperature
- Pre- and post-certification development effort
- Parts repair procedures
- Complexity - basic engine, added features such as variable nozzle, augmentation, ejector, etc.
- Duty cycle
- Environmental factors
- Spare parts price factor
- Specific thrust
- Gas generator airflow
- By-pass ratio

A discussion of each of these parameters is included in Appendix A to this section starting on page 16-15.

After a thorough analysis of the above parameters, Pratt & Whitney Aircraft selected the parameters of specific thrust, gas generator airflow, and bypass ratio as the factors being the most useful for the prediction of engine maintenance materials costs during the current engine study phase. These factors provide a measure of engine size, working level and complexity. These parameters can be used for predicting material cost per hour for subsonic and supersonic turbine engines with the addition of environmental and duty cycle factors applied to the supersonic engine plus variable nozzle, augmentor and ejector.

Other factors such as TBO and premature removal rate have not been included in the proposed method which represents the quantitative aspects of estimating the base-line engine maintenance material cost. This base-line is predicated on subsonic records of a satisfactory premature removal rate representing durable and reliable turbine engines. P&WA subsonic turbine engine records show that, for a well-developed engine, material cost per hour is relatively insensitive to TBO after a brief introductory period. Based on subsonic turbine engine records, price is completely misleading as a factor to predict such costs.

In-flight shutdowns and schedule delays, both of which are related to premature removal rate, can seriously affect aircraft utilization rate. Revenue per aircraft is importantly reduced as a result of a higher rate of unscheduled engine removals, repairs and maintenance procedures which disrupt schedule departures. These factors will directly influence the number of aircraft and spare engines required to support a given travel market: labor and material cost expenditures will also be affected. In addition, the added expense of passenger accommodations, meals, and the detrimental effects of a poor on-time record result from decreased engine reliability and durability. It can be appreciated that the effect of a larger fleet for a given market is by far the major factor of the aforementioned because of the leverage represented by the ratio of total vehicle DOC to engine DOC.

When the base-line material cost per hour has been determined using the proposed formula, it is recommended that the evaluator modify the results by weighing the capability of the manufacturer in such areas as development effort, repair procedures, time between overhauls and premature removal rate based on the current subsonic engine records.

7. ESTIMATE OF ENGINE MATERIALS COSTS

As indicated in the preceding subsection, a study was conducted by Pratt & Whitney Aircraft to determine the minimum numbers of factors necessary to estimate the maintenance material cost per hour for advanced engines. After due evaluation, the parameters of specific thrust, gas generator airflow, and by-pass ratio were selected. These are known factors which are readily available during the engine study phase. The procedure for estimating material costs per hour based on these factors, is discussed in this section. The material cost per hour obtained from the proposed system is intended solely for predicting the target maintenance costs for engines which evolve from a successful engine development program. When using the costs predicted by this formula for advanced engines, consideration must be given to the adequacy of the development program in time, dollars, and service experience to justify the conclusion that the state of art required for an advanced engine can in fact be achieved as planned.

The specific analysis procedure used to develop the method for estimating engine maintenance material costs involved first a review of reported airline costs taken from CAB Form 41 for the time periods shown in Figure 16-8. Account 5246.2 (materials - aircraft engine) and 31.5 per cent of account 5243.2 (aircraft engine repair - outside) were used.

The figure of 31.5 per cent for the material portion of outside repair costs was established by determining the portion comprised of in-house repair. The assumption was then made that this same percentage also applied to outside shops. The reported in-house costs for labor, materials, and one half of the maintenance burden were totaled. Then the percent of this total represented by materials was determined and an average taken over several airlines and aircraft. This cost data is presented in the curves listed below:

Figure 16-9 shows the basic material cost per hour as a function of gas generator airflow for a zero bypass engine. The level of this curve was set by the minimum airline costs for this type of engine.

Figure 16-10 shows the ratio between a specific gas generator and a fan or turboprop engine using the same gas generator. The level of this curve was set by the minimum airline cost for these types of engines.

Figure 16-11 supplies a reference specific thrust versus bypass ratio for all engines. The values are based upon the current state of the art as portrayed by most of the engines now operating with the airlines.

Figure 16-12 provides another cost ratio as a function of a specific thrust ratio. The line on this curve runs through the minimum cost level and well below the cost level for engines which have been operating above the current state of the art or have not been developed to attain the minimum cost level.

An explanation of the use of Figures 16-9 through 16-12 for calculating QEC unit material costs per flight hour is presented in Figure 16-13.

Figure 16-14 shows the percentage increase in material cost estimated to be necessary to account for the difference between subsonic and supersonic environment and duty cycle. The level is based on cost changes due to metal property improvements required as total temperature and pressure increase with cruise Mach number. Figure 16-12 was used in estimating the duty cycle difference.

Figure 16-15 presents the dollars per hour increments for the variable nozzle, augmentor, and ejector reverser portions of the SST engine. The level of this line is based on estimated percentage cost as a function of engine cost and life factors for each of the components.

An explanation of the use of Figures 16-14 and 16-15 for calculating estimated material costs per hour is presented in Figure 16-16.

Additional explanatory notes on the above curves are contained in Appendix B to this section starting on page 16-18 of this report.

During this work it was necessary in many instances to use materials costs for a bare engine instead of for the complete Q.E.C. unit. A ratio of 1.7 was derived for the QEC unit materials costs/bare engine materials costs. Bare engine maintenance costs came from data supplied by the Pratt & Whitney Aircraft Service Department. QEC unit maintenance costs are from ATA statistics reported in Form 41. Ratios were computed for several engines and an average value determined.

C. ECONOMIC FACTORS

The major engine factors affecting direct operating costs were studied during this contract and included the following:

1. Engine-Aircraft Matching
2. Fuel Cost
3. Oil Cost
4. Depreciation
5. Engine Prices
6. Engine Development Costs
7. Engine Labor Cost Estimates
8. Engine Maintenance Material Cost Estimates

A discussion of each of these factors is contained in the paragraphs which follow.

1. ENGINE-AIRCRAFT MATCHING

A major effort during the Phase IIA contract has been the re-examination without prejudice of the advantages and disadvantages of all engine cycles that have been suggested as suitable for a supersonic transport in the Mach 2.7 to 3.0 cruise range. An effort was made to optimize the engine-aircraft match for range-payload, flight speed, take-off and landing conditions, sonic boom overpressures, noise levels, and overall utility and flexibility. Since engines proposed during Phase I were judged to be inadequate to meet the objectives of the SST program, Pratt & Whitney Aircraft has abandoned the limitations imposed by the use of J-58 component hardware and also increased the turbine inlet temperature level for the basic engine specification to 2200°F for cruise and 2300°F for maximum (transonic acceleration). Initial service operation would be conducted at 1900°F cruise/2000°F maximum.

The engine cycles considered in the Phase IIA evaluation and the performance for each are shown in Figure 16-17. In addition to the engine cycles presented in this table, an STF-223 cycle consisting of a turbofan engine configuration with full afterburning augmentation was evaluated. This engine which mixed the flow of the gas generator and fan prior to burning in a common afterburner was found to be non-competitive early in the aircraft studies and dropped from consideration.

The remainder of the cycles were subjected to detail study in optimized aircraft before a final decision was made as to cycle selection and size. The study included the effects of engine performance, engine weight and engine price as these related to the optimized aircraft. These studies were based on comparable component efficiency and performance for each cycle and considered the requirement that all engines be available in the same time period in order to provide a meaningful comparison. Accordingly, while each of these engines entailed development risks in different areas and to different degrees, the time required to reach production status was considered to be equal for all engines. The engine cycle finally selected represents an optimized engine-aircraft configuration designed for minimum operating cost consistent with the performance required.

2. FUEL COSTS

The fuel cost will be the largest of the factors that can be directly associated with the engine. An engine design objective is the capability of operating with a fuel which is equivalent in cost to that of PWA Spec. 522 (ASTM Jet A), the current subsonic fuel. PWA Specification 533 defines the supersonic transport engine fuel characteristics. Preliminary comments from three oil companies indicate it is possible to satisfy all requirements of this specification including those for thermal stability at no increase in cost in the 1970 time period.

3. OIL COST

Pratt & Whitney Aircraft will specify PWA 521 Type II oil for the supersonic transport engine. Since the engine design will have about the same level of oil consumption as current turbine engines (0.4 gals./hr.), the influence on aircraft D.O.C. of this factor is considered insignificant.

4. DEPRECIATION

Engine depreciation, which is a function of engine price, is another factor which will significantly affect aircraft direct operating cost. The prices for the engines being offered and the standards on which these are based can be found on page 16-11 of this section.

5. ENGINE PRICES

Selection of the optimum SST engine by the airframe manufacturers was made after detailed studies of optimized aircraft. Primarily as a result of the difference in aircraft configuration, Lockheed's

selection required an engine sized at 700 lb./sec. while Boeing's selection required one sized at 640 lb./sec. These engines have been designated as the STF-219-L and STF-219-B respectively.

As a result of the selection of these new engines for the SST airplane, it was necessary to establish new engine unit prices. Accordingly, the estimated production unit selling prices in 1964 dollars, calculated in accordance with the Phase II-A SST Economic Model Ground Rules, dated July 10, 1964 are:

STF-219-L per Eng. Spec. No. 2682 - $2,000,000
STF-219-B per Eng. Spec. No. 2681 - $1,825,000

These prices include all standard equipment listed in the engine specification including the ejector and reverser and are based on a program involving 200 aircraft with a stabilized production rate of 2.5 aircraft per month and, in accordance with the FAA's request, include amortization of the company-absorbed estimated development costs subsequent to an assumed aircraft certification by mid-1972 but none of the development cost prior to aircraft certification.

These estimated engine prices are suitable for use in computing the engine depreciation portion of airplane direct operating cost in accordance with the FAA Phase II-A Economic Model Ground Rules. The rules also indicate that these engine prices should be used to estimate engine maintenance material costs by means of a modified ATA formula. It is recommended that, instead of using this method, the estimated maintenance costs described on page 16-12 be used for the STF-219 engines.

6. ENGINE DEVELOPMENT COSTS

As a result of the new engines being proposed at the end of Phase II-A, it has been necessary to revise the development cost estimates. Due to the compressed time schedule for Phase II-A reporting, the following "preliminary" estimated development costs were given to the aircraft contractors and recommended for their use in accordance with the FAA Phase II-A SST Economic Model Ground Rules, dated 10 July 1964:

STF-219-L per Eng. Spec. No. 2682........$970,000,000
STF-219-B " " " " 2681........$880,000,000

These costs include all the engine, ejector and reverser development costs prior to an assumed aircraft certification date of mid-1972 and is based on an effective prototype engine development program go-ahead of December 1, 1964. The cost, in accordance with the FAA's

request, includes the cost of two ground test engines including ejectors and reversers for the aircraft flight test program and their support.

These estimated development costs are suitable for use in evaluating the economic potential of the SST designs in accordance with the FAA Phase II-A Economic Model Ground Rules.

7. ENGINE LABOR COST ESTIMATES

Before calculating labor requirements for the STF-219-L and the STF-219-B engines, it was necessary to determine the expected time between overhauls. Initially, it is anticipated that the target time between overhauls will be 600 hours when the engine is operated at turbine inlet temperatures of 1900°F cruise and 2000°F maximum (transonic acceleration). Subsequent increases in time between overhauls and/or cruise temperature will be dependent on experience and will be worked out with the airline operators to obtain the most economical tradeoffs between time between overhaul and increased temperature. Experience would indicate that time between overhauls would probably increase to approximately 1500 hours before significant increases in turbine inlet temperature will be considered in order not to adversely affect aircraft utilization and make possible the use of a reasonable spare-engine ratio.

If operation were continued at 1900°F for cruise and 2000°F for maximum (transonic operation) it is anticipated that the time between overhauls will increase with additional operating time in the manner shown in Figure 16-18. It is estimated that labor costs for a STF 219 engine will be $7.50 per flight hour when a time between overhauls of 3000 hours is reached. The estimated maintenance costs apply to the engine only and do not cover complete quick engine change costs. Included with the engine are all items of standard equipment such as the gas generator and duct heater fuel system controls, the complete duct heater augmentation system, the variable area exhaust nozzle and controls, the blow-in-door ejector and integral reverser system and its controls.

8. ENGINE MAINTENANCE MATERIAL COST ESTIMATES

Estimates have been prepared of SST engine maintenance costs for the specific engines selected by the airframe contractors for their

Phase II-A engine designs. These estimates are in 1964 dollars and were made for the STF-219-B (Boeing) and the STF-219-L (Lockheed) engines. Inasmuch as there is at present no significant operating experience at the elevated turbine temperature levels required in the SST powerplant, it can be readily appreciated that a careful review and revision of these estimates will be required as experience is gained in the engine development and flight test program.

The turbine inlet temperature for the initial service operation of the STF-219 engine will be a function of the time when airline passenger-carrying service commences operation. If SST service operation should be scheduled to commence during 1972, then the initial service operation of the engine will probably have to be at a 1900°F cruise turbine inlet temperature and a 2000°F transonic acceleration temperature. Turbine inlet temperature will be increased to the 2200°F/2300°F level as soon as it is practical to do so as shown by airline operating experience and concurrent engine development. The step or steps which will be taken in increasing the engine performance to the 2200°F/2300°F level may require significant engine parts changes, and, during this period, engine TBO will increase at a slower rate than if the operating temperature level were to be maintained at the 1900°F/2000°F level.

The following estimates are made in consideration of the probable program as described above:

a. After an initial period of three years, it is estimated that maintenance material costs will be as follows:

   STF-219-L per Eng. Spec. No. 2682...$75.00 per hour
   STF-219-B per Eng. Spec. No. 2681...$70.00 per hour

   These figures apply under the assumption that operation starts and continues at 1900°F for cruise and 2000°F for maximum.

b. Maintenance material costs during the initial period of three years (at 1900°F cruise and 2000°F maximum) may be adversely affected by the requirement for engine part changes associated with the break-in period. Accordingly, it is suggested that a minimum of 50% higher costs be assumed for this period.

c. Once satisfactory levels of maintenance material cost, time between overhaul and utilization have been achieved at 1900°F cruise and 2000°F maximum, the rate of progress to higher turbine inlet temperature will depend on an economic trade-off between the operation-proven effects on aircraft performance, engine maintenance material costs and engine time between overhauls.

The estimated maintenance costs apply to the engine only and do not cover complete quick engine change unit costs. Included with the engine are all items of standard equipment, such as gas generator and duct heater fuel system controls, the complete duct heater augmentation system, variable area exhaust nozzle and controls, and blow-in door ejector and integral reverser system and its controls.

ITEM 16
APPENDIX A

DISCUSSION OF PARAMETERS USED FOR
ESTIMATING MAINTENANCE MATERIAL COST
(Ref. page 16-6)

Time between overhaul - TBO can have a significant effect on material cost per hour but a well-developed engine, after a very brief introductory period should demonstrate a material cost per hour which is effectively constant and unaffected by increasing TBO. This results because the expendable parts cost per hour will decrease while the cost per hour due to those parts which last through two, three, or more overhauls will increase. The rate of TBO increase will be affected by the amount of development effort expended, since an engine with the proper amount of pre- and post-certification development support historically has shown a continually increasing allowable TBO. On an operating hour basis, the material cost would therefore be expected to remain approximately constant as the engine progresses through successive overhauls at greater time intervals.

Premature engine removal rate - This factor will definitely have an effect on material cost per hour of operation but history has shown that a satisfactory post-development effort and a continuing rate of TBO increase combine to reduce the effect of this parameter on engine operating cost. Because premature removal rate (PRR) is basically unknown until operational experience is gained, it is considered difficult to predict this factor at any point prior to operation. The effect of a high premature removal rate on utilization is very important, affecting the overall supersonic transport economics adversely. The extent of this effect is such that it cannot be tolerated. The engine post-certification development must be planned at a high level in order to ensure a capability to provide the prompt engineering changes required during early service operation. This is necessary to achieve a low average PRR.

Engine price - The development of the SST engine represents an effort and an investment which is many times that of previous commercial engine development. Because of the magnitude of this program, the period of time over which it may extend, and the degree of development effort planned, engine price estimates may vary substantially. The degree of price variation could reflect the total approach taken by the

manufacturer in the program foreseen for the design, development, and support of the product. As subsonic commercial engine records will show, engine price alone cannot be depended upon to provide an accurate prediction of engine material costs per hour even if this is biased with TBO or premature removal rate because these factors are difficult to judge for future engines.

Turbine inlet temperature - This factor has a very important effect on material cost per hour since it is a measure of the working level of the engine. The effects of turbine inlet temperature are included in the specific thrust factor of the proposed method.

Pre- and Post-Certification Development Effort - The economic success of any commercial transport engine is dependent on the degree of total effort expended by the manufacturer in the pre- and post-certification periods. This could be an excellent measure of material cost per hour if all proposals were based on the same approach. However, since it is difficult to assess this factor quantitatively, it is recommended that this should be a judgment factor considered by the evaluator after the material cost per hour is calculated using the proposed method.

Parts Repair Procedures - The degree of response of the manufacturer in devising repair procedures will have a definite effect on maintenance material costs per hour. This area is difficult to assess in any simple formula and should be treated as another judgment area by the evaluator when the material cost per hour has been calculated using the proposed method.

Complexity - Complexity of engine design will affect engine material costs per hour. Added complexity such as augmentation, variable nozzle, ejector, etc., peculiar to the SST engine, must also be considered in any method for predicting material cost per hour.

Duty Cycle - The average working level of the SST engine throughout a typical flight is higher than the subsonic turbine engine relative to the maximum rating of each engine. Throughout acceleration and cruise the relative thrust level is higher for the SST engine than it is for the subsonic turbine engine. This duty cycle factor should be included in any method of estimating direct operating costs.

Environmental factors - The acceleration, cruise, and initial descent regimes will subject the SST engine to more severe environmental factors than the subsonic turbine engine. These effects will require the use of more exotic materials and are considered in the proposed method for estimating engine material cost per hour.

Spare parts price factor - Engine material cost per hour is affected by the spare parts pricing level and this should be considered in any evaluation. The average subsonic engine spare parts price factor is included in the proposed method.

Specific thrust - This is considered a very important parameter because the overall effects of turbine inlet temperature, compression ratio, and component efficiency, indeed, the whole basis for the performance level achieved by any engine, is substantially represented by this parameter.

Gas generator airflow - This parameter is a measure of engine size and can be considered a measure of engine maintenance material cost under conditions of comparable design and development support.

By-pass ratio - This factor has a significant effect on specific thrust but a relatively minor effect on material cost. In order to achieve a proper measure of material cost, specific thrust should be biased with by-pass ratio.

ITEM 16
APPENDIX B

EXPLANATORY NOTES FOR ENGINE MATERIAL COST CURVES
(Ref Page 16-8)

Figure 16-9 provides a basic cost per flight hour for any gas generator airflow. This curve is based on a given level of unaugmented specific thrust and will be fairly close for any other level of specific thrust. Regardless of specific thrust level, the airflow to use is that for the unaugmented take-off rating of the engine.

Figure 16-10 provides cost ratio values for all by-pass ratios. The initial ratio at very low by-pass ratio values is quite high but the slope as by-pass ratio increases is low. This is felt to be the true variation above 1.0 by-pass ratio. A new engine with a by-pass ratio less than 1.0 is a remote possibility for any aircraft application at this time.

Figure 16-11 designates a thrust divided by gas generator airflow value for any by-pass ratio at the current level of technology. This is the denominator of the specific thrust ratio abcissa value Figure 16-12.

Figure 16-12 provides a cost ratio for any specific thrust ratio. The numerator of the specific thrust ratio is defined by the characteristics of the engine for which a materials cost estimate is desired. The data points on this curve represent essentially all of the turbine engine data reported to the CAB by domestic airlines. The line in Figure 16-12 represents the material cost per hour performance of the current commercial turbine engines which have established records reflecting proper development levels. Any new engine program should be targeted to obtain material costs that result from similar comprehensive development programs.

Figure 16-9 through 16-12 are used to obtain subsonic quick engine change materials costs. When calculating supersonic engine costs, it is suggested that the materials costs be reduced to the bare engine value by dividing by a factor of 1.7, prior to applying the corrections from Figures 16-14 and 16-15.

Figure 16-14 provides a percentage increment to be added for the supersonic engine reflecting the materials costs attributed to duty cycle and cruise environment effects.

Figure 16-15 was developed to show the estimated material cost attributed to the additional hardware included on the supersonic engine for a 1.3 by-pass ratio turbofan.

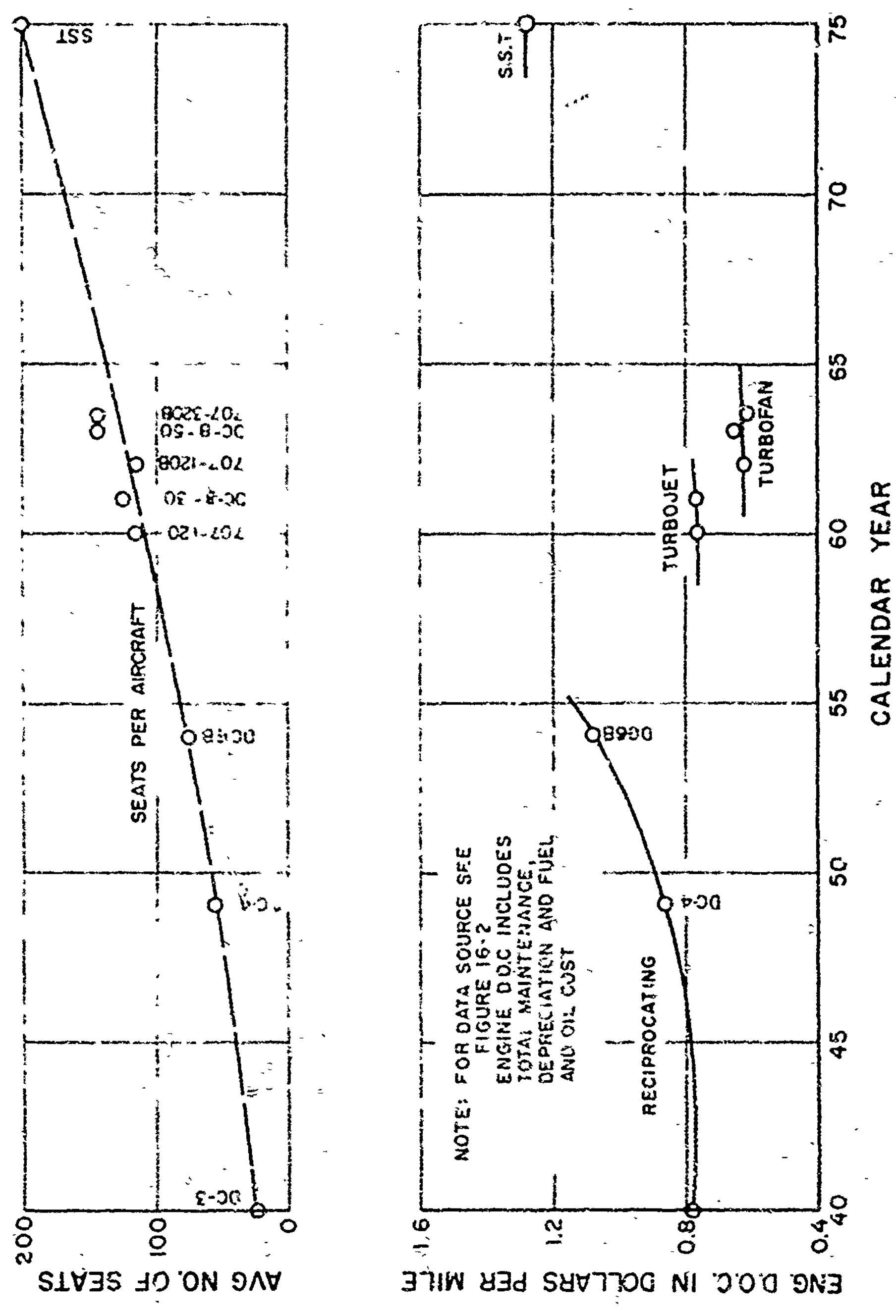

HISTORY OF POWERPLANT CONTRIBUTION TO AIRCRAFT DIRECT OPERATING COST AND AIRCRAFT CAPACITY

Figure 16-1

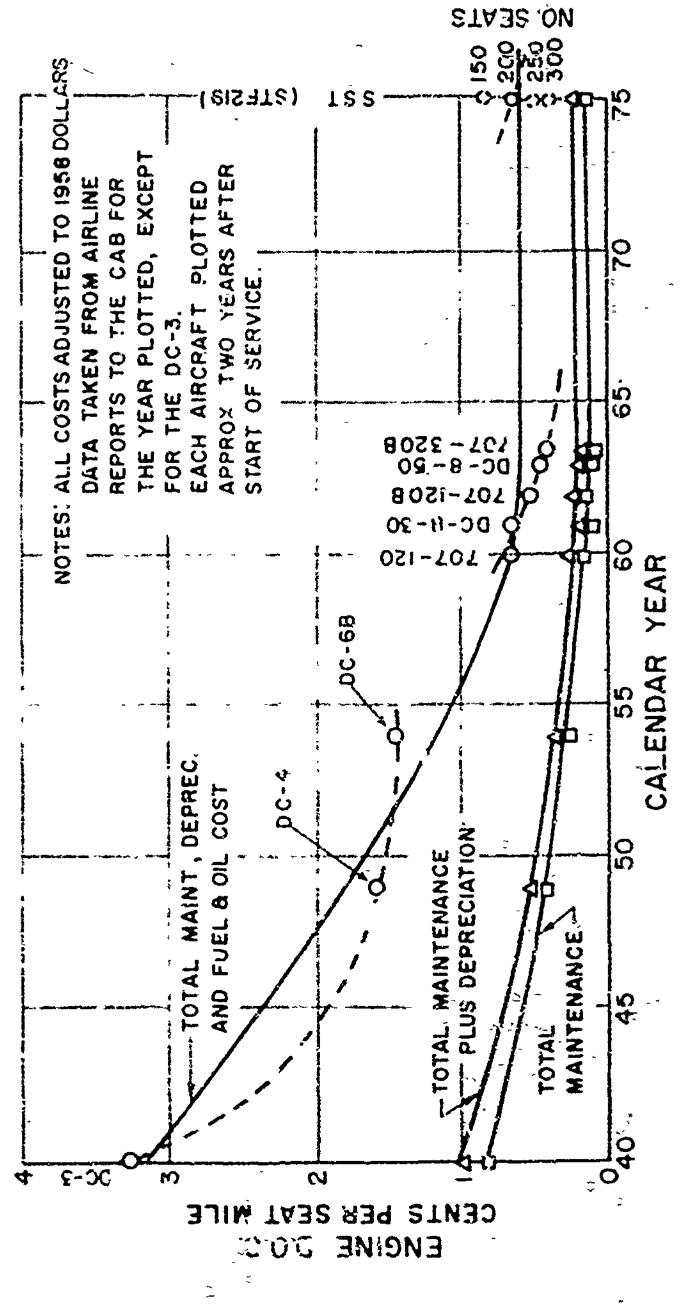

HISTORY OF POWERPLANT CONTRIBUTION TO AIRCRAFT DIRECT OPERATING COST

Figure 16-2

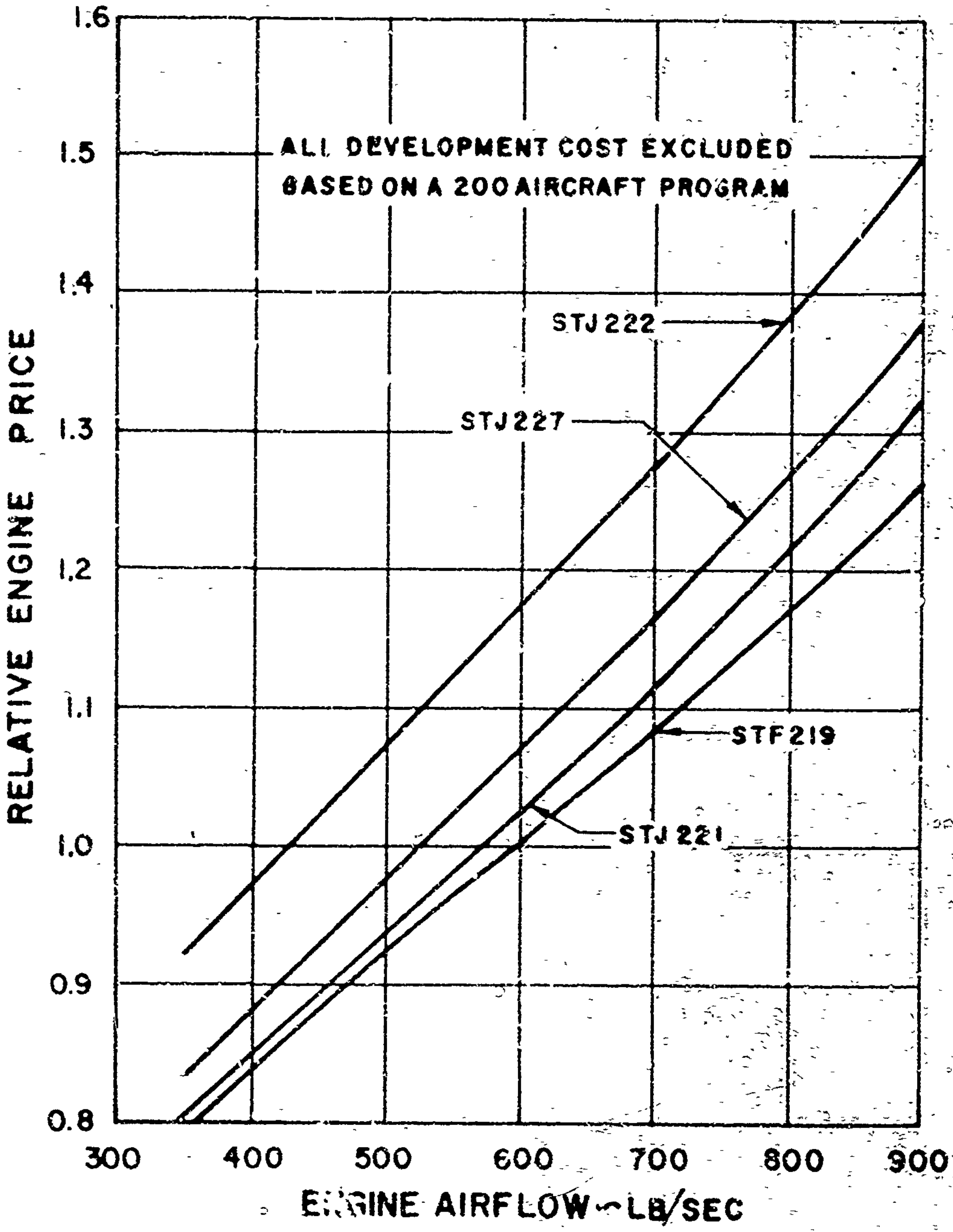

ESTIMATED RELATIVE PRICE OF SST STUDY ENGINES

Figure 16-3

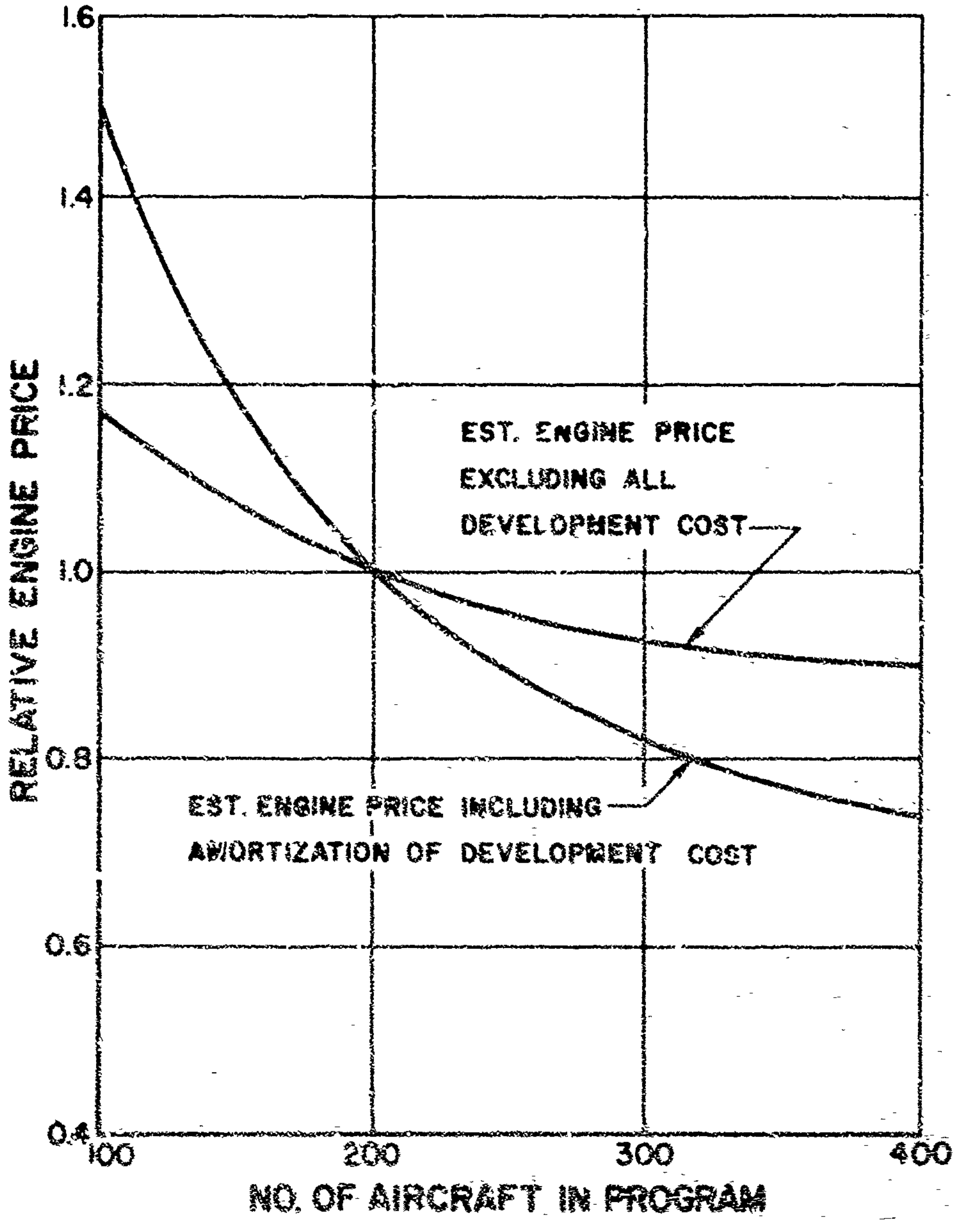

ESTIMATED EFFECT OF PROGRAM SIZE ON SST ENGINE PRICE

Figure 16-4

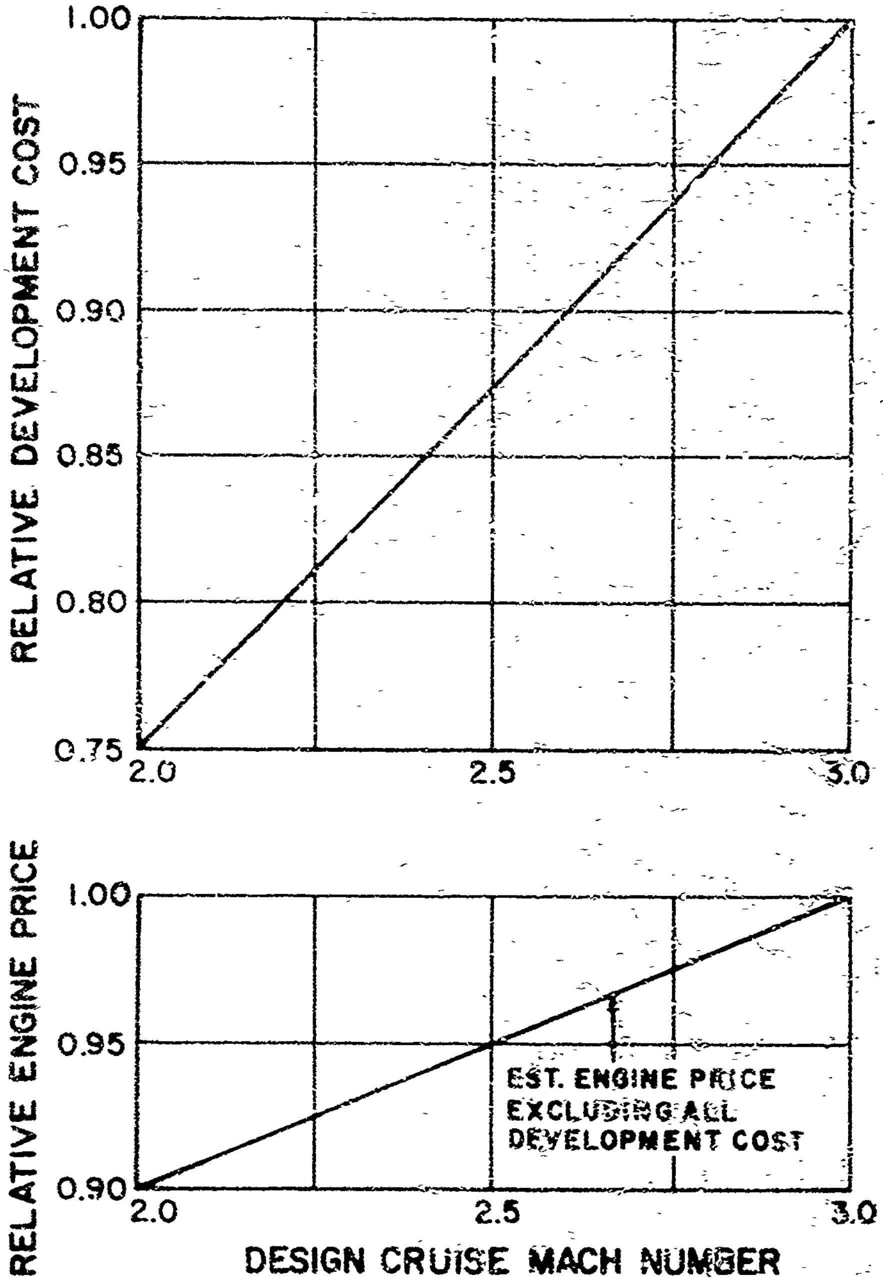

ESTIMATED EFFECT OF DESIGN CRUISE MACH NUMBER ON ENGINE UNIT PRICE AND TOTAL DEVELOPMENT COST

Figure 16-5

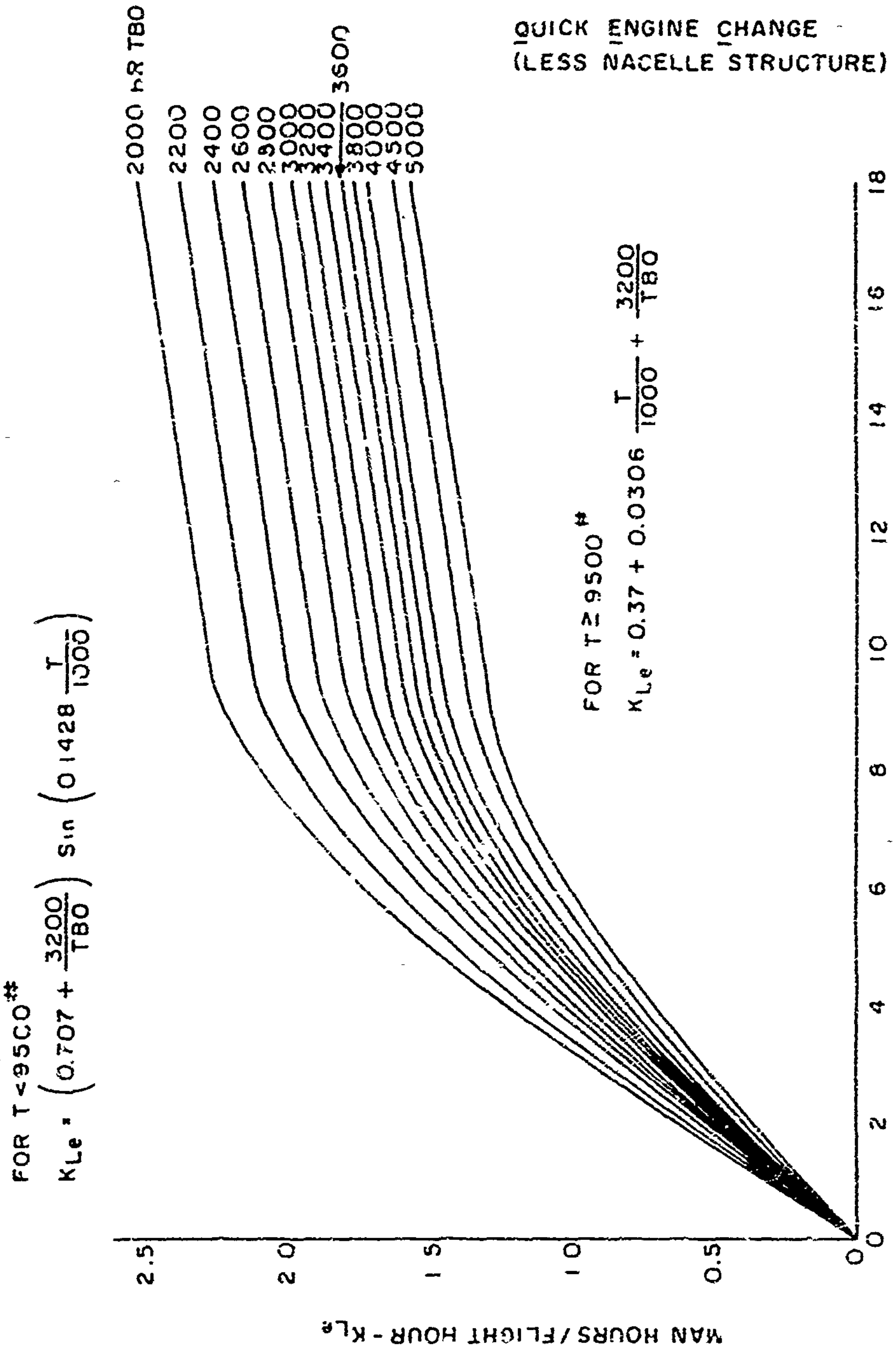

QUICK ENGINE CHANGE (LESS NACELLE STRUCTURE)
UNIT LABOR MAN HOURS PER FLIGHT HOUR -
TURBOJETS AND TURBOFANS

Figure 16-6

ESTIMATION OF AIRCRAFT QUICK ENGINE CHANGE UNIT MAINTENANCE LABOR MAN HOURS

(K_{Le} in ATA Standard Method of Estimating Comparative Direct Operating Costs of Transport Airplanes)

(1) Data Requirements

a. Sea Level static non-augmented take-off thrust - lbs

b. Estimated Time Between Overhaul (TBO) - Hrs

(2) Estimation Procedure

a. Enter Figure 16-6 at take-off thrust, proceed to TBO and read Man Hours/Flight Hour.

b. As an alternate method, use the following equations:

1. For take-off thrust values less than 9500 lbs

$$K_{Le} = (.707 + \frac{3200}{TBO}) \text{Sine} (.1428 \frac{T}{1000})$$

2. For take-off thrust values equal to or greater than 9500 lbs

$$K_{Le} = .37 + .0306 \frac{T}{1000} + \frac{3200}{TBO}$$

(3) Supersonic Engines

a. To estimate labor requirements for a supersonic bare engine plus variable nozzle, augmenter, ejector and reverser, multiply the results of the above calculation by .85.

Figure 16-7

BASIC DATA - AIRLINE REPORTS TO CAB

ENGINE	JT3C-6	JT3C-7	JT3C-12	JT3D	JT4A	CJ805-3	CJ805-23	R.R.DART	AVON 533
Airline	PAA TWA AAL UAL	UAL BN	EAL	UAL AAL TWA PAA	UAL EAL TWA PAA PAG	DAL TWA	AAL	CO UAL	UAL
Dates	Apr.'60 Dec.'63	Apr.'60 Dec.'63	Jan.'61 Dec.'63	Apr.'61 Dec.'63	Apr.'60 Dec.'63	Apr.'60 Dec.'63	Apr.'62 Dec.'63	Apr.'60 Dec.'63	Jan.'61 Dec.'63
Mat'l. Cost $/Hr.*	11.30	7.48	12.85	12.15	9.39	11.67	22.15	2.82	16.15
Fn (S.L.S.T.O.)	13,500	12,000	13,000	17,500	16,800	11,200	16,100	1630 SHP	12,725
Wagg	185	182	187	192.2	253	170	170	22.2	185
B.P.R.	0	0	0	1.365	0	0	1.47	28.5	0
Fn/Wagg	73.0	66.0	69.5	90.9	66.4	66.0	94.7	209	68.8

DEVIATION ANALYSIS

	JT3C-6	JT3C-7	JT3C-12	JT3D	JT4A	CJ805-3	CJ805-23	R.R.DART	AVON 533
Mat'l. Cost $/Hr calculated	13.95	7.06	10.54	13.61	9.35	6.65	13.92	3.19	9.83
% Deviation	+23.5	-6.4	-18.0	+12.1	-0.4	-43.0	-37.2	+13.1	-39.2

*Figures are a weighted average (total costs divided by total hours) for each engine model.

Figure 16-8

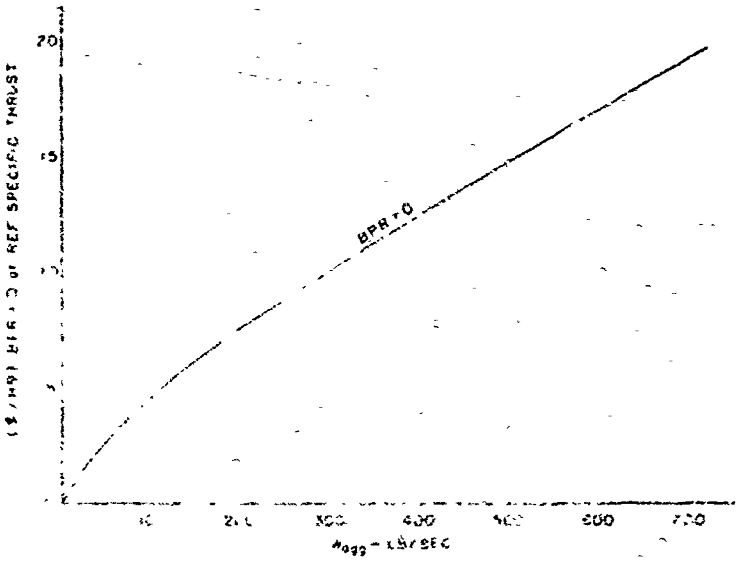

QUICK ENGINE CHANGE (LESS NACELLE STRUCTURE)
UNIT MATERIAL COST PER HOUR VS. GAS GENERATOR
TAKE-OFF AIRFLOW

Figure 16-9

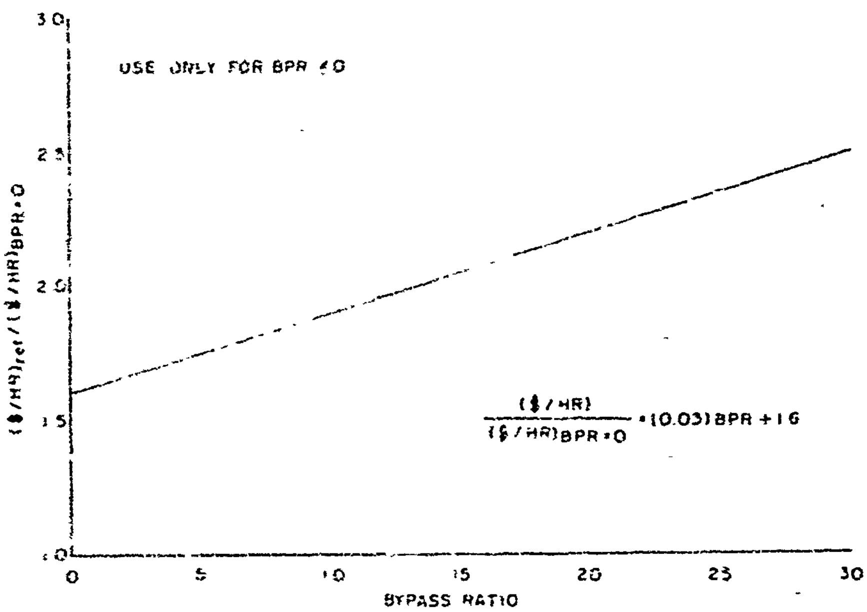

MATERIAL COST RATIO VS. BYPASS RATIO

Figure 16-10

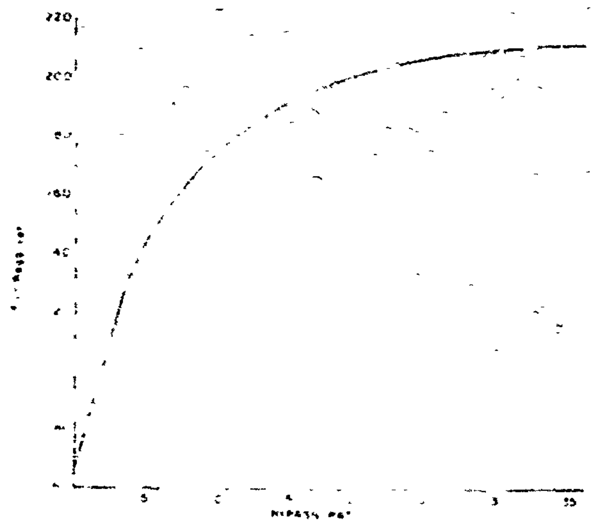

REFERENCE SPECIFIC THRUST VS. BYPASS RATIO

Figure 16-11

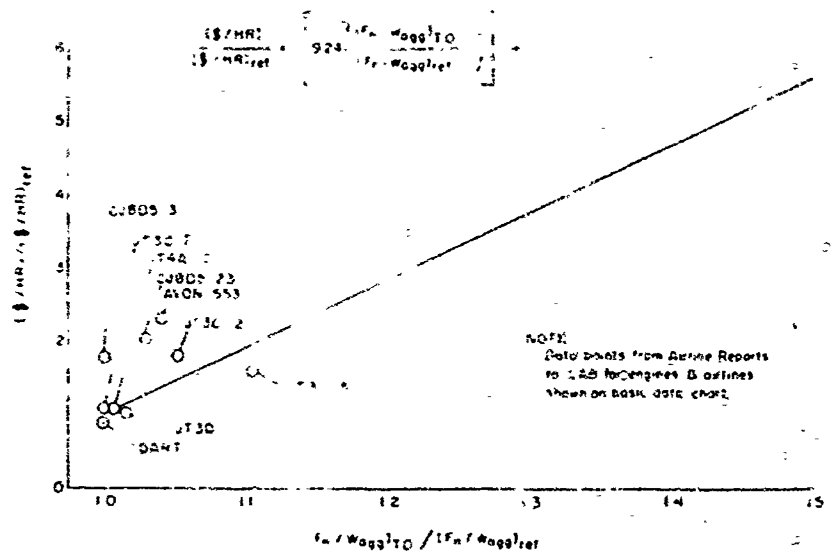

MATERIAL COST RATIO VS. SPECIFIC THRUST RATIO

Figure 16-12

ESTIMATION OF AIRCRAFT QUICK ENGINE CHANGE UNIT MATERIAL COSTS PER FLIGHT HOUR

For a non-augmented fixed convergent nozzle turbine engine

(1) Engine data required - Sea level static take-off

a. Thrust (pounds) - Fn.

b. Airflow (pounds/sec.) - Wa.

c. Bypass ratio - BPR

(2) Calculate:

a. Gas generator airflow - Wagg

Wagg = Wa/(BPR + 1)

b. (Fn/Wagg) T.O.

(3) Estimation procedure

a. Enter Figure 16-9 at Wagg and read $/Hr. for BPR = 0.

b. Enter Figure 16-10 at BPR and read ($/Hr.) ref./($/Hr.) BPR = 0 (Use a value of 1 for BPR = 0).

c. Enter Figure 16-11 at BPR and read (Fn/Wagg) reference.

d. Calculate (Fn/Wagg) T.O. (Step 2b) divided by (Fn/Wagg) ref.

e. Enter Figure 16-12 at (Fn/Wagg) T.O. /(Fn/Wagg) ref. and read ($/Hr.)/($/Hr.) ref.

ESTIMATED Q.E.C. MATERIALS COST PER HOUR

$$\$/\text{Hr} = \underbrace{\left[(\$/\text{Hr.})\ \text{BPR} = 0\right]}_{\text{Figure 16-9}} \times \underbrace{\left[(\$/\text{Hr.})\ \text{ref.}/(\$/\text{Hr.})\ \text{BPR} = 0\right]}_{\text{Figure 16-10}} \times \underbrace{\left[(\$/\text{Hr.})/(\$/\text{Hr.})\ \text{ref.}\right]}_{\text{Figure 16-12}}$$

Figure 16-13

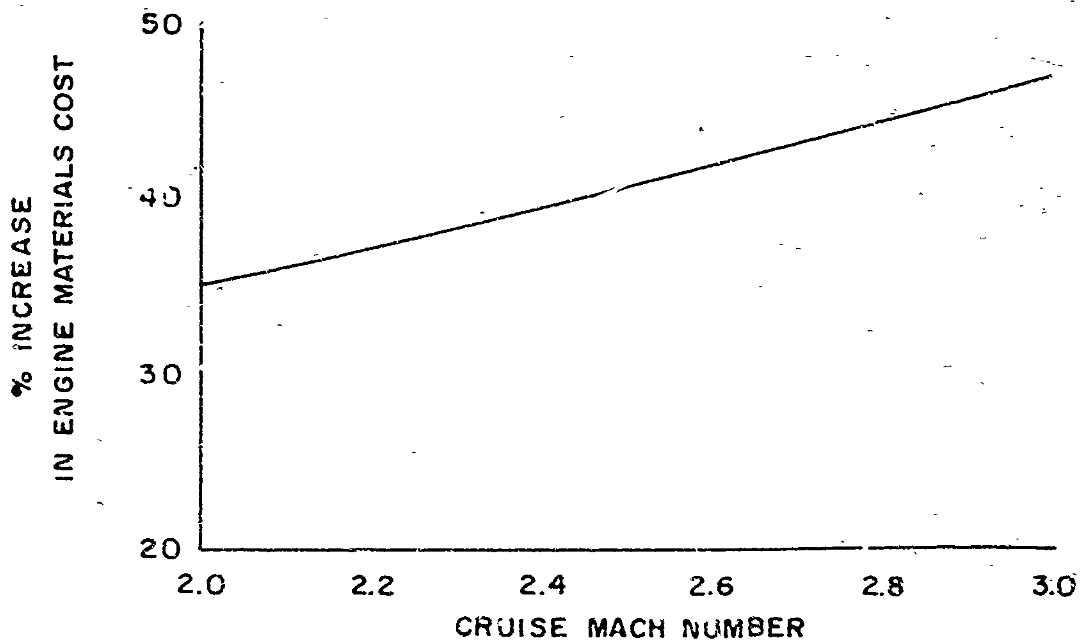

SST CRUISE ENVIRONMENT & DUTY CYCLE MATERIAL COST VS. CRUISE MACH NUMBER

Figure 16-14

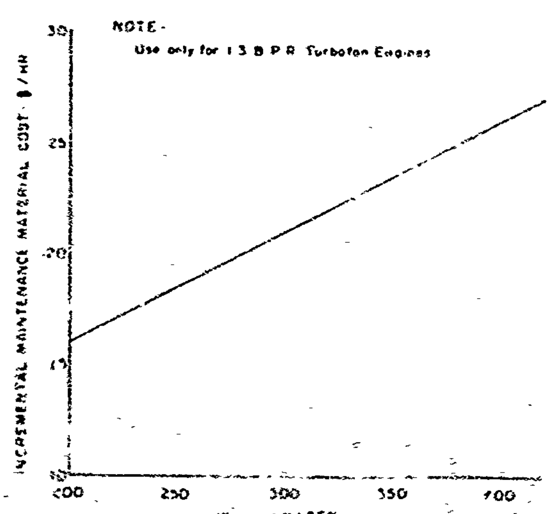

SST ENGINE MAINTENANCE MATERIAL COST INCREMENT FOR VARIABLE NOZZLE, AUGMENTER, EJECTOR AND REVERSER

Figure 16-15

ESTIMATION OF ENGINE MATERIAL COSTS PER FLIGHT HOUR

For an augmented, variable nozzle supersonic turbine engine

(1) Data Requirements

a. Cruise Mach number is required in addition to the requirements shown on Figure 16-13.

(2) Estimation Procedure

a. Use Figure 16-13 to calculate ESTIMATED Q.E.C. MATERIALS COST PER HOUR. Note - use non-augmented take-off thrust.

b. Enter Figure 16-14 at Cruise Mach Number and read % increase in Engine Materials Cost Per Hour.

c. Enter Figure 16-15 at Wagg and read $/Hr. Maintenance Material Cost for nozzle, augmenter, and ejector.

ESTIMATED ENGINE MATERIALS COST PER HOUR

$/Hr. = {(Estimated Q.E.C. Materials Cost Per Hour*/1.7)

*From Figure 16-13

x [1 + (% Increase in Engine Materials Cost**/100)]}

**From Figure 16-14

+ ($/Hr. for Nozzle, Augmenter and Ejector)

Figure 16-15

Figure 16-16

UNINSTALLED PERFORMANCE COMPARISON OF ENGINES STUDIED DURING PHASE II-A EVALUATION

	STJ222	STJ227	STJ221	STF219
Take-Off Maximum Thrust	51900	61000	63000	52500
Nominal Airflow Size	450	690	670	600
Transonic Acceleration, Mach 1.2, 45000 Feet				
Thrust	18300	24500	19600	18200
Specific Fuel Consumption	1.86	1.75	1.25	1.84
Supersonic Cruise, Mach 2.7 at 65000 Feet, Thrust/Transonic Thrust = 0.62				
Specific Fuel Consumption	1.44	1.45	1.46	1.52
Supersonic Cruise, Mach 3.0 at 75000 Feet, Thrust/Transonic Thrust = 0.59				
Specific Fuel Consumption	1.75	1.56*	1.53*	1.79
Subsonic Part Throttle, Mach 0.9 at 36150 Feet, Thrust/Transonic Thrust = 0.42				
Specific Fuel Consumption	1.10	1.09	1.09	0.92
Subsonic Part Throttle, Mach 0.6 at 15000 Feet, Thrust/Transonic Thrust = 0.42				
Specific Fuel Consumption	1.22	1.24	1.30	0.93

*At Max Rating

Figure 16-17

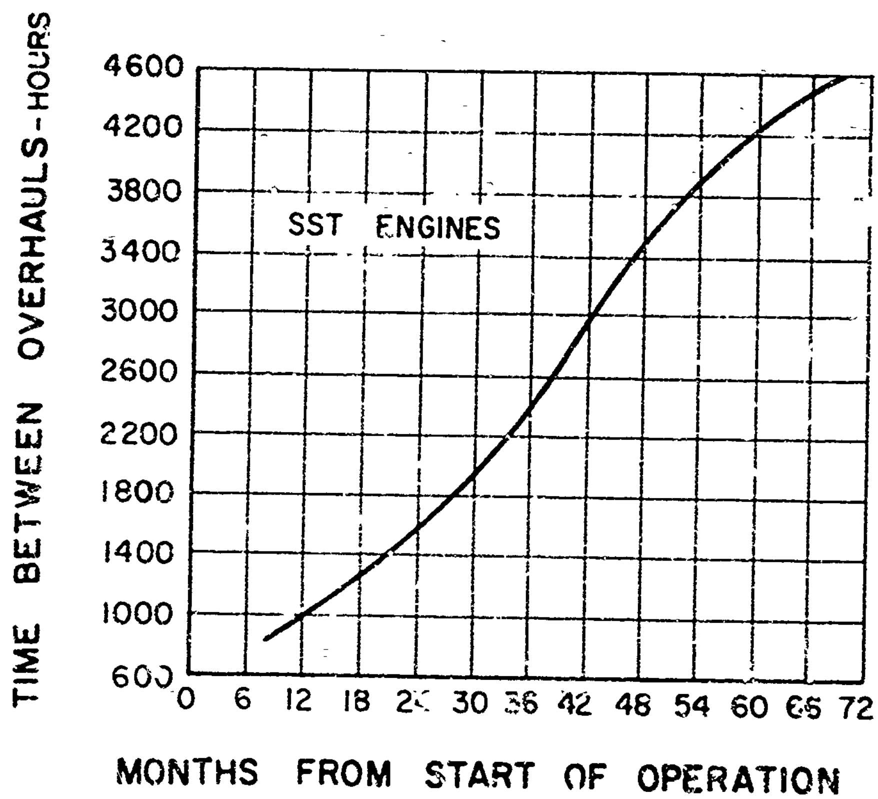

ANTICIPATED RATE OF TBO PROGRESSION

Figure 16-18

ITEM 17 - SUPPORTING DESIGN CONSIDERATIONS

OBJECTIVE

This item of the contract required Pratt & Whitney Aircraft to consider and report on the following factors in the work performed under this contract, and to recommend any improvements to be adopted in Phase II-B and Phase III in the following factors: reliability, configuration management, weight and center of gravity control, value engineering, maintainability, and safety.

A. RELIABILITY

1. INTRODUCTION

During the Phase II-A period of the SST engine program, various studies and analyses were made to assure that the inherent reliability capability of the design was optimized for the SST engine.

The Design Reliability Group conducted a comparative reliability analysis for the various engine configurations to assess the relative reliability capability of the engine cycles under consideration.

A failure mode analysis of the basic engine structure coupled with a design reliability review was carried out. This permitted a critical analysis and review of the detailed design to assure that all possible failure modes were considered in the design and that the design philosophy adopted would be adequate in providing a reliable powerplant.

Design features of the STF219 were compared with current commercial engines. The improved reliability design features were listed based on their expected performance in relation to experience with previous designs. These reliability design features are discussed in paragraph 5.

The following sections give a detailed report of the continued reliability analysis effort for the SST program under Phase II-A.

2. COMPARATIVE RELIABILITY ANALYSIS

A study of the comparative reliability was made for three SST engine cycles, namely, a duct heating turbofan, a nonaugmented turbojet, and a fully augmented turbojet. In assessing the inherent reliability capability of each engine cycle the following definition of failure was used: any malfunction or discrepancy, chargeable to the engine, that would result in the premature removal of the engine from an aircraft. Reliability assessment based on this definition of failure is an indication of the engine availability for service operation and relative maintenance requirements. A reliability assessment based on in-flight shutdowns chargeable to the engine was also conducted.

Commercial turbine engine failure data were utilized in weighing the effect of the various engine components in determining an overall reliability assessment for each cycle. The factors influencing this assessment were the mechanical complexity, operating conditions (temperatures, pressures, rotor speeds, etc.) and relationship of the design to the state-of-the-art.

It is expected that the nonaugmented turbojet would demonstrate the lowest failure rate in commercial SST service operation. The duct heating turbofan and the fully augmented turbojet should exhibit a failure rate higher than the nonaugmented turbojet, with the augmented turbojet showing the highest failure rate. The factors which account for the differences in the expected reliability are: number of main bearings and seals; number of compressor and turbine stages; existence of an inlet case; complexity of combustion system (number of nozzles, etc.); complexity of control, fuel and oil systems; requirement for augmentation; and the temperature of available cooling air for duct heater or afterburner.

3. FAILURE MODE ANALYSIS AND DESIGN REVIEW

a. Failure Mode Analysis

A detailed failure mode analysis has been accomplished for the basic engine structure. Included in the process has been the listing of the predominant failure modes, their causes and consequences, and the design philosophy adopted to preclude such occurrences. Extensive use was made of service records that have been accumulated from commercial and military aircraft engine experience. This includes service experience on engines in aircraft with supersonic capability.

Failure mode analyses contribute to the overall design process in that possible problem areas are considered and eliminated from the design before these problems are exhibited during the development or operational phases of the engine. A typical worksheet used in the failure mode analysis is illustrated in Figure 17-1.

b. Design Review

Special attention has been given to those areas in the engine where problems have existed in previous engine designs or where problems are anticipated in the SST powerplant. The design reliability reviews of the detailed component layouts have been focused particularly on these areas. These reviews were made to provide assurance that adequate preventive measures have been taken and that the latest Pratt & Whitney Aircraft design philosophy has been adopted. The designers were helped in accomplishing this task by maintaining and utilizing in the design effort up-to-date copies of the Design and Drafting Room Manuals. These manuals contain Pratt & Whitney Aircraft standard design practices which reflect the latest state-of-the-art design philosophy for reliable gas turbine engine design. Additionally, standard parts of previously demonstrated reliability have been utilized whenever their use was feasible for inclusion into the design.

4. STF219 ESTIMATED FLIGHT RELIABILITY

A study was conducted to estimate the mean time between in-flight shutdowns (MTBIFS) for the STF219 duct heating turbofan engine. An in-flight shutdown is defined as any malfunction or discrepancy chargeable to the engine which causes or generates a decision to shut down the engine while in flight (i.e., from the moment a take-off roll begins until the landing roll begins). It should be noted that this definition would exclude failures of ancillary equipment not part of the engine as defined by the model specification, maintenance errors, false fire warnings, bird strikes, and other incidents which would not be directly chargeable to the engine.

The MTBIFS for the STF219 engine is estimated to be 10,000 hours. This is estimated for a mature engine installation that will result from an accumulation of operating experience and the incorporation of modifications to eliminate any initial problems that may develop.

This reliability prediction is based on extensive service records from commercial and military operations. Each major section of the engine was analyzed using actual shutdown rates experienced in current engines - 'ljusted by correction factors accounting for the advanced design features, degree of complexity, and operational environment of the SST engine. The failure mode analysis work described in Part 3, above was utilized in this assessment.

5. ENGINE RELIABILITY FEATURES

In improving the inherent reliability capability of the SST engine components, each major section was analyzed and compared in detail with the in-flight shutdown and premature removal experience with current engines. The analysis took into account the more severe operating conditions of the SST powerplant, such as the increased engine inlet temperature at high Mach numbers and the increased turbine inlet temperature.

Many design features have been incorporated to enhance the reliability of the STF219 engine. The following is a breakdown of the engine into its major components. Under each section is listed some of the outstanding reliability features and improvements over current engines.

a. Fan and Compressor Section

Basically, the fan and compressor is a less complicated structure with fewer stages than the JT3D. It consists of a two-stage overhung fan and a five-stage high pressure compressor. The overhung fan does not require inlet case struts with their anti-icing requirements and potential cracking problems. Fan and compressor blades are retained in their disks by either clamping plates or shear pins instead of sheet-metal tablocks. Vibration damping devices, extended blade roots with external centrifugal dampers, are used in the first and last stages of the high pressure compressor to reduce the effect of blade excitation caused by the struts upstream and downstream, respsrctively, from these stages. Abradable shrouds over the blade tips reduce the heat generation in the event of a radial rub during some abnormal operating condition. The high compressor stators are mechanically attached to the inner and outer shrouds. This is an improvement over the contour-rolled strip stock vanes used in current engines which are brazed to the inner and outer shrouds resulting in stress concentrations at the braze locations in the vane root and tip.

An aerodynamic brake is provided behind the second-stage fan rotor. Braking is accomplished with a variable stator that rotates to a closed position restricting the airflow through the engine. Thus, in the event that the engine has to be shut down in flight, the windmilling speed is reduced to a level comparable to that experienced in present commercial subsonic aircraft.

Past engine experience indicates that vibratory and cyclic cracking in and around points of load introduction and discontinuities are the most frequent problems in main structures. All the accumulated experience from such problems on preceding engine designs has been utilized in the design of the intermediate case as well as the other main static structures. Areas of stress concentration have been minimized based on advanced design philosophy and features known to be effective in alleviating trouble areas in past engines. Extensive use of butt welded construction throughout the entire intermediate case reduces stress concentration. Oil from the bearing compartment which drains through the fan-case strut is contained within a tube and does not come in contact with the inner surface of the strut. Thus any crack which may develop in the strut will not effect the oil system. The bearing compartment is isolated from the high pressure fan air.

b. Diffuser and Combustion Section

The diffuser case is also fabricated by means of butt welded construction. Reduced stress concentration at attachments of through-tubes and struts and the transfer of the tower shaft in the cooler front section of the engine will increase the reliability of this case. Oil tubes passing through the diffuser case struts isolate the oil system from the inner surface of the struts. As in the fan case, the oil or the breather system is not seriously affected by high pressure and temperature air leakage through a strut crack.

The combustor incorporates an improved annular design, as differentiated from the can type. The annular combustor provides a more uniform temperature profile of the gases entering the turbine nozzle vanes. Also, improved methods of mixing the fuel and air results in a shorter combustion chamber length and shorter unsupported cooled combustion system walls. Reduced circumferential temperature gradients, fewer hotspots, and a single annular system, all contri-

bute to a reduced incidence of low cycle fatigue cracking. The likelihood of pieces breaking out to cause turbine damage is considerably reduced. The design requires fewer fuel nozzles than the can type, inherently decreasing the probability of clogging and faulty spray patterns. The fuel manifolds are external to the main gas stream and thus are subjected to a lower temperature environment.

c. Turbine Section

The turbine section is expected to present the greatest challenge to reliability in relation to current subs ic engines. This is primarily the result of the increased level of bine inlet temperature for the SST engine, necessitating the use of oled blades and vanes. However, advanced concepts of blade and vane cooling, taking full advantage of improved materials and past experience with oxidation preventative coatings, are being tested in hot rigs to develop a reliable configuration.

The turbine consists of three stages, one high-pressure and two low-pressure stages. This is one less stage than is currently used on the JT3D. The first two turbine stages utilize rotor blades with extended roots and external root dampers, thus eliminating the need for tip shrouds on these stages. Turbine shroud wear has been a particular problem in the past and the elimination of these shrouds from the first two turbine stages with their high operating temperatures should improve turbine reliability.

The more uniform temperature pattern provided by the annular burner, together with positive vane retention, should result in improved turbine nozzle vane reliability. Radial seals on the turbine blade platforms and provisions for between-platform sealing prevent the impingement of the hot main stream gases on the turbine disks.

d. Main Bearings and Seals

Particular design emphasis has been directed toward improving the environmental conditions in the main bearing compartments. The following are ome of the STF219 design features which contribute to improved liability. Only four main bearings are required instead of the six main shaft and two intershaft bearings used in the JT3D. The shorter combustion chamber length required with an annular combustor together with an overhung fan make it possible to support each rotor with only two bearings. No intershaft bearings are needed. The two main thrust bearings are located in the relatively cool section of the engine. The use of single rather than duplex thrust

bearings eliminates the potential problem of skidding of the bearing which could be caused by unequal thrust load distribution between the two bearings of the duplex set at certain operating conditions. All the main shaft bearings are cooled by oil under the races. Face seal plates are also oil cooled. All of these features contribute to longer bearing and seal life.

Carbon face seals with back-up labyrinth seals are used in all bearing compartments. A pressurized and vented labyrinth seal system in the No. 3 and No. 4 bearing compartments isolates the bearing compartments from their relatively high-temperature and high-pressure environment. It is accomplished by introducing comparatively low-temperature and low-pressure fan exit air into a jacket surrounding the bearing compartment. The lower temperature and pressure not only benefit the bearings and seals, but also the overall oil system since the average temperature and amount of air leakage into the oil system will be reduced. As a result, the amount of heat rejection by the oil system will be reduced, and oil coking problems will be minimized.

e. Fan Duct Section

The STF219 utilizes a duct heater for augmentation. Thus it is possible to cool the duct liners with relatively cool fan discharge air. A shield between the duct outer liner and the rear mount ring has been provided to protect the rear mount ring in the event of liner overtemperature during augmentation. Additionally, the shield provides for turbine blade containment. Vibration damping provisions have been incorporated on the aft outer liner to prevent excessive liner vibration and thus reduce the probability of fatigue cracking.

f. Ejector-Reverser System

The ejector-reverser system is designed so that the blow-in doors are positively opened, creating the reverse exhaust path as the reverser flaps are actuated from the stowed to the reverse position. A lock is provided in the actuator to assure that the reverser flaps remain in the stowed position during normal operation of the engine. The twelve reverser flaps are positioned by separate actuators. Thus if one of the actuators or linkages should fail, the reverser capability is not critically influenced. Pressure loading on the reverser flaps causes return to the stowed position in the event of system failure. *

* A more detailed reliability analysis is presented in a letter from D. J. Jordan to G. M. Bain, dated 14 February 1964.

The blow-in doors and tail flaps have been designed so that they are self actuating except in the case of reverser operation of the blow-in doors. The optimum operating position is maintained by the pressure balance of the gases on the blow-in doors and tail flaps.

B. CONFIGURATION MANAGEMENT

1. OBJECTIVE

The objective in the area of configuration control during the SST Phase II-A program was to provide engine configurations based on the various engine cycles being studied, submit preliminary installation drawings for these engines, and maintain close coordination with the two airframe contractors to provide optimum airframe and engine installation compatibility.

2. DISCUSSION

The major areas requiring resolution were those of providing suitable engine mounting arrangements, engine accessory arrangements, provisions for driving airframe accessories, secondary cooling airflow systems, blow-in-door ejector exhaust system configurations to satisfy airframe nacelle contour lines, and thrust reverser configurations to meet the airframe targeting requirements.

A system of SST coordination sheets was established and monitored by Pratt & Whitney Aircraft's Installation Engineering Department to transmit data to and from the airframe contractors. Telephone and telegraph communications were used frequently to maintain liaison and transmit information. These communications were again monitored by Installation Engineering. Frequent meetings were held between Pratt & Whitney Aircraft and the airframe contractors' engineering personnel to discuss and resolve problems. These meetings were held both at Pratt & Whitney Aircraft and at the two airframe contractors' facilities.

Preliminary engine installation drawings were prepared for the basic engine cycles that have been studied. These installation drawings were submitted to each of the two airframe contractors for consideration early in the program. In response to requests from Boeing, information was supplied to define permissible preliminary engine

contours to fit their conical nacelle concept. These lines were further modified to define a nacelle envelope for fixed deflection of the engine exhaust gases. This envelope remained fluid as engine studies progressed, until October when final definition was coordinated with Boeing.

Considerable design effort was required in the area of engine accessory arrangement studies. In response to requests from both airframe contractors, many arrangements of top-mounted, side-mounted, and bottom-mounted engine accessories were studied. The various design arrangements were submitted to the airframe contractors for their consideration, and final configurations were negotiated for each airframe installation.

At the request of both airframe contractors, design studies were initiated to provide an engine-driven power take-off pad for driving the remotely mounted airframe accessories. The designs have been coordinated and accepted by both contractors. At the request of Lockheed Aircraft, an engine-mounted elbow gearbox and flexible shaft decoupler are being provided at the power take-off pad.

Extensive coordination and design effort was necessary to arrive at a suitable engine mounting system for each airframe installation. Since the airframe contractors have different nacelle concepts, the engine mounting arrangement had to be tailored to fit each installation. A number of engine mounting arrangements were proposed for both installations, and acceptable configurations have now been finalized.

The targeting of the thrust reverser exhaust gases required major revisions of the original configurations.

Coordination with both airframe contractors was necessary to establish thrust reversing targeting to satisfy their respective installation requirements. Design arrangements were submitted, and final agreement on reversing configurations was reached.

The secondary air supply for ejector cooling is handled differently for each airframe manufacturer. The Lockheed airplane furnishes a pressurized nacelle for conducting the air rearward between the engine and the nacelle. In the Boeing installation the nacelle is not pressurized and secondary air is ducted back to the ejector. In both installations, the inlet is the source of secondary air.

C. WEIGHT AND CONFIGURATION CONTROL

1. WEIGHT ANALYSIS

The STF219 is an advanced twin-spool, duct burning turbofan engine. The estimated dry weights for the Boeing and Lockheed engines are tabulated in Figures 17-2 and 17-3 including a sectional weight breakdown. Included in the dry engine weight is the following standard equipment:

a) Gearbox for engine accessories

b) Fuel pumps (engine and duct heater)

c) Fuel Controls (engine and duct heater)

d) Fuel check and dump valve

e) Ignition system without power source

f) Hydraulic pump

g) Breather pressurizing valve

h) Exhaust nozzle control

i) Hydraulic actuation for variable area nozzle

j) Oil tank

k) Fuel-oil coolers

l) Oil pump and filter

m) Instrumentation

n) Blow-in-door ejector-reverser

o) In-flight aerodynamic engine brake

p) Fuel boost pump

q) Fuel filter

r) Engine mounting system capable of supporting engine and exhaust system.

Weight of additional equipment and installation features requested by the airframe manufacturers is tabulated in Figures 17-2 and 17-3.

The weight of the STF219 was established at an airflow of 600 pounds per second and scaled to the sizes required by Boeing and Lockheed. The weight of the basic engine was established by calculating the weight of parts from preliminary layouts. Detailed design information was available on all airfoils and rotating parts. The static structure was analyzed and proper thicknesses incorporated into the engine weight analysis. A preliminary Bill of Material was established to assure that all parts were accounted for.

Having established the basic weight of the STF219 at an airflow of 600 pounds per second, the engine weight was then scaled to the required airflow sizes by scaling each major component. Scale factors for each section were based on a thorough study of the necessary changes in blade chords for the compressor and turbine, burner geometry, duct-heater geometry, and blow-in-door ejector-reverser sizes. Materials were also optimized for cruise Mach number requirements of each airframe. The engine mounting system was tailored to meet the requirements established by both Boeing and Lockheed.

2. LIGHTWEIGHT DESIGN FEATURES

Since the requirement for a lightweight propulsion system is important in the SST program, emphasis was placed on optimization and incorporation of all lightweight features without compromising performance, life or reliability objectives. The lightweight features incorporated represent a significant advancement over current commerical turbofan design philosophy and significantly increase the thrust-to-weight ratio. Figure 17-4 illustrates the impact of advanced design concepts on the thrust-to-weight ratios for supersonic engines. All engines shown have been adjusted to the same turbine inlet temperature, pressure ratio, airflow and equipment for purposes of comparison. The ability to obtain thrust-to-weight ratios in this higher range for the STF219 design is already substantiated in part by the STF200 demonstrator engine currently operating at Pratt & Whitney Aircraft. Also, the feasibility of the lightweight features of the STF219 gas generator has been demonstrated by the STF200 engine.

The advanced lightweight features incorporated into the STF219 are as follows:

1) The compressor inlet case support was eliminated by cantilevering the fan rotor. The elimination of the compressor inlet case also eliminated the inlet guide vanes, the front bearing, the bearing support structure and the inlet guide vane anti-icing system.

2) The fan rotor utilizes high aspect ratio blading and an increased stage pressure ratio, thereby permitting thinner disks and fewer stages.

3) The high-pressure compressor rotor employs several lightweight features not incorporated in current turbofan engines. The blade aspect ratios have been increased, thus permitting thinner disks. The stage loading has been increased, thus allowing fewer stages. Also, dual spacer rotor construction is used.

4) A high heat-release-rate annular combustion chamber replaces the conventional can combustion chambers resulting in a significant savings in length, diameter and weight. The diffuser-burner section was further lightened by using the burner liner to aid the diffusion process and reduce the length required for diffusion.

5) The turbine rotor employs high aspect ratio blading in the turbine section. This results in thinner disk sections.

6) The combination of the short annular combustion chamber, the high stage loading and the high aspect ratio blading of the high-pressure compressor rotor reduces the gas generator length permitting the use of two bearings per rotor. This reduces the number of bearings used in present day turbofans from six fixed bearings plus an intershaft bearing to four fixed bearings with no intershaft bearing. The elimination of bearings, bearing supports, and lubrication system components results in weight savings.

7) A cascade type diffuser in the fan duct reduces the overall engine length and weight.

8) The duct heater variable-area nozzle was integrated with the ejector structure, thereby eliminating parts previously required. The nozzle flaps are reduced in length and the system is changed from a floating hinge design to a fixed hinge design. The shorter flaps require less actuation load and stroke, thus saving weight in the actuators.

9) The blow-in-door ejector-reverser has been designed to house the thrust reverser, thus utilizing structure already available.

10) The fuel control for the gas generator and the duct heater are combined in a common housing using common input sensors.

11) Material usage was optimized to provide minimum weight by selection of the best available materials. Extensive use was made of titanium throughout the low temperature regions of the engine and of high-strength, high-temperature materials in the high-pressure compressor, burner and turbine sections.

3. WEIGHT SCALING

Engine weight as a function of engine airflow was supplied to the airframe companies to assist them in selecting the proper engine size. Data on engine center of gravity and mass moment of inertia were also supplied. A study was made to determine the effect of cruise Mach number on engine weight and the information was supplied to both airframe companies.

4. TURBOJET WEIGHT ANALYSIS

Three advanced lightweight single-spool turbojet engines were evaluated. The three configurations are: a) STJ221, a nonaugmented turbojet: b) the STJ222, a fully augmented afterburning turbojet; and c) the STJ227, a partially augmented turbojet. These engines were studied in basic sizes designed to have the same transonic thrust, and weight scale factors were calculated to permit scaling over a range of airflow sizes. Figure 17-5 summarizes the estimated dry weights of the above turbojets. The STF219 is listed for comparative purposes. Estimates of weights for all engines were made in a consistent manner with equivalent equipment included. The Mach number capability, nozzle performance, and the state-of-the-art aerodynamic and mechanical design were maintained at the same level. Figures 17-6 through 17-8 summarize the weight scale factors for the basic engines including the ejector-reverser.

5. MIXED FLOW AFTERBURNING TURBOFAN

A mixed flow afterburning turbofan, the STF223, was briefly evaluated. Since the cycle was eliminated from consideration by Boeing and Lockheed early in Phase II-A, no further design study or weight analysis was done for this engine

D. VALUE ENGINEERING

During Phase II-A, four value engineers were assigned full time to the SST program. Their efforts were supplemented by assistance from the Production Engineering, Industrial Engineering and Purchasing Departments. The work accomplished is summarized in the following paragraphs.

Parametric studies were completed on the relative price versus airflow for the STF219, STJ227, and STJ222 engines, as shown in Figure 17-9. The results of these studies were supplied to Boeing and Lockheed as input data for their direct operating cost studies.

These curves were generated by estimating the cost of each of the engines in the design airflow size. A sampling of purchased finished parts and raw material forms with dimensional scale factors to cover the airflow range were then sent to vendors through the Purchasing Department for price estimates. Based on these estimates, data were developed to scale both raw material and purchased finished parts costs over the total airflow range of 350 to 900 pounds per second. Similar type estimates were generated for the machine shop and assembly labor by the Production and Industrial Engineering Departments. The cost versus airflow data were then applied to the basic engine cost, which was in turn converted to price by the Accounting Department.

A study to determine the effect of flight speed on price was completed from Mach 2.5 to Mach 3.0 and the results are shown in Figure 17-10. These results were achieved by a detailed review of materials selection with the Design, Design Analysis and Engineering Metallurgy Groups. The effect of the flight speed on the materials selection was determined, and the engine costs were adjusted to reflect the materials changes. The relative price versus Mach number curve is applicable to all engines.

As part of the Phase II-A program, the Value Engineering Group worked closely with the SST Design Group reviewing preliminary layouts and recommending more economical design solutions. Economic evaluations were performed for the Design and Project Groups to assist them in the selection of design solutions that assured the maximum in value. These studies included cost-weight trade-offs for alternate disk, shaft and major case materials.

During Value Engineering's design review, experts from Production Engineering's Advanced Methods Group and the Weld Development Laboratory were contacted regarding the machining, fabrication and welding of the advanced materials being considered. Based on these meetings with Production Engineering, at which all major engine parts were reviewed, recommendations regarding construction were made and evaluated to assure that the designs were consistent with the latest manufacturing techniques. Some of the new techniques which were considered included electron beam welding, flo-turning, electric discharge machining, electrical-chemical machining, and explosive forming.

Specialty vendors were contacted to discuss the use and economics of specialty products and processes. These contacts included items such as cooled turbine blades, cooled [illegible], variable stators, honeycomb and wire mesh. Meetings were [illegible] with potential suppliers of the main control system to discuss the [illegible] cost of fuel flow, environmental temperature and fuel temperature.

Throughout the Phase II-A program the preliminary planning estimates on all engines under consideration were revised as the designs were modified, and the Project Manager was kept informed weekly as to the relative and total cost status.

Simultaneously with preliminary costs for planning purposes, final cost estimates were in process. Components that represented more than 80 per cent of the engine costs were examined in detail. Quotations on purchased parts and raw material were obtained from vendors with experience in working with the advanced materials required for the SST. Vendors currently supplying hardware for the JT11D-20 engine were contacted and asked to provide cost estimates on these parts in high volume. These estimates, along with quotations on a sampling of SST hardware and the standard cost data on all current production engines, were correlated and used as the basis for production prices.

E. MAINTAINABILITY

1. INTRODUCTION

This section presents a discussion of the maintenance features of the STF219 powerplant. The maintainability effort applied in the design phase is discussed, including a brief comparison of the maintainability aspects of the various powerplants studied. Specific design features of the STF219 which facilitate both scheduled and unscheduled maintenance requirements are discussed in detail. This discussion is oriented toward flight line maintenance, field repair and overhaul requirements expected for the SST powerplant. The major component assembly procedures and their associated figures presented in Item 2 of this report will help to clarify the descriptions of specific maintenance features described in this section.

2. MAINTAINABILITY ENGINEERING

The engines proposed for the SST powerplant have been designed with careful consideration given to inherent maintainability features. Pratt & Whitney Aircraft's extensive experience with turbofan and turbojet engines was called upon to establish the maintenance concept for the SST powerplant. Service records provided maintenance and overhaul experience used to establish the maintenance requirements for the powerplant, with due consideration for the operating conditions of the SST.

The study engines considered in Phase II-A were constantly reviewed by the Maintainability Engineering Group during the design stages. A preliminary task analysis was performed on each powerplant to assure that the maintenance requirements could be met with minimum down time and maximum safety for maintenance personnel. Uncomplicated assembly procedures, resulting from unit component construction features, simplify maintenance tasks and minimize the personnel skill requirements in all levels of maintenance. No new maintenance techniques or skills are required; therefore, the engine may be maintained by existing aircraft powerplant crews with minimum additional training. The special tooling requirement and the ground equipment will be similar to that used on current powerplants.

3. COMPARISON OF VARIOUS DESIGNS

The basic engine maintenance requirements of all the powerplant studies are the same. The augmented engines require some additional maintenance for the afterburning or duct heating system. Flight line maintenance requirements can be met equally well with all the designs. Those requirements, which would be accomplished with the powerplant removed from the aircraft, i.e. hot section inspection or field repair, present only a small additional disassembly procedure for the duct heating engines since the ducts can be easily removed.

4. FLIGHT LINE MAINTENANCE

The ability to satisfy flight line maintenance requirements depends upon the installation in the aircraft, and detailed co-ordination with the airframe manufacturer has been performed to achieve the full maintainability potential of the engine design. Design features which facilitate the accomplishment of flight line maintenance requirements for the STF219 turbofan powerplant are discussed below.

Visual inspection of the exhaust section may be readily performed. Inspection of the engine inlet is complicated by the design of the aircraft inlet and may require the use of special tooling. Borescope provisions will be incorporated in the STF219 design to facilitate this inspection as required. The powerplant design does not require an inlet case and thus eliminates the need for inlet case maintenance. This feature also eliminates the anti-icing requirement and facilitates inspection of the low compressor for foreign object damage.

The engine accessory gearbox is presently considered in two alternate locations to satisfy the different airframe manufacturers. The accessibility of the engine supplied controls and filters, therefore, depends upon the installation, and these requirements have been co-ordinated with the airframe manufacturers. In either location clearance for inspection, adjustment, or removal of the main oil strainer, fuel filters, and engine supplied accessories is provided by the powerplant design and is considered by the airframe design. The design will employ quick-disconnect mounting where necessary to permit simplified removal of individual engine supplied accessories. The design provides a power take-off pad for the wing mounted airframe accessories.

need for replacement. With the combustion inner liner moved forward, the first-stage nozzle inner case may be telescoped forward to expose the first-stage turbine rotor. The front seal disk and disk rim air-seal ring may then be moved forward. The retaining ring holding the blades in the disk is then removed and any damaged blades may be replaced. All turbine blades are moment-weight classified and may be replaced in pairs without rebalancing the rotor.

The replacement of the combustion liners is considered under the repair concept described below. It should be noted that the use of an annular burner presents a more durable combustion chamber and provides a more uniform temperature pattern, thereby reducing the frequency of unscheduled turbine maintenance. This burner design permits a shorter, lighter engine and is a major factor in permitting the use of two bearings for the support of each rotor. This reduces bearing compartment maintenance and greatly facilitates component disassembly.

6. FIELD REPAIR

The design of the major components of the STF219 engine greatly facilitates disassembly of the engine. This feature makes even the remote areas of the engine readily accessible for maintenance action should the need arise. The major units of disassembly are shown in Figure 17-12.

The absence of an inlet case permits ease of inspection of the blades and vanes of the entire low-pressure compressor, which consists of two fan stages. Should excessive foreign object damage be evident, the entire low compressor may be removed as a unit for maintenance. Any damaged blades or vanes may be individually replaced, and the rotor stages rebalanced. This feature permits the reassembly of the fan rotors without subsequent rebalancing of the complete low rotor assembly.

The high and low rotor thrust bearings are accessible after the fan rotors are removed. The front bearing support is unbolted from the intermediate case. Then, with a proper restraining fixture applied to the low turbine, the low rotor coupling bolt is unthreaded driving the front hub, bearing support and No. 1 bearing and seal forward as a unit.

The high rotor thrust bearing (No. 2 bearing) may be subsequently removed with little additional disassembly. The intershaft seal assembly is removed from the intermediate case, and the retaining nuts, seal plate and towershaft drive gear are withdrawn from the high compressor front hub. The intermediate case is then unbolted from the high compressor case and removed forward carrying the No. 2 bearing and seal. These units may then be disassembled from the intermediate case for maintenance if necessary.

The condition of the ignition system can be determined by testing the igniter plugs individually for spark without disassembly of the plugs or engine cases. These igniter plugs may also be readily removed for inspection or replacement as required without case or duct disassembly.

Exhaust gas temperature-measuring thermocouple probes are designed and located in a manner which permits the use of calibrating equipment without running the engine. A connector is supplied on the engine to provide a means of checking continuity of individual thermocouple leads without removing the thermocouple harness from the engine.

5. HOT SECTION MAINTENANCE

Careful attention was given during design to provide ready accessibility to the burner-turbine area. The maintenance actions required for both scheduled and unscheduled hot section maintenance are described below and are illustrated in Figure 17-11.

The duct outer liner and ejector nozzle case and structure may be readily removed as a unit. The duct inner liner, positioned over the burner and turbine cases, is then withdrawn by removing radial screws and sliding it aft. The aerodynamic flameholder and main burner igniters may be unfastened from the engine case and the intermediate duct section removed in an aft direction. The duct inner liner, positioned over the diffuser case, is then removed in an aft direction to provide access to the fuel manifold and fuel nozzles. The fuel nozzles may be individually removed for inspection or replacement.

To inspect the combustion liners, first-stage nozzle vanes, and first-stage turbine blades, it is necessary to gain access to the internal engine structure. This is accomplished by unbolting the burner rear case and telescoping it in an aft direction over the turbine case. The aft portion of the combustion outer liner is then telescoped forward inside the diffuser case to expose the combustion chamber and first-stage nozzle vanes for inspection. The first-stage nozzle vanes may be individually removed by telescoping the combustion inner liner in a forward direction. The vanes then may be withdrawn in a forward direction out of the inner torque ring. With several adjacent vanes removed, the first-stage turbine blades may be readily inspected.

The design of the STF219 permits replacement of the first-stage turbine blades with little additional disassembly, should inspection indicate the

The low rotor rear bearing (No. 4 bearing) and seal are exposed when the turbine exhaust section is removed. The bearings and seals may then be stripped from the low turbine shaft.

The entire low-pressure turbine, with the exception of the second stage nozzle vanes, may be removed and replaced as a unit without the need for rebalancing. This unit may be disassembled from the engine while attached to the turbine exhaust section or after that section is removed. The rear turbine case must be unbolted from the front turbine case and the rotor coupling nut unthreaded to jack the low turbine unit away from the engine. Second stage vanes are then individually replaceable.

The removal of high turbine blades was described under Hot Section Maintenance above. An alternate means would be to remove them with the high turbine disk. With the low turbine removed, the front turbine case may be unbolted from the burner rear case and removed carrying the second stage nozzle vanes. The high turbine rotor may then be removed in either of two ways. The rotor and shaft may be removed as a unit carrying the bearing and aft seal with it. In this case, the aft seal must be unbolted from the bearing support by gaining access through the combustion section as discussed in the hot section maintenance procedures. The alternate method would be to separate the high turbine rotor from the shaft and remove the disk and blades as a unit.

The removal and replacement of both turbine units may be accomplished without removing either compressor. Replacement of turbine blades is thus simplified. All turbine blades are moment-weight classified and may be replaced in pairs without rebalancing the rotor.

When both turbine units are removed the high rotor rear bearing (No. 3 bearing) compartment is readily accessible for maintenance. The bearing and rear seal are removed with the turbine hub as described above. The bearing support may then be removed to expose the fittings on the bearing compartment oil lines. After disconnecting these fittings the front compartment seal may be removed. The accessibility of this bearing is greatly improved over previous twin spool engine designs.

The three-piece combustion chamber liner may be removed after the low turbine unit and high turbine rotor have been disassembled from the engine. The two-piece nozzle inner case, vane outer support ring, and first-stage nozzle vanes may be removed as a unit. The aft portions of the combustion inner and outer liners may then be withdrawn from the engine. The fuel nozzle adapters and liner retaining pins are then removed, and the forward combustion liner can be withdrawn in an aft

direction. An alternate design of the combustion liners is being studied in an effort to permit liner removal without turbine disassembly. This will be done through the use of an axially split structure. Any maintainability gains resulting from this study will be evaluated with regard to their effect on performance, cost, reliability and weight before considering this design for incorporation into the final powerplant design.

7. OVERHAUL

The component disassembly features described above, plus the fact that the engine can be disassembled in either a horizontal or vertical position, simplify overhaul procedures. A more detailed discussion of the assembly procedures is presented in Item 2 of t report.

8. MAINTENANCE PLAN

The design features discussed above describe the maintenance capability of the engine. The Pratt & Whitney Aircraft maintenance plan for the selected powerplant will be presented in our commercial engine publication as defined in ATA Specification No. 100. This plan will be published six to eight months prior to initial scheduled operation. This maintenance plan will subsequently be reviewed by a maintenance review board composed of members from the participating airlines, the Federal Aviation Agency, and Pratt & Whitney Aircraft. At this time specific maintenance requirements, tasks and frequencies will be established. Any subsequent revisions to the maintenance plan will be subject to approval of the Federal Aviation Agency.

F. SAFETY

1. INTRODUCTION

A primary objective of the overall development program is safety. Extensive effort is directed toward this end. During the Phase II-A period, the safety aspects of the engine design were monitored. The need for fail-safe and redundant features was considered, and recommendations were made for inclusion of these features into the design.

The following sections present a detailed report of the continued effort to enhance safety for the SST powerplant under Phase II-A.

2. MONITORING THE SAFETY ASPECTS OF ENGINE DESIGN

During the failure mode analysis, discussed in the Reliability Section, the various failure modes were analyzed as to their effect on flight safety. The design criteria were reviewed as to their adequacy in reducing the probability of such failures occurring which would affect flight safety. Every effort was made in the design reliability review to assure that possible failures are contained and their consequences neutralized or prevented from progressing into a more serious failure.

The detailed component design layouts were reviewed from a flight safety point of view as well as other reliability considerations. With the aid of commercial in-flight shutdown summaries for various Pratt & Whitney Aircraft engines, particular attention was brought to bear on those areas where particular failures in service resulted in in-flight shutdowns. Investigations were conducted to assure that design improvements have been incorporated in these areas that would reduce the probability of similar failures in the SST engine.

Where feasible, fail-safe features and redundancy have been considered and recommended to assure that certain failures do not result in a more hazardous condition affecting flight safety.

3. FAIL-SAFE AND REDUNDANT FEATURES

The fail-safe and redundant features of the STF219 engine are as follows:

- The rotors, cases, mounts, and bearing supports are designed to withstand the dynamic loads, induced by rotor imbalance caused by blade failure, of a peak magnitude equivalent to the static load of ten per cent of the blades of any one stage.
- Fan blade chords have been established that will provide adequate structural durability in the event of bird ingestion.
- In accordance with FAA requirements, engine cases are designed to contain blades in the event of blade failure.
- Abradable shrouds are used over the compressor and fan blades where blade rub could occur.

- In case of excessive axial movement of the rotors, rubbing will occur at the heavy rim section rather than at the thinner web section of a disk. This will maintain disk integrity and prevent the disk from bursting as a result of separation of the heavy rim section from the web and bore.

- The variable stator behind the second fan rotor, used as an aerodynamic braking device, is aerodynamically balanced in the open position for normal engine operation. In addition, a mechanical lock is provided in the actuator to keep the vanes in the open position.

- Anti-icing problems and the possible failure of inlet struts after long exposure to hot anti-icing air are eliminated because the engine does not require inlet case struts.

- A steel sleeve is used at all thrust bearing locations. In the event of bearing failure, this sleeve will provide protection against the high temperatures and stresses that otherwise might seriously reduce the strength of the shaft. In addition, this sleeve facilitates cooling. Failure of the more lightly loaded radial bearings is not considered critical to the integrity of the shaft.

- Main shaft splines are kept a safe distance from main bearing areas. In this way, in case of a bearing failure, the load carrying capacity of the splines will not be seriously impaired by the heat generated by the failure.

- In the unlikely event of a main shaft failure, braking of the turbine rotor sufficient to preclude disk burst will take place. This is accomplished in the design by ensuring that the free turbine rotor, as it moves rearward due to the resultant axial thrust on it, does not "hang up" on any stationary member that could provide a temporary bearing surface. Contact is designed to occur initially between the blades and vanes, studies and tests have shown that this will stop the turbine rotor before disk burst speeds are reached.

- All main bearing carbon seals have back-up labyrinth seals that would restrict hot gases from entering bearing compartments and possibly causing a fire in the event of carbon seal failure.

- Oil coolers, fuel heaters, and all main filters are provided with bypass valves which open when pressure increases to a prescribed level as the result of plugging by contaminants.

- A fully redundant main oil filter system is used. Two filters are utilized with one intended as a stand-by unit, operating only in the event of plugging of the primary filter. Each filter is provided with pressure taps to which a cockpit warning light system can be connected. Thus the pilot can be warned if filters become plugged.

- A shield between the duct outer liner and the rear mount ring has been incorporated to protect the rear mount ring in the event of an overtemperature of the liner during augmentation. Additionally, the shield improves turbine blade containment capability.

- Both inner and outer ends of the first-stage turbine nozzle vanes are retained so that in the event of a burn-through the vane will be prevented from passing through the turbine causing further damage.

- The engine starter is mounted on the airframe-furnished gearbox. However, a shear section in the starter drive will be recommended to the airframe manufacturer to minimize damage to the critical internal engine parts in case the compressor is not free to rotate during starting as a result of obstruction or binding.

- A redundant ignition system is used. The engine main burner has two spark-igniters and two ignition exciters, although only one of each is normally used for ignition. Automatic ignition is provided for restart in case of engine flame out.

- The twelve reverser flaps are operated by an individual actuator for each flap. Thus, if one or more of the actuators or linkages should fail, only the reverser capability of the affected flaps would result. In the event that failure of the actuation system should occur during reversing operation, the reverser flaps have been designed to return to the stowed position by pressure balance.

- The exhaust nozzle actuation linkage is designed to provide proper actuation of the nozzle flaps even with the failure of as many as half of the actuation cylinders. Axially and circumferentially located rollers on the unison ring prevent cocking and binding of the ring as a result of unsymmetrical loading because of actuation-cylinder malfunction or any other cause. This is also characterisitc of reverser flap actuation system.

- The exhaust nozzle is designed to open in the event of complete actuation failure, thus preventing excessive back pressure on the fan and a dangerous situation in the augmenting condition.

- In case of duct heater flameout, dangerous overspeed is not a matter of concern because duct flow is separate from engine flow and the pressure ratio across the turbine would remain unchanged.

- A mechanical lock is incorporated in reverser actuators to keep the reverser flaps in the stowed position during normal engine operation.

- The reverser flaps can not be actuated until (and unless) the blow-in doors are open to create the reverse exhaust nozzle.

TYPICAL FAILURE MODE ANALYSIS FOR THE STF219

Item	Failure Mode (Ranked According to Probability of Occurrence)	Consequence	Cause	Design Philosophy
Combustion Chamber Liners	Cracked	Maintenance action at overhaul. [illegible] cracking [illegible] tolerated with[illegible] consequence[illegible]	[illegible] induced low cycle fatigue	The combustor [illegible] annular type combustor which [illegible] improved design over the can type. This design results [illegible] circumferential temperature gradients, [illegible] and greater [illegible] flexibility. All of these factors contribute to a reduced incidence of low cycle fatigue cracking. The liners are fabricated with [illegible] the walls away from the flame side and with corrugated porous sheet metal on the flame side walls. [illegible] are scrubbed by [illegible] This provides for cooler metal liner temperatures [illegible] design. The outer rear [illegible] support ring has been designed with flexibility to accommodate differential thermal growth. Liners are fabricated from Hastelloy-X which is readily weldable and maintains its strength at elevated temperatures. [illegible] quality control must be maintained at all welded joint
	Buckled or Distorted	Maintenance action [illegible]	Creep	The inner liner is creep limited due to hoop stress. The liner is designed to a limit of 0.5% creep in 10,000 hours [illegible] operation. The outer liner is creep buckling limited. The liner is designed with a 1.3 margin of safety [illegible] stress in 10,000 hours [illegible] operation
	Worn	Maintenance action at overhaul	Contact stresses at sliding joints	Annular combustor provides an increase in bearing surface at sliding joint locations resulting in reduced contact stresses over the can type. Contact surfaces are hardfaced to reduce wear
	Burned	Performance loss, possible premature engine removal or in-flight shutdown	Impingement of hot gases on liner walls	Perforated sheet metal combined with porous sheet metal reduces hot spots and average metal temperature of the liners relative to earlier designs. Annular combustor eliminates the need for cross-over tubes which are a source creating a local hot spot in the can type
	Piece Broken out	Performance loss, premature engine removal, in flight shutdown, possible resultant damage to turbine airfoils.	Propagation of crack initiated by same cause as for cracked failure mode	Same as noted above for cracked failure mode. Probability of breaking out a large enough piece so that the liner tilts out of position is extremely remote
	Oxidation	Maintenance action	Exposure of metal to elevated temperature	Hastelloy-X material is utilized because of its oxidation resistance at the operating temperatures of the liners.

Figure 17-1

WEIGHT SUMMARY FOR BOEING INSTALLATION
STF219-B

Airflow = 640 lb/sec

Fan rotor, stator, case and front mount	725 lb
Intermediate case	637
High-pressure compressor rotor, stator, case	597
Diffuser and burner	960
Turbine rotor, stator, and shaft	1337
Turbine exhaust	242
Ducts, liners and variable area nozzle	1676
Blow-in-door ejector-reverser	2000
Control components and plumbing	753
Lube system and gearbox	323
Total estimated dry engine weight	9250 lb
*Additional equipment and installation features	540
Engine Specification Weight	9790 lb

*Includes the following items:

1. Lengthened ducts and ejector system to expose rear mount ring
2. Common fuel inlet manifold
3. Reverser null thrust capability
4. Additional tower shaft (power take-off)
5. Secondary air ducts (and valves)
6. Strengthened front mount capable of supporting inlet
7. Ejector cambered six degrees from engine centerline
8. Provisions for supplying air for inlet anti-icing

Figure 17-2

WEIGHT SUMMARY FOR LOCKHEED INSTALLATION
STF219-L

Airflow = 700 lb/sec

Fan rotor, stator, case and front mount	792 lb
Intermediate case	721
High-pressure compressor rotor, stator, case	727
Diffuser and burner	1056
Turbine rotor, stator, and shaft	1570
Turbine exhaust	272
Ducts, liners and variable area nozzle	1814
Blow-in-door ejector-reverser	2080
Control components and plumbing	843
Lube system and gearbox	350
Total estimated dry engine weight	10,225 lb
*Additional equipment and installation features	130
Engine Specification Weight	10,355 lb

*Includes the following items

1. Additional towershaft and angle gearbox for aircraft use
2. Fuel filter and fuel heater

Figure 17-3

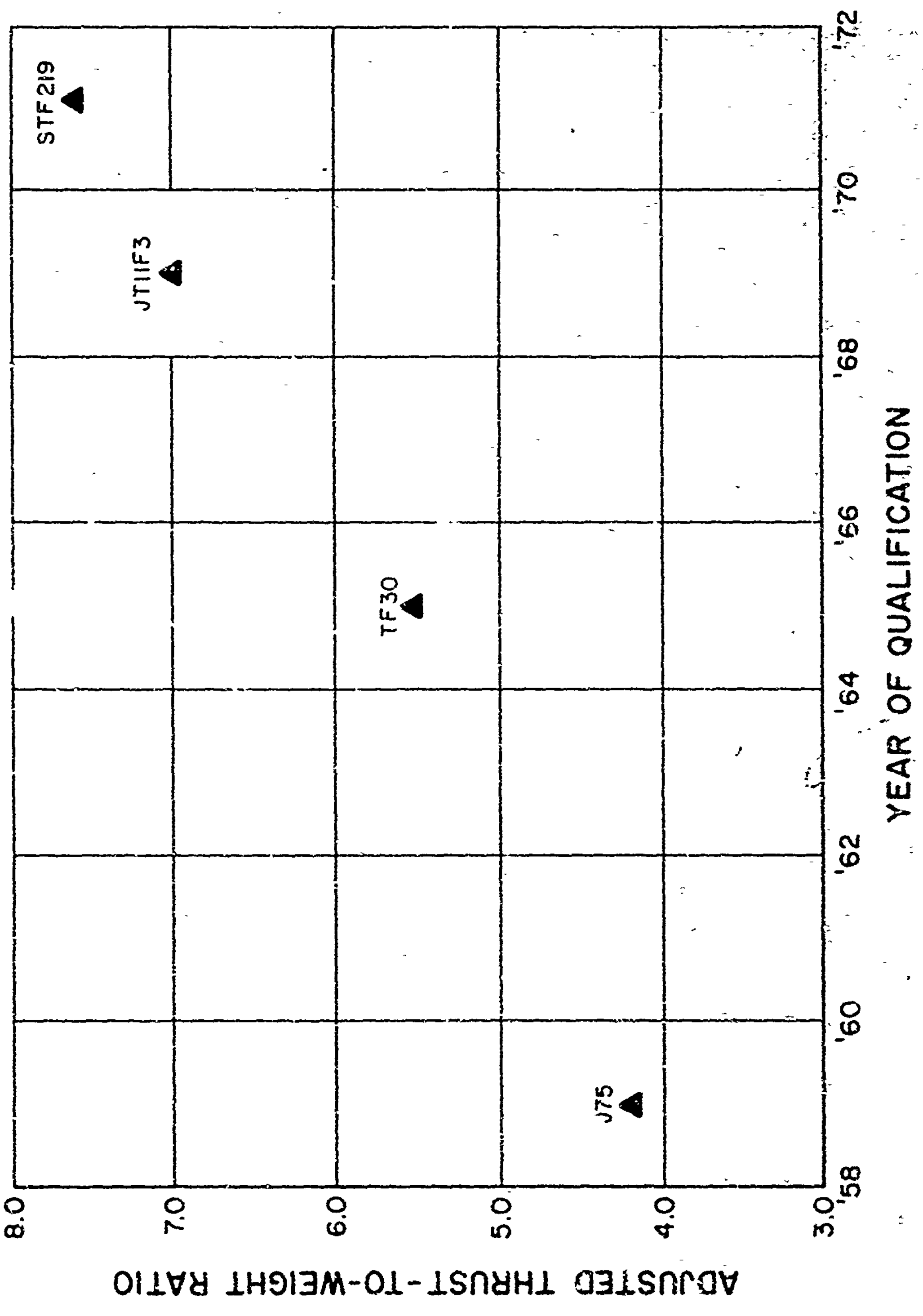

ADJUSTED THRUST-TO-WEIGHT RATIOS VS TIME

FOR SUPERSONIC ENGINES

Figure 17-4

COMPARISON OF ENGINE WEIGHT AND SIZE

Engine Designation	Airflow. lb/sec	Dry Weight, pounds	Ejector Diameter inches
STF219	600	8400	76.3
STJ221	690	11600	87.0
STJ222	450	8300	71.8
STJ227	690	11900	87.0

Figure 17-5

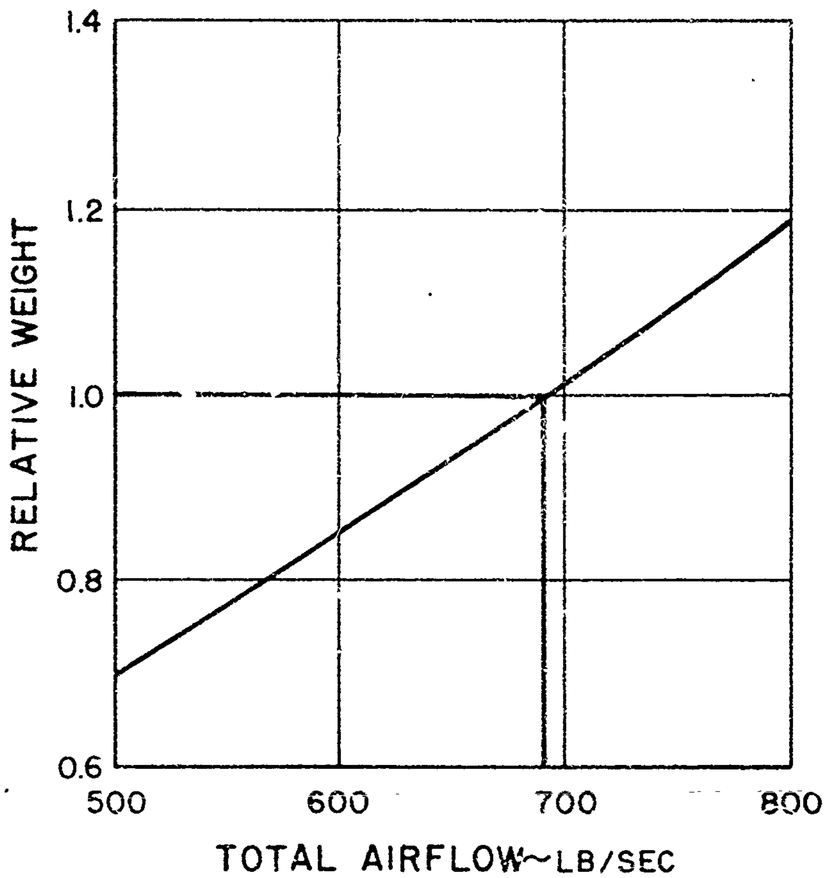

STJ221 ENGINE WEIGHT VS AIRFLOW

Figure 17-6

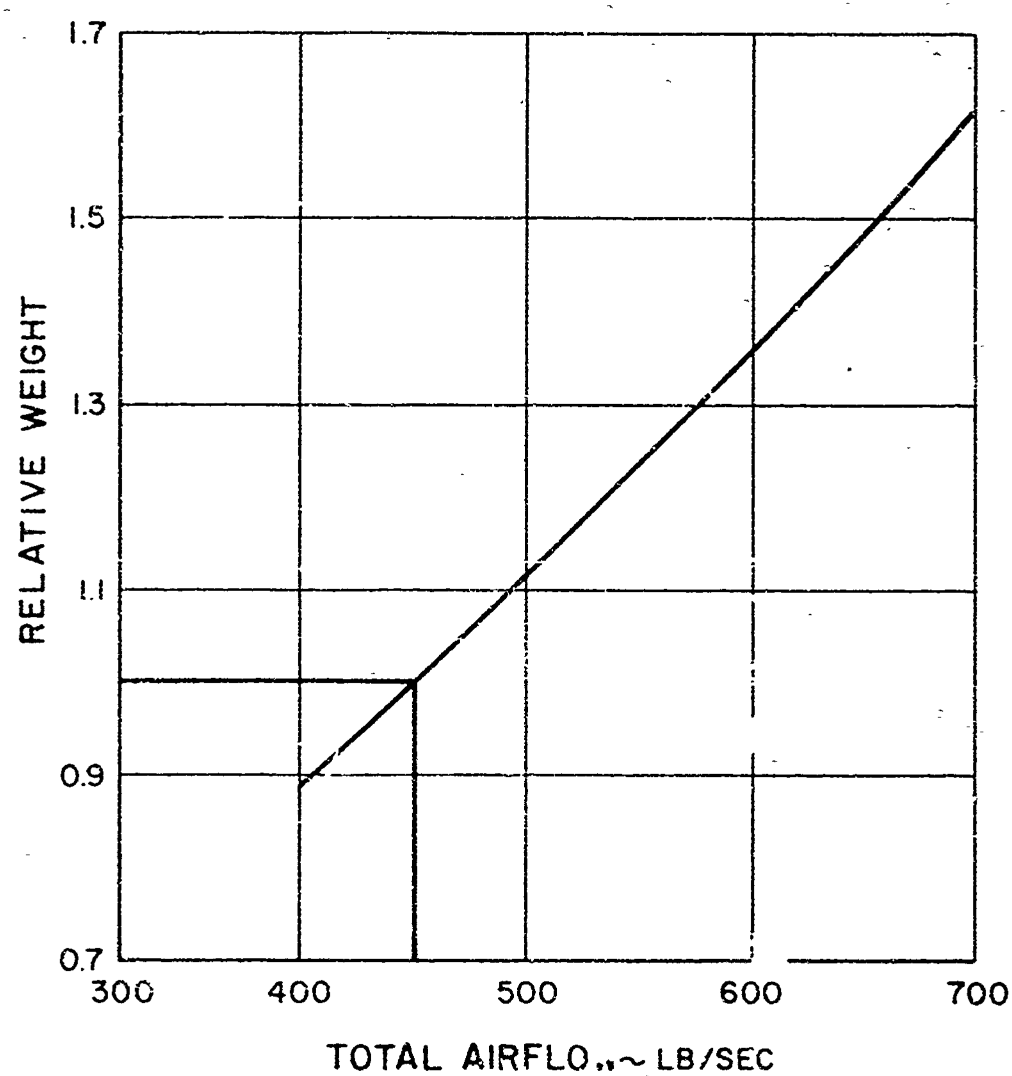

STJ222 ENGINE WEIGHT VS AIRFLOW

Figure 17-7

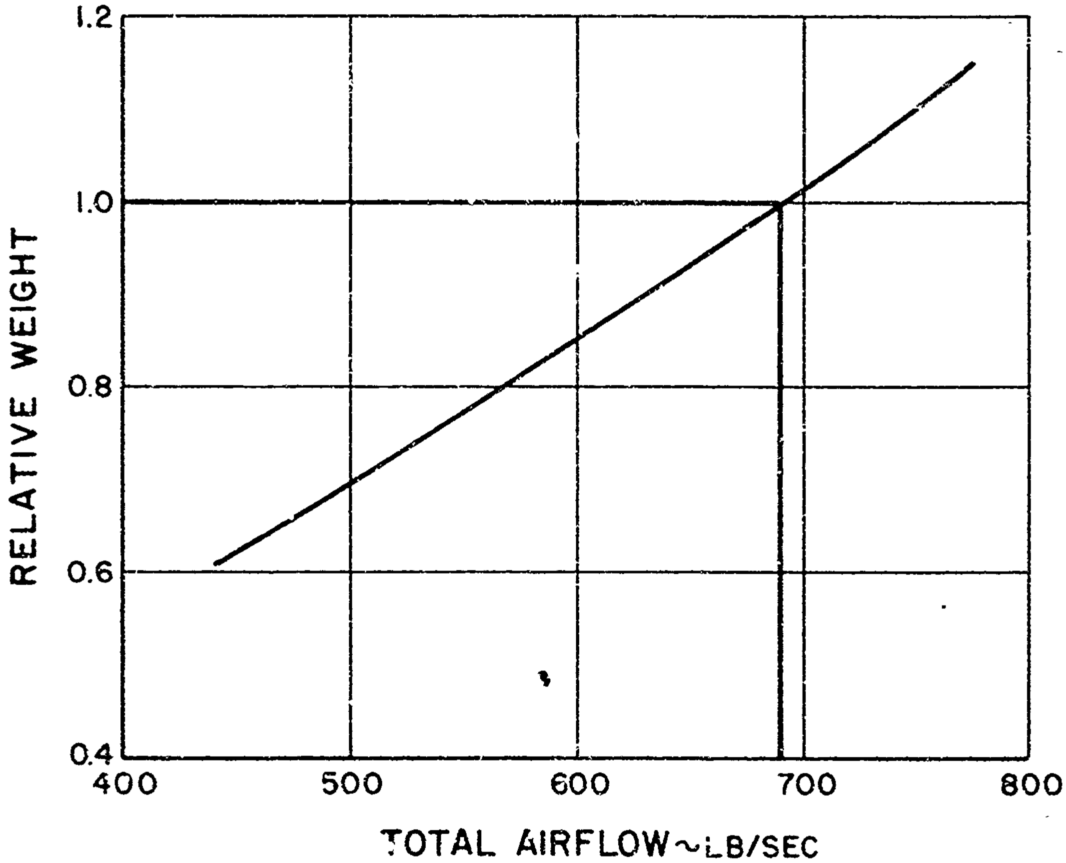

STJ227 ENGINE WEIGHT VS AIRFLOW

Figure 17-8

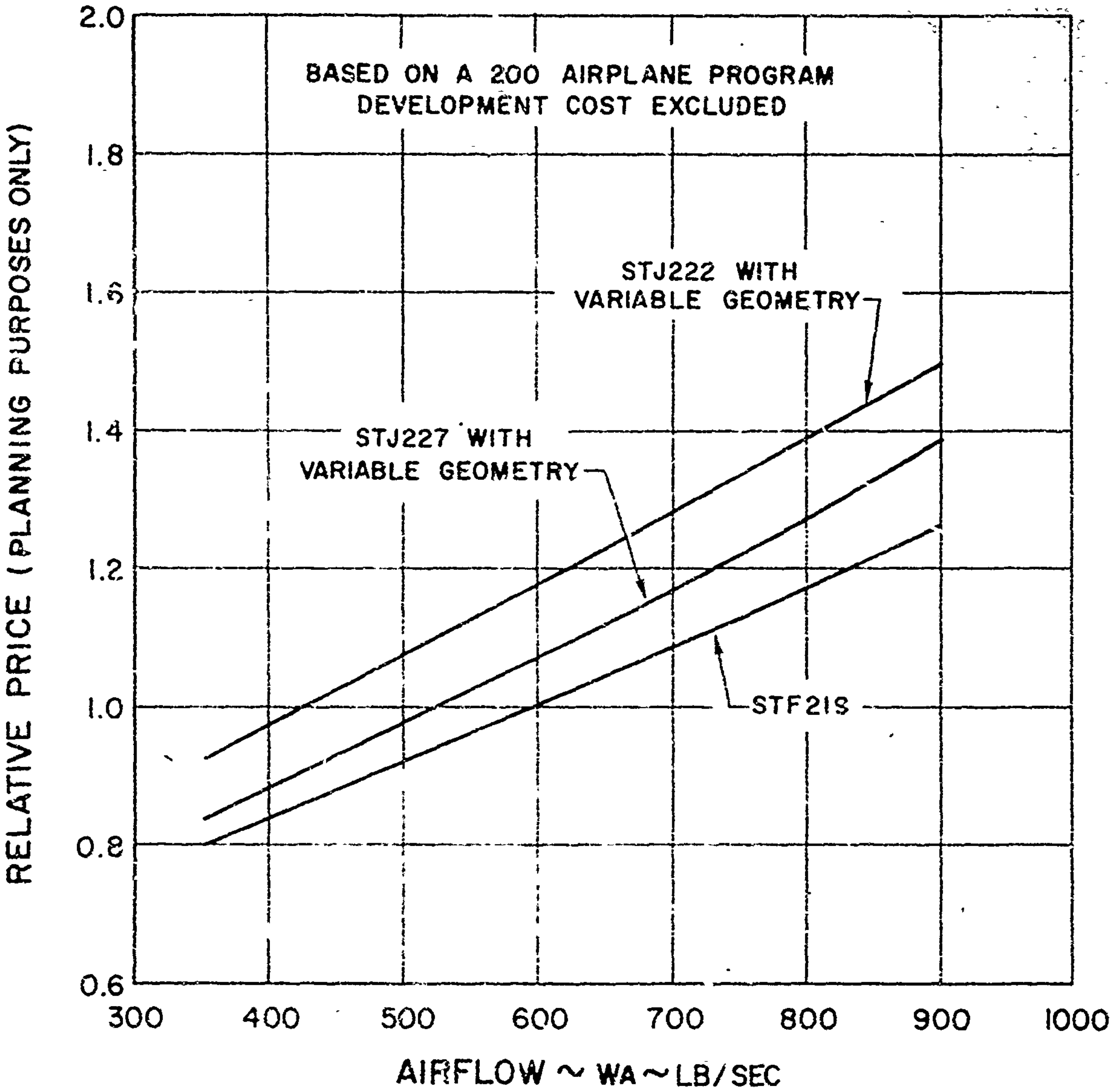

ESTIMATED RELATIVE PRICE VS AIRFLOW OF SST ENGINES INCLUDING EJECTOR REVERSER

Figure 17-9

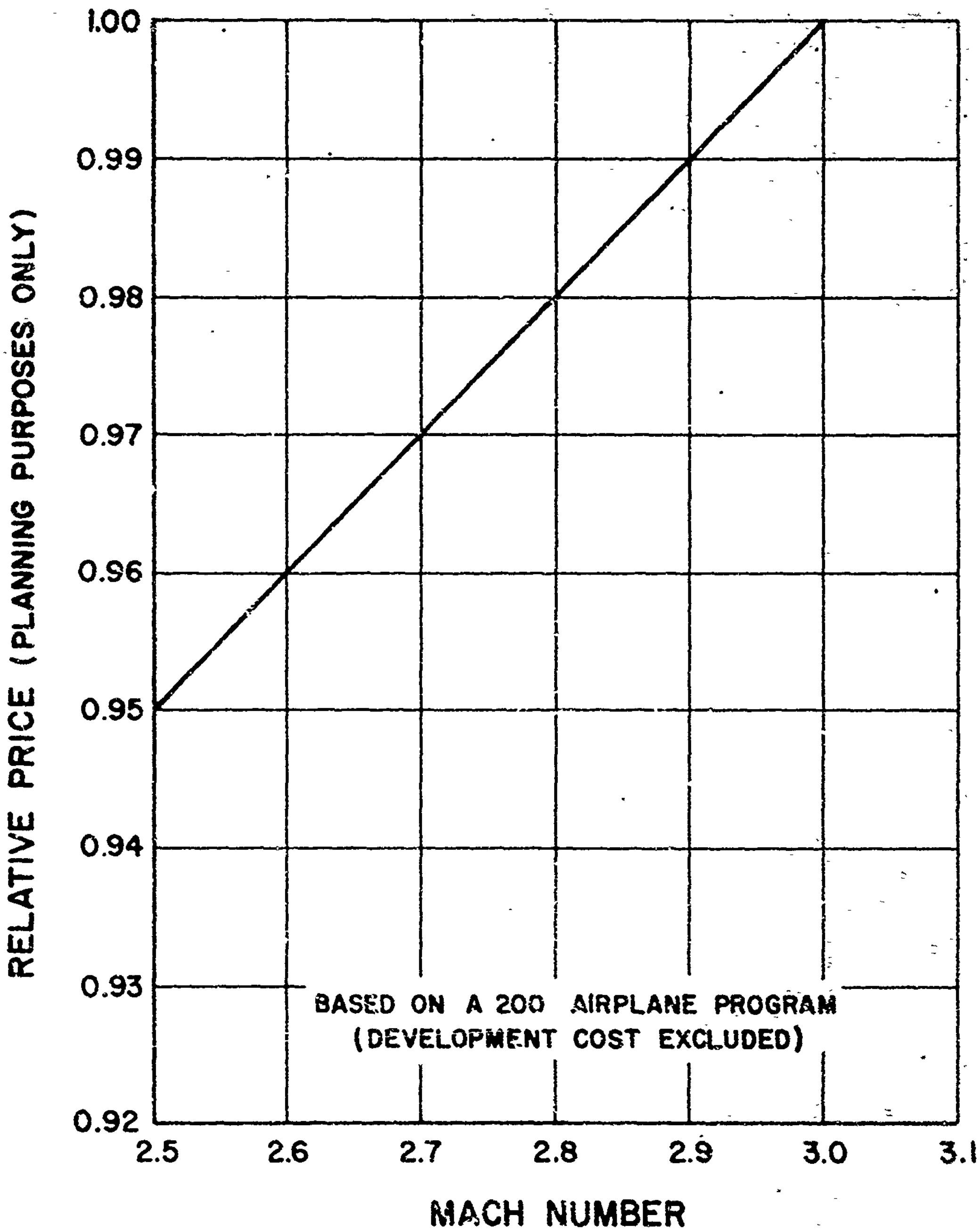

ESTIMATED RELATIVE PRICE VS MACH NUMBER OF SST ENGINES
INCLUDING EJECTOR REVERSER

Figure 17-10

PRATT

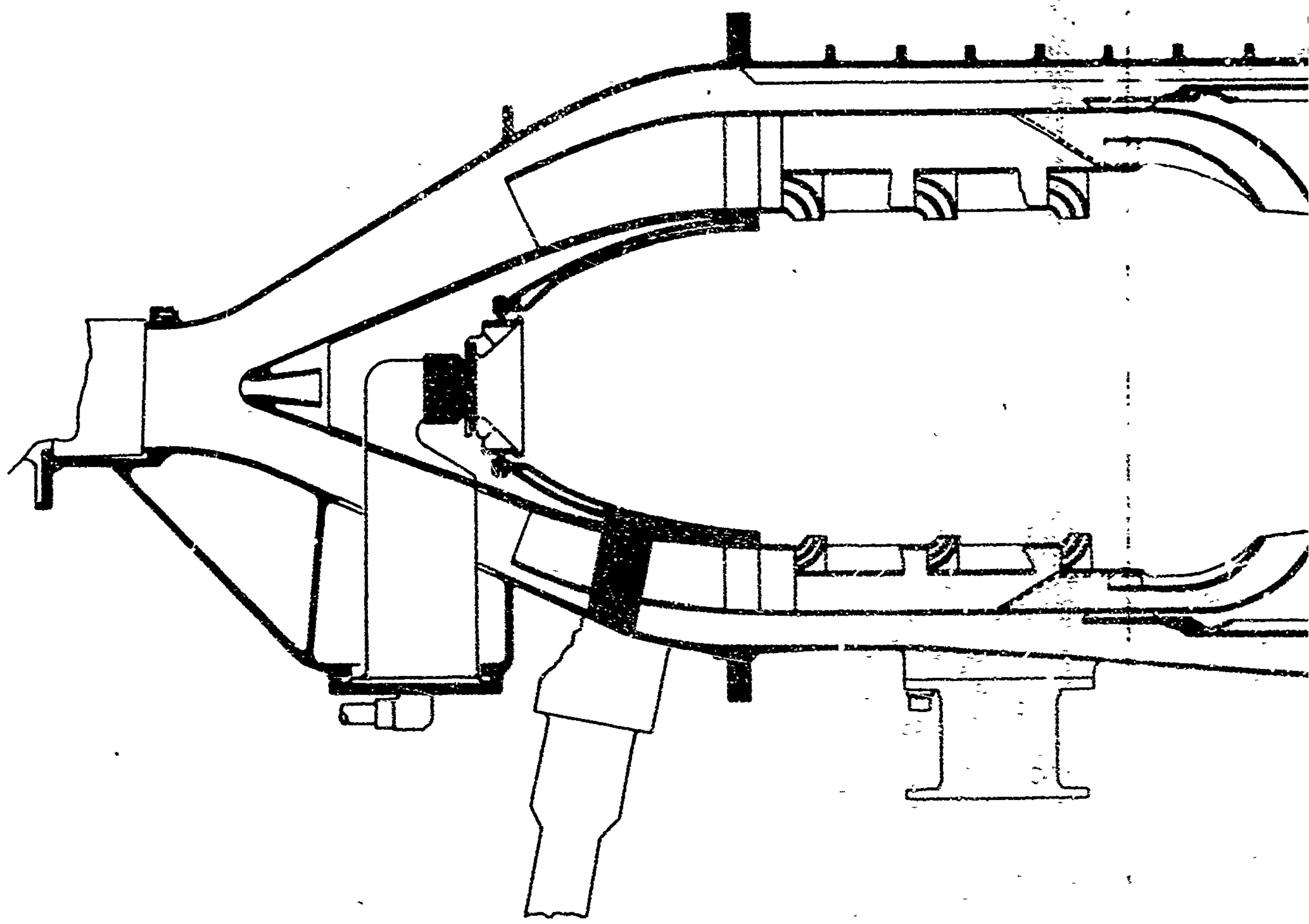

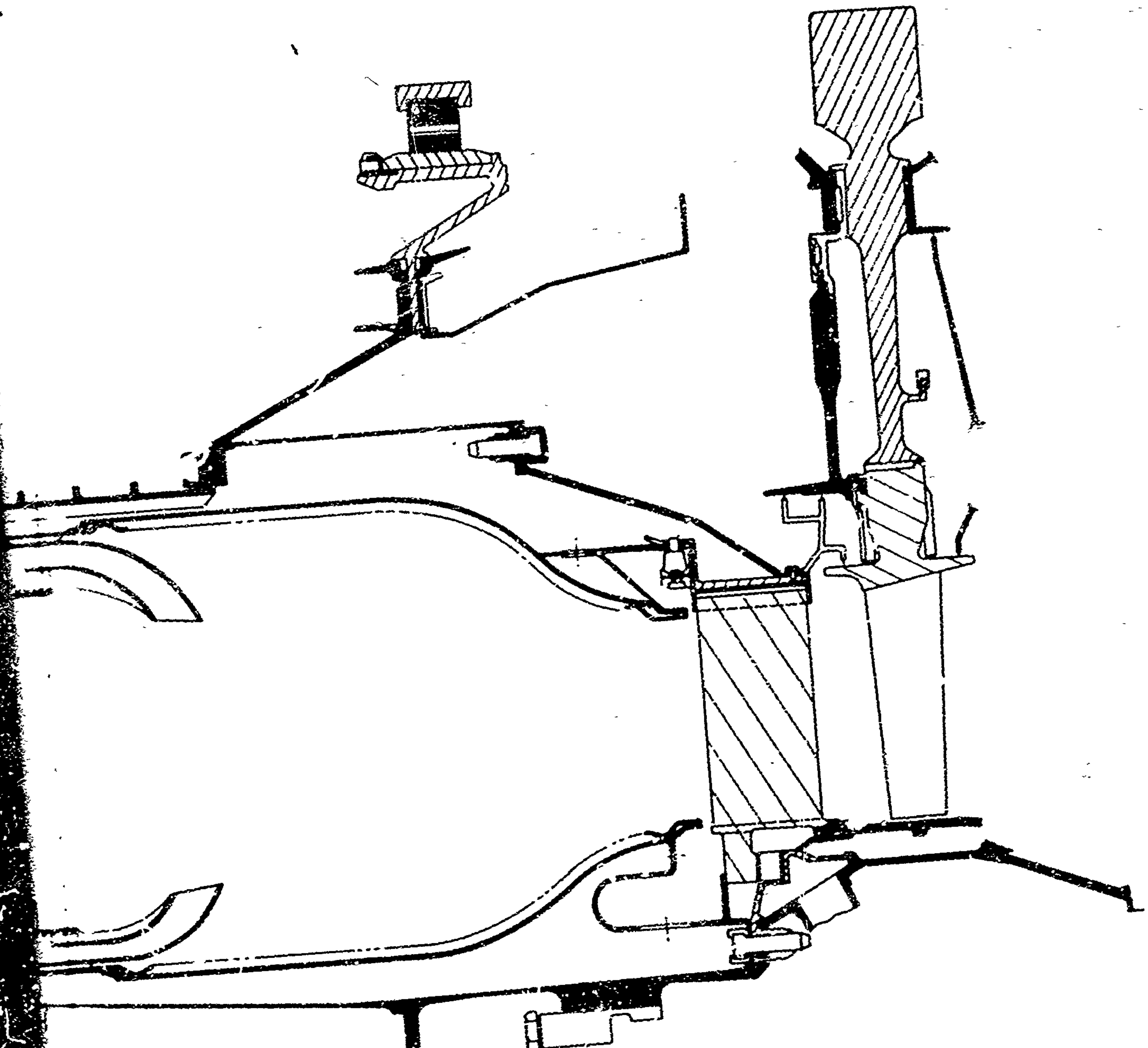

Part I - Engine Hot Section

STF219 HOT SECTION MAINTENANCE

Figure 17-11

Sheet 1 of 5

PRATT & WHITNEY A

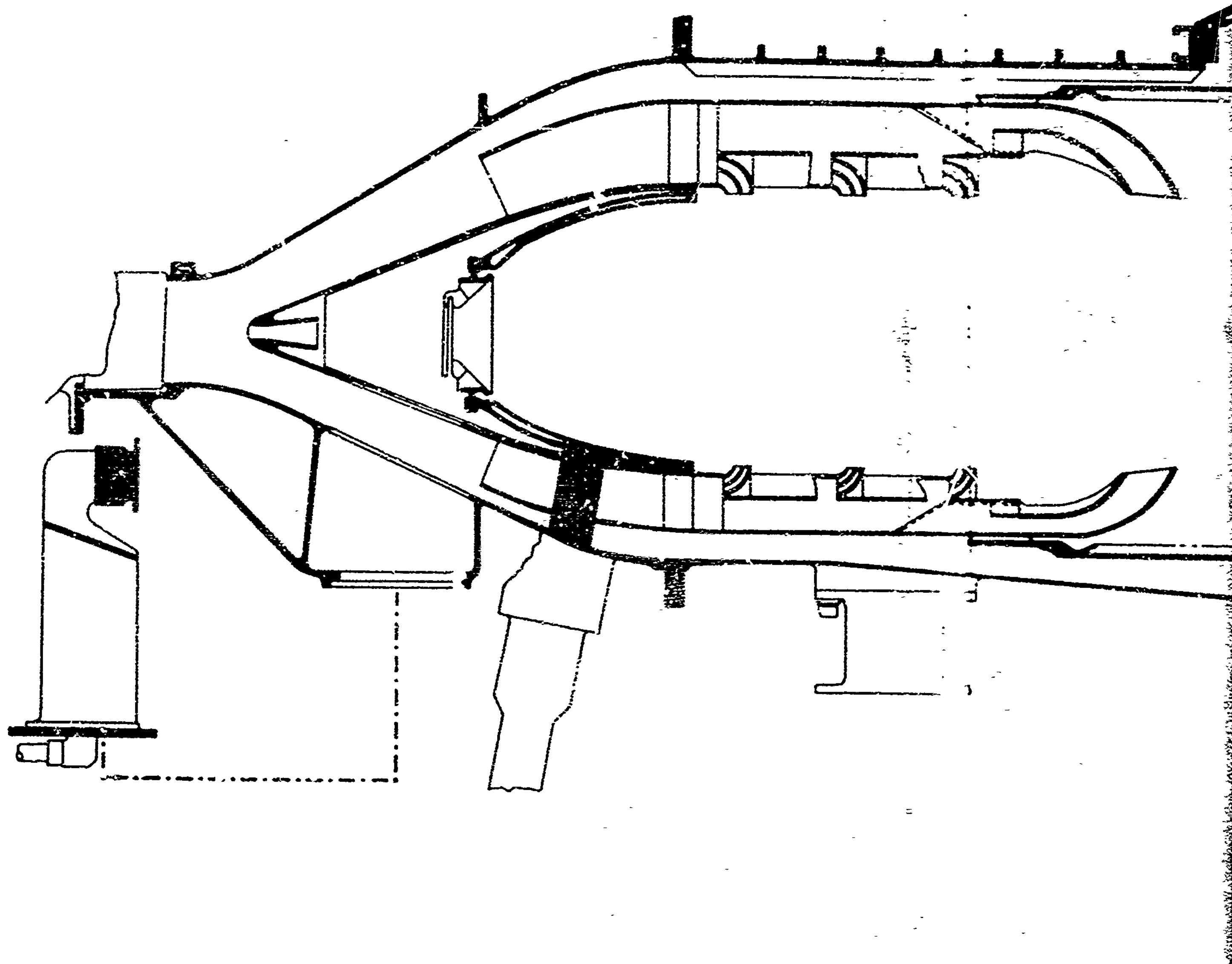

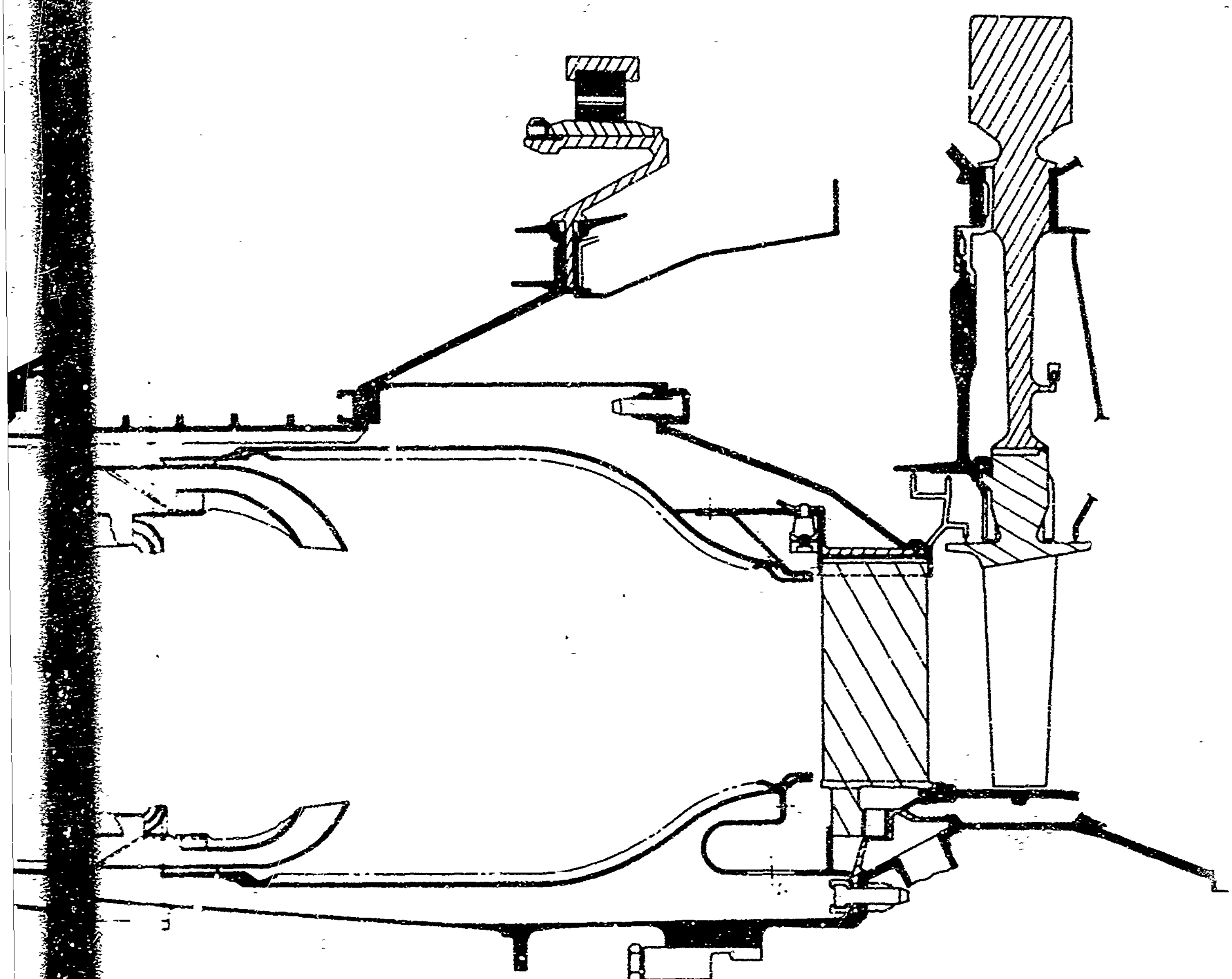

Part 2 - Fuel Nozzle Inspection

STF219 HOT SECTION MAINTENANCE (Cont'd.)

Figure 17-11

Sheet 2 of 5

1

2

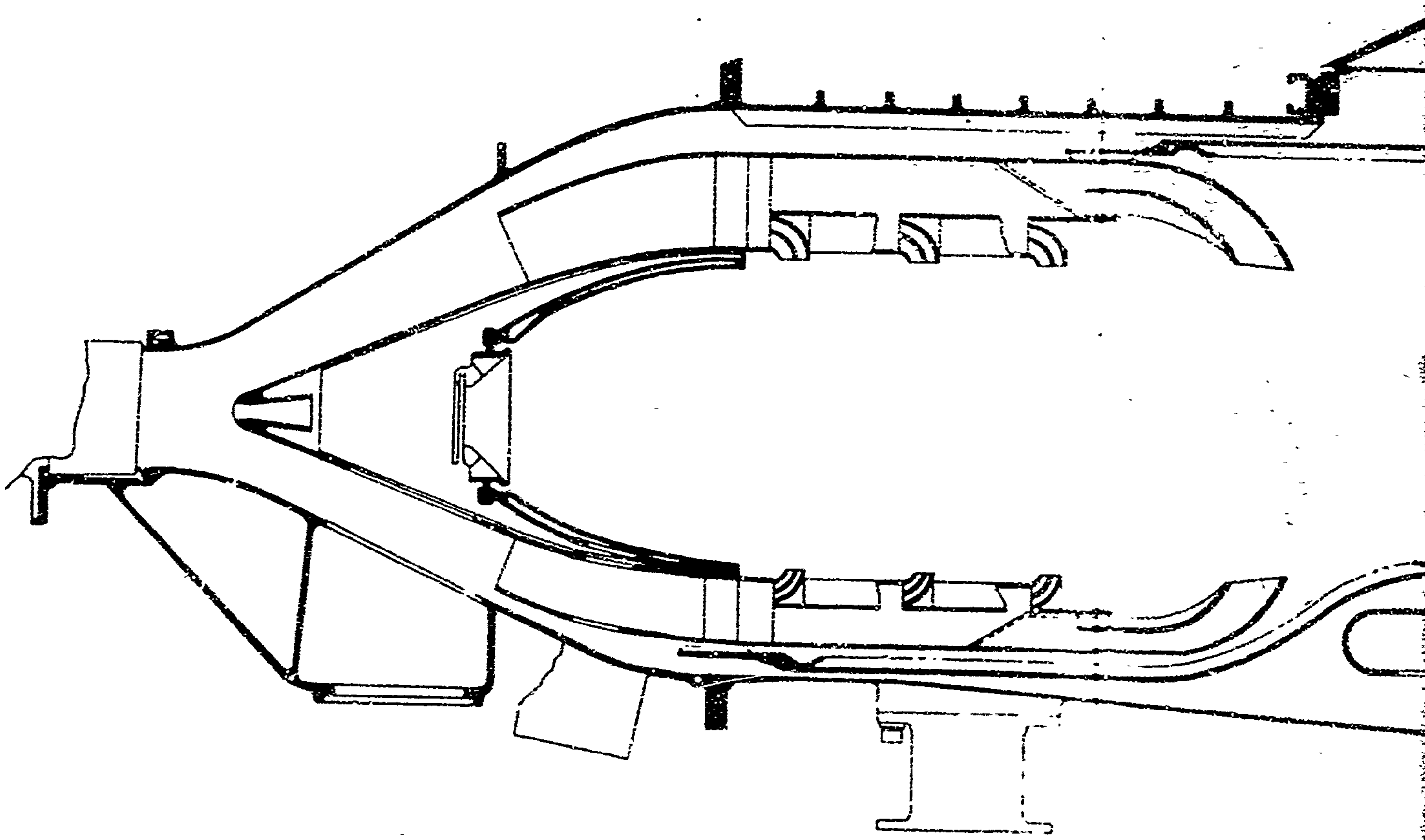

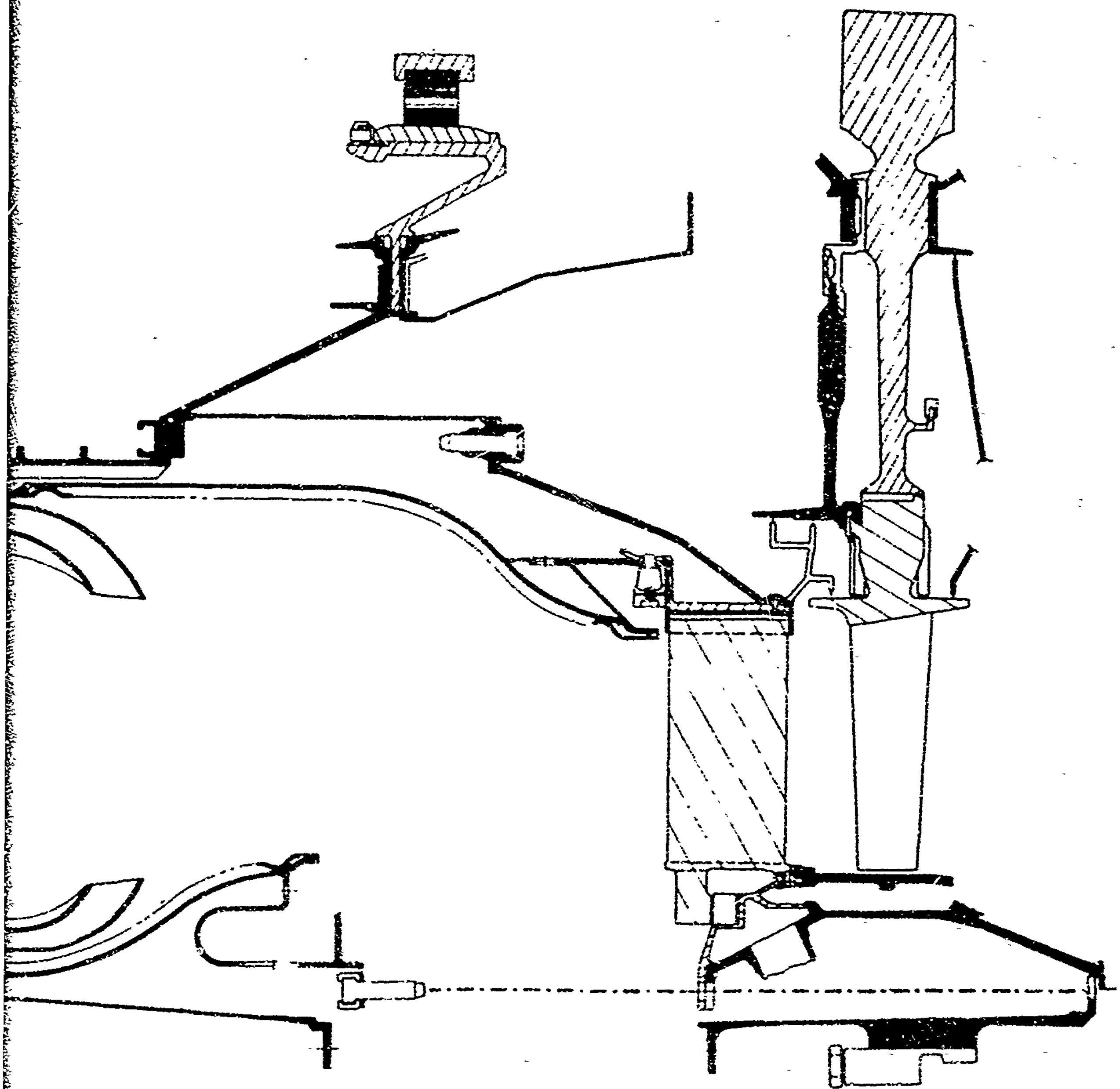

Part 3 - First-Stage Nozzle Vane and Combustion Liner Inspection

STF219 HOT SECTION MAINTENANCE (Cont'd.)

Figure 17-11

Sheet 3 of 5

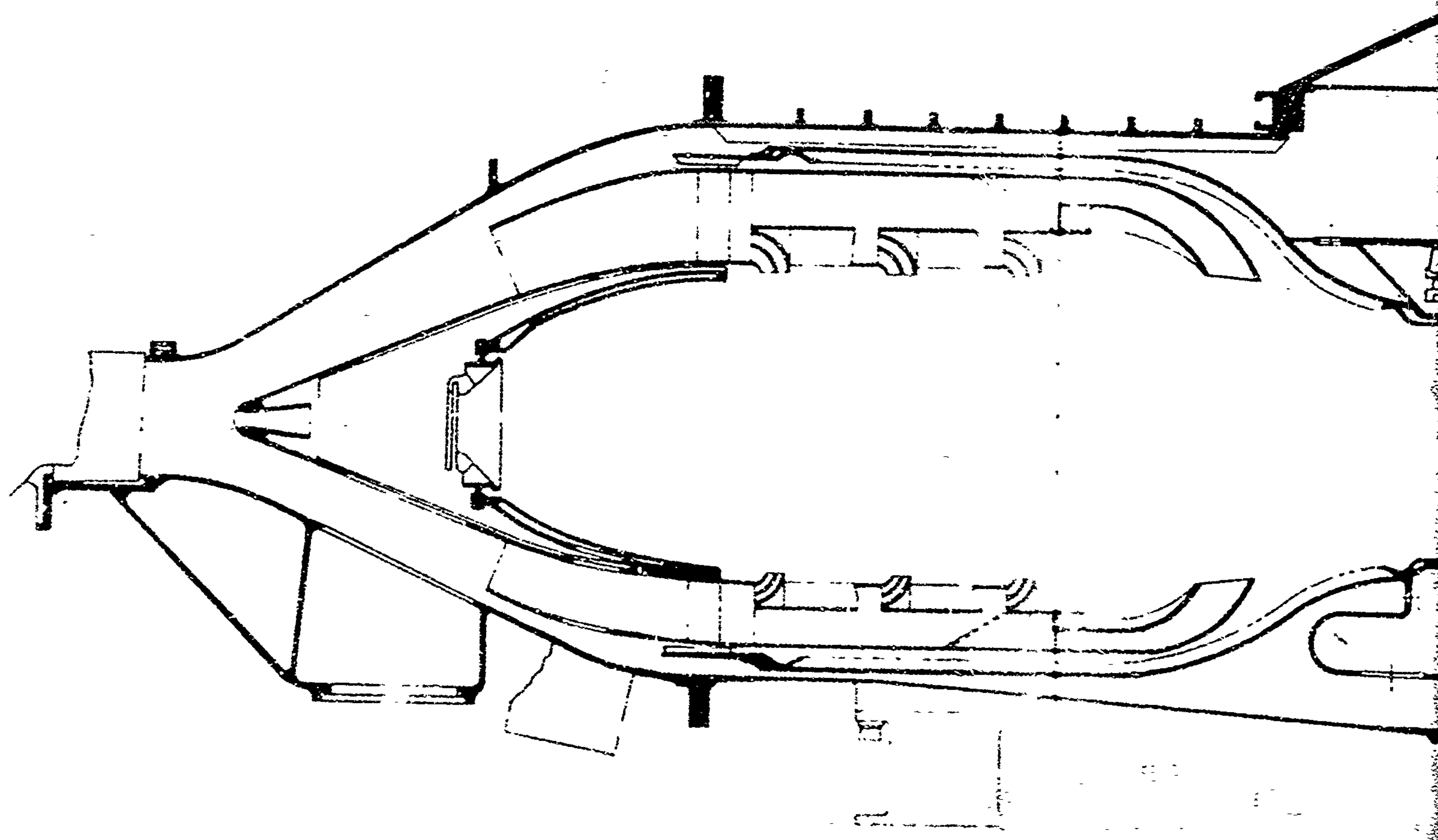

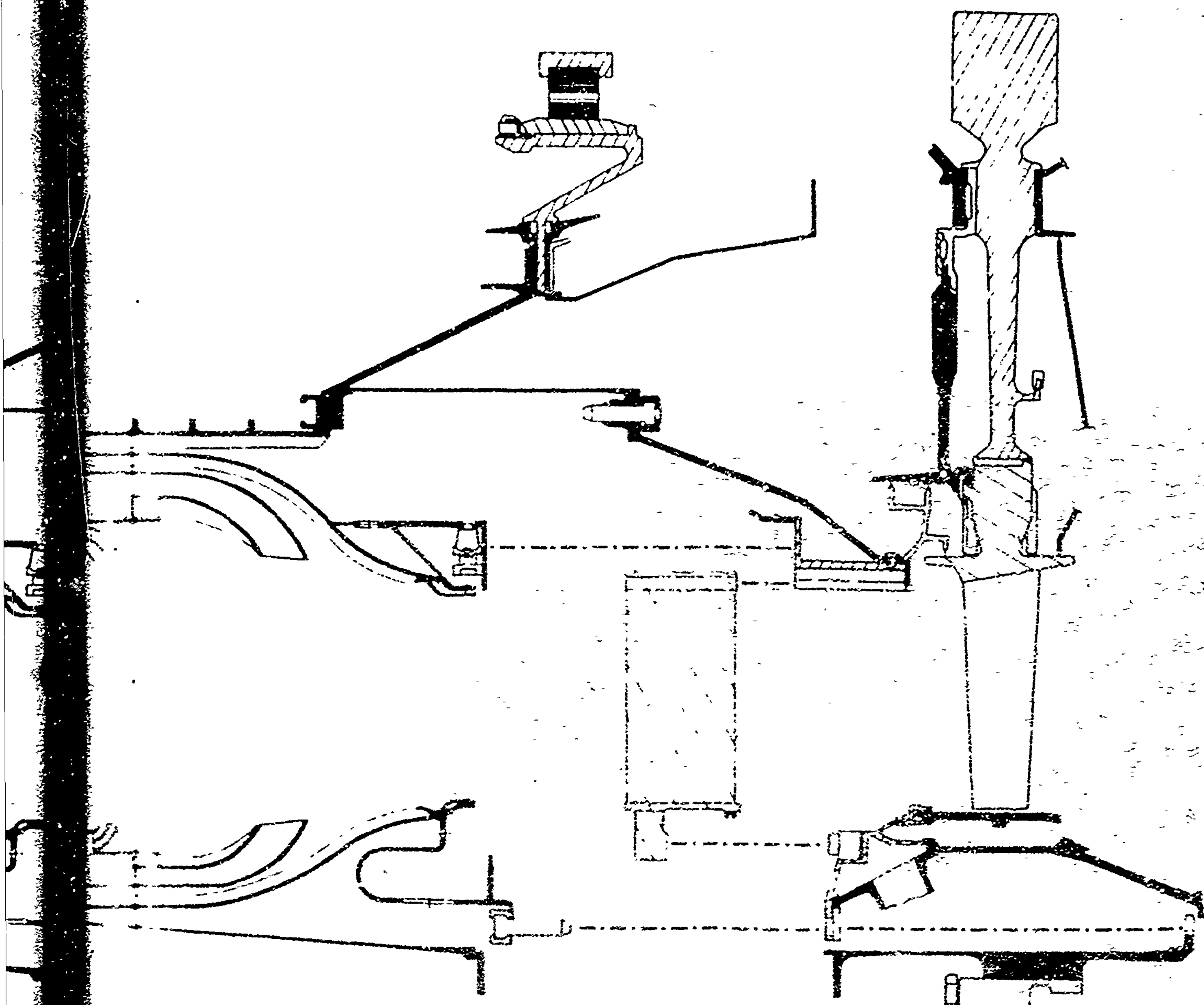

Part 4 - First-Stage Nozzle Vane Removal and First-Stage Turbine Blade Inspection

STEP - HOT SECTION MAINTENANCE (Cont'd)

Figure [illegible]-11

Sheet 1 of [illegible]

2

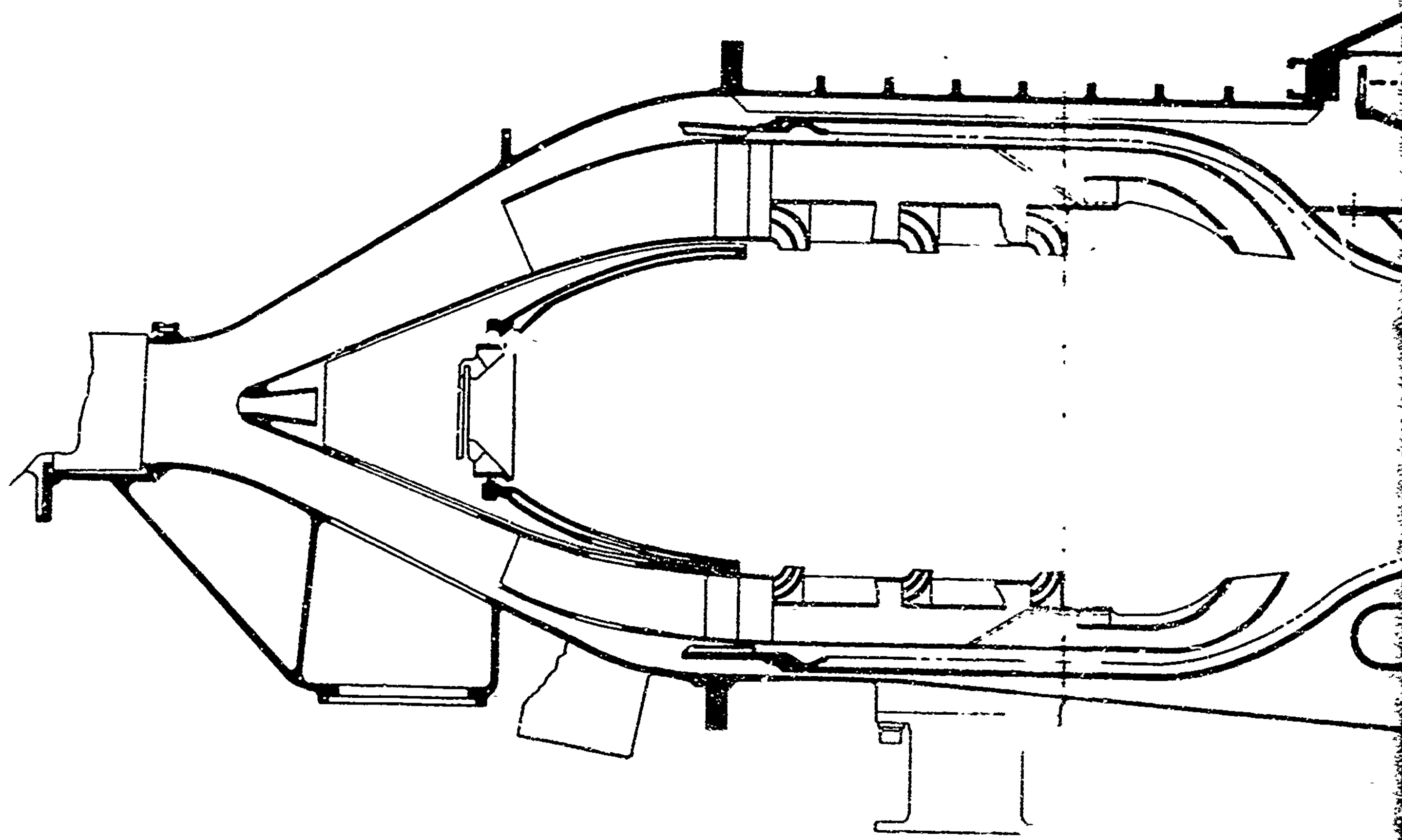

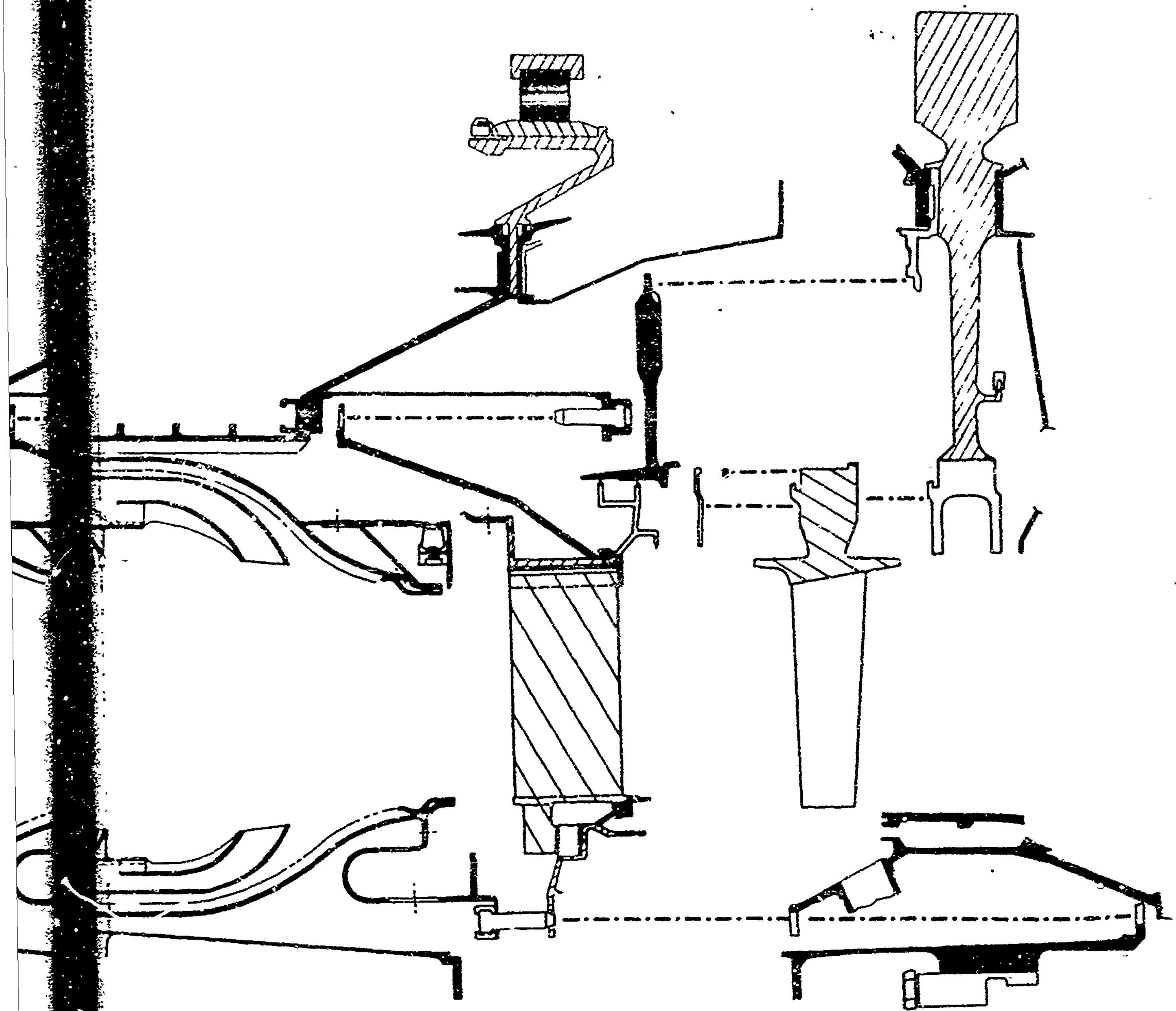

Part 5 - First-Stage Turbine Blade Removal

STF219 HOT SECTION MAINTENANCE (Cont'd.)

Figure 17-11
Sheet 5 of 5

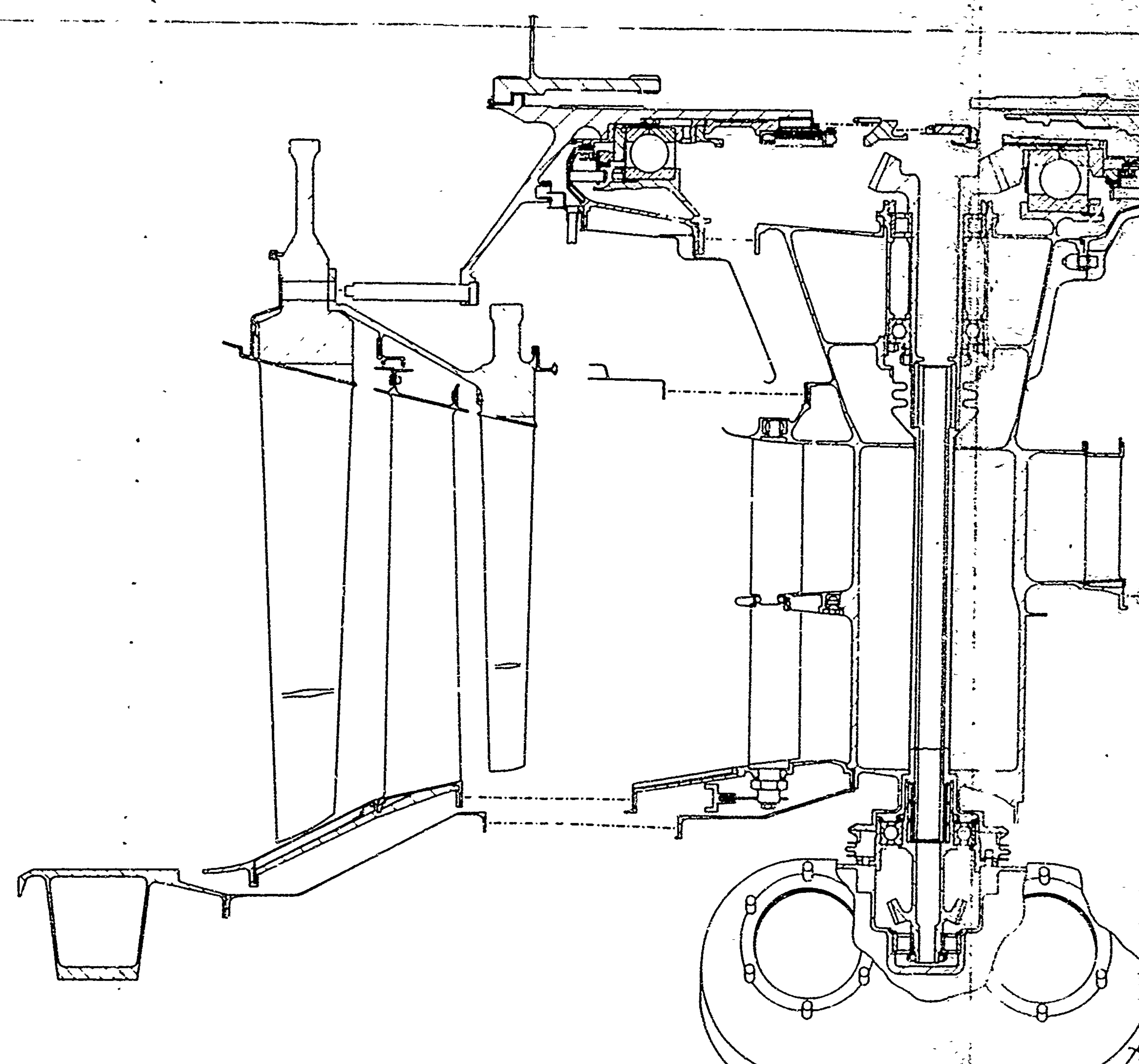

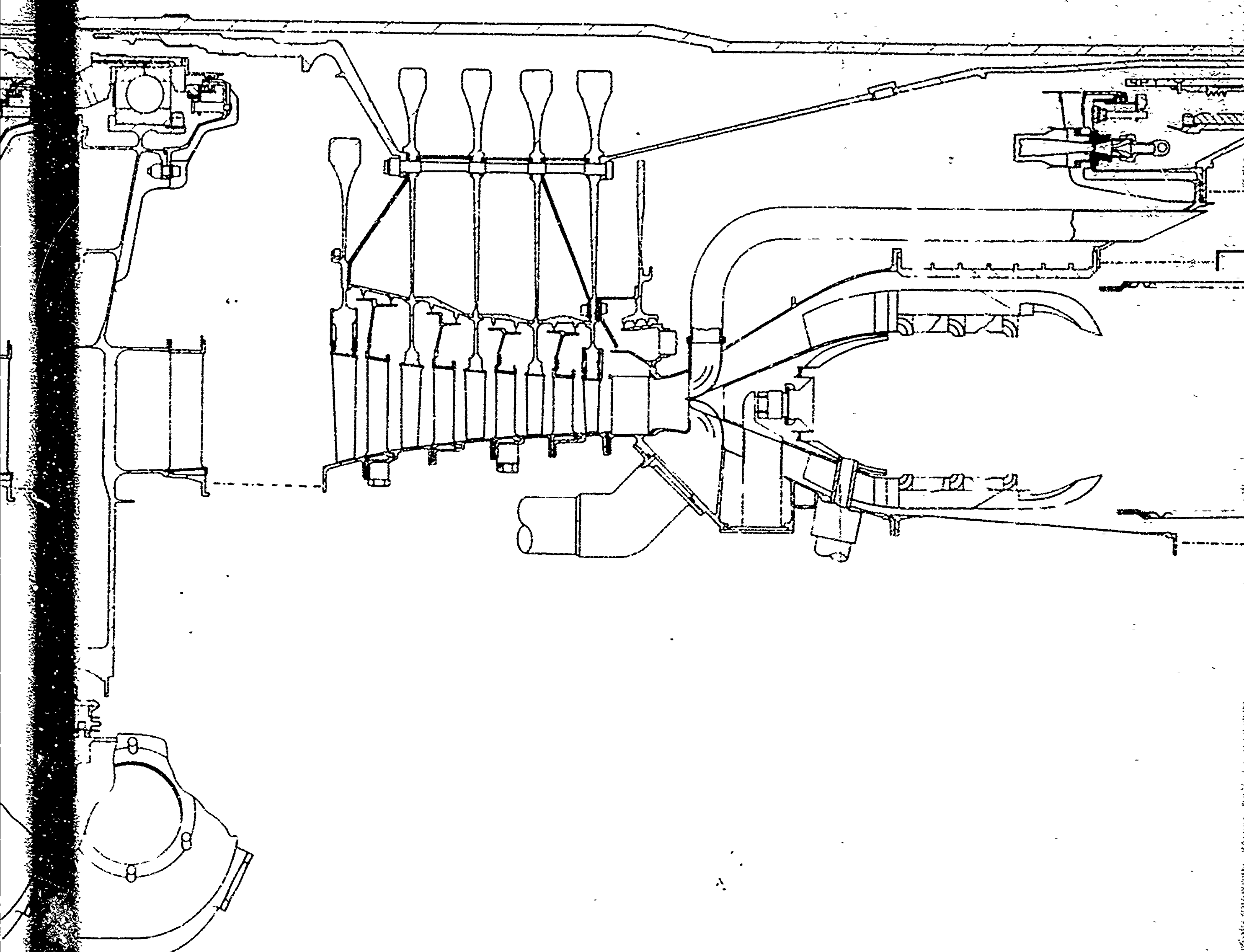

2

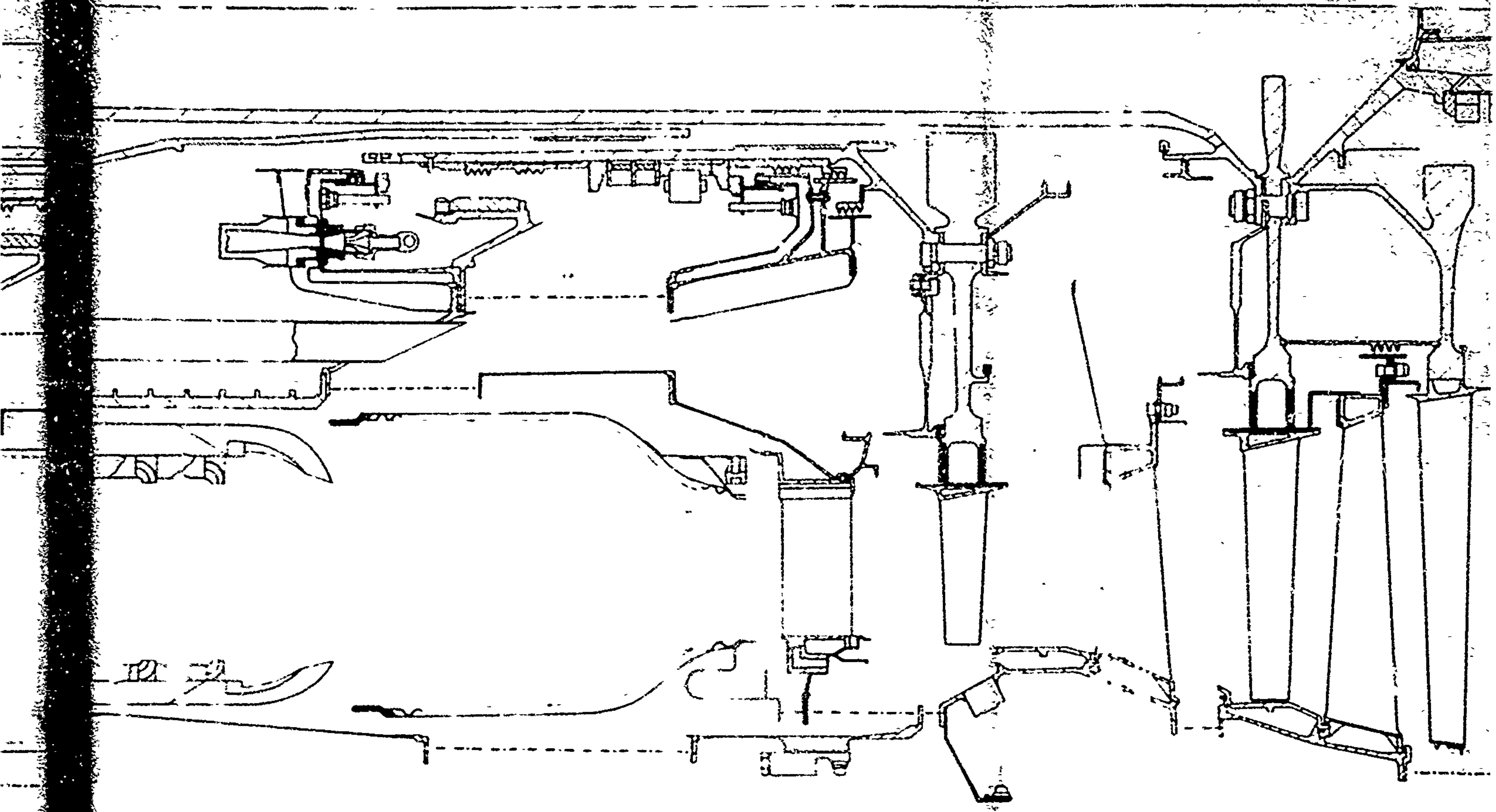

2

3

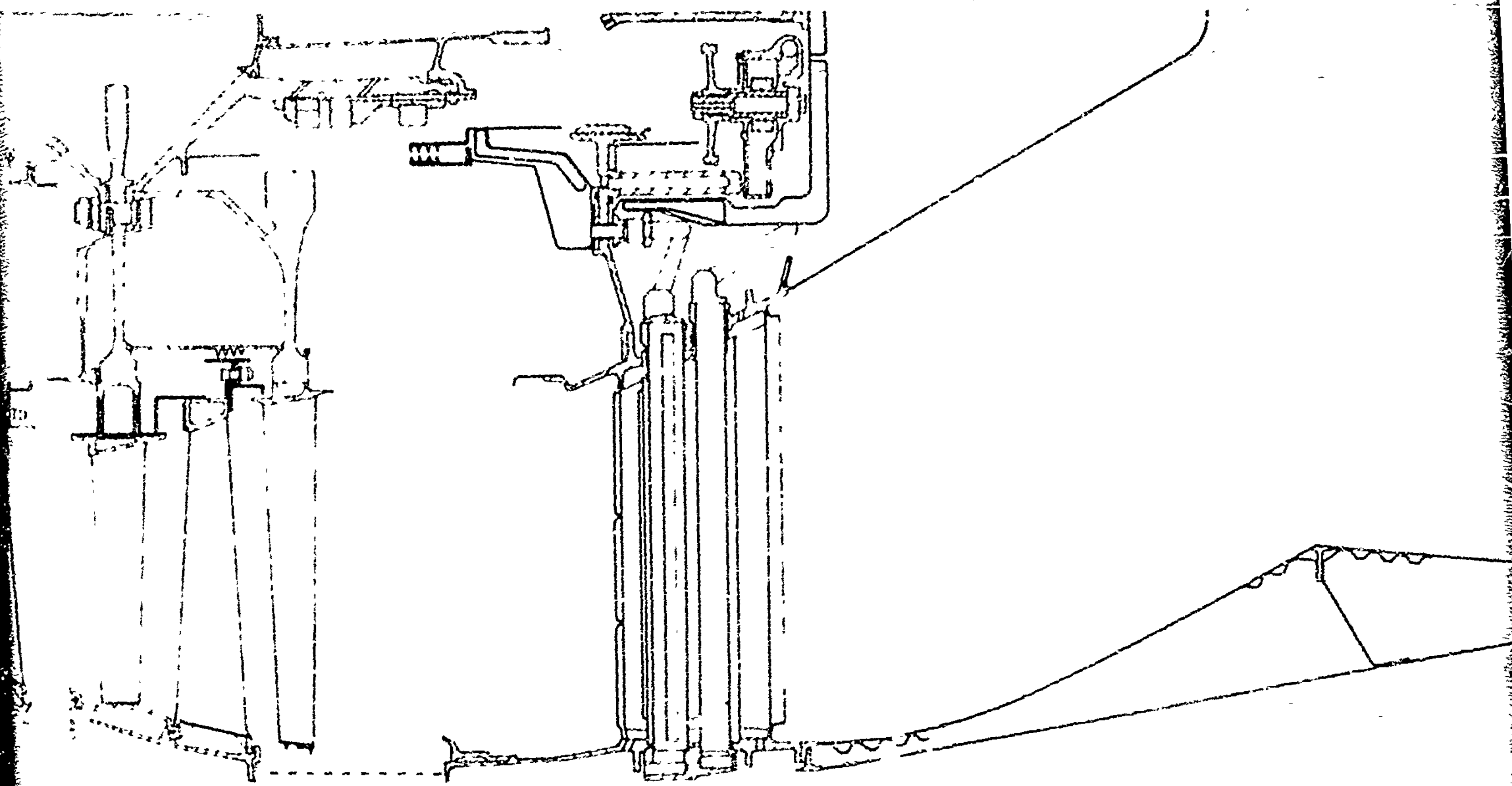

STF219 MAJOR DISASSEMBLY UNIT

Figure 1?-12

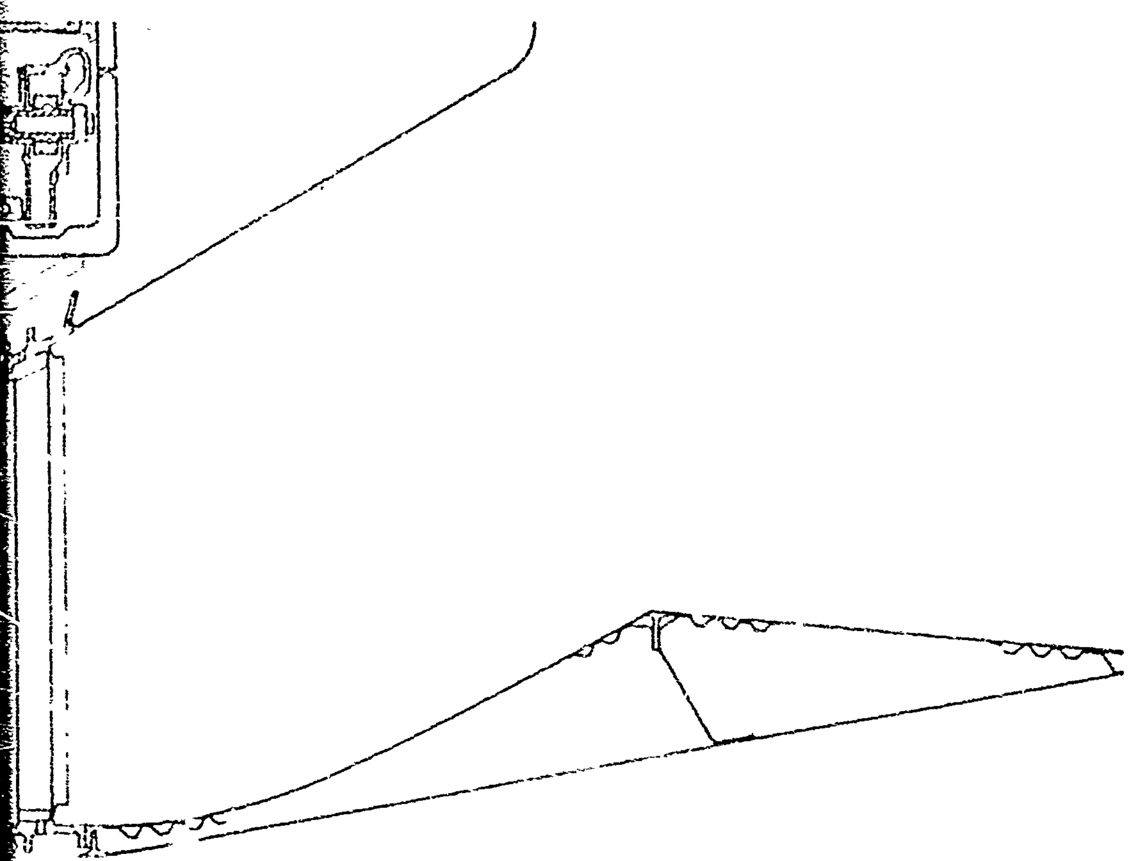

STF-19 MAJOR DISASSEMBLY UNITS

Figure 17-12

5